

ISOTOPES IN ORGANIC CHEMISTRY

W. H. NCEL AND C. C. LEE / EDITORS

VOLUME 3

CARBON-13 IN ORGANIC CHEMISTRY



ELSEVIER



Donated to
TRINITY UNIVERSITY LIBRARY
by
THE EWING HALSELL FOUNDATION
in memory of
GRACE FORTNER RIDER

ISOTOPES IN ORGANIC CHEMISTRY

ELSEVIER SCIENTIFIC PUBLISHING COMPANY
335 Jan van Galenstraat
P.O. Box 211, Amsterdam, The Netherlands

Distributors for the United States and Canada:

ELSEVIER NORTH-HOLLAND INC.
52, Vanderbilt Avenue
New York, N.Y. 10017

Library of Congress Cataloging in Publication Data

Main entry under title:

Carbon-13 in organic chemistry.

(Isotopes in organic chemistry ; v. 3)

Includes bibliographical references and index.

1. Carbon--Isotopes. 2. Chemistry, Organic.

I. Dunn, Gerald Emery, 1919-

II. Series.

QD466.5.C1C317

547.1'388

76-49680

ISBN 0-444-41472-X

With 34 illustrations and 47 tables

© Elsevier Scientific Publishing Company, 1977.

All rights reserved. No part of this publication may be reproduced, stored in a retrieval system or transmitted in any form or by any means, electronic, mechanical, photocopying, recording or otherwise, without the prior written permission of the publisher, Elsevier Scientific Publishing Company, P.O. Box 330, Amsterdam, The Netherlands

Submission of an article for publication implies the transfer of the copyright from the author to the publisher and is also understood to imply that the article is not being considered for publication elsewhere.

Printed in The Netherlands

ISOTOPES IN ORGANIC CHEMISTRY

ADVISORY BOARD

R.P. Bell, F.R.S.	University of Stirling (Scotland)
A.N. Bourns	McMaster University (Canada)
C.J. Collins	Oak Ridge National Laboratory (U.S.A.)
V. Gold, F.R.S.	King's College, University of London (England)
A.J. Kresge	University of Toronto (Canada)
S. Oae	University of Tsukuba (Japan)
W.H. Saunders, Jr.	University of Rochester (U.S.A.)
D.E. Sunko	University of Zagreb (Yugoslavia)
M. Wolfsberg	University of California, Irvine (U.S.A.)
H. Zollinger	Federal Institute of Technology, Zürich (Switzerland)

CONTRIBUTORS TO VOLUME 3

- | | |
|-------------|---|
| G.E. Dunn | Department of Chemistry,
University of Manitoba,
Winnipeg, Manitoba, Canada. |
| A. Fry | Department of Chemistry,
University of Arkansas,
Fayetteville, Arkansas, U.S.A. |
| J. Hinton | Department of Chemistry,
University of Arkansas,
Fayetteville, Arkansas, U.S.A. |
| G. Kunesch | Institut de Chimie des Substances Naturelles,
Gif-sur-Yvette, France. |
| M. Oka | Department of Chemistry,
University of Arkansas,
Fayetteville, Arkansas, U.S.A. |
| A.S. Perlin | Department of Chemistry,
McGill University,
Montreal, Quebec, Canada. |
| C. Poupat | Institut de Chimie des Substances Naturelles,
Gif-sur-Yvette, France. |
| A.W. Willi | Fachbereich Chemie,
Universität Hamburg,
Hamburg, West Germany. |

ISOTOPES IN ORGANIC CHEMISTRY

Edited by

E. BUNCEL

Queen's University, Kingston, Ontario, Canada

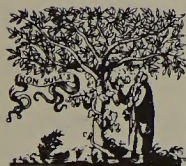
and

C.C. LEE

University of Saskatchewan, Saskatoon, Saskatchewan, Canada

Volume 3

Carbon-13 in organic chemistry



ELSEVIER SCIENTIFIC PUBLISHING COMPANY

AMSTERDAM OXFORD NEW YORK

1977

QD

466.5

C1

C317

605814

ISOTOPES IN ORGANIC CHEMISTRY

Volume 1. Isotopes in molecular rearrangements

N.C. Deno The Pennsylvania State University	Deuterium labeling in carbonium ion rearrangements
W.R. Dolbier, Jr. University of Florida	Isotope effects in pericyclic reactions
J.L. Holmes University of Ottawa	The elucidation of mass spectral fragmentation mechanisms by isotopic labeling
D.H. Hunter University of Western Ontario	Isotopes in carbanion rearrangements
J.S. Swenton The Ohio State University	Utilization of deuterium labeling in organic photochemical rearrangements

Volume 2. Isotopes in hydrogen transfer processes

M.M. Kreevoy University of Minnesota	The effect of structure on isotope effects in proton transfer reactions
G. Lamaty Université de Montpellier	Deuterium exchange in carbonyl compounds
K.T. Leffek Dalhousie University	Proton transfers in nitro compounds
E.S. Lewis Rice University	Isotope effects in hydrogen atom transfer reactions
H. Simon and A. Kraus Technische Universität Munich	Hydrogen isotope transfer in biological processes
P.J. Smith University of Saskatchewan	Isotope effects in elimination reactions
R. Stewart University of British Columbia	Isotopes in oxidation reactions

Volume 4. Tritium in organic chemistry

- | | |
|--|---|
| E. Caspi
The Worcester Foundation for Experimental Biology | Tritium in studies of biosynthesis of sterols and triterpenes |
| A.J. Kresge
University of Toronto | Isotope effects requiring the use of tritium |
| G. Sundstrom, O. Hutzinger and S. Safe
University of Amsterdam and University of Guelph | Tritium labelled aromatics of biological and environmental significance |
| W. Spillane
University College, Galway | Tritium in photochemical and free radical aromatic substitution |
| W.-N. Tang
Texas A & M University | Reactions of energetic tritium atoms with organic compounds |
| D.W. Young
University of Sussex | Stereospecifically tritiated compounds: synthesis and use in biosynthetic/mechanistic studies |

FOREWORD TO VOLUME 1

Organic chemistry is characterized by a vast variety of compounds, structures and reactions realized by a rather limited number of chemical elements. One and the same element is generally represented by a considerable number of atoms, playing several different roles. It is evident that a method enabling us to give the otherwise anonymous atom a kind of identity should be of particular value in this branch of chemistry.

Tracing by means of similar but still chemically discernible groups has been practised in organic chemistry for a long time, and has revealed that organic reactions are far more varied than expected. Isotopes, being chemically identical in a qualitative and usually also in an almost quantitative sense, are far more powerful as tracers, due to this similarity and to the fact that atoms rather than groups are labelled and can be traced as such.

A simple account of the molecular species involved, their structures and configurations, cannot be considered a complete description of a chemical system in equilibrium. We know from studies of non-equilibrium systems that opposite reactions balancing one another are generally taking place. As far as species of different molecular compositions are concerned, this has been realized for more than a century. It is only in the last few decades, however, that we have had at hand the means to measure the amounts of different isotopes and follow the behaviour of systems which are non-equilibrium ones with respect to isotopic composition. This has led to a still more vivid picture of most systems in equilibrium, with several exchange reactions taking place, sometimes at rates too large to be measured on the classical time scale of chemical reactions.

Even this is not enough for the true scientist who wants to go beyond the knowledge of which reactions actually take place and how fast they occur. He feels a desire to know also how the atomic nuclei and electrons behave in the transition called a chemical reaction. His questions come close to the fundamental limit set by the principle of uncertainty. At present the transition state of the rate-determining reaction step seems to be the most complete description attainable. In such studies it is not only the qualitative chemical similarity of isotopes, allowing the identity of atoms in the transition state to be revealed, but also their quantitative chemical dissimilarity which is of importance and allows a study of the force field and hence binding conditions in the transition state itself. Thanks to the fairly low atomic number of most atomic species of importance in organic chemistry, the relative mass differences between isotopes are sufficient to cause differences in quantitative behaviour, rather easily measurable with modern instruments.

Many scientists feel the flood of scientific publications as an encumbrance. The justification for the existence of a series like the one started by the present volume lies in the aid that the surveys it contains may offer the research worker and, perhaps more important, the stimulus for further research that may be provided. The applica-

tion of isotope methods has undoubtedly a very important role in future research in organic chemistry. No attempt at a detailed prediction will be ventured here, however. It may suffice to refer to the development of the nuclear magnetic resonance technique. The studies of ordinary hydrogen nuclei, which have been of outstanding importance for the development of organic chemistry, can be considered as an application of isotope methods according to the ordinary usage of the concept only to the extent that deuterium has been used as a stand-in for protium. In the not-too-distant future, however, most laboratories will have equipment allowing routine studies of the less abundant carbon isotope ^{13}C , and then many chemists will be in possession of a sensitive probe in the centre of atoms of the most important element in organic chemistry. It will reveal not only details of molecular structure in the usual sense but also more subtle details about the electron distribution in the backbone of organic molecules. It is open to discussion, of course, whether this kind of work, which frequently makes use of the natural occurrence of heavy carbon, should be considered as an application of isotope methods. In any case, it utilizes a particular property of an isotope different from the most abundant one.

It is evident from the thoughts expressed in the last paragraph that the borders of the field "Isotopes in Organic Chemistry" are rather indeterminate. The editors' intention to apply as few restrictions as possible on subject matter seems wise, because then the interest taken in the present series by its future readers can be allowed to indicate the position of these borders in practice.

Göteborg

Lars Melander

PREFACE

The publication, in the late 1940's, of a number of monographs on tracer methodology, particularly the authoritative volume on *Isotopic Carbon* by Calvin, Heidelberger, Reid, Tolbert and Yankwich, has given great impetus to tracer studies in organic chemistry. The utilization of kinetic isotope effects as a probe for the transition state also gained in momentum with the publication in 1960 of the monograph *Isotope Effects on Reaction Rates* by Melander. With these developments, and the more recent advent of techniques such as n.m.r. and mass spectrometry, applications of both radioactive and stable isotopes have become extremely useful in many areas of investigation.

It is the intent of this series to bring together information from diverse areas of organic chemistry under the common theme highlighting the use and value of isotopes. Since in the future one can look to increasingly wider opportunities for utilization of isotopic studies, it is our intention to place as few restrictions as possible on the subject matter to be covered. It may also be hoped thereby that the series will aid in providing a stimulus for further research.

It is our plan that each volume should have a central theme as a link for the various chapters. Thus the first volume contained contributions relating to the broad area of *Isotopes in Molecular Rearrangements*, the second volume dealt with *Isotopes in Hydrogen Transfer Processes*, and the present volume is devoted to *Carbon-13 in Organic Chemistry*. Other broad topics to be covered in future volumes will include *Tritium in Organic Chemistry*, *Isotopes in Structural Elucidations*, *Isotopic Sulfur in Organic Chemistry*, etc. Coverage of any one broad topic will not necessarily be limited to one volume. A second volume on molecular rearrangements, for example, is being planned.

We feel honoured in that Professor Lars Melander has consented to write a Foreword to the series. Sincere appreciation is also extended to members of the Editorial Advisory Board for their valuable comments on various aspects of this undertaking, and most importantly, we would like to express our thanks to the contributing authors on whose efforts the success of this series will largely depend.

Kingston, Ontario
Saskatoon, Saskatchewan

E.B.
C.C.L.

CONTENTS

Foreword to Volume 1	ix
Preface	xi
Chapter 1. Carbon-13 kinetic isotope effects in decarboxylation, by G.E. Dunn	1
I. Introduction	1
II. General principles	1
III. Kinetic considerations	4
A. Monocarboxylic acids	5
B. Dicarboxylic acids	6
1. Intramolecular kinetic isotope effect, 7 – 2. Intermolecular carboxyl-carbon isotope effect, 8 – 3. Intermolecular α -carbon isotope effect, 9 –	
IV. Experimental considerations	10
V. Observed ^{13}C kinetic isotope effects	11
A. Monocarboxylic acids, aliphatic	12
1. Formic acid, 12 – 2. Trichloroacetic acid, 12 –	
B. Monocarboxylic acids, aromatic	13
1. Salicylic acid, 13 – 2. 2,4-Dihydroxybenzoic acid, 14 – 3. Anthranilic acids, 15 – 4. Mesitoic acid, 17 – 5. Azulene-1-carboxylic acid, 17 –	
C. Heterocyclic acids	18
1. Pyrrole-2-carboxylic acid, 18 – 2. Picolinic acid, 18 – 3. Quinaldinic acid, 21 –	
D. Dicarboxylic acids	22
1. Oxalic acid, 22 – 2. Malonic acid, 25 – 3. Bromomalonic acid, 29 – 4. Oxaloacetic acid, 29 – 5. Glutamic acid, 30 – 6. Pyridinedicarboxylic acid, 31 –	
VI. Related reactions	32
A. Bromodecarboxylation	32
B. Decarboxylation of esters	33
C. Photodecarboxylation	34
D. Oxidative decarboxylation	36
References	38
Chapter 2. Carbon-13 n.m.r. methodology and mechanistic applications, by J. Hinton, M. Oka and A. Fry	41
I. Introduction	41
II. Experimental techniques	41
III. Quantitative carbon-13 n.m.r. applications	50
IV. Carbon-13 n.m.r. mechanistic applications	66
A. Introduction	66
B. Carbenium ion rearrangements	67

C. Ketone rearrangements	75
D. Carbene and thermal decomposition and rearrangement reactions	80
E. Radical reactions studied by ^{13}C -n.m.r. CIDNP	86
F. Miscellaneous reactions and other mechanistic applications of ^{13}C -n.m.r. spectroscopy	92
References	99

Chapter 3. Biosynthetic studies using carbon-13 enriched precursors, by G. Kunesch and C. Poupat

I. Introduction	105
A. Indirect observation of carbon-13 enrichment: the satellite method	106
B. Direct observation of carbon-13 enrichment: CW and FT techniques	106
II. Incorporation of carbon-13 acetate	107
A. Griseofulvin	107
B. Radicinin	109
C. Latumcidin	111
D. Penicillic acid	113
E. Multicollic and multicolosic acids	116
F. Asperlin	117
G. Asperentin	118
H. Sterigmatocystin	119
I. Mollisin	122
J. Nigrifactin	124
K. Ochrephilone	125
L. Avenaciolide	126
M. Cytochalasanes: cytochalasin B and cytochalasin D	127
III. Combined incorporation of carbon-13 acetate and more elaborate precursors . .	128
A. Tenellin	129
B. Shanorellin	130
C. Nybomycin	131
D. The ansamycins	131
1. Rifamycin S and rifamycin W, 133 – 2. Streptovaricin D, 135 – 3. Geldanamycin, 136 –	
E. Piericidin A	138
F. β -Lactam antibiotics: penicillins and cephalosporins	139
G. Prodigiosin	141
H. Variotin	142
I. Fusaric acid	143
J. Lasalocid A (Antibiotic X-537 A)	144
K. Aureothin	144
L. Ochratoxin	145
M. Sepedonin	145

IV. Terpenes	146
A. Helicobasidin	147
B. Ovalicin	147
C. Ascochlorin	148
D. Virescenol A	149
E. Fusidic acid	150
V. Incorporation of tryptophan	151
A. Pyrrolnitrin	151
VI. The corrins and the porphyrins	152
A. Vitamin B ₁₂ (cyanocobalamin)	152
B. The porphyrins	156
VII. Conclusion	158
References	161
Chapter 4. Application of carbon-13 n.m.r. to problems of stereochemistry, by A.S. Perlin	171
I. Introduction	171
II. General features of ¹³ C n.m.r. spectroscopy	171
A. Proton-decoupled spectra	172
B. Coupled spectra	174
III. Stereochemical aspects of ¹³ C chemical shifts	175
A. Upfield shifts associated with <i>gauche</i> interactions. The γ -effect	175
1. Alkanes, 176 – 2. Methylcyclohexanes, 176 – 3. Other cyclohexane derivatives, 179, – 4. Some acyclic systems. Synthetic polymers. Alkenes, 179 – 5. Other mono- cyclic systems, 183 – 6. Arenes, 189 – 7. Fused and bridged ring compounds, 190 –	
B. Downfield shifts associated with substituents in a 1,5-relationship. δ -Effects	194
C. Upfield shifts associated with <i>anti-periplanar</i> heteroatoms	197
D. Shielding differences associated with the ring size of saturated cyclic com- pounds	199
E. Other examples of stereochemical applications	201
1. Molecular symmetry, 201 – 2. Dynamic systems, 204 – 3. Charged species, 207 –	
IV. Stereochemical aspects of ¹³ C coupling constants	208
A. Measurement of ¹³ C– ¹ H coupling	208
B. Coupling between directly-bonded ¹³ C and ¹ H (¹ J _{C–H})	209
C. Two-bond ¹³ C– ¹ H coupling (² J _{C–H})	212
D. Coupling between vicinal ¹³ C and ¹ H (³ J _{C–H})	215
E. Coupling between ¹³ C and nuclei other than ¹ H	219
1. ¹³ C and ¹³ C, 219 – 2. ¹³ C and ³¹ P, 220 – 3. ¹³ C and ¹⁹ F, 222 – 4. ¹³ C and other nuclei, 223 –	
V. ¹³ C nuclear spin relaxation	224
A. Influence of proton proximity on T ₁	224
B. Influence of molecular motion on T ₁	226

C. Segmental motion	227
D. Intermolecular association	228
References	229
Chapter 5. Kinetic carbon and other isotope effects in cleavage and formation of bonds to carbon, by A.V. Willi	237
I. Introduction and scope of presentation	237
II. Carbon, hydrogen, and other isotope effects in nucleophilic substitution	238
A. Isotope effect and mechanism	238
B. S_N2 reactions	238
1. Isotope effects and transition state properties, 238 – 2. Correlation of KIEs with free energy parameters, 239 – 3. Computer calculations of KIEs, 239 – 4. Isotope effects in S_N2 reactions of benzyl and α -phenylethyl compounds, 248 –	
C. Isotope effects in limiting (S_N1) solvolysis	249
1. Experimental data, 249 – 2. α -Deuterium KIEs in solvolysis, 249 – 3. Carbon KIEs in S_N1 solvolysis, 253 – 4. Chlorine isotope effects, 254 –	
D. The Snee ion-pair mechanism versus the S_N2 and S_N1 mechanisms	254
E. Carbon and hydrogen isotope effects in solvolysis with aryl participation	255
III. Carbon and hydrogen isotope effects in aromatic decarboxylations	257
A. The mechanism of decarboxylation of aromatic acids with electron-releasing substituents	257
1. Rate-determining proton transfer, 257 – 2. Change of the rate-determining step, 259 –	
B. Carboxyl- ^{13}C and D_2O solvent isotope effects in decarboxylations with changing rate-determining step	261
1. Acidity dependence of isotope effects, 261 – 2. The magnitudes of the carbon and hydrogen isotope effects, 264 –	
IV. Carbon and other isotope effects in carbonyl addition reactions	267
A. Heavy atom isotope effects in ester hydrolysis and related reactions	267
1. General, 267 – 2. Experimental data, 267 – 3. Theoretical, 269 –	
B. Heavy atom isotope effects in the formation of derivatives of carbonyl com- pounds	271
C. The Cannizzaro reaction	273
D. Miscellaneous reactions	275
1. Cyclization of <i>o</i> -benzoylbenzoic acid, 275 – 2. Reaction of formaldehyde with 4-hydroxycoumarin, 276 – 3. The Dieckmann condensation, 276 – 4. The thermal deammonation of phthalamide, 277 –	
E. α -Deuterium isotope effects in carbonyl addition reactions of aldehydes	278
References	280
Index	285

Chapter 1

CARBON-13 KINETIC ISOTOPE EFFECTS IN DECARBOXYLATION

G.E. DUNN

Department of Chemistry, University of Manitoba, Winnipeg, Manitoba R3T 2N2 (Canada)

I. INTRODUCTION

From the experimental point of view, decarboxylation is the ideal reaction for studying kinetic carbon-isotope effects. This is primarily because of the particularly desirable properties of the product, carbon dioxide. Its only carbon atom comes from the bond which is ruptured during decarboxylation, so that an isotopic label in the carboxyl group is not diluted by other carbons in the product. It is an unreactive gas which, because of its relatively high freezing point, is easy to collect, measure, and purify in an ordinary vacuum line. For mass-spectrometric analysis it has a convenient molecular weight, gives a strong molecular-ion beam, and does not have a "memory" effect from adsorption on the equipment. It has the advantage over organic molecules that its only other element, oxygen, has a very low natural abundance of ^{17}O , so that it does not interfere with ^{13}C analysis.

The decarboxylation reaction itself has convenient features too. It is easily initiated and interrupted thermally and, at least for decarboxylations occurring at temperatures below 300°C , it is usually "clean". Only rarely is it complicated by concurrent or consecutive side-reactions.

Probably for these reasons, decarboxylation was the first reaction to be examined for heavy-atom isotope effects under kinetic conditions. Within a year of the discovery of isotopic fractionation of carbon in the mass-spectrometric fragmentation of propane in 1948 [1], three groups of investigators reported carbon kinetic isotope effects in decarboxylation reactions. Using malonic acid labelled in the carboxyl group, Yankwich and Calvin [2] found the rate ratio $^{12}\text{C}/^{14}\text{C}$ to be 1.12 ± 0.03 at 150° , while Bigeleisen and Friedman [3] found $^{12}\text{C}/^{13}\text{C}$ to be 1.019 ± 0.001 at 137.5° . Lindsay, et al. [4], using oxalic acid, found the $^{12}\text{C}/^{13}\text{C}$ rate ratio to be 1.034 at 100° . Thus was uncovered the problem of the relative magnitudes of the ^{13}C and ^{14}C kinetic isotope effects which occupied most of the investigators in this area over the next few years.

II. GENERAL PRINCIPLES

Immediately after the first observance of heavy-atom isotope effects three somewhat different approaches to the calculation of kinetic isotope effects appeared [5–7], all based on absolute reaction-rate theory. Of these, the one devised by Bigeleisen and

coworkers has been most widely used. It is authoritatively elucidated in a review by Bigeleisen and Wolfsberg [8], from which the following sketch is abstracted. For heavy atoms such as carbon, it leads to the following expression for the ratio of rate constants of isotopic isomers.

$$\frac{k_1}{k_2} = \frac{\nu_{1L}^\ddagger}{\nu_{2L}^\ddagger} \left[1 + \sum_i^{3n-6} G(u_i) \Delta u_i - \sum_i^{3n^\ddagger-7} G(u_i^\ddagger) \Delta u_i^\ddagger \right] \quad (1)$$

This form of the Bigeleisen equation assumes only one possible reaction site, equal transmission coefficients for light and heavy isotopic isomers, and negligible quantum mechanical tunneling. The superscript \ddagger refers to a property of the transition state, and the subscripts 1 and 2 refer to the light and heavy isotopes, respectively.

$$G(u_i) = \frac{1}{2} - \frac{1}{u_i} + \frac{1}{e^{u_i} - 1}, \quad u_i = u_{i1} - u_{i2}, \quad u_i = \frac{h\nu_i}{kT}$$

where ν_i is the frequency of the i^{th} mode of vibration. In the reactant there are $3n - 6$ normal modes and in the transition state $3n^\ddagger - 7$. The missing mode corresponds to ν_L^\ddagger , the imaginary stretching frequency of the bond being broken.

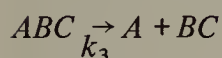
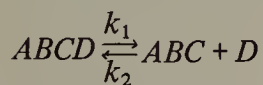
The ratio $\nu_{L1}^\ddagger/\nu_{L2}^\ddagger$ can be replaced by $(m_2^*/m_1^*)^{1/2}$ where m^* is the reduced mass of the activated complex along the axis of the bond undergoing reaction, so the ratio will always be greater than unity and independent of temperature. Whether or not the temperature dependent factor (in brackets) is greater or less than unity will depend on the relative magnitudes of the summation terms corresponding to initial state and transition state. Extensive calculations on model systems by Wolfsberg and Stern [9] have shown that frequencies of vibrations more than two bonds removed from the reacting bond cancel in the two summation terms. For many reactions of heavy-atom isotopes this also applies to bonds more than one bond away from the reaction site. However, for those bonds whose force constants are changed in going from reactant to transition state, cancellation will not occur. If the bond is weakened in the transition state $G(u_i^\ddagger)$ is less than $G(u_i)$ and the temperature-dependent term is greater than unity, so that the heavier isotopic species reacts more slowly than the lighter one — the “normal” isotope effect. In the extreme case that an isotopically labelled atom is tightly bound in the reactant but unbound in the transition state, the $G(u_i^\ddagger)$ terms for this atom will become zero and the isotope effect will be a maximum. For ^{13}C Bigeleisen [10] has calculated this maximum to be about 1.25 at 25°C . In practice, of course, carbon atoms are never free in the transition state, so ^{13}C isotope effects are normally much smaller — in the order of a few percent.

On the other hand, if bonds are strengthened in the transition state the decrease in the temperature-dependent factor may, or may not, be enough to offset the accompanying increase in the temperature-independent factor, so that “inverse” isotope effects are much less common than “normal” ones. For the same reason the temperature dependence of kinetic isotope effects may not be simple. Since the relative importance of the temperature-dependent and temperature-independent factors vary

with temperature, and since the two factors operate in opposite senses, an inverse isotope effect at one temperature may become normal at another. Furthermore, the temperature dependence of vibration frequencies in reactants and transition state are complex and may be sufficiently different to cause inversion in the temperature-dependent factor itself [11].

Since the kinetic isotope effect depends so intimately upon the structure of the transition state, it is obviously a very useful tool for studying reaction mechanisms. Because it concerns only those bonds in the immediate vicinity of the reaction site, it is much more amenable to calculation in large molecules than are absolute rates. Computers have made it possible to calculate isotope effects for various model transition states and, by comparison of these with experiment, to derive considerable understanding of this otherwise inaccessible state [9].

However, most of the work done up to now has been of a much simpler order which requires only the demonstration that isotopic substitution does, or does not, produce an experimentally detectable kinetic isotope effect. Since vibrational changes resulting from isotopic substitution at sites remote from the one where reaction is occurring cancel between reactant and transition state, such isotopic substitution does not produce kinetic isotope effects. Hence, the existence of a kinetic isotope effect shows that the isotopic label is at, or very near, the reaction site. The absence of an isotope effect must be interpreted with more caution. It may mean that the isotopic label is remote from the reaction site, or it may result from compensating effects in the temperature-dependent and temperature-independent factors. It may also mean that, although the isotopic substitution is at the reaction site, force-constant changes in the labelled bond only occur after the rate-determining step of the reaction. For example, consider a reaction



where $ABCD$ represents the atomic skeleton of a molecule. If ABC is an unstable intermediate, the overall rate of reaction is

$$\frac{d[A]}{dt} = \frac{k_1 k_3 [ABCD]}{k_2 [D] + k_3} \quad (2)$$

This reduces to

$$\frac{d[A]}{dt} = k_1 [ABCD] \quad (3)$$

if the first step is rate-determining, or to

$$\frac{d[A]}{dt} = \frac{k_1 k_3 [ABCD]}{k_2 [D]} \quad (4)$$

if the second step is rate-determining. In the absence of neighboring-group effects, isotopic substitution in a heavy atom like carbon at *A* will be too remote to affect the *CD* vibration, so it will not alter k_1 or k_2 . It will, of course, alter k_3 . Hence there will be a kinetic isotope effect in the overall reaction if the rate-determining step is the second one, but not if it is the first. For intermediate cases, where the general rate expression applies, there will obviously be isotope effects varying in magnitude with the ratio of $k_2 [D]$ to k_3 . Such variations in isotope effects as the rate-determining step changes with concentration, temperature, or other reaction conditions, sometimes provide especially revealing clues to mechanism.

Isotopic substitution in *D* will affect k_1 and k_2 but not k_3 . Since k_1 appears in the rate expression no matter which step is rate-determining, there will always be an isotope effect in the overall rate, although it may be smaller for rate-determining second step because of cancellation between k_1 and k_2 . In this connection it may be noted that equilibrium isotope effects are generally smaller than kinetic ones.

Isotopic substitution at *B* will, of course, affect k_3 and produce a kinetic isotope effect in the overall rate if the second step is rate-determining. It will also affect k_1 (although probably to a lesser extent than k_3) if the *BC* bond is altered in the transition state of the first step. This could be the case if, for example, *ABC* is a carbonium ion so that the hybridization of *C*, and consequently the *BC* force constant, changes during this step. There may, therefore, be a small isotope effect in the overall rate even if step one is rate-determining. Similar considerations apply to isotopic substitution at *C*.

The preceding brief discussion will serve to illustrate how kinetic isotope effects can be used in the study of reaction mechanisms. The presence of an isotope effect in a suitably labelled substrate shows that the force constant of a bond to the isotopically substituted atom is altered in or before the rate-controlling step of the reaction. Detailed calculations by the Stern and Wolfsberg [9] or similar treatment may reveal very significant details of the transition state which would produce such an isotope effect, although isotope effects are usually more sensitive to energy and composition than to geometry [9]. In practice, the mere qualitative knowledge that a given bond undergoes alteration in a particular step of the reaction is very useful and is often attainable by no other means. On the other hand, the failure to detect a kinetic isotope effect must be interpreted with more caution. The above discussion has shown that an isotope effect may be absent for any of several reasons. Usually a knowledge of the structure and chemistry of the reactants and products will permit a choice among the various possibilities, but often an element of doubt remains.

III. KINETIC CONSIDERATIONS

In principle the numerical value of a kinetic isotope effect can be determined by independent measurement of the rate constants for the isotopically substituted and unsubstituted reagents. For atoms as heavy as carbon, however, the average isotope effect

at room temperature is barely outside the combined experimental errors in the two rate constants. The only reliable way to determine ^{13}C kinetic isotope effects, therefore, is to allow a mixture of the isotopic isomers to react, and to measure the isotopic ratios before and after a fraction of the mixture has reacted. In a mixture of labelled and unlabelled reactants the reaction mixture will become richer in the slower-reacting isomer as reaction proceeds. The product will initially be richer in the faster-reacting isomer, but as reaction proceeds the isotopic ratio of the accumulated products must approach the initial ratio of reactants. For decarboxylation of ^{13}C -labelled acids it is convenient to measure the isotopic ratio of the product, CO_2 , as indicated in the Introduction, so attention will be focused on this procedure.

Two types of isotopic competition are possible. For monocarboxylic acids, labelled acid molecules may be allowed to compete with unlabelled ones, and the ratio of rate constants for reaction of the isotopic isomers is called the intermolecular kinetic isotope effect. For acids with two or more equivalent carboxyl groups, competition occurs between carboxyl groups within the same molecule, and the ratio of rate constants for decarboxylation of labelled and unlabelled groups is called the intramolecular kinetic isotope effect. The kinetic derivations given below for calculation of the various types of isotope effects follow the procedures derived by Bigeleisen and Wolfsberg [8] and Lindsay et al. [12], although different approximations are sometimes used to arrive at more general expressions.

A. Monocarboxylic acids

If a mixture of isotopically substituted carboxylic acids decarboxylates on reaction with species A , B , etc., so that the reaction is first order with respect to acid and of order a with respect to A , b with respect to B , etc.,



the rates will be

$$\frac{d[\text{CO}_2]}{dt} = k[\text{RCOOH}][A]^a[B]^b \dots \quad (7)$$

$$\frac{d[\text{C}^*\text{O}_2]}{dt} = k^*[\text{RC}^*\text{OOH}][A]^a[B]^b \dots \quad (8)$$

or

$$\frac{d[\text{CO}_2]}{d[\text{C}^*\text{O}_2]} = \frac{k[\text{RCOOH}]}{k^*[\text{RC}^*\text{OOH}]} \quad (9)$$

If $[\text{RCOOH}]$ is taken to be $[\text{RCOOH}]_0$ at $t = 0$ and $[\text{RCOOH}]_0 - [\text{CO}_2]$ at t , the above

equation becomes

$$\frac{d[\text{CO}_2]}{d[\text{C}^*\text{O}_2]} = \frac{k([\text{RCOOH}]_0 - [\text{CO}_2])}{k^*([\text{RC}^*\text{OOH}]_0 - [\text{C}^*\text{O}_2])} \quad (10)$$

which integrates to

$$\frac{k}{k^*} = \frac{\log\left(1 - \frac{[\text{CO}_2]}{[\text{RCOOH}]_0}\right)}{\log\left(1 - \frac{[\text{C}^*\text{O}_2]}{[\text{RC}^*\text{OOH}]_0}\right)} \quad (11)$$

Let the measured fractional conversion be taken as

$$\frac{[\text{CO}_2] + [\text{C}^*\text{O}_2]}{[\text{RCOOH}]_0 + [\text{RC}^*\text{OOH}]_0} = f \quad (12)$$

and the isotopic ratios $[\text{RC}^*\text{OOH}]_0/[\text{RCOOH}]_0$ and $[\text{C}^*\text{O}_2]/[\text{CO}_2]$ be R_0 and R , respectively; then the isotope effect is given by

$$\frac{k}{k^*} = \frac{\log\left[1 - \frac{f(1 + R_0)}{(1 + R)}\right]}{\log\left[1 - \frac{f(1 + R_0)R}{(1 + R)R_0}\right]} \quad (13)$$

If R and $R_0 \leq 0.01$, as is the case when the natural abundance of ^{13}C is used, this equation reduces to

$$\frac{k}{k^*} = \frac{\log(1 - f)}{\log(1 - \frac{fR}{R_0})} \quad (14)$$

Bothner-By and Bigeleisen [13] have also shown that for such small values of R_0 the above equation holds irrespective of the kinetic order with respect to $[\text{RCOOH}]$.

Errors in the measured isotope effect increase with increasing extent of reaction, as shown in Table 1 for a typical ^{13}C isotope effect of 4%. It is evident that errors can be minimized by working at low conversions and determining extent of reaction by measuring the product. At very low conversion k_{12}/k_{13} approaches R_0/R . For the example in Table 1, calculating k_{12}/k_{13} from R_0/R at 1% reaction gives an error of 0.5% in $(k_{12}/k_{13} - 1)100$. Thus, if it is possible to work to 1% conversion or less, it is unnecessary to know f accurately, and calculations are reduced.

B. Dicarboxylic acids

Competition between isotopes in the same molecule is kinetically more complex than competition between isotopic isomers, particularly when, as is usually the case, the isotopic isomers are used in their natural abundances. The kinetics of carbon-iso-

TABLE 1

EFFECT OF ERROR IN MEASUREMENT OF PRODUCT (f), REACTANT ($1 - f$), AND ISOTOPIC RATIOS (R, R_0) ON PERCENT ISOTOPE EFFECT AT VARIOUS PERCENTS OF REACTION

Percentage reaction 100 f	Percentage error in $\left(\frac{k_{12}}{k_{13}} - 1\right) 100$		
	1% error in f	1% error in $(1 - f)$	0.01% error in R, R_0
10	0.05	0.50	0.55
25	0.17	0.53	0.60
50	0.55	0.55	0.76
75	1.79	0.60	1.11

tope competition in dicarboxylic acids were first derived by Bigeleisen for ^{14}C labelling of malonic acid [14], then applied to the natural abundance of ^{13}C in oxalic acid by Lindsay et al. [4], malonic acid by Bigeleisen and Friedman [3], and expanded by Lindsay et al. [12] and Loudon et al. [15]. Their methods will be reviewed and generalized for all dicarboxylic acids in the following paragraphs.

For a dicarboxylic acid of n carbons containing mole fraction M_0 of ^{13}C randomly distributed, the fraction of molecules containing j atoms of ^{13}C is

$$\frac{n!}{j!(n-j)!} M_0^j (1 - M_0)^{n-j} \quad (15)$$

In unenriched material, where M_0 is small ($M_0 \approx 0.01$), M_0^j will be negligible for $j > 1$, so only monolabelled acid need be considered. The fraction of molecules containing ^{13}C in one carboxyl group will be

$$2M_0(1 - M_0)^{n-1}$$

Also, if the acid contains a carbons located α to a carboxyl group, the fraction of molecules containing ^{13}C in one α -position will be

$$aM_0(1 - M_0)^{n-1}$$

If n is not too large ($n < 10$), the fraction of molecules labelled in a carboxyl or α -position is closely approximated by $2M_0$ or aM_0 , respectively, and the fraction not labelled in either of these positions is approximately $1 - (a + 2)M_0$.

1. Intramolecular kinetic isotope effect

For most dicarboxylic acids thermal decarboxylation results in the loss of only one carboxyl group. In what follows, this loss of one carboxyl group will be called com-

plete decarboxylation. In such a complete decarboxylation the unlabelled and α -labelled acid will produce unlabelled carbon dioxide. The carboxyl-labelled acid will produce labelled and unlabelled carbon dioxide in the ratio of the rate constants for cleavage of the labelled and unlabelled carboxyl groups, k/k^* , in the same molecule. This ratio is the intramolecular kinetic isotope effect, i_1 . Then the ratio, R_C , of labelled to unlabelled carbon dioxide in the product of complete decarboxylation will be given by

$$R_C = \frac{C^*O_2}{CO_2} = \frac{\frac{k^*}{k + k^*}(2M_0)}{\frac{k}{k + k^*}(2M_0) + aM_0 + 1 - (a + 2)M_0} \quad (16)$$

from which it follows that

$$i_1 = \frac{k}{k^*} = 2M_0 \left(\frac{1}{R_C} + 1 \right) - 1 = 2 \frac{M_0}{M_C} - 1 \quad (17)$$

Thus, the intramolecular isotope effect can be obtained for any dicarboxylic acid from M_0 , the mole fraction of $^{13}CO_2$ in the carbon dioxide from combustion of the acid (with its ^{13}C distribution demonstrated to be random) and M_C , the mole fraction of $^{13}CO_2$ in the carbon dioxide from complete decarboxylation of the same acid.

2. Intermolecular carboxyl-carbon isotope effect

The intermolecular isotope effect, i_2 , for a dicarboxylic acid is commonly taken to be the ratio of the rate constant for cleavage of CO_2 from unlabelled molecules to that for cleavage of C^*O_2 from molecules labelled in one carboxyl group. Obviously, this cannot be determined by complete decarboxylation. It may, however, be determined for oxalic acid, and approximated for others, from the C^*O_2/CO_2 ratio of the initial decarboxylation product.

The usual assumption that isotopic substitution only affects rate constants when it occurs at bonds undergoing alteration, leads to the conclusion that the three kinetically important species in the decarboxylation of a mono-labelled dicarboxylic acid are (1) unlabelled acid, (2) acid labelled in one carboxyl group and (3) acid labelled in one α -position. As indicated earlier, the mole fractions of these are $M_1 = 1 - (a + 2)M_0$, $M_2 = 2M_0$, and $M_3 = aM_0$. Let the rate constants for formation of unlabelled carbon dioxide from these three species be k_1 , k_2 and k_3 , respectively. Labelled carbon dioxide will be produced by species (2) only, with a rate constant k_2^* . For a first-order reaction the mole fraction of any species remaining after time t is $(1 - e^{-kt})M$, so the ratio of labelled to unlabelled carbon dioxide accumulated up to time t will be given by the following equation.

$$R = \frac{C^*O_2}{CO_2} = \frac{\frac{k_2^*}{k_2 + k_2^*}(1 - e^{-(k_2 + k_2^*)t})M_2}{(1 - e^{-k_1t})M_1 + \frac{k_2}{k_2 + k_2^*}(1 - e^{-(k_2 + k_2^*)t})M_2 + (1 - e^{-k_3t})M_3} \quad (18)$$

At very low conversion ($t \rightarrow 0$) this simplifies to

$$R = \frac{k_2^* M_2}{k_1 M_1 + k_2 M_2 + k_3 M_3} = \frac{2 k_2^* M_0}{k_1 [1 - (a + 2)M_0] + 2 k_2 M_0 + a k_3 M_0} \quad (19)$$

This equation contains four unknowns, k_1, k_2, k_2^*, k_3 , but only two measurable quantities, R and M_0 , so it will be necessary to make some approximations. Since the first term of the denominator is much larger than the other two, small errors in the latter will be acceptable. In the denominator of the ratio then, $2k_2 \approx k_1 \approx k_3$. Use of these approximations leads to the following expression for the intermolecular kinetic isotope effect, where R_0 is the ratio C^*O_2/CO_2 in the starting material ^a.

$$\frac{k_1}{2 k_2^*} \approx \frac{M_0}{R(1 - M_0)} = \frac{R_0}{R} \quad (20)$$

3. Intermolecular α -carbon isotope effect

The effect of isotopic substitution at one α -position of a dicarboxylic acid can be calculated from the ratio, A , of labelled to unlabelled monocarboxylic acid produced initially. Since species (2) and (3) produce labelled acid while (1) and (2) produce unlabelled acid, the ratio A is given by the following equation.

$$A = \frac{\frac{k_2}{k_2 + k_2^*}(1 - e^{-(k_2 + k_2^*)t})M_2 + (1 - e^{-k_3 t})M_3}{(1 - e^{-k_1 t})M_1 + \frac{k_2^*}{k_2 + k_2^*}(1 - e^{-(k_2 + k_2^*)t})M_2} \quad (21)$$

At low conversions this becomes

$$A = \frac{2 k_2 M_0 + a k_3 M_0}{k_1 [1 - (a + 2)M_0] + 2 k_2^* M_0} \quad (22)$$

Substituting previously determined values of the intra- and inter-molecular isotope effects, i_1 and i_2 , leads to

$$A = \frac{k_1 \frac{i_1}{i_2} + a k_3}{k_1 \left(\frac{1}{M_0} - a - 2 \right) + \frac{k_1}{i_2}} \quad (23)$$

from which the following expression is obtained for the intermolecular α -isotope effect.

$$\frac{k_1}{k_3} = \frac{a}{\left(\frac{1}{M_0} - a - 2 + \frac{1}{i_2} \right) A - \frac{i_1}{i_2}} \quad (24)$$

^a For oxalic acid an exact solution is possible, using $a = 0$ and $k_2 = k_2^* i_1$. The data of Lindsay et al. [4] give the exact solution $k_1/2k_2^* = R_0(1 - i_1 R)/R(1 - R_0) = 1.0457$ compared to $R_0/R = 1.0456$ for the approximate one.

IV. EXPERIMENTAL CONSIDERATIONS

Measurement of the ^{13}C kinetic isotope effect in a decarboxylation involves the following steps: reaction is allowed to proceed to the predetermined extent and quenched; the extent of reaction (f) is determined if necessary; the carbon dioxide produced is recovered quantitatively from the reaction mixture, purified without isotopic fractionation, and delivered to the mass spectrometer for measurement of its isotopic ratio $^{13}\text{CO}_2/^{12}\text{CO}_2$ ($=R$). The isotopic ratio (R_0) or mole fraction (M_0) of ^{13}C in the starting material is determined by a similar procedure using either complete decarboxylation (for monocarboxylic acids) or complete combustion (for dicarboxylic acids).

Carbon dioxide is recovered from the reaction mixture either by entrainment in a carrier gas or by the conventional freeze—pump—thaw degassing cycle on a vacuum line. It is collected in base by the former method or in a liquid-nitrogen trap by either method. The freeze method is most convenient for decarboxylations in the melt, but may be difficult when large volumes of solution or low-melting solvents are used. In these circumstances carbon dioxide plus a small amount of solvent may be distilled on the vacuum line from the cold, well-stirred solution. After any method of collection the carbon dioxide is purified from lower-boiling impurities (e.g. air) by several freeze—thaw cycles under vacuum, and from higher-boiling impurities (e.g. solvent) by several distillations from dry-ice—acetone to liquid nitrogen baths under high vacuum.

The extent of reaction, f , may be determined by measuring either the carbon dioxide produced or the carboxylic acid remaining. As was shown in Table 1, for small conversions the same percent uncertainty in measurement produces a smaller error in the calculated isotope effect if carbon dioxide is measured rather than carboxylic acid. However, the isotope effect is much less sensitive to errors in f than to errors in R . Indeed, if it is possible to work at less than 1% conversion, it is not necessary to know f at all. This is a practical procedure when decarboxylating from the melt, for example, but when isotope effects are being correlated with kinetics in dilute solution it may be impossible because the volume of solution required would make quantitative recovery of the carbon dioxide difficult. Carbon dioxide is commonly measured by PV/T measurements in a gas buret on the vacuum line. Unreacted carboxylic acid can be measured spectrophotometrically if it, or its decarboxylation product, contains a suitable chromophore. In some circumstances (buffered solutions, for example) it may be titrated. Needless to say, either method requires that there be no side reactions, and this can best be established by measuring both carbon dioxide and carboxylic acid, at least in some samples.

The purified and measured carbon dioxide is then introduced into the mass spectrometer for measurement of the isotopic ratio, R . Fifty micromoles is a convenient quantity of carbon dioxide, although this can be reduced by a factor of ten with suitable inlet systems. It is much easier to measure isotopic ratios accurately than to measure actual abundances, and a modern ratio-recording mass spectrometer can easily

measure $^{13}\text{CO}_2/^{12}\text{CO}_2$ ratios with an accuracy of 0.01%. R_0 is best determined by analysis of the CO_2 resulting from complete decarboxylation of a monocarboxylic acid, since this gives the ratio of $^{12}\text{C}-^{13}\text{C}$ to $^{12}\text{C}-^{12}\text{C}$ in the bond undergoing reaction, rather than the average isotopic ratio for all C—C bonds and thus avoids any correction for non-random distribution of ^{13}C in the acid. For dicarboxylic acids R_0 may be determined from the CO_2 obtained from complete combustion of the acid, but the question then arises whether this average value of R_0 is the actual value in the bond being ruptured. This is usually answered by comparing the $^{13}\text{C}/^{12}\text{C}$ ratio in the carbon dioxide obtained from combustion of the dicarboxylic acid with that from its monocarboxylic acid residue after decarboxylation. There is an advantage in using the same compound (carbon dioxide) to measure both R and R_0 . Otherwise corrections may be required for differences in isotopic discrimination by the mass spectrometer in different compounds.

The isotopic ratio is most conveniently measured by a ratio-recording mass spectrometer, of which there are several on the market. These are relatively low-cost instruments, since high resolution is not required. They operate by balancing the output from one detector locked on a particular mass (45 in the case of $^{13}\text{CO}_2$) against that from another detector locked on a neighboring mass (44 for CO_2) or, more commonly, on a range of masses (e.g. 41–48) bracketting the first. Thus, a pure sample of carbon dioxide supplies $^{13}\text{C}^{16}\text{O}_2 + ^{12}\text{C}^{16}\text{O}^{17}\text{O}$ at one detector and $^{12}\text{C}^{16}\text{O}_2 + ^{12}\text{C}^{16}\text{O}^{18}\text{O}$ at the other. The corrections for oxygen isotopes are small enough to be ignored in much work, but for accurate measurements it is desirable to equilibrate the carbon dioxide with water of known oxygen-isotopic content before analysis and to make the corresponding corrections.

V. OBSERVED ^{13}C KINETIC ISOTOPE EFFECTS

The remainder of this chapter will be devoted to a summary of the ^{13}C kinetic isotope effects observed in decarboxylation reactions and the conclusions based upon them. These isotopic studies were undertaken with either of two objectives. The early work with oxalic and malonic acids was intended to demonstrate the existence of a ^{13}C kinetic isotope effect, and to compare its magnitude with that of the corresponding ^{14}C effect. Interestingly enough, this latter question seems never to have been answered conclusively by experiment. Investigators appear to agree that the ^{14}C effect is very nearly twice the ^{13}C effect, but no one has taken the trouble to reconcile or correct the conflicting experimental results still standing in the literature on this subject. They will not be reviewed here, since this series is devoted to ^{13}C only.

The second motive for examining ^{13}C isotope effects, and the one applying in most of the literature reports, is to answer a more or less specific question concerning the sequence of steps, or the relative magnitudes of rate constants, in a multi-step reaction mechanism. Less frequently the objective has been more ambitious — to obtain detailed information about the structure and bond strengths of the transition state by

comparing the experimental results with those predicted by various theoretical models. Thus far, such investigations have had rather limited success because of the complexity of the molecules concerned and the difficulty of obtaining experimental results which are precisely reproducible between different laboratories. The theoretical calculations in such investigations are not reviewed in this chapter because the author is not a theoretician, but the experimental results are reported and compared with those from other laboratories.

Observed ^{13}C kinetic isotope effects in decarboxylations are reported here in order of increasing complexity of the acids decarboxylated. Monocarboxylic and dicarboxylic acids are considered separately because the kinetic treatment is different for the two types, and dicarboxylic acids may have an intramolecular isotope effect which is impossible for monocarboxylic acids.

A. Monocarboxylic acids, aliphatic

Simple monofunctional carboxylic acids decarboxylate only on pyrolysis of their salts with alkali — conditions which do not lend themselves to mechanistic study, and therefore have not attracted isotopic investigation. For those more easily decarboxylated acids discussed below, ^{13}C kinetic isotope effects are reported as percent isotope effects $(k_{12}/k_{13} - 1)100$.

1. Formic acid

Thermolysis of formic acid leads to decarbonylation, but decarboxylation can be brought about by enzymic catalysis, and Hoering found the kinetic isotope effect to be 2.6% at “room temperature” in the decarboxylation of formate by dehydrogenylase from a *Clostridium* species [16]. This is a considerably smaller isotope effect than those commonly observed in non-enzymatic decarboxylations of aliphatic acids, and thus suggests that some step other than C—H bond rupture is partially rate-determining.

2. Trichloroacetic acid

The decarboxylation of trichloroacetic acid in aqueous solution has been found to be first order with respect to trichloroacetate ion, and the following mechanism has been proposed [17].



This predicts that there will be a carbon isotope effect in the reaction, and Bigeleisen and Allen found it to be $(3.27 \pm 0.07)\%$ for aqueous sodium trichloroacetate at 70.4°C [18].

Subsequently Lakshmi et al. found the magnitude of the isotope effect to depend

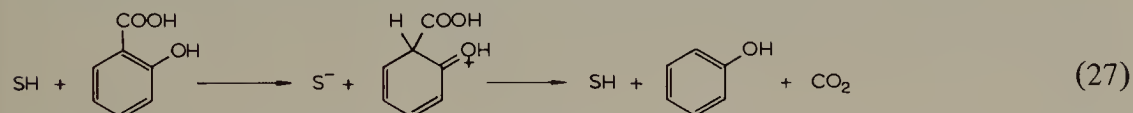
upon the nature of the cation [19]. When trichloroacetic acid was refluxed in aqueous base containing alkaline earth or lanthanide ions (concentrations unspecified) the depletion of ^{13}C in the carbonate precipitated was greater for barium and strontium than for calcium, and greater for praseodymium and neodymium than for lanthanum. The authors attribute this to a greater covalency of calcium and lanthanum trichloroacetates. The actual isotope effects are unavailable, since R_0 and f are not given.

B. Monocarboxylic acids, aromatic

It is among aromatic acids that the ^{13}C kinetic isotope effect has had its most fruitful application as a tool for investigating mechanisms of decarboxylation. Among these acids the rates of C—C bond breaking and C—H bond making are often of the same order of magnitude, so that the rate-determining step may involve either or both of these processes, depending upon conditions. In these circumstances, changes in the magnitude of the carbon isotope effect provide a conveniently sensitive probe for changes in mechanism.

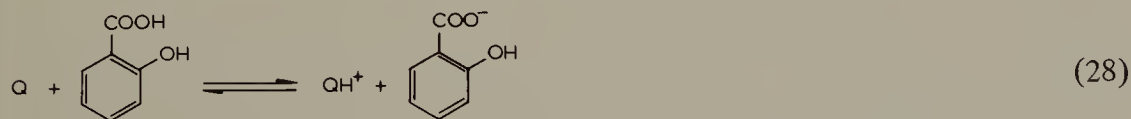
1. Salicylic acid

In contrast to the behavior of aliphatic acids, the decarboxylation of salicylic acid in the protic solvent resorcinol is first order with respect to the acid and the rate is increased by electron-releasing, rather than electron-attracting substituents [20]. This indicates positive charge at the reaction site in the transition state, and suggests that protonation of the α -carbon is at least partly rate-determining [20].



Whether the substrate decarboxylates as acid or anion, and whether the α -protonated form is intermediate or transition state, is not revealed by this evidence.

In the aprotic solvents nitrobenzene and quinoline the kinetic orders with respect to salicylic acid are second and first, respectively, and substituent effects in quinoline solution suggest that the substrate decarboxylates as anion [21].



Again, the α -protonated species could be either intermediate or transition state.

Bourns et al. showed that in dilute solutions of quinoline in nitrobenzene, decarboxylation of salicylic acid is first order with respect to acid and first order with respect to quinoline, as required by the above mechanism, and that the ^{13}C kinetic isotope effect changes from $(2.21 \pm 0.02)\%$ to $(0.73 \pm 0.04)\%$ on changing solvent from pure quinoline to dilute quinoline in nitrobenzene [22]. This is not explicable with the α -protonated species as transition state but, as intermediate, its decomposition could be rate-determining at high quinoline concentration (giving an isotope effect), whereas its formation could be rate-determining at low quinoline concentration (no isotope effect). Thus the observed change in isotope effect with quinoline concentration makes it possible to distinguish between the two-step and three-step mechanisms.

2. 2,4-Dihydroxybenzoic acid

The decarboxylation of various substituted salicylic acids in aqueous solution is first order with respect to acid [23–25] which fits either a unimolecular decomposition of the acid or electrophilic displacement of carbon dioxide from the anion by proton. Rates for the various substituents correlate with Hammett's σ^+ constants, giving $\rho = -4.38$ [25]. This, together with the observation of general acid catalysis [25] and a solvent deuterium isotope effect greater than unity [26], indicates that electrophilic substitution by proton is the correct mechanism, but leaves open the question whether it is a one-step or a two-step mechanism; that is, whether the α -protonated species is a transition state or an intermediate.

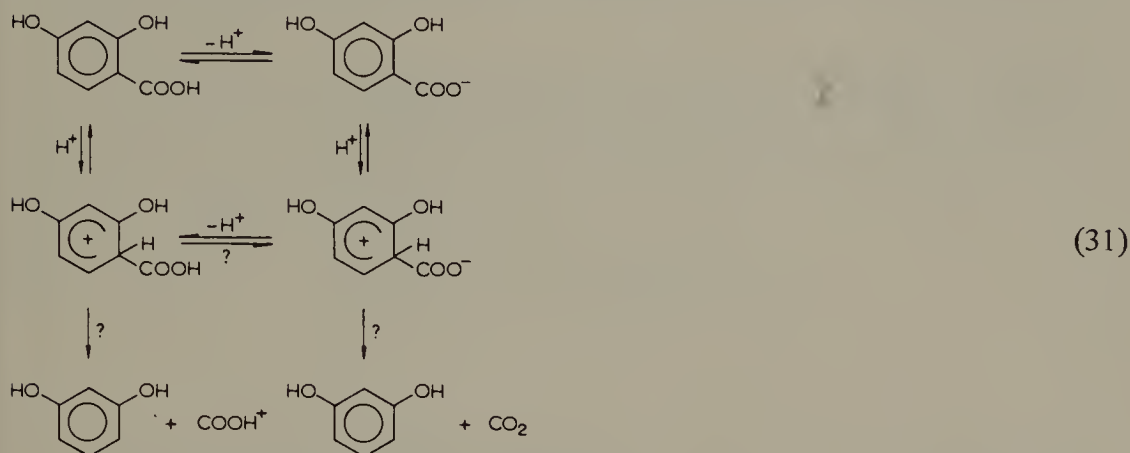
The rate dependence at high acidities shows that the un-ionized acid as well as the anion undergoes decarboxylation through α -protonation [27]. Bourns found the ^{13}C kinetic isotope effect to increase with acidity, as shown in Table 2 [27].

TABLE 2

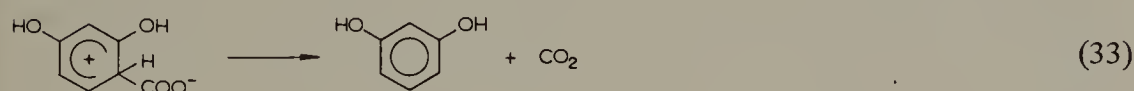
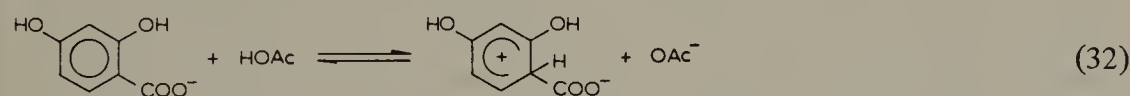
^{13}C KINETIC ISOTOPE EFFECT IN THE DECARBOXYLATION OF 2,4-DIHYDROXYBENZOIC ACID AT 85°C [27]

HClO_4 , M	Percentage isotope effect
0.002	0.63
0.01	0.56
0.02	0.60
0.05	0.62
0.10	0.61
1.10	0.96
3.00	2.18
5.81	3.14
7.81	3.61

This indicates a two-step mechanism in which α -protonation is slow enough to be rate-determining at low acidities, but accelerates at higher acidities until it leaves C—C bond breaking as the rate-determining step. Whether or not the carboxyl group of the α -protonated acid ionizes before it decarboxylates is not clear.



Lynn and Bourns confirmed that the reaction at low acidity is a two-step one by showing that in acetate buffers the ^{13}C isotope effect increases from 0.5% to 1.8% as the acetate concentration of the buffer is increased from 0.067 *M* to 1.00 *M* [28]. At low acetate concentration the steady-state concentration of α -protonated intermediate is large enough that the second step is fast, so there is no isotope effect. At higher acetate concentrations the concentration of intermediate is depressed enough to make the second step rate-limiting, thus producing an isotope effect.

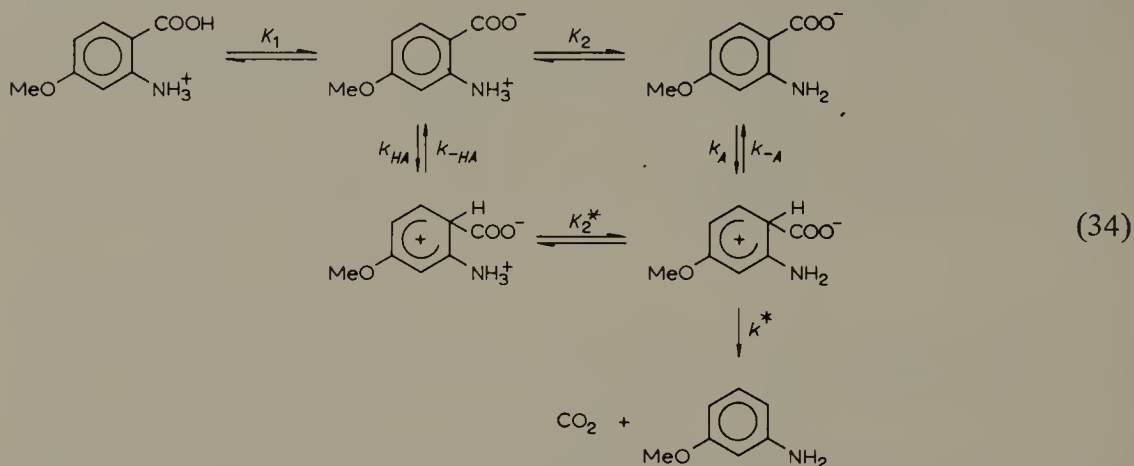


3. Anthranilic acids

The decarboxylation of anthranilic acid in boiling aqueous solution is first order with respect to anthranilic acid [29]. Stevens et al. showed that the reaction is acid catalyzed and that there is no appreciable ^{13}C kinetic isotope effect in water or 1 *N* sulfuric acid at 100°C, or in the melt at 160°C [30]. They therefore concluded that the rate-determining step is protonation of the α -carbon rather than C—C bond breaking.

4-Methoxyanthranilic acid decarboxylates in buffered aqueous solution of ionic strength 0.1 at 60°C with a rate which reaches a maximum at pH = 1.1 and drops off

rapidly at higher and lower pH [31]. Since the isoelectric pH of anthranilic acid under these conditions is 3.33, it is evident that the rate is not determined by the protonation of any one of neutral acid, zwitterion, cation or anion. The following mechanism was therefore proposed, where the isoelectric species could be zwitterion, as shown, or neutral acid.



This mechanism leads to a pH dependence of the required form:

$$k = \frac{k_A K_1 K_2 + k_{HA} K_1 [\text{H}^+]}{K_1 + [\text{H}^+]} \times \frac{1}{1 + \frac{k_{-HA}}{k^* K_2^*} [\text{H}^+]} \quad (35)$$

and predicts that when $[\text{H}^+] \ll k^* K_2^* / k_{-HA}$ there will be no ^{13}C kinetic isotope effect since k^* , which governs the rate of C—C bond breaking, will then contribute negligibly to the overall rate constant. Under these conditions protonation of the α -carbon is rate-determining. At higher acidities, on the other hand, k^* will contribute to the overall rate constant, and there will be a ^{13}C isotope effect. As predicted, Dunn and Bucini found the ^{13}C kinetic isotope effect in the decarboxylation of 4-methoxyanthranilic acid at 60°C and ionic strength 0.50 to be $(0.22 \pm 0.03)\%$ at $\text{pH} = 4.0$, $(1.40 \pm 0.09)\%$ at $\text{pH} = 1.3$, and $(4.17 \pm 0.03)\%$ in 2 N hydrochloric acid [32].

The difference between these results and those of Stevens et al., who failed to find a ^{13}C kinetic isotope effect in the decarboxylation of anthranilic acid at acidities up to 1 M sulfuric acid [30], is accounted for by the fact that $k^* K_2^* / k_{-HA}$ is much larger for anthranilic acid (~ 100) than for its 4-methoxy derivative (~ 0.2). The change-over from rate-determining α -protonation to rate-determining C—C bond breaking should therefore occur at much higher acidities for anthranilic than for 4-methoxyanthranilic acid. Dunn and Dayal confirmed this by showing that the ^{13}C kinetic isotope effect for decarboxylation of anthranilic acid at 115°C changes from $(0.12 \pm 0.02)\%$ in 2 M sulfuric acid to $(3.73 \pm 0.03)\%$ in 10 M sulfuric acid [33].

Zielinski found the ^{13}C kinetic isotope effect in the decarboxylation of anthranilic

This mechanism leads, after approximation and simplification suitable to the region where first-order dependence on acidity is changing to acid independence, to the following rate expression [38].

$$k_{\text{obs}} = \frac{k_1 [\text{H}_3\text{O}^+]}{1 + \frac{k_2 k_6}{k_5 k_7} [\text{H}_3\text{O}^+]} \quad (38)$$

Since k_7 is the rate constant for C—C bond breaking and it is only significant when $[\text{H}_3\text{O}^+] > k_5 k_7 / k_2 k_6$, it follows that there should be a ^{13}C isotope effect in the range of acidity where k_{obs} is independent of acidity, but none in the region where it is proportional to hydrogen ion concentration.

Huang and Long studied the ^{13}C kinetic isotope effect at 25°C as a function of acidity [39]. It was found to increase from $(0.0 \pm 0.8)\%$ to $(3.5 \pm 0.7)\%$ as perchloric acid concentration was increased from 0.01 M to 0.32 M . At a constant ionic strength of 0.5 M , a similar change from $(0.8 \pm 0.8)\%$ in 0.006 M perchloric acid to $(4.3 \pm 0.8)\%$ in 0.32 M perchloric acid was observed. These results are in excellent agreement with the proposed mechanism and thus confirm that α -protonation precedes C—C bond breaking.

C. Heterocyclic acids

1. Pyrrole-2-carboxylic acid

The decarboxylation of pyrrole-2-carboxylic acid in aqueous solution at 50°C is first order with respect to substrate. The first-order rate constant increases slightly as the acidity of the solution is increased from pH 3 to pH 1, then rises rapidly and continuously with further increase of acidity up to 10 M hydrochloric acid [40]. Since pK_1 is large and negative and $pK_2 = 4.39$, it is clear that the species decarboxylating is neither the anion nor the isoelectric species. Because of the chemical resemblance of pyrroles and anilines it is suggested that the mechanism for decarboxylation of pyrrole-2-carboxylic acid is similar to that of anthranilic acid, in which the first step is α -protonation of either the anion or the isoelectric species, followed by loss of carbon dioxide from the α -protonated anion.

Dunn and Lee found the ^{13}C kinetic isotope effect to be $(0.06 \pm 0.02)\%$ at $\text{pH} = 2.63$, and $(2.81 \pm 0.03)\%$ in 4 M hydrochloric acid at 50°C and ionic strength 1.0 [40]. This confirms that the rate-determining step changes from α -protonation in dilute acid to rate-determining C—C bond breaking at high acidity, in accordance with the anthranilic acid mechanism.

2. Picolinic acid

Picolinic acid decarboxylates much more easily than benzoic acid or its own *m*- and *p*-isomers. In the melt or in protic solvents the product of decarboxylation is pyridine, but in the Hammick reaction carbonyl solvents give α -pyridylcarbinols, which has sug-

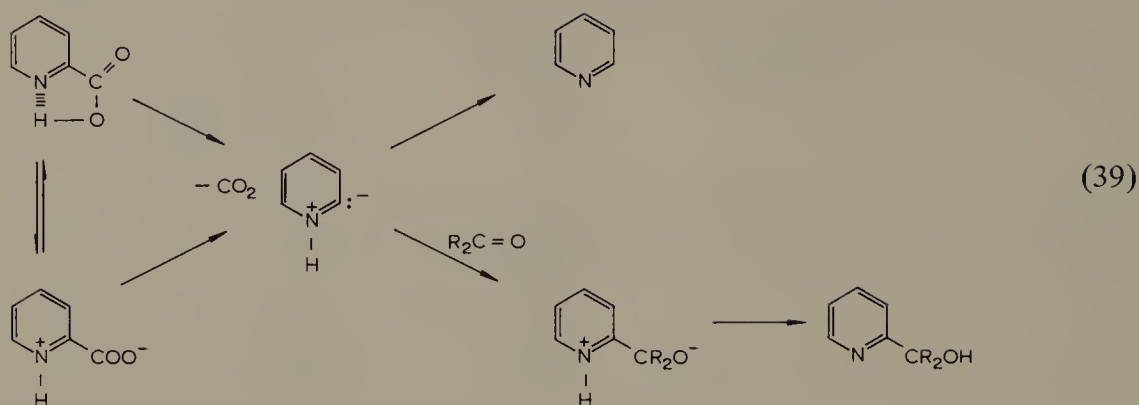
TABLE 3

 ^{13}C KINETIC ISOTOPE EFFECTS IN THE DECARBOXYLATION OF PICOLINIC ACID [44]

Temperature (°C)	$\frac{\text{Mole solvent}}{\text{Mole acid}}$	Percentage reaction (100 <i>f</i>)	Percentage isotope effect $\left(\frac{k_{12}}{k_{13}} - 1\right) 100$
140.5	0	3.21	1.32
141.0	0	1.94	1.32
141.5	0	2.40	1.32
155.5	0	1.38	1.27
155.5	0	3.52	1.25
155.5	0	7.80	1.235
Water			
141.5	0.927	2.33	1.67
141.5	5.8	1.12	1.84
141.5	7.8	2.51	2.20
141.5	12.36	0.90	2.24
142	40.73	1.35	2.31
141.5	45.32	0.84	2.32
141.5	87.53	1.11	2.37
157	11.96	4.21	2.17
157	16.79	7.84	2.10
174.7	8.47	4.69	2.05
174.5	12.27	8.95	2.09
190	19.63	8.14	1.98
Phenol			
141.5	1.088	2.05	1.59
141.5	1.105	1.79	1.61
141.5	2.352	1.41	1.73
141.5	6.979	1.14	1.87
141.5	8	1.11	1.92
142.5	9	1.35	1.95
157	13	2.95	1.88
157	15	5.59	1.92
157	14	6.22	1.88
173	13	4.81	1.86
173	25	12.07	1.93
173	28	17.76	1.90
<i>o</i> -Nitrophenol			
141.5	3.95	6.38	1.29
141.5	7.11	6.38	1.27

References pp. 38–40

gested the following mechanism [41,42].



The positive charge on nitrogen, either preformed in the zwitterion or developing in the transition state from neutral acid, facilitates the formation of carbanion (ylid) by the same inductive effect as that of the chlorines in trichloroacetate.

The proposed mechanism requires a carbon-isotope effect (except in the unlikely event that intramolecular proton transfer is rate-controlling) and both ^{14}C [43] and ^{13}C [44] kinetic isotope effects have been found by Zielinski. The ^{13}C results are shown in Table 3. The isotope effect has the normal temperature dependence and it independent of percent reaction, as expected, but shows a pronounced medium effect. It is larger in water and phenol than in the melt or in *o*-nitrophenol, but in all cases it is considerably less than the intermolecular isotope effect for malonic and most other acids. Zielinski considered the possibility that protonation of the α -carbon is partially rate-determining, but found no carboxyl–tritium isotope effect for decarboxylation in the melt. The lack of a hydrogen-isotope effect was also taken as evidence against an ionization pre-equilibrium. Decarboxylation of a hydrated zwitterion with concurrent proton transfers via the solvating molecules was the favored mechanism [44].

Zielinski also observed an isotope effect in the decarboxylation of picolinic acid hydrochloride [44]. The data are shown in Table 4. Here the isotope effect is smaller and decreases with increasing percent reaction. Zielinski concludes that the decarboxylation of picolinic acid hydrochloride takes place by a “dissociative mechanism”, but does not explain how this lowers the isotope effect.

Dunn et al. studied the decarboxylation of picolinic acid in aqueous solution as a function of pH. The rate profile, at 150°C , shows that the isoelectric species decarboxylates fastest, as required by the Hammick mechanism. The cation does not decarboxylate, but the anion decarboxylates about half as fast as the isoelectric species. ^{13}C kinetic isotope effects at the same temperature and concentration were $(2.25 \pm 0.02)\%$ for the isoelectric species at pH 1.13, in good agreement with Zielinski’s value in water, and $(2.08 \pm 0.02)\%$ for the anion at pH 3.95 [36]. Apparently C–C bond breaking is a smaller component of the activation energy for decarboxylation of the

TABLE 4

¹³C KINETIC ISOTOPE EFFECT IN THE DECARBOXYLATION OF PICOLINIC ACID HYDROCHLORIDE [44]

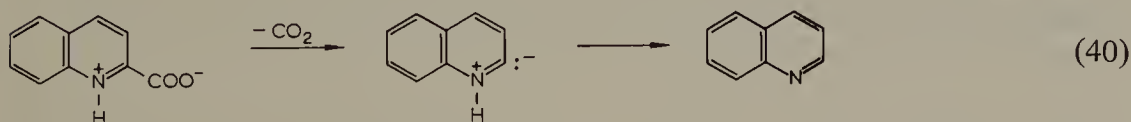
Temperature (°C)	Mole solvent Mole acid	Percentage reaction	Percentage isotope effect
Water			
142	2.733	0.33	1.12
195.5	0.136	1.94	1.11
195.5	0	1.81	1.12
195.5	0	5.43	1.00
195.5	0	12.59	0.87
195.5	0	14.39	0.80
195.5	0	19.96	0.74
210.5	0	28.29	0.63

anion than of the acid. What the other components are was not elucidated.

It is interesting to note that in water the cation did not decarboxylate, although Zielinski reported an isotope effect for decarboxylation of picolinic acid hydrochloride [44]. In aqueous solutions of the hydrochloride, hydrolysis of the cation would be sufficient to permit decarboxylation, but in the melt the hydrochloride must either dissociate to free acid or decarboxylate by a mechanism not available in water. The very small isotope effect suggests that some process other than C—C breaking is largely rate-determining. Possibly it is dissociation.

3. Quinaldinic acid

Quinaldinic acid, like picolinic acid, is believed to decarboxylate by decomposition of the zwitterion into carbon dioxide and a nitrogen ylid [41,42].



Since the first step would doubtless be rate-determining, a ¹³C kinetic isotope effect is expected. Zielinski [45,46] studied decarboxylation of the acid neat and in aqueous solution, and obtained the results shown in Table 5. As in the case of picolinic acid, the isotope effect is considerably larger in aqueous solution than in pure acid. Carbon—carbon bond breaking is more advanced in the aqueous transition state than in that of the pure acid, but no model has been proposed to account for this.

TABLE 5

 ^{13}C KINETIC ISOTOPE EFFECT IN THE DECARBOXYLATION OF QUINALDINIC ACID

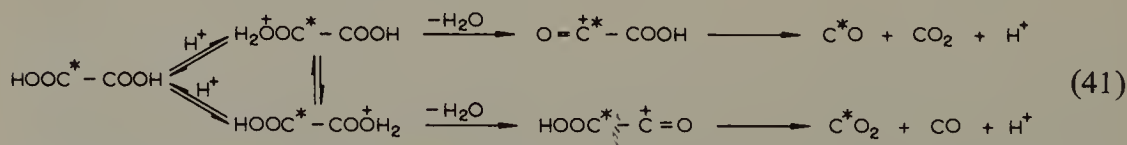
Temperature (°C)	Mole fraction acid in aqueous solution	Percentage isotope effect	Reference
180	1.00	1.09 ± 0.02	45
171	1.00	1.11 ± 0.05	45
161	1.00	1.13 ± 0.06	45
160	1.00	1.19	46
151	1.00	1.09 ± 0.03	45
149	1.00	1.10 ± 0.03	46
142	1.00	1.04 ± 0.04	45
175	0.0128	2.13	46
175	0.0595	1.98	46
157	0.0610	2.10	46
157	0.0128	2.31	46

D. Dicarboxylic acids

Dicarboxylic acids were historically the first in which carbon isotope effects in decarboxylation were examined [2]. Much of the early work was concerned with establishing the existence and magnitude of the kinetic isotope effect, and not particularly with its interpretation.

1. Oxalic acid

The decarboxylation of oxalic acid was the first in which a ^{13}C kinetic isotope effect was observed. Lindsay et al. studied decarboxylation in concentrated sulfuric acid at 100°C and found the intramolecular kinetic isotope effect to be 3.3% and the intermolecular kinetic isotope effect to be 3.4% [4]. They did not concern themselves with the mechanism of the decarboxylation, but it is obvious that C–C bond breaking is well advanced in the transition state. Fry and Calvin obtained similar results under similar conditions: $(2.7 \pm 0.2)\%$ at 103.0° and $(3.3 \pm 0.2)\%$ at 80.1°C [47]. They proposed the following mechanism



with the lower pathway preferred because CO_2 rather than CO becomes enriched in ^{13}C . This implies that loss of water is the rate-determining step.

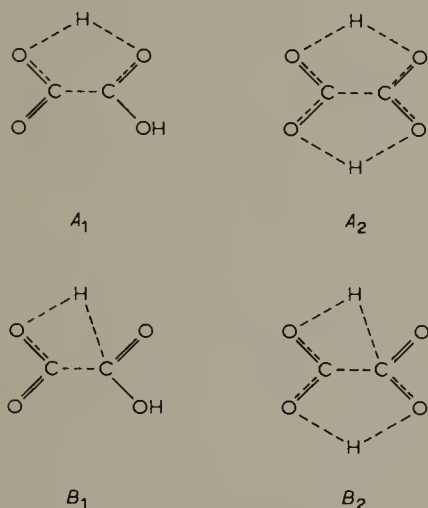
Yankwich and co-workers examined the intramolecular kinetic isotope effect

TABLE 6

¹³C INTRAMOLECULAR KINETIC ISOTOPE EFFECT IN THE GAS-PHASE DECARBOXYLATION OF OXALIC ACID [48,49]

Temperature (°C)	Percentage isotope effect	
	(COOH) ₂	(COOD) ₂
126.6	0.52 ± 0.04	0.42 ± 0.04
134.1	0.17 ± 0.09	0.19 ± 0.06
146.4	-0.06 ± 0.03	-0.01 ± 0.10
155.6	-0.24 ± 0.06	-0.18 ± 0.05
160.0	-0.21 ± 0.04	-0.22 ± 0.02
170.0	-0.20 ± 0.01	-0.36 ± 0.04
180.0	-0.19 ± 0.04	-0.33 ± 0.03

in the gas-phase decarboxylation of oxalic acid [48] and oxalic acid-*d*₂ [49]. The results are given in Table 6. Attention was focussed on the inversion of isotope effect with increasing temperature. They considered that the usual temperature dependence of isotope effects is not large enough to account for inversion in such a narrow temperature range, and postulated that it arises from a change of mechanism. They proposed a transition state like *A*₁ or *A*₂ (possibly on the walls of the reaction vessel) at lower temperatures, and one like *B*₁ or *B*₂ (in the body of the gas) at higher temperatures.



The change of mechanism was supported by the fact that the hydrogen isotope effect (also small) inverts in the same temperature range [50]. Theoretical calculations also failed to account for the inversion on the basis of a single mechanism [51]. Neverthe-

TABLE 7

¹³C KINETIC ISOTOPE EFFECTS IN THE DECARBOXYLATION OF OXALIC ACID IN GLYCEROL SOLUTION [52]

Temperature (°C)	<i>f</i>	Percent isotope effect		
		Intramolecular	Intermolecular	
			Carboxyl	α
98.0	0.965	1.20 ± 0.13	1.5 ± 0.4	2.7 ± 0.5
112.0	0.970–0.995	1.34 ± 0.09	1.2 ± 0.3	2.5 ± 0.4
121.0	0.998	1.48 ± 0.08	1.1 ± 0.3	2.5 ± 0.3
130.0	0.999	1.91 ± 0.07	0.9 ± 0.2	2.8 ± 0.2
135.0	0.950–0.990	2.36 ± 0.07	0.8 ± 0.2	3.2 ± 0.2

less, it would seem prudent to be cautious in the interpretation of such small effects.

Yankwich and co-workers also examined the ¹³C isotope effect in the decarboxylation of oxalic acid in glycerol solution [52]. The initial reaction is first order with respect to oxalic acid, but the rate constant increases in later stages of the reaction, perhaps because of catalysis by the product formic acid. Both intramolecular and intermolecular isotope effects are given in Table 7 but, because the reactions were carried to high conversions (*f*), the intermolecular effects are subject to considerable uncertainty. The abnormal temperature dependence of the intramolecular isotope effect is striking, and again the possibility of its resulting from a change of mechanism was considered. However, the absence of a common inversion temperature for all three isotope effects, or a single enthalpy value which would account for the shift from one mechanism to the other, was taken as evidence against a duality of mechanism [52].

Because the decarboxylation of oxalic acid is kinetically simpler in dioxane than in glycerol or sulfuric acid, Huang et al. studied the ¹³C kinetic isotope effect in dioxane [53]. They found the intermolecular isotope effect to be (3.19 ± 0.07)% at 79.8°, (3.23 ± 0.13)% at 99.2°, (3.50 ± 0.08)% at 111°, (3.37 ± 0.22)% at 123°, (3.08 ± 0.03)% at 127.4°, and (2.74 ± 0.04)% at 131.8°C. Again a complex temperature dependence is noted. This time, however, the authors are not able to offer an explanation in terms of change of mechanism. Extensive theoretical calculations best fitted a transition state in which the carboxyl group which will become carbon dioxide has its C–C bond lengthened, its C–O bond shortened, and either its O–H bond lengthened or its O–C–O angle opened toward linearity. §

Yankwich and co-workers have also studied the ¹³C isotope effect in the pyrolytic decomposition of various heavy metal oxalates.

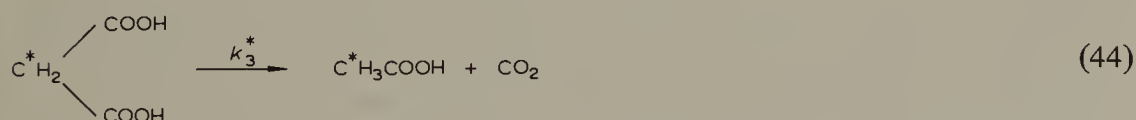
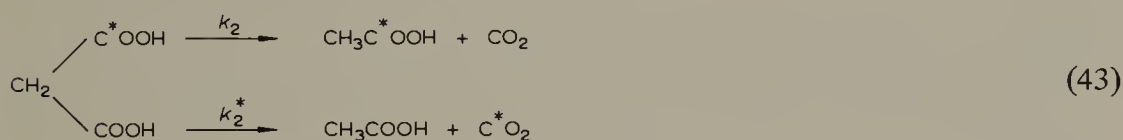
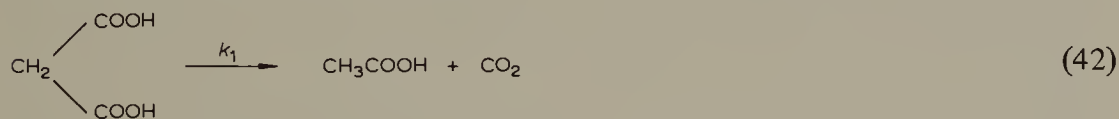


Both intra- and intermolecular isotope effects were examined as functions of metal ion, temperature, and extent of reaction. The intramolecular isotope effect was the same for lead [54], zinc [55], and manganous oxalates [56] on complete decarboxylation, varying from 0.8% at 280°C to 0.4% at 500°C. For samples prepared from manganous chloride and oxalic acid the isotope effect depended upon the extent of decarboxylation. At 300°C the intramolecular effect was 2.1% during the first 2% of reaction, 1.0% during the second 2% of reaction and 0.7% on complete decarboxylation. At the same temperature the intermolecular isotope effect varied from 1.4% during the first 2% of reaction to 0.9% during the second 2% of reaction. When the manganous oxalate was prepared from manganous chloride and sodium oxalate, the dependence upon extent of reaction disappeared for the intramolecular effect but not for the intermolecular one. At 300° the intermolecular isotope effect varied from 1.2% in the first 2% of reaction to 0.3% in the second. The temperature dependence of the intermolecular isotope effect was also abnormal, increasing with temperature. Similar, but not as extensive, results were obtained with zinc and lead oxalates. The usual difficulties in interpretation of solid-state kinetics are encountered in trying to explain these isotope effects.

2. Malonic acid

Malonic is the acid for which ^{13}C kinetic isotope effects have been most thoroughly examined. As the classic example of an easily decarboxylated acid, it was used in early work to compare the magnitudes of ^{13}C kinetic isotope effects with theoretical predictions and with the corresponding ^{14}C effects.

Using the symbolism developed in Section III.B.2, the decarboxylation of malonic acid may be represented as follows.



Bigeleisen and Friedman used the methods indicated in Section II to calculate theoretical values for the intramolecular (k_2/k_2^*) and the carboxyl intermolecular ($k_1/2k_2^*$) ^{13}C kinetic isotope effects [3]. Later, Stern and Wolfsberg used computer meth-

TABLE 8

PERCENT ^{13}C KINETIC ISOTOPE EFFECTS IN THE DECARBOXYLATION OF MALONIC ACID IN THE MELT

	T, °C	k_2/k_2^*	$k_1/2k_2^*$	k_1/k_3^*	$k_1/2k_2$
Theory					
Bigeleisen and Friedman [3]	137.5	1.98	2.1		0.12
Stern and Wolfsberg [57]	2	2.90	3.28	4.00	0.34
	127	1.86	2.22	2.60	0.35
	227	1.40	1.74	2.00	0.34
Experiment		CO ₂	HOAc		
Bigeleisen and Friedman [3]	137.5	2.0	3.7		1.7
Lindsay et al. [58]	138	2.8	2.4	4.6	1.8, 2.1
	138	2.1			
Lindsay et al. [12]	137	2.1	3.4		1.3
	149		4.1		2.0
	173		3.4		1.3
	196		3.6		1.5
Bernstein [59]	160	3.33			
Yankwich and Stivers [60]	137	2.9	2.5		
Zielinski [61]	112	3.49		4.10	0.59
	121.5	3.35			
	136	3.16		3.63	0.46
	148	3.01			
	181	2.75			
Yankwich and Promislow [62]	140	2.92	2.90		
Loudon et al. [15]	150	2.5	2.8	4.0	1.7
					1.5

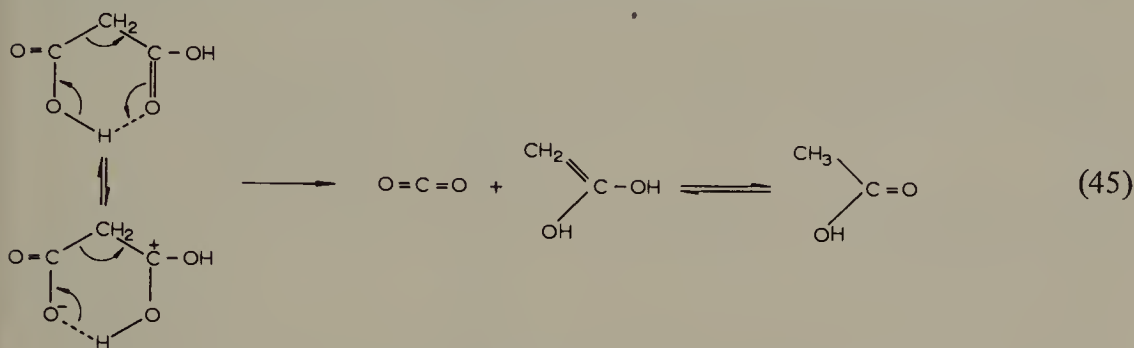
ods to obviate some of the approximations used by the earlier workers, and to calculate the α intermolecular isotope effect (k_1/k_3^*) [57]. Their predictions may be compared with the experimental values obtained by various authors in Table 8.

The early work in the melt was not particularly concerned with the mechanism of the reaction. However, some mechanistic assumptions were made. The theoretical isotope effects listed in Table 8 are based on a model in which the transition state differs from the reactant only in that the stretching force constant for the breaking C—C bond vanishes [57]. This model works reasonably well for the intramolecular isotope effect, but its prediction for the intermolecular isotope effect is too small. Nevertheless, it shows that the carboxyl-to-methylene C—C bond is largely broken in the transition state.

Because different isotope effects are observed for the intramolecular (k_2/k_2^*) and intermolecular carboxyl ($k_1/2k_2^*$) competitions, it is clear that there is an isotope ef-

fect ($k_1/2k_2$), here called the β isotope effect, arising from isotopic substitution in the carboxyl group not undergoing rupture. Values of this isotope effect calculated from the original authors' data are shown in the last column of Table 8. Except for Zie-
linski's, they are much larger than predicted by the simple model described above and, as several authors have pointed out [8,15], would seem to indicate some significant bond changes at the carbon most remote from the reaction site. Perhaps these figures should be treated with caution, however, since they include the errors present in both the inter- and intramolecular isotope effects.

Nevertheless, it is interesting to note that the commonly accepted mechanism of malonic acid decarboxylation does involve considerable reorganization of the bonding around the terminal carbon atom. Largely by analogy with β -ketoacids, which have been more thoroughly studied, the mechanism is supposed to be the following.



Yankwich and co-workers have pointed out that decarboxylation in the melt may proceed to a significant extent before the melt becomes homogeneous. They have therefore measured isotope effects in solution, where the reaction is also accessible to kinetic studies [63–66]. Their results are shown in Table 9. It is noteworthy that, where both were measured, the intra- and intermolecular carboxyl isotope effects are so similar as to make any β isotope effect negligibly small. The evidence on this point from different workers is sufficiently varied that a direct examination of the β isotope effect would perhaps be warranted.

From the facts that the temperature dependences shown in Table 9 are greater than those predicted by the simple form of the Bigeleisen theory [14], and that the isotope effect at a given temperature is larger in quinoline than in other solvents, Yankwich and co-workers conclude that decarboxylation is preceded by some kind of rapid equilibrium with its own isotope effect. From the fact that the rate constants for decarboxylation in dioxane solution are linearly related to the concentration of added quinoline [66] they conclude that the pre-equilibrium involves complex formation between malonic acid and quinoline, and that the formation constant has a 1% isotope effect. Insofar as this conclusion rests on a discrepancy between experiment and the simple theory, it should be accepted with caution, since the simple theory is often not in precise agreement with experiment (see Table 8).

The monoanion of malonic acid decarboxylates about one-tenth as fast as the acid

TABLE 9

¹³C KINETIC ISOTOPE EFFECTS IN THE DECARBOXYLATION OF MALONIC ACID IN SOLUTION

Reference	Solvent	T, °C	k_2/k_2^*	$k_1/2k_2^*$
Yankwich et al. [63]	80% Sulfuric acid	56		4.53 ± 0.06
		79		3.76 ± 0.09
		100		3.48 ± 0.04
		129		3.36 ± 0.07
Yankwich and Belford [64]	Quinoline	34		5.67 ± 0.11
		59		4.94 ± 0.11
		79		4.38 ± 0.02
		99		4.09 ± 0.08
		118		3.79 ± 0.09
Yankwich and Belford [65]	Quinoline	86	4.45 ± 0.08	
		100	4.10 ± 0.09	
		110	3.73 ± 0.01	
		123	3.56 ± 0.02	
		138	3.17 ± 0.06	
Yankwich and Ikeda [66]	Dioxane	40.3		4.33 ± 0.01
		50.3		4.15 ± 0.07
		60.2		3.98 ± 0.04
		71.3		3.82 ± 0.04
		80.4		3.58 ± 0.07
		88.8		3.38 ± 0.03
		99.1		3.20 ± 0.02

TABLE 10

APPARENT ¹³C KINETIC ISOTOPE EFFECTS IN THE DECARBOXYLATION OF HYDROGEN MALONATE ION

Reference	Solvent	T, °C	k_2/k_2^*	$k_1/2k_2^*$
Yankwich and Weber [68]	Quinoline	67.5		4.17 ± 0.06
		79		4.15 ± 0.01
		98		3.91 ± 0.07
		119		3.77 ± 0.05
Yankwich and Weber [69]	Quinoline	79	3.54 ± 0.03	
		89.5	3.68 ± 0.08	
		102.5	3.52 ± 0.08	
		115.5	3.32 ± 0.04	
		138	3.28 ± 0.08	
Buddenbaum et al. [70]	Water	100		4.33 ± 0.10

itself [67], and Yankwich and co-workers have also examined the ^{13}C kinetic isotope effect in this decarboxylation [68–70]. Their results are given in Table 10. In quino-line the isotope effect is larger than predicted by the simple theory, and Yankwich and co-workers propose that part of the apparent kinetic isotope effect is really a thermo-dynamic isotope effect in the equilibrium by which hydrogen malonate ion is formed from malonic acid and 1-butylpiperidine. They point out that, if this is true, there should be a similar isotope effect in the ionization of hydrogen malonate ion to malonate ion. Since malonate ion does not decarboxylate, they predict that the ap-parent kinetic isotope effect should vary with the extent of hydrogen malonate ion dissociation, i.e. with pH. In aqueous solution they find this to be true [60] with

$$\frac{k_1}{2k_2^* \text{ apparent}} = (1.0433 \pm 0.0010) - \rho(0.0085 \pm 0.0014) \quad (46)$$

where ρ is the mole fraction of malonate ion. Consideration of various models leads them to prefer one in which the hydrogen malonate ion is weakly complexed with solvent, and the reaction



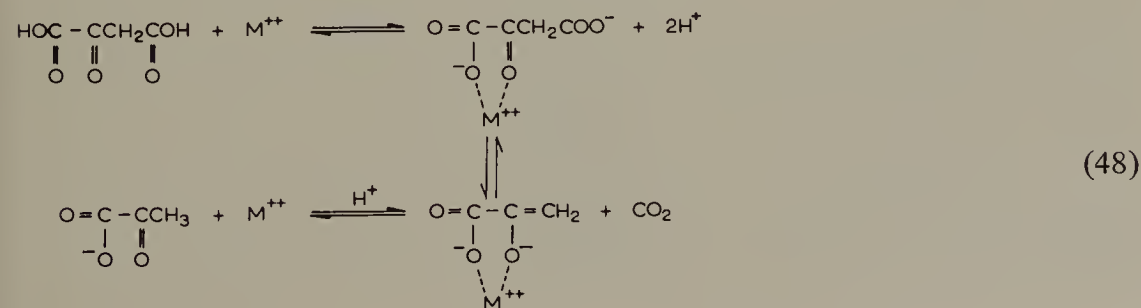
has an equilibrium constant of 1.01 at 100°C . They point out that other interpreta-tions are possible.

3. Bromomalonic acid

Yankwich and Stivers studied the ^{13}C intramolecular kinetic isotope effect of bro-momalonic acid in the melt in order to compare it with the ^{14}C effect [60]. By anal-ysis of the carbon dioxide from complete decarboxylation they found a ^{13}C isotope effect of $(2.4 \pm 0.6)\%$. By analysis of the acetic acid they obtained $(2.4 \pm 0.2)\%$. The temperature was unspecified. These results are very similar to those found for malonic acid itself [60].

4. Oxaloacetic acid

The decarboxylation of oxaloacetic acid and, more importantly, its reverse, the car-boxylation of pyruvic acid, are important biological reactions whose mechanisms have been extensively studied. The reaction is catalyzed by metal ions and by metal ions plus enzymes. By analogy with dimethyloxaloacetic acid the mechanism of the non-enzymatic reaction is believed to be as follows [71].



The uncatalyzed and metal-ion-catalyzed reactions both have ^{13}C kinetic isotope effects which in preliminary work appeared to be larger for paramagnetic than for diamagnetic ions [72]. However, the final results showed this not to be the case. Wood, using ^{13}C -enriched oxaloacetic acid, found isotope effects of $(4.5 \pm 0.4)\%$ for the uncatalyzed reaction and $(3.5 \pm 0.3)\%$ in the presence of a ten-fold excess of any one of yttrium, dysprosium or gadolinium ion [73]. Apparently C—C bond breaking (the second step in the above mechanism) is rate-determining in both the uncatalyzed and metal-ion-catalyzed decarboxylations.

Westheimer and co-workers studied the reaction as catalyzed by Mn^{2+} or Cu^{2+} ions and by a micrococcal decarboxylase, again using ^{13}C enriched substrate [74]. For the reaction catalyzed by 0.001 *M* metal ion alone they found the ^{13}C kinetic isotope effect to be 6.0% using Mn^{2+} and 5.6% using Cu^{2+} . In the presence of Mn^{2+} and enzyme the rate was increased by a factor of 10^8 , but the ^{13}C isotope effect disappeared. Clearly the rate-determining step changes from C—C bond breaking in the non-enzymatic reaction to some earlier step in the enzymatic one. Westheimer et al. suggest several possible mechanisms for the enzyme-catalyzed reaction in which decarboxylation of an enzyme-substrate complex is so rapid that formation of the complex becomes rate-determining.

5. Glutamic acid

Hoering found the ^{13}C kinetic isotope effect in decarboxylation of glutamic acid catalyzed by crystalline glutamate decarboxylase to be 2.59%, and noted that this is considerably smaller than isotope effects in uncatalyzed decarboxylations of similar acids [16].

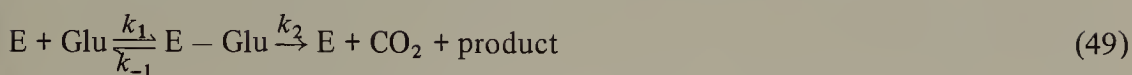
O'Leary et al., also using glutamate decarboxylase, found an even smaller isotope effect which varied with pH [75,76]. Their results are shown in Table 11. Their explanation of the small isotope effect follows the same lines as Westheimer's explanation of the zero isotope effect in the decarboxylation of oxaloacetic acid [74].

TABLE 11

^{13}C KINETIC ISOTOPE EFFECTS IN THE ENZYMATIC DECARBOXYLATION OF GLUTAMIC ACID AT 37°C [75,76]

pH	Buffer	Percentage isotope effect
3.6	Isonicotinamide—HCl	1.56 ± 0.07
4.0		1.44 ± 0.04
4.4		1.38 ± 0.08
4.4	Pyridine—HCl	1.55 ± 0.05
4.7		1.66 ± 0.11
5.2		1.88 ± 0.03
5.5		2.22 ± 0.05

Decarboxylation is assumed to occur in an enzyme-substrate complex



for which

$$k_{\text{obs}} = \frac{k_1 k_2}{k_{-1} + k_2} \quad (50)$$

If the first step is insensitive to isotopic substitution,

$$\text{then } \frac{k_{\text{obs}}}{k_{\text{obs}}^*} = \frac{k_2}{k_2^*} \left(\frac{k_{-1} + k_2^*}{k_{-1} + k_2} \right) \quad (51)$$

Consequently, there will be an isotope effect if $k_{-1} \gg k_2$, but not if $k_{-1} \ll k_2$. The small observed effect can be accounted for if k_2/k_{-1} lies in the range 1–3. Its variation with pH could arise from a pH dependence of k_2/k_{-1} ; a reasonable hypothesis since both the enzyme and glutamic acid contain basic groups whose degree of protonation could easily influence the stability of the complex.

6. Pyridinedicarboxylic acids

Zielinski has examined ^{13}C isotope effects in the decarboxylation of the 2,3-, 2,4- and 2,6-pyridinedicarboxylic acids in the melt [77]. In the 2,3- and 2,4- acids only the 2-carboxyl group decarboxylates at the temperatures used, so they were treated kinetically as monocarboxylic acids. The results are shown in Table 12.

Dunn et al. studied the decarboxylation of pyridine-2,3-dicarboxylic acid as a function of pH in aqueous solutions of ionic strength 1.0 [36]. The rate profile was very similar to that for picolinic acid (Section V.C.2) with the maximum at a pH of about 1. They considered the possibility of a change of mechanism with pH similar to that found for anthranilic (Section V.B.3) and azulene-1-carboxylic acids (Section V.B.5), but the ^{13}C isotope effect turned out to be essentially independent of pH [36]. In aqueous solutions of ionic strength 1.0 at 95°C they found the ^{13}C kinetic isotope effect to be $(2.84 \pm 0.03)\%$ at pH = 0, $(2.73 \pm 0.02)\%$ at pH = 2.63 and $(2.67 \pm 0.01)\%$ at pH = 3.95. These results are very similar to those for picolinic acid, and it seems probable that the Hammick mechanism (eqn. 39) applies to both.

It is noteworthy that the ^{13}C isotope effect for pyridine-2,3-dicarboxylic acid is considerably larger in aqueous solution [36] than in the melt [77]. Zielinski found this to be true for picolinic acid as well (Table 3). It would appear that C–C bond breaking is not entirely rate-determining in the decarboxylation of pyridinecarboxylic acids, and less so in the melt than in protic solvents. It is tempting to suppose that proton transfer is partially rate-determining, but the lack of a tritium isotope effect in Zielinski's experiments with picolinic acid (Section V.C.2) argues against this. Of course, it must be remembered that the *absence* of an isotope effect is never conclusive evidence in itself.

TABLE 12

¹³C KINETIC ISOTOPE EFFECTS IN THE DECARBOXYLATION OF PYRIDINEDICARBOXYLIC ACIDS IN THE MELT [77]

Acid	T, °C	Percentage reaction	Percentage isotope effect
2,3-	168	2.04	0.98
		38.50	1.13
		57.56	1.14
	155	2.08	0.94
		4.60	0.96
		22.45	1.05
		32.74	1.08
		43.73	1.10
	139.5	0.27	0.87
		9.22	0.97
		33.30	1.09
2,4-	220	4.78	1.25
		7.50	1.22
		8.20	1.24
	209.5	9.12	1.27

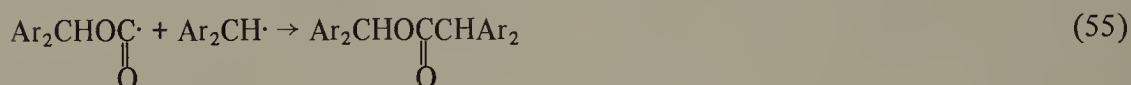
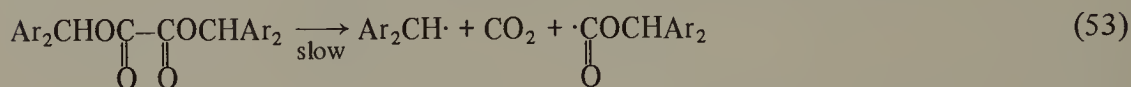
Zielinski has also examined the decarboxylation of pyridine-2,6-dicarboxylic acid in the melt and found ¹³C kinetic isotope effects approaching 2% [77]. These are distinctly larger than those for the other pyridinedicarboxylic acids and picolinic acid under comparable conditions. However, the isotope effects for pyridine-2,6-dicarboxylic acid were calculated on the assumption that the second carboxyl group decarboxylates much more readily than the first [77], whereas Dunn et al. subsequently found the initial rate constants for decarboxylation of picolinic and pyridine-2,6-dicarboxylic acids in aqueous solution to be nearly the same [36]. If, as seems probable, these rate constants are also alike in the melt, the amount of second decarboxylation after 1% decomposition of pyridine-2,6-dicarboxylic acid will be negligible, so that the kinetic isotope effect can be calculated from eqn. 20 like any other dicarboxylic acid. Recalculation by eqn. 20 using those data [77] obtained at 5% conversion or less yields ¹³C kinetic isotope effects of $(0.86 \pm 0.03)\%$ at 228°C, $(0.88 \pm 0.04)\%$ at 210°C and $(0.80 \pm 0.10)\%$ at 196°C. These results are not very different from those obtained from the other pyridinedicarboxylic acids or from picolinic acid.

VI. RELATED REACTIONS

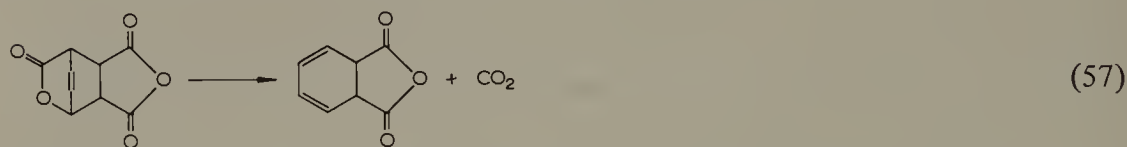
A. Bromodecarboxylation

Since decarboxylation is an electrophilic displacement of carbon dioxide, it is apparent that other electrophiles besides proton should be able to effect the displace-

average kinetic isotope effects of 2.8% for ^{13}C and 1.6% for ^{18}O , using four different substituted benzhydryl oxalates, they concluded that a C—C and a C—O bond are broken in concert. Of course, isotope effects cannot distinguish homolytic from heterolytic bond breaking, but they conclude on other grounds that thermolysis is a radical process with considerable polar character at the transition state.



Goldstein and Thayer in a study of the mechanism of the Diels—Alder reaction chose the thermolysis of the Diels—Alder adduct of α -pyrone and maleic anhydride because it yields carbon dioxide ready for isotopic analysis [81].



Dimethylphthalate solutions of the adduct (0.1 *M*) at 130.2°C gave a ^{13}C kinetic isotope effect of $(3.0 \pm 0.3)\%$ and an ^{18}O kinetic isotope effect of $(1.4 \pm 0.2)\%$.

Detailed calculations of the type devised by Schachtschneider [82] and Wolfsberg [9] indicated that the observed isotope effects are most simply accommodated by a transition state in which the C—C bond is broken, the C=O bond is tightened, and the oxygen-to-bridgehead-carbon bond is nearly intact. This shows that the C—C and C—O bonds are not broken precisely simultaneously, but does not prove the existence of an intermediate. Goldstein and Thayer conclude that the reaction takes place in two stages but not necessarily in two steps. This is a very interesting use of isotope effects to obtain information about the transition state of a reaction for which mechanistic information has long been difficult of access.

C. Photodecarboxylation

Yankwich and Buddemeier have studied the uranyl nitrate sensitized photodecarboxylation of oxalic acid [83]. They found a *reverse* intramolecular isotope effect of $(2.4 \pm 0.1)\%$ for a solution containing 3.00 *M* sulfuric acid, 0.33 *M* oxalic acid, and 0.0168 *M* uranyl nitrate irradiated in a Pyrex vessel with a General Electric AH-5 mer-

cury lamp. It is an inverse isotope effect in the sense that ^{13}C concentrates in the lighter fragment, CO, whereas in thermal decarboxylation it concentrates in the heavier one, CO_2 [4]. Their data also suggest that there is no intermolecular isotope effect. Although the preliminary report [83] offers no interpretation of these results, the significance of an intra- without an inter-molecular carbon isotope effect is clear enough: the nature of the products is determined in a step which involves C—C bond breaking, but the rate is not. The most obvious interpretation of this would be that photo-excitation has no isotope effect and every excited molecule goes to product (quantum yield = 1). However, the observed quantum yield is about 0.6 [84], so the mechanism must be more complex. One possibility is that the initial excited state may, without isotope effect, either decay to ground state or convert irreversibly to an intermediate which goes completely to product *via* C—C bond rupture. The distribution of ^{13}C between CO_2 and CO is determined in the last step, whereas the rate and quantum yield are determined in the earlier ones.

Gamma-radiation-induced decarboxylation of higher dicarboxylic acids has been studied by Hosaka et al. [85]. Their results are shown in Table 13. It is noticeable that some of the dicarboxylic acids have considerably larger isotope effects than others or any of the monocarboxylic acids. The authors correlate this with contiguity of the two carboxyl groups in a molecule, either through methylene groups (as in malonic acid) or by ring closure (as in adipic acid). They speculate that contiguity facilitates energy exchange, but do not explain why the excitation energy is localized in the carboxyl groups or how exchange causes increased isotope effects.

TABLE 13

INTERMOLECULAR ^{13}C ISOTOPE EFFECTS IN THE RADIATION-INDUCED DECARBOXYLATION OF CARBOXYLIC ACIDS IN THE SOLID STATE [85]

Acid	Percentage isotope effect ± 0.3
$\text{C}_6\text{H}_5\text{CH}(\text{COOH})_2$	2.1
NCCH_2COOH	0.6
$\text{CH}_3\text{CH}=\text{CHCOOH}$	0.7
$\text{HOOCCH}_2\text{COOH}$	1.9
$\text{HOOC}(\text{CH}_2)_2\text{COOH}$	1.3
$\text{HOOC}(\text{CH}_2)_3\text{COOH}$	0.6
$\text{HOOC}(\text{CH}_2)_4\text{COOH}$	2.0
$\text{HOOC}(\text{CH}_2)_5\text{COOH}$	2.0
$\text{HOOC}(\text{CH}_2)_8\text{COOH}$	0.7
<i>cis</i> $\text{HOOCCH}=\text{CHCOOH}$	2.4
<i>trans</i> $\text{HOOCCH}=\text{CHCOOH}$	1.1

TABLE 14

¹³C KINETIC ISOTOPE EFFECTS IN THE OXIDATION OF AQUEOUS OXALIC ACID [86]

Reagent	No. of runs	Percentage isotope effect	
		Mean	Variation
Br ₂	5	2.2	1.8–2.4
H ₂ O ₂ + Fe ²⁺	8	1.8	1.6–2.2
KMnO ₄	7	2.6	1.7–3.0
KMnO ₄ + Mn ²⁺	4	3.5	3.2–3.6

D. Oxidative decarboxylation

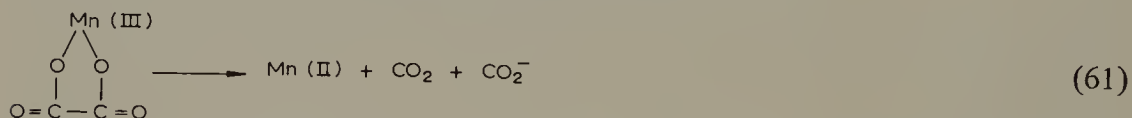
Carbon-13 kinetic isotope effects in the oxidation of oxalic acid to carbon dioxide were first studied by Bunton and Llewellyn [86]. From their results, shown in Table 14, they conclude that C–C bond breaking is at least partially rate-determining, since electron-transfer from oxygen should not be appreciably dependent on the presence of carbon isotopes. The isotope effect is particularly variable when the oxidizing agent is permanganate, which is probably due to a variable induction period. It is believed that the rate-controlling step during the induction period is



followed by a two-electron transfer to Mn(VI) or Mn(IV) from oxalate.



The rate is slow during the induction period because of the lack of Mn(II), but as Mn(II) accumulates, or is added, the rate-controlling process becomes the one-electron oxidative decomposition of an oxalate–Mn(III) complex [87].



It is noticeable that in the presence of Mn²⁺ the ¹³C isotope effect is larger and much less variable, which suggests that the isotope effect is smaller for oxidation by Mn(VI) or Mn(IV) than for oxidation by Mn(III).

Betts and Buchannon studied the ¹³C isotope effect in permanganate oxidation of oxalic acid as a function of percent reaction [88]. Their results are shown in Table 15. The isotope effect is constant at (3.7 ± 0.1)% after about 0.5% reaction where the decomposition of Mn(III) complex is presumably rate-determining, but is smaller in the

TABLE 15

^{13}C KINETIC ISOTOPE EFFECTS IN THE OXIDATION AT 2°C OF 0.05 M OXALIC ACID BY 0.02 M POTASSIUM PERMANGANATE IN 0.9 M SULFURIC ACID [88]

Percentage oxalic acid reacted	No. of runs	Percentage isotope effect
0.00–0.16	1	2.90
0.16–0.32	1	3.18
0.00–0.32	3	3.04 ± 0.02
0.32–0.48	1	3.36
0.32–0.64	3	3.37 ± 0.08
0.48–0.64	1	3.57
0.64–0.96	4	3.59 ± 0.08
0.96–1.28	4	3.72 ± 0.15
1.28–1.60	2	3.76 ± 0.06
1.60–1.92	1	3.70
1.92–2.24	1	3.74
2.24–2.56	1	3.73
2.56–2.88	1	3.76
2.88–3.20	1	3.75

initial stages where oxalate is oxidized by Mn(VI) and Mn(IV). When Mn(III) oxidation is inhibited completely by the addition of excess fluoride ion the observed ^{13}C isotope effect is $(0.0 \pm 0.6)\%$, indicating that C–C bond breaking is not rate-determining in the two-electron oxidation by Mn(VI) and Mn(IV) [88].

TABLE 16

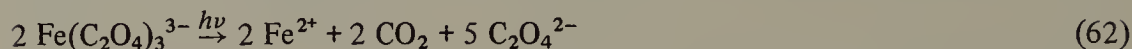
^{13}C KINETIC ISOTOPE EFFECTS IN THE PHOTO-INITIATED DECOMPOSITION OF 0.01 M $\text{K}_3\text{Fe}(\text{C}_2\text{O}_4)_3 \cdot 3\text{H}_2\text{O}$ IN 0.25 M SULFURIC ACID [88]

$T, ^\circ\text{C}$	λ, nm	Quantum yield ^a	Percentage isotope effect
19 ± 1	365	0.60	0.11
	403	0.55	1.67
	410	0.54	1.62
	441	0.51	2.69
	481	0.42	3.96
	507	0.23	4.94
	520	0.07	5.04
2 ± 1	403	0.50	1.62
	441	0.50	3.00
	481	0.40	4.00
	520	0.05	5.54

^a For decomposition of oxalate ion [89]

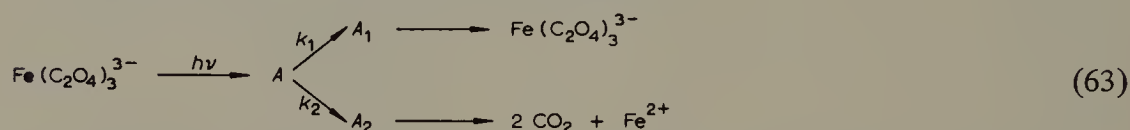
References pp. 38–40

In a search for other examples of oxalate oxidation where C—C bond breaking is not rate-controlling, Betts and Buchannon studied the photo-initiated oxidation of oxalate by ferric ion [88].



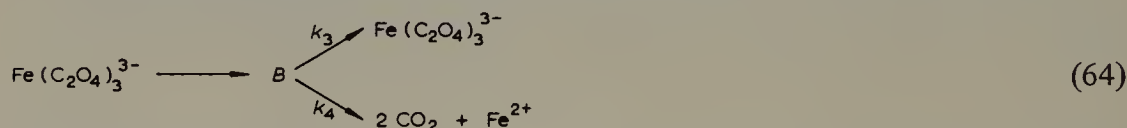
Their results are shown in Table 16. To explain the variation of isotope effect with wavelength, they propose two decomposition pathways, one with no isotope effect which predominates at short wavelength, and a second with a large isotope effect at longer wavelengths.

At short wavelengths the proposed mechanism is



where the excited state A decays either to ground state (rate constant k_1), or to a second intermediate A_2 (rate constant k_2) whose only fate is the formation of carbon dioxide by C—C bond breaking. Since neither k_1 nor k_2 concern C—C bond breaking, A_2 has the same isotopic composition as starting material, and since every A_2 molecule decomposes to product, there will be no isotope effect. The quantum yield is determined by $k_2/(k_1 + k_2)$, and is therefore less than unity.

At longer wavelengths only one intermediate is necessary to explain the results.



The rate constant k_4 , which concerns C—C bond breaking, will be greater for ^{12}C than for ^{13}C , and the excess of heavy isotopic isomer can decay to ground state *via* k_3 . In support of their mechanism Betts and Buchannon cite other work [90] which postulates that the short-wavelength excitation is associated with a primary electron transfer, whereas the long-wavelength one is associated with ligand excitation and has a much lower extinction coefficient.

ACKNOWLEDGEMENT

The author is grateful to Dr. R.H. Betts for permission to use his data prior to publication, and for numerous fruitful discussions.

REFERENCES

- 1 O. Beeck, J.W. Otvos, D.P. Stevenson and C.D. Wagner, J. Chem. Phys., 16 (1948) 225.
- 2 P.E. Yankwich and M. Calvin, J. Chem. Phys., 17 (1949) 109.

- 3 J. Bigeleisen and L. Friedman, *J. Chem. Phys.*, 17 (1949) 998.
- 4 J.G. Lindsay, D.E. McElcheran and H.G. Thode, *J. Chem. Phys.*, 17 (1949) 589.
- 5 J. Bigeleisen, *J. Chem. Phys.*, 17 (1949) 675.
- 6 K.S. Pitzer, *J. Chem. Phys.*, 17 (1949) 1341.
- 7 L. Melander, *Ark. Kemi*, 2 (1950) 211.
- 8 J. Bigeleisen and M. Wolfsberg, *Adv. Chem. Phys.*, 1 (1958) 15.
- 9 M. Wolfsberg and M.J. Stern, *Pure Appl. Chem.*, 8 (1964) 225, 325 and subsequent papers.
- 10 J. Bigeleisen, *Science*, 110 (1949) 14.
- 11 T.T.S. Huang, W.J. Cass, W.E. Buddenbaum and P.E. Yankwich, *J. Phys. Chem.*, 72 (1968) 4431.
- 12 J.G. Lindsay, A.N. Bourns and H.G. Thode, *Can. J. Chem.*, 29 (1951) 192.
- 13 A.A. Bothner-By and J. Bigeleisen, *J. Chem. Phys.*, 19 (1951) 755.
- 14 J. Bigeleisen, *J. Chem. Phys.*, 17 (1949) 425.
- 15 A.G. Loudon, H. Maccoll and D. Smith, *J. Chem. Soc. Faraday Trans.*, (1973) 849.
- 16 T.C. Hoering, Carnegie Inst. Wash., Papers Geophys. Lab. No. 1361, (1960–61) 200, [*Chem. Abstr.*, 57 (1962) 3778].
- 17 F.H. Verhoek, *J. Am. Chem. Soc.*, 56 (1934) 571.
- 18 J. Bigeleisen and T.L. Allen, *J. Chem. Phys.*, 19 (1951) 760.
- 19 Lakshmi, N.V. Pillai, T. Sharma and U. Agarwala, *Inorg. Nucl. Chem. Lett.*, 7 (1971) 383.
- 20 B.R. Brown, D.L. Hammick and A.J.B. Scholefield, *J. Chem. Soc.*, (1950) 778.
- 21 G.E. Dunn, E.G. Janzen and W. Rodewald, *Can. J. Chem.*, 46 (1968) 2905.
- 22 A.N. Bourns, J. Buccini, G.E. Dunn and W. Rodewald, *Can. J. Chem.*, 46 (1968) 3915.
- 23 B.R. Brown, W.W. Elliott and D.L. Hammick, *J. Chem. Soc.*, (1951) 1384.
- 24 W.M. Schubert and J.D. Gardiner, *J. Am. Chem. Soc.*, 75 (1953) 1401.
- 25 A.V. Willi, *Trans. Faraday Soc.*, 55 (1959) 433.
- 26 A.V. Willi, *Z. Naturforsch., Teil A*, 13 (1958) 997.
- 27 A.N. Bourns, *Trans. Roy. Soc. Can., Sect. 4*, 2 (1964) 277.
- 28 K.R. Lynn and A.N. Bourns, *Chem. Ind. (London)*, (1963) 782.
- 29 L. McMaster and R.L. Shriner, *J. Am. Chem. Soc.*, 45 (1923) 751.
- 30 W.H. Stevens, J.M. Pepper and M. Lounsbury, *Can. J. Chem.*, 30 (1952) 529.
- 31 G.E. Dunn, P. Leggate and I.E. Scheffler, *Can. J. Chem.*, 43 (1965) 3080.
- 32 G.E. Dunn and J. Buccini, *Can. J. Chem.*, 46 (1968) 563.
- 33 G.E. Dunn and S.K. Dayal, *Can. J. Chem.*, 48 (1970) 3349.
- 34 M. Zielinski, *Rocz. Chem.*, 42 (1968) 1725.
- 35 W.M. Schubert, *J. Am. Chem. Soc.*, 71 (1949) 2639.
- 36 G.E. Dunn, G.K.J. Lee and H.F. Thimm, *Can. J. Chem.*, 50 (1972) 3017.
- 37 F.A. Long in A.K. Covington and P. Jones, *Hydrogen-bonded Solvent Systems*, Taylor and Francis, London, 1968, p. 293.
- 38 J.L. Longridge and F.A. Long, *J. Am. Chem. Soc.*, 90 (1968) 3092.
- 39 H.H. Huang and F.A. Long, *J. Am. Chem. Soc.*, 91 (1969) 2872.
- 40 G.E. Dunn and G.K.J. Lee, *Can. J. Chem.*, 49 (1971) 1032.
- 41 P. Dyson and D.L. Hammick, *J. Chem. Soc.*, (1934) 1724.
- 42 M.F.R. Ashworth, R.P. Daffern and D.L. Hammick, *J. Chem. Soc.*, (1939) 809.
- 43 I. Zlotowski and M. Zielinski, *Nukleonika*, 6 (1961) 511.
- 44 M. Zielinski, *Nukleonika*, 14 (1969) 29.
- 45 M. Zielinski, *J. Chem. Phys.*, 41 (1964) 3646.
- 46 M. Zielinski, *J. Chem. Phys.*, 47 (1967) 3868.
- 47 A. Fry and M. Calvin, *J. Phys. Chem.*, 56 (1952) 897.
- 48 G. Lapidus, D. Barton and P.E. Yankwich, *J. Phys. Chem.*, 70 (1966) 3135.
- 49 G. Lapidus, D. Barton and P.E. Yankwich, *J. Phys. Chem.*, 70 (1966) 1575.

- 50 G. Lapidus, D. Barton and P.E. Yankwich, *J. Phys. Chem.*, 70 (1966) 407.
- 51 P.E. Yankwich and W.E. Buddenbaum, *J. Phys. Chem.*, 71 (1967) 1185.
- 52 W.E. Buddenbaum, M.A. Haleem and P.E. Yankwich, *J. Phys. Chem.*, 71 (1967) 2929.
- 53 T.S. Huang, R.W. Kidd and P.E. Yankwich, *J. Chem. Phys.*, 62 (1975) 4757.
- 54 P.E. Yankwich and J.L. Copeland, *J. Am. Chem. Soc.*, 79 (1957) 2081.
- 55 P.E. Yankwich and P.D. Zavitsanos, *J. Phys. Chem.*, 68 (1964) 1275.
- 56 P.E. Yankwich and P.D. Zavitsanos, *Pure Appl. Chem.*, 8 (1964) 287.
- 57 M.J. Stern and M. Wolfsberg, *J. Chem. Phys.*, 39 (1963) 2776.
- 58 J.G. Lindsay, A.N. Bourns and H.G. Thode, *Can. J. Chem.*, 30 (1952) 163.
- 59 R.B. Bernstein, *J. Phys. Chem.*, 56 (1952) 893.
- 60 P.E. Yankwich and E.C. Stivers, *J. Chem. Phys.*, 21 (1953) 61.
- 61 M. Zielinski, *Nukleonika*, 10 (1965) 337.
- 62 P.E. Yankwich and A.L. Promislow, *J. Am. Chem. Soc.*, 76 (1954) 4684.
- 63 P.E. Yankwich, R.L. Belford and G. Fraenkel, *J. Am. Chem. Soc.*, 75 (1953) 832.
- 64 P.E. Yankwich and R.L. Belford, *J. Am. Chem. Soc.*, 75 (1953) 4178.
- 65 P.E. Yankwich and R.L. Belford, *J. Am. Chem. Soc.*, 76 (1954) 3067.
- 66 P.E. Yankwich and R.M. Ikeda, *J. Am. Chem. Soc.*, 81 (1959) 5054.
- 67 G.A. Hall, Jr., *J. Am. Chem. Soc.*, 71 (1949) 2691.
- 68 P.E. Yankwich and H.S. Weber, *J. Am. Chem. Soc.*, 77 (1955) 4513.
- 69 P.E. Yankwich and H.S. Weber, *J. Am. Chem. Soc.*, 78 (1956) 564.
- 70 W.E. Buddenbaum, W.G. Koch and P.E. Yankwich, *J. Phys. Chem.*, 70 (1966) 673.
- 71 R. Steinberger and F.H. Westheimer, *J. Am. Chem. Soc.*, 71 (1949) 4158, 73 (1951) 429.
- 72 E. Gelles and R.I. Reed, *Nature (London)*, 176 (1955) 1262.
- 73 A. Wood, *Trans. Faraday Soc.*, 60 (1964) 1263.
- 74 S. Seltzer, G.A. Hamilton and F.H. Westheimer, *J. Am. Chem. Soc.*, 81 (1959) 4018.
- 75 M.H. O'Leary, *J. Am. Chem. Soc.*, 91 (1969) 6886.
- 76 M.H. O'Leary, D.T. Richards and D.W. Hendrickson, *J. Am. Chem. Soc.*, 92 (1970) 4435.
- 77 M. Zielinski, *Rocz. Chem.*, 43 (1969) 1547.
- 78 E. Grovenstein and U.V. Henderson, *J. Am. Chem. Soc.*, 78 (1956) 569 and references cited therein.
- 79 E. Grovenstein and G.A. Ropp, *J. Am. Chem. Soc.*, 78 (1956) 2560.
- 80 J. Warkentin and D.M. Singleton, *Can. J. Chem.*, 45 (1967) 3035.
- 81 M.J. Goldstein and G.L. Thayer, *J. Am. Chem. Soc.*, 87 (1965) 1933.
- 82 R.G. Snyder and J.H. Schachtschneider, *Spectrochim. Acta*, 19 (1963) 85, 117.
- 83 P.E. Yankwich and R.W. Buddemeier, *J. Chem. Phys.*, 30 (1959) 861.
- 84 W.G. Leighton and G.S. Forbes, *J. Am. Chem. Soc.*, 52 (1930) 3139.
- 85 A. Hosaka, A. Sugimori and G. Tsuchihashi, *Bull. Chem. Soc. Jpn*, 40 (1967) 1803.
- 86 C.A. Bunton and D.R. Llewellyn, *Res. Appl. Ind.*, 5 (1952) 443.
- 87 S.J. Adler and R.M. Noyes, *J. Am. Chem. Soc.*, 77 (1955) 2036.
- 88 R.H. Betts and W.D. Buchannon, private communication.
- 89 C.G. Hatchard and C.A. Parker, *Proc. Roy Soc. London, Ser. A*, 235 (1956) 518.
- 90 G.B. Porter, J.G.W. Doering and S. Karanka, *J. Am. Chem. Soc.*, 84 (1962) 4027.

Chapter 2

CARBON-13 NMR METHODOLOGY AND MECHANISTIC APPLICATIONS

J. HINTON, M. OKA, and A. FRY

Department of Chemistry, University of Arkansas, Fayetteville, Ark. 72701 (U.S.A.)

I. INTRODUCTION

This chapter has been written to illustrate the uses of carbon-13 nuclear magnetic resonance spectroscopy in quantitative analysis and mechanistic investigations of organic reactions. The literature coverage is selective with no attempt being made to review critically all of the papers relevant to the subjects of interest. Although ^{13}C n.m.r. spectroscopy has proven to be an extraordinarily powerful tool for the elucidation of molecular structure, for the determination of the motional characteristics of molecules through T_1 measurements, and for the investigation of reaction dynamics, its use in mechanistic and quantitative studies has been rather limited thus far. With the advent and present availability of ^1H broadband decoupling and pulsed FT techniques, the use of ^{13}C n.m.r. spectroscopy in these areas is certain to increase. It is the authors' desire, therefore, that this chapter serve as a guide for the use of ^{13}C in such investigations and that it serves a heuristic purpose as well. The chapter is divided into three sections: experimental techniques, quantitative analysis and mechanistic studies. Obviously, there exists overlap between the last two sections; however, the authors have attempted to arrange the papers discussed for illustrative purposes. We apologize for any conflict between this arrangement and the intent of the original authors.

II. EXPERIMENTAL TECHNIQUES

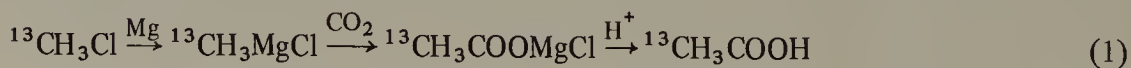
Since carbon-12, the most abundant isotope of carbon, has no nuclear spin, the use of carbon as an n.m.r. probe depends on the existence of an isotope that is n.m.r. "active", namely carbon-13. Carbon-13 has a nuclear spin of $1/2$, a natural abundance of 1.108%, and a relative sensitivity, compared to a proton, of 1.59×10^{-2} . The last two properties of the ^{13}C nucleus served as both a blessing and a curse in the early development of n.m.r. spectroscopy. The low natural abundance drastically reduced the possible multiplicity in the ^1H spectra, making the detection and analysis of those spectra less difficult. The combined effect of these two properties reduces the overall sensitivity to detection of a ^{13}C nucleus compared to a ^1H nucleus by a factor of 5700. Consequently, the development of ^{13}C -n.m.r. spectroscopy lagged far behind that of the more sensitive nuclei (i.e. ^1H , ^{19}F , ^{31}P) until the advent of pulsed-FT and ^1H broadband decoupling techniques. Since that time ^{13}C -n.m.r. spectroscopy has undergone a phenomenal growth.

References pp. 99–104

There are two n.m.r. methods that may be employed to monitor the presence of a ^{13}C nucleus in a molecule: (i) direct observation of the ^{13}C nucleus using CW or FT techniques; and (ii) indirect observation using ^{13}C satellite analysis of the ^1H spectra. Both of these methods will be discussed briefly with respect to their application to mechanistic studies and quantitative analysis.

Since the ^{13}C nucleus has a spin quantum number of $1/2$, protons adjacent or bonded to this nucleus will experience the effect of the two spin states of the carbon nucleus when placed in a magnetic field. The proton resonance signal will be split into a doublet because of the ^1H – ^{13}C spin–spin coupling. This coupling is not usually observed in ^1H -n.m.r. spectra because only 1.108% of the carbons are the ^{13}C isotope. If, however, the proton spectra are not too complex and if the spectra are recorded at high amplitude, it is possible to observe the protons bonded (H – ^{13}C) or adjacent (H – C – ^{13}C) to ^{13}C nuclei. Their doublets, called satellite spectra, will be 1.108% as intense as the (H – ^{12}C) proton peak, and almost symmetrically positioned about it. The doublet actually will be shifted slightly to high-field because of the carbon isotope effect on the proton resonance position.

The appearance of ^{13}C satellites at the natural abundance level can be illustrated in the spectra of acetic acid shown in Fig. 1. Figure 1(A) shows the normal ^1H spectrum of acetic acid and the higher amplitude spectrum of the methyl group ^{13}C satellite doublet, $J(^{13}\text{C}$ – $\text{H}) = 127$ Hz. The satellite doublet $J(^{13}\text{C}$ – C – $\text{H}) = 7.3$ Hz corresponding to the two bond coupling (H – C – ^{13}C) between the carbonyl carbon and the methyl protons is shown in Fig. 1(B). One must take the precaution of distinguishing the satellite spectra from the spinning side bands which are also very pronounced at high amplitudes. Although the spinning side bands and the satellites have the same appearance (i.e. multiplet patterns) they are distinguishable in two ways: (i) the spinning side bands are *symmetrically* positioned about the (^1H – ^{12}C) signal; (ii) their position is a function of the sample tube spinning rate. The complexity of a proton spectrum or the fortuitous overlap of the position of a satellite peak with some other resonance peak frequently prevents the distinct observation of both portions of the satellite spectrum, as shown in Fig. 2. Here, the low-field portion of the ^{13}C satellite spectrum is obscured by accidental overlap with the peak from the methyl group attached to the carbonyl carbon and the hydrogen on the central carbon of the isopropyl group. In quantitative analysis, however, this unobserved portion obviously must be taken into account. If there is a large number of different types of proton in a molecule and the spin–spin coupling among the protons is extensive, it may be impossible to use satellite analysis satisfactorily. In general, satellite analysis is most usefully employed in quantitative and mechanistic investigations for systems that are enriched in ^{13}C . The effect of ^{13}C enrichment on satellite spectra can be illustrated with acetic acid. Consider the preparation of acetic acid by the use of a Grignard reagent with the ^{13}C enrichment coming from different sources



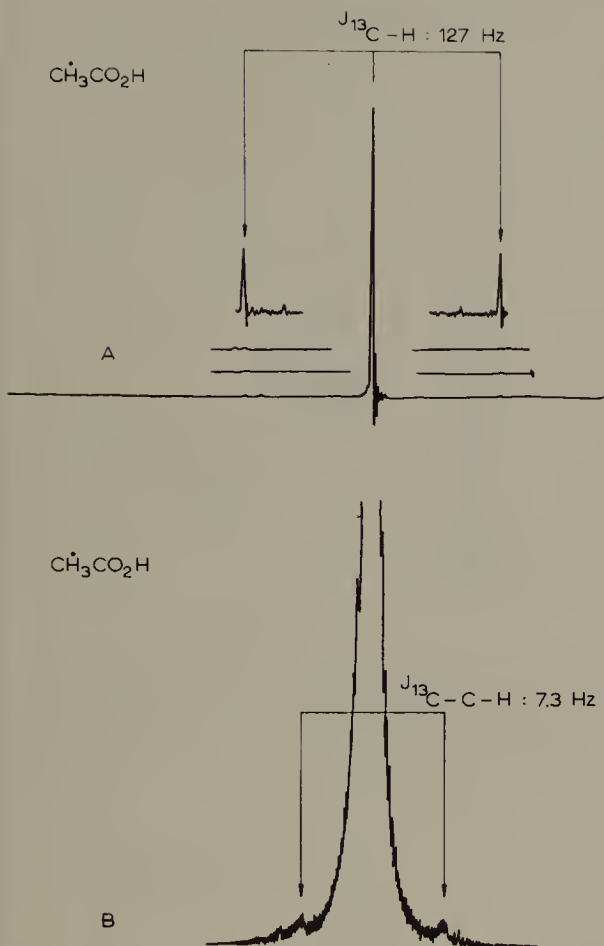
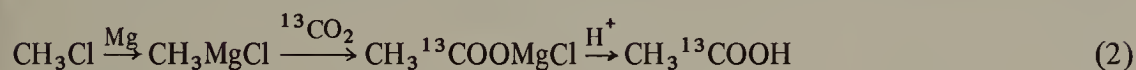


Fig. 1. (A) ^1H -n.m.r. spectrum of the methyl group protons showing one bond C-H coupling in the ^{13}C satellite doublet. (B) ^1H -n.m.r. spectrum of the methyl group protons showing two bond C-H coupling in the ^{13}C satellite doublet.



The ^1H -n.m.r. spectra of approximately 90% ^{13}C -enriched acetic acid ^a prepared in reactions (1) and (2) are shown in Figs. 3(B) and 3(C), respectively. Here for the 90% enriched material, it is seen that the "satellite" peaks have become the main peaks. When acetic acid is prepared from CH_3Cl and CO_2 which are *both* approximately 90% ^{13}C -enriched, reaction (3), the proton spectrum of the doubly-labeled acetic acid is that shown in Fig. 3(D). The satellite spectra not only provide the unequivocal assignments



^a We are grateful to Dr. T.W. Whaley of the Los Alamos Laboratory for providing the labeled acetic acid.

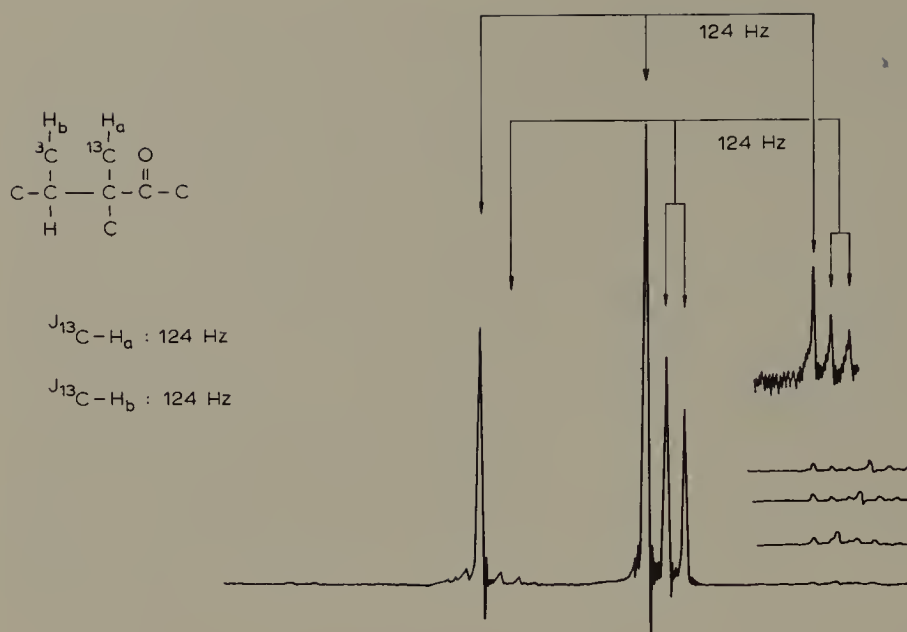


Fig. 2. ^1H -n.m.r. spectrum of 3,3,4-trimethyl-2-pentanone showing the masking of the low-field portion of the ^{13}C satellite doublet.



Fig. 3 (A) Natural abundance ^1H -n.m.r. spectrum of the methyl group protons of acetic acid. (B) ^1H -n.m.r. spectrum of the methyl group protons of acetic acid with the methyl carbon enriched to 90% with ^{13}C . (C) ^1H -n.m.r. spectrum of the methyl group protons of acetic acid with the carboxyl carbon enriched to 90% with ^{13}C . (D) ^1H -n.m.r. spectrum of the methyl group protons of acetic acid with 90% ^{13}C enrichment at both carbons.

of the positions of enrichment, but also the integrated intensities of the ^{13}C satellites and the ^1H – ^{12}C proton peaks give the percent enrichment at each position. It is these two features of satellite spectra that make quantitative analysis and mechanistic studies possible. The high percent enrichment used to obtain the satellite spectra of acetic acid shown here was for illustrative purposes and should not be viewed as the level of enrichment necessary for quantitative analysis or mechanistic investigations. In general, 10% or less enrichment is sufficient to obtain satisfactory data.

The use of satellite analysis for non-quantitative mechanistic investigations requires the identification of the satellite peaks of interest for the reactants and/or products with and without enrichment. The increase in the peak height or area of a satellite group then provides information about the position of enrichment and from this mechanistic inferences can be drawn. If, however, one wants to determine quantitatively the extent of reaction from the amount of ^{13}C enrichment at a given position in a reaction product, the satellite peak areas or heights must be accurately measured. The accurate measurement of ^1H -n.m.r. peak heights or areas has been thoroughly discussed in the literature [1–10]; therefore, only a brief discussion will be given here with emphasis placed on potential difficulties.

The reason ^1H -n.m.r. peaks can be used to make quantitative measurements is that the observed signal is directly proportional to the number of nuclei per unit volume, N , producing the signal. It can be shown [10] that under optimum conditions, the peak voltage of the adsorptions signal is

$$V \propto N \left(\frac{I+1}{I} \right) \left(\frac{\mu}{T} \right)^2 \omega_0 H_0 \left(\frac{T_2}{T_1} \right)^{1/2} \quad (4)$$

where I is the spin quantum number, μ the magnetic moment, ω_0 the resonance frequency, H_0 the applied magnetic field, T_2 the transverse relaxation time and T_1 the longitudinal relaxation time. For a given experiment at constant temperature, assuming $T_1 = T_2$, the signal strength or peak intensity at a given frequency is proportional to

$$N(I+1)\mu\omega_0^2 \quad (5)$$

or for a given field strength

$$\frac{N(I+1)\mu^3 H_0^2}{I^2} \quad (6)$$

Since one can use either peak height or area in mechanistic investigations or quantitative analyses, it is important to be aware of how the intensity measured by the area under an n.m.r. peak compares to that obtained from a peak height. The area of a peak is

$$A \propto \frac{X_0 H_1}{(1 + \gamma^2 H_1^2 T_1 T_2)^{1/2}} \quad (7)$$

and the corresponding peak height is

$$P.H. \propto \frac{X_0 H_1 T_2}{1 + \gamma^2 H_1^2 T_1 T_2} \quad (8)$$

where H_1 is the r.f. field, X_0 the magnetic susceptibility of the sample and γ is the magnetogyric ratio. A comparison of the equations for peak area and height shows that at low (H_1) r.f. power the area of the signal does not depend on T_2 but the peak height is proportional to T_2 . The peak height equation also indicates that at low H_1 , peak height comparisons are valid only for identical T_2 values. If one is observing weak signals, as is often the case with satellite spectra, H_1 is usually increased to obtain a more intense signal. Under this condition it is important to use peak area instead of peak height because the area depends less critically on H_1 . In fact, increasing H_1 tends to make the area become constant while the peak height diminishes to zero. Under high power conditions, the peak area is an accurate measurement of relative intensity only if the $T_1 T_2$ product is the same for all peaks. It is also advisable to keep the viscosity of the sample low so that T_1/T_2 approaches unity.

The areas of peaks can be determined in several ways. They can be determined with a planimeter or by cutting out the peaks and weighing them, which method requires replication to achieve satisfactory precision. With care, a precision of about $\pm 5\%$ can usually be obtained. The measurement of peak areas can be more accurately accomplished with electronic integration. Alexander and Koch [6] have concluded that the integration is within 1% of the theoretical value if 3–4 mequiv of protons are available (i.e., about 60 mg for a compound of molecular weight 200 with 10 protons per molecule).

Although satellite analysis takes advantage of the higher sensitivity of ^1H relative to ^{13}C and the fact that an ^1H -n.m.r. spectrometer might be more readily available than one designed for ^{13}C , the direct observation of ^{13}C used as a tracer has some distinct advantages over satellite analysis. Carbon-13 spectra are normally obtained under ^1H broadband decoupled conditions; therefore, each nonequivalent carbon appears as a single resonance peak. Since the chemical shift range of ^{13}C is much greater than that of ^1H , the problem of overlapping signals is seldom encountered; consequently, reaction mechanisms may be studied without the laborious task of separation and degradation common to ^{14}C tracer work. Also ^{13}C enrichment is not required in some instances, the natural abundance level being sufficient.

The use of direct ^{13}C observation for quantitative analysis is not as straight-forward as with ^1H observation because ^{13}C peak intensities often do not correlate directly with the number of carbon nuclei producing the peaks. An example of this can be seen in the ^{13}C -proton decoupled spectrum of 1,2-dibromopropane (Fig. 4). Each peak in this spectrum is generated by a single ^{13}C nucleus, yet the signal intensities are not the same. The failure of the peak intensities to correlate directly with the number of nuclei results from variable nuclear Overhauser signal enhancements (NOE) and different spin-lattice relaxation times, T_1 .

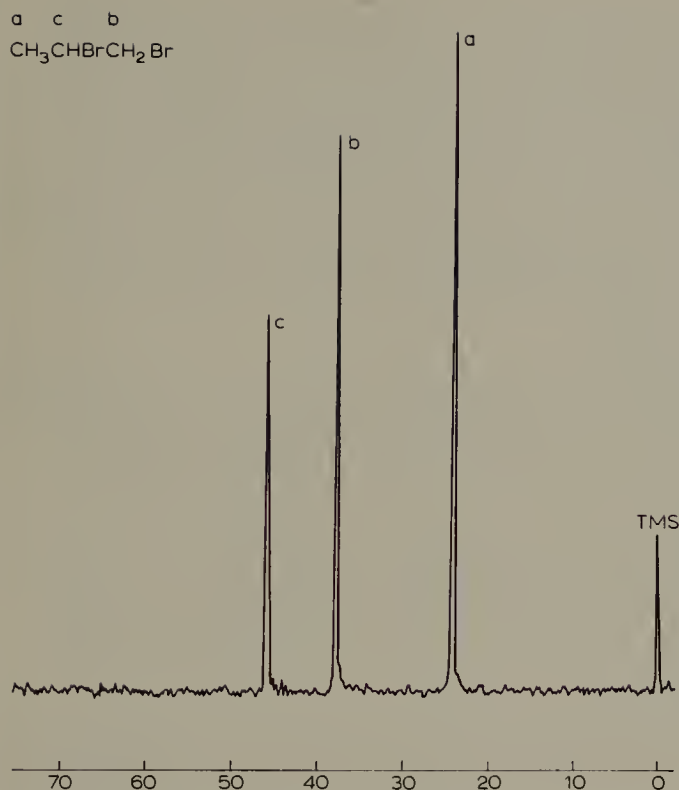


Fig. 4. Proton decoupled ^{13}C -n.m.r. spectrum of 1,2-dibromopropane.

In the normal ^{13}C pulsed FT experiment, the delay time between pulses is of the order of a second. Carbon-13 nuclei with long T_1 values will remain partially saturated, resulting in lower observed peak intensities relative to those nuclei with shorter T_1 values. Since the Boltzmann distribution of spin states is restored to 99% of its thermal equilibrium value after five T_1 times, the problem of partial saturation may be overcome by employing a “wait” time between pulses of at least five times the longest T_1 value in the molecular system.

The NOE observed in ^1H decoupled spectra depends on the nature and the environment of the individual carbon nuclei; consequently, the enhancement may not be the same for each of the nuclei. For compounds of molecular weight 100–200 it has been shown that the NOE is usually complete for all protonated carbons [11,12]; in larger rigid molecules the non-protonated carbons often show the complete NOE [13]. It has been shown experimentally and theoretically that paramagnetic species when added to a solution can suppress the NOE so that quantitative measurements can be made accurately [14–17]. This technique is particularly useful for making quantitative measurements on low molecular weight compounds. Shoolery and Jankowski [18] have used simultaneously gated decoupling [19] and the addition of paramagnetic reagents to improve the precision of quantitation.

Levy and Edlund [20], however, have shown that with medium and large size organic molecules (molecular weight > 200) NOE suppression can be incomplete and variable because efficient ^{13}C — ^1H dipole—dipole relaxation is able to successfully compete with electron—nuclear relaxation from the paramagnetic relaxation agent. In order to obtain quantitative results it is necessary to have an estimate of the spin—lattice times for the sample to determine how much paramagnetic relaxation reagent is needed to quench the NOE. In those cases where the dipole—dipole interaction is sufficiently efficient it will be impossible to suppress effectively the NOE's with relaxation reagent without producing very significant line broadening.

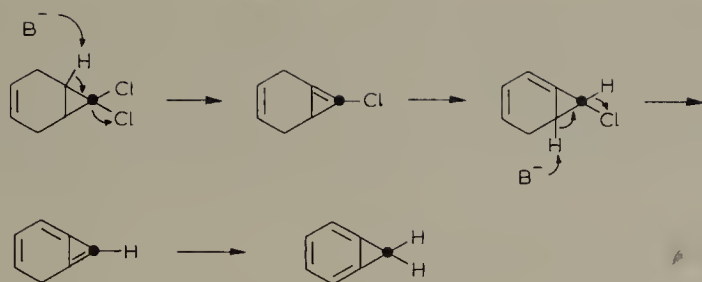
Levy and Edlund [21] have also shown recently that quantitative ^{13}C investigations performed at high or moderately high magnetic field strengths may be less accurate than expected because of variable NOE's for nonprotonated carbons that can have anisotropic tensors.

Even though one eliminates the T_1 and NOE problems, Levy and Nelson [22] point out that there are two possible instrumental contributions to error in peak area measurements that should be considered: the pulse amplifier must be powerful enough to produce a uniform excitation over the complete spectral width, and problems might arise from limited computer storage.

For many years tremendous effort has gone into bringing ^{13}C -n.m.r. spectroscopy to the point that today it is relatively easy to obtain natural abundance ^{13}C spectra. There is now developing an interesting and, in the light of the aforementioned effort, amusing twist to the use of ^{13}C -n.m.r. spectroscopy in mechanistic studies. Instead of using a ^{13}C -enriched precursor and identifying the enhanced resonance line or lines as is normally done, it has been proposed that ^{12}C -labeled (^{13}C -depleted) precursors be used with the subsequent identification of a line that has *disappeared* [23]. An excellent illustration of this technique is that of the elucidation of the mechanism of the formation of benzocyclopropene [24]. Two mechanisms have been proposed for the formation of benzocyclopropene on basic dehydrochlorination of 7,7-dichlorobicyclo[4.1.0]hept-3-ene. Since only route B involves skeletal rearrangement, ^{12}C labeling should provide a means of determining which mechanism is correct. The $[7\text{-}^{12}\text{C}]$ compound was prepared from $^{12}\text{CDCl}_3$ and subjected to dehydrohalogenation. The natural abundance ^{13}C -n.m.r. spectrum (A) of the benzocyclopropene product, together with that (B) from the ^{12}C -labeled product are shown in Fig. 5. From a comparison of the spectra, mechanism B involving skeletal rearrangement obviously may be ruled out.

The advantages of ^{12}C over ^{13}C labeling are the lack of complication due to ^{13}C — ^{13}C coupling as found with highly enriched ^{13}C material and the potential hazard to man of elevated ^{13}C concentrations in metabolic studies. A recent study, however, of substantial replacement of the body carbon with ^{13}C in mice indicated that the subjects maintained normal health throughout the experiments, and examination of tissues revealed no abnormalities [25]. Another advantage would seem to be the reduced cost of ^{12}C enriched material compared to that for material enriched in ^{13}C . Simpson [26] points out, however, that this cost advantage might not always be valid. In a mechanis-

Route A



Route B

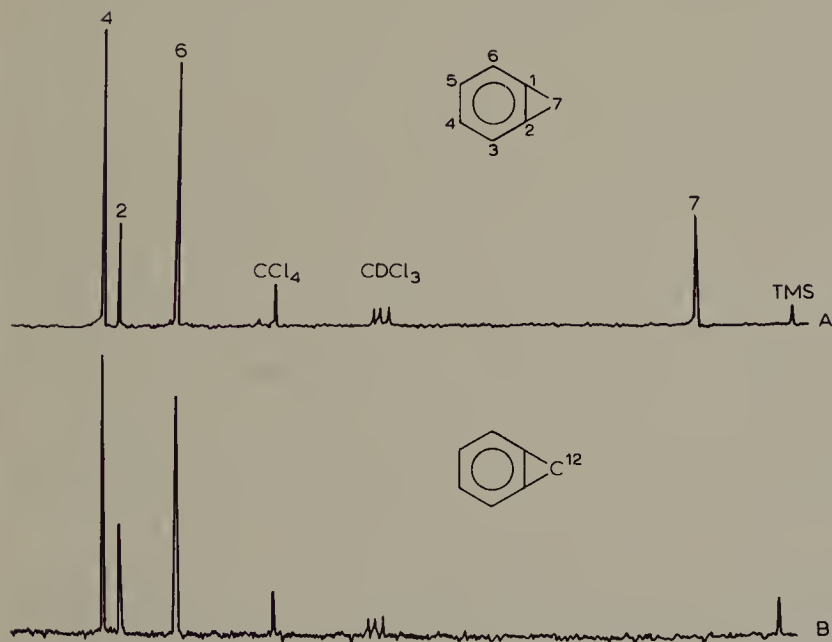
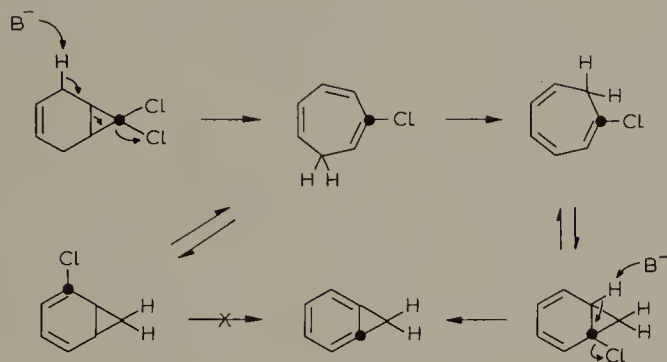


Fig. 5. (A) Natural abundance ^{13}C -n.m.r. proton decoupled spectrum of benzocyclopropene [24].
 (B) ^{13}C -n.m.r. proton decoupled spectrum of the ^{12}C -labeled benzocyclopropene [24].

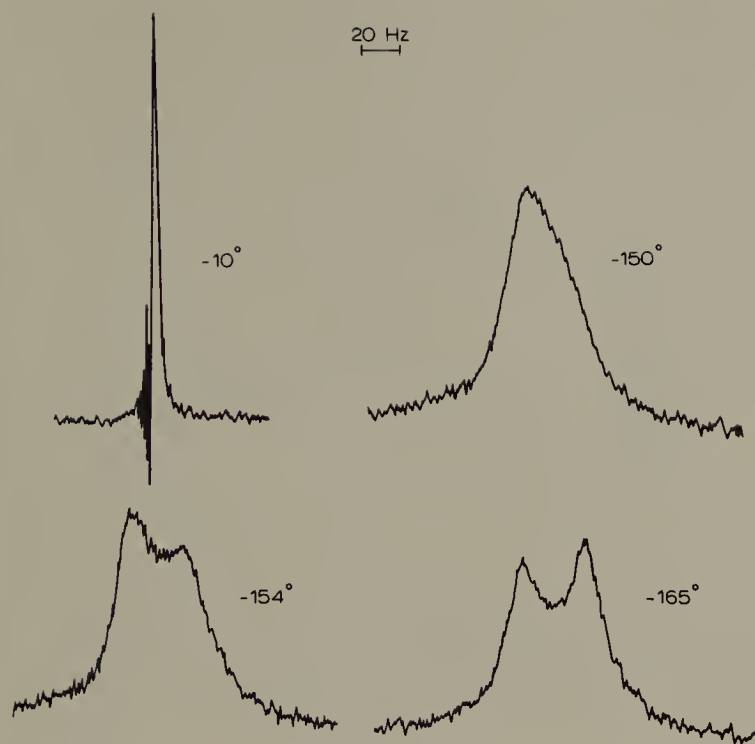
tic investigation, a precursor with effectively 100% ^{12}C at the requisite position is required to obtain a significant result using the ^{12}C labeling technique. However, to achieve the equivalent result with ^{13}C labeling (i.e. 100% enhancement of a signal as opposed to 100% elimination) only 1.1% ^{13}C above natural abundance is required. The cost, therefore, of 2.2% ^{13}C material might compare favorably with 100% ^{12}C material.

III. QUANTITATIVE CARBON-13-NMR APPLICATIONS

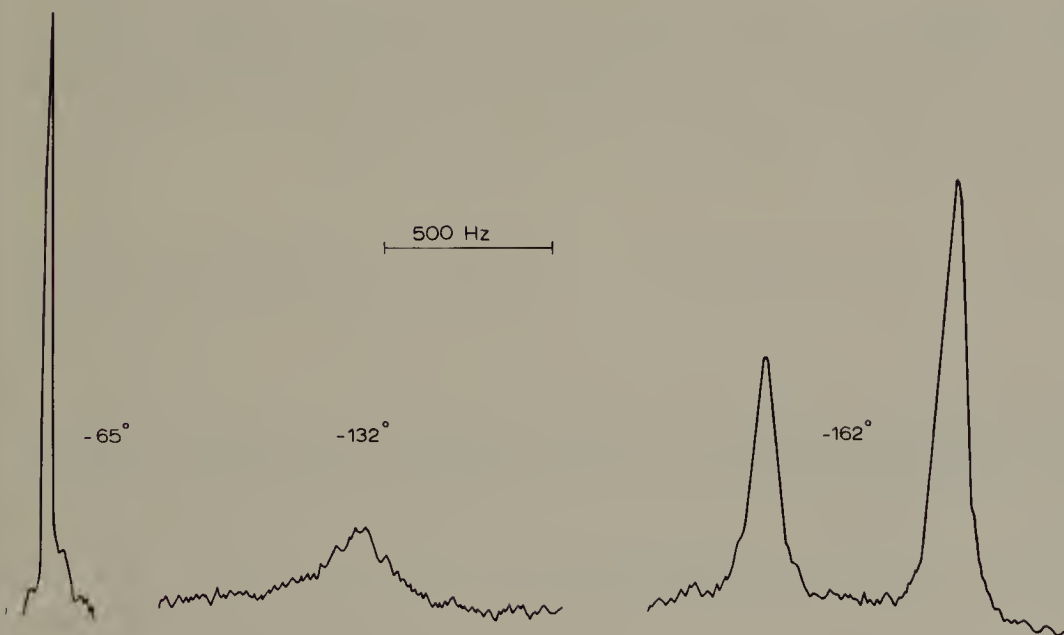
Carbon-13 n.m.r. spectroscopic techniques have been applied to a wide variety of problems in which quantitative information (i.e. thermodynamic parameters, rate constants, equilibrium constants and isomer ratios) was sought. The very large chemical shift range of ^{13}C , 600 p.p.m., compared to that of ^1H , 20 p.p.m., and the marked dependence of ^{13}C chemical shifts on molecular geometry makes ^{13}C -n.m.r. spectroscopy an extremely useful tool for the quantitative determination of subtle changes and differences in molecules in a stable condition or undergoing dynamic change. In dynamic studies ^{13}C -n.m.r. has several advantages over ^1H -n.m.r. in that the chemical shift differences between signals associated with the exchanging sites are much larger, in general, and the spectra are usually less complicated since one normally decouples protons and observes carbon singlets only.

The advantages of ^{13}C -n.m.r. spectroscopy over that of proton-n.m.r. spectroscopy can be illustrated by the work of Anet and Wagner [27] on the conformation of cyclo-nonane. A comparison of the proton spectrum at 251 MHz with that of the ^{13}C -n.m.r. spectrum at 63.1 MHz as a function of temperature dramatically shows the resolving power of ^{13}C -n.m.r. (Fig. 6(A) — ^1H -n.m.r. and 6(B) — ^{13}C -n.m.r.). The two ^{13}C resonance peaks at -162° are separated by 9 p.p.m. with an intensity ratio of 2 : 1. An analysis of the spectra gave a value for the free energy barrier of about 6 kcal mol^{-1} for the conformational process being observed. Another example of the resolving power of ^{13}C -n.m.r. spectroscopy is shown in Fig. 7 where the axial conformer of methylcyclohexane can be directly observed [28]. The direct observation of both axial and equatorial forms made possible the determination of the equilibrium constant $K_{e/a} \approx 100$ for this system at -100° . At low temperatures where the rate of conformational inversion is slow on the n.m.r. time scale, resonance signals characteristic of each conformer may be observed and their relative intensities provide a direct measure of the equilibrium constant. This low temperature technique was also used to study the conformational equilibria of cyclohexylmercury(II) derivatives [29]. At -90° , peak height measurements of the ^{13}C signals of both the axial and equatorial forms of cyclohexylmercury(II) acetate gave an equilibrium constant, $K_{a/e} = 2.3$. The n.m.r. results revealed that such mercury compounds exist preferentially in the axial forms.

Chadwick et al. [30] have used low temperature ^{13}C -n.m.r. to study the rotational isomerism of furan-, thiophen-, and *N*-methylpyrrole-2-carbaldehydes, 2-acetylfuran, furan-2-carbonyl chloride, and *tert*-butyl furan-2-carboxylate. Below -60° , furan-2-carbaldehyde (*I*), in $\text{CH}_2\text{Cl}_2/\text{CD}_2\text{Cl}_2$, shows two C-3 resonances (separation of 9 p.p.m.)



A



B

Fig. 6. (A) The 251-MHz ^1H -n.m.r. spectra of a 1.5% solution of cyclononane in a 2 : 1 mixture of CHCl_2 and CHF_2Cl at various temperatures [27]. (B) The 63.1 MHz ^{13}C FT-n.m.r. spectra of a 4% solution of cyclononane in a 3 : 1 mixture of CHCl_2 and $\text{CH}_2=\text{CHCl}$ at various temperatures [27].

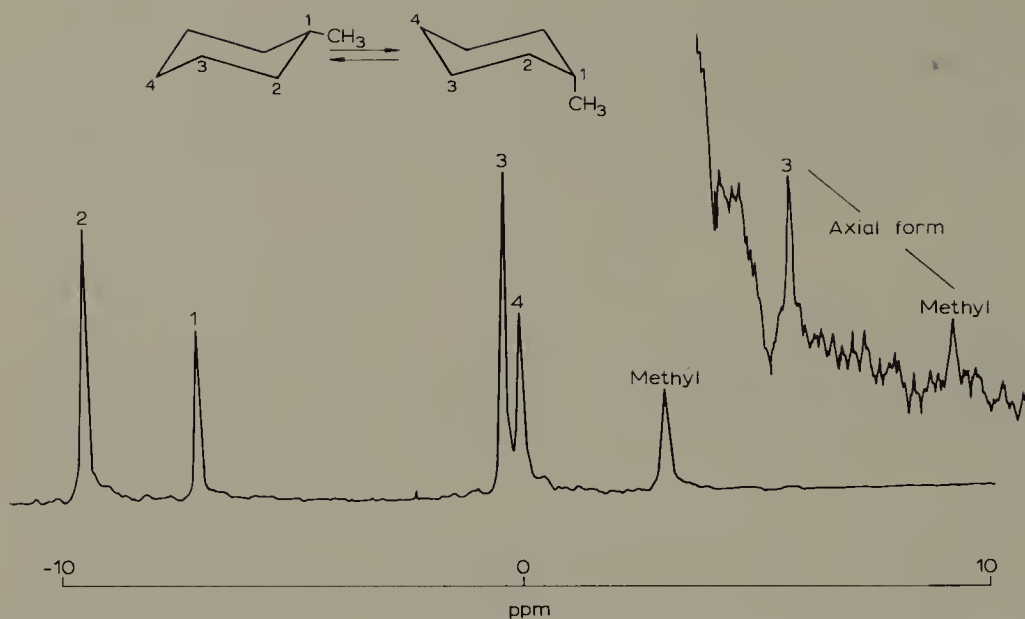
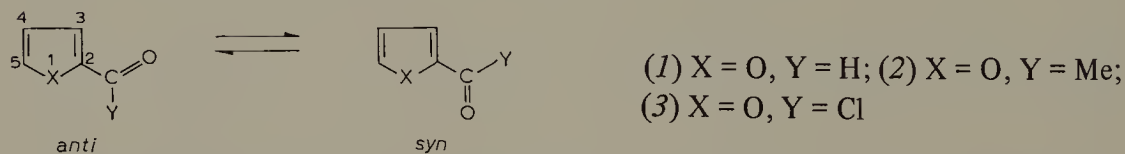
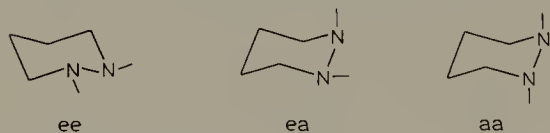


Fig. 7. 63.1-MHz ^{13}C -n.m.r. spectrum of neat methylcyclohexane at -110° . The spectrum represents 96 scans on a Varian CAT [28].

and two $\text{C}=\text{O}$ resonances (separation of 3 p.p.m.). Using a CDCl_3 solution of $\text{Cr}(\text{acac})_3$ to minimize differences in relative Overhauser enhancements, an equilibrium constant, $K_{\text{syn/anti}} = 5$, was obtained. In a similar manner furan ketone (2) and acid chloride (3) showed separate signals for the *syn* and *anti* forms at -80° from which equilibrium constants of $K_{\text{syn/anti}}$ (2) = 3.5 and $K_{\text{syn/anti}}$ (3) = 10 were obtained.



Variable temperature ^{13}C -n.m.r. was used to investigate the conformational populations of 1,2-dimethylhexahydropyridazine [31]. At ambient temperature the ^{13}C -n.m.r.



spectrum contains three sharp lines indicating rapid conformational interconversion. At -53° , six lines are observed: a set of three lines (set A) which remain sharp as the temperature is lowered and a second set of three lines (set B). The lines of set B sharpen until about -85° ; however, subsequent lowering of the temperature produces broadening and at -100° they disappear. As the temperature is lowered a new set of five lines

(set C) appears. Using chemical shift arguments, set A was assigned to the ee conformer. At -53° , ee is interconverting slowly enough with the other conformation to permit resolution of the interconverting conformers ae, aa and ea as set B signals. At the lowest temperature, the five lines of set C are attributed to the freezing out of the ea (= ae) conformation with no evidence being obtained for the presence of aa. By comparison of the areas of set A and set B peaks in the -53 to -68° region, estimates between 60 and 70% ee were obtained, with an apparent increase as the temperature is lowered.

The ability to observe directly individual conformers in an interconverting system at low temperatures can obviously provide very important quantitative information. It is, however, not always possible to work at the slow exchange limit; or one might be interested in determining the thermodynamic parameters for the conformational inversion process, in which case spectra must be analyzed as a function of temperature. At the high temperature or fast exchange limit, the rate of interconversion is much greater than the chemical shift difference between resonance signals corresponding to the individual conformers. Consequently, the exchanging carbons produce a single signal whose position depends upon the relative populations at the different environments. A rigorous discussion of line shape analysis in the intermediate exchange range is beyond the scope of this chapter; however, detailed discussions are in the literature [32–34]. The concepts involved in this type of analysis can be demonstrated with the following example.

Consider the exchange of a nucleus between sites A and B. The residence times at each site are designated τ_A and τ_B and the rates of transfer from each site are given by first-order rate constants which are the reciprocals of these quantities



If the fractional populations of the A and B sites are P_A and P_B , respectively, then

$$\frac{\tau_A}{\tau_B} = \frac{P_A}{P_B} = \frac{k_B}{k_A} \quad (10)$$

where k_A is the first-order rate constant for the conversion of site A to site B and k_B corresponds to the process of conversion from B to A. If it is assumed that there is an equal probability of the nucleus being in the two sites and that spin–spin relaxation can be neglected at each site, the line shape can be expressed in convenient form over the entire range of rates, from two separated peaks, through coalescence into a broadened resonance and collapse to a narrow singlet. The V-mode signal line shape is described by the equation

$$V = -\frac{M_0}{4} \frac{\gamma H_1 \tau (\nu_A - \nu_B)^2}{[\frac{1}{2}(\nu_A - \nu_B) - \nu]^2 + 4\pi^2 \tau^2 (\nu_A - \nu)^2 (\nu_B - \nu)^2} \quad (11)$$

It is apparent that the line shape depends on $\tau(\nu_A - \nu_B)$ where ν_A and ν_B are the reso-

nance frequencies corresponding to site A and B, respectively. Under these conditions

$$\frac{1}{\tau} = k = \frac{2}{\tau_A} = \frac{2}{\tau_B} = 2 k_A = 2 k_B \quad (12)$$

where k is the rate constant for the reaction in both directions. When eqn. (11) is plotted for a series of values of the quantity $\tau(\nu_A - \nu_B)$ a spectral series is generated where two peaks are observed for large values of $\tau(\nu_A - \nu_B)$ and a single line appears for small values of this quantity. When $\tau(\nu_A - \nu_B) = 1/(\pi\sqrt{2})$ the peaks coalesce to produce a flat-topped resonance signal. A comparison of actual spectra as a function of temperature with the theoretical spectra generated for various $\tau(\nu_A - \nu_B)$ values enables one to determine τ and hence k as a function of temperature. An Arrhenius type plot then gives the activation parameters for the process.

The first line-shape kinetic analysis with ^{13}C -n.m.r. was that of Gansow et al. [35] on the hindered internal rotation of *N,N*-dimethyltrichloroacetamide. Actual and computer simulated ^{13}C -n.m.r. spectra at several temperatures are shown in Fig. 8. The τ values were obtained from the computer simulated signal shape analysis. An Arrhenius plot of

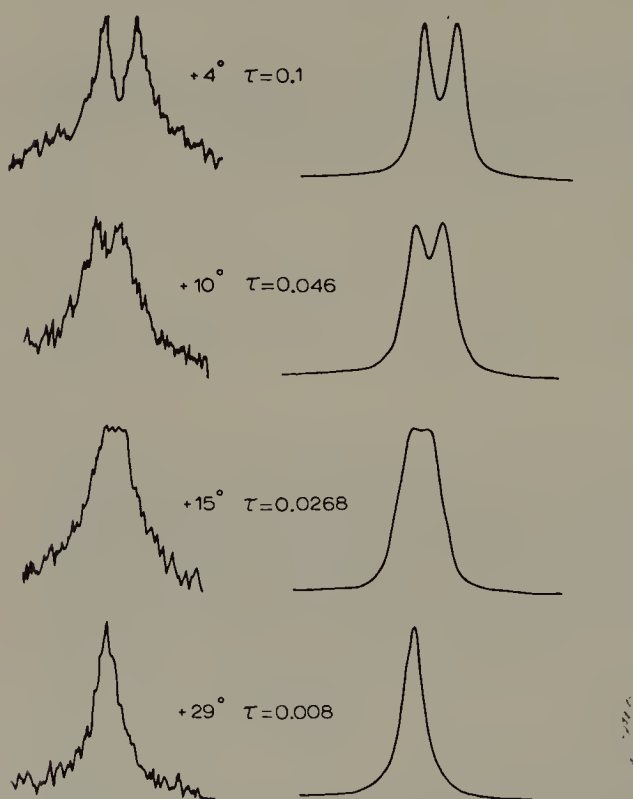
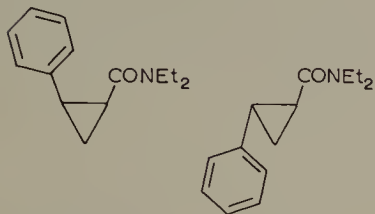


Fig. 8. Actual and computer simulated ^{13}C -n.m.r. spectra of *N,N*-dimethyltrichloroacetamide at various temperatures [35].

the data gave an activation energy, $E_a = 16.6 \text{ kcal mol}^{-1}$. At the coalescence temperature (15°), the free energy of activation was calculated to be $17.6 \text{ kcal mol}^{-1}$.

The barriers to internal rotation for the *cis*- and *trans*-isomers of 2-phenylcyclopropanecarboxylic acid *N,N*-diethylamides have been determined from ^{13}C -n.m.r. spectra line shape analysis [36]. From the temperature dependence of the alkyl carbon reso-



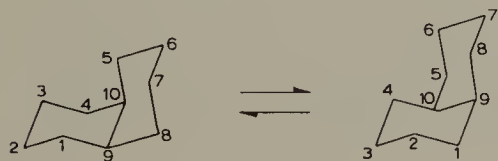
nance signals the free energy of activation or barrier energy was determined for both the *cis*- and *trans*-isomers. For the *cis*-isomer, $(\nu_A - \nu_B)_{\text{CH}_2} = 39.2 \text{ Hz}$, $(\nu_A - \nu_B)_{\text{CH}_3} = 43.6 \text{ Hz}$, $\Delta G_{25^\circ}^\ddagger = 17.6 \text{ kcal mol}^{-1}$ and for the *trans*-isomer, $(\nu_A - \nu_B)_{\text{CH}_2} = 27.3 \text{ Hz}$, $(\nu_A - \nu_B)_{\text{CH}_3} = 39.2 \text{ Hz}$, $\Delta G_{25^\circ}^\ddagger = 16.9 \text{ kcal mol}^{-1}$.

The barrier for rotation about the C–N nitroso bond in *p*-nitroso-*N,N*-dimethylaniline has also been determined with ^{13}C -n.m.r. spectroscopy using the *meta* carbon resonance signal for which $(\nu_A - \nu_B) = 79.7 \text{ Hz}$ at 25.2 MHz [36]. A value of $\Delta G_{25^\circ}^\ddagger = 13.3 \text{ kcal mol}^{-1}$ was obtained for this system.

The rotational barrier of benzaldehyde has been determined from line shape analysis of the temperature dependent ^{13}C -n.m.r. spectra of the aromatic carbons [37]. The aromatic carbon spectra are shown in Fig. 9. At -134° the *ortho* and *meta* carbons are not equivalent. At -124° the signals of the *meta* carbons coalesce whereas those of the *ortho* carbons broaden; at -109° the lines of the *ortho* carbons are so broad that they are barely detectable and they become fully equivalent at -60° . Line shape analysis gives the thermodynamic parameters, $E_a = 8.6 \text{ kcal mol}^{-1}$, $\Delta H^\ddagger = 8.3 \text{ kcal mol}^{-1}$ and $\Delta S^\ddagger = 3.6 \text{ e.u.}$

The temperature dependence of ^{13}C -n.m.r. spectroscopy resonance signals has been used to determine the activation parameters for conformational inversion of a number of alicyclic systems [38–41] as shown in Table 1.

There are a number of other similar investigations for monosubstituted cyclooctanones [42], 5-oxocanone [43], cyclodecane [44], cyclododecane [44], cyclotetradecane [44] and a [10]-annulene [45]. In general the temperature dependent spectra of these systems are a little more complex than the ones discussed previously. *Cis*-decalin for example, exists as a 1 : 1 mixture at room temperature, exhibiting only three ^{13}C resonance signals [38]. At -29° five signals appear with one much narrower than the rest.



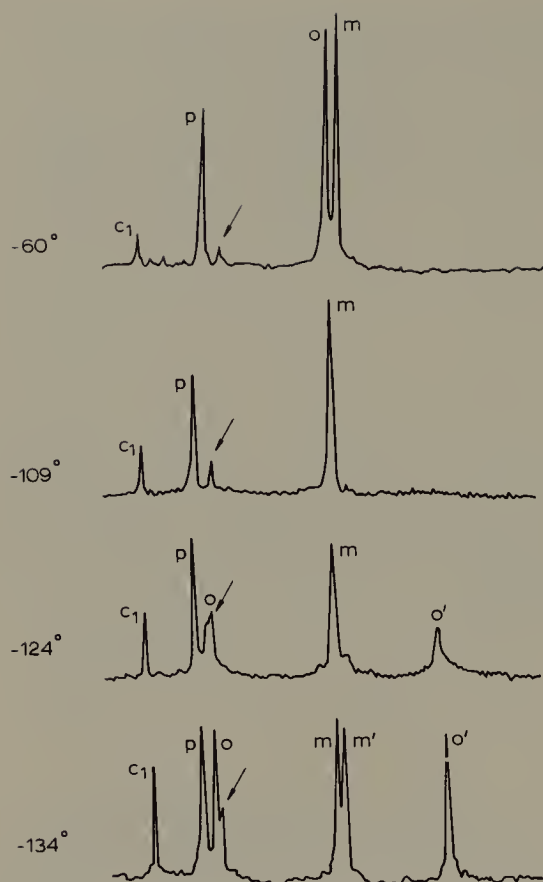


Fig. 9. The ^{13}C -n.m.r. spectra of benzaldehyde at various temperatures. The arrow denotes an impurity [37].

TABLE 1

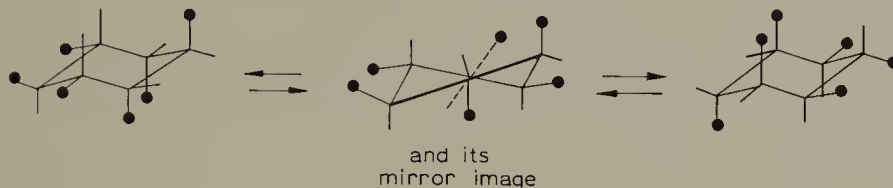
ACTIVATION PARAMETERS FOR CONFORMATIONAL INVERSIONS OF ALICYCLIC SYSTEMS

Compound ^a	ΔG^\ddagger (kcal mol ⁻¹)	ΔH^\ddagger (kcal mol ⁻¹)	ΔS^\ddagger (eu)
<i>cis</i> -Decalin [38]	12.6 (298 K)	13.6	3.5
<i>cis</i> -9-Methyldecalin [38]	12.6 (298 K)	12.4	-0.7
γ -Benzene hexachloride [41]	11.9 (298 K)	9.9	-7.7
1,1,3,3-Tetramethylcyclohexane [40]	9.0	6.4	-13.2
<i>trans</i> -1,3-Dimethylcyclohexane [38]	9.8 (298 K)	11.1	4.5
<i>cis</i> -1,4-Dimethylcyclohexane [38]	9.8 (298 K)	11.0	4.1
2,2,6,6-Tetramethyl-1,1-difluorocyclohexane [40]		9.8	-1.0
3,3,5,5-Tetramethyl-1,1-difluorocyclohexane [40]		5.8	-9.0
1,1-Dimethylcyclohexane [38]	10.2 (298 K)	11.3	3.7
<i>cis</i> -1,2-Dimethylcyclohexane [38]	10.3 (298 K)	9.3	-3.5

^a Nos. in square brackets are references.

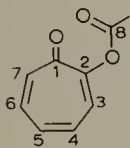
Carbons 9 and 10 are equivalent in each conformer; however, the other carbons form four nonequivalent pairs (C-1,5; C-4,8; C-3,7; C-2,6). The ^{13}C spectrum of γ -1,2,3,4,5,6-hexachlorocyclohexane as a function of temperature is shown in Fig. 10 [41].

At room temperature only two lines appear in the spectrum with an intensity ratio of 2 : 1. Below -40° three lines with relative intensities of 3 : 2 : 1 appear with the line of intensity 3 being a superposition of two lines with an intensity ratio of 2 : 1. If one represents the ring inversion of this compound as



then there are four nonequivalent carbon atoms and thus four different sites, two with a population of 2 and the other two with a population of one. With ring inversion, the spin at the site with a population of 2 transfers to the other site with a population of 2 but never to the sites with a population of one. The same is true for the spins at the sites with a population of one. A proper line shape analysis of the temperature spectra then permits the calculation of the activation parameters for these rather complex systems.

Tautomeric equilibria have also been investigated using temperature ^{13}C -n.m.r. spectra and line shape analysis to obtain thermodynamic parameters. The free energy of activation, $\Delta G^\ddagger = 10.8 \text{ kcal mol}^{-1}$, was obtained for the migration of the acetyl group in the acetate of tropolone [46].



At -70° , nine lines are present in the ^{13}C -n.m.r. spectrum which coalesce into three lines at room temperature. At the higher temperatures the lines of carbons 1 and 2 coincide with that of 8 while those of 4 and 6 and 3 and 7 coalesce with that of 5, the third signal being that of the methyl carbon. The solution to this problem involves dealing with three sets of two site exchange processes each having a different $(\nu_A - \nu_B)$ value. There are other similar systems which have also been studied with equal success [47–49].

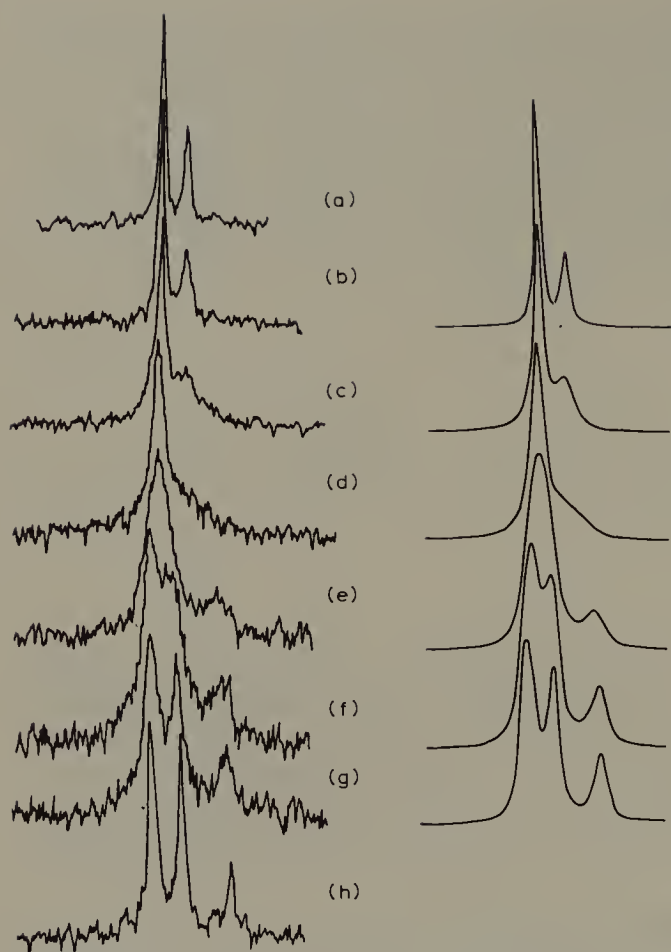


Fig. 10. The observed (left) and the calculated (right) ^{13}C -n.m.r. spectra of γ -benzenehexachloride at various temperatures. The chemical shifts are temperature dependent, but the frequency scale of each spectrum is appropriately offset so that the main peak is always at the same position. At (a) 294.5 K, (b) 275 K, (c) 261 K, (d) 254.5 K, (e) 244.5 K, (f) 237 K, (g) 231 K and (h) 211.5 K [41].

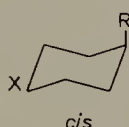
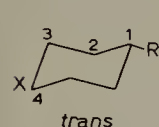
The keto-enol tautomerism of the compounds

	Calculated from	% Enol
$\begin{array}{ccccccc} & \text{O} & & \text{O} & & & \\ & \parallel & & \parallel & & & \\ \text{CH}_3 & - \text{C} & - & \text{CH}_2 & - & \text{C} & - \text{CH}_3 \\ 1 & 2 & 3 & 4 & 5 & & \end{array}$	C-1	78
	C-3	78
$\begin{array}{ccccccc} & \text{O} & & \text{O} & & & \\ & \parallel & & \parallel & & & \\ \text{CH}_3 & - \text{C} & - & \text{CH}_2 & - & \text{C} & - \text{O} - \text{CH}_2\text{CH}_3 \\ 4 & 3 & 2 & 1 & 5 & 6 & \end{array}$	C-2	11
	C-4	9
	C-5	14
$\begin{array}{c} \text{O} \\ \parallel \\ \text{H}_3\text{C} - \text{C}_6\text{H}_4 - \text{C} - \text{CH}_2 \\ \quad \quad \quad \\ \text{H}_3\text{C} \quad \text{C}_5 \quad \text{C}_4 \quad \text{C}_3 \\ \quad \quad \quad \\ \text{CH}_2 \quad \text{C} = \text{O} \\ \parallel \\ \text{O} \end{array}$	C-2	60
	C-6	53

has been studied by ^{13}C -n.m.r. spectroscopy [50]. In each case only one enol was observed, and the percentage of enol form at 42° was calculated by comparing the integrated peak intensity of the indicated carbon in the enol to the total from enol plus keto.

There are many other systems for which quantitative data may be obtained at one temperature (i.e. the normal probe temperature), a number of which will be discussed briefly. O'Neill and Pringuer [51] have shown that isomeric mixtures of 2,4- and 2,6-diisocyanatotoluene may be quantitatively analyzed by peak height measurements without the use of gated decoupling or the addition of paramagnetic reagents. The percentages of the 2,4-isomer in mixtures of 2,4- and 2,6-isomers are shown in Table 2, the spectra being obtained on two different spectrometers.

The accuracy of quantitative ^{13}C -n.m.r. spectroscopy was also shown in the determination of the amount of *trans* isomer in mixtures of *cis* and *trans*-4-*tert*-butylcyclo-



hexane derivatives using both ^{13}C -n.m.r. line intensities of the two isomers and g.l.c. [52]. The results are shown in Table 3. The agreement between the two techniques is obviously good.

A systematic study of the configurations of oximes has been performed by Hawkes et al. [53] using ^{13}C -n.m.r.



TABLE 2
PERCENTAGE OF 2,4-DI-ISOCYANATOTOLUENE IN MIXTURES OF 2,4- AND 2,6-ISOMERS

Sample	Stated composition	^{13}C -n.m.r. Spectroscopy		
		JEOL Integration	JEOL Peak height	Bruker
1	100	a	97.0	96.8
2 ^b	90	91.1	90.3	c
3	80	c	c	80.6
4	65	66.9	66.4	65.0

^a Peak area not integrated.

^b 1 : 1 mixture of 1 and 3.

^c Sample not run.

TABLE 3

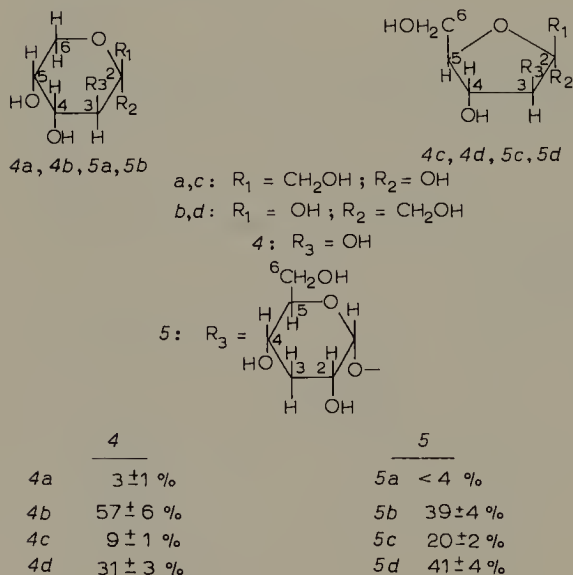
PERCENTAGE OF *trans*-ISOMER DETERMINED BY ^{13}C -NMR AND GLC

Calculated from	R = OH	O ₂ CCH ₃	NH ₂	Br
C-1	71	33	83	43
C-2	66	35	82	40
C-3	69	29	83	44
C-4	69	35	76	38
Mean value	68 ± 1	33 ± 1.5	80 ± 1.5	40 ± 1.5
G.l.c.	67	33	80	40

In order to determine quantitatively the *syn-anti* composition of the oximes, $\text{Cr}(\text{acac})_3$ was used to quench the differential NOE. The data were obtained at 35°. The results and comparison with other literature values for some of the compounds studied are shown in Tables 4 and 5. Again the agreement is quite satisfactory.

Voelter et al. [54] have quantitatively investigated the *cis-trans*-isomerism of thyrotropin releasing hormone (TRH) in aqueous solution, at room temperature, by comparison ^{13}C -n.m.r. peak intensities of both forms. It was found that aqueous solutions of TRH contain 10–20% of the *cis* isomer.

From ^{13}C -n.m.r. investigation of the anomeric equilibrium of *D*-fructose and *D*-furanose in water at 36°, the following compositions were determined by measurement of integrated peak intensities [55].



The complex formation reaction between nickel(II) and acetate ions in aqueous solution has been studied by ^{13}C -n.m.r. spectroscopy [56]. Equilibrium quotients for the

TABLE 4

KETOXIME ISOMER DISTRIBUTIONS DETERMINED FROM THE ^{13}C -NMR SPECTRA

Ketoximes ^b	Carbons ^c	% of major isomers ^a			ΔG° ^f
		With Cr-(acac) ₃ ^d	Pulse delay ^e	Lit. [53]	
$\begin{array}{c} \text{HO}-\text{N} \\ \parallel \\ \text{CH}_3-\text{C}-\text{CH}_2\text{CH}_3 \\ \text{1} \quad \text{2} \quad \text{3} \quad \text{4} \end{array}$	C-3	78	73	74	0.77
$\begin{array}{c} \text{N}-\text{OH} \\ \parallel \\ \text{CH}_3-\text{C}-\text{CH}_2\text{CH}_3 \end{array}$	C-4	77	76		
	C-1	71	68		
$\begin{array}{c} \text{HO}-\text{N} \\ \parallel \\ \text{CH}_3-\text{C}-\text{CH}(\text{CH}_3)_2 \\ \text{1} \quad \text{2} \quad \text{3} \quad \text{4} \end{array}$	C-3	86	88	86	1.11
$\begin{array}{c} \text{N}-\text{OH} \\ \parallel \\ \text{CH}_3-\text{C}-\text{CH}(\text{CH}_3)_2 \end{array}$	C-1	86	84		
$\begin{array}{c} \text{HO}-\text{N} \\ \parallel \\ \text{CH}_3-\text{C}-\text{CH}_2\text{C}(\text{CH}_3)_3 \\ \text{1} \quad \text{2} \quad \text{3} \quad \text{4} \quad \text{5} \end{array}$	C-3	83	81	82	0.93
$\begin{array}{c} \text{N}-\text{OH} \\ \parallel \\ \text{CH}_3-\text{C}-\text{CH}_2\text{C}(\text{CH}_3)_3 \end{array}$	C-1	80	82		
$\begin{array}{c} \text{HO}-\text{N} \\ \parallel \\ \text{CH}_3\text{CH}_2-\text{C}-\text{CH}(\text{CH}_3)_2 \\ \text{1} \quad \text{2} \quad \text{3} \quad \text{4} \quad \text{5} \end{array}$	C-3	78	78	78	0.78
$\begin{array}{c} \text{N}-\text{OH} \\ \parallel \\ \text{CH}_3\text{CH}_2-\text{C}-\text{CH}(\text{CH}_3)_2 \end{array}$	C-4	78	78		
$\begin{array}{c} \text{HO}-\text{N} \\ \parallel \\ \text{CH}_3-\text{C}-\text{CH}_2\text{C}_6\text{H}_5 \\ \text{1} \quad \text{2} \quad \text{3} \end{array}$	C-3	74	71	74	0.58
$\begin{array}{c} \text{N}-\text{OH} \\ \parallel \\ \text{CH}_3-\text{C}-\text{CH}_2\text{C}_6\text{H}_5 \end{array}$	C-1	70	70		

^a The uncertainties of the values determined from the ^{13}C -n.m.r. spectra are probably of the order $\pm 5\%$.

^b Presumed major isomer listed first.

^c The ^{13}C -n.m.r. signals used for peak height measurements.

^d From ^{13}C -n.m.r. spectra, obtained with added $\text{Cr}(\text{acac})_3$ to reduce differential NOE effect.

^e From ^{13}C -n.m.r. spectra without $\text{Cr}(\text{acac})_3$, but with a 12-sec pulse delay.

^f Free energies (kcal mol^{-1}) at 35° ; these were determined from mean values.

TABLE 5

ALDOXIME ISOMER DISTRIBUTION OBTAINED FROM ^{13}C -NMR SPECTRA

Aldoximes ^a	Percentage of major isomer	
	^{13}C -n.m.r. data ^b	Lit. [53]
$\begin{array}{c} \text{HO}-\text{N} \\ \parallel \\ \text{CH}_3-\text{CH} \end{array} \quad \left. \vphantom{\begin{array}{c} \text{HO}-\text{N} \\ \parallel \\ \text{CH}_3-\text{CH} \end{array}} \right\}$ $\begin{array}{c} \text{N}-\text{OH} \\ \parallel \\ \text{CH}_3-\text{CH} \end{array}$	64	61
$\begin{array}{c} \text{N}-\text{OH} \\ \parallel \\ \text{CH}_3\text{CH}_2\text{CH}_2-\text{CH} \end{array} \quad \left. \vphantom{\begin{array}{c} \text{N}-\text{OH} \\ \parallel \\ \text{CH}_3\text{CH}_2\text{CH}_2-\text{CH} \end{array}} \right\}$ $\begin{array}{c} \text{HO}-\text{N} \\ \parallel \\ \text{CH}_3\text{CH}_2\text{CH}_2-\text{CH} \end{array}$	56	54
$\begin{array}{c} \text{N}-\text{OH} \\ \parallel \\ (\text{CH}_3)_2\text{CH}-\text{CH} \end{array} \quad \left. \vphantom{\begin{array}{c} \text{N}-\text{OH} \\ \parallel \\ (\text{CH}_3)_2\text{CH}-\text{CH} \end{array}} \right\}$ $\begin{array}{c} \text{HO}-\text{N} \\ \parallel \\ (\text{CH}_3)_2\text{CH}-\text{CH} \end{array}$	71	70
$\begin{array}{c} \text{N}-\text{OH} \\ \parallel \\ \text{C}_6\text{H}_5\text{CH}_2-\text{CH} \end{array} \quad \left. \vphantom{\begin{array}{c} \text{N}-\text{OH} \\ \parallel \\ \text{C}_6\text{H}_5\text{CH}_2-\text{CH} \end{array}} \right\}$ $\begin{array}{c} \text{HO}-\text{N} \\ \parallel \\ \text{C}_6\text{H}_5\text{CH}_2-\text{CH} \end{array}$	49	54

^a Presumed major isomer listed first.^b 12-sec pulse delay.

formation of the monoacetatonickel(II) complex were calculated from the relative areas of distinct bulk and coordinated acetate signals over a temperature range of -5 to $+20^\circ$ and were found to be constant over this range. Using acetic acid enriched to 90.0 atom % ^{13}C in the carboxyl position, spectra of the type shown in Fig. 11 were obtained. The equilibrium quotients obtained by ^{13}C -n.m.r. methods were in good agreement with results obtained using polarographic techniques.

The solvation number of Al^{3+} ion in aqueous organic mixtures and the amount of each solvent component in the first solvation shell has been determined using ^1H - and ^{13}C -n.m.r. spectroscopy [57]. In these solutions separate signals were observed for bulk and coordinated solvent molecules; consequently, their relative areas could be used to determine quantitatively the composition of the first solvation shell.

Carbon-13-n.m.r. spectroscopy has been used to measure quantitatively the *cis* and

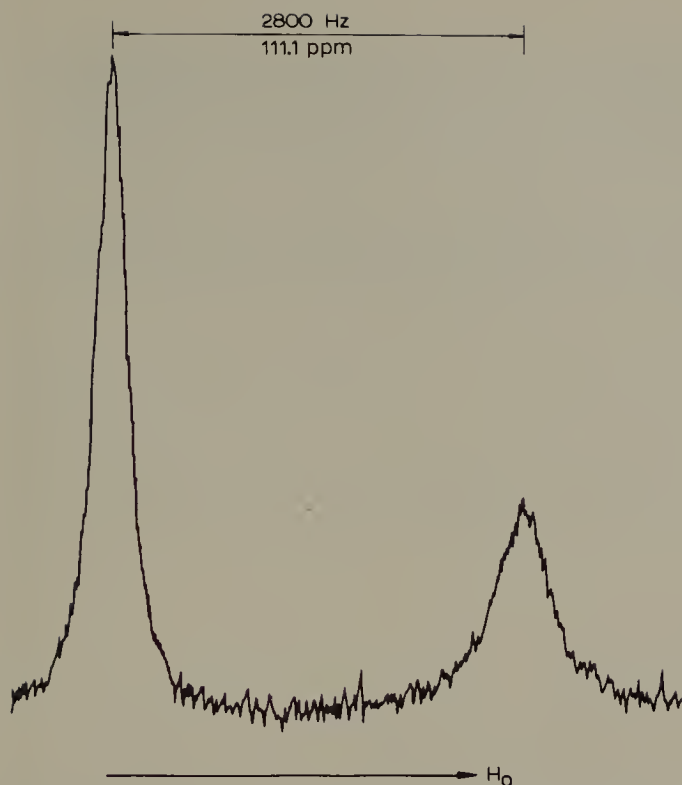
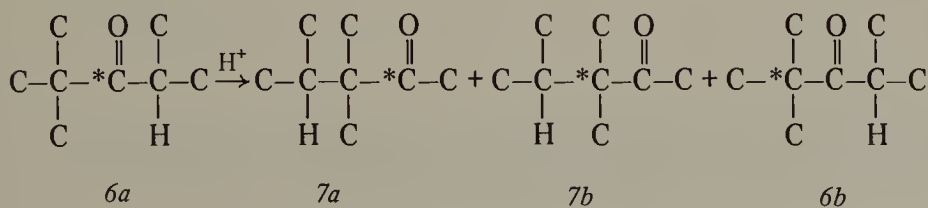


Fig. 11. The 25.2-MHz ^{13}C -n.m.r. spectrum at 0° of a D_2O solution containing 0.701 m $\text{Ni}(\text{ClO}_4)_2$ and 0.552 m $\text{CH}_3^{13}\text{COOH}$. The downfield and upfield signals represent bulk acetate and mono-acetatonickel(II), respectively [56].

trans contents in a series of eight polypentenamers by peak area analysis [58]. The analytical use of ^{13}C -n.m.r. spectroscopy has been suggested, and used to a limited extent, to measure quantitatively stereoconfiguration and monomer sequence distribution [59–64]. A quantitative analytical method for determining the composition of fats and oils using ^{13}C -n.m.r. spectroscopy has been discussed by Shoolery [65].

The quantitative use of ^{13}C satellite p.m.r. spectra can be illustrated with the acid catalyzed ketone rearrangement studies of Oka et al. [66]. In the acid catalyzed ketone rearrangement of 2,2,4-trimethyl-3-pentanone to 3,3,4-trimethyl-2-pentanone, it was predicted that two competing mechanisms, alkyl group migration vs. oxygen function rearrangement, would be involved during the rearrangement. In order to examine the prediction, the rearrangement of ^{13}C -labeled 2,2,4-trimethyl-3-pentanone-3- ^{13}C (6a) was carried out.

Prediction



In a typical experiment, the rearrangement of 91% ^{13}C -enriched *6a* was carried out in concentrated sulfuric acid at 71° for two hours. The recovered ketonic material consisted of 14.8% of 2,2,4-trimethyl-3-pentanone-X- ^{13}C (*6*) and 85.2% of 3,3,4-trimethyl-2-pentanone-X- ^{13}C (*7*).

The ^{13}C -n.m.r. spectrum of the reaction product clearly indicated that the recovered ketones were mixtures of isotopic isomers *7a* (major) and *7b* (minor), and *6a* (major) and *6b* (minor).

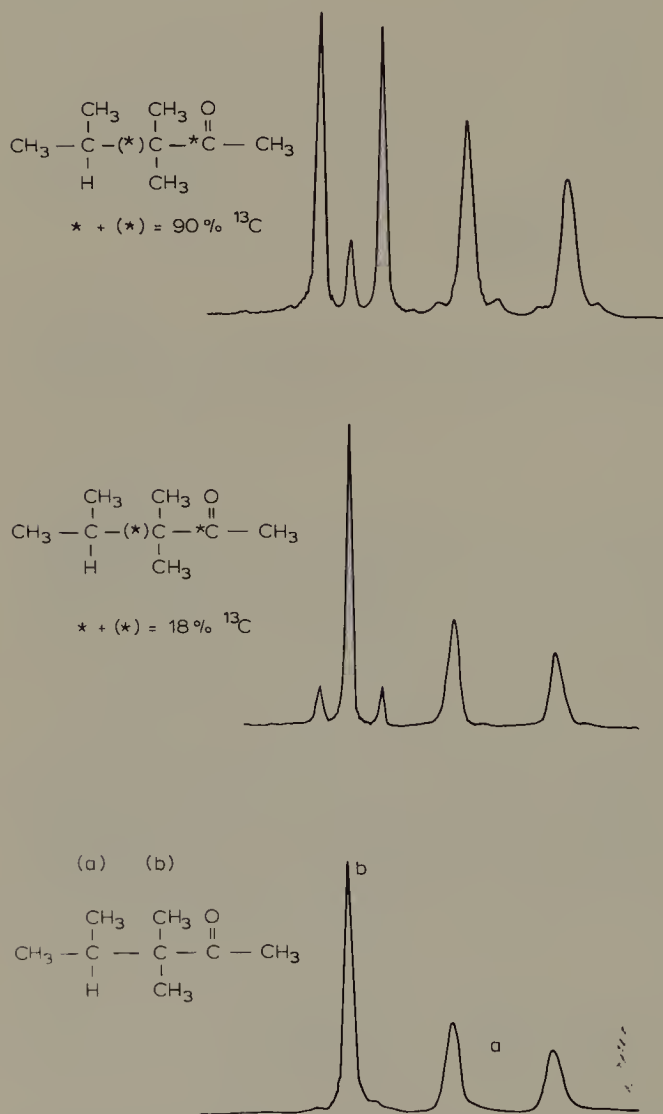


Fig. 12. ^1H -n.m.r. spectra of high-field signals of unlabeled 3,3,4-trimethyl-2-pentanone and of $\sim 18\%$ ^{13}C and $\sim 90\%$ ^{13}C -enriched 3,3,4-trimethyl-2-pentanone-X- ^{13}C .

The upfield part of the p.m.r. spectrum of unlabeled 3,3,4-trimethyl-2-pentanone is shown in Fig. 12, together with the corresponding spectra for the ^{13}C -enriched ketones recovered from the rearrangement reaction. Figure 13 shows the upfield part of the p.m.r. spectrum of the ^{13}C -enriched starting ketone, 2,2,4-trimethyl-3-pentanone, together with that for the same compound recovered from the rearrangement reaction. Analysis of the ^{13}C -satellites in these spectra shows the presence in the rearranged material of the minor isomers *6b* and *7b* along with the major isomers *6a* and *7a*. In Fig. 12, for the 90% enriched material the small amount of *7b* can be seen as the two sets of ^{13}C -satellites flanking the peaks of the methyl doublet of the isopropyl group. These satellites are due to $J_{13\text{CCH}}$. For both the ca. 18% and ca. 90% enriched materials the major isotopic isomer *7a* is shown by the ^{13}C -satellites flanking the (b) methyl groups peak ($J_{13\text{C}=\text{OCCH}}$). Quantitative estimates from both the ^{13}C -n.m.r. and ^{13}C -satellite p.m.r. data show the rearranged ketone mixture to be about 93% *7a* and 7% *7b*.

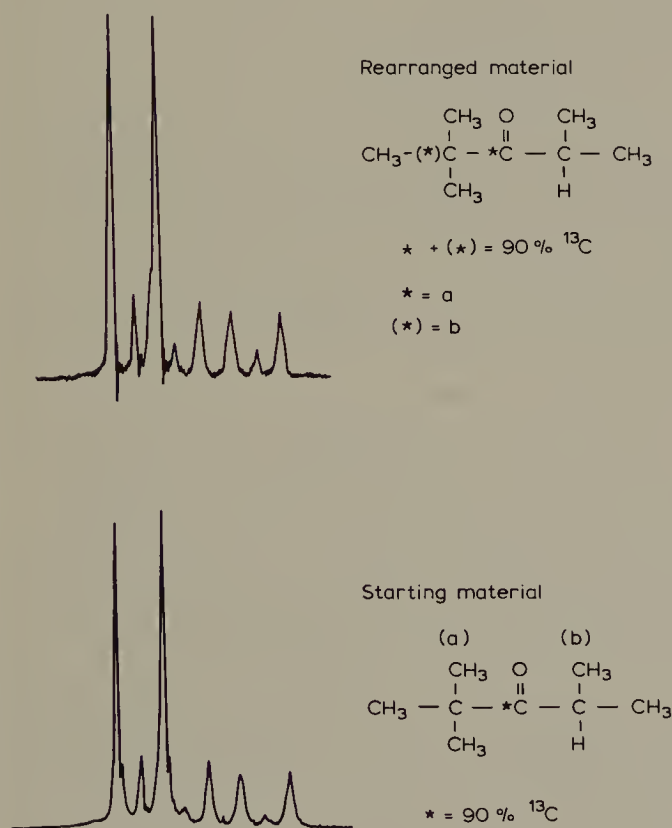


Fig. 13. ^1H -n.m.r. ^{13}C satellite spectra of high field signals of $\sim 90\%$ ^{13}C enriched 2,2,4-trimethyl-3-pentanone-3- ^{13}C (starting material) and $\sim 90\%$ ^{13}C -enriched 2,2,4-trimethyl-3-pentanone-X- ^{13}C (rearranged material). A portion of the isopropyl satellite spectrum is masked by the $(\text{CH}_3)_\text{a}$ peaks.

Although no additional satellite for *6b* in Fig. 13 can be seen, the presence of *6b* can be deduced by comparing the relative signal intensities of the protons (b) of the isopropyl group. In the starting material, $^{12}\text{CH}/^{13}\text{CH}$ is 9/91, while in the recovered (rearranged) starting material $^{12}\text{CH}/^{13}\text{CH}$ is 15/81. This indicates the loss of ^{13}C enrichment at the carbonyl carbon in the recovered ^{13}C labeled 2,2,4-trimethyl-3-pentanone. Thus the recovered material was a mixture of *6a* (major) and *6b* (minor). Mechanistic details of this reaction will be considered in a later section.

The quantitative use of ^{13}C -satellite p.m.r. spectra was also employed in determining the mechanism of thermal rearrangement of *p*-tolylcarbene to benzocyclobutene and styrene [67].

The examples of the quantitative use of ^{13}C -n.m.r. spectroscopy briefly discussed above certainly do not represent a comprehensive review of all the investigations in this area; however, it is hoped that the nature and scope of this technique have been sufficiently illustrated to indicate the potential of quantitative studies using ^{13}C -n.m.r. spectroscopy.

IV. CARBON-13 NMR MECHANISTIC APPLICATIONS [68]

A. Introduction

A very large fraction of ^{13}C -n.m.r. research is involved in one way or another with the study of reaction mechanisms. Most reaction mechanisms are constructed on the basis of the knowledge of the structure of reaction products and intermediates, and it is in this structural area where ^{13}C -n.m.r. spectroscopy has had its greatest impact. Carbon exists in a wide variety of chemical environments, and there is a close, understandable and predictable relationship between a carbon's chemical surroundings and its chemical shift. Excellent data and additivity relationships are now available for almost all classes of compounds, so solutions to many structural problems are now quite routine. The selective use of spin-spin coupling to other elements nicely supplements the chemical shift structural information. The use of substrates selectively enriched with carbon-13 or deuterium enables the investigator using ^{13}C -n.m.r. spectroscopy to follow an individual center throughout the course of a reaction, and the use of this powerful technique is increasing rapidly in both chemical and biochemical systems. Mechanistic applications of ^{13}C -n.m.r. spectroscopy to biochemical problems are dealt with elsewhere in this volume, and will not be covered in this chapter.

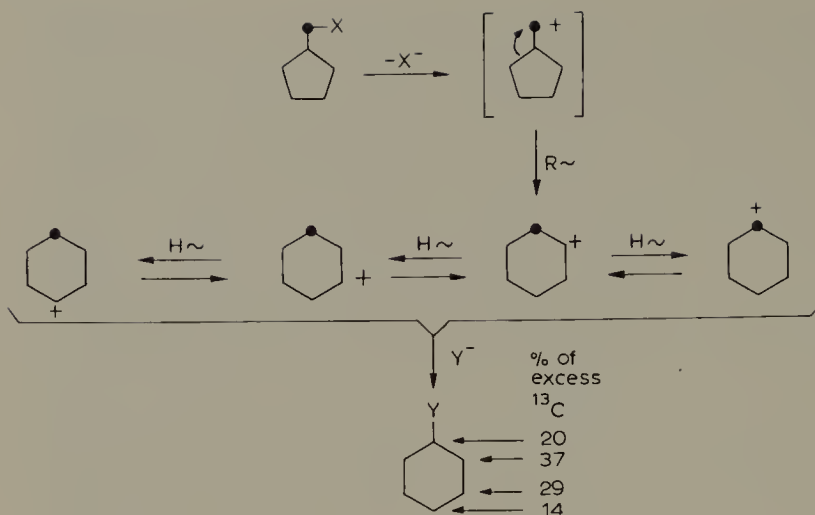
In many ways the study of reactive intermediates, especially carbenium and carbonium ions, has been revolutionized by ^{13}C -n.m.r. spectroscopy [69]. Most of the research in this area has involved the determination of structure; for instance, for most chemists the question of whether or not the norbornyl cation can have a nonclassical structure was only answered satisfactorily by the ^{13}C -n.m.r. data [70]. (However, the question of whether the usual reactions of norbornyl derivatives proceed through classical or nonclassical intermediates is by no means settled [71].)

Carbon-13 n.m.r. spectroscopy is well suited to studies of conformational equilibria and equilibria of various other kinds, since it provides excellent structural data for identifying the species present as well as for establishing the positions of such equilibria. The more quantitative aspects of this area have been dealt with earlier in this chapter, and the various examples selected for coverage in the following sections on mechanistic applications were chosen because they involve structural rearrangements as distinguished from conformational changes or geometry about multiple bonds. For example anomeric equilibria of ketoses in water are particularly susceptible to analysis by ^{13}C -n.m.r. techniques [55]. A useful investigation of keto–enol tautomerism has been carried out [50], but Elguero et al. [72] concluded that ^{13}C chemical shifts are of only limited value in determining the positions of tautomeric equilibria for rapidly interconverting azole tautomers. Closely related to tautomeric equilibria studies is the question of the site of protonation in systems having more than one basic center. Carbon-13 n.m.r. techniques are of much value in such studies, and a later section of this chapter reviews several examples of that subject. Also closely related to such subjects is the delocalization of electrons in conjugated systems, often expressed in terms of relative contributions of individual cononical forms to a resonance hybrid. The use of ^{13}C -n.m.r. chemical shift data for such purposes is perhaps most useful in carbocation structure studies. Some studies dealing with relative contributions of resonance structures in anions and neutral molecules are discussed in a later section.

The main emphasis in the remainder of this chapter will be on the study of molecular rearrangements by ^{13}C -n.m.r. techniques. The material will be organized into sections on carbenium ion rearrangements, ketone rearrangements, carbene and thermal decomposition and rearrangement reactions, radical reactions studied by ^{13}C -n.m.r. CIDNP, and miscellaneous reactions and other mechanistic applications of ^{13}C -n.m.r. spectroscopy.

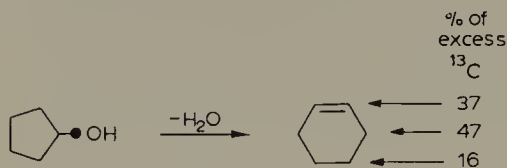
B. Carbenium ion rearrangements

Following earlier similar work using carbon-14 tracer techniques, Reutov and co-workers [73] first demonstrated the great utility of using carbon-13 enriched materials and ^{13}C -n.m.r. analytical methods to study rearrangement reactions [74]. The main advantage of carbon-13 over carbon-14 is that it is not necessary to degrade the rearranged product in order to identify the position of the labeled atom. In the solvolytic rearrangement of cyclopentylcarbinyl-1- ^{13}C derivatives to cyclohexyl derivatives, there was considerable scrambling of the label among all the ring positions, indicating extensive hydride shifts in the intermediate cyclohexyl cation. The percentage of excess ^{13}C figures given for the product (see diagram overleaf) are for the formolysis of the cyclopentylcarbinyl tosylate. The corresponding figures for the acetolysis of the tosylate and of the *p*-nitrobenzenesulfonate [75] were quite different from each other and from the formolysis results, indicating that the natures of the leaving group and medium are both important factors in determining the extent of the hydride shifts. When cyclopentyl-



carbinol-1-¹³C and cyclopentylcarbinyl-1-¹³C chloride were converted to cyclohexyl chloride by treatment with Lucas reagent at 50° for 6 h and aluminum chloride at -30° for 30 min, respectively, essentially complete scrambling of the label to all ring positions was observed [76].

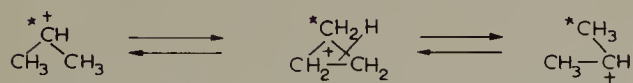
The dehydration of cyclopentylcarbinol-1-¹³C with boric acid at 340° also gave cyclohexene in which the label was scrambled among all the ring positions [77], pre-



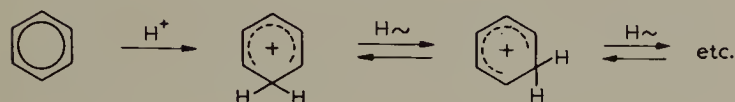
sumably by a carbenium ion rearrangement similar to that outlined above. Another advantage of the carbon-13 tracer technique compared to corresponding carbon-14 studies is shown by this experiment. The cyclohexene product was contaminated with 1-methylcyclopentene and methylenecyclopentane, but the chemical shifts of the three compounds were sufficiently different so that the cyclohexene could be analyzed without separating the mixture.

Hydride shifts such as the above, and skeletal rearrangements as well, are commonly observed for cations generated in superacid solutions. Carbon-13 n.m.r. much of it involving the INDOR method, has been a mainstay in the study of these reactions. This research area was reviewed by Olah [69] in 1973. As an example of the use of ¹³C-enriched compounds in such rearrangement studies, Olah and White [78] dissolved 2-chloropropane-2-¹³C in SO₂ClF-SbF₅, and found that at -60° the carbon-13 label was scrambled, with a half life of one hour, among the three positions of the isopropyl cation which was formed. The mechanism presumably involves an intermediate pro-

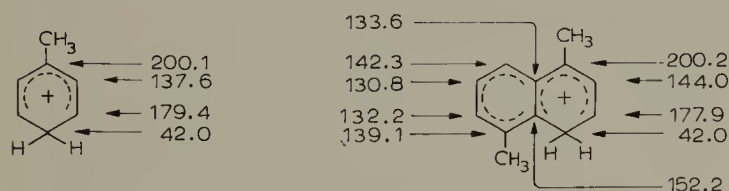
tonated cyclopropane [79], although no evidence was presented against the intermediacy of the *n*-propyl cation with successive hydride, methyl, and hydride shifts.



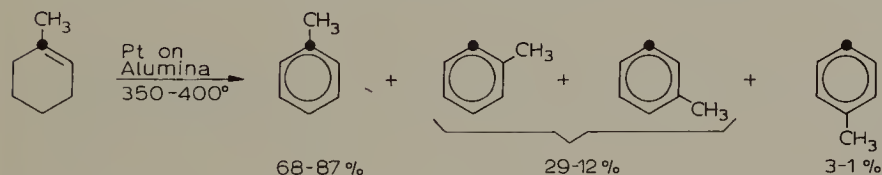
The benzenium ion, obtained by solution of benzene in $\text{HF-SbF}_5\text{-SO}_2\text{ClF}$ at -78° , showed single ^{13}C -n.m.r. and p.m.r. peaks [80], showing rapid equilibration of the various hydride shifted structures.



On the other hand, for ions derived from toluene and other alkylbenzenes [80], alkyl-naphthalenes [81], and alkylacenaphthalenes [82], such hydride shifts are not rapid, and the sites of protonation are easily established by the ^{13}C -n.m.r. chemical shifts.



Hydride and alkyl shifts in this type ion may, however, be the cause for the scrambling of the label observed by Marshall et al. [83] in the catalytic dehydrogenation of 1-methylcyclohexene-1- ^{13}C over 0.5% platinum on alumina at $350\text{--}400^\circ$.

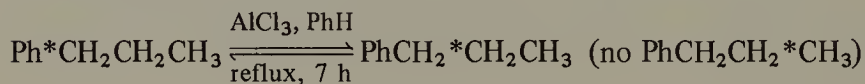


This finding has much significance for researchers using specifically carbon-13 or carbon-14 labeled aromatic compounds, since the preparation of many such compounds involves such a catalytic dehydrogenation step.

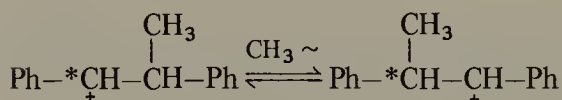
The original report [84] of isotopic scrambling among all ten positions (automerization) of carbon-14 labeled naphthalene in the presence of aluminum chloride was shown to be incorrect by Staab and Haenel [85] and later by the original investigators [86] using naphthalene-1- ^{13}C and ^{13}C -n.m.r., ^{13}C -satellite p.m.r., e.s.r., and mass spectrometry. Apparently (although from the reported details it seems very strange), the original

erroneous report resulted from incomplete purification of the degradation products from trace amounts of very high activity impurities, which illustrates, in a backhanded way, one of the major advantages of carbon-14 over carbon-13 in tracer work, its greater sensitivity, but at the same time, one of the possible pitfalls of carbon-14 work.

Carbon-14 tracer experiments have shown [87] that the α - and β -carbons in *n*-propylbenzene are equilibrated upon treatment with AlCl_3 in moist benzene under conditions where no significant amount of isopropylbenzene is formed.

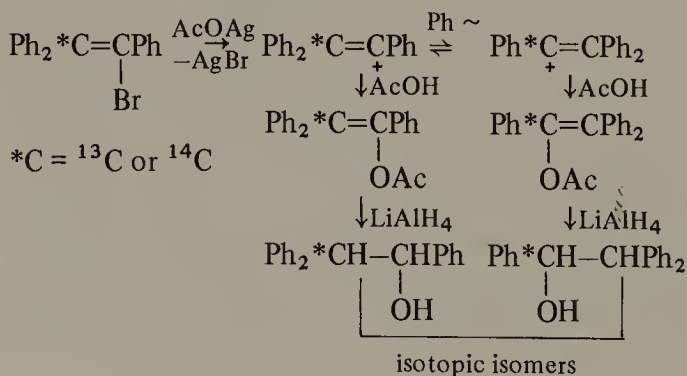


The mechanism for this interesting reaction favored by Roberts et al. [88] involves diphenylpropane as a key intermediate. It is formed by alkylation of benzene by a carbenium ion derived from the reactant. The key step in the rearrangement is scrambling of the α - and β -carbons by a methyl migration in a cation formed from the diphenylpropane.



Reversal of the process, utilizing the rearranged cation, gives the rearranged β -labeled *n*-propylbenzene. Under no conditions would this mechanism give unlabeled or dilabeled molecules from the labeled reactant. On the other hand, from an alternate "bimolecular" mechanism [89] involving diphenylhexyl cations, both dilabeled and unlabeled *n*-propylbenzene would be expected from the labeled reactant. Roberts and Gibson [90] utilized 1-phenylpropane-1- ^{13}C to differentiate between these two mechanisms. They found the expected α,β -scrambling, but no dilabeled molecules and no increase in the amount of unlabeled material, using mass spectrometric, ^{13}C -n.m.r. and ^{13}C -satellite p.m.r. analytical procedures, thus eliminating the "bimolecular" mechanism as a possibility. Olah et al. [80] suggest a "bond to bond carbonium ion rearrangement mechanism" for this reaction, but they provide no details.

Rummens et al. [91] have recently carried out a detailed comparative analysis of the use of carbon-13 and carbon-14 in studying the extent of rearrangement in the reaction of triphenylvinyl-2- ^{13}C (or -2- ^{14}C) bromide with silver acetate in acetic acid.



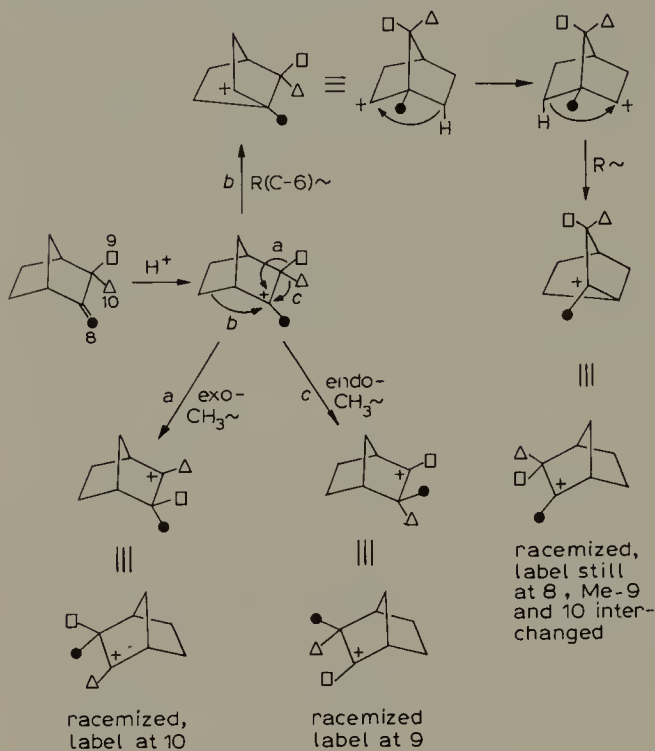
For ease of degradation or n.m.r. analysis, the vinyl esters were reduced to the corresponding saturated alcohols. The carbon-13 analyses were carried out using both direct ^{13}C -n.m.r. and ^{13}C -satellite p.m.r. spectroscopy. The extent of isotopic scrambling (phenyl shift from C-2 to C-1) was found to be $7.6 \pm 0.4\%$ by direct ^{13}C -n.m.r. analysis, $6.1 \pm 0.6\%$ by satellite analysis, and $6.5 \pm 0.3\%$ by carbon-14 analysis. The agreement is clearly satisfactory, and the carbon-13 methods have the great advantage of not requiring a time-consuming degradation. On the other hand, the precision is better with the carbon-14 method, and in addition this method permits the use of liberal amounts of inactive carriers in aiding the isolation and purification of the desired products. Furthermore, if the amount of rearrangement had been very small, the advantage of the much greater sensitivity of the carbon-14 method would have been paramount.

Oka and Lee [92] carried out a similar carbon-13 study using trianisylvinyl-2- ^{13}C bromide and silver acetate—acetic acid or silver trifluoroacetate—trifluoroacetic acid. The amount of rearrangement (*p*-anisyl shift) in the more nucleophilic acetic acid was 20%, and in trifluoroacetic acid scrambling was complete (50% rearrangement). The greater extent of rearrangement of anisyl compared with phenyl reflects the greater migratory aptitude of the former, and probably also a longer lifetime for the more stable trianisylvinyl cation (or ion pair) as compared with the triphenylvinyl cation. The greater degree of rearrangement in trifluoroacetic than in acetic acid reflects the lower nucleophilicity of the former in competing with the neighboring aryl group for the cationic center. This interpretation is fully in line with the results of earlier carbon-14 results [93] on the solvolyses of triphenylvinyl-2- ^{14}C trifluoromethanesulfonate in acetic acid (6.7% rearrangement), formic acid (7.7% rearrangement), and trifluoroacetic acid (27.0% rearrangement).

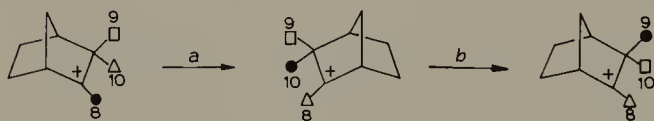
In the case of the *cis*- and *trans*-1,2-dianisyl-2-phenylvinyl-2- ^{13}C bromides, no observable phenyl migrations could be detected by ^{13}C -n.m.r. analyses [94]. The greater sensitivity of carbon-14 than carbon-13 studies would certainly make the detection of a small amount of phenyl migration more feasible.

A recent carbon-13 tracer study [95] of the mechanism of acid-catalyzed racemization of camphene has attempted to answer the interesting question of whether or not *endo*-methyl migration is involved (path *c* below). Carbon-14 tracer studies [96] many years ago showed that at least two paths were involved, (*a* and *b* below) but the degradative procedures used did not enable the amount of label at positions 9 and 10 to be determined separately. Using (—)-camphene-8- ^{13}C (ca. 46% enrichment), David et al. [95], carried out the racemization and measured the amount of ^{13}C -enrichment at positions 8, 9, and 10 using direct ^{13}C -n.m.r. and ^{13}C -satellite p.m.r. analytical techniques. In agreement with the earlier carbon-14 work, the label rearranged extensively (path *a* below) from position 8 to position 10 (but not as fast as the racemization, requiring path *b* below); and in addition, after a time, enrichment also appeared at position 9. A detailed kinetic analysis of the data led to the conclusion that path *a* was followed to the extent of 53%, path *b* 41%, and path *c*, *endo*-methyl migration, to a small but significant extent (some minor rearrangement via a tricyclene formation mechanism was

also postulated). These conclusions are in accord with the mechanism outlined below (● identifies the initial ^{13}C -label at position 8, while □ and △ identify the methyl groups originally at positions 9 and 10, respectively; for illustrative purposes, the question of non-classical ions is ignored).



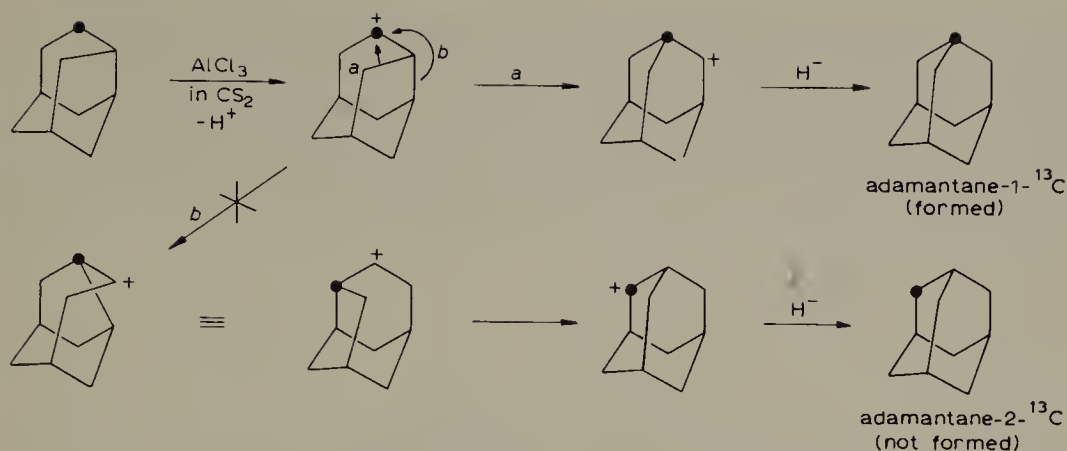
However, since Me-9 and 10 are interchanged by path *b*, *exo*-methyl migration, path *a*, followed by path *b* will also result in a label at position 9.



Even with such paths as this included, Vaughan and co-workers' analysis [95] led to the conclusion that *endo*-methyl migration was involved to a minor extent. However, in a reanalysis of the same data, Collins and Lietzke [97] challenged this conclusion, and maintained that paths *a* and *b* alone were sufficient to explain the data.

Recently Farcasiu et al. [98] have prepared protoadamantane-4- ^{13}C and rearranged it to adamantane. All of the excess carbon-13 was found in the 1-position of the adamantane (path *a*), showing clearly that the degenerate 4-protoadamantyl-4-protoadamantyl rearrangement [99] (path *b*), which would scramble the label, does not compete with the conversion to adamantane. (See diagram on next page).

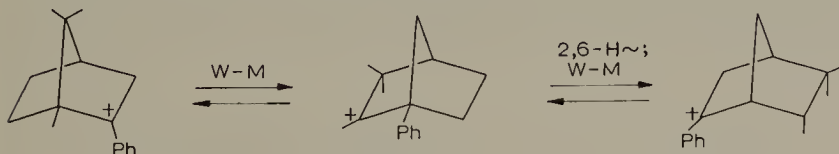
Holden and Whittaker [100] have used ^{13}C -n.m.r. spectroscopy to identify the



products from the rearrangements of the tosylates of isothujol (α -OTs) and neoiso-thujol (β -OTs) in $\text{SO}_2\text{--HSO}_3\text{F}$ solution. Their proposed mechanism for the rearrange-ments involves a trishomocyclopropenyl cation.



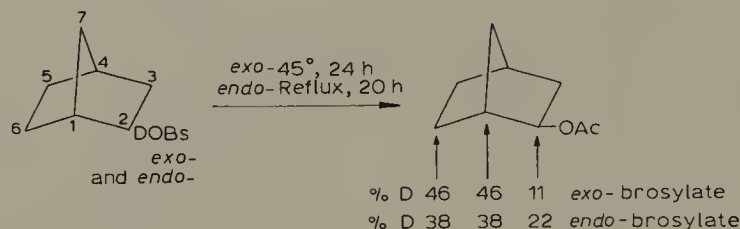
In a similar fashion, the 2-phenylbornyl cation was shown [101] to undergo rapid Wagner–Meerwein skeletal and hydrogen shift rearrangements in $\text{HSO}_3\text{F--SO}_2\text{ClF}$ at -70° to an isomeric tertiary benzylic ion in which the non-bonded interactions between phenyl and methyl are eliminated.



One of the important ways in which ^{13}C -n.m.r. has been used in mechanistic studies is as a probe for the position of deuterium, supplementing the usual p.m.r., i.r., and mass spectral analytical methods. The chemical shifts of deuterated carbons are about 0.12 p.p.m. higher than those of the corresponding protonated carbons. These isotope shifts make it easy to locate the positions of the deuterium atoms, and when used in conjunction with geminal and vicinal C–D coupling information, can provide very detailed structural information. As compared to tritium work, these deuterium methods have the same advantages (and sensitivity disadvantages) as carbon-13 tracer studies have over similar studies with carbon-14. The savings in time and effort in terms of product separation and degradation can be very great.

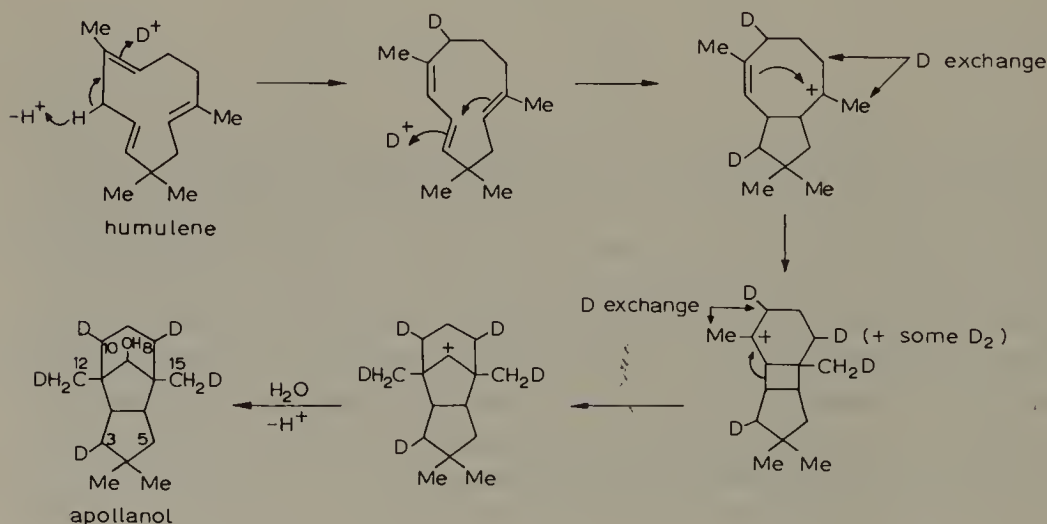
For example, both carbon-14 and tritium tracers have been used to study the skele-

tal rearrangements of *exo*- and *endo*-norbornyl brosylates during acetolysis [102]. Stothers' group repeated this work using *exo*- and *endo*-2-*d*-2-norbornyl brosylates and natural abundance ^{13}C -n.m.r. spectroscopy for analysis [103]. The results showed that deuterium in the product was located *only* at C-1, C-2, and C-6 resulting from skeletal shifts of C-6 from C-1 to C-2 or hydride shifts from C-6 to C-2.



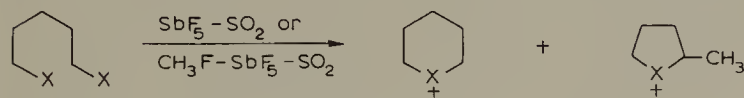
The results are in general agreement with the tritium values [102]. The fact that the residual signal at C-1 in the acetate was *completely* (within $\pm 3\%$) isotope shifted led Stothers to conclude [68] that no (within $\pm 3\%$) C-3 to C-2 hydride shift could have occurred, since that would place H adjacent to the new C-1 carbon (the original C-4 carbon). (The C-3, C-5, and C-7 signals in the acetate each consisted of two signals, one shifted upfield by the deuterium on the adjacent carbon.)

The mechanism of the acid-catalyzed rearrangement of humulene to apollanol proposed by Corey and Nozoe [104] was supported by the findings of a similar study [103] of the positions of incorporation of deuterium into the product when the reaction was carried out in deuteriosulfuric acid. The mechanism [104] involved a prototropic double bond shift to a conjugated triene, followed by carbenium ion ring closures and skeletal rearrangements. The deuterium was located *only* at the position of initial deuterium attack on the conjugated system, C-3(5), and at the non-bridgehead (exchangeable) positions, C-8(10) and C-12(15), *alpha* to the carbenium ion centers in the proposed intermediates.

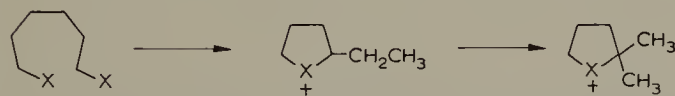


The detection of dideuteration of C-8(10) by ^{13}C -n.m.r. measurements was noteworthy.

Rearrangements during the formation of halonium ions from dihalides in superacid solutions have been studied with the aid of ^{13}C -n.m.r. spectroscopy. For example, in $\text{SbF}_5\text{--SO}_2$, or using $\text{CH}_3\text{F--SbF}_5\text{--SO}_2$, 1,5-dihalopentanes give varying amounts of the six-membered ring halonium ions and the rearranged five-membered ring 1-methyl halonium ions, depending on the experimental conditions and the halogen [105].

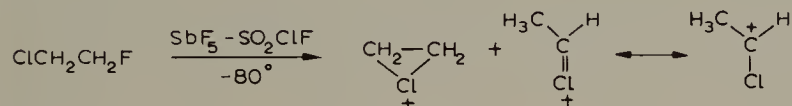


One of the most interesting results of the research of Peterson's group [106] in this area is the report that 1,6-dihalohexanes do not give the seven-membered ring halonium ions, but rather 1-ethyltetramethylene halonium ions, which upon standing, rearrange further to 1,1-dimethyltetramethylenehalonium ions.



The authors speculate that the first product may be formed by two successive 1,2-hydride shifts in the cation formed as one halogen is abstracted, or possibly through the intermediacy of a protonated cyclopropane. As for the product of the second step, the authors say only, "Such an ion cannot be formed via simple hydride shifts, but must result from rearrangement of the carbon skeleton itself." Again, a hydride shift in a protonated cyclopropane intermediate may be involved.

Olah et al. [107], using ^{13}C -n.m.r. and p.m.r. spectroscopy showed that, depending on conditions, various mixtures of dimethylenechloronium ion and methylchlorocarbenium ion were formed upon treatment of 1-chloro-2-fluoroethane with $\text{SbF}_5\text{--SO}_2\text{--ClF}$ at -80° .

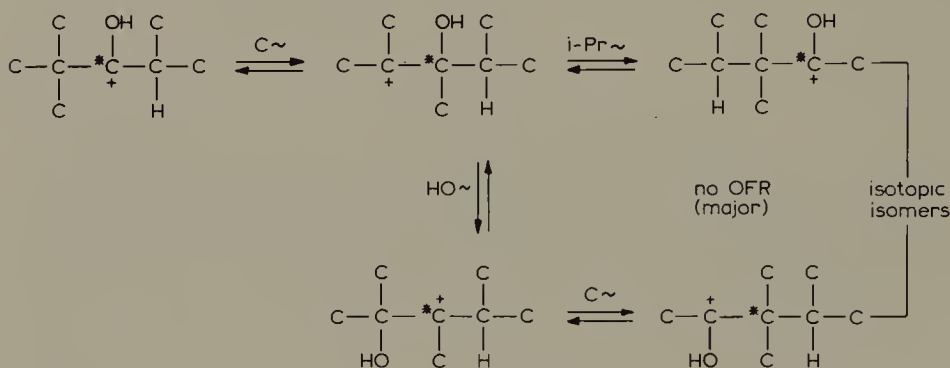


A 1,2-hydride shift is obviously involved in the formation of the latter compound, but the two ions were not thought to be interconvertible.

C. Ketone rearrangements

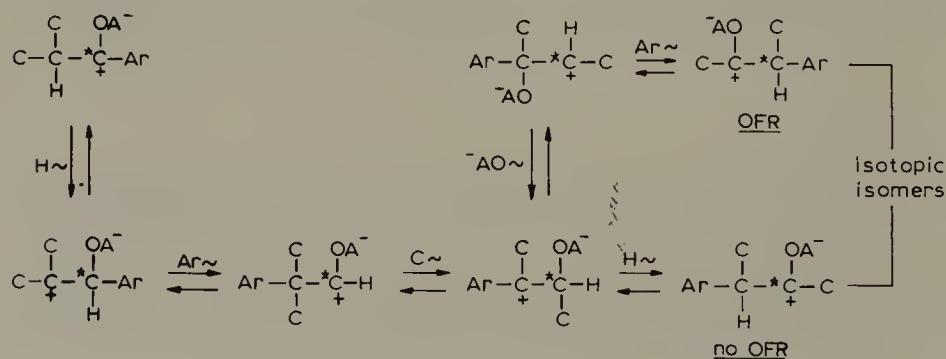
The mechanisms of acid-catalyzed rearrangements of aldehydes and ketones have been studied very extensively for many years by carbon-14 tracer techniques [108], and in recent years carbon-13 and ^{13}C -n.m.r. analytical procedures have been used as well. The existence of an oxygen function rearrangement (OFR) path was demonstrated [66], using both ^{13}C -n.m.r. and ^{13}C -satellite p.m.r. techniques, in the rearrangement,

in sulfuric acid at 70° for 2 hours, of 2,2,4-trimethyl-3-pentanone-3-¹³C. The isotopic isomers, 3,3,4-trimethyl-2-pentanone-2-¹³C (major product) and 3,3,4-trimethyl-2-pentanone-3-¹³C (minor product), were obtained. The mechanism proposed involves competitive alkyl and oxygen function shifts (probably OH shifts; other OFR possibilities exist [108]) in the conjugate acids of the ketones and tertiary carbenium ions derived from them.



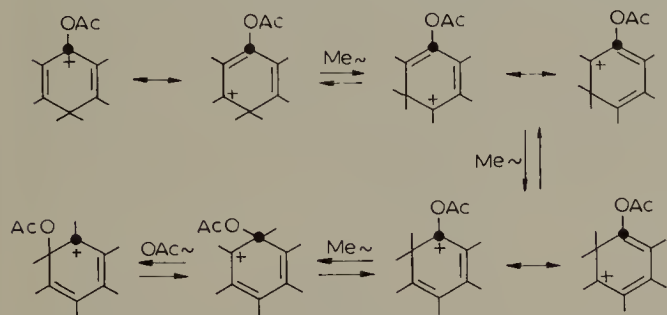
A small amount of the isotopic isomer of the starting material, 2,2,4-trimethyl-3-pentanone-2-¹³C, was also detected, showing the reversibility of the process with the groups migrating in a different order. The main advantage of carbon-13 over carbon-14 for tracer experiments of this type is that the position of the label can be determined without the tedious and time-consuming degradation of the product. Equally important in this case was the fact that the ¹³C-n.m.r. analysis could be carried out directly on the *mixture* of the two ketones, eliminating the necessity for a preparative gas chromatographic separation.

In a similar kinetic and equilibrium study [109] of oxygen function rearrangement in the aluminum chloride-catalyzed rearrangement of *p*-chloroisobutyrophenone to 3-(*p*-chlorophenyl)-2-butanone, both carbon-13 and carbon-14 analytical procedures were used. The same qualitative results were obtained with both isotopes, but the precision of the carbon-14 data was superior. In this case the favored mechanism of the reaction (based in part on oxygen function rearrangement data for carbon-14 labeled *p*-methylisobutyrophenone) involved the intermediacy of an aldehyde conjugate acid and competi-



tive shifts of hydrogen and aryl, alkyl, and $(\text{O}-\text{AlCl}_3)^-$ $(\text{OA})^-$ groups (alternative paths involving initial methyl migrations would involve secondary carbenium ions).

Oxygen function rearrangement was also observed by Isaev et al. [110] in the treatment of 2,3,4,5,6-hexamethylcyclohexadienone-1- ^{13}C with $\text{Me}_2\text{O} \cdot \text{BF}_3$ at 130° for 50 hours. The carbon-13 label was completely scrambled among all the ring positions. The proposed mechanism involved a series of methyl and oxygen function (OA) shifts in the ketone conjugate acid and tertiary carbenium ions derived from it.

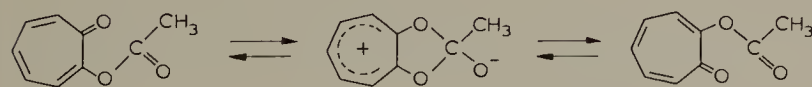


The oxygen function rearrangement may then be repeated to all ring positions. It would be interesting to see if methyl group scrambling is faster than ring carbon scrambling.

One of the simplest of "ketone rearrangements" is the tautomerism of tropolone.



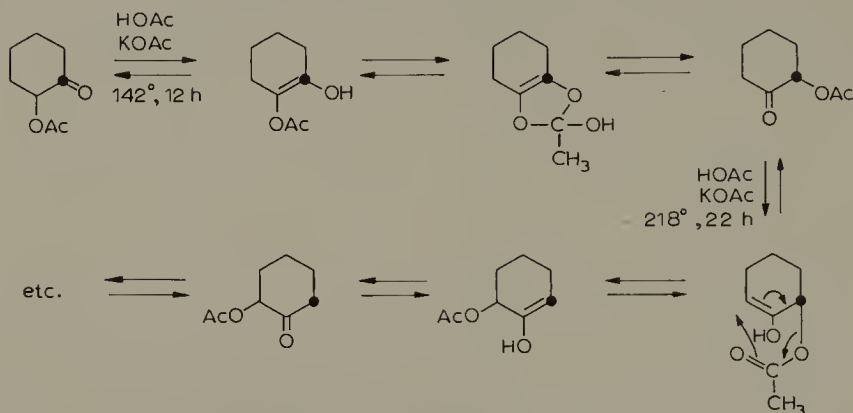
The proton-decoupled ^{13}C -n.m.r. spectrum of tropolone consists of only four singlets [111], showing clearly that the above interconversion is rapid at room temperature. The acetate of tropolone was also shown to be rapidly equilibrating at 50° (only three lines were resolved), but at -70° singlets for all nine carbons were obtained [46]. The mechanism of the exchange undoubtedly involves attack of the ring carbonyl oxygen on the acetate carbonyl carbon.



ΔG^\ddagger for the exchange was calculated to be $10.8 \text{ kcal mol}^{-1}$. Similarly, the 2-butyldimethylsilyl ether of tropolone was shown [112] to be undergoing rapid exchange on the n.m.r. time scale, even at temperatures as low as -70° . The observation of separate ^{13}C -n.m.r. peaks for the two methyl groups in the rapidly rearranging system demonstrates that the silyl shift is occurring with retention of configuration at silicon, since any migration with inversion or racemization would interchange the methyl environments. It was concluded that the rearrangement must involve a five membered ring

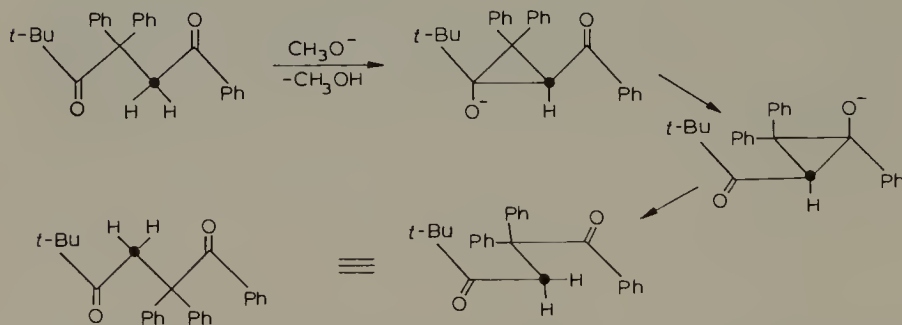
intermediate with the two oxygens bound to trigonal-bipyramidal silicon by one apical and one equatorial bond. A similar study was reported [112] for the 2-butyldimethylsilyl enol ether of acetylacetone.

An interchange somewhat similar to those described above, but now involving in addition transfer of ring hydrogens was revealed in the ^{13}C -n.m.r. study [113] of the scrambling at 142° for 12 h of the 1- and 2-positions (only) of 2-acetoxycyclohexanone-1- ^{13}C , presumably via the acetate of the enediol.



Under more drastic conditions, 218° for 22 h, the label-scrambling extended to the other ring carbons as well. This reaction probably has a similar mechanism involving the 1,6-enediol, but an intermolecular reaction has not been completely ruled out.

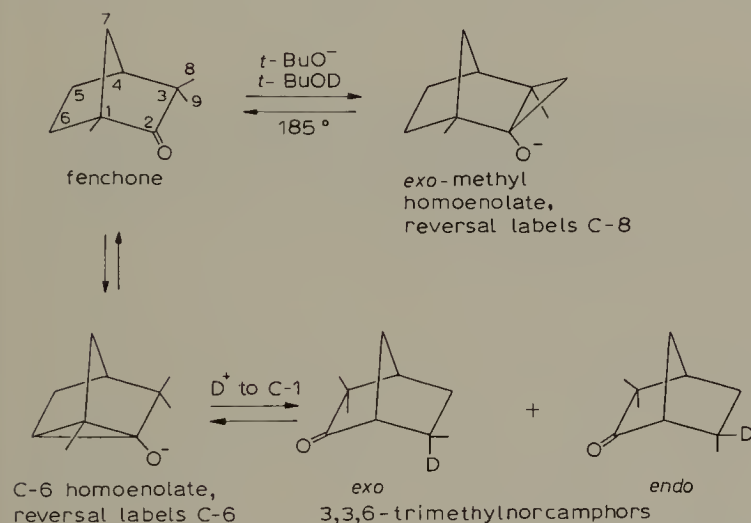
By a carbon-13 tracer experiment using ^{13}C -satellite p.m.r. spectroscopy as the analytical method, Betts and Yates [114] demonstrated that a homoenolate rather than a 1,2-phenyl shift mechanism was involved in the rearrangement of 1,3,3-triphenyl-5,5-dimethyl-1,4-hexanedione-2- ^{13}C to 1,2,2-triphenyl-5,5-dimethyl-1,4-hexanedione-3- ^{13}C .



In agreement with the established mechanism involving a cyclopropanone intermediate, Knutsson [115] found that the label was equally distributed between the α - and β -positions in the product acid from the Favorskii rearrangement of 1,1,3-tribromoacetone-3- ^{13}C .

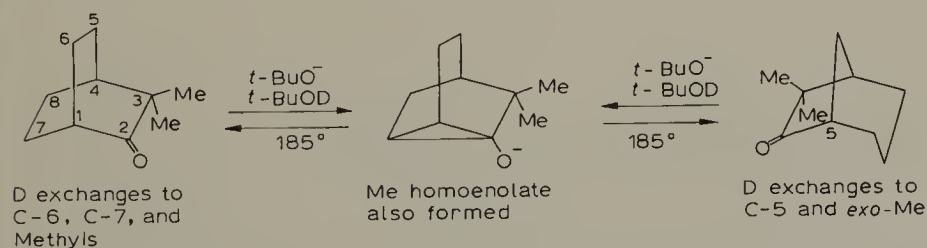
The use of ^{13}C -n.m.r. spectroscopy as a probe for deuterium has also been used to advantage in studies of base catalyzed ketone rearrangements and homoenolizations

[116,117]. Upon treatment with *tert*-BuOK–*tert*-BuOD at 185° for various times, fenchone was found to undergo slow deuterium exchange at C-6, and also slower exchange at C-8 (*exo*-methyl). Within the sensitivity of the ^{13}C -n.m.r. method for deuterium analysis, no exchange was detected at any other position in the molecule. In their more recent work, Johnson et al. [117], using ^2H -n.m.r. spectroscopy, found small amounts of additional very slow exchange at C-9 and C-10. Their paper offers an excellent exposition of the advantages of ^2H -n.m.r., and the pitfalls of ^{13}C -n.m.r. spectroscopic methods for deuterium analysis. One of the biggest advantages of ^2H -n.m.r. spectroscopy is that exchange at the 6-*exo*- and 6-*endo*-positions in fenchone can be studied independently, so that the stereoselectivity of the exchange can be determined. In addition to deuterium exchange, fenchone was also found to undergo a rearrangement (5–6%) to a 3 : 1 mixture of *exo*- and *endo*-3,3,6-trimethylnorcamphor. The proposed mechanisms for these reactions are shown below.



The labeling at C-9 and C-10 presumably involves less readily formed homoenolates at those positions.

Similar studies were carried out on deuterium exchange and skeletal rearrangements via homoenolization for a series of bicyclooctanones [118]. The bicyclo[2.2.2] system is readily converted to the bicyclo[3.2.1] system.

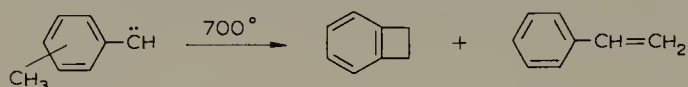


When a 5,6-double bond was introduced into the bicyclo[2.2.2] substrate, the deuterium

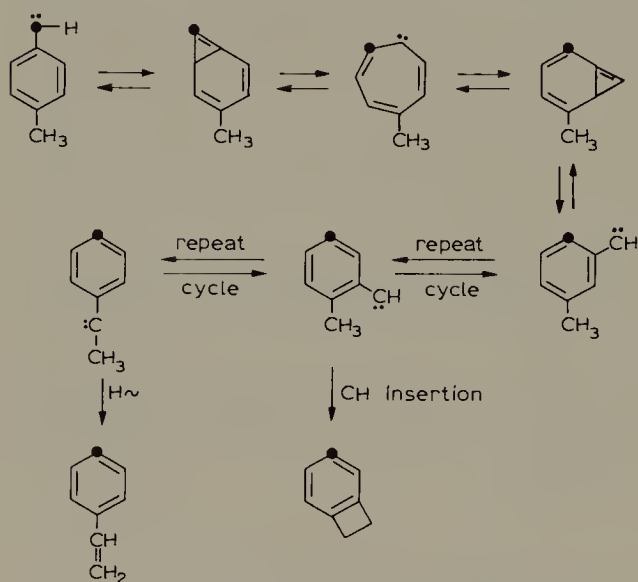
exchange and skeletal rearrangements were similar in nature but much faster. In this case, deuterium was incorporated into both olefinic positions. The mechanism by which exchange takes place at olefinic position C-3 in the bicyclo[3.2.1] products was not established.

D. Carbene and thermal decomposition and rearrangement reactions

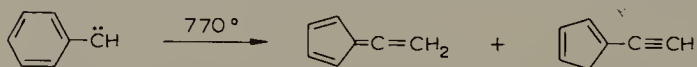
The mechanisms of several carbene reactions have been studied using ^{13}C -n.m.r. techniques. Hedaya and Kent [67] found that *o*-, *m*-, and *p*-tolylcarbenes all rearranged at high temperatures to give about 50% yields of mixtures of benzocyclobutene and styrene.



When *p*-tolylcarbene was generated from *p*-tolyl diazomethane- ^{13}C by flash vacuum pyrolysis at 700° , all of the label appeared at the 4-position in both the benzocyclobutene and the styrene, as shown by ^{13}C -n.m.r. and ^{13}C -satellite p.m.r. spectroscopy. These results were interpreted in terms of a mechanism proposed by Baron et al. [119], an alternate mechanism [67] being unacceptable.

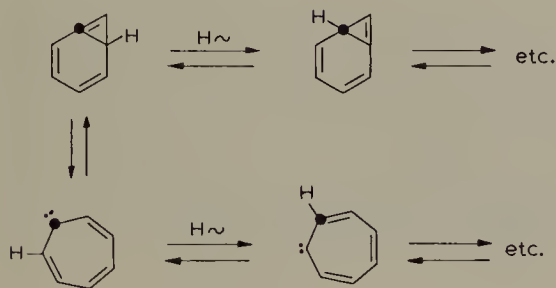


It is known [120] that phenylcarbene undergoes ring contraction reactions at high temperatures to give fulvenallene and ethynylcyclopentadiene.



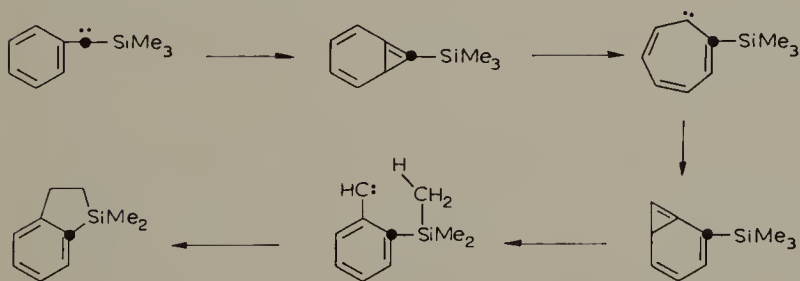
Crow and Paddon-Row [121] carried out a carbon-13 tracer study of this interesting

reaction, using $\text{Ph}^{13}\text{CH}_3$, and, using a derivative of the hydrocarbon products to facilitate ^{13}C -n.m.r. analysis, found that the two products were *uniformly labeled*. If the rearrangement mechanism mentioned in the previous paragraph is applied to carbon-13 labeled phenylcarbene itself, the eventual result is to scramble the label uniformly among all of the carbons *except C-1* of the ring. In order to explain their results, Crow and Paddon-Row [121] proposed that the above mechanism be modified by including hydrogen shift steps.



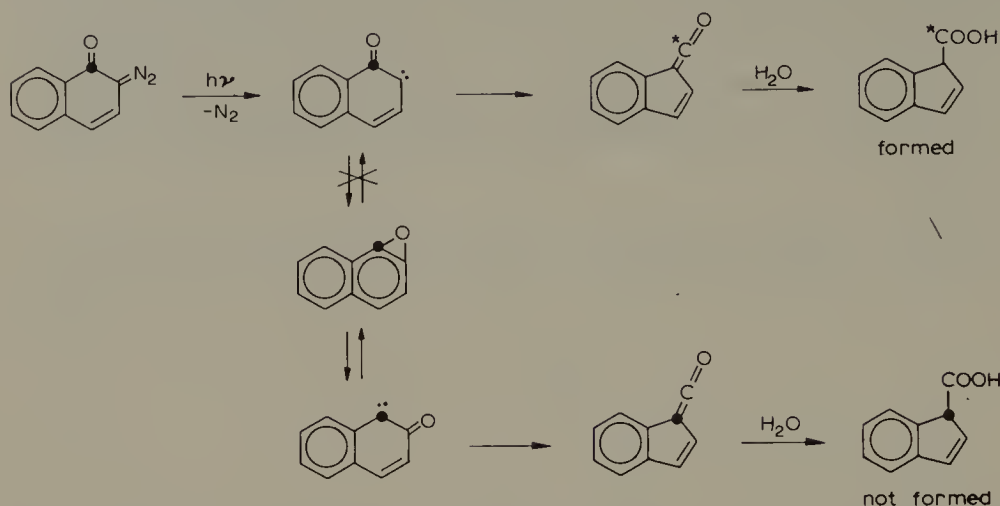
They suggest that the reason Hedaya and Kent [67] did not observe such hydrogen shifts in their tolylcarbene experiments is that the rate of hydrogen shifts may be much slower than the rate of carbene migration, but that both processes are much faster than the rate of ring contraction. More work obviously needs to be done on these fascinating reactions.

Further support for bicyclic and cycloheptatrienylidene intermediates of the above type comes from the carbon-13 tracer study by Barton et al. [122] who generated phenyltrimethylsilylcarbene by pyrolysis of (i) carbon-13 labeled phenyltrimethylsilyldiazomethane and (ii) the lithium salt of the tosylhydrazone of carbon-13 labeled phenyl trimethylsilyl ketone, leading eventually to benzodimethylsilacyclopentane. As shown by ^{13}C -n.m.r. and mass spectrometry, all of the carbon-13 label was found in a single position in the aromatic ring, and none in the saturated ring. This finding rules out an alternate mechanism involving a silacyclopropane ring [123], and supports the mechanism shown below.



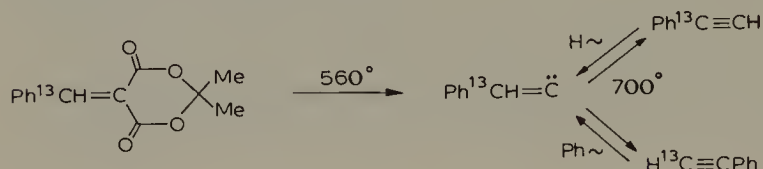
Using ^{13}C -n.m.r. and mass spectrometry, Zeller [124] has recently demonstrated that oxirene formation is not involved in the photolytic Wolff rearrangement of 2-diazonaphthalene-(2 H)-one-1- ^{13}C . All of the carbon-13 initially at the 1-position of the naphthalene ring was found in the carboxyl group of the product indene-1-carboxylic

acid; none was found in the indene ring as would be expected if an oxirene intermediate had been formed.



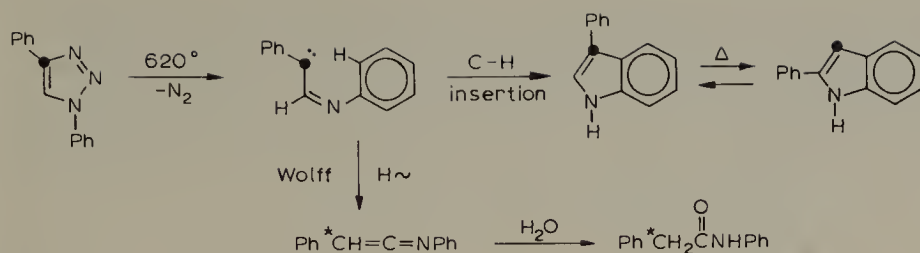
Alternatively, the oxirene ring might be an incidental side intermediate, opening only in the way it had originally formed; or the loss of nitrogen and migration of the ring carbon might be concerted.

Brown et al. [125], using ^{13}C -satellite p.m.r. analysis found that carbon-13 labeled benzyldenecarbene, generated from a benzyldene malonate at 560° and 0.1 mm Hg in a flow system, rearranged to a mixture of 1- and 2-labeled phenylacetylene. They also found that the two alkyne carbons in 1-phenylacetylene-1- ^{13}C were completely scrambled in a similar experiment at 700° , which they interpreted as involving reversible formation of the carbene.

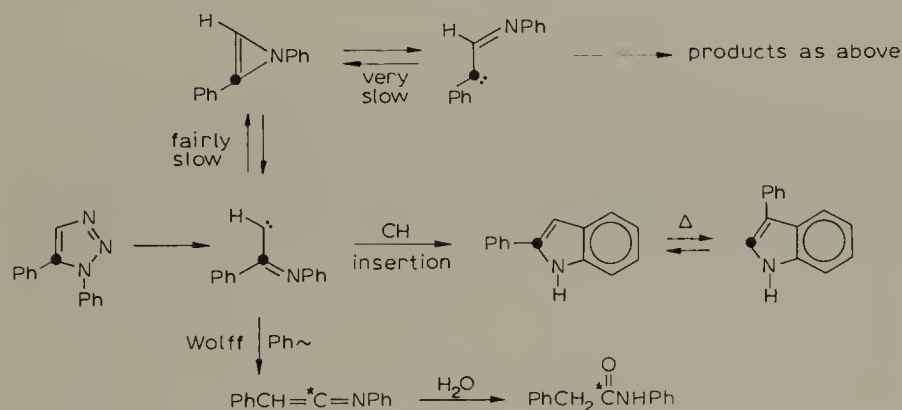


An earlier study [126] of the possible anionic rearrangement of phenylacetylene-1- ^{13}C showed no alkyne carbon scrambling at temperatures up to 178° , even in the presence of strong bases.

In a detailed carbon-13 tracer study of the pyrolysis of 1,4- and 1,5-diphenyl-1,2,3-triazoles, Gilchrist et al. [127] found that the major products were 2- and 3-phenylindole, and phenylacetanilide (formed by hydrolysis during workup of the identified intermediate *N*-(phenylvinylidene)-aniline; small amounts of 1-phenylindole were also found). The 2- and 3- phenylindoles were shown to interconvert under the reaction conditions. The distribution of carbon-13 in the products of the pyrolysis (620° , 0.01 mm Hg) of 1,4-diphenyl-1,2,3-triazole-4- ^{13}C was consistent with the following mechanism involving an iminocarbene which could undergo Wolff rearrangement or insertion into an aromatic C-H bond.



However, the pyrolysis of 1,5-diphenyl-1,2,3-triazole-5- ^{13}C had a more complex mechanism, as shown by the fact that the 2- and 3-phenylindoles were both labeled at *both* the 2- and 3- positions; also, the phenylacetanilide was labeled in *both* the methylene and carbonyl carbons. In order to explain these results, in addition to a mechanism of the above type, closure of the carbene to an azirine ring was postulated, which could open to give the carbene shown above, and the products derived from it.

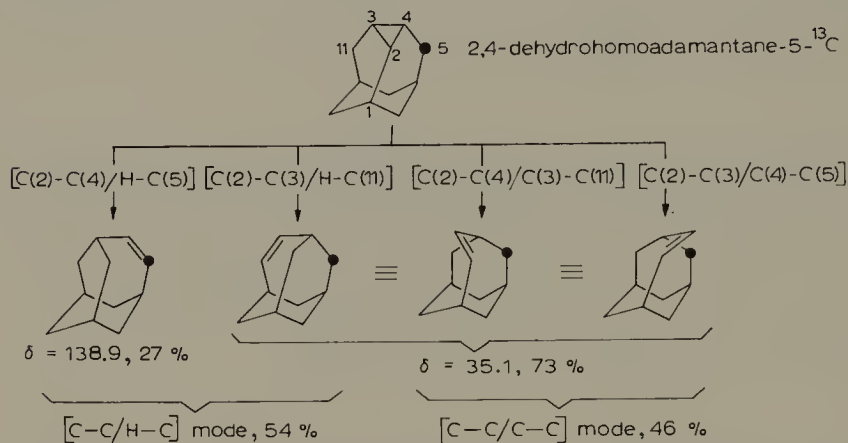


The authors suggest that the steric effects of the adjacent phenyl groups in the carbene formed from the 1,5-substituted compound facilitate closure of the azirine ring, and that such a closure for the isomeric carbene should be very slow.

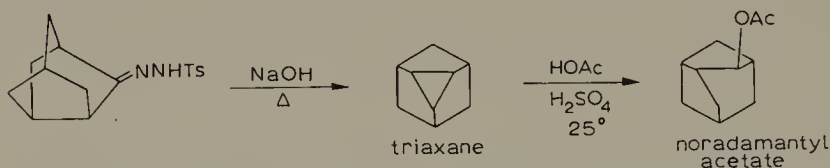
Brown and Butcher [128] used ^{13}C -satellite p.m.r., together with infrared and mass spectroscopy, (but not the more definitive ^{13}C -n.m.r. spectroscopy) to show that the benzonitrile obtained as one of many products in the pyrolysis (850° , 0.7 mm Hg) of oxindole-3- ^{13}C was ring labeled, presumably about randomly. None of the label was found in the nitrile carbon. Mechanisms postulated to rationalize the results involved arylnitrenes and arylcarbenes and their rearrangements by ring expansion and contraction.

Baldwin and Grayston [129] have studied the pyrolytic (ca. 400°) ring opening reactions of the conformationally restricted cyclopropane rings in 2,4-dehydroadamantane and 2,4-dehydrohomoadamantane-5- ^{13}C , to protoadamantene and homoadamantene, respectively (see below). They found that the reactions proceed 20–80 times more rapidly than the analogous “unrestricted” ring opening of methylcyclopropane to 1-butene. Cyclopropane ring opening reactions have been thought to involve 1,3-

diradicals with the terminal groups in the plane of the carbon atoms, but the results of this study seem to indicate that such a mechanism is not necessary, and that the bonding changes are concerted. Furthermore, in these reactions, $[C-C/C-C]$ rearrangement modes were shown to be competitive with $[C-C/H-C]$ modes by the carbon-13 results.

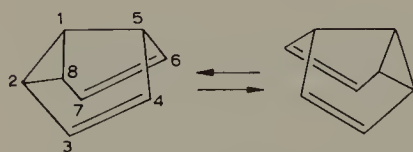


Carbon-13-n.m.r. spectroscopy played a leading role in the discovery by Nickon and Pandit [130] of the interesting tetracyclic hydrocarbon triaxane. In synthesizing triaxane the sodium salt of the *p*-toluenesulfonylhydrazone shown below was pyrolyzed, and the carbene so formed underwent a C-H insertion reaction to give the cyclopropyl ring.



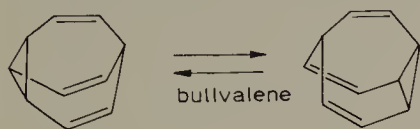
The proton decoupled ^{13}C -n.m.r. spectrum of the highly symmetrical triaxane consisted of only three peaks of equal intensity. Opening of the cyclopropyl ring took the normal course to give noradamantyl derivatives.

The (thermal) rearrangements involved in valence tautomerism can be studied very effectively by the use of ^{13}C -n.m.r. spectroscopy. For instance, at room temperature, (or -95°) semibullvalene shows a simple three line spectrum [131,132], corresponding to rapid valence tautomerism, but at -160° the five line spectrum [132] of the individual tautomers appears.



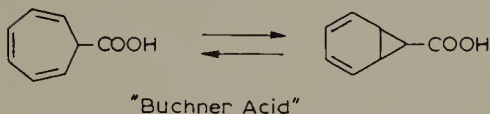
-95°		-160°	
Carbons	δ	Carbons	δ
2,8		2,8	42.2
1,5	50.7	1	48.0
2,4,6,8	87.2	5	53.1
3,7	121.7	3,7	121.7
		4,6	131.8

Analysis of the variation of ^{13}C -n.m.r. line shapes with temperature enables the activation parameters to be determined for such degenerate bonding changes as those involved in the Cope rearrangements of bullvalene [133,134], and cyclooctatetraene dimer [135].



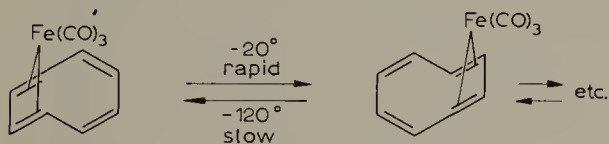
$$\begin{aligned}\Delta G^\ddagger &= 12.6 \text{ kcal mol}^{-1} \\ \Delta H^\ddagger &= 13.9 \text{ kcal mol}^{-1} \\ \Delta S^\ddagger &= 4.4 \text{ e.u.}\end{aligned}$$

Using ^{13}C -n.m.r. and p.m.r. spectroscopy and deuterium labeled compounds, Wehner and Gunther [136] have recently demonstrated the valence tautomerism between the cycloheptatriene and norcaradiene structures of one of the "Buchner Acids".

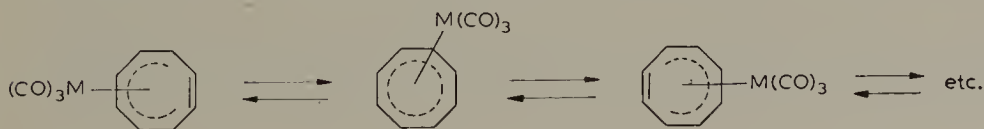


The same type of behavior was also observed for a number of esters of related structure [137].

The valence tautomerism of the cyclooctatetraene (COT) and tetramethylcyclooctatetraene (TMCOT) rings complexed in tricarbonylmetal compounds has also been studied utilizing the temperature dependence of ^{13}C -n.m.r. spectra. The general field has been reviewed recently by Cotton [138]. At least two quite different kinds of behavior have been noted, one involving 1,2-shifts [139] and the other random shifts [140]. At -20° the (proton coupled) ^{13}C -n.m.r. spectrum of the COT ring in (COT)- $\text{Fe}(\text{CO})_3$ consists [141] only of a doublet ($J_{^{13}\text{C-H}} \cong 158 \text{ Hz}$), showing rapid valence tautomerism of the 1,2-shift type.



At -120° this doublet was split into four well separated doublets corresponding to the four different types of carbons in the "frozen" molecule. The behavior of (TMCOT)- $\text{Cr}(\text{CO})_3$ was similar [140]. On the other hand, for (COT) $\text{M}(\text{CO})_3$ for $\text{M} = \text{Cr}, \text{Mo},$ or W , based on the fact that the four peaks representing the four different kinds of carbons in the COT ring all broadened at the same rate as the temperature was changed, a 1,2-shift mechanism was ruled out [140]. Instead a mechanism was invoked involving random shifts in a nearly planar "piano stool" intermediate or transition state.



Carbonyl group scrambling also takes place, independently of the above ring rearrangements.

Another kind of thermal rearrangement was observed by Schmidbaur et al. [142] in the temperature dependent ^{13}C -n.m.r. spectrum of tetramethylmethoxyphosphorane. The compound has a trigonal bipyramidal structure with the methoxy group at one of the axial positions. At -90° the proton decoupled ^{13}C -n.m.r. spectrum shows a clear high intensity doublet, $J_{\text{PC}} = 116.0$ Hz, corresponding to the three equatorial methyls, and two well separated lower intensity doublets, $J_{\text{PC}} = 7.3$ and 6.8 Hz, corresponding to the axial methyl and the methoxy methyl, respectively. When the temperature was increased to $+35^\circ$, the coupling disappeared from the methoxy signal, and the separate axial and equatorial methyl signals were replaced by a new doublet at the weighted average chemical shift and with the weighted average coupling constant (88 Hz). Clearly, the axial and equatorial methyls are undergoing rapid intramolecular scrambling at the higher temperature. (Intermolecular exchange of the methoxy group by reversible decomposition to methanol and trimethylmethylenephosphorane was postulated to account for features of the p.m.r. and non-proton-decoupled ^{13}C -n.m.r. spectra.)

E. Radical reactions studied by ^{13}C -n.m.r. CIDNP

The use of chemically induced dynamic nuclear polarization, CIDNP, to study the mechanisms of radical reactions has become well established in p.m.r. spectroscopy [143–145] and several examples have appeared recently in which ^{13}C -n.m.r. spectroscopy has been used. In these reactions positive (absorption, *A*) or negative (emission, *E*) enhancements of the normal n.m.r. signals are observed in the just formed products of the reactions. These *A* and *E* enhancements arise when the odd electrons of a pair of dissimilar radicals interact with the nuclear magnetic moments of the atoms near the reaction site. This interaction can induce singlet–triplet mixing in the caged radical pair, and the mixing will generally be faster for one carbon-13 nuclear state than for the other, depending on the difference in the electronic *g* factors for the two radicals and the sign and magnitude of the hyperfine coupling constant, *a*, for the particular radical of interest. Thus the populations of the two nuclear states in the singlet radical pair will be different from those in the triplet pair. If reaction to form products then “sorts” between singlet and triplet pairs, the product will contain an excess or a deficiency of one nuclear state at the molecular site of interest, which will appear as *A* or *E* enhancement in the n.m.r. spectrum. This “sorting” in caged radical pairs often involves radical–radical combination reactions to produce singlet state products. The longer lived triplet radicals, with the excess or deficiency of a particular nuclear state reversed, have a larger probability of escaping from the cage and being scavenged by solvent, etc., or of reacting by encounters with other free radicals. These products would then have the sense (sign) of the enhancement reversed relative to those from the caged pair reactions. It is this framework that permits mechanistic conclusions to be drawn from the sense of the enhancement, i.e. does a product arise from a cage re-

reaction, or from an encounter between two presorted free radicals?

Because of the several factors involved in predicting the sense of the enhancement for a particular mechanistic path, it is convenient to use the "Kaptein rules" [145] for the signs of the polarization for radical pair interactions. For carbon-13 work, if proton decoupling is used there are no complications from spin coupled multiplets and the sign of the net polarization at a given product site, + for absorption, *A*, and – for emission, *E*, is given by multiplying the signs of the individual terms in the expression,

$$\text{net polarization} = \mu\epsilon\Delta g a$$

where μ and ϵ enter with the following signs.

$$\mu \begin{cases} - & \text{when the radical pair is formed from a singlet precursor, as in thermal bond} \\ & \text{rupture;} \\ + & \text{when the pair is formed from a triplet precursor, as in phototriplet produc-} \\ & \text{tion, or by encounter of previously "sorted" free radicals;} \end{cases}$$

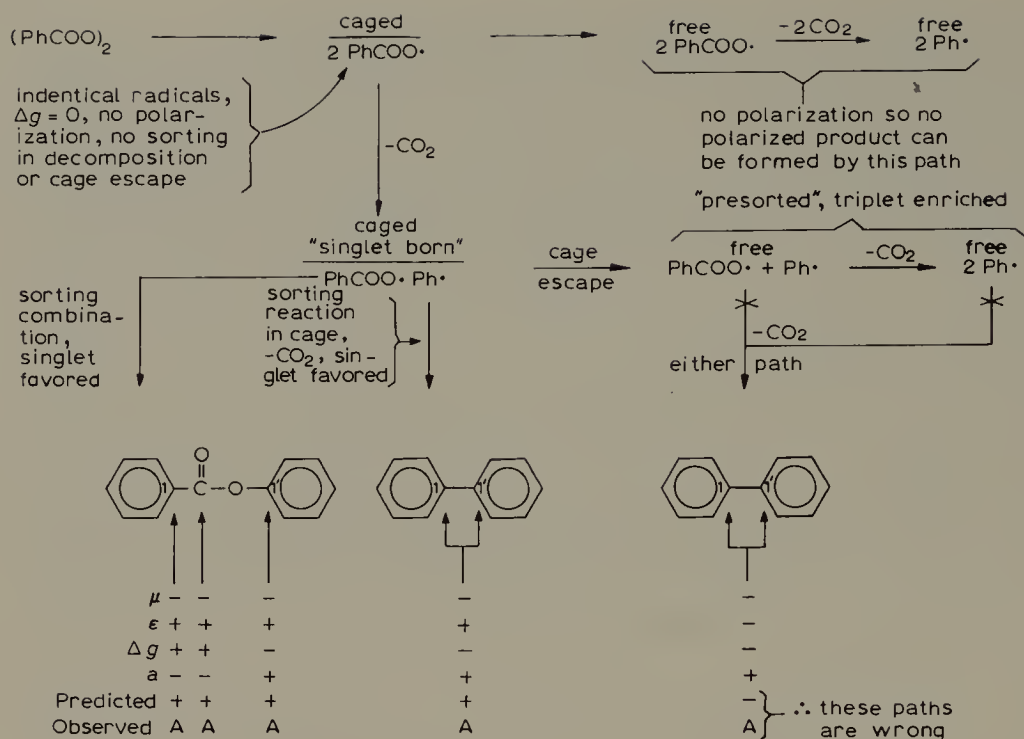
$$\epsilon \begin{cases} + & \text{for combination or disproportionation products arising from caged "sort-} \\ & \text{ing" reactions;} \\ - & \text{for products arising from radicals escaped from the cage (radical transfer,} \\ & \text{addition, coupling, etc.).} \end{cases}$$

The Δg term is the electronic *g* value for the radical site being considered minus the *g* value for the other radical of the caged pair. The *a* term is the hyperfine coupling constant for the radical being considered. The *g* and *a* terms are usually available or estimatable from e.s.r. data.

In 1970 Lippmaa et al. [146] first reported the use of ^{13}C -n.m.r. CIDNP techniques to study the decomposition of benzoyl peroxide and acetyl benzoyl peroxide. For benzoyl peroxide, absorption signals (*A*) were noted for the central (1,1') carbons of diphenyl and for the three central carbons (1, carbonyl, and 1') of phenyl benzoate; emission signals (*E*) were observed for benzene and carbon dioxide; the benzoic acid product was not polarized. For acetyl benzoyl peroxide the results were similar, although no polarized benzene was detected. Subsequently, a more detailed ^{13}C -n.m.r. CIDNP study of the decomposition of benzoyl peroxide in tetrachloroethylene appeared [147] with the results for the most part confirming those reported above. Again, no polarized benzene was detected, and strong emission signals were noted for the chlorobenzene and trichlorostyrene produced.

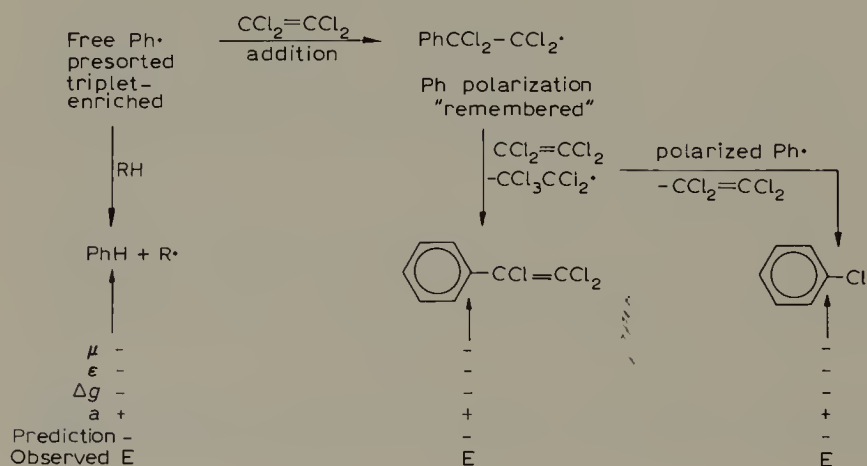
Several aspects of the mechanisms of these reactions were clarified by comparison of the experimental results with those predicted by application of the Kaptein rule [145], and for illustrative purposes these reactions are treated in some detail below. (Many other details of the mechanisms are not treated here.)

It is seen that all of the indicated carbons in phenyl benzoate show enhanced absorption (+, *A*) as predicted by the Kaptein rule for reaction through the caged radical pair $\text{PhCOO}\cdot\text{Ph}\cdot$. The fact that the biphenyl shows enhanced absorption clearly indicates



that it is formed, at least in part, by CO_2 extrusion and concerted collapse within the caged radical pair $\text{PhCOO}\cdot \text{ Ph}\cdot$. As indicated, other likely paths to biphenyl should give emission (negative enhancement), so such paths are incorrect, at least as its sole source. Since the CO_2 formed showed emission, at least some of it must have come from the presorted triplet enriched $\text{PhCOO}\cdot$ radical.

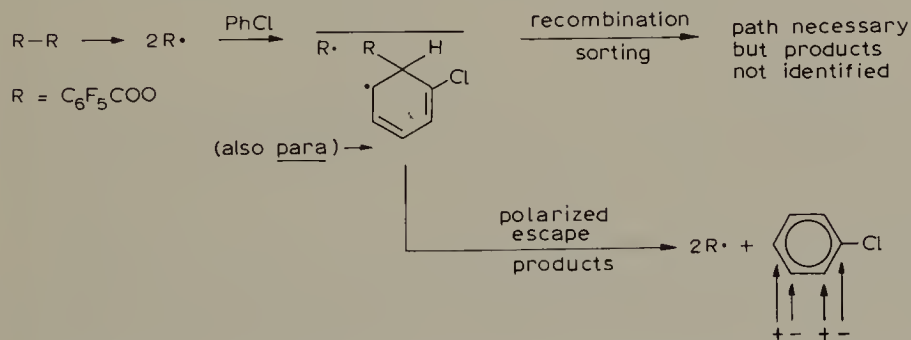
The likely origins of the benzene (*E*), chlorobenzene (*E*), and trichlorostyrene (*E*) are indicated below.



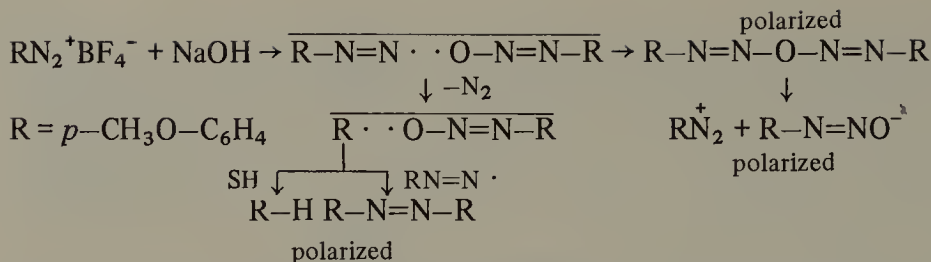
In the work of Lippmaa et al. [146] the decomposition was carried out in cyclohexanone, an excellent hydrogen source (RH on the arrow at the left above), so *E* benzene is readily formed. However in the more recent work [147], no easily available hydrogen source was present, and the polarized Ph^\bullet would have time to relax before a productive encounter to form benzene could take place. Therefore it is not surprising that polarized benzene was not detected.

Kaptein et al. [148] have carried out a detailed proton, deuterium, and enriched carbon-13 CIDNP spectral study of the decomposition of acetyl peroxide, and have determined the mechanism to be very similar to that described above. One of the main conclusions from the enriched carbon-13 experiments was that the methyl acetate was formed by an intramolecular caged radical pair reaction of the type described above, rather than by an intermolecular reaction.

The ^{13}C -n.m.r. CIDNP spectrum of chlorobenzene, increased absorption at C-2 and C-4, and decreased absorption at C-1 and C-3, observed during the photolysis of perfluorobenzoyl peroxide in CDCl_3 –30% chlorobenzene, provided evidence for the reversible formation of a σ -complex of the perfluorobenzoyloxy radical with chlorobenzene [149]. Application of the Kaptein rule [145] to the individual preferential polarizations in the chlorobenzene led to the conclusion that attack was predominantly at the *ortho* and *para* positions.

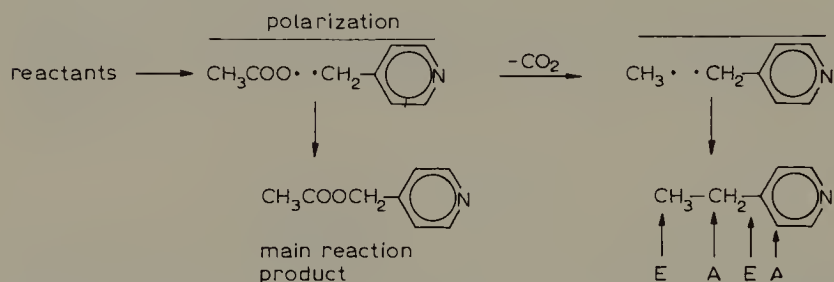


Berger et al. [150] demonstrated the great advantage of the pulsed Fourier transform technique, especially for fast reactions, in a ^{13}C -n.m.r. CIDNP study of the reaction of *p*-methoxyphenyldiazonium tetrafluoroborate in acetonitrile with methanolic sodium hydroxide. The main product of the reaction, anisole, showed CIDNP emission at C-4, as did the coupling side product 4,4'-dimethoxyazobenzene, (emission at the same position, C-1 in this compound). A strong positive enhancement appeared at C-1 of the original diazonium salt, so it is obviously undergoing a reversible unsymmetrical caged radical pair reaction of some sort. (Phenyl- and *p*-nitrophenyldiazonium salts did not exhibit similar behavior.) The authors speculate that the polarized diazonium ion might be formed by recombination of the caged radical pair $\text{R}-\text{N}=\text{N}^\bullet \cdot \text{O}-\text{N}=\text{N}-\text{R}$ to form the diazoanhydride, and thence the diazonium ion. The anisole and azoanisole would then be formed by loss of nitrogen, followed by appropriate free radical encounters.



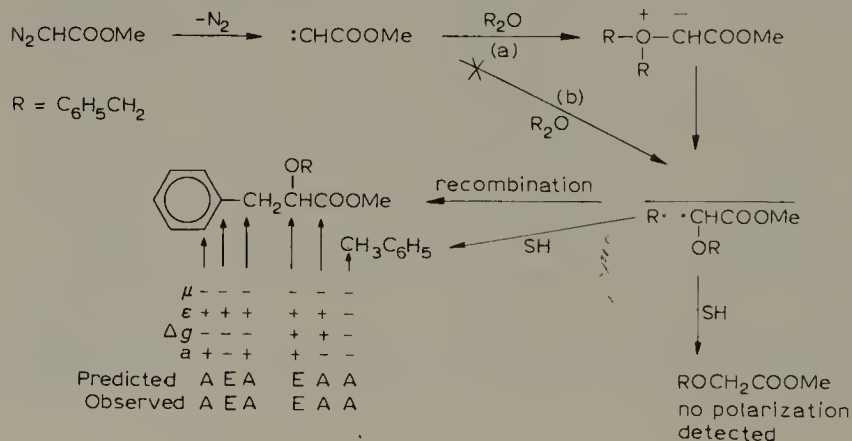
Using estimated values of a and g , the authors show that this mechanism is in accord with Kaptein's rule [145]. Other possible routes to the polarized diazonium ion are also mentioned.

The pulsed Fourier transform technique was also used [151] to study the growth and decay, all within 300 sec, of the ^{13}C -n.m.r. CIDNP spectrum during the reaction of 4-picoline-*N*-oxide with acetic anhydride to form 4-ethylpyridine. Using the Kaptein rule [145] the authors proposed that the mechanism involved polarization in the 4-picolyl-acetoxy radical pair, rather than in the 4-picolyl-methyl radical pair, since Δg would be ca. 0 in the latter pair.



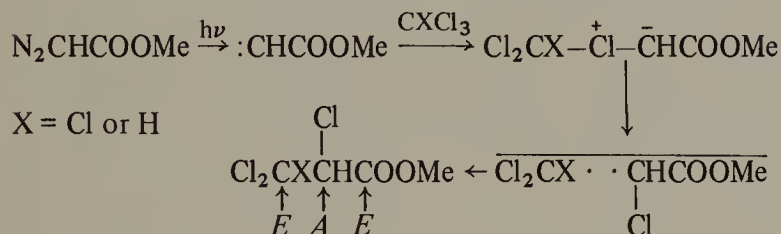
The A and E enhancements as shown were in agreement with the Kaptein rule predictions.

On the basis of p.m.r. and ^{13}C -n.m.r. CIDNP data, together with product studies, Iwamura et al. [152] concluded that both ylide and caged radical pair intermediates were involved in the reaction of methyl diazoacetate with dibenzyl, benzyl phenyl, and benzyl ethyl ethers. With dibenzyl ether, the ether insertion product had the ^{13}C CIDNP enhancements shown below. The ^{13}C results were interpreted in terms of the following mechanism path (a) with the Kaptein rule [145] analysis as indicated.



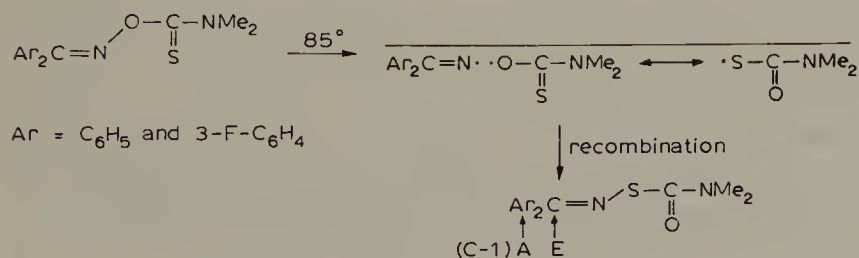
The direct formation of the caged radical pair, path (b), rather than through the ylide, path (a), was ruled out because of the greater yield of methyl benzyloxyacetate than of methyl ethoxyacetate in the case where the reactant was benzyl ethyl ether, and because of the failure to detect CIDNP in the methyl benzyloxyacetate. If direct radical pair formation were the main path, the more stable benzyl radical would be expected to form more readily, leading to higher yields of the methyl ethoxyacetate. Presumably the methyl benzyloxyacetate is formed by a normal Hoffmann-type β -elimination of ethylene from the ylide, and thus no CIDNP would be expected. It is puzzling that no CIDNP was observed in the methyl benzyloxyacetate produced when dibenzyl ether was used, since the toluene was polarized and the Hoffmann-type β -elimination from the ylide is not an available path.

On the basis of ^{13}C -n.m.r. CIDNP data, formation of a chloronium ylide which undergoes intramolecular rearrangement through a caged radical pair was supported [153] as the mechanism of the photolysis of methyl diazoacetate in various halomethanes.



The enhancements indicated are as predicted by Kaptein's rule [145] for recombination of the caged radical pair shown. When the solvent was CH_2Cl_2 , no ^{13}C -n.m.r. CIDNP was observed, since Δg was estimated to be near zero. When the solvent was CFCl_3 , Δg was also near zero, and the emission observed at C-3 was interpreted in terms of a multiplet effect of C-3 coupling with the fluorine atom. The authors argue against a radical chain mechanism on the basis that a radical chain carrier such as $\text{CXCl}_2\cdot$ would be expected to relax its initial polarization during the chain process, leading to non-polarized products, and that such a chain process would not lead to polarization at positions other than C-3.

The rearrangement of oxime derivatives to thiooxime derivatives was shown to be an intramolecular radical cage recombination reaction by a ^{13}C -n.m.r. CIDNP study [154]. The signs of the enhancements observed were in accord with this mechanism, as analyzed by Kaptein's rule [145].

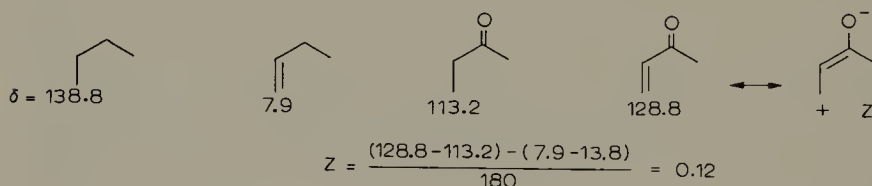


Some of the other aromatic carbons were also polarized, but these were not analyzed. No polarization could be found for the minor product, $\text{Ar}_2\text{C}=\text{N}-\text{N}=\text{CAr}_2$, the dimer of the cage escape iminyl radical $\text{Ar}_2\text{C}=\text{N}\cdot$, nor for the dimeric products of the other cage escape radical. The authors suggest that since the iminyl radical has a relatively long life, nuclear relaxation takes place before dimerization.

F. Miscellaneous reactions and other mechanistic applications of ^{13}C -n.m.r. spectroscopy

The delocalization of electrons in cationic systems has been studied extensively by ^{13}C -n.m.r. techniques, especially by Olah et al. [69,155], and the results have often been couched in terms of contributions of specific canonical structures to a resonance hybrid. Basically, these are structural studies of carbenium and carbonium ions, and as such will not be dealt with further in this chapter.

Numerous authors have couched their analyses of such charge distributions in neutral molecules in these same terms, and some of these applications are reviewed here. For conjugated unsaturated ketones Levin and Weingarten [156] have developed a simple formula for evaluation of the contribution of the 1,4-dipolar valence bond structure to the resonance hybrid by relating the observed chemical shifts of the conjugated ketone to the chemical shifts of the corresponding alkenes, alkanes, and saturated ketones and the chemical shift to be expected from a full π -electron deficiency, taken as 180 p.p.m. For instance, for vinyl methyl ketone, the contribution, Z , of the 1,4-dipolar structure to the resonance hybrid is 0.12.

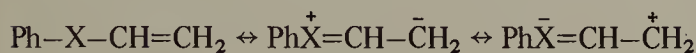


Such calculations for a series of enones lead to values and trends of Z in agreement with qualitative expectation, and hopefully such approaches can lead to predictions of chemical reactivity as well as to simply understood electronic descriptions of molecules, and perhaps also can focus attention on anomalies.

There is undoubtedly a strong correlation between chemical reactivity and electron deficiency at a given site, as measured by ^{13}C -n.m.r. chemical shift relationships such as that indicated above. Many "Hammett type plots" of chemical shifts vs. σ or σ^+ show good linear correlations. For instance Olah et al. [157] showed such a relationship between σ^+ and the chemical shifts of the cationic carbon for a series of *m*- and *p*-substituted cumyl carbenium ions in $\text{SbF}_5\text{-SO}_2$ solution. But simple correlations between carbon-13 chemical shifts, electron density, and chemical reactivity should be approached with caution. There are many factors besides electron density which con-

tribute to carbon-13 shielding. Brown and Peters [158] have pointed out that rates of solvolysis of a series of substituted tertiary esters of *p*-nitrobenzoic acid do not correlate at all well with the carbon-13 chemical shifts of the corresponding tertiary carbenium ions.

The carbon-13 chemical shifts for both the α - and β -carbons in both phenyl vinyl ethers and phenyl vinyl sulfides containing various *m*- and *p*-substituents give good linear correlations with σ (the ρ values are of opposite sign for the α - and β -positions) [159]. However the chemical shift differences between the α - and β -positions for the ethers were much larger than those for the sulfides. This was interpreted in terms of resonance structures for the sulfide in which the sulfur can accept additional pi electrons from the vinyl double bond ($d\pi-p\pi$ overlap).

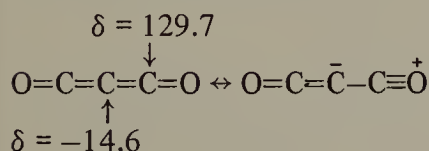


important for
X = S and O

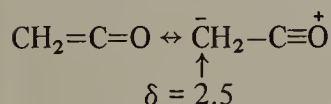
important only
for X = S

The bonding between phosphorus and carbon in phosphorus ylides has also been studied by ^{13}C -n.m.r. techniques in an effort to evaluate similar $d\pi-p\pi$ interactions [160].

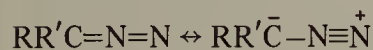
The interesting molecule C_3O_2 , carbon suboxide, has recently been shown [161] to have very high shielding of the central carbon, presumably due to resonance interaction of the type shown.



The very high shielding of the terminal carbon in ketene was interpreted in terms of a large contribution from a similar resonance structure [162].



More recently, Firl et al. [163] have shown that the corresponding carbon in a series of substituted diazomethanes also is very highly shielded.



$\delta = 23.1$ for $\text{R} = \text{R}' = \text{H}$, ranging upward to 62.5 for $\text{R} = \text{R}' = \text{Ph}$

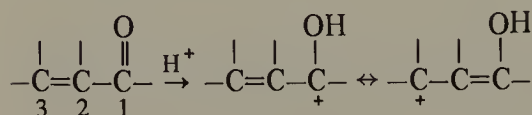
The site of protonation of molecules containing more than one basic center, usually as part of a conjugated system, has obvious mechanistic implications. Carbon-13 n.m.r. spectroscopy has been a particularly valuable tool in studying this matter, since the chemical shifts are very sensitive to the positive charge density on carbon and other environmental considerations. An early interesting example of the use of enriched carbon-13 (56%) in such studies was the demonstration by Olah and White [164] that the

protonated form of carbonic acid was the symmetrical trihydroxycarbenium ion. The carbon-13 spectrum was a clear quartet with $J = 4.5$ Hz, showing coupling to the three equivalent hydroxyl hydrogens.

Acids [165–167] and esters [165,168] protonate on the carbonyl oxygen rather than the hydroxyl or ether oxygens. Sulfoxides protonate on oxygen [169]. The observation of a doublet methyl signal in the ^{13}C -n.m.r. spectrum of *N,N*-dimethylformamide in from 0 to 100% sulfuric acid demonstrates that the predominant protonated form at all acidities is the O-protonated amide [170].

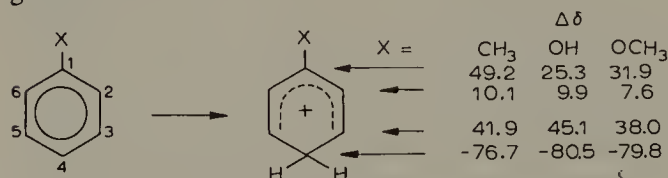


Unsaturated aldehydes and ketones protonate on oxygen [171] to form hydroxy-allylcarbenium ions.



The ^{13}C -n.m.r. downfield shift upon formation of the protonated species was always greater at C-3 than at C-1, corresponding to greater positive charge density at C-3. There was little change in chemical shift at C-2 upon protonation.

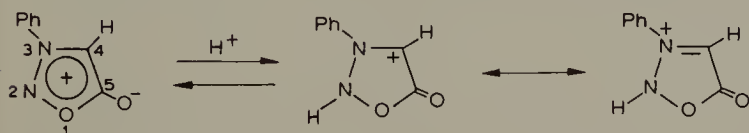
Olah and Mo [172] have carried out an extensive investigation of the sites of protonation of mono-, di-, and trihydroxy- and methoxybenzenes in various superacid solutions and have found evidence for both C- and O-protonation, sometimes in the same acid medium. They also found diprotonated species present in the strongest acid solutions of the polysubstituted compounds. Most of their conclusions were drawn from p.m.r. spectral data, but the ^{13}C -n.m.r. data on the protonation products from phenol and anisole show clearly that they are C-protonated to give the *p*-hydroxy- and *p*-methoxybenzenium ions. The details of the changes in chemical shifts, $\Delta\delta$ (downfield shifts positive), upon protonation provide valuable insight into the nature of the extensive positive charge delocalizations. Corresponding data for protonated toluene are also given.



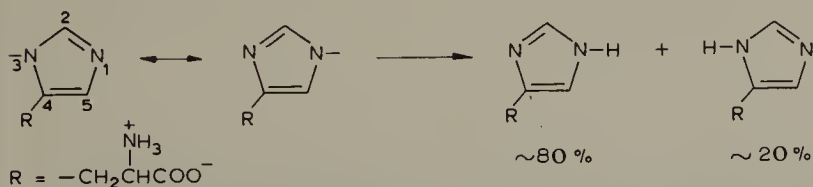
The upfield shifts of C-4 in all three compounds, and the downfield shifts of the other ring carbons, especially C-1 and C-3, show that C-4 is the position of protonation and that the positions *ortho* and *para* to the site of protonation bear most of the positive

charge. In anisole, the methoxy carbon is shifted downfield by 91.0 p.p.m. ($\Delta\delta = +91.0$), clearly indicating a substantial delocalization of the positive charge to the methoxy oxygen. (This delocalization of the charge to oxygen also "freezes" the methoxy group on one side of the ring and makes the methoxybenzenium ion unsymmetrical, so that the $\Delta\delta$ values for C-5 and C-6 are somewhat different from those for C-3 and C-2.) The smaller downfield shifts of C-1 in phenol and anisole than in toluene again show the electron donating ability of the hydroxy and methoxy oxygens.

On the basis of p.m.r. spectroscopic data in trifluoroacetic acid and $\text{HSO}_3\text{F}-\text{SbF}_5-\text{SO}_2$, Olah et al. [173] concluded that 3-phenylsydnone was protonated on the carbonyl oxygen. However, more recently Buglass [174], on the basis of ^{13}C -n.m.r. and ^{15}N -n.m.r. spectral data on this and related compounds contend that sydnones are protonated at N-2 in deuteriosulfuric acid. On shifting from CDCl_3 to deuteriosulfuric acid the downfield shift of the C-4 resonance was 11 p.p.m., while that for the carbonyl carbon was only 5 p.p.m. On shifting from $(\text{CD}_3)_2\text{CO}$ to 60% $\text{H}_2\text{SO}_4-\text{D}_2\text{O}$, the downfield shift for N-2 in 3,4-diphenylsydnone-2- ^{15}N (96% enrichment) was 29.9 p.p.m. Buglass also suggests that the downfield p.m.r. shift of the sydnone ring proton supports N-2 protonation.



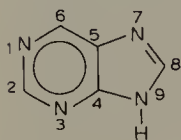
By showing that the ^{13}C -n.m.r. chemical shift vs. pH profiles for C-2, C-4, and C-5 in L-histidine were nearly the same as corresponding curves for 1-methyl-L-histidine and very different from those for 3-methyl-L-histidine, Reynolds et al. [175] concluded that the 1-H tautomer is the predominant tautomeric form of the imidazole ring in L-histidine.



This method should be of general applicability in determining the sites of protonation, or positions of tautomeric equilibria, of di- or polyfunctional compounds. Several other compounds containing the histidine ring, including some polypeptides, showed behavior similar to that of histidine.

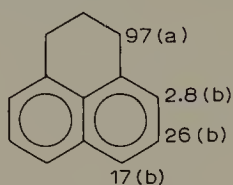
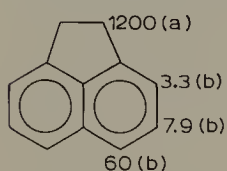
The same procedure, the use of *N*-methyl derivatives as model compounds to "freeze" the tautomeric equilibria of amidines, guanidines, and related compounds was used by Jackman and Jen [176] to systematize the use of ^{13}C -n.m.r. and p.m.r. spectroscopy in determining the predominant tautomeric forms present in such compounds.

On the basis of ^{13}C -n.m.r. data, Pugmire and Grant [177] concluded that the anion of purine was protonated with nearly equal facility at tautomeric positions N-7 and N-9, and that cation formation from the neutral molecule took place in the six membered ring by protonation at N-1.

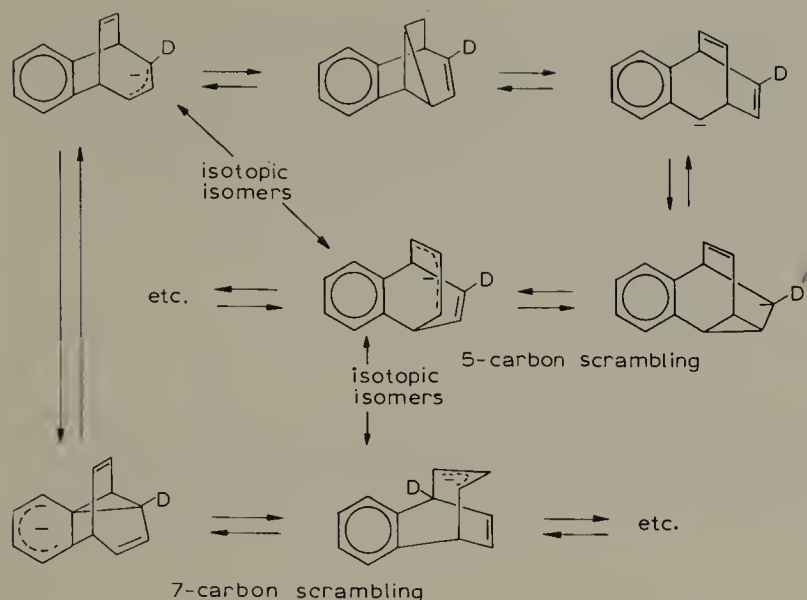


In much the same way that ^{13}C -n.m.r. spectroscopy can be used to assess the degree of positive charge at various positions in a carbocation, it can also be used to evaluate the delocalization of the charge in carbanions. In an early study [178] of six delocalized carbanions, it was found that all of the odd numbered carbons in all of the penta-dienyl and 3-vinylpentadienyl systems absorb at higher field than the even numbered carbons, as expected from resonance or molecular orbital theory. By comparison of the chemical shifts with those for alkenes, the authors concluded that there was very little charge density at all on the even numbered carbons. They noted a rough correlation between charge density as indicated by chemical shift and reactivity in nucleophilic displacement reactions.

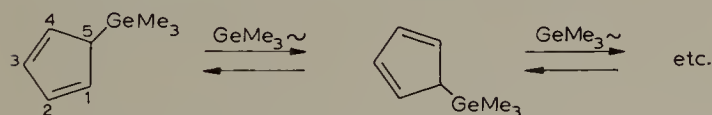
The base-catalyzed hydrogen–deuterium exchange rates for the various hydrogens in acenaphthene and related hydrocarbons has been studied [116,179] using ^{13}C -n.m.r. spectroscopy to monitor the positions and amounts of deuterium uptake. The exchange rates are controlled by carbanion stability and reactivity, and are quite sensitive to ring strain effects. Rate constants, $k_1 \times 10^7 \text{ s}^{-1}$ at 120.4° (a) or 204° (b) for two of the compounds studied are shown below.



The mechanism of the degenerate rearrangement of the 6,7-benzobicyclo[3.2.2]-nonatrienyl anion has been studied by Moncur et al. [180] using deuterium labeled substrate and ^{13}C -n.m.r. spectroscopy to measure the label scrambling. The anion was generated by treating the 2-deuterio-2-methylether with sodium–potassium alloy at 0° , and the reaction was run at 32° . The result was essentially statistical scrambling of deuterium into all nonbenzo positions (except for some perturbation due to an isotope effect). This finding required not only “5-carbon scrambling”, but also “7-carbon scrambling” in which a phenyl migration is involved. (See diagram on next page.) Upon quenching only 6,7-benzobicyclo[3.2.2]-2,6,8-nonatriene was formed, leading the authors to conclude that the benzylic anion (top right above) is less stable than the isomeric allylic anion by at least 2 kcal mol^{-1} .



Metal cyclopentadienyl complexes are of interest in that the carbon–metal bonding may be of the π or the σ type, and, if of the σ type, may or may not undergo rapid exchange reactions involving the other ring carbons (metallotropic rearrangements). At lower temperatures, the proton-decoupled ^{13}C -n.m.r. spectra of the cyclopentadienyl rings of many $\text{C}_5\text{H}_5\text{MR}_a\text{X}_b$ compounds consisted of three lines, characteristic of the three types of carbon in σ -bonded compounds [181]. For instance, for $\text{C}_5\text{H}_5\text{GeMe}_3$ at -20° , lines at $\delta = 52.1$ (C-5), 129.8 (C-2 and C-3), and 133.9 (C-1 and C-4) were observed. At higher temperatures many of these compounds undergo line broadening and degenerate rearrangements to give σ -compounds with only a single ^{13}C -n.m.r. line; for instance $\text{C}_5\text{H}_5\text{GeMe}_3$ shows only a single line, $\delta = 117.7$ at 125° . The rearrangement is thought to involve a series of 1,2 shifts.



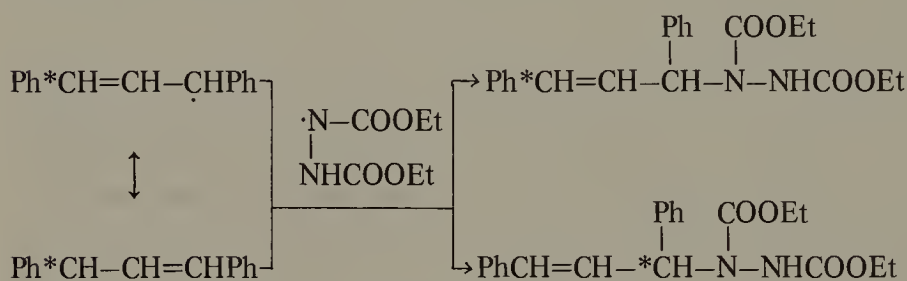
The rearrangement is believed to be intramolecular. Similar rearrangements were noted for cyclopentadienyl compounds of Sn, Si, Fe, and Hg. For $\sigma\text{-C}_5\text{H}_5\text{Fe}(\text{CO})_2\text{-}\pi\text{-C}_5\text{H}_5$, two ring signals were observed, at δ 113.1, corresponding to the weighted average of the three individual low-temperature signals of the σ -bonded ring, and at δ = 87.1, corresponding to the aromatic π -bonded ring.

The use of isotopic tracers to distinguish among mechanistic pathways in allylic systems, e.g., $\text{S}_{\text{N}}1$, $\text{S}_{\text{N}}2$, and $\text{S}_{\text{N}}2'$, is well known, and the procedure has been generalized by Shemyakin et al. [182] in connection with their study of the additions of $\text{Ph}^{13}\text{CH}=\text{CHCH}_2\text{Ph}$ and $\text{Ph}^{13}\text{CH}=\text{N}-\text{CH}_2\text{Ph}$ to diethyl azodicarboxylate. The reactions were carried out by refluxing in benzene for 4–5 h. The positions of the carbon-13 in the starting materials and products were determined by ^{13}C -n.m.r. and mass spectro-

copy. In both cases the position of the carbon-13 label in the recovered starting material was the same as in the initial reactant, eliminating any possibility of isotopic scrambling by reactant tautomerism. In the addition of the 1,3-diphenylpropene-1- ^{13}C , 85–88% of the label was in the 3-position, indicating predominant reaction by allylic inversion, perhaps by way of a six membered cyclic transition state.

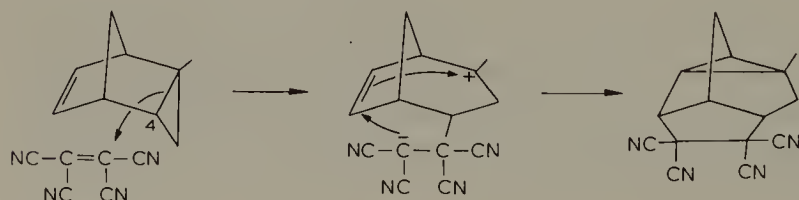


The remainder of the product was labeled in the 1-position possibly by way of a direct addition of the C-3-carbon–hydrogen bond to the nitrogen–nitrogen bond, or, more likely, by some path involving an allylic radical, in which case the 1- and 3-positions would be scrambled.



If this were the secondary mechanism of the reaction, since both 1- and 3-labeled products are necessarily formed, the allylic inversion path would account for only about 70% of the product. The results of the reaction with $\text{Ph}^{13}\text{CH}=\text{N}-\text{CH}_2\text{Ph}$ were similar, with the allylic inversion mechanism again being predominant.

Coxon et al. [183], have shown that the ^{13}C -n.m.r. spectrum of the addition product of tetracyanoethylene and 2-*exo*-methyl-*endo*-tricyclo-[3.2.1.0^{2,4}]oct-6-ene is consistent with that formed by regiospecific corner attack at C-4, and not with that formed by a $[\pi^2 + \pi^2]$ cycloaddition process.



Using ^{13}C -n.m.r. spectroscopy as the primary analytical tool, Stothers et al. [184] showed that the products of the reaction of azibenzil with sulfur dioxide were those arising from a $[4 + 2]$ cycloaddition of the first formed intermediates, diphenyl ketene and phenylbenzoylsulfene, rather than those derived by a $[2 + 2]$ cycloaddition as earlier proposed [185].

Using ^{13}C -n.m.r. techniques to determine the amount and position of deuterium incorporated into $\Delta^{8(14)}$ -cholesten-3-ol upon treatment with deuterium in the presence of palladium black, Siegel et al. [186] concluded that the exchange mechanism proposed earlier [187] was not acceptable in this case. There are five allylic hydrogens in this molecule, one at C-9 and two each at C-7 and C-15. The Rooney—Gault—Kemball mechanism [187] would have all five of these hydrogens exchanging readily through a metal— π -allylic complex which could abstract deuterium both from the metal surface on one side of the complex and from a molecule of deuterium positioned above the complex on the other side. A comparison of the ^{13}C -n.m.r. and mass spectral data showed that only one deuterium was exchanged at each of the C-7 and C-15 positions (plus the one at C-9).

The use of ^{12}C -labeling, the analysis depending on the disappearance of a ^{13}C -n.m.r. signal, to study the mechanism of a base catalyzed elimination reaction was discussed in the introduction to this chapter [24].

ACKNOWLEDGEMENTS

The financial support of the University of Arkansas, the National Science Foundation, and the United States Atomic Energy Commission, which made possible some of the authors' research described in this chapter, is gratefully acknowledged.

REFERENCES

- 1 R.B. Williams, *Ann. N. Y. Acad. Sci.*, 70 (1958) 890.
- 2 F. Kasler, *Quantitative Analysis by NMR Spectroscopy*, Academic Press, New York, 1973.
- 3 D.M. Rackham, *Talanta*, 17 (1970) 895.
- 4 A.F. Cockerill, R.C. Harden, G.L.O. Davies and D.M. Rackham, *Org. Magn. Reson.*, 6 (1974) 452.
- 5 W.B. Smith, *J. Chem. Educ.*, 41 (1964) 97.
- 6 T.G. Alexander and S.A. Koch, *Appl. Spectrosc.*, 21 (1967) 181.
- 7 J.L. Jungnickel and J.W. Forbes, *Anal. Chem.*, 35 (1963) 938.
- 8 C.A. Reilly, *Anal. Chem.*, 32 (1960) 221R.
- 9 R.B. Williams, *Conference on Molecular Spectroscopy*, Pergamon Press, New York, 1959, p. 26.
- 10 J.A. Pople, W.G. Schneider and H.J. Bernstein, *High-Resolution Nuclear Magnetic Resonance*, McGraw-Hill, New York, 1959.
- 11 G.C. Levy, *J. Chem. Soc., Chem. Commun.*, (1972) 47.
- 12 G.C. Levy, D.M. White and F.A.L. Anet, *J. Magn. Reson.*, 6 (1972) 453.
- 13 A. Allerhand, D.D. Doddrell and R. Komovski, *J. Chem. Phys.*, 55 (1971) 189.
- 14 G.N. LaMar, *J. Am. Chem. Soc.*, 93 (1971) 1040.
- 15 G.N. LaMar, *Chem. Phys. Lett.*, 10 (1971) 230.
- 16 D.F.S. Natusch, *J. Am. Chem. Soc.*, 93 (1971) 2567.
- 17 R. Freeman, K.G.R. Pachler and G.N. LaMar, *J. Chem. Phys.*, 55 (1971) 4586.
- 18 J.H. Shoolery and W.C. Jankowski, *Varian Applications Note*, NMR 73/74.
- 19 R. Freeman, H.D.W. Hill and R. Kaptein, *J. Magn. Reson.*, 7 (1972) 327.

- 20 G.C. Levy and V. Edlund, *J. Am. Chem. Soc.*, 97 (1975) 4482.
- 21 G.C. Levy and V. Edlund, *J. Am. Chem. Soc.*, 97 (1975) 5031.
- 22 G.C. Levy and G.L. Nelson, *Carbon-13 Nuclear Magnetic Resonance for Organic Chemists*, Wiley-Interscience, New York, 1972.
- 23 S.B.W. Roeder, *J. Magn. Reson.*, 12 (1973) 343.
- 24 J. Prestien and H. Günter, *Angew. Chem. Int. Ed. Eng.*, 13 (1974) 276.
- 25 C.T. Gregg, J.Y. Hutson, J.R. Prine, D.C. Ott and J.E. Furchner, *Life Sci.*, 13 (1973) 775.
- 26 T.J. Simpson, *J. Magn. Reson.*, 17 (1975) 262.
- 27 F.A.L. Anet and J.J. Wagner, *J. Am. Chem. Soc.*, 93 (1971) 5266.
- 28 F.A.L. Anet, C.H. Bradley and G.W. Buchanan, *J. Am. Chem. Soc.*, 93 (1971) 258.
- 29 F.A.L. Anet, J. Krane, W. Kitching, D. Doddercl and D. Praeger, *Tetrahedron Lett.*, (1974) 3255.
- 30 D.J. Chadwick, G.D. Meakins and E.E. Richards, *Tetrahedron Lett.*, (1974) 3183.
- 31 S.F. Nelsen and G.R. Weisman, *J. Am. Chem. Soc.*, 96 (1974) 7111.
- 32 C.S. Johnson, Jr., *Adv. Magnetic Resonance*, Vol. 1, Academic Press, New York, 1965.
- 33 J.W. Emsley, J. Feeney and L.H. Sutcliffe, *High Resolution Nuclear Magnetic Resonance Spectroscopy*, Chapter 9, Pergamon Press, Oxford, 1965.
- 34 J.A. Pople, W.G. Schneider and H.J. Bernstein, *High Resolution Nuclear Magnetic Resonance*, Chapters 10 and 13, McGraw-Hill, New York, 1959.
- 35 O.A. Gansow, J. Killough and A.R. Burke, *J. Am. Chem. Soc.*, 93 (1971) 4297.
- 36 Y.K. Greshin, N.M. Sergeyev, O.A. Subbotin and Y.A. Ustynyuk, *Mol. Phys.*, 25 (1973) 297.
- 37 L. Lunazzi, D. Macciantelli and A.C. Boicelli, *Tetrahedron Lett.*, (1975) 1205.
- 38 D.K. Dalling, D.M. Grant and L.F. Johnson, *J. Am. Chem. Soc.*, 93 (1971) 3678.
- 39 H.J. Schneider, R. Price and T. Keller, *Angew. Chem.*, 10 (1971) 730.
- 40 D. Doddrell, C. Charrier, B.L. Hawkins, W.O. Crain, L. Harris and J.D. Roberts, *Proc. Nat. Acad. Sci. U.S.*, 67 (1970) 1588.
- 41 O. Yamamoto, M. Yanagisawa, K. Hayamizu and G. Kotowycz, *J. Magn. Reson.*, 9 (1973) 216.
- 42 H.J. Schneider, T. Keller and R. Price, *Org. Magn. Reson.*, 4 (1972) 907.
- 43 F.A.L. Anet and P.J. Degen, *Tetrahedron Lett.*, (1972) 3613.
- 44 F.A.L. Anet, A.K. Cheng and J.J. Wagner, *J. Am. Chem. Soc.*, 94 (1972) 9250.
- 45 S. Masamune, K. Hojo, G. Bigam and D.L. Rabenstein, *J. Am. Chem. Soc.*, 93 (1971) 4966.
- 46 S. Masamune, A.V. Kemp-Jones, J. Green, D.L. Rabenstein, M. Yasunami, K. Takase and T. Nozoe, *J. Chem. Soc., Chem. Commun.*, (1973) 283.
- 47 L. Weiler, *Can. J. Chem.*, 50 (1972) 1975.
- 48 H.J. Reich and D.A. Murcia, *J. Am. Chem. Soc.*, 95 (1973) 3418.
- 49 W.F. Reynolds, I.R. Peat, M.H. Freedman and J.R. Lyerla, Jr., *J. Am. Chem. Soc.*, 95 (1973) 328.
- 50 J.H. Billman, S.A. Sojka and P.R. Taylor, *J. Chem. Soc., Perkin Trans. 2*, (1972) 2034.
- 51 I.K. O'Neill and M.A. Pringuer, *Org. Magn. Reson.*, 6 (1974) 398.
- 52 H.J. Schneider, D. Heiske, V. Hoppen and M. Schommer, *Tetrahedron Lett.*, (1974) 1971.
- 53 G.E. Hawkes, K. Herwig and J.D. Roberts, *J. Org. Chem.*, 39 (1974) 1017.
- 54 W. Voelter, O. Oster and K. Zech, *Angew. Chem. Int. Ed. Eng.*, 13 (1974) 131.
- 55 D. Doddrell and A. Allerhand, *J. Am. Chem. Soc.*, 93 (1971) 2779.
- 56 R. Fuentes, L.O. Morgan and N.A. Matwiyoff, *Inorg. Chem.*, 14 (1975) 1837.
- 57 D. Canet, J.J. Delpuech, M. R. Khaddar and P. Rubini, *J. Magn. Reson.*, 15 (1974) 325.
- 58 C.J. Carman and C.E. Wilkes, *Macromolecules*, 7 (1974) 40.
- 59 J. Schaefer, *Macromolecules*, 2 (1969) 210.
- 60 J. Schaefer, *Macromolecules*, 2 (1969) 533.
- 61 C.J. Carman, A.R. Tarpley and J.H. Goldstein, *Macromolecules*, 4 (1971) 445.
- 62 J. Schaefer, *Macromolecules*, 4 (1971) 107.
- 63 C.J. Carman and C.E. Wilkes, *Rubber Chem. Technol.*, 44 (1971) 781.

- 64 C.E. Wilkes, C.J. Carman and R.A. Harrington, *J. Polym. Sci., Part C*, (1973).
- 65 J.N. Shoolery, Varian Applications Note, NMR-75-3.
- 66 M. Oka, A. Fry, T.W. Whaley and J.F. Hinton, unpublished results, c.f. M. Oka Ph.D. Dissertation, University of Arkansas, 1973.
- 67 E. Hedaya and M.E. Kent, *J. Am. Chem. Soc.*, 93 (1971) 3283.
- 68 An excellent review of this topic has recently appeared by J.B. Stothers in *Topics in ¹³C-NMR Spectroscopy*, G.C. Levy, Ed., Vol. 1, Chap. 6, Wiley, New York, 1974, p. 229–286.
- 69 For an excellent and highly personalized recent review of this field see G.A. Olah, *Angew. Chem. Int. Ed. Eng.*, 12 (1973) 173.
- 70 G.A. Olah, A.M. White, J.R. DeMember, A. Commeyras and C.Y. Lui, *J. Am. Chem. Soc.*, 92 (1970) 4627.
- 71 H.C. Brown and K.T. Liu, *J. Am. Chem. Soc.*, 97 (1975) 600, and previous work cited there.
- 72 J. Elguero, C. Marzin and J.D. Roberts, *J. Org. Chem.*, 39 (1974) 357.
- 73 For leading references see T.N. Shatkina, E.V. Leont'eva and O.A. Reutov, *Dokl. Akad. Nauk SSSR*, 173 (1967) 113.
- 74 O.A. Reutov, T.N. Shatkina, E. Lippmaa and T. Pehk, *Dokl. Akad. Nauk SSSR*, 181 (1968) 1400; *Tetrahedron*, 25 (1969) 5757.
- 75 O.A. Reutov, T.N. Shatkina, E.V. Leont'eva, E. Lippmaa and T. Pehk, *Dokl. Akad. Nauk SSSR*, 183 (1968) 846.
- 76 A.N. Lovtsova, T.N. Shatkina, O.A. Reutov, E. Lippmaa and T. Pehk, *Dokl. Akad. Nauk SSSR*, 192 (1970) 346.
- 77 T.N. Shatkina, A.N. Lovtsova, O.A. Reutov, E. Lippmaa and T. Pehk, *Izv. Akad. Nauk SSSR, Ser. Khim.*, (1970) 726.
- 78 G.A. Olah and A.W. White, *J. Am. Chem. Soc.*, 91 (1969) 5801.
- 79 M. Saunders and E.L. Hagen, *J. Am. Chem. Soc.*, 90 (1968) 6881.
- 80 G.A. Olah, R.H. Schlosberg, R.D. Porter, Y.K. Mo, D.P. Kelly and G.D. Mateescu, *J. Am. Chem. Soc.*, 94 (1972) 2034.
- 81 G.A. Olah, G.D. Mateescu and Y.K. Mo, *J. Am. Chem. Soc.*, 95 (1973) 1865.
- 82 G.A. Olah, G. Liang and P. Westerman, *J. Am. Chem. Soc.*, 95 (1973) 3698.
- 83 J.A. Marshall, D.E. Miller and A.M. Ihrig, *Tetrahedron Lett.*, (1973) 3491.
- 84 A.T. Balaban and D. Farcasiu, *J. Am. Chem. Soc.*, 89 (1967) 1958.
- 85 H.A. Staab and M. Haenel, *Angew. Chem. Int. Ed. Eng.*, 7 (1968) 548.
- 86 A.T. Balaban, D. Farcasiu, V.A. Koptiyug, I.S. Isaev, M.I. Gorfinkel and A.I. Rezvukhin, *Tetrahedron Lett.*, (1968) 4757.
- 87 For leading references see R.M. Roberts and J.E. Douglas, *J. Org. Chem.*, 28 (1963) 1225.
- 88 R.M. Roberts, A.A. Khalaf and R.N. Greene, *J. Am. Chem. Soc.*, 86, (1964) 2846; see also A. Streitwieser, Jr., and L. Reif, *J. Am. Chem. Soc.*, 86 (1964) 1988.
- 89 D. Farcasiu, *Rev. Chim. (Bucharest)*, 10 (1965) 457.
- 90 R.M. Roberts and T.L. Gibson, *J. Am. Chem. Soc.*, 93 (1971) 7340.
- 91 F.H.A. Rummens, R.D. Green, A.J. Cessna, M. Oka and C.C. Lee, *Can. J. Chem.*, 53 (1975) 314.
- 92 M. Oka and C.C. Lee, *Can. J. Chem.*, 53 (1975) 320.
- 93 C.C. Lee, A.J. Cessna, B.A. Davis and M. Oka, *Can. J. Chem.*, 52 (1974) 2679.
- 94 C.C. Lee and M. Oka, *Can. J. Chem.*, 54 (1976) 604.
- 95 C.W. David, B.W. Everling, R.J. Kilian, J.B. Stothers and W.R. Vaughan, *J. Am. Chem. Soc.*, 95 (1973) 1265.
- 96 J.D. Roberts and J.A. Yancey, *J. Am. Chem. Soc.*, 75 (1953) 3165; W.R. Vaughan and R. Perry, Jr., *J. Am. Chem. Soc.*, 75 (1953) 3168; W.R. Vaughan, C.T. Goetschel, M.H. Goodrow and C.L. Warren, *J. Am. Chem. Soc.*, 85 (1963) 2282.
- 97 C.J. Collins and M.H. Lietzke, *J. Am. Chem. Soc.*, 95 (1973) 6842.
- 98 M. Farcasiu, D. Farcasiu, J. Slutsky and P. von R. Schleyer, *Tetrahedron Lett.*, (1974) 4059.

- 99 D. Lenoir, R.E. Hall and P. von R. Schleyer, *J. Am. Chem. Soc.*, 96 (1974) 2138.
- 100 C.M. Holden and D. Whittaker, *J. Chem. Soc., Chem. Commun.*, (1974) 353.
- 101 J.M. Coxon, A.J. Jones, C.P. Beeman, M.V. Hasan and I.D. Rae, *Tetrahedron Lett.*, (1975) 577.
- 102 J.D. Roberts, C.C. Lee and W.H. Saunders, *J. Am. Chem. Soc.*, 76 (1954) 4501; C.C. Lee and L.K.M. Lam, *J. Am. Chem. Soc.*, 88 (1966) 2831; C.C. Lee, B.S. Hahn and L.K.M. Lam, *Tetrahedron Lett.*, (1969) 3049.
- 103 J.B. Stothers, C.T. Tan, A. Nickon, F. Huang, R. Sridhar and R. Weglein, *J. Am. Chem. Soc.*, 94 (1972) 8581.
- 104 E.J. Corey and S. Nozoe, *J. Am. Chem. Soc.*, 87 (1965) 5733.
- 105 P.E. Peterson, B.R. Bonazza and P.M. Henricks, *J. Am. Chem. Soc.*, 95 (1973) 2222.
- 106 P.M. Henricks and P.E. Peterson, *J. Am. Chem. Soc.*, 95 (1973) 7449.
- 107 G.A. Olah, D.A. Beal and P.W. Westerman, *J. Am. Chem. Soc.*, 95 (1973) 3387.
- 108 For a recent review see A. Fry in *Mechanisms of Molecular Migrations*, Vol. IV, B.S. Thyagarajan (Ed.), Interscience, New York, 1971, p. 113.
- 109 N. Staudenmayer-Coudoux and A. Fry, unpublished results; c.f. N. Staudenmayer-Coudoux, Ph.D. Dissertation, University of Arkansas, 1974.
- 110 I.S. Isaev, T.G. Egorova, I.A. Shleider, E. Lippmaa, T. Pehk and V.A. Koptug, *Dokl. Akad. Nauk SSSR*, 189 (1969) 1258.
- 111 L. Weiler, *Can. J. Chem.*, 50 (1972) 1975.
- 112 H.J. Reich and D.A. Murcia, *J. Am. Chem. Soc.*, 95 (1973) 3418.
- 113 J.B. Stothers, I.S.Y. Wang, D. Ouchi and E.W. Warnhoff, *J. Am. Chem. Soc.*, 93 (1971) 6702; see also I.S.Y. Wang and E.W. Warnhoff, *J. Chem. Soc., Chem. Commun.*, (1969) 1158.
- 114 M.J. Betts and P. Yates, *J. Am. Chem. Soc.*, 92 (1970) 6982.
- 115 L. Knutsson, *Chem. Scr.*, 2 (1972) 227.
- 116 D.H. Hunter, A.L. Johnson, J.B. Stothers, A. Nickon, J.L. Lambert and D.F. Covey, *J. Am. Chem. Soc.*, 94 (1972) 8582; leading references are given to previous homoenolization studies.
- 117 A.L. Johnson, J.B. Stothers and C.T. Tan, *Can. J. Chem.*, 53 (1975) 212.
- 118 D.M. Hudyma, J.B. Stothers and C.T. Tan, *Org. Magn. Reson.*, 6 (1974) 614.
- 119 W.J. Baron, M. Jones, Jr. and P.P. Gaspar, *J. Am. Chem. Soc.*, 92 (1970) 4739.
- 120 P.O. Schissel, M.E. Kent, D.J. McAdoo and E. Hedaya, *J. Am. Chem. Soc.*, 92 (1970) 2147; J.A. Myers, R.C. Joines and W.M. Jones, *J. Am. Chem. Soc.*, 92 (1970) 4740; C. Wentrup and K. Wilczek, *Helv. Chim. Acta*, 53 (1970) 1459.
- 121 W.D. Crow and M.N. Paddon-Row, *J. Am. Chem. Soc.*, 94 (1972) 4746.
- 122 T.J. Barton, J.A. Kilgour, R.R. Gallucci, A.J. Rothschild, J. Slutsky, A.D. Wolf and M. Jones, Jr., *J. Am. Chem. Soc.*, 97 (1975) 657.
- 123 W. Ando, A. Sekiguchi, T. Hagiwara and T. Migita, *J. Chem. Soc., Chem. Commun.*, (1974) 372.
- 124 K. Zeller, *J. Chem. Soc., Chem. Commun.*, (1975) 317.
- 125 R.F.C. Brown and K.J. Harrington, *J. Chem. Soc., Chem. Commun.*, (1972) 1175; R.F.C. Brown, K.J. Harrington and G.L. McMullen, *J. Chem. Soc., Chem. Commun.*, (1974) 123; see also G.W. Van Dine and R. Hoffmann, *J. Am. Chem. Soc.*, 90 (1968) 3227.
- 126 J. Casanova, Jr., M. Geisel and R.N. Morris, *J. Am. Chem. Soc.*, 91 (1969) 2156.
- 127 T.L. Gilchrist, C.W. Rees and C. Thomas, *J. Chem. Soc., Perkin Trans. 1*, (1975) 8.
- 128 R.F.C. Brown and M. Butcher, *Tetrahedron Lett.*, (1970) 3151; *Aust. J. Chem.*, 25 (1972) 149.
- 129 J.E. Baldwin and M.W. Grayston, *J. Am. Chem. Soc.*, 96 (1974) 1629, 1630.
- 130 A. Nickon and G.D. Pandit, *Tetrahedron Lett.*, (1968) 3663.
- 131 E. Wenkert, E.W. Hagaman, L.A. Paquette, R.E. Wingard, Jr. and R.K. Russell, *J. Chem. Soc., Chem. Commun.*, (1973) 135.

- 132 A.K. Cheng, F.A.L. Anet, J. Mioduski and J. Meinwald, *J. Am. Chem. Soc.*, 96 (1974) 2887.
- 133 H. Nakanishi and O. Yamamoto, *Tetrahedron Lett.*, (1974) 1803.
- 134 H. Gunther and J. Ulmen, *Tetrahedron*, 30 (1974) 3781.
- 135 H. Nakanishi and O. Yamamoto, *Chem. Lett.*, (1973) 1273.
- 136 R. Wehner and H. Gunther, *J. Am. Chem. Soc.*, 97 (1975) 923.
- 137 H. Gunther, W. Peters and R. Wehner, *Chem. Ber.*, 106 (1973) 3683.
- 138 F.A. Cotton in *Dynamic Nuclear Magnetic Resonance Spectroscopy*, L.M. Jackman and F.A. Cotton (Eds.), Academic Press, New York, 1975.
- 139 F.A.L. Anet, H.D. Kaesz, A. Maasbol and S. Winstein, *J. Am. Chem. Soc.*, 89 (1967) 2489.
- 140 F.A. Cotton, D.L. Hunter and P. Lahuerta, *J. Am. Chem. Soc.*, 96 (1974) 4723, 7926.
- 141 G. Rigatti, G. Boccalon, A. Ceccon and G. Giacometti, *J. Chem. Soc., Chem. Commun.*, (1972) 1165.
- 142 H. Schmidbaur, W. Buchner and F.H. Kohler, *J. Am. Chem. Soc.*, 96 (1974) 6208.
- 143 R. Kaptein and L.J. Oosterhoff, *Chem. Phys. Lett.*, 4, (1969) 195, 214; G.L. Closs, *J. Am. Chem. Soc.*, 91 (1969) 4552; G.L. Closs and A.D. Trifunac, *J. Am. Chem. Soc.*, 92 (1970) 2183, 7227.
- 144 H.R. Ward, *Acc. Chem. Res.*, 5 (1972) 18; R.G. Lawler, *Acc. Chem. Res.*, 5 (1972) 25.
- 145 R. Kaptein, *J. Chem. Soc., Chem. Commun.*, (1971) 732; *J. Am. Chem. Soc.*, 94 (1972) 6251, 6262.
- 146 E. Lippmaa, T. Pehk, A.L. Buchachenko and S.V. Rykov, *Chem. Phys. Lett.*, 8 (1970) 521; *Dokl. Akad. Nauk SSSR*, 195 (1970) 632.
- 147 E.M. Schulman, R.D. Bertrand, D.M. Grant, A.R. Lepley and C. Walling, *J. Am. Chem. Soc.*, 94 (1972) 5972.
- 148 R. Kaptein, J. Brokken-Zijp and F.J.J. de Kanter, *J. Am. Chem. Soc.*, 94 (1972) 6280.
- 149 R. Kaptein, R. Freeman and H.D. Hill, *J. Chem. Soc., Chem. Commun.*, (1973) 953.
- 150 S. Berger, S. Hauff, P. Niederer and A. Rieker, *Tetrahedron Lett.*, (1972) 2581.
- 151 H. Iwamura, M. Iwamura, M. Imanari and M. Takeuchi, *Tetrahedron Lett.*, (1973) 2325.
- 152 H. Iwamura, Y. Imahashi and K. Kushida, *Tetrahedron Lett.*, (1975) 1401.
- 153 H. Iwamura, Y. Imahashi, M. Oki, K. Kushida and S. Satoh, *Chem. Lett.*, (1974) 259.
- 154 C. Brown, R.F. Hudson and A.J. Lawson, *J. Am. Chem. Soc.*, 95 (1973) 6500.
- 155 For instance, see G.A. Olah, P.W. Westerman and D.A. Forsyth, *J. Am. Chem. Soc.*, 97 (1975) 3419; G.A. Olah and J.L. Grant, *J. Am. Chem. Soc.*, 97 (1975) 1546; G.A. Olah and R.J. Spear, *J. Am. Chem. Soc.*, 97 (1975) 1539; G.A. Olah and P. Westerman, *J. Am. Chem. Soc.*, 95 (1973) 3706.
- 156 R.H. Levin and L. Weingarten, *Tetrahedron Lett.*, (1975) 611.
- 157 G.A. Olah, C.J. Jeuell and A.M. White, *J. Am. Chem. Soc.*, 91 (1969) 3961.
- 158 H.C. Brown and E.N. Peters, *J. Am. Chem. Soc.*, 95 (1973) 2400.
- 159 O. Kajimoto, M. Mobayshi and T. Fueno, *Bull. Chem. Soc. Jpn.*, 46 (1973) 1422.
- 160 T.A. Albright, W.J. Freeman and E.E. Schweizer, *J. Am. Chem. Soc.*, 97 (1975) 940; G.A. Gray, *J. Am. Chem. Soc.*, 95 (1973) 5092, 7736.
- 161 E.A. Williams, J.D. Cargioli and A. Ewo, *J. Chem. Soc., Chem. Commun.*, (1975) 366.
- 162 J. Firl and W. Runge, *Angew. Chem. Int. Ed. Eng.*, 12 (1973) 668.
- 163 J. Firl, W. Runge and W. Hartmann, *Angew. Chem. Int. Ed. Eng.*, 13 (1974) 270.
- 164 G.A. Olah and A.M. White, *J. Am. Chem. Soc.*, 90 (1968) 1884.
- 165 G.E. Maciel and D.D. Traficante, *J. Phys. Chem.*, 69 (1965) 1030.
- 166 D.D. Traficante and G.E. Maciel, *J. Phys. Chem.*, 70 (1966) 1314.
- 167 G.A. Olah and A.M. White, *J. Am. Chem. Soc.*, 89 (1967) 7072.
- 168 G.A. Olah and P.W. Westerman, *J. Org. Chem.*, 38 (1973) 1986.
- 169 G. Gatti, A. Levi, V. Lucchini, G. Modena and G. Scorrano, *J. Chem. Soc., Chem. Commun.*, (1973) 251.

- 170 R.A. McClelland and W.F. Reynolds, *J. Chem. Soc., Chem. Commun.*, (1974) 824.
- 171 G.A. Olah, Y. Halpern, Y.K. Mo and G. Liang, *J. Am. Chem. Soc.*, 94 (1972) 3554.
- 172 G.A. Olah and Y.K. Mo, *J. Am. Chem. Soc.*, 94 (1972) 5341; *J. Org. Chem.*, 38 (1973) 353.
- 173 G.A. Olah, D.P. Kelly and N. Suciú, *J. Am. Chem. Soc.*, 92 (1970) 3133.
- 174 A.J. Buglass, *J. Chem. Soc., Chem. Commun.*, (1974) 313.
- 175 W.F. Reynolds, I.R. Peat, M.H. Freedman and J.R. Lyster, Jr., *J. Am. Chem. Soc.*, 95 (1973) 328.
- 176 L.M. Jackman and T. Jen, *J. Am. Chem. Soc.*, 97 (1974) 2811.
- 177 R.J. Pugmire and D.M. Grant, *J. Am. Chem. Soc.*, 93 (1971) 1880.
- 178 R.B. Bates, S. Brenner, C.M. Cole, E.W. Davidson, G.D. Forsythe, D.A. McCombs and A.S. Roth, *J. Am. Chem. Soc.*, 95 (1973) 926.
- 179 D.H. Hunter and J.B. Stothers, *Can. J. Chem.*, 51 (1973) 2884.
- 180 M.V. Moncur, J.B. Grutzner and A. Eisenstadt, *J. Org. Chem.*, 39 (1974) 1604.
- 181 Y.K. Grishin, N.M. Sergeyev and Y.A. Ustynyuk, *J. Organomet. Chem.*, 22 (1970) 361; *Org. Magn. Reson.*, 4 (1972) 377.
- 182 M.M. Shemyakin, L.A. Neiman, S.V. Zhukova, Y.S. Nekrasov, T.J. Pekh and E.T. Lippmaa, *Tetrahedron*, 27 (1971) 2811.
- 183 J.M. Coxon, M. de Bruijn and C.K. Lau, *Tetrahedron Lett.*, (1975) 337.
- 184 J.B. Stothers, L.J. Danks and J.F. King, *Tetrahedron Lett.*, (1971) 2551.
- 185 T. Nagai, M. Tanaka and N. Tokura, *Tetrahedron Lett.*, (1968) 6293.
- 186 S. Siegel, V. Ku and R. Clough, private communication.
- 187 J.J. Rooney, F.G. Gault and C. Kemball, *Proc. Chem. Soc. London*, (1960) 407; F.G. Gault, J.J. Rooney and C. Kemball, *J. Catal.*, 1 (1962) 255.

BIOSYNTHETIC STUDIES USING CARBON-13 ENRICHED PRECURSORS

G. KUNESCH and C. POUPAT

(Chargés de Recherche au CNRS)

Institut de Chimie des Substances Naturelles du C.N.R.S., 91190 - Gif-sur-Yvette (France)

I. INTRODUCTION

Since radioisotopes became available in the late forties, the study of the biosynthesis of natural products has made tremendous progress. Practically all we know about primary and secondary metabolism [1] is the result of tracer studies. The combined use of carbon-14 and tritium as well as the introduction of scintillation counting [2] brought biosynthetic studies to their present level of refinement.

The rapid progress of tracer studies was essentially due to several advantages of radioactive labels (^{14}C , ^3H in almost all cases) the most important being extremely high sensitivity, low cost detection equipment (particularly in comparison to ^{13}C -n.m.r.) and the rapidly growing number of commercially available precursors. The major disadvantage of labelling with radioactive isotopes lies in the fact that extensive and tedious degradations are often necessary in order to locate the label within the radioactive molecule.

For this reason the use of ^{13}C -n.m.r. in the study of biosynthesis was early recognized as a potentially powerful tool. Indeed, the positions of the label can be determined directly from the spectrum without any chemical degradation being necessary. Nevertheless, a one-to-one assignment of all signals of the spectrum must be obtained beforehand.

Another important factor should not be neglected: the current trend towards spectroscopic methods in the structure determination of natural products set a problem to biosynthetic research because of the generalized decrease in degradation reactions due to the routine use of n.m.r. and mass spectrometry.

The advantages of ^{13}C -n.m.r. far outweigh the disadvantages of this technique: complicated, expensive equipment, rather low sensitivity and the necessity of feeding large amounts of precursor (the latter may alter metabolic pathways which will be discussed in more detail below).

In spite of the above mentioned limitations, the possibility of obtaining information on the location of carbon-13 labels without degradation gave rise to a rapidly increasing interest in this technique; the now available literature establishes ^{13}C -n.m.r. as an excellent tool in the elucidation of biosynthetic pathways. Nevertheless, the sensitivity problem has not yet found a satisfactory solution. Indeed, the majority of biosynthetic investigations using ^{13}C labelled precursors have been done with microorganisms producing physiologically active or toxic compounds for which optimum yield conditions

had been previously established. (If these conditions are unknown, a ^{14}C tracer assay should be undertaken beforehand).

Several review articles [3] concerning the use of ^{13}C -n.m.r. in the elucidation of biosynthetic pathways have been published and the classical textbooks on ^{13}C -n.m.r. [4] contain chapters discussing the biosynthetic aspects of ^{13}C -n.m.r. spectroscopy. For this reason, the need for another review on this topic may be questioned. On the other hand, the rapid growth in the number of publications dealing with this subject hopefully justifies this contribution.

Three different techniques — the satellite method, the continuous wave (CW) and Fourier transform (FT) technique — have been used in biosynthetic studies for the determination of the level and location of ^{13}C enrichment. These technical aspects of the problem will be discussed only briefly below since detailed accounts can be found elsewhere [4] and in any case would be beyond the scope of this article.

A. Indirect observation of Carbon-13 enrichment: the satellite method

Although the satellite method is used less frequently today, it was the first n.m.r. method applied for measuring ^{13}C enrichments.

^{13}C with a nuclear spin of $I = 1/2$ shows spin coupling with attached hydrogen atoms, the coupling constant being in the range of 100–250 Hz. In a normal ^1H -n.m.r. spectrum each proton resonance is accompanied by two satellite bands on both sides of the main signal, their distance corresponding to $J^{13}\text{C-H}$. At natural abundance of ^{13}C (1.1%) these signals have an intensity of 0.55%. For this reason, they cannot be measured in a single sweep and computer assisted multiscan averaging techniques must be used.

The major advantages of the “satellite method” are that it is non-degradative and less expensive than the currently employed CW or FT techniques.

Nevertheless, very early on, severe limitations of the satellite method became apparent:

(i) In order to be detectable, a hydrogen atom must be attached to the labelled carbon atom, which prevents the study of quaternary carbon atoms. (This problem can be resolved by conversion to suitable derivatives, e.g. reduction of carbonyl groups, which diminishes the advantages of a non-degradative technique).

(ii) One of the signals may be hidden under a hydrogen signal (of much greater intensity) or another satellite which renders the determination of the intensity of the satellites difficult or even impossible.

These two problems would disappear if ^{13}C resonances could be observed directly, but the necessary equipment was not commercially available before the late sixties.

B. Direct observation of Carbon-13 enrichment: CW and FT techniques

The ^{13}C -n.m.r. spectra of the first papers on biosynthesis using ^{13}C labelled precursors (early 1970) were measured in the continuous wave technique (CW). This method

allows the direct observation of ^{13}C resonances, but it suffers from the major disadvantage of low sensitivity. This is due to the fact that at a given instant only one frequency can be observed, which means that for a given shift range of about 5000 Hz (200 p.p.m.) each 1 Hz wide resonance line would be measured for only 1/5000 of the total acquisition time. Thus, a great number of scans is necessary. Although rapid sweeps increase sensitivity, they also diminish resolution.

The solution to these problems was the application of FT techniques to ^{13}C -n.m.r. A short (ca. 50 μsec) broad-band radio-frequency (r.f.) pulse excites the entire range of nuclear precession frequencies simultaneously. (The very high r.f. power is required in order to excite the sample in such a short period.) The sample absorbs individual frequency components and these frequencies — the precession frequencies — are detected by the receiver and the resultant free induction signal is measured as a function of time. Fourier transformation of the accumulated signals finally gives the spectrum. Practically, the FT method allows the recording of spectra in a much shorter time (about 2 orders of magnitude) with significantly improved sensitivity (about 1 order of magnitude).

In the following, a certain number of published investigations have been selected in order to illustrate the use of ^{13}C -labels in the study of biogenetic pathways. Due to the great structural diversity of the investigated compounds, this chapter will be arranged as far as possible in the order of increasing complexity of the precursors used. Nevertheless, some important groups of natural products — such as the corrins, the porphyrins and the terpenes — will be discussed independently of the ^{13}C -precursor incorporated.

II. INCORPORATION OF CARBON-13 ACETATE

Radiotracer investigations have revealed the existence of several principal biosynthetic pathways, each of these being ramified in many ways. Three primary compounds are found at the starting point of each pathway: acetic acid as its coenzyme A ester, shikimic acid and γ,γ -dimethylallyl alcohol as its pyrophosphate ester.

As in the case of the ^{14}C tracer studies, the first ^{13}C -label experiments were undertaken using acetate as a simple, commercially available precursor. Several examples will be discussed in some detail in the following section ^a.

A. *Griseofulvin* (1)

The incorporation of $[2\text{-}^{13}\text{C}]$ -acetate into griseofulvin (1) was the first reported application of ^{13}C to the study of a biosynthetic problem [5].

Historically, the biosynthesis of griseofulvin (1) is also among the most thoroughly studied biosynthetic problems using ^{14}C . In their classical paper, A.J. Birch et al. [6]

^a Throughout the formulae and schemes, ^{14}C -label will be represented, except where otherwise stated, by * and ^{13}C -label in the following manner: $\overset{\bullet}{\text{C}}\text{H}_3\overset{\bullet}{\text{C}}\text{OOH}$.

source of all carbon atoms, the principal progress of the above study was to demonstrate the feasibility of biosynthetic investigations using ^{13}C labelled precursors. Several other applications of the satellite method will be discussed below.

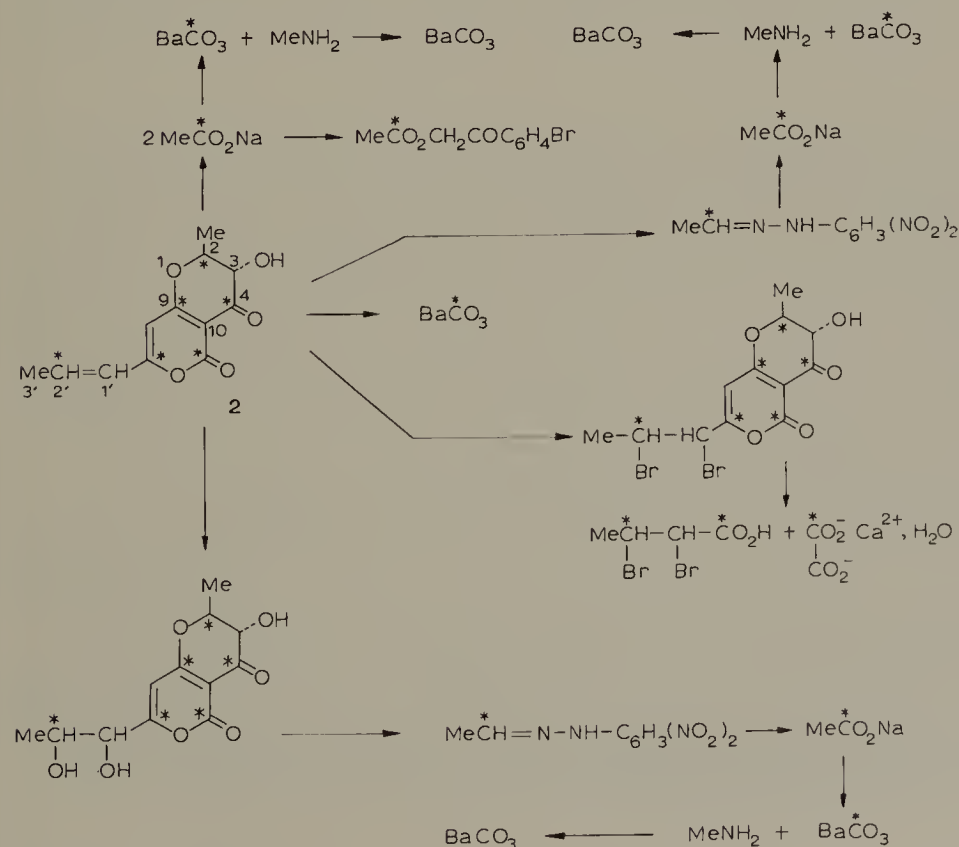
B. Radicinin (2)

The biosynthesis of radicinin (2), a pyranopyrone metabolite from the fungus *Stemphylium radicinum*, was the first to be studied by the "direct technique".

Previously, Grove [8] had extensively investigated the biosynthesis of radicinin using ^{14}C as a tracer. In his incorporation experiments, particular emphasis was made on the distinction between starter units (acetyl CoA) and building units (malonyl CoA) and the final labelling pattern was consistent with the formation of radicinin by the combination of two chains assembled from acetate-malonate-derived two-carbon units.

In contrast to the case of griseofulvin, where the ^{14}C study, although lengthy and tedious, gave more complete results, the comparison of the conventional ^{14}C -method and the ^{13}C -n.m.r. investigation of the biosynthesis of radicinin provides a striking demonstration of the superiority of the latter technique for certain problems. Scheme II illustrates the great number of degradation steps necessary for a relatively small molecule (12 carbon atoms only).

SCHEME II



References pp. 161-166

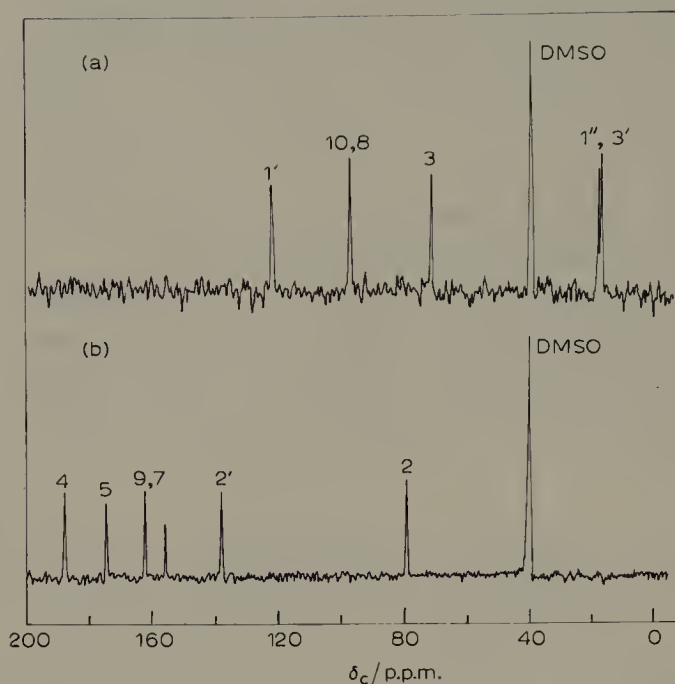


Fig. 1. (a) Incorporation of $^{13}\text{CH}_3\text{COONa}$ in (2). (b) Incorporation of $\text{CH}_3\text{ }^{13}\text{COONa}$ in (2). (Reprinted with permission from M. Tanabe, H. Seto and L. Johnson, *J. Am. Chem. Soc.*, 92 (1970) 2157, copyright by the American Chemical Society).

Tanabe et al. [9] administered $[1\text{-}^{13}\text{C}]$ -acetate and $[2\text{-}^{13}\text{C}]$ -acetate in 2 separate experiments to the culture broth of *Stemphylium radicinum* and the isotope enriched radicinins isolated after 3 weeks were analysed by c.m.r. The spectra were obtained in the CW swept mode and the solvent peak was the homonuclear lock signal. The sample isolated after administration of $[2\text{-}^{13}\text{C}]$ -acetate furnished a spectrum (Fig. 1a) showing 6 strong signals corresponding to carbon atoms 3, 8, 10, 1', 3' and 1''. Due to the high enrichment value of 17% (determined by integration of the proton- ^{13}C satellite bands of the two methyl groups) only these 6 signals are visible and the peaks from carbon atoms at natural abundance are obscured by noise.

The 6 other signals became apparent in the spectrum (Fig. 1b) obtained from $[1\text{-}^{13}\text{C}]$ -acetate labelled material, corresponding to C-2, 4, 5, 7, 9 and 2'.

In a parallel study, off-resonance decoupling had been applied to the assignment of carbon signals, confirming the quaternary character of C-4, 5, 7 and 9 which remained singlets and the methine character of C-2 and C-2' which split into doublets.

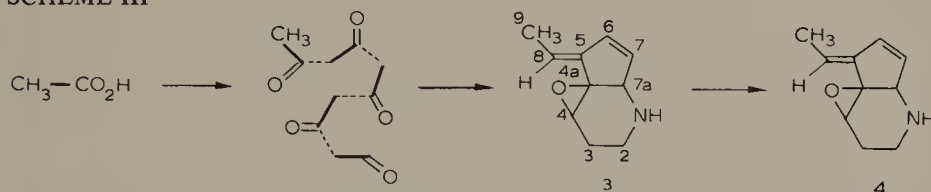
The importance of these results was not only the confirmation of the above mentioned ^{14}C tracer experiments, but also the demonstration of the superiority of the direct c.m.r. method over the satellite method, since all 12 carbon atoms could be observed without any chemical degradation step.

C. Latumcidin (3)

Latumcidin (3) is an antibiotic produced by *Streptomyces reticuli* var. *latumcidicus*. The biosynthesis of this metabolite (isolated in the form of the more stable dihydroderivative (4) which is a naturally occurring intermediate) has been studied extensively using several differently labelled precursors ($[1-^{13}\text{C}]$, $[2-^{13}\text{C}]$, $[1,2-^{13}\text{C}]$ as well as a 1 : 1 mixture of the two singly labelled acetates). The results obtained will be discussed in some detail.

Scheme III shows that this antibiotic can reasonably be derived from 5 acetate units via polyketide intermediates, using $[1-^{13}\text{C}]$ -acetate (56% enrichment) and $[2-^{13}\text{C}]$ -acetate (61% enrichment) [10].

SCHEME III



Seto et al. [10] obtained highly enriched samples (17.3 and 6.6% respectively, measured by direct comparison of the signal intensities of C-6 and C-7 since these two peaks are completely identical in the spectrum of natural abundance). Figure 2 gives the spectra of dihydrolatumcidin at natural abundance (a) and after labelling (b: ^{13}C -methyl and c: ^{13}C -carboxyl acetate). These spectra clearly demonstrate that latumcidin is biosynthesized from 5 acetate units as shown above. Previously, all peaks had been assigned unambiguously with the aid of off-resonance and selective proton decoupling experiments.

In agreement with Scheme III, the carbon atoms 4a and 5 are both derived from methyl carbons of acetate: thanks to the high enrichment rate the relevant spectrum (Figure 2b) clearly shows coupling between these carbon atoms ($J = 57\text{ Hz}$).

However, further informations on the other C—C bonds formed by condensation of acetates may be obtained in two different ways.

Firstly, administration of uniformly labelled $[1,2-^{13}\text{C}]$ -acetate allows the observation of $^{13}\text{C}\text{--}^{13}\text{C}$ couplings between the carbons directly derived from intact acetate units, thus providing a proof for the absence of bond fission during biosynthesis.

Secondly, feeding of an equimolecular mixture of $^{13}\text{CH}_3\text{COOH}$ and $\text{CH}_3^{13}\text{COOH}$ should give information on C—C bonds formed by condensation of acetate units (among the four possible combinations, only one: $\text{CH}_3^{13}\text{CO} \dots ^{13}\text{CH}_3\text{CO} \dots$ will provide $^{13}\text{C}\text{--}^{13}\text{C}$ coupling).

In order to test these two methods, latumcidin was the model of choice. Incorporation of $[1,2-^{13}\text{C}]$ -acetate (90% enrichment) led to the isolation of a sample whose spectrum is shown in Figure 3a.

Administration of a 1 : 1 mixture of highly enriched (90%) specifically labelled acetates gave a material from which the spectrum 3b was obtained.

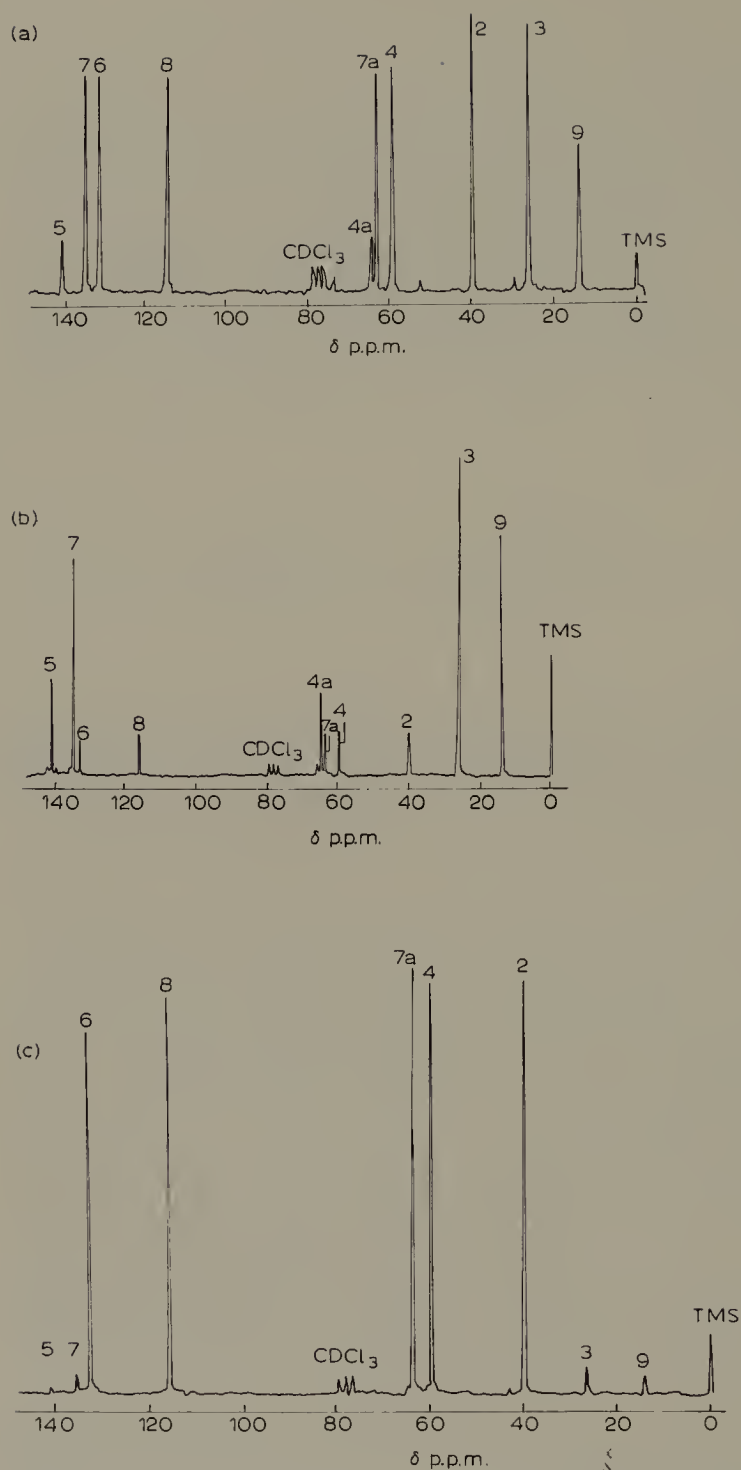


Fig. 2. ^{13}C -n.m.r. Spectra of (4). (a) At natural abundance, (b) after incorporation of $[2\text{-}^{13}\text{C}]$ -acetate and (c) after incorporation of $[1\text{-}^{13}\text{C}]$ -acetate. (Spectra reproduced with permission from H. Sato, T. Satō, H. Yonehara and W.C. Jankowski, *J. Antibiot.*, 26 (1973) 609.)

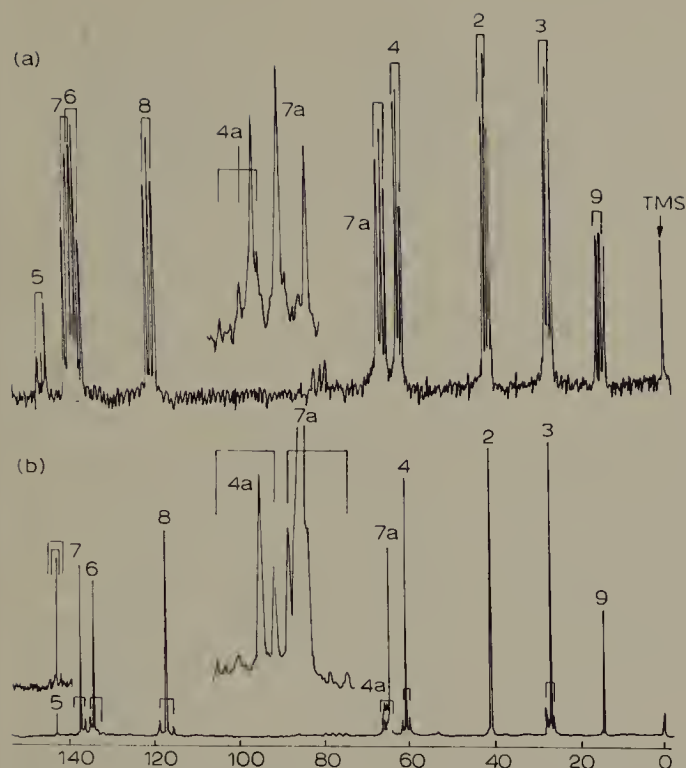


Fig. 3. ^{13}C -n.m.r. Spectra of (3). (a) After incorporation of $[1,2-^{13}\text{C}]$ -acetate and (b) after incorporation of a 1 : 1 mixture of $[1-^{13}\text{C}]$ - and $[2-^{13}\text{C}]$ -acetate.

(Spectra reprinted with permission from H. Sato, T. Satō and H. Yonehara, J. Am. Chem. Soc., 95 (1973) 8462, copyright by The American Chemical Society.)

Coupling between C_9-C_8 , C_5-C_6 , C_7-C_{7a} , $\text{C}_{4a}-\text{C}_4$ and C_3-C_2 is observed in spectrum 3a due to the intact incorporation of acetate. In contrast, spectrum 3b shows coupling between C_8-C_5 , C_6-C_7 , $\text{C}_{7a}-\text{C}_{4a}$, C_4-C_3 and C_4-C_5 while the methyl group of the starter unit and the carboxyl group of the terminal acetate unit remain singlets.

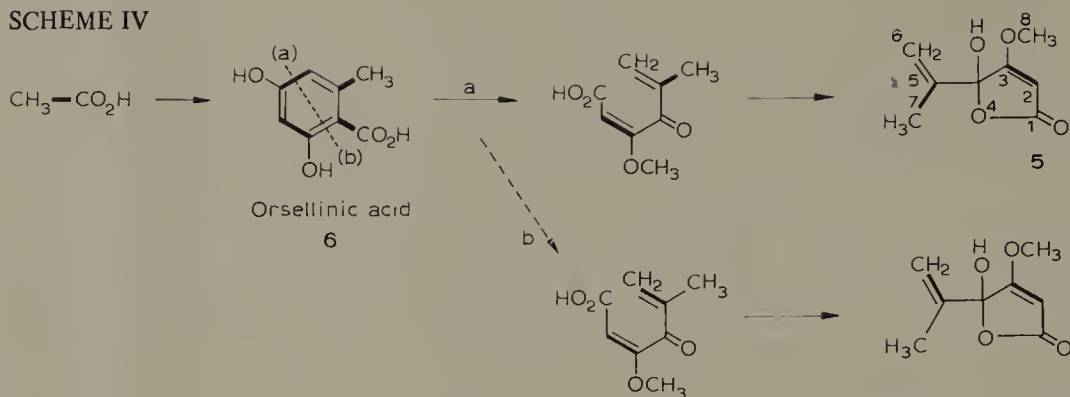
It should be emphasized that these two methods are complementary and that a great deal of structural information may be obtained in this manner.

D. Penicillic acid (5)

The biosynthesis of penicillic acid (5), a wide spread metabolite of *Penicillium* species, has been the subject of active interest.

The co-occurrence and structural similarity of orsellinic (6) and penicillic (5) acids suggested very early a biogenetic relationship [11] as depicted in Scheme IV. Incorporation of ^{14}C -labelled orsellinic acid (^{14}C -2 and carboxyl) led to the isolation of radioactive penicillic acid which was carefully degraded in order to locate the label [12].

SCHEME IV



The results obtained in this manner demonstrated that orsellinic acid is an effective precursor of penicillic acid. Furthermore, the location of the label shows that the obligatory fission of the aromatic ring takes place along pathway (a).

The use of ^{13}C - ^{13}C coupling in combination with the FT-c.m.r. technique can greatly facilitate the investigation of mechanisms involved in biosynthesis. Since the fission of the aromatic ring along pathway (a) occurs between two carbon atoms derived from the same acetate unit, it seemed interesting to apply this non-degradative method to this problem.

After addition of [1,2- ^{13}C]-acetate to surface cultures of *Penicillium cyclopium* enriched penicillic acid was isolated [13]. The proton noise-decoupled c.m.r. spectrum of this sample (Figure 4) shows ^{13}C - ^{13}C coupling between carbon atoms 2 and 3

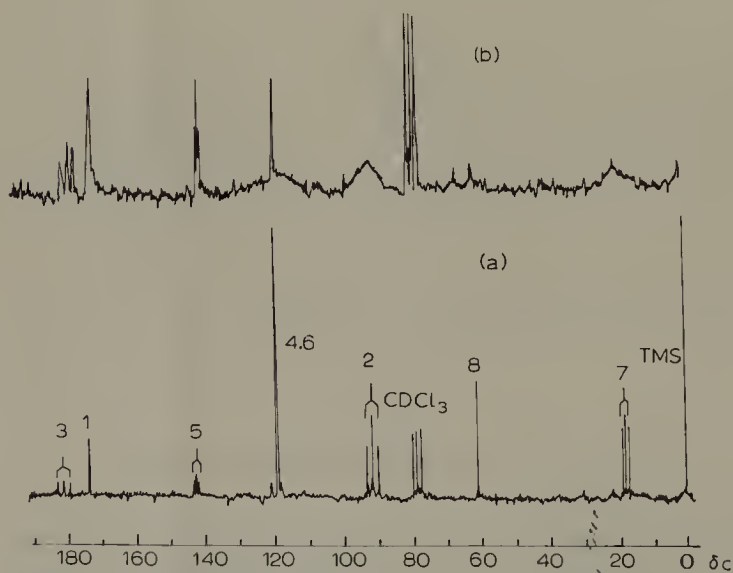


Fig. 4. (a) Proton-noise decoupled spectrum of (5) in CDCl₃. (b) Undecoupled spectrum of (5) in CDCl₃.

(Reproduced with permission from H. Seto, L.W. Cary and M. Tanabe, J. Antibiot., 27 (1974) 558).

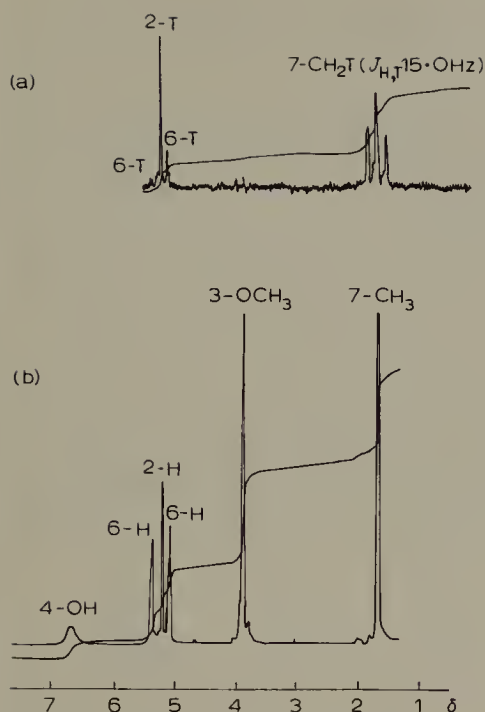


Fig. 5. (a) ^3H -n.m.r. spectrum of labelled (5). (b) ^1H -n.m.r. spectrum of (5). (Reproduced with permission from J.M.A. Al-Rawi, J.A. Elvidge, D.K. Jaiswal, J.R. Jones and R. Thomas, *J. Chem. Soc. Chem. Commun.*, (1974) 220.)

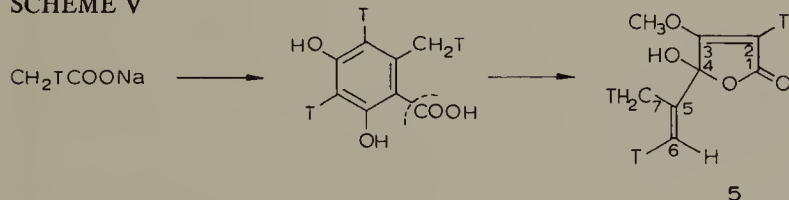
($J = 78$ Hz) and between carbon atoms 5 and 7 ($J = 45$ Hz). Increased signal intensities (relative to the unlabelled methoxy carbon signal) for carbon atoms 1, 4 and 6 demonstrate the incorporation of acetate into the whole molecule. This result constitutes an independent and elegant proof for the existence of pathway (a) since ^{13}C – ^{13}C coupling between carbon atoms 1 and 2 as well as between 3 and 4 should have been observed in addition to the coupling between C-5 and C-7 in the case of pathway (b).

As mentioned above, the biosynthesis of penicillic acid has raised considerable interest and it may be interesting to note that it represents the first application of ^3H -n.m.r. spectroscopy to a biosynthetic investigation.

In this study [14], [^3H]-acetate of very high specific activity (2.4 Ci mmol^{-1}) was incorporated into penicillic acid by *P. cyclopium*. The ^3H -n.m.r. (96.02 MHz) of this sample of penicillic acid (35 mg of about $98 \text{ m Ci mmol}^{-1}$) is shown in Fig. 5 together with the corresponding p.m.r. spectrum.

For the sake of clarity the biogenetic scheme (Scheme V) leading from acetate via

SCHEME V



orsellinic acid to penicillic acid is repeated in order to indicate the location of the tritium label in these compounds.

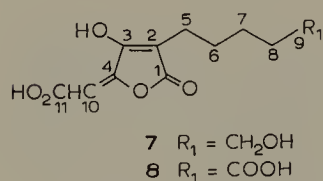
As a matter of course, the labelling pattern observed is in agreement with the mechanism involving a 4–5 cleavage of orsellinic acid. A hydrolytic cleavage (instead of the more general oxidative scission) of the 4–5 bond has been proposed by Mosbach [12], although no method was available to test his postulate.

The presence of ^3H in position 7 of penicillic acid is a strong argument in favour of this hypothesis.

In general, the ^3H -n.m.r. study of the biosynthesis of penicillic acid demonstrates not only the feasibility of this new technique, but it also shows that its results may be complementary to ^{13}C and ^{14}C -studies in carefully chosen examples. In addition, radioactivity may serve as a monitor of isotopic content. Furthermore, a large amount of chemical shift and coupling data is available from ^1H -n.m.r. and can be directly utilized for ^3H -n.m.r. Finally the (almost total) absence of natural isotope content results automatically in greater ease of detection.

E. Multicollic (7) and multicolosic (8) acids

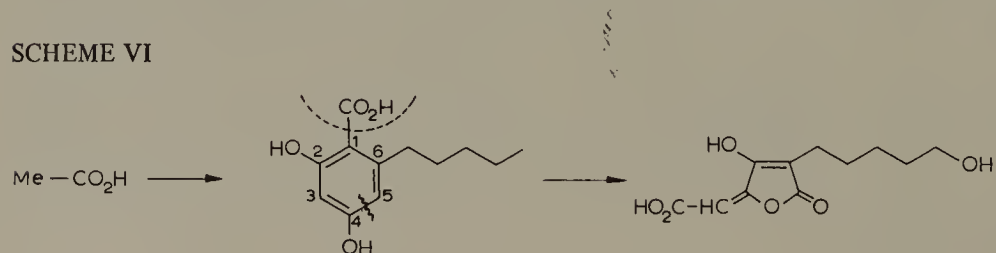
Multicollic (7) and multicolosic (8) acids were isolated from *Penicillium multicolor* and their structure determined by chemical and spectroscopic methods [15] including ^{13}C -n.m.r. spectroscopy and lanthanide induced shift studies with $\text{Eu}(\text{fod})_3$.



In the parallel biosynthetic investigation, $[1\text{-}^{13}\text{C}]$ -, $[2\text{-}^{13}\text{C}]$ - and $[1,2\text{-}^{13}\text{C}]$ -acetic acids were added to cultures of *P. multicolor*. Carbon atoms 2, 4, 6, 8 and 11 showed increased signal intensities after incorporation of $[1\text{-}^{13}\text{C}]$ -acetate, while carbon atoms 1, 3, 5, 7, 9 and 10 were enriched by $[2\text{-}^{13}\text{C}]$ -acetate (Fig. 6).

In spite of the great structural similarities of both metabolites with penicillic acid (see page 113), this distribution of label indicated a different biogenetic pathway. The results of the incorporation of $[1,2\text{-}^{13}\text{C}]$ -acetate support a pathway via an oxidative cleavage (as compared with the hydrolytic cleavage occurring during penicillic acid biosynthesis) of an aromatic precursor, probably 6-pentylresorcylic acid (Scheme VI).

SCHEME VI



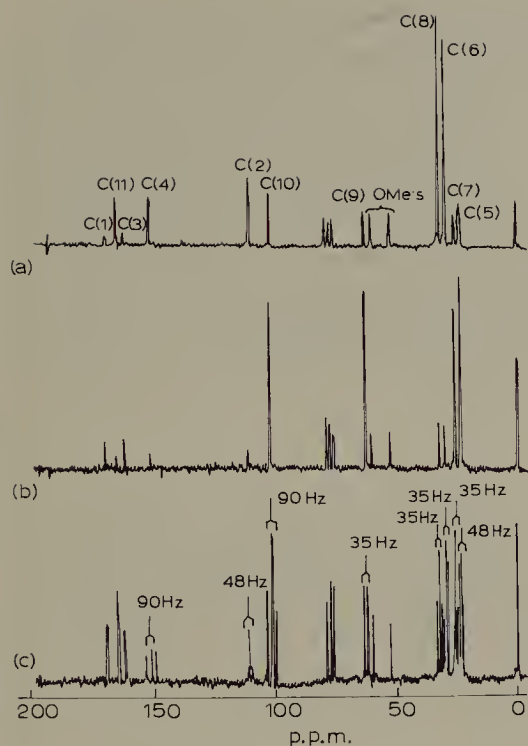
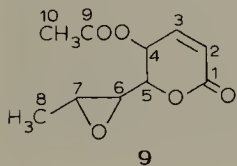


Fig. 6. The proton-noise decoupled F.T. ^{13}C -n.m.r. spectra of methyl O-methyl-multicolate labelled with: (a) $\text{CH}_3^{13}\text{COONa}$ (b) $^{13}\text{CH}_3\text{COONa}$ and (c) $^{13}\text{CH}_3^{13}\text{COONa}$ (in CDCl_3). (Reproduced with permission from J.A. Gudgeon, J.S.E. Holker and T.J. Simpson, *J. Chem. Soc. Chem. Commun.* (1974) 636.)

Lactone formation takes place between carbon atoms 2 and 5 (between C-1 and C-4 in the corresponding intermediate of penicillic acid biosynthesis) after 4,5-fission of the aromatic precursor. This scheme not only explains the distribution of ^{13}C -label, but also the couplings observed ($J_{8,9}$, $J_{6,7}$, $J_{2,5}$, and $J_{4,10}$) in the sample isolated after incorporation of $[1,2\text{-}^{13}\text{C}]$ -acetate.

F. Asperlin (9)

A δ -lactone, asperlin (9), has been isolated from *Aspergillus nidulans* (NRLL 3134) and its structure determined [16].



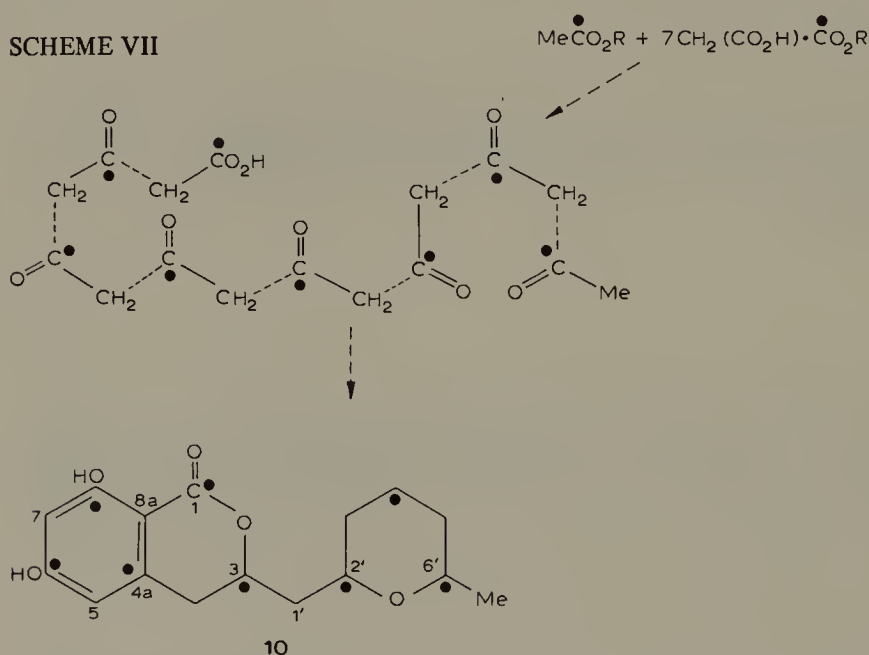
Addition of $[2\text{-}^{13}\text{C}]$ -acetate to a culture medium of *A. nidulans* furnished labelled asperlin showing 5 signals (corresponding to carbon atoms number 2, 4, 6, 8 and 10) of enhanced activity [17]. Assignments of carbon resonances were facilitated by taking off-resonance spectra in different solvents and by measuring residual coupling constants.

From the c.m.r. spectrum (taken in the CW-mode) a 9% ($\pm 1\%$) enrichment was estimated by comparison of signal intensities. A similar enrichment level (ca. 10%) was determined using the satellite-method. Finally both n.m.r. results concerning the enrichment level of asperlin were checked by a detailed mass spectrometry analysis. By measuring the difference in the ratios $M + 1/M$ of labelled and unlabelled asperlin an average of 7.3% ^{13}C -enrichment at each of five positions was calculated.

G. Asperentin (10)

The structure of asperentin (10) [18] isolated from an entomogenous strain of *A. flavus* suggests a direct biosynthesis from eight acetates. Labelling experiments with $[2\text{-}^{14}\text{C}]$ -malonate and $[1\text{-}^{13}\text{C}]$ -acetate have confirmed this simple biogenetic pathway (Scheme VII).

SCHEME VII



The biogenetic study of this compound [19] is discussed in more detail because the authors describe a technique for minimizing the Overhauser enhancement in ^{13}C -n.m.r. spectroscopy. In fact, a preliminary examination by standard FT-n.m.r. procedures of the metabolite indicated an approximately two-fold enrichment. Since this enrichment is well within the range of theoretical Overhauser enhancements, the authors investigated a modification of the classical FT-n.m.r. technique i.e. the gated decoupling technique [20].

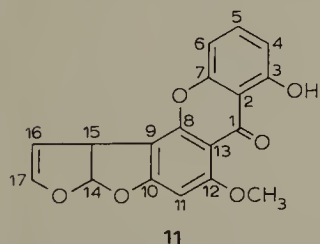
The integrals of ^{13}C spectra are not sufficiently reliable for two main reasons: firstly because of the Overhauser effect, and secondly because of the use of a too high mean radiofrequency power. Both effects are related to relaxation times. While the gated decoupling technique allows the Overhauser effect to be eliminated, the effects of the second problem — associated with r.f. power — can be diminished by increasing the delay between two pulses.

Although unit areas for each carbon atom were not achieved by this technique, the ratio between values for any two carbon atoms in the natural and labelled compounds was of sufficient accuracy.

Other methods designed to eliminate the effects resulting in different peak intensities are described below.

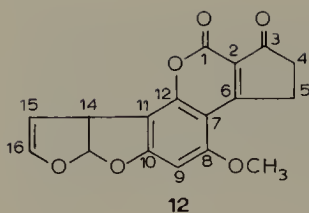
H. Sterigmatocystin (11)

Sterigmatocystin was isolated from *Aspergillus versicolor* and its structure has been determined in 1962 by E. Bulloch et al. [21]. Structural considerations suggested an involvement of the acetate—malonate pathway, although the formation of the bisdihydrofuran moiety could not be explained by any of the usual biogenetic pathways.



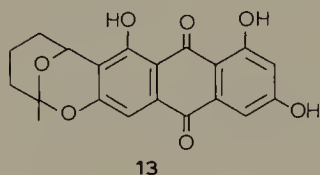
In 1968, Holker et al. [22] published a radiocarbon investigation on the biosynthesis of sterigmatocystin using $[1-^{14}\text{C}]$ -acetate as a precursor. The labelled sterigmatocystin (11) was subjected to a series of degradation reactions in order to determine the distribution of the label in the metabolite. The results obtained supported the acetate—malonate hypothesis for the origin of the xanthone-part in sterigmatocystin (11). Although the branched four-carbon unit of the bisdihydrofuran moiety was equally derived from acetate, it was more surprising to note that the C—C bond joining this part of the xanthone was apparently formed between carbon atoms derived from the methyl groups of acetate. Small differences in the radioactivity level in the two parts of the molecule were interpreted in favor of a biosynthesis from two preformed ketide units, although the mechanism of this combination remained obscure.

The biosynthesis of a structurally related group of *Aspergillus* metabolites, the aflatoxins, has also been a topic of much speculation [23]. The radiocarbon study of the biosynthesis of aflatoxin- B_1 (12) [24] was essentially centered on the problem of the bisdihydrofuran part in order to compare the distribution of the label in this part of the molecule with that predicted by the published postulates. Degradative studies on radioactive aflatoxin- B_1 (12) isolated after administration of $[1-^{14}\text{C}]$ - and $[2-^{14}\text{C}]$ -ace-



tates fixed the origin of 13 out of the 16 carbon atoms of the skeleton. In addition, the level of radioactivity at each site suggested that aflatoxin-B₁ is derived from a single polyacetate chain. Furthermore, careful determination of the distribution of the isotope in the bisdihydrofuran portion established firmly that the vicinal carbon atoms C-11 and C-14 were both derived from a methyl group of acetate. The distribution of the label was not in agreement with any of the previously proposed biogenetic schemes, particularly because the fermentation of *A. flavus* in the presence of radioactive sterigmatocystin produced inactive aflatoxin-B₁.

Independently, ¹⁴C-tracer studies by Hsieh et al. [25] showed once more that negative incorporation results must be interpreted with caution. Starting from the observation that a mutant of *A. parasiticus* ATCC 15517 incapable of aflatoxin biosynthesis had been found to accumulate averufin (13), they suggested that this pigment should



be an intermediate in aflatoxin formation. They prepared ¹⁴C-labelled averufin (13) and found that it was efficiently converted into aflatoxin-B₁. Using the same techniques, they added to the mycelium of *A. parasiticus* ¹⁴C-labelled sterigmatocystin, which was also incorporated into aflatoxin-B₁ [26]. By taking into account all the information available, a biogenetic sequence starting from a C₂₀-polyketide and leading via averufin and sterigmatocystin to aflatoxin was proposed.

Meanwhile, the great number of degradation steps necessary in radiocarbon studies had encouraged the use of ¹³C-label. Growing cultures of *A. versicolor* in the presence of [1-¹³C]- and [2-¹³C]-acetates [27] led to the isolation of two ¹³C-enriched samples of sterigmatocystin. Each carbon appeared as a singlet in the noise decoupled spectrum obtained in the CW mode (Fig. 7).

Spectrum 7 (a) (from [1-¹³C]-acetate) shows nine and spectrum 7 (b) (from [2-¹³C]-acetate) eight signals of enhanced activity. This result is in full agreement with the above mentioned radiocarbon studies. In addition, C—C coupling is observed in spectrum (b) between C-9 and C-15 (although the resolution of the downfield C-9 splitting is insufficient). This particular difficulty was overcome by recording the FT spectrum at 55.33 MHz. In this spectrum (7c) the C-9 signal is well resolved with $J_{13C9-15} = 48$ Hz. This observation provided an elegant proof that these two carbon atoms are both derived

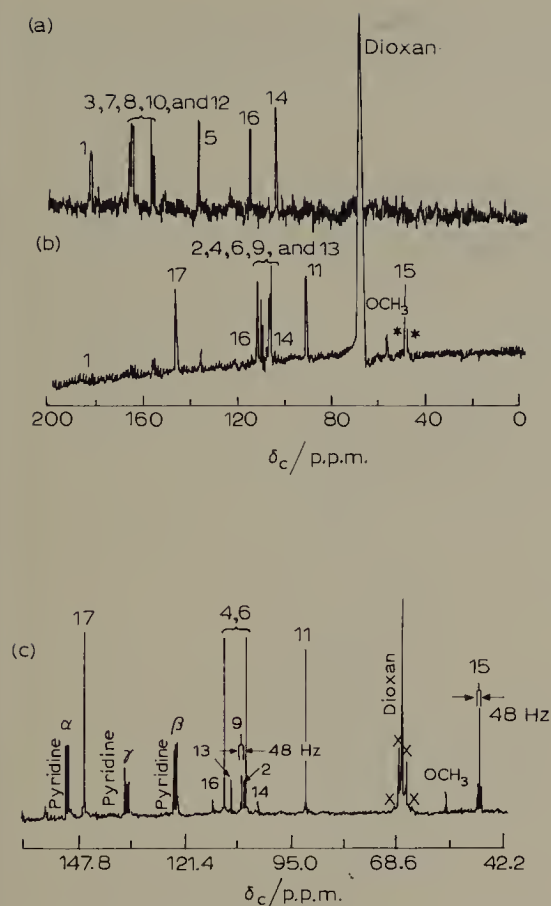


Fig. 7. (a) CW ^{13}C -n.m.r. spectrum of (11) after incorporation of $[1\text{-}^{13}\text{C}]$ -acetate. (b) CW ^{13}C -n.m.r. of (11) after incorporation of $[2\text{-}^{13}\text{C}]$ -acetate. (c) FT ^{13}C -n.m.r. of (11) after incorporation of $[2\text{-}^{13}\text{C}]$ -acetate recorded at 55.33 MHz.

(Spectra (a) and (b) reproduced with permission from M. Tanabe, T. Hamasaki, H. Seto and L. Johnson, *Chem. Commun.*, (1970) 1539)

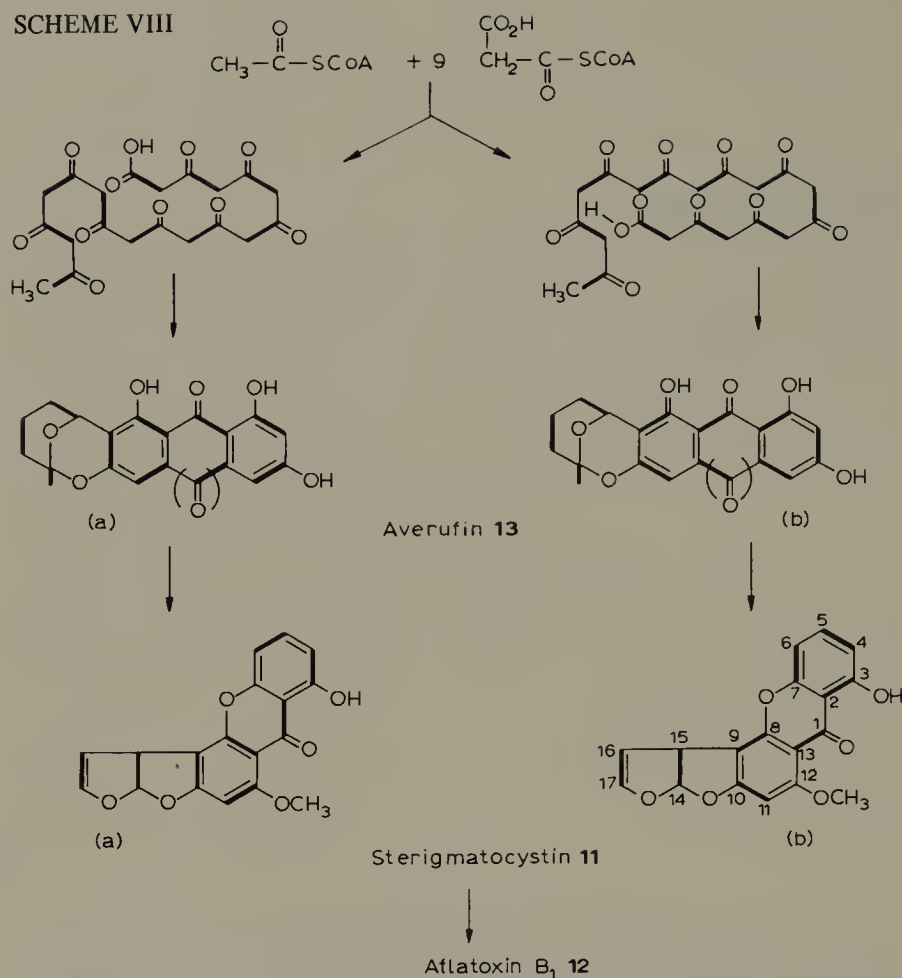
(Spectrum (c) from M. Tanabe in *Biosynthesis*, Vol. 2, Chemical Society, London, 1973, p. 267.)

from the methyl groups of acetate. Furthermore, the aromatic resonances at C-4 and C-6 could be distinguished.

Incorporation of $[1,2\text{-}^{13}\text{C}]$ -acetate (90% enriched) into sterigmatocystin formed by *A. versicolor* [28] furnished conclusive information concerning the folding pattern of the hypothetical C_{20} -polyketide precursor of averufin (Scheme VIII).

Although both pathways (a) and (b) are in agreement with the previously determined distribution of label, only pathway (b) leads to sterigmatocystin showing the observed ^{13}C – ^{13}C coupling pattern. C_4 – C_5 and C_6 – C_7 couplings are of crucial importance for the distinction between (a) and (b).

SCHEME VIII



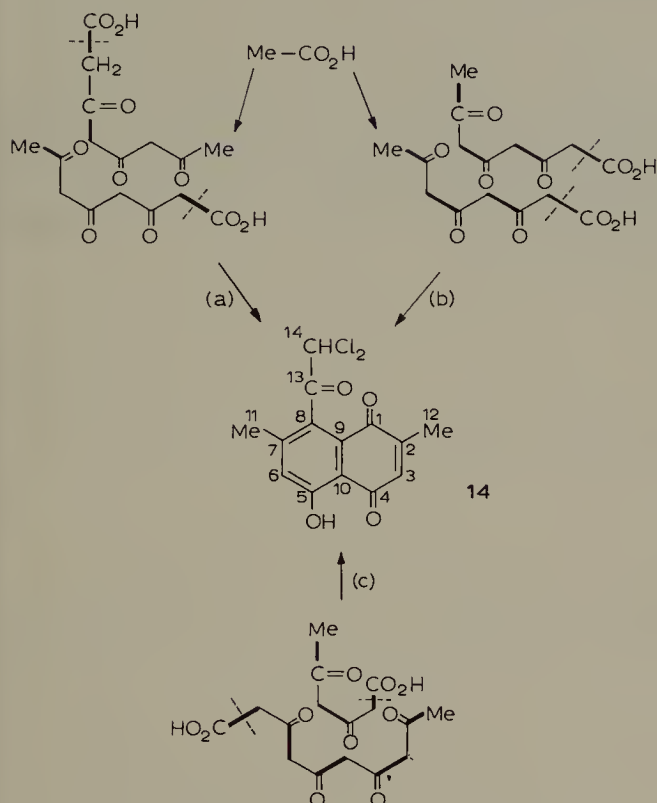
I. Mollisin (14)

A certain number of results had been obtained in an earlier ^{14}C study [29] of the biosynthesis of the naphthoquinone pigment mollisin (14). Labelled acetate and malonate were good precursors, while $[^{14}\text{CH}_3]$ -methionine, mevalonate and labelled chloroacetic and bromoacetic acids were not utilized for the biosynthesis of mollisin (14). Kuhn–Roth oxidation of a sample of the pigment isolated after administration of $[1-^{14}\text{C}]$ -acetate yielded acetic acid containing one third of the activity in the carboxyl group (corresponding to carbon atoms 2 and 7 of mollisin). If these two carbon atoms comprise half of the total activity, six labelled carbon atoms derived from $[1-^{14}\text{C}]$ -acetate should be present in the whole molecule, which is a rather unexpected result for a C_{14} -compound, especially since the two methyl groups are not labelled by methionine.

On the basis of this result two slightly different pathways have been proposed for the biosynthesis of mollisin: both pathways (a and b) explain the formation of the metabolite from two simultaneously formed polyketide chains. In order to be consistent with

the distribution of label mentioned above the loss of two carboxyl groups must be assumed (Scheme IX).

SCHEME IX



The first ^{13}C -investigation of the biosynthesis of mollisin [30] was performed with the aid of the satellite method. After addition of $[2\text{-}^{13}\text{C}]$ -acetate to a culture of *Mollisia caesia* ^{13}C -enriched mollisin was isolated and analysed. Enrichment at 5 different sites was observed (carbon atoms number 3, 4, 6, 11 and 12) and this result was in agreement with the radiocarbon study, but still no distinction was possible between pathways (a) and (b).

A surprising result was obtained in the second ^{13}C study [31]. An enriched sample of mollisin (14) was isolated after administration of generally labelled $[1,2\text{-}^{13}\text{C}]$ -acetate (90% enrichment). In a noise decoupled FT spectrum ^{13}C — ^{13}C coupling should be seen between C-11 and C-7, and between C-12 and C-2 if pathway (a) takes place. In contrast, in the case of pathway (b) coupling between C-11 and C-7, and between C-14 and C-13 should be visible while C-12 should remain a singlet. Several couplings could be determined in the spectrum of mollisin (14) enriched with generally labelled acetate. Although C-2, C-4, C-7 and C-13 couplings could not be measured because of a low enrichment resulting in a poor signal to noise ratio, ^{13}C — ^{13}C coupling constants could be determined for C-12 ($J_{2,12} = 45.0$ Hz), C-3 ($J_{3,4} = 52.5$ Hz), C-6 ($J_{6,7} = 61.3$ Hz) and for C-14 ($J_{13,14} = 47.5$ Hz). This demonstrates beyond doubt that the corresponding

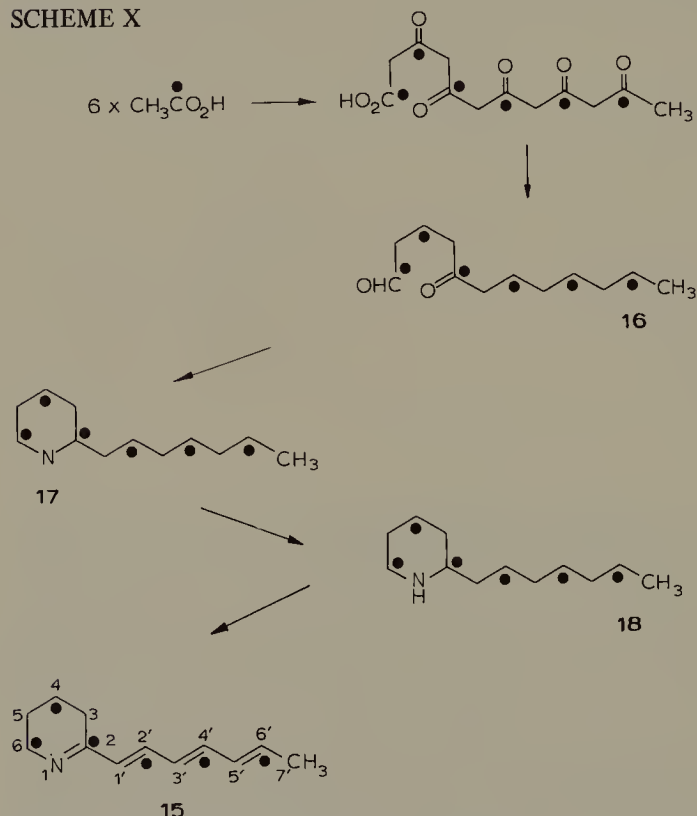
carbon atoms are derived from intact acetate units. Furthermore, this result excludes pathways (a) and (b); a completely different pathway (c) seems to be involved in the biosynthesis of mollisin.

J. Nigrifactin (15)

The isolation and structure determination of several simple piperidine alkaloids from microorganisms [32] raised questions as to their biosynthesis: in fact, the piperidine ring can be derived in nature from lysine, acetate or terpenoids [33].

Addition of $[1-^{13}\text{C}]$ -acetate to the culture of *Streptomyces nigrifaciens* var. FFD-101 led to the isolation of labelled nigrifactin (15) [34].

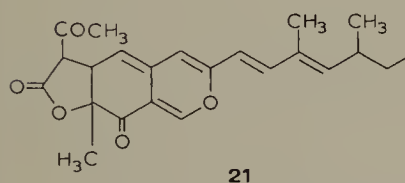
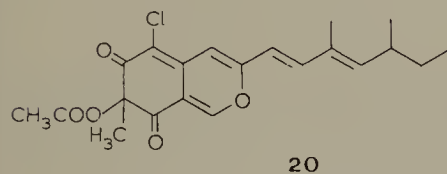
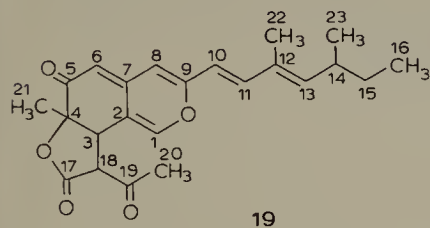
SCHEME X



Its ^{13}C -n.m.r. spectrum shows clearly the enhancement of 6 signals (corresponding to carbon atoms 6, 4, 2, 2', 4' and 6') suggesting a polyketide origin in close analogy to the hemlock alkaloids. In parallel ^{14}C -investigations using specifically labelled precursors, several probable intermediates $[1-^{14}\text{C}]$ -5-oxododecanal (16), $[6-^{14}\text{C}]$ -2-n-heptylpiperidine (17) and $[6-^{14}\text{C}]$ -2-n-heptylpiperidine (18) were synthesized and fed to *Streptomyces nigrifaciens*. The fact that the latter compound is an efficient precursor suggests that the double bonds of nigrifactin are formed in the last steps of the biogenetic pathway (Scheme X).

K. Ochrephilone (19)

A new metabolite, ochrephilone (19), was isolated from *P. multicolor* (NRRL 2060) in addition to the already known constituents sclerotiorin (20) [35] and rotiorin (21) [36]. Early chemical and spectroscopic studies of the new compound suggested a close similarity with these two co-metabolites whose polyketide origin had been established previously by ^{14}C tracer investigations [37]. Nevertheless, several tentative structures were in agreement with the data obtained. Finally, ^{13}C -n.m.r. spectroscopy and the information furnished by ^{13}C - ^{13}C coupling enabled structure (19) to be assigned to ochrephilone [38].



Ten signals of enhanced intensities can be detected in the spectrum of ochrephilone isolated after incorporation of $[2\text{-}^{13}\text{C}]$ -acetate, indicating the presence of a decaaketide. (The remaining 3 carbon atoms C-21, C-22 and C-23 should be derived from the C_1 -pool, in analogy with the results obtained with ^{14}C -tracers for sclerotiorin and rotiorin). In the spectrum of the sample obtained after administration of $[1,2\text{-}^{13}\text{C}]$ -acetate, several coupling constants could be measured, the most important being $J_{1,2} = 78 \text{ Hz}$ suggesting the presence of an oxygen substituent at C-1.

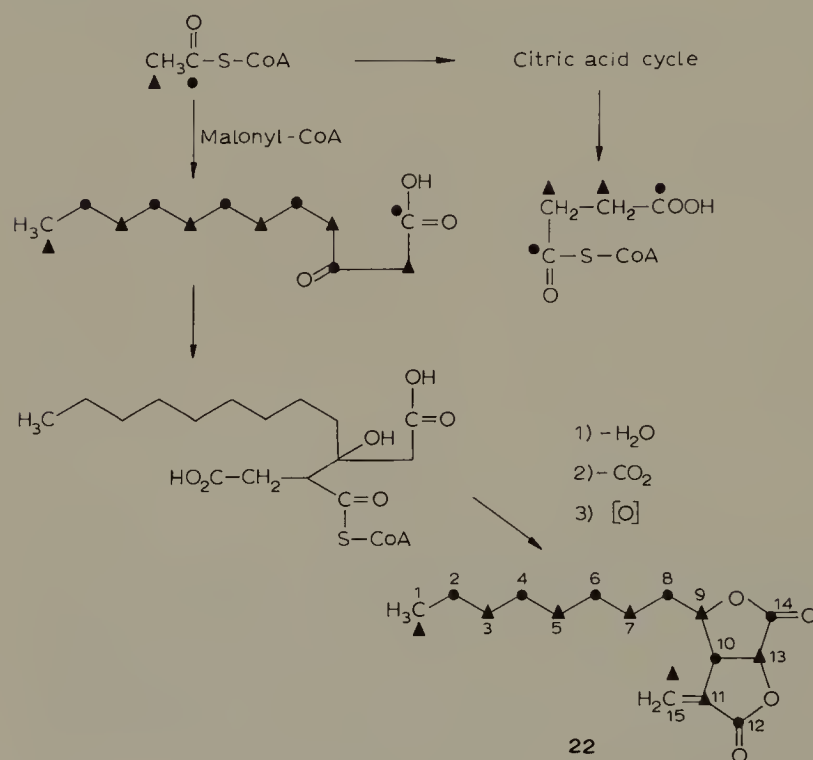
Further confirmation of structure (19) for ochrephilone was obtained by a labelling experiment using a 1 : 1 mixture of $[1\text{-}^{13}\text{C}]$ - and $[2\text{-}^{13}\text{C}]$ -acetates, both highly enriched (90%). As discussed in some detail, in the case of dihydrolatumcidin (see page 111), incorporation of $[1,2\text{-}^{13}\text{C}]$ -acetate provides information on carbon atoms originating from intact acetate units, while the alternative double labelling method (administration of 1 : 1 mixture of $[1\text{-}^{13}\text{C}]$ - and $[2\text{-}^{13}\text{C}]$ -acetates) furnishes coupling data concerning the C—C bonds formed by condensation of 2 acetate units. From

this point of view the structure determination of ochrephilone is an excellent demonstration of the advantages of biosynthetically enriched metabolites in structural investigations.

L. Avenaciolide (22)

Several possible pathways have been proposed [39] for the biosynthesis of the bislactone avenaciolide (22) [40] produced by *Aspergillus avenaceus* G. Smith (CMI, 161440). Tanabe et al. [41] administered $[1-^{13}\text{C}]$ - and $[2-^{13}\text{C}]$ -acetates to cultures of *A. avenaceus* and demonstrated that this bislactone (22) is biosynthesized by condensation of 3-oxodecanoic acid (acetate-malonate pathway) with succinate derived equally from acetate via the citric acid cycle (Scheme XI).

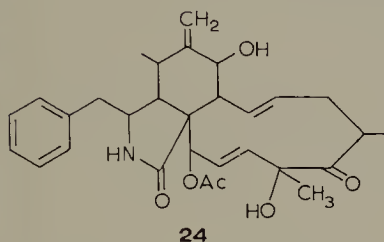
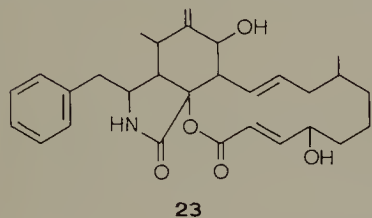
SCHEME XI



The ^{13}C -n.m.r. spectrum of avenaciolide (22) isolated after administration of $[2-^{13}\text{C}]$ -acetate shows enhanced signal intensities for C-1, 3, 5 and 7 in the *n*-octyl side-chain as well as for C-9, 13, 11 and 15 in the bislactone moiety. In addition, ^{13}C - ^{13}C coupling ($J = 75 \text{ Hz}$) is observed between C-11 and C-15, which confirms that $[2-^{13}\text{C}]$ -acetate is incorporated into succinate via the citric acid cycle. In contrast, carbon atoms 2, 4, 6, 8, 10 and 14 of avenaciolide (22) are labelled by $[1-^{13}\text{C}]$ -acetate in agreement with Scheme XI.

M. Cytochalasanes: Cytochalasin B (23) and Cytochalasin D (24)

The cytochalasanes are chemically related metabolites isolated recently from several microorganisms. The new structural type of these compounds (examples: cytochalasin B (23) isolated from *Phoma* sp. S298 [42], and cytochalasin D (24) a metabolite of



Zygosporium masonii [43]) raised interest in their biosynthesis. A series of radiotracer experiments was undertaken [44] which showed that cytochalasin B (23) (or phomin) was formed from one molecule of phenylalanine (without loss of the carboxyl group), 2 molecules of methionine and 9 acetate units. Three methionine-derived methyl groups were incorporated into cytochalasin D (24) [45]. Chemical degradations of compounds (23) and (24) demonstrated specific incorporations of phenylalanine and methionine, but only a few carbon atoms were accessible by chemical degradative methods in the acetate derived moiety.

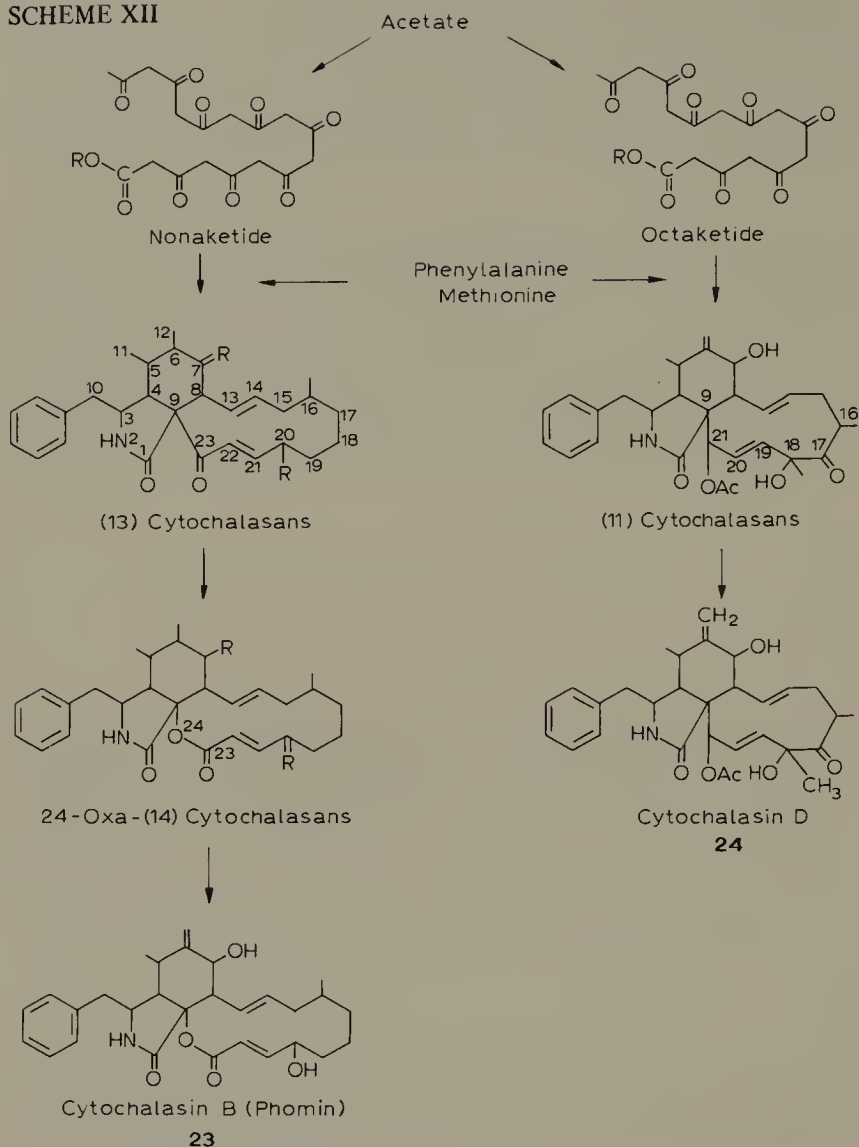
Tamm and co-workers [46] therefore repeated the incorporation of acetate using ^{13}C as a label. Previously, an extensive ^{13}C -n.m.r. study of these compounds at natural abundance was undertaken, including single frequency decoupling and partially relaxed FT, which allowed unambiguous assignments of almost all carbon signals, while ^{13}C -incorporation results have been used for the remaining carbon signals.

Addition of $[2\text{-}^{13}\text{C}]$ -acetate to cultures of *Phoma* sp. S298 led to the isolation of cytochalasin B (23) labelled in positions 11, 6, 8, 9, 14, 16, 18, 20 and 22. Labelling in position 16 is corroborated by earlier results from degradations of cytochalasin B (23) isolated after feeding of ^{14}C labelled acetate. This finding allows in turn the attribution of the signals due to C-15 and C-17.

In a similar manner, $[1\text{-}^{13}\text{C}]$ -acetate and $[2\text{-}^{13}\text{C}]$ -acetate were incorporated into cytochalasin D (24) produced by cultures of *Zygosporium masonii* and the assignment of the ^{13}C -n.m.r. spectrum could be completed in this way.

Viewed together with the previously mentioned ^{14}C tracer studies, these experiments support the biosynthetic pathway of cytochalasanes described in Scheme XII.

SCHEME XII



Further examples of purely acetate derived metabolites whose biosynthesis has been investigated using ^{13}C tracers include the following: fatty acids [47]; epoxydon [48]; thermozymocidin [49]; scytalone [50]; tajixanthone [51]; cerulenine [52].

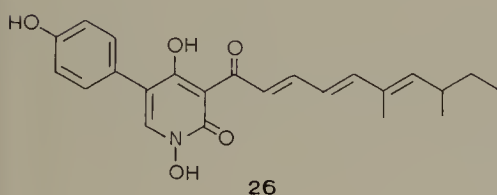
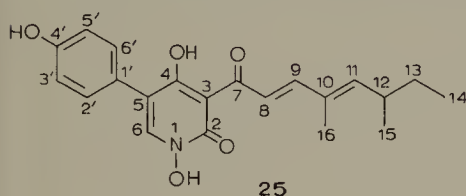
III. COMBINED INCORPORATION OF CARBON-13 ACETATE AND MORE ELABORATE PRECURSORS

In the previous section several examples were discussed where the incorporation of [^{13}C]-acetates provided a significant contribution to the elucidation of a biosynthetic pathway. Before 1970, only a small number of ^{13}C -labelled precursors was commercially available and therefore an increasing number of investigators interested in the application of ^{13}C -label began to synthesize appropriate ^{13}C -labelled molecules, taking advantage

of the great amount of work devoted to the synthesis of specifically labelled ^{14}C -compounds. This progress in synthesis and the increasing number of commercial products allowed incorporation studies on a series of metabolites originating from a greater variety of precursors. Some of the more interesting studies are discussed in greater detail below.

A. Tenellin (25)

The insect pathogenic fungi *Beauveria tenella* (Delacroix) Siem. and *Beauveria bassiana* (Bals.) Vuill. produce the pigments tenellin (25) and bassianin (26). Their structures were established by chemical and spectroscopic methods; ^{13}C -n.m.r. as well as bio-synthetic labelling with ^{15}N - and ^{13}C -labelled precursors were used in this study [53].



The investigation [54] of the biosynthesis of these metabolites was preceded by ^{14}C -tracer experiments which indicated acetate, phenylalanine and methionine as very efficient precursors. Advantage was taken of these findings in the subsequent ^{13}C -tracer investigation.

As predicted, *L*-[^{13}C - CH_3]-methionine labels carbon atoms 15 and 16 of tenellin, whereas carbon atoms 2–3 and 7–14 were alternately labelled by [1- ^{13}C]- and [2- ^{13}C]-acetates, but no enrichment was observed at C-4. Administration of [1,2- ^{13}C]-acetate provided a confirmation of the intact incorporation of five acetate units at the above mentioned sites.

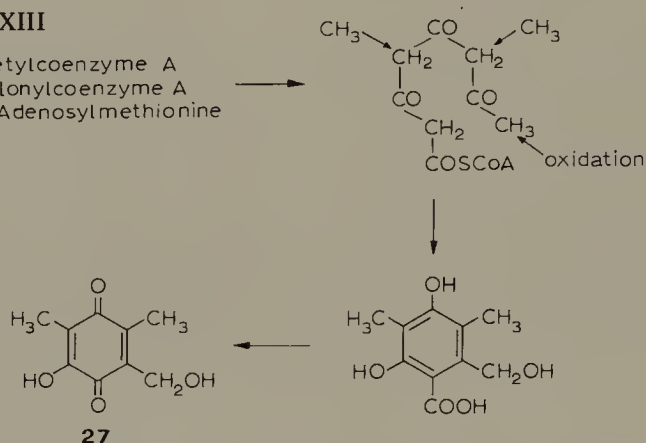
The question concerning the origin of the remaining carbon atoms was resolved by the successful incorporation of [1- ^{13}C]- and [2- ^{13}C]-phenylalanine which labelled C-4 and C-6 respectively. The intact incorporation of a phenylalanine molecule obviously requires the migration of its carboxyl group to the adjacent carbon atom at some stage of the biogenetic pathway. (Similar rearrangements have been observed before in tropic acid [55] and pulvic acid [56] biosynthesis). It should be noted that only a relatively small number of incorporation experiments provided such a great amount of information on the biosynthesis of these two pigments.

B. Shanorellin (27)

Carbon-14-tracer studies on the biosynthesis of shanorellin (27), a benzoquinone pigment isolated from *Shanorella spirotricha* Benjamin, showed that acetate and methionine were good precursors of this substance, while propionate, 2-methylmalonate, shikimate, phenylalanine and tyrosine were not incorporated [57]. Kuhn–Roth oxidation of radioactive shanorellin (27) obtained after incorporation of $[1-^{14}\text{C}]$ -acetate, $[2-^{14}\text{C}]$ -acetate and $[^{14}\text{CH}_3]$ -methionine furnished inactive acetic acid for the first, but radioactive acetic acid for the other two samples, the label being located in the carboxyl in $[2-^{14}\text{C}]$ -acetate-derived shanorellin (27) while methionine labelled the methyl group, suggesting that both methyl groups of shanorellin originate from the C_1 -pool. On the basis of these results, Scheme XIII was proposed for the biosynthesis of shanorellin.

SCHEME XIII

1 mol Acetylcoenzyme A
3 mol Malonylcoenzyme A
2 mol S-Adenosylmethionine



The result of the ^{13}C -tracer study of shanorellin biosynthesis is in complete agreement with the hypothesis [58]. The optimum isotope incorporation had been determined previously by adding increasing amounts of precursor to the culture medium: addition of 5 mM of acetate decreased the yield of shanorellin, but resulted in the lowest isotope dilution. On the other hand, addition of methionine at concentrations above 0.3 mM completely suppressed shanorellin biosynthesis. This observation is important in the whole field of biosynthetic studies using ^{13}C -labelled precursors: the high quantities of samples needed for recording the spectra in turn necessitates relatively large amounts of precursor which may – as illustrated by shanorellin (27) – either completely suppress or only diminish the biosynthesis of the metabolite under investigation. Even the induction of a completely different pathway has been observed in a study of the biosynthesis of showdomycin [59].

Three series of ^{13}C -tracer incorporations have been undertaken: ^{13}C -formate, $[1-^{13}\text{C}]$ - and $[2-^{13}\text{C}]$ -acetates. As expected, formate labels the two methyl groups of shanorellin, while the $[2-^{13}\text{C}]$ -acetate label can be detected in the CH_2OH group and in carbon atoms 2, 4 and 6. Finally, $[1-^{13}\text{C}]$ -acetate incorporation leads to increased signal intensities for carbon atoms 1, 3 and 5, in agreement with Scheme XIII.

C. Nybomycin (28)

The unique heterocyclic system of nybomycin (28), an antibiotic isolated from *Streptomyces* sp. D-57 [60], stimulated speculation on its biogenetic origin [61].



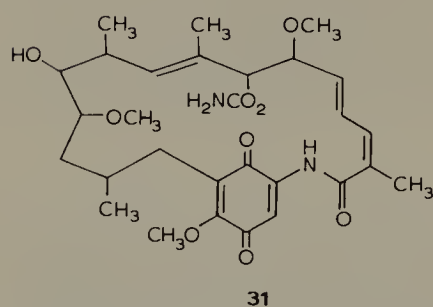
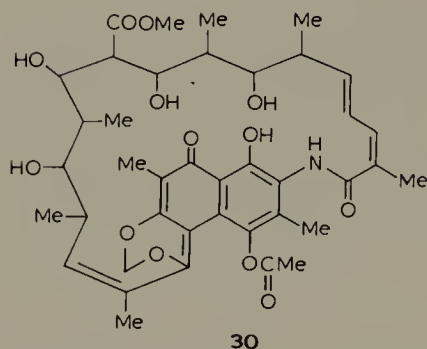
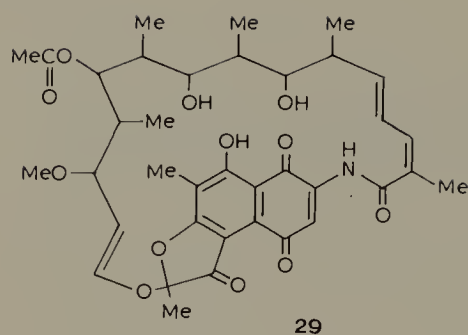
The use of radiotracers allowed the source of carbon atoms 2, 11', 6', 8', 6 and 8 to be determined [62]. C-2 and C-11' were shown to be derived from the C₁-pool by incorporation of [¹⁴CH₃]-methionine; the location of the label was demonstrated by a series of degradation reactions. The precise determination of the amount of radioactivity at each position after the incorporation of [1-¹⁴C]- and [2-¹⁴C]-acetates was much more difficult, especially since the existing degradation schemes for nybomycin (28) do not give access to all carbon atoms.

Consequently, the authors [62] turned to the application of ¹³C-tracers. Carbon-13-enriched nybomycin (28) was isolated after administration of [1-¹³C]-acetate to the culture medium of *Streptomyces* sp. D-57. The ¹³C-n.m.r. spectrum of this sample of nybomycin (28) showed clearly four enhanced signals corresponding to carbon atoms 4, 6, 8 and 10, confirming the earlier ¹⁴C-data. Again, no label could be detected in the central ring of nybomycin (28), thus excluding a precursor of phloroglucinol type.

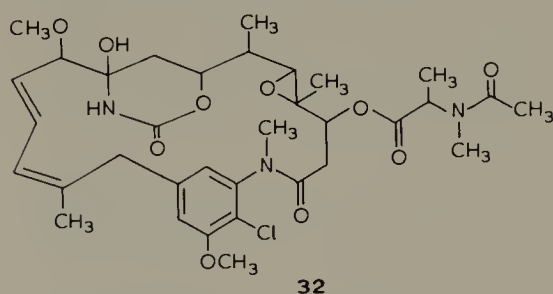
D. The ansamycins

Although ansamycins have been known since 1957 and in spite of the great biological importance of these compounds (antiviral and antibacterial activity as well as inhibition of RNA dependent DNA polymerase) [63] no biosynthetic study had been published before 1973, when Prelog and co-workers announced their ¹⁴C-tracer study on rifamycin S (29) [64] and White et al. [65] and Rinehart and co-workers [66] their ¹³C-tracer investigations on rifamycin S (29) and streptovaricin D (30), respectively. The reason for this relatively long delay may be found in the rather complex structure of these molecules, which rendered the systematic degradation of ¹⁴C-labelled ansamycins extremely difficult.

Nevertheless some preliminary results had been obtained relatively easily: [¹⁴CH₃]-methionine labelled only the methoxyl group of rifamycin S (29) while propionate and acetate were well incorporated. Finally, the ¹³C-tracer studies on rifamycin S (29), streptovaricin (30) and geldanamycin (31) gave a complete picture of ansamycin biosynthesis. These studies demonstrated convincingly that the ansamycins are not only a structurally but also a biogenetically related group of natural products (no investigation



has been undertaken at the time of writing concerning the biosynthesis of maytansin (32), which is a higher plant product).



While the *ansa*-portion of these compounds was shown to be derived from propionate and acetate, no definitive results concerning the C₇N-chromophore – common to all

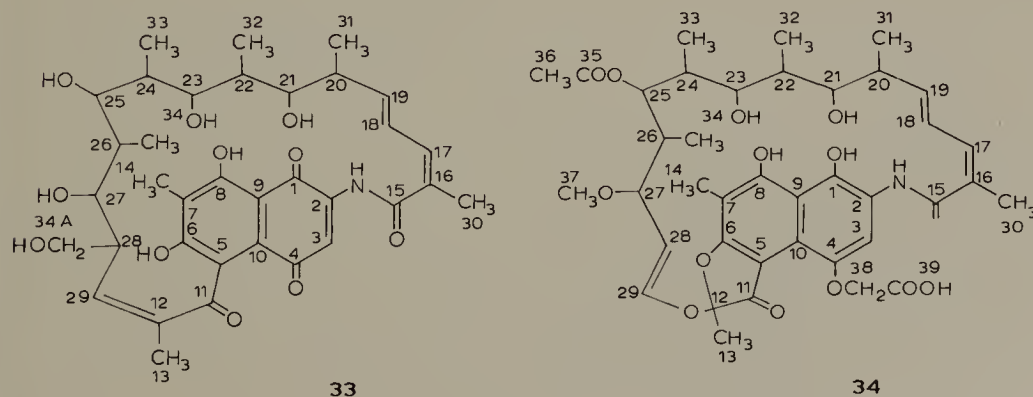
ansamycins – was obtained for a long time, although its carbon skeleton suggested some relationship with shikimic acid (which is a very poor precursor).

1. Rifamycin S (29) and rifamycin W (33)

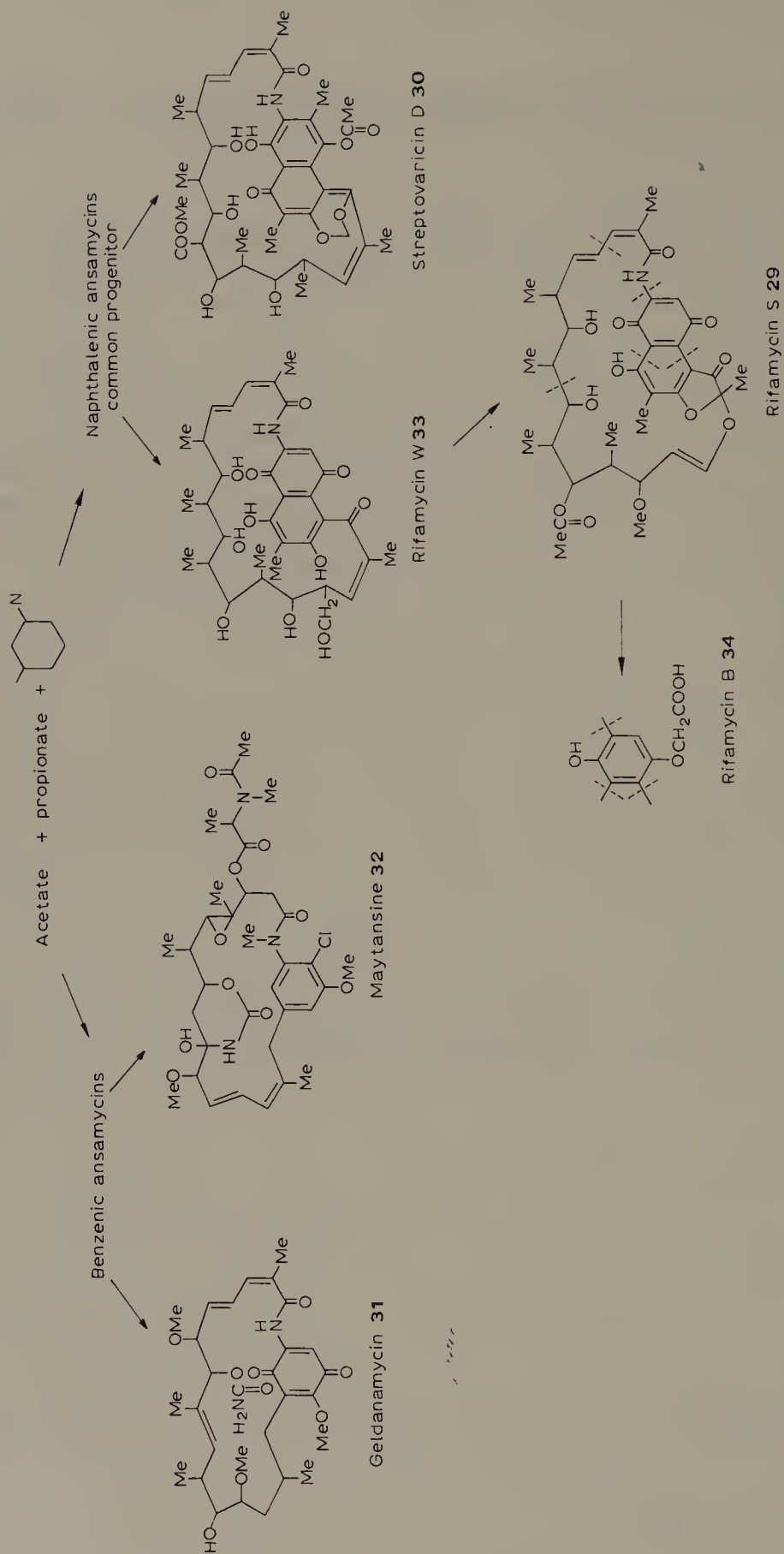
As mentioned above, the incorporation of a great number of ^{14}C - and $^{14}\text{C}/^3\text{H}$ -labelled precursors into *Nocardia mediterranei* led to isolation of radioactive rifamycin S (29) of which degradation partially confirmed an earlier hypothesis formulated by Corcoran and Chick [67].

As soon as complete assignments of the ^{13}C -spectra of the rifamycins (as well as of a great number of derivatives) were available [68], an extensive study of their biosynthesis using ^{13}C -labelled precursors was undertaken [65]. The signals due to carbon atoms 6, 15, 19, 21, 23, 25, 27 and 29 were found to be derived from C-1 of propionate, carbon atoms 7, 12, 16, 20, 22, 24, 26 and 28 from C-2 of propionate and carbon atoms 13, 14, 30, 31, 32, 33 and 34 originate from C-3 of propionate. Thus eight propionate units have been incorporated into rifamycin S (29). One propionate (corresponding to carbon atoms 27 and 28) lost its C-3 methyl group, an observation which would have been very difficult to obtain with the same precision by non-spectroscopic methods. As far as the problem of the direction of chain growth is concerned, the orientation of the two acetate units inserted into the *ansa*-chain was of crucial importance and unambiguous assignments for carbon atoms 17, 18 and 19 had to be established by specific proton decouplings. Since it is C-18 which is derived from the methyl group of acetate, the seven carbon aromatic moiety must be the starting unit of the mixed propionate–acetate condensation. The interruption of the carbon chain by an ether bridge between C-12 and C-29 corresponds to the oxidative splitting between C-1 and C-2 of a propionate unit. These results are independently supported by the structure elucidation and the biosynthesis of rifamycin W (33), which is discussed briefly below.

In a parallel investigation, the same authors [69] succeeded in isolating a new ansamycin, rifamycin W (33) from a mutant strain of *Nocardia mediterranei*. Its structural similarity with the other known rifamycins and the streptovaricins is obvious. Compared to rifamycin S (29), two structural features were particularly interesting: the



SCHEME XIV



absence of an ether bridge between C-12 and C-29 and the presence of a hydroxy-methyl substituent on C-28.

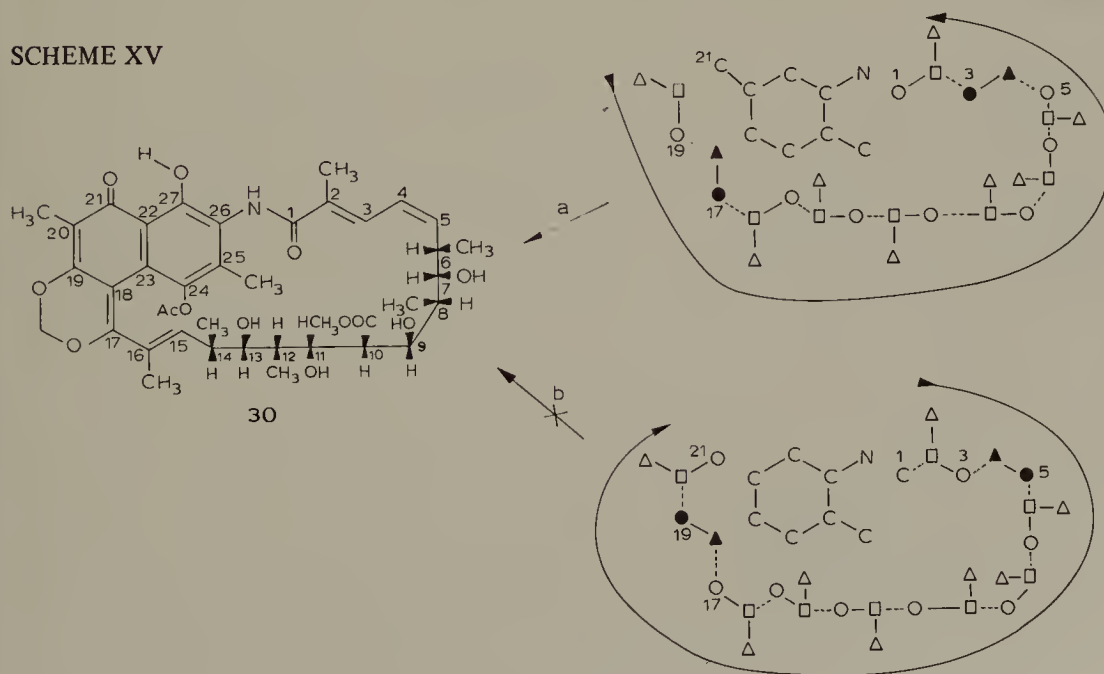
Two series of incorporation experiments were undertaken. In the first, ^{13}C -labelled propionates ($[1-^{13}\text{C}]$ -, $[2-^{13}\text{C}]$ - and $[3-^{13}\text{C}]$ -propionates) as well as $[1-^{13}\text{C}]$ -acetate were incorporated into rifamycin W (33) and the results obtained were in perfect agreement with a mixed propionate–acetate origin of the *ansa*-portion of this metabolite (8 intact propionates and 2 acetates). In the second, ^{14}C -rifamycin W was shown to be converted efficiently into rifamycin B (34) [70] by the mycelium of a rifamycin B-producing strain of *Nocardia mediterranei*.

Thus, rifamycin W (33) represents some kind of a missing link in the biosynthetic pathway of the rifamycins and the above mentioned results underline the importance of mutant strains in the study of biosynthetic pathways (Scheme XIV).

2. Streptovaricin D (30)

Streptovaricin D (30) is an ansamycin structurally related to the rifamycins and this metabolite can be isolated from *Streptomyces spectabilis*. Preliminary ^{14}C -tracer studies [66] ($^{14}\text{CH}_3$ -methionine, ^{14}C -malonate and ^{14}C -propionate) had suggested a mixed propionate–acetate origin for the *ansa*-bridge. As for the rifamycins, the two terminal propionates can be arranged in two different ways: one where the amide carbonyl is derived from the carboxyl group of propionate (Scheme XV) (pathway a), the other where the amide carbonyl would originate from a one-carbon source (pathway b). It should be noted that the ^{14}C -tracer experiments had not allowed for the distinction between pathways (a) and (b) (Scheme XV).

SCHEME XV



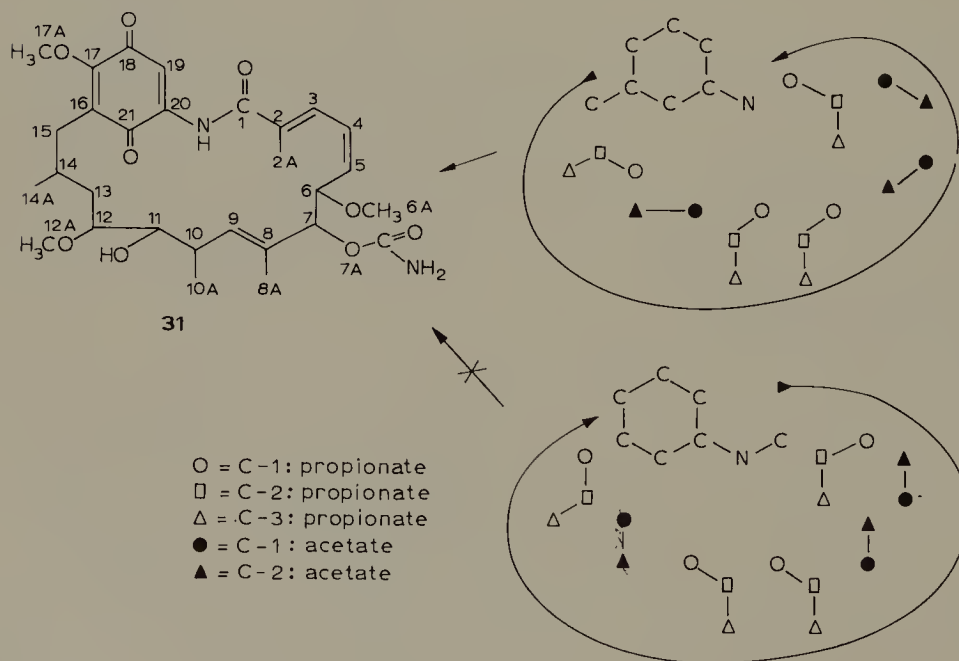
In order to settle this question, $[1-^{13}\text{C}]$ -propionate was added to cultures of *Streptomyces spectabilis* and the enriched streptovaricin D (30) was isolated and investigated by ^{13}C -n.m.r. As can be seen from Scheme XV, the key carbon atoms which allow one to distinguish between these two possibilities are the amide carbon C-1 and carbon atoms 3 and 5.

In the ^{13}C -n.m.r. spectrum of labelled streptovaricin D (30), 8 signals of enhanced activity were observed, assigned to carbon atoms 1, 5, 7, 9, 11, 13, 15 and 19, establishing clearly and elegantly that pathway (a) is followed. In analogy with rifamycin biosynthesis, one of the ring carbons (C-19) is labelled by the carboxyl group of propionate and the quinone carbonyl C-21 is again unlabelled. No indications concerning the C_7N moiety could be obtained. (According to unpublished results by the same authors [66], they have evidence that the methyl group on C-25 is derived from methionine, which is consistent with the non-incorporation of propionate at this particular site). Viewed together, the information available from rifamycin and streptovaricin biosynthetic studies demonstrated the existence of close structural and biogenetic relationship within the ansamycins. In order to complete these data, incorporation results on a benzenoid ansamycin were desirable.

3. Geldanamycin (31)

Two benzenoid ansamycins, geldanamycin (31) [71] and maytansin (32) [72] are known actually and it was interesting to see whether their biosynthesis was analogous to that of the rifamycins and streptovaricin D. Geldanamycin (31) was the compound

SCHEME XVI

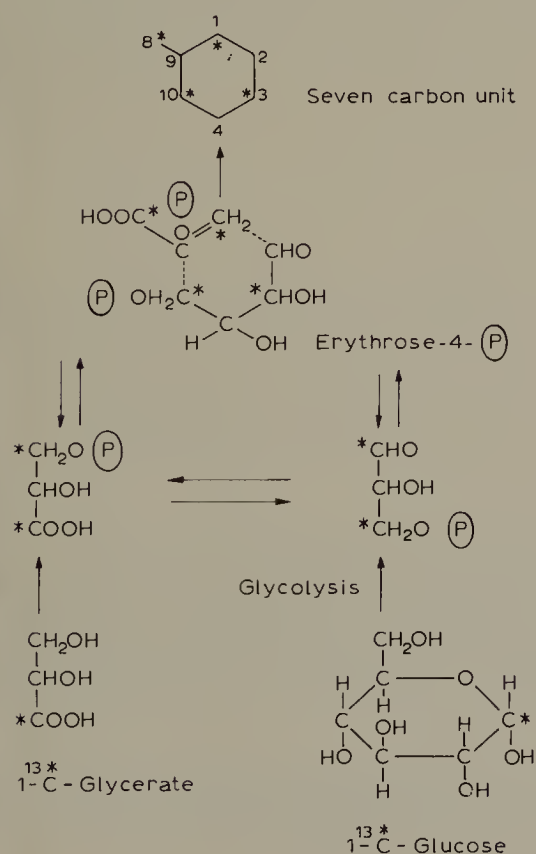


of choice since maytansin is a higher plant product and therefore difficultly amenable to ^{13}C -tracer studies.

In preliminary incorporation experiments several ^{14}C -labelled precursors ($[^{14}\text{CH}_3]$ -methionine and $[1\text{-}^{14}\text{C}]$ -propionate) were added to cultures of *Streptomyces hygroscopicus* var. *geldanus* var. *nova* [73]. Both were well incorporated, acetate and malonate much less. These observations indicated a certain similarity of its biosynthesis with that of the previously discussed ansamycins. This was elegantly demonstrated by the use of ^{13}C -precursors. Administration of $[^{13}\text{CH}_3]$ -methionine yielded labelled geldanamycin (31) whose ^{13}C -n.m.r. spectrum showed that only the three methoxyl groups were enriched by ^{13}C -labelled precursors. Curiously, the carbamate carbon at position 7A was not labelled. In the experiment with $[1\text{-}^{13}\text{C}]$ -propionate, C-1, C-7, C-9 and C-13 were enriched, which corresponds again to an amide-head direction of the biosynthesis of the *ansa*-moiety of geldanamycin and indicates a continuous sequence of propionate—acetate units from C-14 through C-1. This is in agreement with the above mentioned results concerning rifamycins and streptovaricin biosynthesis (Scheme XVI).

At this stage of progress in ansamycin biosynthesis a general scheme became apparent. While the mixed origin from propionate—acetate of the *ansa*-chain was quite clearly

SCHEME XVII



established (the importance of ^{13}C -tracers in this work must be emphasized), only a few hints were available concerning the central C_7N -unit. Preliminary ^{14}C -tracer studies of a great number of potential precursors (including glucose, glucosamine, myoinositol and shikimate) provided no conclusive results [74]. Further progress in this problem only became possible when considerable improvements in incorporation and spectra-recording techniques had been achieved. As soon as this became possible, White and Martinelli [75] obtained significant incorporation of $[1\text{-}^{13}\text{C}]$ -glucose into rifamycin S (29) whose ^{13}C -n.m.r. spectrum showed enhanced signals for carbon atoms C-1 and C-10. Further evidence concerning the biogenetic origin of the C_7N -chromophore came from studying the incorporation of $[1\text{-}^{13}\text{C}]$ -glycerate which labelled two positions, C-3 and C-8. These observations were interpreted in favour of a shikimate-type origin of the chromophore, apparently contradicting earlier negative results with ^{14}C -shikimate. In order to explain the observed labelling pattern, a scheme was proposed based on known metabolic pathways of the two specifically incorporated precursors, avoiding a passage through shikimate (Scheme XVII).

A major advantage of this scheme lies in the fact that the immediate precursor of the ansamycin chromophore readily explains the ring closure with the aliphatic bridge to form the naphthalenic unit (Figure 8).

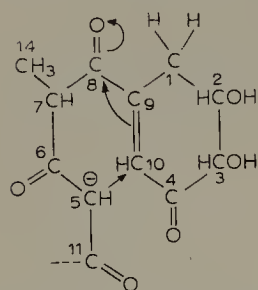


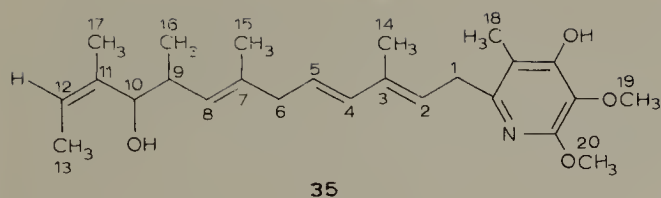
Fig. 8. Proposed mechanism of ring closure to give the naphthalenic chromophore of rifamycin S (29).

Although the corresponding results concerning the biosynthesis of the C_7N -unit of streptovaricin D (30) and geldanamycin (31) are not yet available, a similar pathway can be predicted for these compounds.

E. Piericidin A (35)

Piericidin A (35), a naturally occurring insecticide, is produced by *Streptomyces mobaraensis* and ^{14}C -tracer studies furnished some indications concerning its biogenetic origin. Indeed, acetate, propionate and methionine were well incorporated, but no definitive results could be obtained, especially since acetate had been heavily randomised prior to incorporation [76].

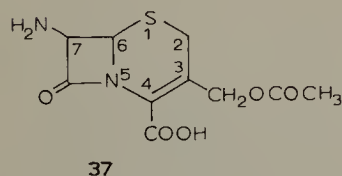
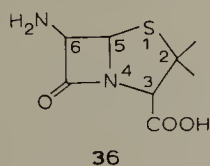
In their ^{13}C -tracer study on the biosynthesis of piericidin A (35), Tanabe et al. [77] added $[3\text{-}^{13}\text{C}]$ -propionate to *Streptomyces mobaraensis* fermentations and analysed the metabolite (35) by the satellite method. In the ^1H -n.m.r. spectrum of (35) the methyl



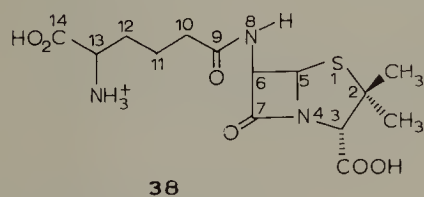
signals of C-14, 15, 16, 17 and 18 were well resolved and could be assigned. The data obtained show that these five methyl groups are derived from propionate; subsequent incorporation of [$^{13}\text{CH}_3$]-methionine allowed the determination of the origin of the OCH_3 groups. No label from propionate was detected in C-13. Furthermore, the equal intensity of the satellite bands favours a pathway involving a single polyketide chain. Nevertheless, from the now available information, the loss of a propionate derived methyl group at C-5 cannot be excluded and needs further investigation.

F. β -Lactam antibiotics: penicillins and cephalosporins

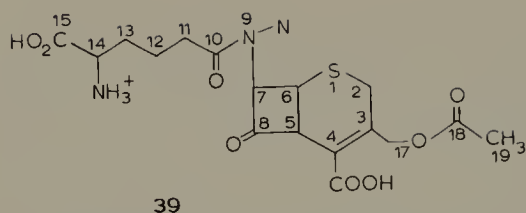
The penicillins are *N*-acyl derivatives of 6-aminopenicillanic acid (36) possessing a β -lactam thiazolidine ring system, which is replaced in the cephalosporins by a β -lactam-dihydrothiazine ring system (7-aminocephalosporanic acid (37)). The importance of the biological properties of the β -lactam antibiotics in the treatment of various infections has stimulated considerable interest not only in their synthesis, but also in their biosynthesis.



As a matter of course, the earlier studies of the biosynthesis of β -lactam antibiotics were undertaken using ^{14}C -tracers, and their results have been reviewed by Abraham and Newton [78]. Exogenous [$2\text{-}^{14}\text{C}$]- and [$6\text{-}^{14}\text{C}$]- α -aminoadipic acids were shown to be the precursors of the acyl side chain of penicillin N (38) and cephalosporin C (39), and intact cysteine and valine were incorporated into the heterocyclic moiety.



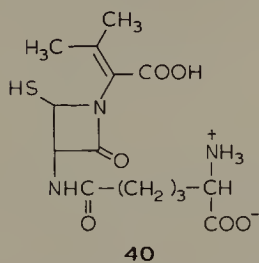
References pp. 161–166



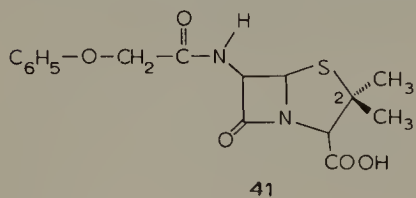
The use of ^{13}C -precursors provides confirmation of results obtained previously with the radiotracers. Thus, addition of $[1\text{-}^{13}\text{C}]$ -acetate to a culture medium of *Cephalosporium acremonium* mutant M 8650-3 led to the isolation of cephalosporin C (39) labelled in positions 10, 15 and 18, while $[2\text{-}^{13}\text{C}]$ -acetate labelled carbon atoms 11, 12, 13, 14 and 19.

It should be noted that the enrichment level at C-13, C-12 and C-11 is about half of that at C-14 suggesting that the acyl side chain is formed by condensation of α -keto-glutarate and acetate via the Krebs cycle [79,80].

Even more interesting information was obtained in the course of the investigations using ^{13}C -labelled valine as precursor. First, DL- $[1\text{-}^{13}\text{C}]$ -valine and DL- $[2\text{-}^{13}\text{C}]$ -valine were shown to enrich specifically positions 16 and 4 of cephalosporin C (39) [80]. On the basis of this result the synthesis of valine possessing a chiral ^{13}C -label was undertaken as a probe for the stereochemical fate of its isopropyl group during conversion into the β -lactam antibiotics [81]. In particular, a great deal of information could be expected concerning the proposal that an α,β -dehydrovaline derivative of the tripeptide (40) was the precursor of these compounds.



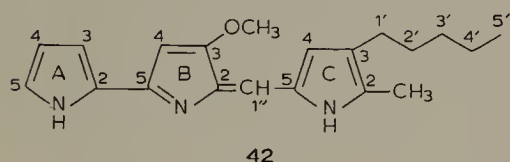
(2RS,3R)- $[4\text{-}^{13}\text{C}]$ -valine, when added to submerged cultures of *C. acremonium* (mutant M-8650-3), furnished labelled cephalosporin C. A five-fold enhanced intensity was detected for the signal assigned to C-2 without any other observable change in the spectrum [82]. In a parallel experiment, the same precursor had been administered to cultures of *Penicillium chrysogenum* which gave labelled penicillin V (41) showing an approximately two-fold enhancement of the $\beta\text{-CH}_3$ at C-2 [82].



Independently, Sih and co-workers [83] had synthesized (2S,3S)-[4- ^{13}C]-valine, which they added to a culture medium of *C. acremonium* (mutant C 91) producing penicillin N (38) along with cephalosporin C (39). The α -methyl signal was enhanced in the ^{13}C -n.m.r. spectrum of penicillin N (38) by about 20%, but no significant amount of label above natural abundance could be detected in the β -methyl signal, which means that (2S, 3S)-[4- ^{13}C]-valine is incorporated into penicillin N (38) with retention of configuration. In the sample of cephalosporin C (39), the ^{13}C -label was located at C-17 providing a complementary result to the above mentioned investigation.

G. Prodigiosin (42)

Prodigiosin (42), which can be isolated from *Serratia marcescens*, was the first natural product whose biosynthesis was studied by applying the FT technique. Tracer studies [84] showed excellent incorporation rates of acetate, glycine, proline and methionine into this metabolite and the first ^{13}C -n.m.r. study [85] confirmed the incorporation of acetate and allowed location of the label in positions B₃, C₃, C₅, 2' and 4' when [1- ^{13}C]-acetate was the precursor, and in positions B₄, C₄, 1', 3' and 5' after incorporation of [2- ^{13}C]-acetate. No label at all could be detected in ring A.

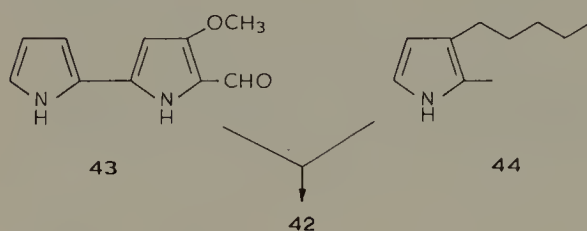


The origin of the remaining carbon atoms was determined by administration of specifically labelled alanine, glycine, proline and serine [86]. For instance, when [carboxy- ^{13}C]-proline was fed to *Serratia marcescens* only the signal due to carbon B₅ was enhanced, supporting a pathway where ring A and carbon B₅ are derived from an intact molecule of proline. As expected, [$^{13}\text{CH}_3$]-methionine is well incorporated into the methoxy group. When [3- ^{13}C]-alanine was administered, prodigiosin (42) showed six sites of incorporation and the pattern of labelling was identical with that observed after incorporation of [2- ^{13}C]-acetate, but one additional incorporation (corresponding to the methyl group of ring C) was observed. These results suggest that C₂ and C₂-Me are derived from alanine (corroborated by ^{14}C -tracer experiments) and that part of the fed alanine is transaminated to pyruvate which is then decarboxylated oxidatively to acetate along known metabolic pathways. Finally, feeding experiments with specifically labelled glycine and serine showed that carbon atoms B₂ and 1'' of prodigiosin (42) are derived from carbons 2 and 3 of serine or from its immediate precursor, glycine.

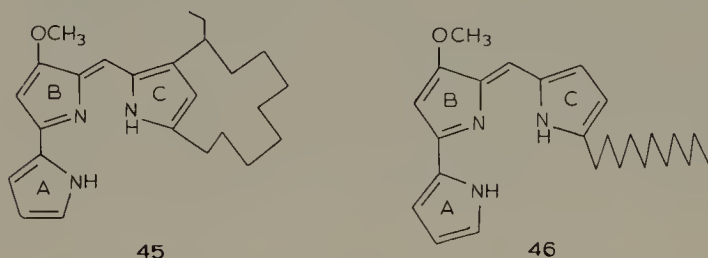
From these results and on the basis of earlier studies which had shown [87] that prodigiosin biosynthesis involved the condensation of two building blocks, a methoxy-bipyrrole carboxaldehyde (43) and a methylamyl pyrrole (44), Scheme XVIII was

proposed. This pattern of pyrrole biosynthesis is unusual in nature and its elucidation is essentially due to recent progress in ^{13}C -n.m.r.

SCHEME XVIII

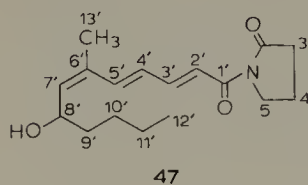


Taking advantage of the available information, the structure and biosynthesis of two related tripyrrole metabolites of *Streptomyces longisporus*, metacycloprodigiosin (45) and undecylprodigiosin (46), were investigated [88]. The slightly different incorporation pattern observed for glycine and acetate might find an explanation in an increased turnover via the Krebs cycle and incorporation of $[1,2-^{13}\text{C}]$ -acetate might be of great help in such a study.



H. Variotin (47)

Variotin (47) is an antifungal antibiotic produced by *Paecilomyces varioti* Bainier var. *antibioticus* [89]. A series of ^{14}C -tracer studies including a large number of chemical degradation steps led to a determination of the distribution of label in the side chain, and these results suggested the incorporation of six acetate units by head-to-tail linkage [90].

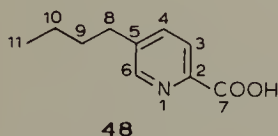


In two separate experiments, $[1-^{13}\text{C}]$ - and $[2-^{13}\text{C}]$ -acetate were administered to cultures of *Paecilomyces varioti* and the samples of ^{13}C -enriched variotin (47) isolated were analysed by the "satellite method" [91]. The satellite bands of 7 carbon atoms could be measured by this technique and the results obtained were in perfect agree-

ment with the ^{14}C -tracer study. In addition, the incorporation of $[\text{}^{13}\text{CH}_3]$ -methionine furnished highly enriched variotin (47) and the label could be located at position 13'. Neither acetate nor methionine were incorporated into the pyrrolidone ring. This is in perfect agreement with the results obtained by Tanaka [90] who had shown with the aid of ^{14}C -tracers that glutamic acid forms the pyrrolidone moiety after loss of its C-1 carboxyl group.

I. *Fusaric acid* (48)

Fusaric acid (48) was among the first compounds (1968) whose biosynthesis was studied with ^{13}C -labelled precursors. The early date also explains the use of the "satellite method" in this case.



Previous ^{14}C -tracer investigations [92] on this phytotoxic metabolite isolated from *Fusarium oxysporum* Schlecht had suggested that the pyridine ring of fusaric acid (48) was derived from acetate via aspartate, although the amounts of radioactivity at different carbon atoms were not entirely consistent with this hypothesis, probably due to the great number of degradation reactions required.

Desaty et al. [93] reinvestigated this problem using doubly labelled ($^{14}\text{C}/^{15}\text{N}$) aspartic acid as precursor. In this experiment the ^{15}N of aspartic acid was incorporated more efficiently than ^{14}C suggesting that aspartic acid is partially metabolised to fusaric acid (48) via oxalacetate and that L-aspartate serves predominantly as a nitrogen-donor.

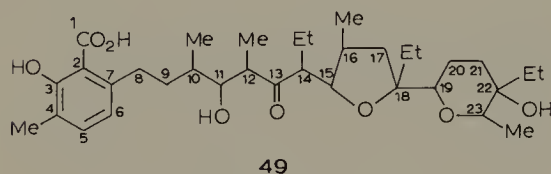
In order to obtain further information on the biosynthesis of the pyridine ring, the same authors [93] incorporated ^{13}C -labelled precursors. In the spectrum of fusaric acid isolated after incorporation of $[1\text{-}^{13}\text{C}]$ -acetate the satellite peaks due to carbon atoms 4, 6, 8 and 10 were measured, C-4 showing a smaller enrichment than the other three labelled carbon atoms, which implies a difference in its biogenetic origin. A reduced sample of fusaric acid ($\text{COOH} \rightarrow \text{CH}_2\text{OH}$) allowed the determination of the level of incorporation at C-7, which was found to be similar to that at C-4. In agreement with this observation, administration of $[2\text{-}^{13}\text{C}]$ -acetate led to a smaller enrichment at C-3 than at C-11 while the values for C-4 and C-7 were much higher than those for C-6. These results are consistent with a biogenetic formation of fusaric acid from two different biological building blocks: one directly derived from acetate and accounting for carbon atoms 5, 6, 8, 9, 10 and 11, the other being a four-carbon dicarboxylic acid formed from acetate and providing carbon atoms 7, 2, 3 and 4.

Further evidence for this scheme was obtained by the incorporation of $[4\text{-}^{13}\text{C}]$ -aspartate: apparently, some equilibration between C-1 and C-4 of aspartate had occurred

prior to the incorporation in fusaric acid, which constitutes a strong argument against direct incorporation of this amino acid.

J. Lasalocid A (Antibiotic X-537 A) (49)

Lasalocid A (49), a metabolite of *Streptomyces lasaliensis*, is among the most interesting examples whose biosynthesis has been investigated using ^{13}C -n.m.r. It is unique in nature in possessing three C-ethyl groups and it is the only polyether antibiotic so far reported with an aromatic chromophore.

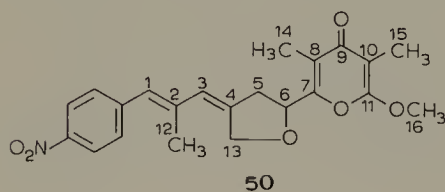


Three different ^{13}C -labelled precursors were administered to *S. lasaliensis* and the following results were obtained: [$1\text{-}^{13}\text{C}$]-acetate is incorporated into carbon atoms 1, 7, 5, 19 and 23. [$1\text{-}^{13}\text{C}$]-propionate enhances the signals due to carbon atoms 3, 9, 11 and 15 and [$1\text{-}^{13}\text{C}$]-butyrate increases the intensity of the resonances arising from carbon atoms 13, 17 and 21 [94,95]. Thus, lasalocid A (49) is biosynthesized from five acetates, four propionates and three butyrates. While the incorporation of propionate accounts for the methyl groups (except the one at C-23 which is apparently part of the chain initiating acetate unit), that of butyrate provides the three C-ethyl groups.

More recently, the same group of authors succeeded in the isolation from *S. lasaliensis* fermentations of a complex mixture of lasalocid A homologs called lasalocid B, C, D and E. These metabolites arise by replacement of one of the four propionate derived methyl groups of (49) by an ethyl group [96]. These results confirm and complete the earlier studies [97] with variously labelled [^{14}C]-propionate and [^{14}C]-butyrate.

K. Aureothin (50)

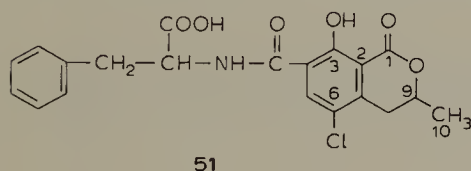
The involvement of *p*-amino- and *p*-nitro-benzoic acids in the biosynthesis of aureothin (50), a metabolite of *Streptomyces luteoreticuli* Katoh et Arai (strain KS2-74) has been reported [98]. These acids (or their biological equivalents) could reasonably be supposed to condense with a polyketide to form aureothin (50). Nevertheless, two possible routes to (50) had to be taken into consideration: one, where methionine-derived C_1 -units are introduced into an acetate-malonate derived polyketide, the other, where the "extra methyls" originate from C-3 of propionate.



The first pathway could be easily excluded since radioactive aureothin (50) isolated after incorporation of [$^{14}\text{CH}_3$]-methionine contained all its label in the methoxy group [99]. This result supported the existence of a pathway involving propionate. Incorporation experiments with [$3\text{-}^{13}\text{C}$]-propionate were performed. Comparison of the ^{13}C -n.m.r. spectra of aureothin (50) at natural abundance and enriched by propionate showed that four carbon atoms (12, 13, 14 and 15) were derived from C-3 of propionate. The question of whether carbon atoms 6 and 7 are provided by propionate (after loss of a methyl group) or by acetate must await further incorporation experiments.

L. Ochratoxin (51)

Steyn et al. [100] studied the biosynthesis of ochratoxin A (51) by experiments with [^{14}C]-phenylalanine, [^{14}C]-acetate and [^{14}C]-methionine. In particular, they demonstrated that the latter compound was specifically incorporated into the amide carboxyl group, a result which was confirmed later by Yamazaki and co-workers [101] with the aid of [$^{13}\text{CH}_3$]-methionine.



M. Sepedonin (52)

Sepedonin (52), a metabolite of *Sepedonium chrysospermum*, is structurally related to stipitatic acid, a naturally occurring tropolone isolated from *Penicillium stipitatum* [102]. In analogy with the latter compound, [^{14}C]-acetate and [^{14}C]-formate were excellent precursors of sepedonin (52) and a series of incorporation experiments with ^{13}C -precursors, using the satellite method for analysis, was undertaken [103]. After enrichment with [$2\text{-}^{13}\text{C}$]acetate only five carbon atoms could be measured (CH_3 , C-4, C-1, C-5 and C-8) by this method, but the ^{13}C -n.m.r. spectrum of the same sample was recorded later on, providing convincing evidence that sepedonin (52) is formed by insertion of a one-carbon unit into a ten-carbon polyketide chain derived from acetate [104].

[$2\text{-}^{13}\text{C}$]-Acetate enhanced the signals due to CH_3 , C-4, C-5, C-9a and C-7 (spectrum A, Fig. 9) and [$1\text{-}^{13}\text{C}$]-acetate labelled C-1, C-3, C-4a, C-6 and C-9 (spectrum B). Finally, administration of [^{13}C]-formate gave sepedonin (52) highly enriched in position 8 (spectrum C). These results are in full agreement with the biogenetic pathway depicted in Scheme XIX. It may be noted that the incorporation of [$1,2\text{-}^{13}\text{C}$]-acetate into (52) could furnish a further confirmation, since according to the scheme, C-7 and

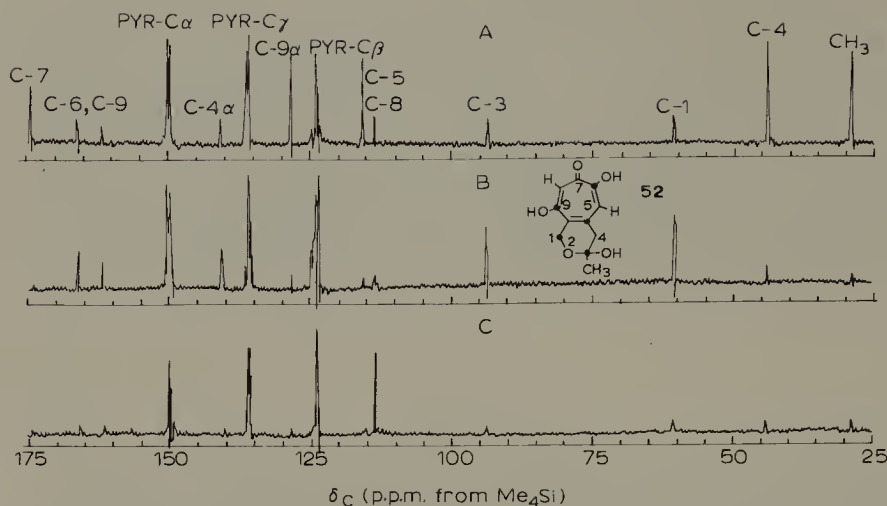
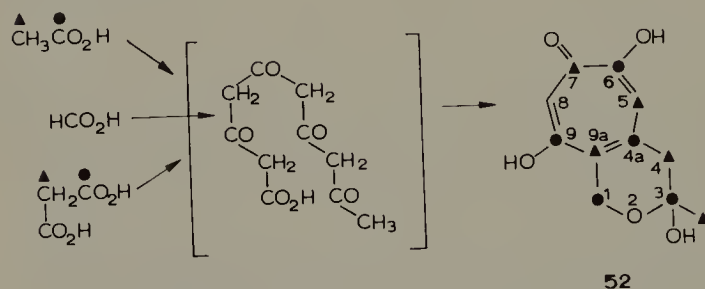


Fig. 9. Incorporation of $[2-^{13}\text{C}]$ -acetate (Spectrum A), $[1-^{13}\text{C}]$ -acetate (Spectrum B) and ^{13}C -formate into sepedonin (52). (Spectra reproduced with permission from A.G. McInnes, D.G. Smith, L.C. Vining and L. Johnson, *Chem. Commun.*, (1971) 325.)

C-9 are derived from the same acetate group, but should appear as singlets in the spectrum.

SCHEME XIX



IV. TERPENES

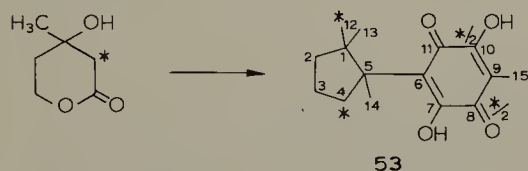
The terpenes constitute one of the largest and structurally most variable classes of secondary metabolites and hold an important place in organic chemistry and biosynthesis. A detailed discussion of the chemical, biogenetic and enzymological studies on terpenes, particularly associated with the work of Bloch, Lynen and Cornforth, is beyond the scope of this article. Comprehensive accounts of isoprenoid biosynthesis — synthesis of mevalonate from acetate, formation of polyisoprene chains via phosphate derivatives and cyclisation, can be found in the literature [105].

It is therefore rather surprising — considering the importance of terpenes in nature

— that the first ^{13}C -biosynthetic study of a terpene, Wenkert's analysis of the virescens enriched by $[1\text{-}^{13}\text{C}]$ - and $[2\text{-}^{13}\text{C}]$ -acetates, was not published before 1972 [106]. Nevertheless, this paper was soon followed by a rapidly increasing number of investigations, some of which will be discussed in more detail.

A. *Helicobasidin* (53)

The fungal sesquiterpene, helicobasidin (53), can be isolated from cultures of *Helicobasidium mompa* [107]. Investigations using ^3H - and ^{14}C -labels have shown that helicobasidin (53) is biosynthesized along a pathway implying a direct cyclisation of farnesyl pyrophosphate. The ^{13}C -study by Tanabe et al. [108] not only confirmed these earlier results, but it also represents a fine example of the application of paramagnetic complexes in the course of biosynthetic investigations.



Incorporation of $[2\text{-}^{13}\text{C}]$ -mevalonate gave enriched helicobasidin (53), which showed easily detectable signal enhancements for carbon atoms 12 and 4, but no definitive increase in intensity was observable for the signals due to carbon atoms 8 and 10, which should be equally labelled because of the symmetry in the quinone moiety. In fact, the C-8 and C-10 signals were diminished due to the absence of attached hydrogen atoms. In order to overcome these limitations paramagnetic *tris* (acetylacetonato) chromium(III) $[\text{Cr}(\text{acac})_3]$ was added, which resulted in the obtention of a spectrum showing equally enhanced intensities for C-8 and C-10. *Tris* (acetylacetonato) chromium(III) not only quenches the nuclear Overhauser effect (NOE), but also decreases relaxation time to more uniform values and helps in this way to eliminate the two major causes of intensity differences in FT ^{13}C -n.m.r. spectroscopy. This method may be useful in cases where only low incorporation rates can be obtained.

B. *Ovalicin* (54)

The determination of the biosynthetic origin of ovalicin (graphinone) — a sesquiterpene from *Pseudeurotium ovalis* [109] — is a good example of the usefulness of $[1,2\text{-}^{13}\text{C}]$ -acetate in biosynthetic studies, since, with a single feeding experiment, the biosynthetic origin of all fifteen carbon atoms of ovalicin (54) was established [110].

When *P. ovalis* was cultured in the presence of $[1,2\text{-}^{13}\text{C}]$ -acetate, enriched ovalicin (54) was isolated and analysed by FT ^{13}C -n.m.r. Twelve coupled carbon signals can be observed in the spectrum (Fig. 10) of ovalicin (54), corresponding to the incorporation of six intact acetate units. These signals were assigned by taking advantage of known chemical shift data, the observed C—C coupling constants and the multiplicities of the

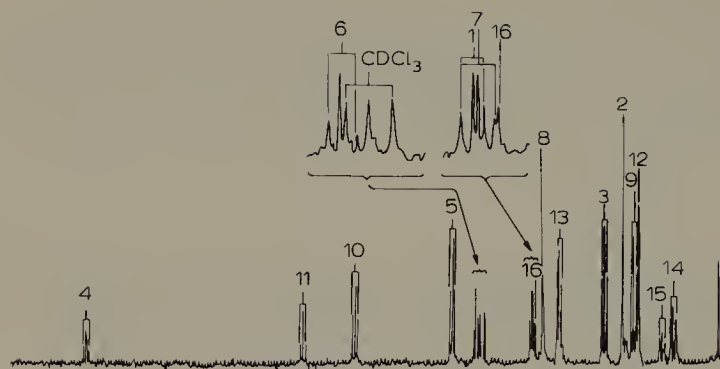
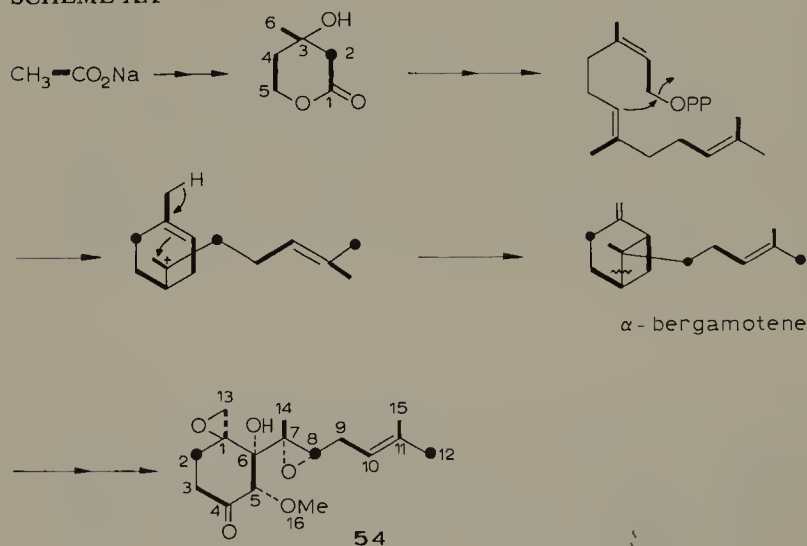


Fig. 10. FT ^{13}C -NMR spectrum of ovalicin (54) after incorporation of $[1,2\text{-}^{13}\text{C}]$ -acetate. (Spectrum reproduced with permission from M. Tanabe and K.T. Suzuki, *Tetrahedron Lett.*, (1974) 4420.)

off-resonance decoupled spectrum of the unlabelled metabolite.

In agreement with Scheme XX, the signals due to the carbon atoms derived from C-2 of mevalonate (C-2, C-8 and C-12) appear as enriched singlets. This pattern of acetate incorporation suggests a biogenetic pathway through cyclisation of *cis*-farnesylpyrophosphate to α -bergamotene, followed by ring opening of the cyclobutane intermediate to give finally ovalicin (54).

SCHEME XX



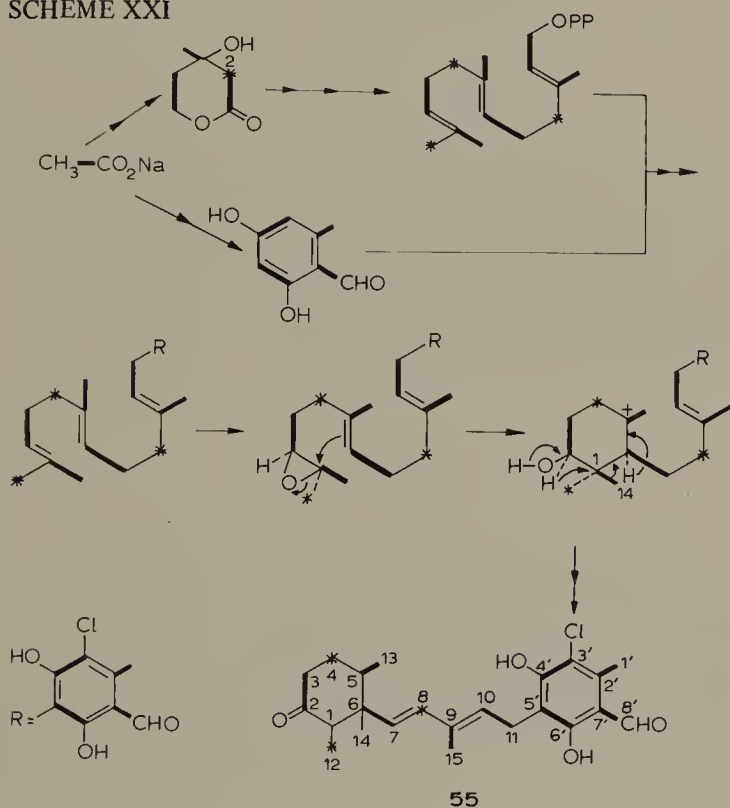
C. Ascochlorin (55)

The investigation of the biosynthesis of ascochlorin (55) — a triprenylphenol from *Nectria coccinea* — is a further application of $[1,2\text{-}^{13}\text{C}]$ -acetate in the elucidation of

biogenetic pathways [111]. Indeed the analysis of only one ^{13}C -n.m.r. spectrum allows the detection of a C—C bond fission followed by a stereospecific migration of a methyl group.

Eighteen signals with C—C couplings were observed in the FT ^{13}C -n.m.r. spectrum of ascochlorin (55) after administration of $[1,2-^{13}\text{C}]$ -acetate, indicating the presence of 9 intact acetate units. Only 5 of them could be attributed to the terpenoid moiety, in particular C-14 and C-1 appeared only as enriched singlets. This result favors the biosynthetic pathway outlined in Scheme XXI.

SCHEME XXI

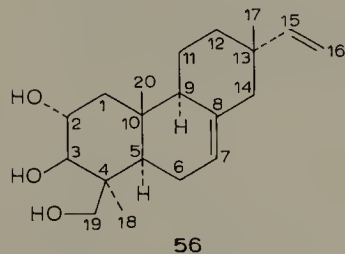


In agreement with this scheme, C-4, C-8 and C-12, which originate from C-2 of mevalonate, appear as singlets of increased intensity. Furthermore, the four C—C couplings in the chloroorseellinic aldehyde part are consistent with its biogenesis through a polyketide.

D. Virescensol A (56)

As already mentioned in the discussion of ovalicin (54) and ascochlorin (55) biosynthesis (see above), the incorporation of $[1,2-^{13}\text{C}]$ -acetate into terpenoids via mevalonate allows one to determine whether a particular ^{13}C -n.m.r. signal originates from C-2 or C-6 of mevalonate. Indeed, carbons derived from C-2 of mevalonate give rise to

singlets while those derived from C-6 show coupling with those coming from C-4. Of course, specifically labelled mevalonate ($[2-^{13}\text{C}]$ -mevalonate for example) would provide the same information — as demonstrated in the case of helicobasidin (53) — but this precursor is still much more expensive.



It was therefore of interest to apply this technique to the problem of the biogenetic origin of the two substituents on C-4 of virescenol A (56) [112]. Tedious degradation experiments had been necessary in the past with ^{14}C -labelled compounds [113]. In the ^{13}C -n.m.r. spectrum of virescenol A (56), one of the substituents on C-4 previously assigned to C-18 shows no coupling, indicating that it is derived from C-2 of mevalonate.

E. Fusidic acid (57)

Fusidic acid (57) is a triterpene antibiotic used in the treatment of staphylococcal infections [114]. From a chemical point of view it was interesting to investigate this compound by ^{13}C -n.m.r. because the fusidane skeleton differs from the androstane and cholestane steroids by having ring B in a boat conformation [115].

In order to assign all carbon signals of the ^{13}C -n.m.r. spectrum of fusidic acid (57), a series of derivatives was prepared and their spectra recorded. Finally, supplementary information was obtained after incorporation of $[1-^{13}\text{C}]$ -acetate by growing *Fusidium coccineum* Fuckel — K. Tubaki in the presence of this precursor [116].

In spite of a relatively low incorporation (ca. 1%), the ^{13}C -n.m.r. spectrum of enriched fusidic acid (57) allowed confirmation of the assignment of a certain number of signals; the sites of label are in full agreement with the known biosynthetic pathways. In addition, the observation of C—C couplings between C-11 and C-12 as well as between C-8 and C-14 — although of limited value in this study — may well prove extremely useful in future applications of ^{13}C -precursors to biosynthetic studies.

The biosynthesis of some other terpenoids has been studied using ^{13}C -labelled precursors and the corresponding references are as follows: C_{16} -terpenoid lactone [117]; coriolin [118]; trichothecolone [119]; hirsutic acid C [120].

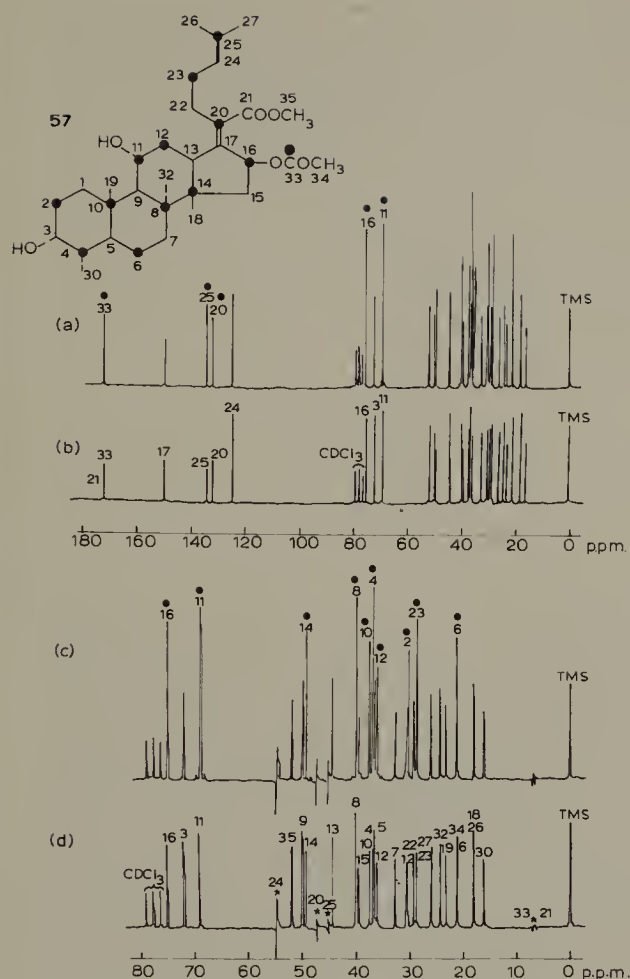


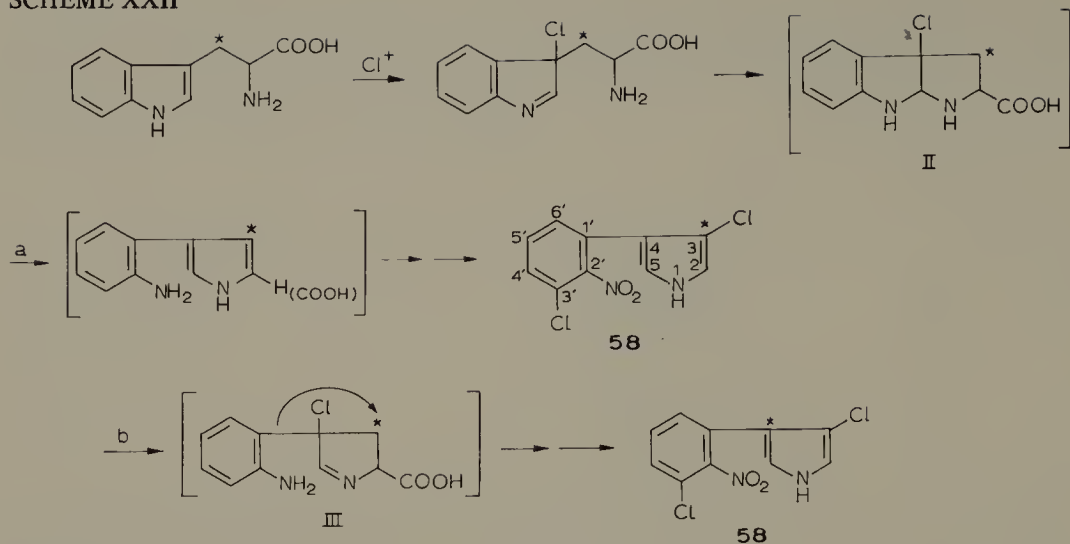
Fig. 11. (a) and (c): ^{13}C -FT n.m.r. of (57) biosynthetically enriched by $\text{CH}_3^{13}\text{COONa}$. (b) and (d): ^{13}C -FT n.m.r. of (57) at natural abundance. (Reproduced with permission from T. Riisom, H.J. Jakobsen, N. Rastrup-Anderson and H. Lorck, *Tetrahedron Lett.*, 26 (1974) 2247.)

V. INCORPORATION OF TRYPTOPHAN

A. Pyrrolnitrin (58)

The incorporation of tryptophan into the antifungal antibiotic pyrrolnitrin (58), a constituent of *Pseudomonas aureofaciens*, has been reported [121]. These studies showed that C-2 of the indole nucleus is retained and that the amino nitrogen furnishes the pyrrole nitrogen, while the indole nitrogen is at the origin of the nitro group. The retention of tritium on C-2 of the alanyl chain of L-tryptophan was also demonstrated. In agreement with these results a biosynthetic sequence (Scheme XXII, path-

SCHEME XXII



way a) was proposed, which suggested that the two chlorine atoms were introduced at a late stage in the biogenesis of pyrrolnitrin (58), although electrophilic substitution of a pyrrole ring in position 3 is rather unusual.

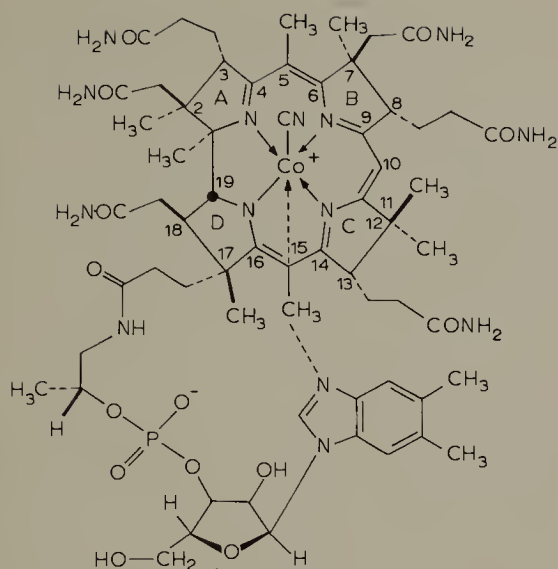
In order to overcome this problem, an alternative pathway (b) was suggested including a 1,2-aryl shift in close analogy to the isoflavone biosynthesis [122]. To settle this question, Floss and co-workers [123] fed DL-[alanyl-3- ^{13}C]-tryptophan to cultures of *P. aureofaciens*. In the ^{13}C -n.m.r. spectrum of the pyrrolnitrin (58) isolated, only the signal due to C-3 showed significant enhancement indicating that it originates from C-3 (side chain) of tryptophan. In addition, degradation experiments with radioactive (58) obtained after incorporation of [^{14}C]- and [$^3\text{H}/^{14}\text{C}$]-tryptophan were in full agreement with the ^{13}C -data, ruling out a rearrangement process involving a 1,2-aryl shift.

VI. THE CORRINS AND THE PORPHYRINS

The corrin and porphyrin heterocyclic ring systems are parts of several important natural products like vitamin B_{12} , haem, the cytochromes and the chlorophylls, and the investigation of their biosynthesis provides perhaps the most important contribution of ^{13}C -tracers.

A. Vitamin B_{12} (cyanocobalamin) (59)

This compound highlighted a major progress in organic chemistry at every stage of its investigation, including its isolation [124], structure determination [125], and its recently achieved total synthesis [126]. As a matter of course, its biosynthesis has been the subject of much speculation [127] and the most important results obtained before the advent of ^{13}C -n.m.r. will be summarized briefly.



59

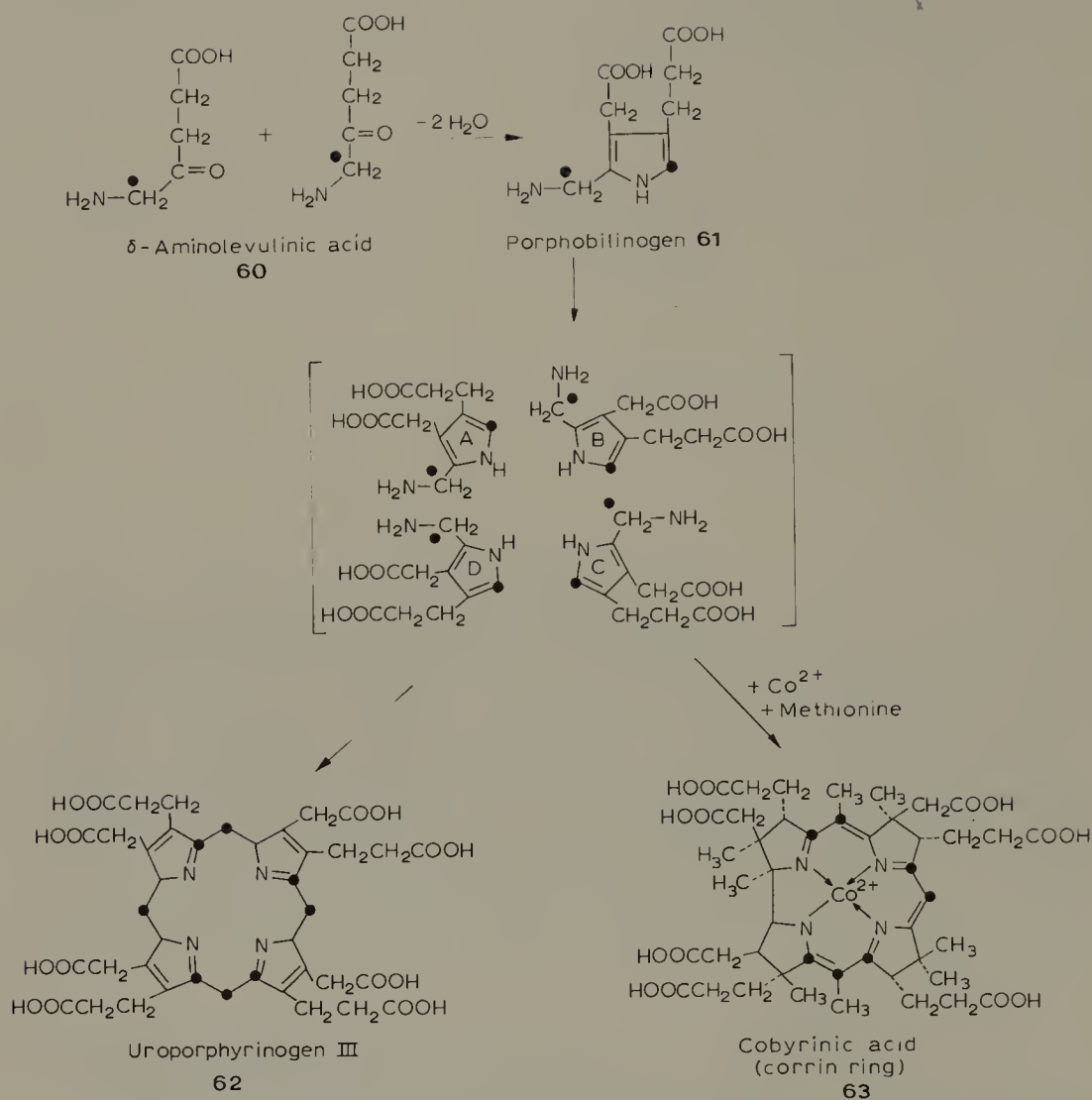
Shemin's incorporation experiments [128] with variously ¹⁴C-labelled δ -amino-levalulinic acids (ALA) (60) indicated that the tetrapyrrole pathway was involved, but no rigorous solution was achieved because of the great experimental problems associated with the degradation of such a complicated molecule. Further evidence concerning the biosynthesis of vitamin B₁₂ (59) was obtained when ¹⁴C-labelled porphobilinogen (PBG) (61) was incorporated into vitamin B₁₂ [129], although once more the location of the radioactivity could not be determined. Finally [¹⁴CH₃]-methionine was incorporated and Kuhn-Roth oxidation experiments seemed in agreement with the introduction of six "extra" methyl groups [130]. From these results the C-1 methyl group was supposed to be derived from C-5 of ALA (60) and one of the methyl groups at C-12 from C-2 of ALA.

In the course of their more recent studies of vitamin B₁₂ biosynthesis, Scott et al. [131], like other authors [132], were inspired by the structural relationship between uroporphyrinogen III (uro'gen III) (62) and cobyrinic acid (63) (in spite of the absence of one methine bridge in the latter compound).

The proposed intermediacy of uro'gen III (62) in vitamin B₁₂ biosynthesis was particularly attractive since it allowed for a biogenetic scheme wherein the corrin and porphyrin pathways diverge *after* the formation of uro'gen III (62). Indirect evidence for such a scheme comes from the fact that uro'gen III is a known metabolite of vitamin B₁₂ producing organisms [133].

In order to test this hypothesis, [8-¹⁴C]-PBG (61) was synthesized and condensed with HCl to yield the statistical mixture of uroporphyrin isomers containing 50% of uroporphyrin III [131]. This mixture was reduced to the corresponding uro'gens immediately before administration to selected strains of vitamin B₁₂ producing *Propionibacterium shermanii*.

SCHEME XXIII



Improved culture conditions were tested with [8- ^{14}C]-PBG (61) and finally incorporation experiments with the [^{14}C]-uroporphyrin and [^{14}C]-uro'gen mixtures performed. A positive incorporation of the latter into vitamin B₁₂ (59) was observed while the uroporphyrin mixture yielded only inactive material. Hydrolysis and Kuhn–Roth oxidation of radioactive cyanocobalamin (59) showed that the ^{14}C -label had not randomised into the nucleotide segment or into carbon atoms yielding acetic acid by oxidation.

Since conflicting results were published at the same time [132], a method of determination of the location of labelled centers in vitamin B₁₂ became desirable. Fortunately, partial assignment of the ^{13}C -FT spectra of vitamin B₁₂ had become available [134]. In addition, these spectra showed an approximately equal intensity for al-

most all carbon signals, making enrichment measurements at low incorporation rates feasible.

[2- ^{13}C]-ALA, [5- ^{13}C]-ALA, [8- ^{13}C]-PBG, [$^{13}\text{CH}_3$]-methionine and [^{13}C]-urogens I–IV were prepared and fed to resting cells of *P. shermanii* [135]. Excellent and specific incorporations into vitamin B₁₂ were achieved with all precursors. The spectra of vitamin B₁₂ (59) enriched by [2- ^{13}C]-ALA (60) were in good agreement with the above mentioned ^{14}C -tracer results. In particular, proof of the intact incorporation of 8- ^{13}C -PBG (61) and [^{13}C]-urogen mixture prepared from it was obtained, providing strong support for the intermediacy of urogen III in corrin biosynthesis.

Results from the [5- ^{13}C]-ALA and [$^{13}\text{CH}_3$]-methionine incorporation experiments were surprising. It was completely unexpected that no enrichment at all could be detected for the C-1 methyl group after incorporation of 5- ^{13}C -ALA (60) (Scheme XXIII). This corresponds to a complete loss of one of the CH_2NH_2 groups of ALA in the course of the formation of the corrin ring, whereas all carbon atoms of ALA are still retained in the biosynthesis of urogen III (62). For this reason, the C-1 methyl group must come from another source and the surprising solution of this problem was found after the incorporation of [$^{13}\text{CH}_3$]-methionine. In fact, the ^{13}C -FT spectrum of dicyanocobalamin showed *seven* signals, one of which was assigned to the C-1 methyl group.

In addition, the stereochemical assignments of the geminal methyl groups on C-12

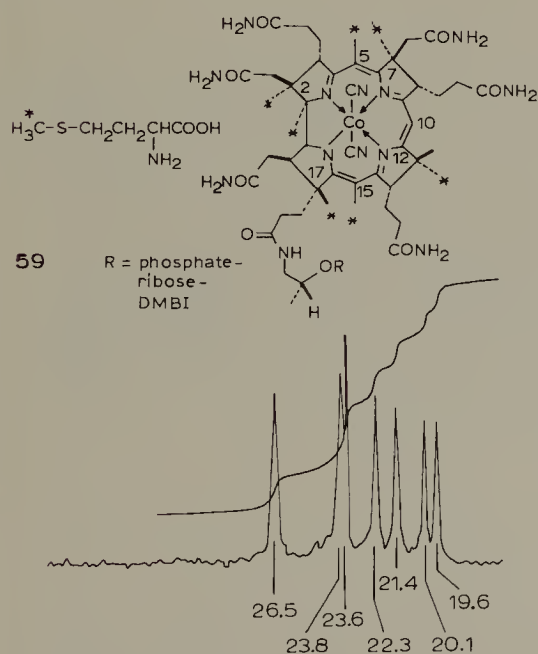
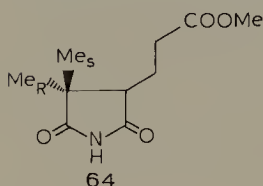


Fig. 12. ^{13}C -FT n.m.r. spectrum of [^{13}C]-L-methionine enriched dicyanocobalamin.

(Reprinted with permission from A.I. Scott, C.A. Townsend, K. Okada, M. Kajiware, R.J. Cushley and P.J. Whitman, J. Am. Chem. Soc., 96 (1974) 8074. Copyright by the American Chemical Society.)

could be firmly established and the methionine derived methyl group on ring C was shown to have the pro-R configuration.

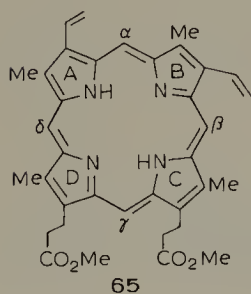
Independent investigations by Battersby et al. [136] led to similar conclusions. They isolated enriched vitamin B₁₂ (59) after incorporation of [5-¹³C]-ALA and [¹³CH₃]-methionine, degraded it via heptamethyl cobyrinate to the amide (64) which was analysed by ¹H-n.m.r. They again established that the pro-R methyl group on C-12 of vitamin B₁₂ (59) is derived from methionine. Since these results were in contradiction to those published by Shemin and co-workers [137] (based on correlation of ¹³C resonances with assigned proton signals), it was desirable to exclude any possibility of an inversion on C-13 of vitamin B₁₂ (59) during degradation. The signals of labelled and natural abundance heptamethyl cobyrinate were compared and it was shown [138] that the seven signals due to the enriched methyl groups coincided with those of the authentic ester, but differed in chemical shift from those shown by heptamethyl 13-epi-cobyrinate [139], confirming the original assignments by Scott et al. [140] and by Battersby.



B. The porphyrins

Although the early steps of their biogenetic pathways are identical, the corrins and the porphyrins are discussed separately. As in the case of vitamin B₁₂, a great number of ¹⁴C-tracer studies have been performed but due to the equally difficult degradation problems, no definitive results, in particular for the later steps, have been obtained.

In the course of their intensive study of the biosynthesis of the porphyrins, Battersby et al. [141] undertook the synthesis of a series of specifically labelled precursors. More importantly, they prepared three protoporphyrin IX dimethyl esters (65) specifically ¹³C-labelled in positions β , γ and δ by unambiguous routes which allowed them to assign the four carbon signals from the *meso*-carbons.

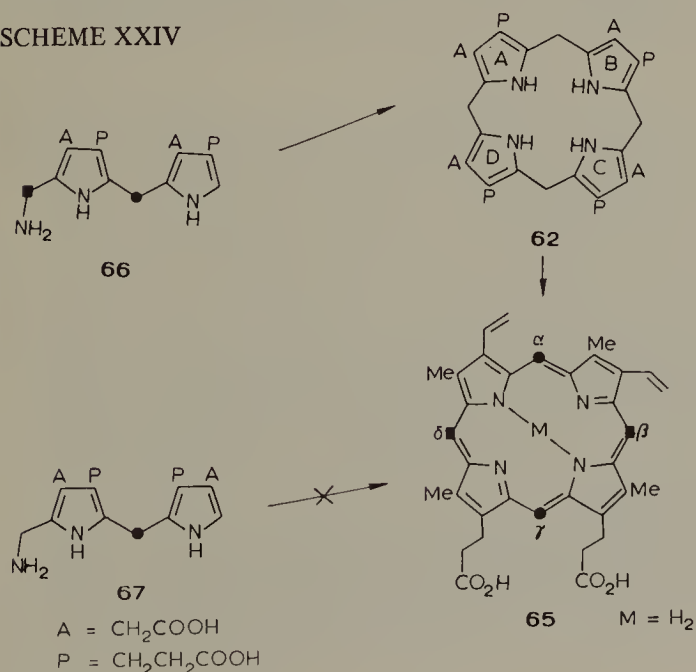


With the aid of ^{14}C -tracers, the biosynthesis of the porphyrin macrocycle from ALA (60) via PBG (61) had been established previously [127]. Incorporation of $[11\text{-}^{13}\text{C}]$ -PBG (61) by an enzyme system from *Euglena gracilis* gave labelled protoporphyrin IX isolated as its methyl ester (65). Its ^{13}C -n.m.r. spectrum showed four signals of equal intensity, demonstrating equal labelling of all four *meso*-carbons within the accuracy of the technique.

On the basis of this result $[2,11\text{-}^{13}\text{C}]$ -PBG was synthesized from $[5\text{-}^{13}\text{C}]$ -ALA (enrichment 90%). Mass spectral analysis of a derivative of $[2,11\text{-}^{13}\text{C}]$ -PBG confirmed that two labelled sites were present and that approximately 81% of PBG carried two ^{13}C atoms. A diluted sample of this ^{13}C -PBG was converted enzymically into protoporphyrin IX via uroporphyrinogen III (62), again isolated as its ester (65). Careful analysis of the intensity and the splitting pattern of the signals assigned to the *meso*-carbons allowed the authors to draw the important conclusions that the PBG-unit D undergoes intramolecular rearrangement during the biosynthesis of the type-III macrocycle and that the PBG units A, B and C are incorporated intact. Most of the over twenty schemes proposed [142] for the mechanism of this rearrangement can be eliminated with the help of these findings [143].

Thus, reliable information was available concerning several steps of the biosynthesis of type-III porphyrins, but further understanding required research on possible intermediates. The ^{14}C -pyrromethanes (66) and (67) were synthesized and incubated with enzyme preparations from *Euglena gracilis* and duck's blood [144]. Only the pyrromethane (66) gave radioactive porphyrin ester (65). (Part of the haemin isolated from the experiment with duck's blood was converted by known methods into a separable mixture of biliverdin-IX esters [145] which allowed the specificity of incorporation to be checked). (Scheme XXIV).

SCHEME XXIV



Later on, pyrromethane (66) labelled at ● with ^{13}C was incorporated. The ^{13}C -FT n.m.r. of (65) showed that the label was specifically located in the α - and γ -*meso* positions. In addition, when (66) specifically enriched at position ■ was incorporated, the complementary β - and δ -*meso* carbons showed enhanced intensity.

In order to exclude a non-enzymic rearrangement leading from the pyrromethane (66) to uro'gen III (which would then be converted enzymically into protoporphyrin IX), ^{14}C -labelled (66) and (67) were treated in separate experiments at pH 7.4 and pH 8.2 and the resulting uroporphyrin mixture isolated. While (67) yielded only the expected isomer II, it was quite surprising to note that pyrromethane (66) gave, after transformation in small yield, a fraction containing rearranged type-III and type-IV isomers. The mechanism of this rearrangement is of great interest and the continued use of ^{13}C -tracers will undoubtedly provide further information in the near future.

VII. CONCLUSION

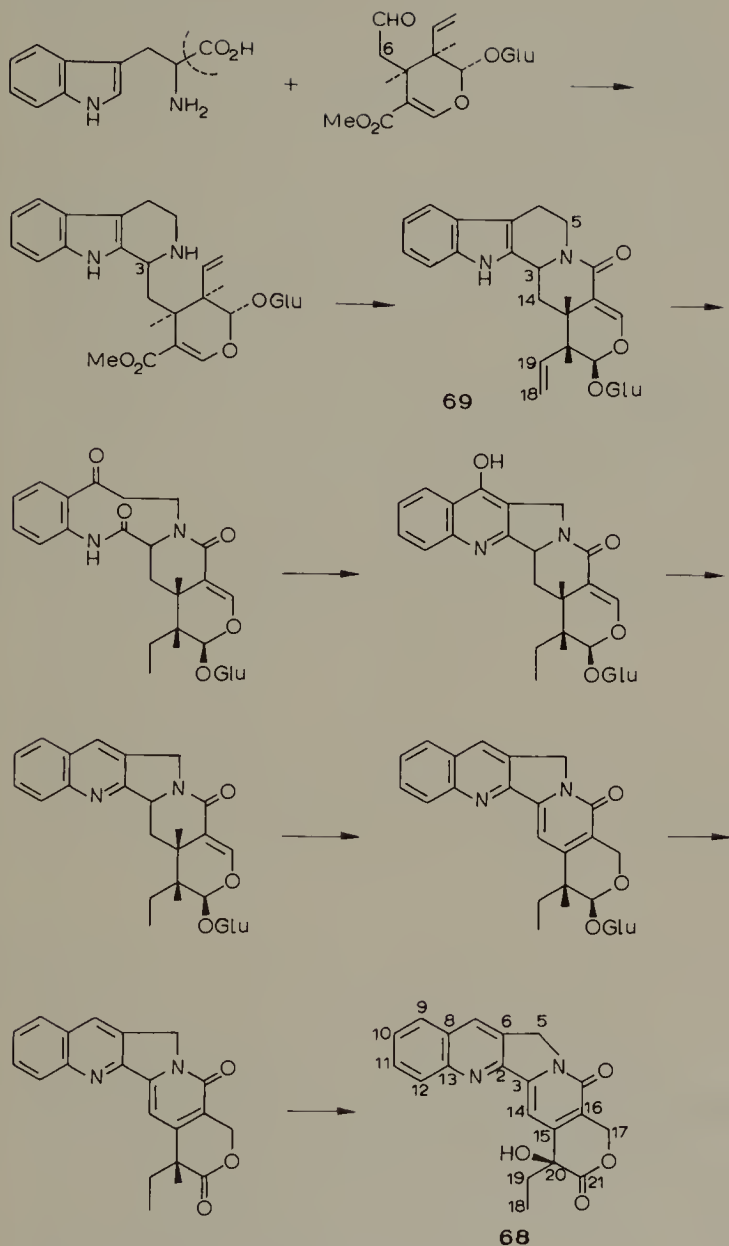
While the first applications of ^{13}C -tracers essentially confirmed earlier ^{14}C -studies, the more recent investigations were preferentially directed towards problems inaccessible to classical methods. One of the major reasons for the rapid increase in the use of ^{13}C in the study of biogenetic pathways is linked to instrumental progress (from the "satellite method" via "continuous wave" to FT technique within less than ten years), highly ^{13}C -enriched precursors (enrichment rates increased from about 50% to approximately 90% within a few years) and the use of paramagnetic reagents like $\text{Cr}(\text{acac})_3$.

After the administration of simple commercially available precursors like acetate, more and more complex molecules were synthesized, as more and more complicated problems had to be resolved. The investigations on the biosynthesis of the β -lactam antibiotics, the rifamycins, the porphyrins and vitamin B_{12} are good examples for this assertion.

The main barrier to a generalised use of ^{13}C -labelled precursors in this field remains the sensitivity problem. As a result, all the investigations discussed until now in this article concerned metabolites from microorganisms or purified enzyme systems. Several methods have been tried in order to avoid this sensitivity problem without durable success. For instance, a greater amount of precursor in the culture medium may increase the incorporation rate, but as discussed in the case of shanorellin (27) [58], the inhibition of the formation of the metabolite by relatively small amounts of a "true" precursor may be encountered as well and changes in "natural" biogenetic pathways have been observed [59]. This explains sufficiently why only two studies have been published concerning higher plant products, where the dilution of labelled material by endogenous material is particularly high.

Several hypotheses [146,147] have been advanced concerning the biosynthesis of camptothecin (68). Hutchinson et al. [148] suggested a lactam intermediate of type (69) and incorporation experiments with ^{14}C - and ^3H -labelled (69) were in good agree-

SCHEME XXV



ment with the proposed pathway, but once more no degradation experiments could be performed (Scheme XXV). [^{13}C]-Lactam (69) was synthesized from [$1\text{-}^{13}\text{C}$]-tryptamine and it could be shown to be specifically incorporated, in spite of a rather low incorporation rate.

The other published application of ^{13}C -tracers to higher plant product biosynthesis [149] again uses a highly elaborate precursor. In continuing their biosynthetic studies [150] on colchicine (70), Battersby et al. prepared (RS)-[$1\text{-}^{13}\text{C}$]-autumnalin (71) which was fed to *Colchicum autumnale* (Liliaceae).

SCHEME XXVI

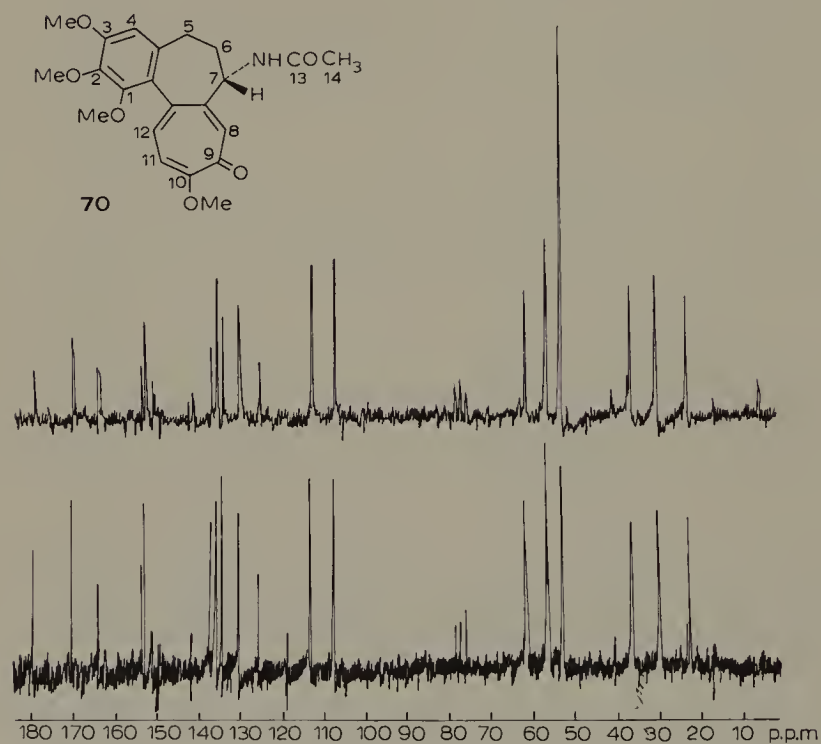
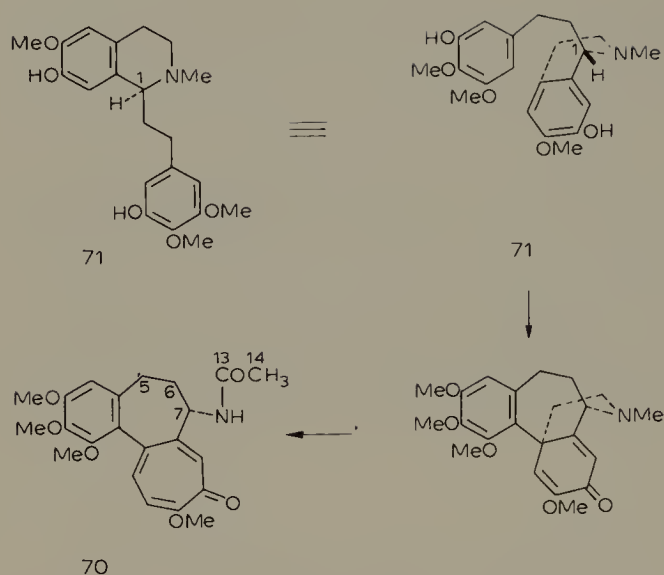


Fig. 13. FT ¹³C-n.m.r. spectra of colchicin (70) at natural abundance (lower spectrum) and after incorporation of (RS)-[1-¹³C]-autumnalin (71) (upper spectrum).

(Reproduced with permission from A.R. Battersby, P.W. Sheldrake and J.A. Milner, *Tetrahedron Lett.*, (1974) 3317.)

Figure 13 shows the spectrum of the labelled alkaloid (top spectrum) compared with that at natural abundance. Attention should be drawn to the fact that the observed incorporation rate of 6% is very exceptional in higher plant studies.

A technically rather complicated solution of the sensitivity problem has been proposed by Scott [3]. The culture of plants in an artificial atmosphere containing ^{13}C -free CO_2 would provide products showing no (or almost no) natural abundance spectrum. In this manner it would be possible to measure enrichment levels as low as 0.2%, which would correspond to a gain in sensitivity of almost one order of magnitude.

The elucidation of biogenetic pathways is not the only application of ^{13}C -enriched precursors. In several cases addition of ^{13}C -enriched compounds to a culture medium contributed decisively to the structure determination of a new metabolite and in other investigations ^{13}C -enriched tracers were incorporated in order to facilitate the assignment of carbon signals. An example of this type of application is the assignment of the ^{13}C -n.m.r. spectrum of gramicidin S-A [151]. Similar studies should prove the usefulness of this method in the peptide field. Carbon-13-tracers could also be used where radioactive compounds cannot be administered, because of possible health hazards, and rapid progress can be expected from ^{13}C -n.m.r. in metabolic studies of mammalian and human biochemistry.

ACKNOWLEDGEMENTS

We wish to thank Mrs. Névot, Mr. Pica and the "Service de Photographie du Groupe des Laboratoires du C.N.R.S. de Gif-sur-Yvette" for their help and excellent cooperation.

REFERENCES

- 1 a. D.M. Greenberg, *Metabolic Pathways*, Academic Press, New York and London, 4 volumes, 3rd edn., 1967–1970.
- b. P. Bernfeld, *Biogenesis of Natural Compounds*, Pergamon Press, Oxford, 2nd edn., 1967.
- c. R. Robinson, *The Structural Relations of Natural Products*, Clarendon Press, Oxford, 1955.
- d. J.D. Bu'Lock, *The Biosynthesis of Natural Products*, McGraw-Hill, London, 1965.
- e. T.A. Geissman and D.H.G. Crout, *Organic Chemistry of Secondary Plant Metabolism*, Freeman-Cooper, San Francisco, 1969.
- 2 a. E.D. Bransome, Jr., (Ed.), *The Current Status of Liquid Scintillation Counting*, Grune and Stratton, New York, 1971.
- b. D.L. Horrochs and C.T. Peng (Eds.), *Organic Scintillators and Liquid Scintillation Counting*, Academic Press, New York, 1971.
- c. M.A. Crook, P. Johnson and B. Scales (Eds.), *Liquid Scintillation Counting*, Vol. 2, Heyden, London, 1972.
- 3 a. G. Lukacs, *Bull. Soc. Chim. Fr.* (1972) 351.
- b. J.B. Grutzner, *Lloydia*, 35 (1972) 375.
- c. H.G. Floss, *Lloydia*, 35 (1972) 399.
- d. M. Tanabe, *Biosynthesis*, Vol. 2, The Chemical Society, London, 1973, p. 241.

- e. A.I. Scott, *Science*, 184 (1974) 760.
- f. U. Séquin and A.I. Scott, *Science*, 186 (1974) 101.
- 4 a. J.B. Stothers, *Carbon-13 NMR Spectroscopy*, Academic Press, New York and London, 1972, p. 485.
- b. G.C. Levy and G.L. Nelson, *Carbon-13 Nuclear Magnetic Resonance for Organic Chemists*, Wiley-Interscience, New York, 1972, p. 169.
- c. E. Breitmaier and W. Voelter, *Carbon-13 NMR Spectroscopy*, Verlag Chemie, Weinheim, 1974, p. 268.
- G.C. Levy, *Topics in ^{13}C NMR Spectroscopy*, Wiley, New York, 1974.
- 5 M. Tanabe and G. Detre, *J. Am. Chem. Soc.*, 88 (1966) 4515.
- 6 A.J. Birch, R.A. Massy-Westropp, R.W. Rickards and H. Smith, *J. Chem. Soc.*, (1958) 360.
- 7 D.J.P. Hockenhall and W.F. Faulds, *Chem. Ind. (London)* (1955) 1390.
- 8 J.F. Grove, *J. Chem. Soc. (C)* (1970) 1860.
- 9 M. Tanabe, H. Seto and L. Johnson, *J. Am. Chem. Soc.*, 92 (1970) 2157.
- 10 a. H. Seto, T. Satō, H. Yonehara and W.C. Jankowski, *J. Antibiotics*, 26 (1973) 609.
- b. H. Seto, T. Satō and H. Yonehara, *J. Am. Chem. Soc.*, 95 (1973) 8461.
- 11 A.J. Birch, G.E. Blance and H.J.J. Smith, *J. Chem. Soc.*, (1958) 4582.
- 12 K. Mosbach, *Acta Chem. Scand.*, 14 (1960) 457.
- 13 H. Seto, L.W. Cary and M. Tanabe, *J. Antibiot.*, 27 (1974) 558.
- 14 J.M.A. Al-Rawi, J.A. Elvidge, D.K. Jaiswal, J.R. Jones and R. Thomas, *J. Chem. Soc. Chem. Commun.*, (1974) 220.
- 15 J.A. Gudgeon, J.S.E. Holker and T.J. Simpson, *J. Chem. Soc. Chem. Commun.*, (1974) 636.
- 16 A.D. Argoudelis and J.F. Zieserl, *Tetrahedron Lett.*, (1966) 1969.
- 17 M. Tanabe, T. Hamasaki, D. Thomas and L. Johnson, *J. Am. Chem.*, 93 (1971) 273.
- 18 J.F. Grove, *J. Chem. Soc. Perkin Trans. 1* (1972) 2400.
- 19 L. Cattell, J.F. Grove and D. Shaw, *J. Chem. Soc. Perkin Trans. 1*, (1973) 2626.
- 20 D. Shaw, *Chemical Society Specialist Periodical Reports, NMR*, London, 1973, Vol. 2, p. 283.
- 21 E. Bulloch, J.C. Roberts and J.G. Underwood, *J. Chem. Soc.*, (1962) 4179.
- 22 J.S.E. Holker and L.J. Mulheirn, *Chem. Commun.*, (1968), 1576.
- 23 a. D.P. Moody, *Nature (London)*, 202 (1964) 188.
- b. J.G. Heathcote, J.J. Child and M.F. Dutton, *Biochem. J.*, 95 (1965) 23P.
- c. J.S.E. Holker and J.G. Underwood, *Chem. Ind. (London)* (1964) 1865.
- d. R. Thomas, *Biogenesis of Antibiotic Substances*, Z. Vanék and Z. Hošťálek (Ed.), Academic Press, New York, 1965, p. 155.
- 24 M. Biollaz, G. Büchi and G. Milne, *J. Am. Chem. Soc.*, 92 (1970) 1035.
- 25 M.T. Lin and D.P.H. Hsieh, *J. Am. Chem. Soc.*, 95 (1973) 1668.
- 26 D.P.H. Hsieh, M.T. Lin and R.C. Yao, *Biochem. Biophys. Res. Commun.*, 52 (1973) 992.
- 27 M. Tanabe, T. Hamasaki, H. Seto and L. Johnson, *Chem. Commun.*, (1970) 1539.
- 28 H. Seto, L.W. Cary and M. Tanabe, *Tetrahedron Lett.*, (1974) 4491.
- 29 R. Bentley, S. Gatenbeck, *Biochemistry*, 4 (1965) 1150.
- 30 M. Tanabe and H. Seto, *Biochemistry*, 9 (1970) 4851.
- 31 H. Seto, L.W. Cary and M. Tanabe, *J. Chem. Soc. Chem. Commun.*, (1973) 867.
- 32 a. A.I. Gurevich, M.N. Kolosov, V.G. Korobko and V.V. Onopreinko, *Tetrahedron Lett.*, (1968) 2209.
- b. T. Terashima, Y. Kuroda and Y. Kaneko, *Tetrahedron Lett.*, (1969) 2535.
- c. S. Umezawa, K. Tatsuta, Y. Horiuchi and T. Tsuchiya, *J. Antibiot.*, 23 (1970) 28.
- 33 E. Leete, *Acc. Chem. Res.*, 4 (1971) 100.
- 34 T. Terashima, E. Idaka, Y. Kishi and T. Goto, *J. Chem. Soc. Chem. Commun.*, (1973) 75.
- 35 F.M. Dean, J. Staunton and W.B. Whalley, *J. Chem. Soc.*, (1959) 3004.
- 36 J.S.E. Holker, J. Staunton and W.B. Whalley, *J. Chem. Soc.*, (1963) 3641.

- 37 A.J. Birch, A. Cassera, P. Fitton, J.S.E. Holker, H. Smith, G.A. Thompson and W.B. Whalley, *J. Chem. Soc.* (1962) 3583.
- 38 H. Seto and M. Tanabe, *Tetrahedron Lett.*, (1974) 651.
- 39 W.B. Turner, *Fungal Metabolites*, Academic Press, London and New York, 1971, p. 292.
- 40 D. Brookes, B.K. Tidd and W.B. Turner, *J. Chem. Soc.*, (1963) 5385.
- 41 M. Tanabe, T. Hamasaki, Y. Suzuki and L. Johnson, *J. Chem. Soc. Chem. Commun.*, (1973) 212.
- 42 a. W. Rothweiler and Ch. Tamm, *Experientia*, 22 (1966) 750.
b. D.C. Aldridge, J.I. Armstrong, R.N. Speake and W.B. Turner, *Chem Commun.*, (1967) 26.
- 43 a. D.C. Aldridge and W.B. Turner, *J. Antibiot.* 22 (1969) 170.
b. H. Minato and M. Matsumoto, *J. Chem. Soc. C* (1970) 38.
- 44 a. M. Binder and Ch. Tamm, *Angew. Chem. Int. Ed. Eng.*, 12 (1973) 370.
b. M. Binder, J.R. Kiechel and Ch. Tamm, *Helv. Chim. Acta*, 53 (1970) 1797.
- 45 C.R. Lebet and Ch. Tamm, *Helv. Chim. Acta*, 57 (1974) 1785.
- 46 W. Graf, J.-L. Robert, J.C. Vederas, Ch. Tamm, P.H. Solomon, I. Miura and K. Nakanishi, *Helv. Chim. Acta*, 57 (1974) 1801.
- 47 a. A.L. Burlingame, B. Balogh, J. Welch, S. Lewis and D. Wilson, *J. Chem. Soc. Chem. Commun.*, (1972) 318.
b. J.E. Cronan Jr. and J.G. Batchelor, *Chem. Phys. Lipids*, 11 (1973) 196.
- 48 K. Nabeta, A. Ichihara and S. Sakamura, *J. Chem. Soc. Chem. Commun.*, (1973) 814.
- 49 F. Aragozzini, M.G. Beretta, G.S. Ricca, C. Scolastico and F.W. Wehrli, *J. Chem. Soc. Chem. Commun.*, (1973) 788.
- 50 D.C. Aldridge, A.B. Davies, M.R. Jackson and W.B. Turner, *J. Chem. Soc. Perkin Trans. 1*, (1974) 1540.
- 51 J.S.E. Holker, R.D. Lapper and T.J. Simpson, *J. Chem. Soc. Perkin Trans. 1*, (1974) 2135.
- 52 S. Omura and G. Lukacs, unpublished results.
- 53 A.G. McInnes, D.G. Smith, C.-K. Wat, L.C. Vining and J.L.C. Wright, *J. Chem. Soc. Chem. Commun.*, (1974) 281.
- 54 A.G. McInnes, D.G. Smith, J.A. Walter, L.C. Vining and J.L.C. Wright, *J. Chem. Soc. Chem. Commun.*, (1974) 282.
- 55 M.L. Loudon and E. Leete, *J. Am. Chem. Soc.*, 84 (1962) 4507.
- 56 W.S.G. Maass and A.C. Neish, *Can. J. Bot.*, 45 (1967) 59.
- 57 a. C.-K. Wat and G.H.N. Towers, *Phytochemistry*, 10 (1971) 103.
b. C.-K. Wat and G.H.N. Towers, *Phytochemistry*, 10 (1971) 1355.
- 58 C.-K. Wat, A.G. McInnes, D.G. Smith and L.C. Vining, *Can. J. Biochem.*, 50 (1972) 620.
- 59 E.F. Elstner, R.J. Suhadolnik and A. Allerhand, *J. Biol. Chem.*, 248 (1973) 5385.
- 60 K.L. Rinehart Jr., G. Leadbetter, R.A. Larson and R.M. Forbis, *J. Am. Chem. Soc.*, 92 (1970) 6994.
- 61 K.L. Rinehart Jr., R.A. Larson, R.M. Forbis and G. Leadbetter, *Abstracts, 5th Int. Symp. Chem. Nat. Prod.*, IUPAC, London, July 1968, p. 79.
- 62 W.M.J. Knöll, R.J. Huxtable and K.L. Rinehart Jr., *J. Am. Chem. Soc.*, 95 (1973) 2703.
- 63 K.L. Rinehart Jr., *Acc. Chem. Res.*, 5 (1972) 57.
- 64 M. Brufani, D. Kluepfel, G.C. Lancini, J. Leitich, A.S. Mesentsev, V. Prelog, F.P. Schmook and P. Sensi, *Helv. Chim. Acta*, 56 (1973) 2315.
- 65 R.J. White, E. Martinelli, G.G. Gallo, G. Lancini and P. Beynon, *Nature (London)*, 243 (1973) 273.
- 66 B. Milavetz, K. Kakinuma, K.L. Rinehart Jr., J.P. Rolls and W.J. Haak, *J. Am. Chem. Soc.*, 95 (1973) 5793.
- 67 J.W. Corcoran and M. Chick, *Biosynthesis of Antibiotics*, J.F. Snell (Ed.), Vol. 1, Academic Press, New York, 1966, p. 159.
- 68 a. E. Martinelli, R.J. White, G.G. Gallo and P.J. Beynon, *Tetrahedron*, 29 (1973) 3441.
b. H. Fuhrer, *Helv. Chim. Acta*, 56 (1973) 2377.

- c. E. Martinelli, R.J. White, G.G. Gallo and P.J. Beynon, *Tetrahedron Lett.*, 15 (1974) 1367.
- 69 E. Martinelli, G.G. Gallo, P. Antonini and R.J. White, *Tetrahedron*, 30 (1974) 3087.
- 70 R.J. White, E. Martinelli and G. Lancini, *Proc. Nat. Acad. Sci. U.S.A.*, 71 (1974) 3260.
- 71 K. Sasaki, K.L. Rinehart Jr., G. Slomp, M.F. Grostic and E.C. Olson, *J. Am. Chem. Soc.*, 92 (1970) 7591.
- 72 S.M. Kupchan, Y. Komoda, W.A. Court, G.J. Thomas, R.M. Smith, A. Karim, C.J. Gilmore, R.C. Haltiwanger and R.F. Boyan, *J. Am. Chem. Soc.*, 94 (1972) 1354.
- 73 R.D. Johnson, A. Haber and K.L. Rinehart Jr., *J. Am. Chem. Soc.*, 96 (1974) 3316.
- 74 A. Karlsson, G. Sartori and R.J. White, *Eur. J. Biochem.*, 47 (1974) 251.
- 75 R.J. White and E. Martinelli, *FEBS Letters*, 49 (1974) 233.
- 76 N. Takahashi, Y. Kimura and S. Tamura, *Tetrahedron Lett.*, 45 (1968) 4659.
- 77 M. Tanabe and H. Seto, *J. Org. Chem.*, 35 (1970) 2087.
- 78 E.P. Abraham and G.G.F. Newton, *Antibiotics*, D. Gottlieb and P.D. Shaw (Eds.), Vol. 2, Springer-Verlag, Berlin, Heidelberg, New York, 1967, p. 1.
- 79 N. Neuss, C.H. Nash, P.A. Lemke and J.B. Grutzner, *J. Am. Chem. Soc.*, 93 (1971) 2337.
- 80 N. Neuss, C.H. Nash and J.B. Grutzner, *Proc. R. Soc. Lond.*, 179 (1971) 335.
- 81 J.E. Baldwin, J. Löfger, W. Rastetter, N. Neuss, L.L. Huckstep and N. de la Higuera, *J. Am. Chem. Soc.*, 95 (1973) 3796, 6511.
- 82 N. Neuss, C.H. Nash, J.E. Baldwin, P.A. Lemke and J.B. Grutzner, *J. Am. Chem. Soc.*, 95 (1973) 3797 and 6511.
- 83 H. Kluender, C.H. Bradley, C.J. Sih, P. Fawcett and E.P. Abraham, *J. Am. Chem. Soc.*, 95 (1973) 6149.
- 84 S.M. Qadri and R.P. Williams, *Biochim. Biophys. Acta*, 230 (1971) 181.
- 85 R.J. Cushley, D.R. Anderson, S.R. Lipsky, R.J. Sykes and H.H. Wasserman, *J. Am. Chem. Soc.*, 93 (1971) 6284.
- 86 H.H. Wasserman, R.J. Sykes, P. Peverada, C.K. Shaw, R.J. Cushley and S.R. Lipsky, *J. Am. Chem. Soc.*, 95 (1973) 6874.
- 87 a. M.T.M. Rizki, *Proc. Nat. Acad. Sci. U.S.A.*, 40 (1964) 1057.
b. H.H. Wasserman, J.E. McKeon and U.V. Santer, *Biochem. Biophys. Res. Commun.*, 3 (1960) 146.
- 88 H.H. Wasserman, C.K. Shaw and R.J. Sykes, *Tetrahedron Lett.*, 33 (1974) 2787.
- 89 S. Takeuchi and H. Yonehara, *Tetrahedron Lett.*, (1966) 5197.
- 90 N. Tanaka, *Antibiotics*, D. Gottlieb and P.D. Shaw (Eds.), Vol. 2, Springer Verlag, Berlin, 1967, p. 216.
- 91 M. Tanabe and H. Seto, *Biochim. Biophys. Acta*, 208 (1970) 151.
- 92 R.D. Hill, A.M. Unrau and D.T. Canvin, *Can. J. Chem.*, 44 (1966) 2077.
- 93 D. Desaty, A.G. McInnes, D.G. Smith and L.C. Vining, *Can. J. Biochem.*, 46 (1968) 1293.
- 94 J.W. Westley, D.L. Pruess and R.G. Pitcher, *J. Chem. Soc. Chem. Commun.*, (1972) 161.
- 95 J.W. Westley, R.H. Evans Jr., G. Harvey, R.G. Pitcher, D.L. Pruess, A. Stempel and J. Berger, *J. Antibiot.*, 27 (1974) 288.
- 96 J.W. Westley, W. Benz, J. Donahue, R.H. Evans Jr., C.G. Scott, A. Stempel and J. Berger, *J. Antibiot.*, 27 (1974) 744.
- 97 J.W. Westley, R.H. Evans Jr., D.L. Pruess and A. Stempel, *Chem. Commun.*, (1970) 1467.
- 98 a. Y. Koyama, Y. Fukakusa, N. Kyomura, S. Yamagishi and T. Arai, *Tetrahedron Lett.*, (1969) 355.
b. S. Kawai, K. Kobayashi, T. Oshima and F. Egami, *Arch. Biochem. Biophys.*, 112 (1965) 537.
- 99 M. Yamazaki, F. Katoh, J.-I. Ohishi and Y. Koyama, *Tetrahedron Lett.*, 26 (1972) 2701.
- 100 P.S. Steyn, C.W. Holzapel and N.P. Ferreira, *Phytochemistry*, 9 (1970) 1977.
- 101 Y. Maebayashi, K. Miyaki and M. Yamazaki, *Chem. Pharm. Bull.*, 20 (1972) 2172.
- 102 P.V. Divekar, H. Raistrick, T.A. Dobson and L.C. Vining, *Can. J. Chem.*, 43 (1965) 1835.
- 103 a. A.G. McInnes, D.G. Smith, L.C. Vining and J.L.C. Wright, *Chem. Commun.*, (1968) 1669.

- b. J. Wright, D.G. Smith, A.G. McInnes, L.C. Vining and D.W.S. Westlake, *Can. J. Biochem.*, 47 (1969) 945.
- 104 A.G. McInnes, D.G. Smith, L.C. Vining and L. Johnson, *Chem. Commun.*, (1971) 325.
- 105 a. K. Bloch, *Science*, 150 (1965) 19.
b. G. Popják, D.S. Goodman, J.W. Cornforth, R.H. Cornforth and R. Ryhage, *J. Biol. Chem.*, 236 (1961) 1934.
c. F. Lynen, H. Eggerer, U. Henning and I. Kessel, *Angew. Chemie*, 70 (1958) 738.
- 106 J. Polonsky, Z. Baskevitch, N. Cagnoli-Bellavita, P. Ceccherelli, B.L. Buckwalter and E. Wenkert, *J. Am. Chem. Soc.*, 94 (1972) 4369.
- 107 S. Natori, H. Nishikawa and H. Ogawa, *Chem. Pharm. Bull. (Japan)*, 12 (1974) 236.
- 108 M. Tanabe, K.T. Suzuki and W.C. Jankowski, *Tetrahedron Lett.*, 47 (1973) 4723.
- 109 P. Bollinger, H.P. Sigg and H.P. Weber, *Helv. Chim. Acta*, 56 (1973) 819.
- 110 M. Tanabe and K.T. Suzuki, *Tetrahedron Lett.*, 49–50 (1974) 4417.
- 111 M. Tanabe and K.T. Suzuki, *J. Chem. Soc. Chem. Commun.*, (1974) 445.
- 112 J. Polonsky, G. Lukacs, N. Cagnoli-Bellavita and P. Ceccherelli, *Tetrahedron Lett.*, (1975) 481.
- 113 D. Arigoni, *Experientia*, 14 (1958) 153.
- 114 W.O. Godtfredsen, W. Von Daehne, S. Vangedal, A. Marquet, D. Arigoni and A. Melera, *Tetrahedron*, 21 (1965) 3505.
- 115 A. Cooper and D.C. Hodgkin, *Tetrahedron*, 24 (1968) 909.
- 116 T. Riisom, H.J. Jakobsen, N. Rastrup-Andersen and H. Lorck, *Tetrahedron Lett.*, 26 (1974) 2247.
- 117 H. Kakisawa, M. Sato, T.I. Ruo and T. Hayashi, *J. Chem. Soc. Chem. Commun.*, (1973) 802.
- 118 M. Tanabe, K.T. Suzuki and W.C. Jankowski, *Tetrahedron Lett.*, 26 (1974) 2271.
- 119 J.R. Hanson, T. Marten and M. Sivers, *J. Chem. Soc. Perkin Trans.*, 1, (1974) 1033.
- 120 T.C. Feline, G. Mellows, R.B. Jones and L. Phillips, *J. Chem. Soc. Chem. Commun.*, (1974) 63.
- 121 H.G. Floss, P.E. Manni, R.L. Hamill and J.A. Mabe, *Biochem. Biophys. Res. Commun.*, 45 (1971) 781.
- 122 H. Grisebach, *Biochemistry of Plant Pigments*, T.W. Goodwin (Ed.), Academic Press, New York, 1964, p. 233.
- 123 L.L. Martin, C.-J. Chang, H.G. Floss, J.A. Mabe, E.W. Hagaman and E. Wenkert, *J. Am. Chem. Soc.*, 94 (1972) 8942.
- 124 a. E.L. Rickes, N.G. Brink, F.R. Koniuszy, T.R. Wood and K. Folkers, *Science*, 107 (1948) 396.
b. E.L. Smith, *Nature (London)*, 162 (1948) 144.
c. E.L. Smith and L.F.J. Parker, *Biochem. J.*, 43 (1948) viii.
- 125 D. Hodgkin, J. Kamper, M. Mackay, J. Pickworth, K.N. Trueblood and J.G. White, *Nature (London)*, 178 (1956) 64.
- 126 a. R.B. Woodward, *IUPAC Chemistry of Natural Products*, Vol. 3 (New Delhi) Butterworths, London, 1972, p. 145.
b. A. Eschenmoser, *IUPAC 23rd Congress, Special Lectures*, Vol. II, (Boston) Butterworths, London, 1971, p. 69.
- 127 B.F. Burnham in *Metabolic Pathways*, Vol. 3, D.M. Greenburg (Ed.), Academic Press, New York, N.Y., 3rd edn., 1969, Chapter 18.
- 128 D. Shemin, J.W. Corcoran, C. Rosenblum and I.M. Miller, *Science*, 124 (1956) 272.
- 129 S. Schwartz, K. Ikeda, I.M. Miller and C.J. Watson, *Science*, 129 (1959) 40.
- 130 R.C. Bray and D. Shemin, *J. Biol. Chem.*, 238 (1963) 1501.
- 131 A.I. Scott, C.A. Townsend, K. Okada and M. Kajiwarra, *J. Am. Chem. Soc.*, 96 (1974) 8054.
- 132 G. Müller and W. Dieterle, *Hoppe-Seyler's Z. Physiol. Chem.*, 352 (1971) 143.
- 133 B.F. Burnham and R.A. Plane, *Biochem. J.*, 98 (1966) 13c.

- 134 D. Doddrell and A. Allerhand, *Proc. Nat. Acad. Sci. U.S.A.*, 68 (1971) 1083.
- 135 A.I. Scott, C.A. Townsend, K. Okada, M. Kajiware, R.J. Cushley and P.J. Whitman, *J. Am. Chem. Soc.*, 96 (1974) 8069.
- 136 A.R. Battersby, M. Ihara, E. McDonald, J.R. Stephenson and B.T. Golding, *J. Chem. Soc. Chem. Commun.*, (1973) 404.
- 137 C.E. Brown, D. Shemin and J.J. Katz, *J. Biol. Chem.*, 248 (1973) 8015.
- 138 A.R. Battersby, M. Ihara, E. McDonald, J.R. Stephenson and B.T. Golding, *J. Chem. Soc. Chem. Commun.*, (1974) 458.
- 139 R. Bonnett, J.M. Godfrey and V.B. Math, *J. Chem. Soc. (C)*, (1971) 3736.
- 140 A.I. Scott, C.A. Townsend, R.J. Cushley, *J. Am. Chem. Soc.*, 95 (1973) 5759.
- 141 a. A.R. Battersby, J. Moron, E. McDonald and J. Feeney, *J. Chem. Soc. Chem. Commun.*, (1972) 920.
b. A.R. Battersby, E. Hunt, E. McDonald and J. Moron, *J. Chem. Soc. Perkin Trans. 1* (1973) 2917.
c. A.R. Battersby, G.L. Hodgson, M. Ihara, E. McDonald and J. Saunders, *J. Chem. Soc. Chem. Commun.*, (1973) 441.
d. A.R. Battersby, G.L. Hodgson, M. Ihara, E. McDonald and J. Saunders, *J. Chem. Soc. Perkin Trans. 1* (1973) 2923.
- 142 A.R. Battersby, E. Hunt and E. McDonald, *J. Chem. Soc. Chem. Commun.*, (1973) 442.
- 143 J.H. Mathewson and A.H. Corwin, *J. Am. Chem. Soc.*, 83 (1961) 135.
- 144 A.R. Battersby, K.H. Gibson, E. McDonald, L.N. Mander, J. Moron and L.N. Nixon, *J. Chem. Soc. Chem. Commun.*, (1973) 768.
- 145 R. Bonnett and A.F. McDonald, *J. Chem. Soc. Perkin Trans. 1* (1973) 881.
- 146 E. Wenkert, K.G. Dave, R.G. Lewis and P.W. Sprague, *J. Am. Chem. Soc.*, 89 (1967) 6741.
- 147 E. Winterfeldt, *Justus Liebigs Ann. Chem.*, 745 (1971) 23.
- 148 C.R. Hutchinson, A.H. Heckendorf, P.E. Daddona, E. Hagaman and E. Wenkert, *J. Am. Chem. Soc.*, 96 (1974) 5609.
- 149 A.R. Battersby, P.W. Sheldrake and J.A. Milner, *Tetrahedron Lett.*, 37 (1974) 3315.
- 150 a. A.C. Barker, A.R. Battersby, E. McDonald, R. Ramage and J.H. Clements, *Chem. Commun.*, (1967) 390.
b. A.R. Battersby, R.B. Herbert, E. McDonald, R. Ramage and J.H. Clements, *J. Chem. Soc. Perkin Trans. 1* (1972) 1741.
- 151 J.A. Sogn, L.C. Craig and W.A. Gibbons, *J. Am. Chem. Soc.*, 96 (1974) 3306.

APPENDIX

Several articles concerning the use of ^{13}C -n.m.r. in biosynthetic studies have been published since the submission of the manuscript, demonstrating the continuing interest in this field. Their titles and references are listed below arranged according to the scheme used above.

A. Review articles

The quantitative analysis of carbon-carbon coupling in the ^{13}C NMR spectra of molecules biosynthesized from ^{13}C enriched precursors.

R.E. London, V.H. Kollman and N.A. Matwiyoff, *J. Am. Chem. Soc.*, 97 (1975) 3565.

Use of ^{13}C magnetic resonance spectroscopy for biosynthetic investigations.

A.G. McInnes and J.L.C. Wright, *Acc. Chem. Res.*, 8 (1975) 313.

Utilization of ^{13}C — ^{13}C coupling in structural and biosynthetic studies. Double labeling method.

H. Seto, T. Satō and H. Yonehara, *Agric. Biol. Chem.*, 39 (1975) 1667.

^{13}C -n.m.r. in biosynthetic studies.

T.J. Simpson, *Chem. Soc. Rev.*, 4 (1975) 497.

The use of ^{13}C labeling in the study of antibiotic biosynthesis.

N. Neuss in *Methods in Enzymology*, J.H. Hash (Ed.), Vol. 43, Academic Press, New York, 1975, p. 404.

B. Incorporation of ^{13}C -acetate

Revised assignment of the ^{13}C -n.m.r. spectrum of radicinin.

H. Seto and S. Urano, *Agric. Biol. Chem.*, 39 (1975) 915.

Study of the biosynthesis of sterigmatocystin and reassignment of ^{13}C -n.m.r. spectrum.

K.G.R. Pachler, P.S. Steyn, R. Vleggaar and P.L. Wessels, *J. Chem. Soc. Chem. Commun.*, (1975) 355.

^{13}C -n.m.r. spectra of aflatoxin B_1 derived from acetate.

D.P.H. Hsieh, J.N. Seiber, C.A. Reece, D.L. Fitzell, S.L. Yang, J.I. Dalezios, G.N. la Mar, D.L. Budd and E. Motell, *Tetrahedron*, 31 (1975) 661.

Biosynthesis of aflatoxin B_1 from $[2\text{-}^{13}\text{C}]$ - and $[1,2\text{-}^{13}\text{C}]$ -acetate.

P.S. Steyn, R. Vleggaar, P.L. Wessels and D.B. Scott, *J. Chem. Soc. Commun.*, (1975) 193.

Biosynthesis of epoxydon and related compounds by *Phyllosticta* sp.

K. Nabeta, A. Ichihara and S. Sakamura, *Agric. Biol. Chem.*, 39 (1975) 409.

^{13}C Fourier transform n.m.r. IX. Complete assignments of some prodigiosins. Bioincorporation of label.

R.J. Cushley, R.J. Sykes, C.-K. Shaw and H.H. Wasserman, *Can. J. Chem.*, 53 (1975) 148.

Homonuclear ^{13}C decoupling in ^{13}C n.m.r. studies of biosynthesis using doubly labelled precursors. Assembly pattern of the acetate units in Bikaverin.

A.G. McInnes, D.G. Smith, J.A. Walter, L.C. Vining and J.L.C. Wright, *J. Chem. Soc. Chem. Commun.*, (1975) 66.

The ^{13}C -n.m.r. spectrum of a pyrone metabolite of *Aspergillus melleus*. Biosynthetic incorporation of single and doubly labelled [^{13}C]-acetate.

T.J. Simpson, *Tetrahedron Lett.* (1975) 175.

The biosynthesis of a pyrone metabolite of *Aspergillus melleus*. An application of long-range ^{13}C — ^{13}C coupling constants.

T.J. Simpson, J.S.E. Holker, *Tetrahedron Lett.* (1975) 4693.

Biosynthesis of terrein, a metabolite of *Aspergillus terreus* Thom.

R.A. Hill, R.H. Carter (née Rayner) and J. Staunton, *J. Chem. Soc. Chem. Commun.*, (1975) 380.

Biosynthesis of capsidiol in sweet peppers (*Capsicum frutescens*) infected with fungi: evidence for methyl group migration from ^{13}C -n.m.r. spectroscopy.

F.C. Baker, C.J.W. Brooks and S.A. Hutchinson, *J. Chem. Soc. Chem. Commun.*, (1975) 293.

Biosynthesis of metabolites of *Periconia macrospinoso* from [$1\text{-}^{13}\text{C}$]-, [$2\text{-}^{13}\text{C}$]-, and [$1,2\text{-}^{13}\text{C}$]-acetate.

J.S.E. Holker and K. Young, *J. Chem. Soc. Chem. Commun.*, (1975) 525.

A ^{13}C -n.m.r. study of the biosynthesis of islandicin from $^{13}\text{CH}_3$ $^{13}\text{COONa}$.

R.C. Paulick, M.L. Casey, D.F. Hillenbrand, H.W. Whitlock, Jr., *J. Am. Chem. Soc.*, 97 (1975) 5303.

Biosynthesis of ravenelin from [$1\text{-}^{13}\text{C}$]- and [$1,2\text{-}^{13}\text{C}$]-acetate.

A.J. Birch, T.J. Simpson and P.W. Westerman, *Tetrahedron Lett.*, (1975) 4173.

Preparation of ^{13}C - and ^3H -labelled cerulenin and biosynthesis with ^{13}C -n.m.r.

J. Awaya, T. Kesado, S. Ōmura and G. Lukacs, *J. Antibiot.*, 28 (1975) 824.

Nanaomycins, new antibiotics produced by a strain of *Streptomyces*

II. Structure and biosynthesis.

H. Tanaka, Y. Koyama, T. Nagai, H. Marumo and S. Ōmura, *J. Antibiot.*, 28 (1975) 868.

Fungal products. Part XVIII. ^{13}C -n.m.r. spectrum and biosynthesis of colletodiol.

M.W. Lunn and J. McMillan, *J. Chem. Soc. Perkin Trans. 1*, (1976) 184.

C. Incorporation of ^{13}C -acetate and/or more elaborate precursors

The use of ^{13}C n.m.r. to establish that the biosynthesis of tenellin involves an intramolecular rearrangement of phenylalanine.

E. Leete, N. Kowanko, R.A. Newmark, L.C. Vining, A.G. McInnes and J.L.C. Wright, *Tetrahedron Lett.*, (1975) 4103.

Biosynthetic studies on piericidin A and its structural revision.

S. Yoshida, S. Shiraishi, K. Fujita and N. Takahashi, *Tetrahedron Lett.*, (1975) 1863.

Application of ^{13}C -n.m.r. to the biosynthetic investigations. II. Biosynthesis of aureothin and related nitro-containing metabolites of *Streptomyces luteoreticuli*.

M. Yamazaki, Y. Maebayashi, H. Katoh, J.-I. Ohishi and Y. Koyama, *Chem. Pharm. Bull. (Japan)*, 23 (1975) 569.

Biosynthesis of cytochalasans. Part 4. The mode of incorporation of common naturally-occurring carboxylic acids into Cytochalasin D.

J.C. Vederas, W. Graf, L. David and C. Tamm, *Helv. Chim. Acta*, 58 (1975) 1886.

Biosynthesis of cercosporin.

A. Okubo, S. Yamazaki and K. Fuwa, *Agric. Biol. Chem.*, 39 (1975) 1173.

Biosynthesis of anthramycin. Determination of the labeling pattern by the use of radioactive and stable isotope techniques.

L.H. Hurley, M. Zmijewski and C.-J. Chang, *J. Am. Chem. Soc.*, 97 (1975) 4372.

Biosynthetic studies using ^{13}C enriched precursors on the 16-membered macrolide antibiotic leucomycin A_3 .

S. Ōmura, A. Nakagawa, H. Takeshima, K. Atusmi, J. Miyazawa, F. Piriou and

G. Lukacs, *J. Am. Chem. Soc.*, 97 (1975) 6600.

A ^{13}C -n.m.r. study of the biosynthesis of the 16-membered macrolide antibiotic tylosin.

S. Ōmura, A. Nakagawa, H. Takeshima, J. Miyazawa, C. Kitao, F. Piriou and G. Lukacs, *Tetrahedron Lett.*, (1975) 4503.

Use of ^{13}C -n.m.r. to establish that the biosynthesis of tropic acid involves an intramolecular rearrangement of phenylalanine.

E. Leete, N. Kowanko and R.A. Newmark, *J. Am. Chem. Soc.*, 97 (1975) 6826.

^{13}C evidence for the stereochemistry of streptomycin biosynthesis from glucose.

M.H.G. Munro, M. Taniguchi, K.L. Rinehart, Jr., D. Gottlieb, T.H. Stoudt, T.O. Rogers, *J. Am. Chem. Soc.*, 97 (1975) 4782.

A c.m.r. study of the biosynthesis of chloramphenicol.

M.H.G. Munro, M. Taniguchi, K.L. Rinehart, Jr., D. Gottlieb, *Tetrahedron Lett.*, (1975) 2659.

D. Terpenes

Application of ^{13}C magnetic resonance to isoprenoid biosynthesis. I. Ovalicin.

D.E. Cane, R.H. Levin, *J. Am. Chem. Soc.*, 97 (1975) 1282.

The biosynthesis of the sesquiterpenoids, cyclonerodiol and cyclonerotriol.

R. Evans, J.R. Hanson and R. Nyfeler, J. Chem. Soc. Chem. Commun., (1975) 814.

Biosynthesis of the diterpene antibiotic, aphidicolin, by radioisotope and ^{13}C -n.m.r. methods.

M.R. Adams and J.D. Bu'lock, J. Chem. Soc. Chem. Commun., (1975) 389.

The ^{13}C -n.m.r. spectra of some gibberellins.

R. Evans, J.R. Hanson and M. Sivers, J. Chem. Soc. Perkin Trans. 1, (1975) 1514.

Fusicoccin. Part V. The biosynthesis of fusicoccin from $[1\text{-}^{13}\text{C}]$ - and $[2\text{-}^{13}\text{C}]$ -acetate.

K.D. Barrow, R.B. Jones, P.W. Pemberton and L. Phillips, J. Chem. Soc. Perkin Trans. 1, (1975) 1405.

Biosynthesis of oleanene- and ursene-type triterpenes from $[4\text{-}^{13}\text{C}]$ mevalonic acid in tissue cultures of *Isodon japonicus* Hara.

S. Seo, Y. Tomita and K. Tori, J. Chem. Soc. Chem. Commun., (1975) 270.

Biosynthesis of ursene-type triterpenes from sodium $[1,2\text{-}^{13}\text{C}]$ acetate in tissue cultures of *Isodon japonicus* Hara and reassignments of ^{13}C NMR signals in urs-12-enes.

S. Seo, Y. Tomita and K. Tori, J. Chem. Soc. Chem. Commun., (1975) 954.

Biosynthesis of the sesquiterpenoids botrydial and dihydrobotrydial.

J.R. Hanson and R. Nyfeler, J. Chem. Soc. Chem. Commun., (1976) 72.

Biosynthesis of bisabolene by callus cultures of *Andrographis paniculata*. K.H. Overton and D.J. Picken, J. Chem. Soc. Chem. Commun., (1976) 105.

E. Porphyrins

Concerning the intermediacy of Uro'gen III and of a heptacarboxylic Uro'gen in corrinoid biosynthesis.

A.I. Scott, N. Georgopapadakou, K.S. Ho, S. Klioze, E. Lee, S.L. Lee, G.H. Temme, III, C.A. Townsend and I.M. Armitage, J. Am. Chem. Soc., 97 (1975) 2548.

Concerning the biosynthesis of vitamin B_{12} .

A.I. Scott, Tetrahedron, 31 (1975) 2639.

Biosynthesis of porphyrins and related macrocycles. Part VI. Nature of the rearrangement process leading to the natural type III porphyrins.

A.R. Battersby, G.L. Hodgson, E. Hunt, E. McDonald and J. Saunders, J. Chem. Soc. Perkin Trans. 1, (1976) 273.

Biosynthesis of porphyrins and related macrocycles. Part VII. Synthesis of specifically labelled $[^{14}\text{C}_1]$ uroporphyrin-III and of $[10,14\text{-}^{13}\text{C}_2]$ -Uroporphyrin-III. Conversion of the latter into $[10,14\text{-}^{13}\text{C}_2]$ protoporphyrin-IX; biosynthetic significance of its ^{13}C -n.m.r. spectrum.

A.R. Battersby, M. Ihara, E. McDonald, J. Saunders and R.J. Wells, J. Chem. Soc. Perkin Trans. 1, (1976) 283.

APPLICATION OF CARBON-13 N.M.R. TO PROBLEMS OF STEREO-CHEMISTRY

ARTHUR S. PERLIN

Dept. of Chemistry, McGill University, Montreal (Canada)

I. INTRODUCTION

Until the late 1960's, most organic chemists associated the term "n.m.r. spectroscopy" with proton studies. Since it has been relatively easy for some time to obtain proton spectra, it is understandable that the enormous value of this technique should have gained universal application. During the same period very few measurements of carbon magnetic resonance were made, although in principle they should be even more appropriate for organic molecules, due largely to restrictions imposed by the low natural abundance (1.1%) and low sensitivity of the magnetically-active carbon isotope, i.e., ^{13}C . However, recent methodology has greatly expedited the detection of ^{13}C resonances, and consequently ^{13}C spectroscopy is rapidly gaining prominence comparable to that of protons.

For studies in stereochemistry, the gain is more than proportional to the new n.m.r. information acquired, because ^{13}C and ^1H data can strongly reinforce each other. *Together*, they afford several kinds of shielding and coupling parameters which must constitute a wholly self-consistent set, and thereby can define molecular geometry more rigorously than is possible with either ^{13}C or ^1H n.m.r. independently.

In dealing here with stereochemical aspects of ^{13}C n.m.r. the objective has not been to present a comprehensive coverage of the subject. Two excellent texts [1,2] contain a detailed treatment of material up to 1972; there are also a number of valuable review articles [3–9] on selected topics, and recent applications to natural products are described elsewhere in this volume. Hence, this article attempts to provide an overall view of steric influences on the characteristics of ^{13}C spectra, and data have been chosen accordingly to illustrate as many specific aspects as possible.

II. GENERAL FEATURES OF ^{13}C NMR SPECTROSCOPY

An especially valuable feature of ^{13}C n.m.r., which became apparent in the earliest studies [10–16], is the wide range of chemical shifts observable — more than 25-fold that of protons. As a result, it is usually possible to detect each of the carbon resonance signals produced by even highly complex molecules, which makes for a measurement of exceptional sensitivity and sophistication.

Spin–spin interactions between ^{13}C and neighbouring magnetic nuclei give rise to

important coupling information. Usually, this means values of J_{C-H} ^a, which are strongly diagnostic of stereochemistry. Sometimes the same $^{13}C-^1H$ coupling information can be derived from the (weak) ^{13}CH satellite signals in proton spectra and, in fact, a large body of such data was obtained [17,18], although for rather simple molecules, long before there was substantial activity in the field of ^{13}C n.m.r. per se. Enrichment is frequently used to enhance the measurement of splittings in such satellite signals, and also to allow for the ready observation in ^{13}C spectra of coupling between carbons (Section IV. A,E)^b.

Major barriers to the acquisition of good spectra within a reasonable time have been substantially overcome by recent advances in technique and instrumentation, e.g., the introduction of effective signal accumulators for continuous wave spectra, the use of 1H -decoupling [22] to intensify signals by the removal of splitting and through nuclear Overhauser enhancement, and, most importantly, the development of pulse Fourier transform (FT) spectroscopy [23]. Relatively inexpensive and highly serviceable spectrometers are finding a wide market and bringing ^{13}C n.m.r. within the reach of most organic chemists. This in no way infers that the technique is as yet on a par with proton spectroscopy — a much longer time is required to obtain a ^{13}C spectrum (or a much more concentrated solution must be used), and a full interpretation of a ^{13}C spectrum is a good deal more challenging. Nevertheless, the present state of the art may, perhaps, be compared favourably with the early period of greater expansion in 1H spectroscopy in the late fifties and early sixties.

A. Proton-decoupled spectra

At the present time, the measurement of a ^{13}C spectrum is usually carried out with simultaneous decoupling of spin-spin interactions with all protons, by intense broad-band irradiation at the appropriate 1H frequency. As a result, the *proton-decoupled* spectrum consists only of a group of narrow singlets (Fig. 1a). With an obtainable resolution of at least 0.1 p.p.m., this simple format generally allows for an easy determination of the number of non-equivalent carbons represented as well as of their chemical shifts, and hence greatly facilitates the detection of elements of symmetry in a molecule, or of the individual species in a mixture of molecules. Another very valuable application of 1H -decoupled spectra is in the measurement of relaxation characteristics of ^{13}C nuclei (Section V).

Identification of the resonances of various classes of carbons (alkyl, aryl, carbonyl,

^a Or of coupling with such abundant magnetic nuclei as ^{19}F , ^{31}P , etc., when present. $^{13}C-^{13}C$ coupling is barely detectable because there can rarely be more than one ^{13}C nucleus in a molecule, or in a monomeric unit of a polymer.

^b A related and very fruitful development is the use of ^{13}C , in place of ^{14}C , as a tracer in biosynthetic studies [19–21]. Since both the location and quantity of the isotope incorporated may be determined by direct examination of the ^{13}C spectrum (or, possibly, the 1H spectrum) a great advantage over radioisotope methodology in this area can be realized (see Chapter 3).

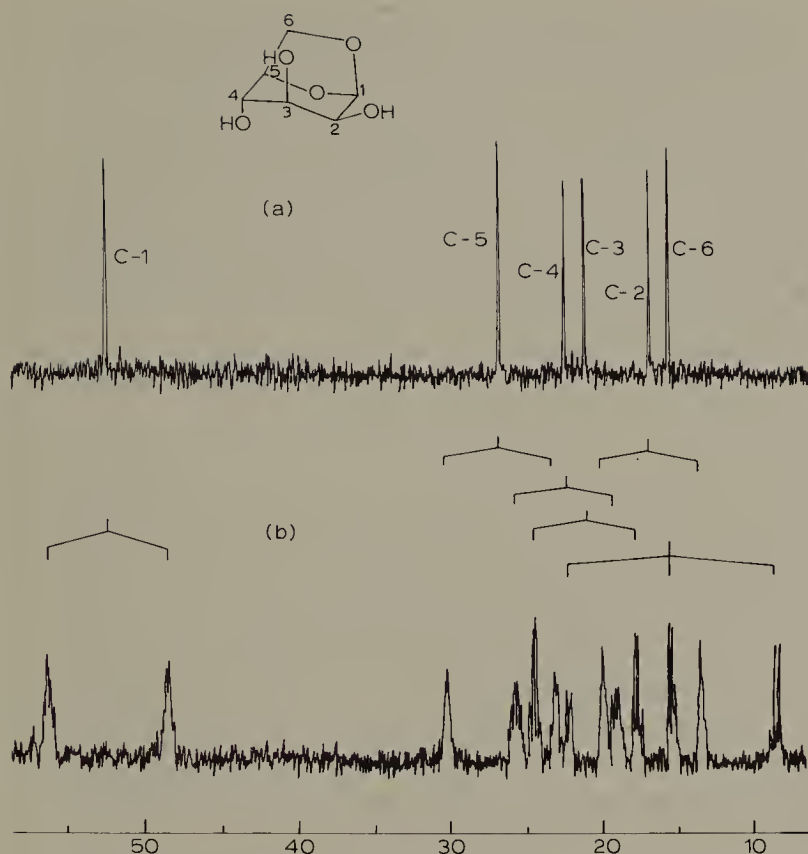


Fig. 1. ^{13}C n.m.r. spectrum (22.63 MHz) of 1,6-anhydro- β -D-mannopyranose in 95% deuterium oxide at 30°C : (a) proton-decoupled (pulse angle, 90° ; repetition time, 2.8 s; total acquisition time, 1 h); (b) proton-coupled with "gated" decoupling (pulse angle, 90° ; repetition time, 3.8 s (2.8 s ^1H -coupled, 0.9 s decoupled); total acquisition time, 16 h). (Spectra recorded by R.G.S. Ritchie and N. Cyr.)

etc.) is straightforward because of the large characteristic chemical shift differences between them. It is less easy to differentiate between individual carbons within a class, although this task is becoming more routine with the availability of a wealth of ^{13}C chemical shift data and of information about the magnitude of shielding produced by various substituents and stereochemical changes. However, in comparison with a well-resolved ^1H spectrum, a complete ^{13}C analysis is likely to require a good deal of experimental manipulation. That is, while the splitting pattern of a ^1H spectrum can clearly define the locations of the protons within a molecule, a decoupled ^{13}C spectrum gives no comparable information (although, in principle, this should be contained in the extremely weak ^{13}C – ^{13}C satellite signals). Hence, the assignment of signals in the spectrum is frequently made in an indirect manner.

For example: (a) a substituent group is introduced to alter the shielding of a particular carbon; (b) deuteration of a specific carbon is carried out, which leads either to

marked broadening [11,12,24], or to a detectable ^{13}C – ^2H splitting [25], of the resonance signal; (c) selective decoupling [26], i.e., coupling between a particular proton and the carbon appended to it is disrupted by irradiation at the (already known) absorption frequency of the proton, thus leading to a disproportionate increase in the relative intensity of only that specific ^{13}C signal. The applicability of such techniques for the identification of resonances obviously depends on chemical and/or instrumental limitations. Because such limitations are not trivial, especially with complex molecules, many signal assignments reported in the literature are tentative, and the correction of earlier assignments is not an infrequent occurrence.

B. Coupled spectra

In the absence of proton decoupling, the ^{13}C spectrum is much more complex (Fig. 1b); an overlap of signals is a common feature, because of the large size (ca. 150 Hz or more) of direct bond ^{13}C – ^1H coupling, and sometimes leads to a serious increase in the complexity of the spectra ^a. In general, however, valuable information is available which is otherwise lost when proton-decoupling is employed. Thus, each type of coupling between ^{13}C and ^1H , i.e., through one, two or three bonds (1J , 2J or 3J), is stereochemically dependent, affording three additional criteria of molecular geometry. Also, the splitting pattern can help materially with signal assignments; i.e., a carbon bearing zero, one, two or three protons produces, respectively, a singlet, doublet, triplet or quartet ^b, and these signals may exhibit finer, long-range, splitting dependent upon the proximity, number and orientation of other protons ^c. Hence, the overall coupling pattern can help, at least partly in a manner analogous to the splitting of ^1H spectra, to define the spatial relationship of each ^{13}C nucleus with respect to other magnetic nuclei in the molecule ^c.

Although by far the majority of ^{13}C spectra now recorded are ^1H -decoupled, it is highly likely that much more attention will be given in the future to coupled spectra, particularly in stereochemical studies. Here again, advances in technique and instrumentation are critical. The recent introduction of “gated” decoupling [30], by allowing for most of the nuclear Overhauser enhancement gained in the fully-decoupled spectrum, goes far in alleviating the problem of excessively long experimentation periods, and other developments will undoubtedly enhance the availability and quality of coupled ^{13}C spectra.

^a As with ^1H spectra added complexity may be introduced by second-order effects [27,28], such as those associated with an ABX spin system consisting of two protons (AB) and a ^{13}C nucleus (X) [28].

^b Off-resonance decoupling [29] is an elegant way to produce this basic outline of splitting that arises from interaction between directly-bonded ^{13}C and ^1H .

^c When there is additional splitting due to the presence of other kinds of magnetic nuclei (Y), it is obviously far easier to determine the ^{13}C –Y couplings (Section IV.E) from the proton-decoupled spectrum.

III. STEREOCHEMICAL ASPECTS OF ^{13}C CHEMICAL SHIFTS

Carbon-13 shielding changes associated with the introduction of substituent groups are extensively documented, particularly for derivatives in the alkane, alkene, alicyclic and aromatic series [1,2]. Substituent parameters that have been derived from these data are found to be largely additive and allow for the calculation of ^{13}C chemical shifts with reasonable confidence. Certain of these parameters have come to be linked specifically with steric effects, and extensive use is made of them in the application of ^{13}C n.m.r. to problems of molecular geometry. The general features of these empirical inter-relationships are described in this section, and an attempt is made to emphasize characteristics that are especially distinctive for individual classes of compounds. With this in mind, much of the data is presented in the form of Figures illustrating *differences* in chemical shifts ($\Delta\delta$) between isomeric species, rather than as extensive compilations of individual chemical shifts. Furthermore, because a configurational or conformational change is almost always associated with shielding changes for *several* nuclei, it is useful and convenient to compare an "overall" difference — i.e., the sum of chemical shift differences ($\Sigma\Delta\delta$) between corresponding nuclei of isomers or conformers. This device is used frequently here to help provide an overview of the nature of steric influences.

A. Upfield shifts associated with *gauche* interactions. The γ -effect

Sterically-induced chemical shifts attributable to non-bonded interactions were quickly recognized [11–16], and subsequent research has found that similar kinds of effects apply for many classes of organic molecules. This will be evident in the following discussion, from the consistency with which certain characteristics recur. However, there are a number of anomalies, sometimes within a given series of isomeric compounds, which are grouped together in Sections III. B–E.

TABLE 1

CHANGES IN ^{13}C SHIELDING ($\Delta\delta$) ASSOCIATED WITH SEQUENTIAL REPLACEMENT OF H BY CH_3 ¹⁴

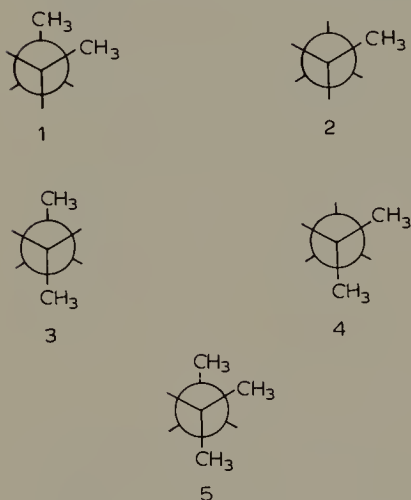
	δ	$\Delta\delta$	
	(p.p.m.)	(p.p.m.)	
$^{13}\text{CH}_3\text{—H}$	−2.1		
$^{13}\text{CH}_3\text{—CH}_3$	5.9	α -effect,	8.0
$^{13}\text{CH}_3\text{—CH}_2\text{—CH}_3$	15.6	β -effect,	9.7
$^{13}\text{CH}_3\text{—CH}_2\text{—CH}_2\text{—CH}_3$	13.2	γ -effect,	−2.4
$^{13}\text{CH}_3\text{—CH}_2\text{—CH}_2\text{—CH}_2\text{—CH}_3$	13.7	δ -effect,	0.5

References pp. 229–235

1. Alkanes

Treating the alkanes listed in Table 1 as a sequence in which H is repeatedly replaced by a methyl group, it is found that the carbon α - or β - to the substituent introduced experiences a decrease in shielding (" α - or β -effect"), whereas the γ carbon becomes more shielded (" γ -effect"). The δ carbon shows slight deshielding, and more remote carbons are essentially unaffected [14].

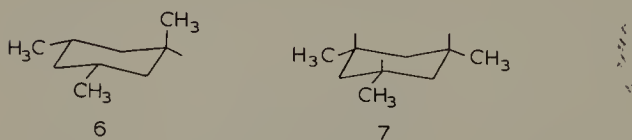
It is generally felt that the α - and β -effects are primarily inductive in nature. The γ -effect, however, is regarded as predominantly steric and as having its origin in non-bonded interactions. Thus, the $^{13}\text{CH}_3$ group of *n*-butane experiences a *gauche* interaction (1) that is not present in propane (2), it being assumed that an *antiperiplanar*



$^{13}\text{CH}_3$ (3) makes no contribution to the shielding change. Similarly, a comparison of 2-methylpropane (4) with 2-methylbutane (5) indicates an increase in shielding of the methyl ^{13}C (by 2.3 p.p.m.) which, by analogy with (1), may be attributed to the *gauche* interaction depicted in (5). Since only about one-third of the rotamer population of butane [31] is represented by (1) (and its mirror image) the full shielding effects are expected to be proportionately greater than the measured values.

2. Methylcyclohexanes

Consistent with the latter possibility, a much stronger γ -effect shows up in methylcyclohexanes [32,33]. For example, the C-3 and C-5 signals of the a,e,e isomer of



1,3,5-trimethylcyclohexane (6) are 6.3 p.p.m. upfield of those of the all-equatorial

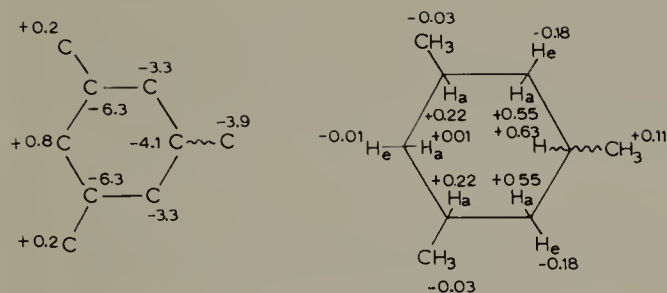
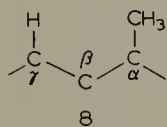


Fig. 2. ^{13}C and ^1H chemical shift differences ($\Delta\delta$, p.p.m.) between the a,e,e and e,e,e isomers of 1,3,5-trimethylcyclohexane, (6) and (7), corresponding to the shielding changes observed when the orientation of CH_3 -1 is altered from eq. to ax. (–, upfield shift; +, downfield shift).

isomer (7), presumably due to the *gauche* (1,3-diaxial) interaction between the ax. CH_3 and CH -3 and -5. The effect on the methyl carbon is not reciprocal, for δCH_3 (eq.)- δCH_3 (ax.) is only 4 p.p.m., (although in methylcyclohexane itself at -110° the corresponding value is 6 p.p.m.) [34]. In addition to these differences, however, C-1, -2 and -6 of (6) also exhibit upfield positions; i.e., a widespread increase in shieldings of ^{13}C nuclei accompanies the eq. \rightarrow ax. change in orientation, as depicted in Fig. 2 [35].

A model has been proposed by Grant and Cheney [33,36,37] to account for these γ -effects in terms of a *gauche* orientation of substituents. Central to this model is a polarization of the C–H bonds, caused by a repulsive interaction between the hydrogen atoms (8), such that the shielding of carbon is increased, and of hydrogen de-



creased. Experimentally, in fact, it is found [32,38] that the γ - and CH_3 -protons experience a downfield shift (Fig. 2) when an eq. \rightarrow ax. orientational change occurs, as in (7) \rightarrow (6). Also, as seen with carbon, other positions are affected; of the β (2,6) protons, the axials become more strongly deshielded, whereas the equatorial ones become slightly more shielded [38]. The downfield shift of H-1 is to be expected, in any event, because an ax. \rightarrow eq. change is involved ^a. Effects on the 4-protons and those of the 3- and 5-methyl groups are minor, which also runs parallel to the results of the corresponding carbons (Fig. 2).

The same type of pattern of ^{13}C and ^1H chemical shift differences is found for other diastereoisomeric pairs of methyl cyclohexanes – 1,2-, 1,3- and 1,4-dimethyl and

^a Although the chemical shift difference between an eq. H and ax. H is attributed primarily to magnetic anisotropy changes associated with the ring, in the light of the other chemical shift changes cited above, it seems possible that the substituent orientation may be a significant factor.

1,2,4-trimethyl [32]. Again one finds that most of the ^{13}C nuclei are more shielded, and the protons less shielded, in the isomer bearing the axial CH_3 . Such characteristics may be conveniently expressed as the *overall* shielding change [35] for each pair — i.e., the sum of the chemical shift differences found between all corresponding nuclei within the pair ($\Sigma\Delta\delta$; e.g., the values from Fig. 2 are -26.0 (^{13}C) and $+1.6$ (^1H) p.p.m.). On this basis, an eq. $\text{CH}_3 \rightarrow$ ax. CH_3 transformation within any of the five pairs cited is accompanied by a relatively consistent spectral change: a total upfield shift of the ^{13}C resonances by $30.3 (\pm 4.3)$ p.p.m., and a total downfield shift of the ^1H resonances by $1.8 (\pm 0.6)$ p.p.m.

If non-bonded interactions do in fact account for these changes, it is pertinent that the enthalpy difference for each of these five pairs is uniformly in the region of $1.8 \text{ kcal mol}^{-1}$. Furthermore, both the $\Sigma\Delta\delta$ values for ^{13}C and the enthalpies increase in the following sequences [35].

$$1,3(\text{e,e}) = 1,4(\text{e,e}) < 1,2(\text{e,e}) < 1,1(\text{e,a}) < 1,3(\text{e,a}) = 1,4(\text{e,a}) < 1,2(\text{e,a});$$

$$\text{and } 1,3,5(\text{e,e,e}) < 1,2,5(\text{e,e,e}) < 1,1,3(\text{e,a,e}) < 1,2,3(\text{e,e,e}) < 1,3,5(\text{e,e,a}) < 1,1,2(\text{e,a,e}) < 1,2,4(\text{e,e,a})$$

Hence these data support the idea that *gauche* interactions are the source of the upfield shifts for α, β, γ and CH_3 carbons (and downfield shifts for protons appended to them). According to the Cheney and Grant model for the γ -effect, repulsive forces between the C—H bonds in (8) cause an increase in the charge density on those carbons. That is, an electron expansion occurs, and the resulting increase in the distance between the nucleus and the p electrons leads to a decrease in the $1/r^3$ component of the (negative) paramagnetic term (σ^p) for nucleus N (eqn.1) [39]; hence there is an increase in shielding.

$$\sigma_{\text{N}} = \sigma^d + \sigma^p \text{ (+ other contributions)} \quad (1)$$

Although it is generally agreed [1,12,39–41] that carbon screening (σ_{N}) is determined mainly by σ^p , it is not clear that changes in the latter term account for the relatively small differences of $\sim 4\text{--}5$ p.p.m. of concern here. For example, calculations by IEHT or CNDO methods infer that eq. and ax. methylcyclohexane do not differ sufficiently in charge density to account for the $\Delta\delta$ actually observed [42]. Such calculations, however, incorporate the assumption of standard geometries and hence may not be sufficiently realistic. Alternatively, the diamagnetic term (σ^d) may be regarded as geometry-dependent [43,44] if the contributions of electrons of other atoms in the molecule are considered [43–46]; the proximity of a *gauche* (or ax.) CH_3 as compared with an *anti* (or eq.) CH_3 would then lead to an increase in this term and a con-

sequent upfield shift ^a. Contributions of changes in carbon hybridization and bond angles may, of course, be of primary importance, but have yet to be quantitatively assessed. However, it has been suggested [47] that an increase in the C_β—C_γ bond length (in 8) is the source of the increase in shielding of the carbon β to the ax. CH₃.

3. Other cyclohexane derivatives

Analogous effects are found with substituents other than alkyl groups. For example, the α,β, and γ carbons of *cis*-4-*t*-butylcyclohexanol [35,47–49] (9) resonate upfield



of those of the *trans* isomer (10), and the increase in shielding of each of these carbons (~4 p.p.m.) is of the same order as for methylcyclohexanes.

Results for a series of monosubstituted cyclohexanes at 180–200 °K afford a broad comparison of eq. → ax. substituent differences [50]. This study has shown that the γ-effect does not increase with substituent size (as measured by Δ*G*[°]) (Table 2), and thereby has raised some doubt as to the relative contribution of steric crowding to an increase in shielding. Nevertheless, when the data are examined in terms of *overall* differences in shielding (ΣΔδ) they are found to correspond moderately well to the substituent free energies (Table 2). Although chlorine, bromine and iodine are unique among the group in that they exhibit no influence (Cl) or a deshielding (Br and I) on the α-C, their β- and γ-effects are shielding. In fact, they appear to induce a greater increase in shielding at these latter positions than do the other substituents, so that in the overall context only iodine departs noticeably from the progression represented by Table 2.

Hence it appears reasonable to associate upfield ¹³C chemical shifts in this series, as with alkanes and methylcyclohexanes, with steric perturbations of the *gauche* butane type. Many other classes of compounds, some far more complex in structure, exhibit clear evidence of this same kind of interrelationship between shielding changes and *gauche* interactions. This widespread consistency accounts for the important fact that so many applications of ¹³C n.m.r. to problems of configuration and conformation have been based primarily on this simple, empirical, premise. Some representative examples from the large body of data available are considered in succeeding sections.

4. Some acyclic systems. Synthetic polymers. Alkenes

The notion of shielding differences such as those between 2-methylpropane (4) and

^a Although, as noted above, calculated charge densities do not differ sufficiently to account for Δδ, values obtained for the σ^d term are not inconsistent with the observed differences in chemical shifts. Thus, σ^d values calculated [44] for the three diastereoisomeric pairs of dimethylcyclohexanes are consistently of the same sign and of a similar order of magnitude as the corresponding Δδ values. Hence, the γ-effect may be more closely related to variations in σ^d, than in σ^p.

TABLE 2

VARIATIONS IN γ EFFECTS, OVERALL DIFFERENCES IN SHIELDING ($\Sigma\Delta\delta$) AND FREE ENERGIES OF MONOSUBSTITUTED CYCLOHEXANE CONFORMERS

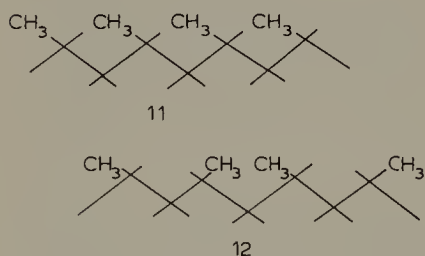
Substituent	γ -effect ^a (p.p.m.)	ΔG° (cal/Mol) ^b	$\Sigma\Delta\delta$ ^c (p.p.m.)
CN	-2.6	152 (200)	-13.9
NC	-4.2	182 —	-14.6
F	-3.8	360 (250)	-15.8
I	-6.6	455 (400)	-15.3
Br	-6.8	585 (750)	-18.1
Cl	-6.6	620 (500)	-20.6
OCH ₃	-4.4	750 (750)	-19.0
OCOCH ₃	-4.0	885 (1000)	-18.3
OH	-4.9	>1400 (1250)	-20.3
CH ₃	-5.4	>1400 (1700)	-26.7

^a Data from ref. 50; difference in chemical shift of the γ -carbon, associated with an eq. \rightarrow ax. change of the substituent.

^b Determined at 180–200 °K [50]; values in brackets are from other studies as compiled in ref. 51.

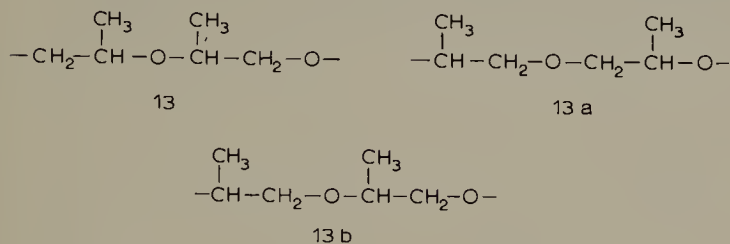
^c Sum of the differences in chemical shifts [50] for *all* of the carbons, associated with an eq. \rightarrow ax. change of the substituent.

2-methylbutane (5), when extended to the polymer level, is consistent with the fact that ¹³C n.m.r. spectroscopy is highly sensitive to changes in conformational sequence, or tacticity [52–56]. Because variations in tacticity must involve a greater or lesser number of *gauche* interactions, chemical shifts of synthetic polymers are expected to reflect the relative orientation of substituents appended to the polymer backbone. For example, by treating polypropylene as a substituted propane, and assuming a shielding of 4.3 p.p.m./*gauche* interaction, good agreement has been obtained between calculated and observed spectra for isotactic (11) and syndiotactic (12) forms of polyalkanes



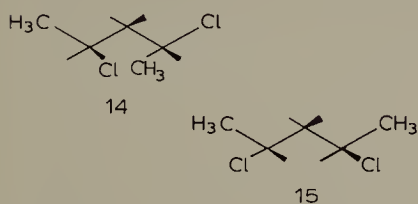
[57]. With the superior resolution obtainable at 69 MHz, it has been shown [57] that a detailed analysis of (up to) pentad sequences in atactic polypropylene is feasible — a remarkably sensitive measure of polymer fine structure.

With some types of synthetic polymers and copolymers, steric influences are superimposed upon those due to structural isomerism. Thus, poly(propylene oxide) may incorporate head-to-head (13) tail-to-tail (13a), or head-to-tail (13b) dyads and thereby



introduce a shielding variable in addition to that associated with tacticity [52,56]. Nevertheless, sterically-induced shifts similar to those already described have been recognized in the ^{13}C spectra of such polymers and successful analyses achieved in cases that could not be analyzed by ^1H n.m.r.

Spectra of poly(vinyl chloride) have been interpreted by reference to chemical shift differences between *meso*- and *rac*-2,5-dichloropentanes [58]. Considering (14) (or its



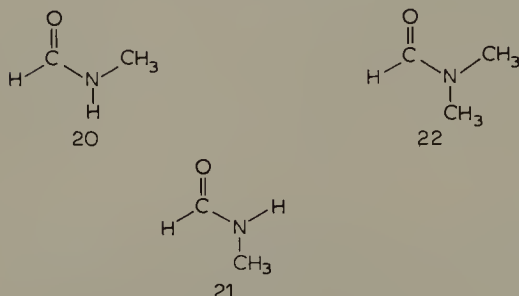
enantiomer) as likely to be the preferred *meso* conformer and (15) that of the racemic modification, the upfield position of the CH_3 and CH signals of (14) relative to those of (15) (by 1.0 and 1.1 p.p.m., respectively) can be interpreted as follows: the methyl and methine carbons of (15) bear only *anti* relationships, whereas in (14) there is one *gauche* and one *anti* arrangement.

The etherification of an alcohol provides an interesting example of an increase in shielding attributable to the *gauche* type of interaction [59]. Hence the ^{13}C resonance signal of the $\text{O}-\text{CH}_3$ group in the series CH_3OR , where $\text{R} = \text{CH}_3$ (16), C_2H_5 (17) (CH_3) $_2\text{CH}$ (18) and $(\text{CH}_3)_3\text{C}$ (19), moves progressively upfield by 11 p.p.m., as the

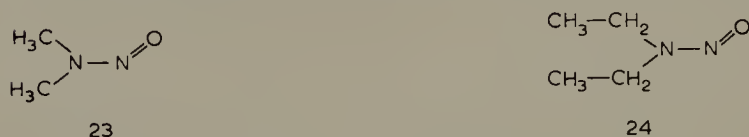


contributions of *gauche* arrangements increase. The carbinyl carbon also becomes more shielded.

Restricted rotation about bonds showing partial double-bond character, as in amides or nitrosamines, permits a ready distinction of *syn* from *anti* arrangements [60–63]. For *N*-methylformamide [60,61], the C=O and CH₃ carbons of the *syn* isomer (20) resonate about 3.3 p.p.m. upfield of those of the *anti* (21)^a. The CH₃

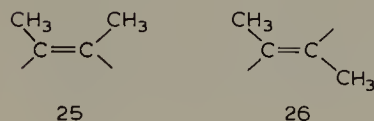


carbons of *N,N*-dimethylformamide (22), being non-equivalent at room temperature, differ by 5 p.p.m. (in chloroform); again, the *syn* orientation is associated with greater shielding [60,61]. Similarly, the spectrum of *N*-nitrosodimethylamine (23) shows two CH₃ resonances 7.9 p.p.m. apart [62]. An appreciable effect on more distant alkyl



groups in related compounds is evident as well: e.g., the methyl carbons of (24) differ by 3.0 p.p.m. and the methylene by 8.9 p.p.m.

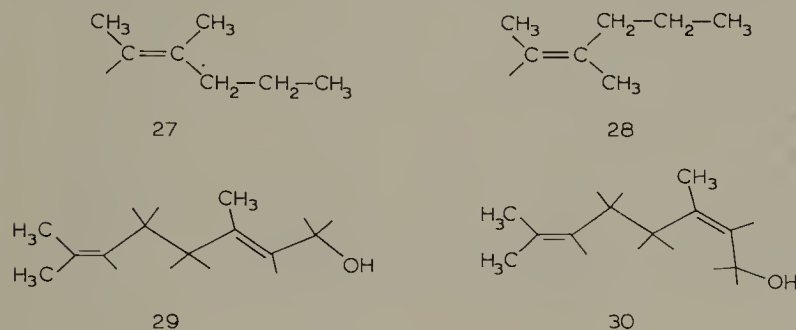
Acyclic alkenes are interesting in this context, because geometric isomers show shielding differences attributable to a similar kind of steric origin [64,65]. Typically, the carbons of *cis*-2-butene (25) are more shielded than those of *trans* (26), and



although the *sp*² carbons differ by only 1.4 p.p.m., signals of the α-carbons of (25) are 5.5 p.p.m. upfield of those of (26). Other isomeric pairs give closely similar data. Indeed, linear regression analysis [65] has shown that the effect on α-carbons is sufficiently large (~5 p.p.m.) and consistent to permit a ready distinction between any *cis-trans* pair of

^a The fact that the *syn* isomer is more stable than the *anti* (*syn* : *anti* = 10 : 1) shows that geometric proximity is not necessarily destabilizing.

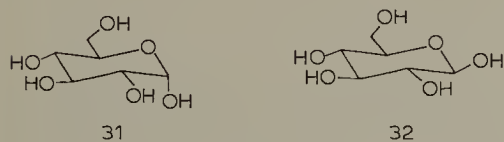
alkenes ^a, including E (27) and Z (28) isomers [64–66] ^b. A comparison of geraniol (29) [65] and nerol (30) [67] illustrates the shielding effects on the various kinds of α -carbons: in both instances, the *cis* terminal CH_3 carbon is more shielded than the



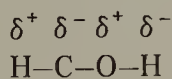
trans (by ~ 8 p.p.m.), the C-3 methyl of (29) (*cis* interaction) is more shielded (by 6.8 p.p.m.) than that of (30), and C-4 is more shielded (by 8.2 p.p.m.) in (30) (*cis* interaction) than in (29); by contrast, the chemical shift remains essentially constant for C-1, which is *cis* to an α -carbon in each molecule. Hence, the eclipsing (or nearly so) of two allylic $\text{H}-\text{C}$ (sp^3) structures in alkenes leads to a strong increase in the shielding of both carbons involved. However, the sp^2 carbons themselves are not comparably affected, and in this respect the *cis*-interaction differs notably from the *gauche* type.

5. Other monocyclic systems

Orientational effects of substituents in aldopyranoses [68–70] show a close correspondence to those encountered with cyclohexane derivatives. As exemplified by α -



and β -D-glucose (31) and (32) [35,68], an eq. $\text{OH} \rightarrow$ ax. OH transformation is associated with upfield shifts for C-2, -3 and -5, whereas C-4 and C-6 are not appreciably affected (Fig. 3). The appended protons show a concomitant downfield shift, but the hydroxyl protons are affected in the opposite manner [35]. Overall, these patterns infer that the ax. OH perturbation may promote a bond polarization extending through the system



^a In the absence of the geometric isomer, the configuration of a 1,2-disubstituted alkene or polyalkene (including terpenes) can be determined with confidence by reference to the corresponding alkane and use of the appropriate shift parameters [65].

^b The 3- CH_3 of (27) is the more shielded by 7.9 p.p.m., whereas C-4 of (28) is the more shielded by 8.5 p.p.m.

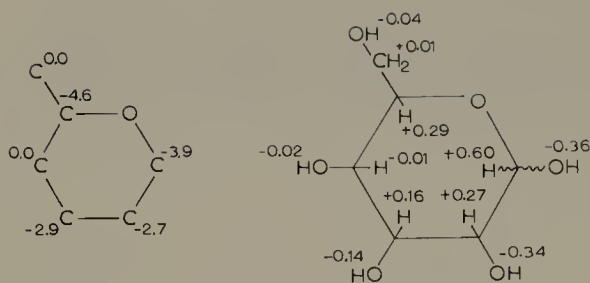
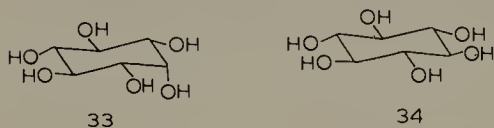


Fig. 3. ^{13}C and ^1H chemical shift differences ($\Delta\delta$, p.p.m.) between α - and β -D-glucopyranose, (31) and (32), corresponding to the shielding changes observed when the orientation of the anomeric hydroxyl group is altered from eq. to ax. (–, upfield shift; +, downfield shift).

Shielding parameters for the various members of the aldopyranose, and also ketopyranose [71–74], series show a moderately good additivity. The differences between (31) and (32) are somewhat greater (an average of 3.7 p.p.m./ring carbon) than the general value of 2.5–3.0 p.p.m./carbon associated with a vicinal *gauche* or 1,3-diaxial C–O, C–H interaction^a. A comparable geometric pair among the hexahydroxycyclohexanes, *myo*- and *scyllo*-inositol (33) and (34), is characterized [75] by smaller upfield shifts for the axial isomer (averaging 1.4 p.p.m./carbon). Although the relatively short ring C–O bonds of (31) may bring ax. OH-1 into closer proximity with H-3 and H-5, and thus induce greater shielding, the difference between (33) and (34)



is also small when compared with less substituted cyclohexanes — e.g., the ring carbons of (9) and (10), or of *cis* and *trans*-1,2-cyclohexanediol, show an average $\Delta\delta$ of about 3.2 p.p.m. Possibly the high incidence of electronegative O atoms introduce a “dampening” effect on C–H bond polarization.

Chemical shift patterns paralleling those for the aldopyranoses are found for their alkyl [69,70] and aryl glycosides [76], 2-amino-2-deoxy analogs [77], deoxy-nitro [78] and deoxy-chloro derivatives [79], which emphasizes that shielding differences between diastereomers are primarily of steric origin. Also, as noted above for cyclohexane derivatives, an increase in the number of *gauche* and *vic* interactions in the sugars, and hence an increase in ΔG of the compounds, is generally matched by an overall ($\Sigma\Delta\delta$) greater shielding of carbons and lesser shielding of protons [70].

It may be more than coincidence that variations in the rate of bromine oxidation at C-1 of reducing sugars show a close correspondence with differences in the ^{13}C -1

^a Values for 1,3-diaxial C–O, C–O interactions are somewhat smaller (see Section III. B).

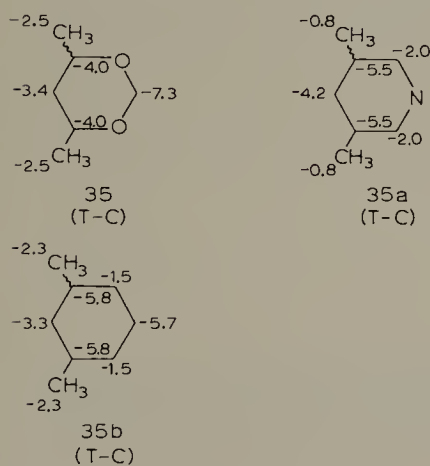
TABLE 3

 ^{13}C and ^1H CHEMICAL SHIFTS OF ALDOPYRANOSES AND RATES OF BROMINE OXIDATION

Aldopyranose	$^{13}\text{C-1}$ (δ)	H-1 (δ)	Relative rates
α -L-Arabinose	97.7	4.60	52
β -D-Xylose	97.6	4.65	52
β -D-Galactose	97.5	4.68	50
β -D-Glucose	96.8	4.74	39
β -D-Mannose	94.4	4.97	24
β -D-Lyxose	95.0	4.94	14
β -D-Ribose	95.3	4.99	6.1
α -D-Lyxose	95.0	5.08	4.9
β -L-Arabinose	93.5	5.34	3.0
α -D-Xylose	93.1	5.26	2.8
α -D-Mannose	94.9	5.25	1.6
α -D-Galactose	93.2	5.34	1.3
α -D-Glucose	93.0	5.32	1.0

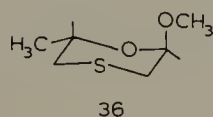
chemical shifts (Table 3) [80]. For example, the rate of oxidation of (32) is thirty-nine times that of (31). Since the rate determining step of the reaction appears to involve a flow of electrons from C towards H, if the C–H bond of (32) is initially more polarized in this direction (less shielded C, more shielded H), then there is a closer relationship between the ground and transition states than would apply for (31). In addition to the rather consistent trend exhibited by carbon, it is noteworthy that the H-1 chemical shifts, by showing the opposite interrelationship with the oxidation rates, are consistent with the bond polarization concept.

Shielding influences ascribable to *gauche* interactions are also found with other saturated 6-membered ring heterocycles. Typical data are afforded by a comparison ($\Delta\delta$) of the ^{13}C chemical shifts for the *trans* and *cis* isomers (T–C) of 4,6-dimethyl-1,3-dioxane (35) [81] and 3,5-dimethylpiperidine (35a) [82], which shows that most



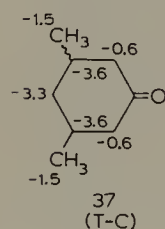
References pp. 229–235

carbons of the e,a (*trans*) isomer resonate upfield of their e,e (*cis*) counterparts. Clearly, the results are analogous to those for such isomeric pairs as *cis*- and *trans*-1,3-dimethylcyclohexane (35b) [32]. Aside from the small $\Delta\delta$ value for the CH₃ carbons of (35a) (which is considered further in Section III.C), the three patterns of shielding changes are not dissimilar. Correlations obtained for ¹³C shielding differences among 1,4-oxathiane derivatives (e.g., (36)), including the 4-oxide (sulfoxide) of 1,4-oxathiane, have taken account of γ *gauche* effects induced by axial ring substituents and an axial S=O group, in helping to define preferred conformations in this series [83]. Com-



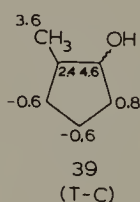
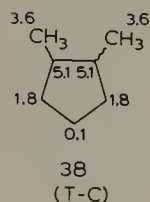
pound (36), for example, has been found to exist preponderantly (~95%) in the conformation shown.

The pattern of chemical shift differences in six-membered ring compounds is not altered grossly by the introduction of an sp^2 carbon. Thus, a comparison of $\Delta\delta$ values for *cis*- and *trans*-3,5-dimethylcyclohexanone (37) shows once again that substantial

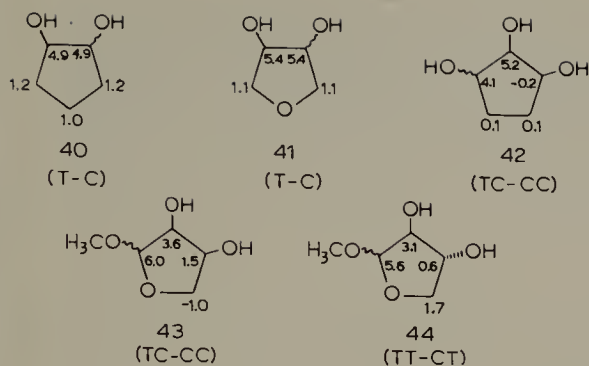


upfield shifts are associated with the species bearing the axial substituent [84]. Analogous data are available also for *cis*- and *trans*-3,4-dimethylcyclohexanone [84].

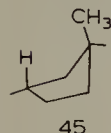
In derivatives of five-membered ring compounds, a close approach of substituent groups is accompanied by upfield shifts [44,85,86]. As shown below, there are relatively consistent shielding differences between 1,2-*cis*- and *trans* isomers of cyclopentane and tetrahydrofuran derivatives; *vic* substituents represented are CH₃/CH₃ (38),



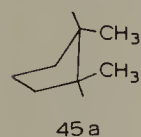
CH₃/OH (39), OH/OH (40), (41) and (42) and OH/OCH₃ (43) and (44). Clearly, in these compounds the effect is closely confined to the site of the interacting groups.



Because of relatively small energy differences between conformers in this series, the various envelope and twist forms interconvert readily. Consequently, accepting that a diaxial interaction between a substituent and a γ C—H (45) is energetically disfavoured,

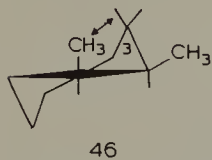


the only close correspondence to the situation in 6-membered rings is the *pseudo-gauche* interaction of *cis*-1,2 substituents (45a). Also consistent with this picture is the



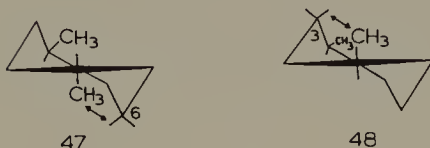
fact that no appreciable effects are observed when the substituents are in a 1,3-relationship^a.

Cycloheptane derivatives, like those of cyclopentane, can assume a number of favourable conformations (most likely twist chairs) in which substituents are mainly equatorial in character [87]. Not surprisingly then, differences in substituent effects between *cis* and *trans* cycloheptanes are smaller than in cyclohexane analogs [87]. Up-field shifts found for CH₃, C-1 (or C-2) and C-3 of the *cis*-1,2-dimethyl isomer as compared with the *trans* may originate in an important contribution by twist chair (46),



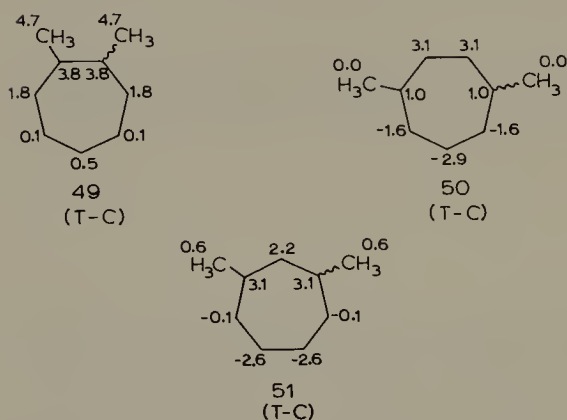
^a However, when the ring bears four substituents, as in cyclopentane tetrols and especially in aldofuranoses, small shielding influences attributable to 1,3-interactions are found (Section III.B).

which incorporates *gauche* interactions. By contrast, in various conformations regarded as favourable for the *trans* isomer, the methyls occupy only equatorial positions. Other γ -effects, such as the greater shielding of C-6 in the *trans*-1,4 compound than in the *cis*, may be accounted for by an interaction as in conformer (47); and of



C-3 of the *cis*-1,4 isomer, as depicted in (48). Similar relationships may be visualized for the 1,3-isomers [87].

Patterns of chemical shift differences between geometric isomers of this series (49), (50), (51) are quite distinctive as compared with examples described above. That is, a group of ^{13}C nuclei of one isomer of a pair (e.g., C-1 to C-4 of (50)) exhibits upfield shifts, while for the second isomer a different group (C-5 to C-7) is similarly affected. As a consequence, the overall differences in shielding ($\Sigma\Delta\delta$) for (50) and (51) are



small — only 4.2 p.p.m. for the 1,3 pair and 2.1 p.p.m. for the 1,4 — in comparison with a total of 21.5 p.p.m. for the 1,2 (49) (or a difference of ~ 30 p.p.m. for each *cis-trans* pair of dimethylcyclohexanes). It is worth noting, therefore, that the enthalpy difference [88] between *cis*- and *trans*-1,3- and -1,4-dimethylcycloheptanes is close to zero, whereas it is 0.7 kcal/mole for the 1,2 pair (and 1.8–1.9 kcal/mole for each geometric pair of dimethylcyclohexanes). Hence, as seen with substituted cyclohexanes and aldopyranoses, ^{13}C shielding changes in these alicyclic molecules reflect the destabilization introduced by vicinal and *gauche* types of interactions.

Shielding effects in spiro compounds attributable to steric factors are not unlike those encountered with simpler alicyclic compounds [89]. Compare, for example, the γ effects (in p.p.m.) illustrated in Fig. 4.

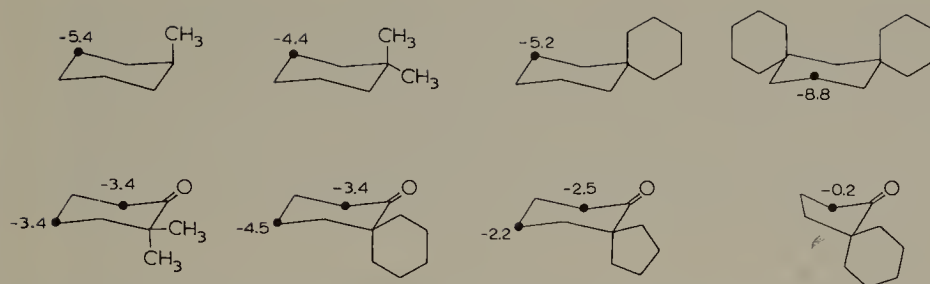


Fig. 4. γ -Gauche effect (upfield shift in p.p.m.) for the designated ^{13}C nucleus. (●), associated with axial substituents in spiro and related alicyclic compounds.

6. Arenes

Disubstituted benzenes show relatively small shielding changes attributable to steric interactions. The methyl carbons of *o*-xylene resonate upfield of those of *m*- and *p*-xylene by 1.0 and 1.5 p.p.m., respectively [11,90]. These differences account for most

TABLE 4
OVERALL DIFFERENCES IN SHIELDING ($\Sigma\Delta\delta$) BETWEEN ISOMERIC ARENES

Compound	$\Sigma\Delta\delta^a$ (p.p.m.)	$\Sigma\Delta\delta \text{ CH}_3$ (p.p.m.) ^a
<i>o</i> -Xylene		
<i>m</i> -Xylene	0.8	2.0
<i>p</i> -Xylene	3.8	3.0
<i>o</i> -Cresol		
<i>m</i> -Cresol	6.2	4.2
<i>p</i> -Cresol	4.5	3.9
1,2-Dimethoxybenzene		
1,3-Dimethoxybenzene	-3.0	-1.0
1,4-Dimethoxybenzene	0.6	0.6
1,2-Dimethylnaphthalene		
1,3-Dimethylnaphthalene	9.4	
1,4-Dimethylnaphthalene	-0.5 (-14.0) ^b	-1.6
1,5-Dimethylnaphthalene	1.1 (-12.4) ^b	-0.8
1,6-Dimethylnaphthalene	8.8	
1,7-Dimethylnaphthalene	9.7	
1,8-Dimethylnaphthalene	34.6	
2,3-Dimethylnaphthalene	13.5	
2,6-Dimethylnaphthalene	19.1 (5.6) ^b	3.0 ^b
2,7-Dimethylnaphthalene	17.6 (4.1) ^b	3.2 ^b

^a Values relative to those of 1,2-isomer in the series.

^b Values relative to those of 2,3-isomer in the series.

References pp. 229–235

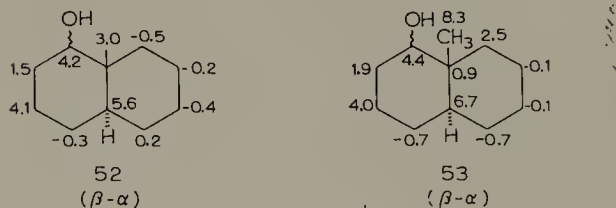
of the overall difference ($\Sigma\Delta\delta$) of a few p.p.m. between the isomers (Table 4). A similar effect is found on comparing *o*-, *m*- and *p*-cresol (Table 4); again $\Delta\delta$ for the methyl carbons accounts for most of the overall differences observed [11]. Perhaps because the methyl groups of 1,2-dimethoxybenzene are too remote from the site of the O—O interaction, their ^{13}C chemical shifts are essentially the same as for the 1,3- and 1,4-compounds [11]. In this latter series, furthermore, the overall shift differences are relatively small (Table 4).

A wider array of effects are possible with dimethylnaphthalenes [91]. As with xylenes, the methyl ^{13}C resonances of the 2,3-isomer are upfield of those of such isomers as the 2,6- or 2,7-isomer by 1.5 and 1.6 p.p.m., respectively. Once again, these differences (3.0 and 3.2 p.p.m.) account for most of the overall increase in shielding that differentiates the *ortho* isomer from others (Table 4). When a methyl group is in a position to interact with nuclei on the adjacent ring, larger upfield shifts are observed than those associated with *o*-methyls. In these circumstances, however, only a small part of the difference is evident in the chemical shifts of the methyl carbons themselves. Hence, the overall difference between the 1,4- or 1,5-isomer and the 2,3-isomer is ~ 13 p.p.m., although $\Delta\delta$ for the CH_3 group is relatively small (Table 4). The 1-methyl carbon experiences an especially strong shielding increase (by ~ 5 p.p.m.) — and, presumably, extra crowding — in the 1,2-isomer. Because of this additional upfield contribution the overall chemical shift difference value for the latter compound is close to those of the 1,4- and 1,5-isomers (Table 4). Values of $\Sigma\Delta\delta$ in the Table listed for other isomers form a series consistent with the effects already noted. Hence, the 2,6- and 2,7-isomers, the methyls of which cannot interact with another substituent nor with the adjacent ring possess, on the whole, nuclei that resonate furthest downfield. Nevertheless, 1,8-dimethylnaphthalene provides [91] a striking exception to these data, as discussed in Section III.B.

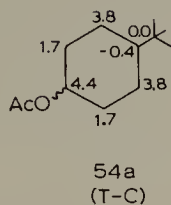
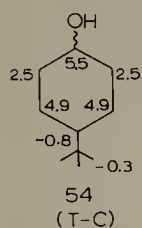
7. Fused and bridged ring compounds

The relative rigidity of bicyclic and polycyclic systems allows for an examination of steric influences on ^{13}C chemical shifts with the benefit of geometries that are more precisely defined than in monocyclic systems. It is reassuring, then, that the general characteristics described above are readily recognized in the spectra of fused and bridged ring compounds, although overall shielding patterns vary in distinctive ways.

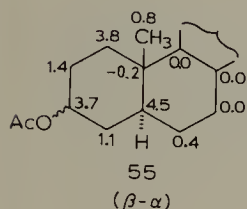
Chemical shift differences between α - and β -1-hydroxy-*trans*-decalins (52) and α - and β -1-hydroxy-9-methyl-*trans*-decalins (53) bear a strong resemblance to the pattern



for 4-*t*-butylcyclohexanol (54) [92]. Close analogies are also found [92,93] between

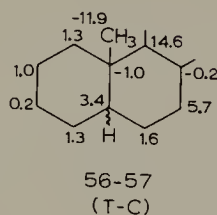
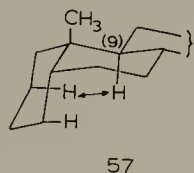
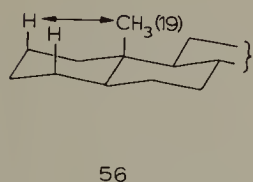


the patterns for *O*-acetates of the latter (54a) and cholestane-3- α - and β -yl acetates (55); (the C and D rings, not shown, are essentially unaffected). In all instances, there



are widespread upfield shifts associated with the presence of an axial, as compared with an equatorial, substituent. Similarly (although not illustrated here), introduction of the 9-methyl substituent (53) is accompanied by relatively uniform upfield shifts for several carbons in both cyclohexane rings, in comparison with the appropriate isomer in (52).

Changes in configuration at the ring juncture, i.e., as in *cis*- and *trans*-decalin and derivatives, or *cis*- and *trans*-isomerism involving the A/B ring fusion in steroids, leads to shielding differences that, again, are readily accounted for in similar terms [94-97].

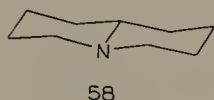


Thus, cholestane (*trans* A/B) (56) and coprostan (*cis* A/B) (57) differ as might be expected (56-57). The large net upfield shift of the CH₃-19 resonance^a can be attributed to the presence of 1,3-diaxial interactions in (56) that are absent in (57), whereas the reverse situation holds for CH-9. A knowledge of characteristics such as these has

^a This value (-11.9 p.p.m.) is close to that (-12.4 p.p.m.) for CH₃-9 of *cis*- and *trans*-9-methyldecalins, and about twice the value for *e*- and *a*-methylcyclohexanes.

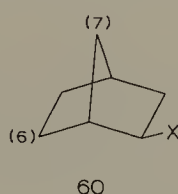
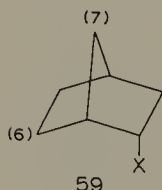
proven invaluable for stereochemical studies on a large array of steroids [93,95–98].

An examination of a variety of monomethyl derivatives of quinolizidine (58) has demonstrated [99] a close analogy between this series and *trans*-decalins. Allowing for

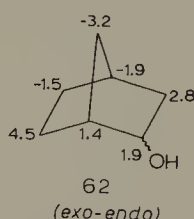
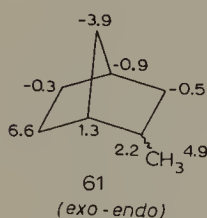


a characteristic chemical shift difference imposed by the bridgehead N in place of CH, chemical shift parameters for α, β and γ carbons were found to be nearly interchangeable with those of strictly related decalins. These findings provide a basis for ^{13}C spectral assignments in alkaloids bearing the quinolizidine structure.

Substituted bicyclo[2.2.1]heptanes (norbornanes) have been particularly extensively examined for possible steric effects [100,101]. A substituent at C-2 is 1,3-diaxially disposed towards CH-6 when *endo* (59) whereas it is quasi *gauche* towards CH-7 when *exo* (60). Since the orientational change is less marked with respect to the other car-



bons, the chemical shifts of C-6 and C-7 dominate the effects observed in this series (61), (62). With the shielding changes for C-6 and C-7 taking opposite directions, overall differences ($\Sigma\Delta\delta$) between isomers turn out to be much smaller than in the cyclohexane series. Values in p.p.m. for *exo* minus *endo* are as follows for a series of 2-substituents (including those in (61), (62)):



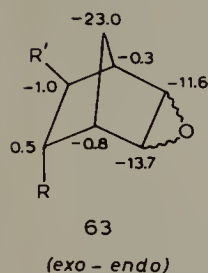
9.4(CH_3), 4.0(CH_2OH), 3.4(COOH), 3.0(COOCH_3), 5.3(NH_2), 4.0(OH), 4.4(OCH_3), 5.3(CN), 2.8(Br) and 5.5(Cl).

Although there is no apparent correspondence between these values and the conformational free energies of the substituents ^a, as for monosubstituted cyclohexanes, it is

^a Substituent free energies are not available, however, from measurements on norbornanes.

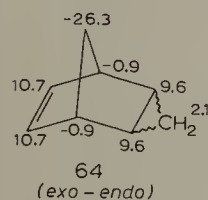
noteworthy that the *endo* substituent is always associated with a net *upfield* shift value.

Interesting effects are observed on fusion of a three-membered ring to the bicyclo-[2.2.1]heptane system [102]. An *exo*-oriented 5,6-epoxy ring induces large upfield shifts for C-5, 6 and 7 relative to those of the *endo*-isomer, as shown by the $\Delta\delta$ pattern (*exo* minus *endo*) in (63) ($R=\text{COOCH}_3$, $R'=\text{H}$); other carbons are affected little by this



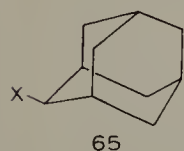
configurational change. Closely similar results are given when $R'=\text{CH}_2\text{Cl}$ in (63). Perhaps these increases in the shielding of the *exo* compound are attributable to a *quasi* eclipsing between the C-5, O, C-6 and C-1, C-7, C-4 arrays of nuclei (although on this basis upfield shifts might have been expected also for C-1 and C-4). In any event, interactions between the *endo* oxirane structure and the *endo* methoxycarbonyl group or CH_3 would appear to be of a lesser nature (see Section III.B).

Notably different results are obtained when a cyclopropyl ring is fused to norbornene in an *exo* or *endo* orientation ((64), *exo* minus *endo*) [103]. The bridgehead



carbon experiences a remarkably large increase in shielding when the cyclopropane ring is *exo*, similar to the results with the epoxide. Here, however, no mutual effect is evident for the carbons of the small ring. Rather, it appears as if, in the *endo* orientation, these cyclopropyl carbons are strongly influenced by a shielding interaction with the π system, which also results in upfield shifts for the olefinic carbons.

The spectra of 2-substituted adamantanes (65), (where X is CH_3 , OH, halogen,



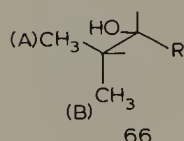
NH_2 , COOH or CN) contain two signals that may be assigned to carbons γ to the sub-

stituent [104]. The γ -effect exhibited by the signal further downfield averages 0 ± 1.3 p.p.m., whereas it is -6 ± 1.4 p.p.m. for the second signal. The latter is, accordingly, ascribed to the γ *syn* carbons and the downfield resonance to the γ *anti* carbons.

B. Downfield shifts associated with substituents in a 1,5 relationship. δ Effects

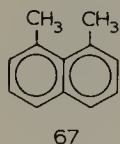
As mentioned earlier (p. 176), the substituent parameter for the δ carbon in alkanes is slightly deshielding: regression analysis of ^{13}C data for 23 linear and branched alkanes gives a value of $+0.3 (\pm 0.1)$ p.p.m. [105]. For acyclic alkenes, this “ δ effect” [91] is larger, being $+1.1 (\pm 0.3)$ p.p.m. for π carbons and $+0.7 (\pm 0.4)$ p.p.m. for σ carbons [106].

A related observation [107] concerns the methyl carbons of isopropyl alkyl carbinols, the isopropyl methyls of which are magnetically non-equivalent because of the asymmetric carbinol centre. In this series, (66) is regarded as the most favoured



rotamer. On changing R from methyl to ethyl, one of the isopropyl resonances moves upfield by ~ 0.7 p.p.m., and the other downfield by ~ 0.8 p.p.m. However, when these carbons are δ with respect to additional CH_3 groups (i.e., R = isopropyl or *tert*-butyl), one (possibly A) remains substantially unchanged whereas the other (B) becomes less shielded by 2.7 p.p.m. (for isopropyl) or 6.9 p.p.m. (for *tert*-butyl).

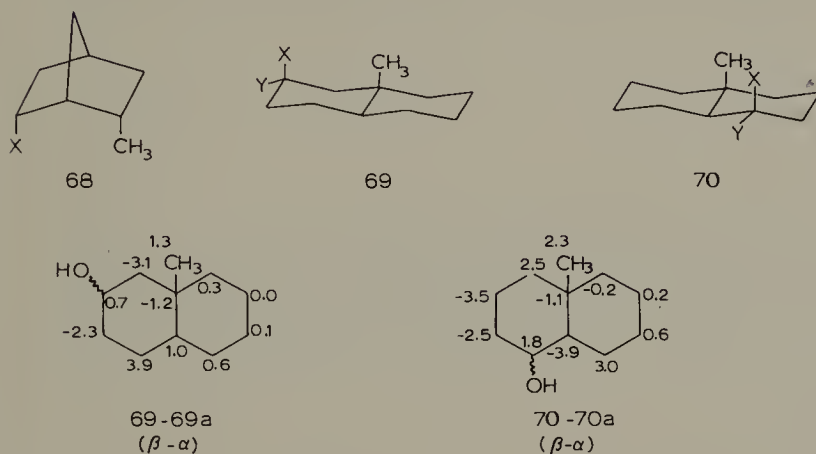
Accordingly a 1,5 (δ) $\text{CH}_3\text{—CH}_3$ relationship may lead to a downfield shift when these groups are suitably oriented with respect to each other. That a close spatial proximity is favourable for this kind of effect has been strikingly demonstrated with 1,8-dimethylnaphthalene (67) [91]. In (67), where the methyl groups most closely



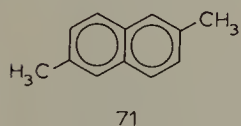
approach each other in a 1,5-relationship, the CH_3 resonances are at 25.9 p.p.m. whereas the chemical shifts of the methyl carbons of 1- or 2-methylnaphthalene are at 19.2 or 21.6 p.p.m., respectively.

A comparison of *endo*-2-methylnorbornane ((68), X=H) with *endo*-6-methyl-*endo*-2-norbornanol ((68), X=OH) shows [108] that the *syn* diaxial arrangement in the latter is associated with a 2.0 p.p.m. downfield shift for the CH_3 group. Similarly, for 9-methyl-*trans*-2- β - ((69), X=OH, Y=H) or 4- β -decalinol ((70), X=OH, Y=H), wherein

the CH_3 and OH groups are *syn* diaxial, the methyl ^{13}C is less shielded by 1.2 or 2.3 p.p.m., respectively, than that of its eq. ($\alpha\text{-OH}$) epimer ((69a) or (70a), $\text{X}=\text{H}$, $\text{Y}=\text{OH}$) [92].

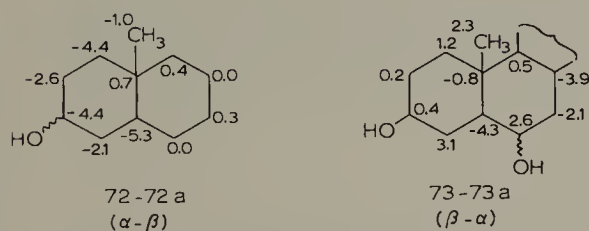


The δ effect in 1,8-dimethylnaphthalene (67) [91] appears to be confined largely to the CH_3 groups themselves, somewhat paralleling the upfield shifts associated with *ortho*-dimethyl derivatives (Section III.A.6). Thus, in comparison with an isomer that is not expected to incorporate upfield or downfield shifts, e.g., the 2,6 isomer (71),



the overall chemical shift difference ($\Sigma\Delta\delta$, (67)–(71)) is +12.7 p.p.m., of which +8.4 p.p.m. is contributed by the two CH_3 groups of (67).

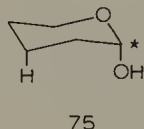
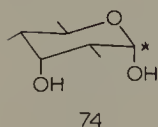
Deshielding changes are more widespread over the substituted decalin molecules [92], as can be seen from the $\Delta\delta$ patterns for (69–69a) and (70–70a), particularly in relation to the pattern for the 3-hydroxy analogs (72–72a) where only *gauche* ef-



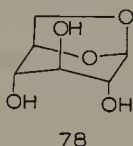
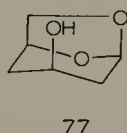
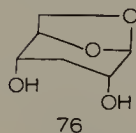
fects should apply. As a consequence, the corresponding $\Sigma\Delta\delta$ values for the first two pairs are only –6.5 and –0.8 p.p.m., whereas that for (72–72a) is –18.4 p.p.m., i.e.,

close to the "typical" $\Sigma\Delta\delta$ values of -19.1 p.p.m. for *cis*- and *trans*-4-*t*-butylcyclohexanol (Section III.A.3) ^a.

Syn-diaxial hydroxyl groups in pyranoses (74) have for long been associated with a small deshielding change in comparison with the 1,3 OH—H interaction (75) [69,70,



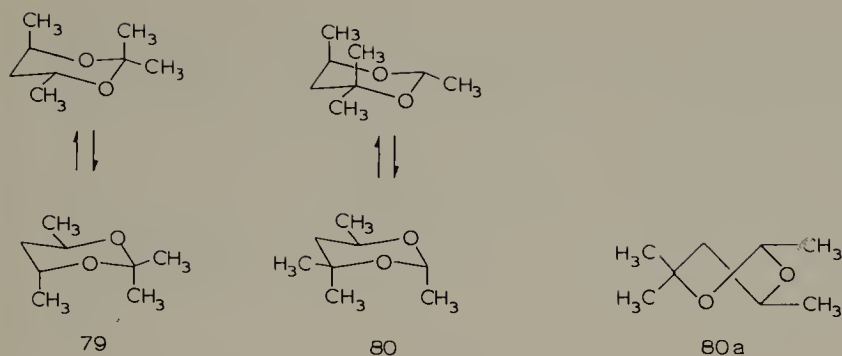
75]. Hence the latter is expected to induce an upfield shift averaging ~ 2.5 – 3.0 p.p.m. for the starred carbon, whereas the OH—OH interaction appears to cause an upfield shift of only about ~ 1.5 – 2.0 p.p.m. Although *syn*-diaxial hydroxyls in a 1,6-anhydro-pyranose (76) exhibit a similar effect, C-6 of these anhydrides experiences little if any



deshielding in the presence of an opposing OH-3 (77) [109]. However, the carbons of the all-axial isomer (1,6-anhydro-D-glucopyranose, (78)) are less shielded on the average than expected by comparison with the chemical shifts of other isomers in this series.

In striking contrast to the data for substituted 1,3-dioxanes described in Section III.C, which conform closely to the general pattern associated with *gauche* interactions, several 1,3-dioxanes containing methyl groups that are expected to be *syn*-diaxial show evidence of sterically induced downfield shifts. For example, C-2 and C-5 of (79) and (80) are less shielded by 1–4 p.p.m. than C-2 and C-5 of their 4,6- or 2,6-*cis*-isomers, and similar results have been obtained for related penta- and hexamethyl derivatives. These findings have been proposed [110] as evidence that such compounds as (79) and (80) exist to some extent in non-chair conformations, and confirmatory data are available for (80) from p.m.r. spectra favouring major contributions from twist-boat conformers (e.g., (80a)) [110].

^a A $\Delta\delta$ pattern closely mirroring that of (70–70a) is seen in (73–73a) for the A and B rings of cholestan-3 β -6 α - (73) and -6 β - (73a) diols (reading clockwise in this instance and counterclockwise in (70–70a)). Similarly, the $\Sigma\Delta\delta$ values for the steroidal pair is the same (-0.8 p.p.m.) as for (70–70a).



On this basis, the ^{13}C deshielding effects observed with the 1,3-dioxanes need not be attributed to *syn*-diaxial $\text{CH}_3\text{--CH}_3$ interactions because in (80a), for example, such interactions are relieved by the departure from a chair conformation. There is no evidence that decalinols (69) and (70) adopt non-chair conformations, but it has been pointed out [92] that *syn*-diaxial interactions in these compounds and related steroids may be reduced by skeletal twist. Distortions in molecular geometry might be a factor also in the 1,3 OH—OH type of relationship of (74), although they are less likely to be important in bicyclic systems such as (68) and (76) (as noted above, however, deshielding of C-6 is *not* evident in (77)). Different considerations may apply for 1,8-dimethylnaphthalene (67) — here it is possible that relief from steric strain is achieved by a coupling (“cog-wheel”) interplay between the rotating methyl groups [111].

It seems reasonable, therefore, to associate at least some of these examples of δ deshielding changes with induced alterations of molecular geometry arising from unfavourable 1,5-interactions between substituents. Although there is ample evidence that *gauche* interactions are accompanied by upfield shifts ^a, steric crowding *per se* obviously need not be ^b. However, those situations that are associated with downfield shifts are characterized also by a spatial relationship of substituents that is distinctly different from the *gauche* interaction. From the standpoint of stereochemical applications of ^{13}C n.m.r. spectroscopy, such a distinction is all important.

C. Upfield shifts associated with anti-periplanar heteroatoms

The eq. 5-methyl resonance of *trans*-2-*t*-butyl-5-methyl-1,3-dioxane (81) is at higher field (δ , 12.4 p.p.m.) than the ax. 5-methyl resonance of the *cis* epimer (82) (δ , 15.9



^a However, see the following Section for some exceptions.

^b By the same token, non-bonded interactions need not be destabilizing but, rather, are characterized by the overall balance between repulsive and attractive contributions [112,113].

TABLE 5

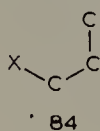
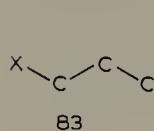
UPFIELD ^{13}C SHIFTS ASSOCIATED WITH THE INTRODUCTION OF AN ANTIPERIPLANAR HETEROATOM IN PLACE OF C OR H

	Carbon ^a	$\Delta\delta$
	$\text{CH}_3\text{-}3,5$	-5.9 ($\text{X}=\text{O}$) -3.6 ($\text{X}=\text{N}$) -0.4 ($\text{X}=\text{S}$)
	$\text{C-}3,5$	-2.3 ($\text{X}=\text{OH}$) -2.3 ($\text{X}=\text{NH}_3 + \text{Cl}^-$) -2.7 ($\text{X}=\text{F}$) -0.2 ($\text{X}=\text{Cl}$)
	$\text{CH}_3\text{-}5$	-7.3

^a Specified carbon is designated by solid circle.

p.p.m.) [114]. Since this situation is the converse of the γ -effect found for methylcyclohexanes (e.g., *trans*- and *cis*-1,4-dimethylcyclohexane), it has been proposed [115] that the *anti-periplanar* positioning of the oxygen atoms in (81) promotes an increase in shielding of the γ methyl ^{13}C nucleus ^a. Many other instances of this type of effect have now been recognized, some examples of which are listed in Table 5.

As a generalization, upfield shifts are found for the γ carbon in the conformational array (83) (as compared with (84)), when $\text{X}=\text{O}$, N , or F (compared with $\text{X}=\text{C}$ or H)

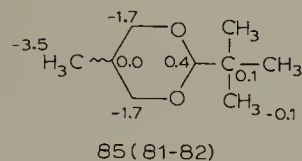


except when X is located at the bridge of a bicyclic compound. When X is Cl or S , no appreciable shifts are found — i.e., second row heteroatoms are effective, whereas those of the third row are not. It has been suggested that there is a partial π bond involvement of the free electron pair and a resulting transfer of charge from the heteroatom to the *trans* γ carbon. This mechanism appears to be favoured by the second row

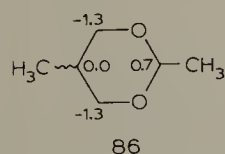
^a The original suggestion [114] that the ring O may have a deshielding effect on the *ax.* 5-methyl substituent is now considered less likely.

elements because of a shorter C—X bond and more compatible radial dimensions [115].

It is important to note that the presence of an axial substituent in (82), as well as in isomers of the compounds listed in Table 5, is associated with an upfield γ shift just as in the many other instances described above for *gauche* interactions. What distinguishes these geometric pairs is the apparent *increased* shielding in the presence of the *trans* heteroatom. Although the effect on γ carbons is especially pronounced, other carbons also appear to be influenced. Thus, the $\Delta\delta$ pattern (85) for the chemical shifts of (81) minus those of (82) suggests the possibility that the strong upfield shift of the eq. CH₃



resonance is also accompanied by lesser increases in shielding at C-4, -5 and -6. That is, an upfield shift for C-5 of (82) is to be expected normally because this atom bears an ax. CH₃; perhaps this is matched in (81) by a screening contribution to the shift of C-5, giving a net $\Delta\delta$ of ~ 0 p.p.m. Similarly, the shifts of C-4 and C-6 in (82), expected by analogy with other cyclic systems to be upfield of those in (81) by ~ 4 p.p.m. (see (35)), are only upfield by 1.7 p.p.m. Closely similar $\Delta\delta$ values are found for *trans*- and *cis*-2,5-dimethyl-1,3-dioxane (86), (data are not available for the methyl ¹³C resonances) [81]. Hence, it appears that all carbons of structure (83) (relative to those of



(84)) experience an increase in shielding, and that the effect is intensified as the distance from the heteroatom increases.

D. Shielding differences associated with the ring size of saturated cyclic compounds

Carbon-13 chemical shifts of alicyclic compounds [116–118], with the striking exception of cyclopropane, differ by only a few p.p.m.; a similar set of data are found [116–118] for saturated heterocycles (Table 6). The far upfield position of the three-membered ring signals has been attributed primarily to the diamagnetic contribution of a ring current.

Although the chemical shift of cyclopentane is slightly smaller than that of cyclohexane, a comparison of structural isomers in the two series shows that ¹³C nuclei of

TABLE 6

¹³C CHEMICAL SHIFTS FOR SATURATED CYCLIC COMPOUNDS OF DIFFERENT RING SIZE [116–118]

Ring size	Compound ^a		
	(CH ₂) _n	O(CH ₂) _n	CH ₃ N(CH ₂) _n
3	−2.6	39.7	28.7
4	23.3	72.8 (C-2,4)	57.9 (C-2,4)
		23.1 (C-3)	17.7 (C-3)
5	26.5	68.6 (C-2,5)	56.9 (C-2,5)
		26.7 (C-3,4)	24.6 (C-3,4)
6	27.8	69.7 (C-2,6)	57.4 (C-2,6)
		27.9 (C-3,5)	26.6 (C-3,5)
		25.1 (C-4)	26.6 (C-4)
7	29.0	—	—

^a In col. 2, *n* = ring size; in cols. 3 and 4, *n* = ring size − 1.

the five-membered ring compounds are less shielded on the average than those of the cyclohexanes. Thus the overall difference ($\Sigma\Delta\delta$) between the chemical shifts of methylcyclopentane (C₆H₁₂) and cyclohexane (C₆H₁₂) is 16.6 p.p.m. (Table 7), corresponding to an increase in the shielding of each cyclohexane carbon by 2.8 p.p.m. Similar results are obtained by comparing *trans*-1,3-dimethylcyclopentane with methyl-

TABLE 7

OVERALL DIFFERENCES ($\Sigma\Delta\delta$) IN THE SHIELDING OF FIVE- AND SIX-MEMBERED RING COMPOUNDS

Pair of structural isomers	$\Sigma\Delta\delta$ (p.p.m.) ^a
Methylcyclopentane — cyclohexane	16.6
<i>trans</i> -1,3-Dimethylcyclopentane — methylcyclohexane	19.3
<i>trans</i> -3-Methylcyclopentanol — cyclohexanol	38.2
Cycloheptane — methylcyclohexane	−5.2
Methylcycloheptane — <i>trans</i> -1,4-dimethylcyclohexane	−2.3
β -D-Fructofuranose — β -D-fructopyranose	25.9
Methyl β -D-xylofuranoside — methyl β -D-xylopyranoside	19.6
Methyl β -D-ribofuranoside — methyl β -D-ribopyranoside	18.8
Methyl α -D-glucofuranoside — methyl β -D-glucopyranoside	19.9
Methyl α -D-galactofuranoside — methyl β -D-galactopyranoside	37.3
Methyl α -D-mannofuranoside — methyl β -D-mannopyranoside	33.4

^a $\Sigma\delta$, five (or seven) membered ring isomer *minus* $\Sigma\delta$, six membered ring isomer.

cyclohexane, or *trans*-3-methylcyclopentanol with cyclohexanol (Table 7); here, the 1,3-substituents are not expected to introduce sterically-induced shifts, and only minor contributions can be expected from axial conformers of the cyclohexanes. On the same basis, the pairing of methylcyclohexane with cycloheptane, or of 1,4-*trans*-dimethylcyclohexane with methylcycloheptane, shows that there are relatively small differences in shielding.

If such comparisons seem to be somewhat artificial, the question becomes more realistic when furanose and pyranose forms of sugars are examined. For example, D-fructose in water consists of a mixture of two five- and two six-membered ring forms in thermodynamic equilibrium. Although the chemical shifts of tetrahydrofuran differ little from those of tetrahydropyran (Table 6) β -D-fructofuranose is readily distinguished from its six-membered ring counterpart in that almost all of its ^{13}C resonance signals are downfield of those corresponding carbons in the β -pyranose [71] — by 4.3 p.p.m. on the average (Table 7). Similarly, other comparisons of furanoses with pyranoses show [44,72,86] invariably that a large shielding change accompanies the inter-conversion of one ring form into the other (Table 7).

It has been suggested [43,44] that differences in diamagnetic contributions (σ^d) to the chemical shifts of five- and six-membered ring analogs may help to account for the more shielded ^{13}C nuclei of the latter. That is, calculations of σ^d suggest that the influence of the diamagnetic term on the chemical shifts of cyclohexane derivatives is substantially larger than for cyclopentane derivatives, although the difference is expected to vary with the particular envelope or twist conformation of the five-membered ring considered.

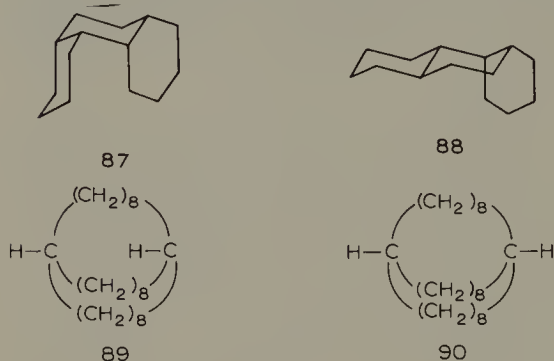
E. Other examples of stereochemical applications

The preceding sections deal with a number of cases in which use has been made of interrelationships between ^{13}C chemical shift differences and stereochemical changes. Many related examples may be cited, especially from such areas as natural products, synthetic polymers and conformational analysis. Reference is made here to several kinds of applications that have not specifically been dealt with above. Although, generally speaking, p.m.r. spectroscopy is also used for these purposes, in certain circumstances ^{13}C n.m.r. has unique value: either protons are lacking or, more commonly, the p.m.r. spectrum is too complex; in others, much larger differences in the shieldings of carbon than of protons allow for a greater precision of measurement. Aside from these advantages, the ^{13}C data have merit if only as a means of checking the p.m.r. results.

1. Molecular symmetry

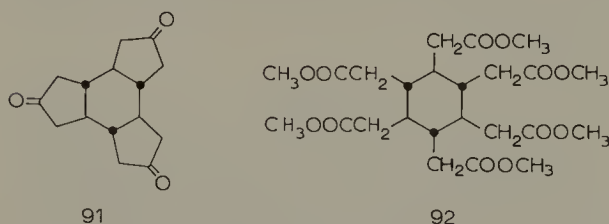
The differentiation of stereoisomers based on symmetry considerations is a valuable application for which ^{13}C n.m.r. is especially well-suited because, so often, all or most of the individual ^{13}C signals in a spectrum can be identified. Hence, *cis-syn-cis-per-*

hydrophenanthrene (87) is readily distinguished from its *trans-syn-cis* isomer (88) by the fact that the former produces a signal for each of the seven non-equivalent carbons in the molecule, whereas 12 out of a possible 14 peaks are resolved in the spectrum of the



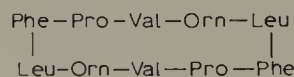
latter [119]. Analogously, two atropisomers of bicyclo[8.8.8]hexacosane are known, one of which produces five ^{13}C signals of appropriate intensity, and the other 10 peaks [120]. Since the latter obviously possesses the lower degree of symmetry it has been confidently assigned an “out, in” stereochemistry (89), and the other the “out, out” (90) (or “in, in”) configuration. As will be readily appreciated, proton spectra of compounds such as these, even at high frequencies, are exceedingly complex by comparison.

The result of what was designed to be a stereospecific synthesis of a chiral triketone (91) possessing D_3 symmetry was nicely checked by ^{13}C n.m.r. [121]. An all-*trans*



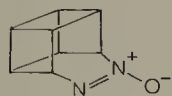
configuration for the immediate precursor of (91), i.e., cyclohexane-hexa-acetic acid (hexamethyl ester) (92), was confirmed by the fact that the spectrum of (92) consisted of only four signals [δ , 172.9(C=O); 51.6(OCH₃); 42.0(CH₂); 35.8(CH)]. Analogously, following the cyclization step (92) \rightarrow (91), the spectrum of product (91) consisted of only three signals (δ , 214.8(C=O), 48.2(CH₂); 43.5(CH)], showing that the all-*trans* configuration has been retained [121].

Gramicidin-S (93), a cyclic polypeptide is composed of five pairs of amino acid residues, and the fact that its ^{13}C spectrum contains peaks for only five carbonyl, five



α - and five β -carbons is clear evidence that there are two identical sequences of amino acids, and hence a plane of symmetry in the molecule [122].

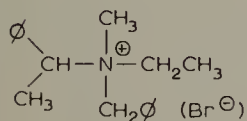
An attempted synthesis of the *N*-oxy derivative of diazabasketene (94) afforded a product that appeared to have a symmetrical structure, because its p.m.r. spectrum



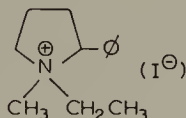
94

consisted of only two broad singlets. However, molecular asymmetry in the structure expected ((94)) was confirmed subsequently by the observation of five separately resolved ^{13}C resonances [123].

Detection of the magnetic non-equivalence of protons situated close to an asymmetric centre is feasible, but the chemical shift differences may be small, and possibly inadequate for such applications as the determination of the optical purity of diastereomers. ^{13}C n.m.r. should be advantageous in such circumstances because of its high sensitivity in distinguishing between different stereochemical environments. An example of the large chemical shift differences attainable has been cited above: i.e., the methyl ^{13}C resonances of the isopropyl group in (66) are 2.7 p.p.m. apart, and they are 7.2 p.p.m. apart in $(\text{CH}_3)_2\text{CHCH}(\text{CH}_3)\text{C}(\text{CH}_3)_3$ [107]. In a recent application [124], the ratio of diastereomeric forms of various quaternary ammonium compounds (e.g., (95) and (96)), has been readily determined. An important aspect of this applica-



(95)

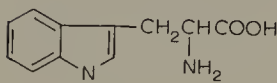


(96)

tion lay in the fact that the individual diastereomers were identified by their ^{13}C chemical shift patterns (i.e., the more shielded carbons were ascribable to those expected to experience a *gauche* type of interaction).

In macromolecules, the individual building units may be subjected to different stereochemical environments, as described above for synthetic polymers (Section III. A.4). Proteins commonly contain many residues of a given amino acid, situated in non-equivalent sites due to differences in the nature of the adjacent amino acids or to variations in chain folding. The associated chemical shift differences have been found sufficiently large in some instances to resolve single carbon resonances of the individual residues of the amino acid [125]. For example, native hen egg-white lysozyme contains six residues of tryptophan (97), and although there is a total of 613 carbons in the protein, its ^{13}C spectrum exhibits five well resolved peaks due to the six γ carbons of the tryp-

tophans (i.e., only two have the same chemical shift). An analytical capacity of such sophistication, naturally, is finding wide usage in chemical and biological studies on enzymes, and proteins in general ^a. For the same reason, ¹³C n.m.r. spectroscopy is of

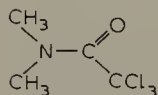


97

great value for the structural elucidation of other macromolecules, such as polysaccharides [126–129].

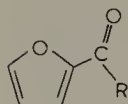
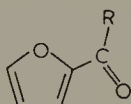
2. Dynamic systems

Non-equivalence arising from restricted rotation about a bond is sometimes readily detectable, as noted for *N,N*-dimethylformamide (22) (Section III.A.4). The experimental temperature, however, is an important factor. Thus, *N,N*-dimethyltrichloroacetamide (98) produces a single methyl resonance at ambient temperature, but two clearly separated signals attributable to the *syn* and *anti* forms are observed at 5° [130]. By



98

using such measurements the free energy of activation that characterizes this rotational barrier may be calculated from the temperature at which the signals coalesce (“coalescence temperature”) [131]. In applications of this kind, the G^\ddagger values can be more precise than those given by p.m.r. data because of the greater ¹³C, than ¹H, chemical shift differences attainable and the larger number of signals that may be observed. Such advantages have been cited [132] in the study of rotational barriers of heterocyclic aldehydes and ketones (99) and (100): in the vicinity of 160–180°K, there were two complete sets of readily identifiable signals — some pairs as much as 10 p.p.m.

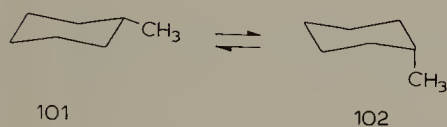
99 (*cis*)100 (*trans*)

^a For this type of application, it is desirable to have especially high sensitivity; one practical means of attaining it is through the use of unusually large n.m.r. tubes, i.e., 20 mm in diameter rather than the more conventional 10–12 mm tube [125].

apart — permitting several concurrent measurements of the coalescence temperature to be made with convenience ^a.

Related applications are those involving the interconversion of conformers of alicyclic compounds. Although ¹H studies have been — and are — invaluable in this context, they frequently must make use of specifically deuterated molecules in order to simplify the spectra. This is not usually necessary for ¹³C studies. Equilibrium and free energy parameters have been estimated from the time-average ¹³C chemical shifts for rapidly interconverting forms of cyclohexane derivatives, by reference to the chemical shifts of an appropriate model compound that is expected to exist essentially in only one chair conformation [134].

Alternatively, these thermodynamic data are available — and probably more reliable — from direct observations at low temperatures [34]. For example, the ¹³C spectrum of methylcyclohexane is resolved at -110° into signals ascribable to a 100 : 1 mixture of eq. and ax. methylcyclohexane ((101) and (102), respectively). Furthermore, measurements of coalescence temperatures in such experiments have afforded activation



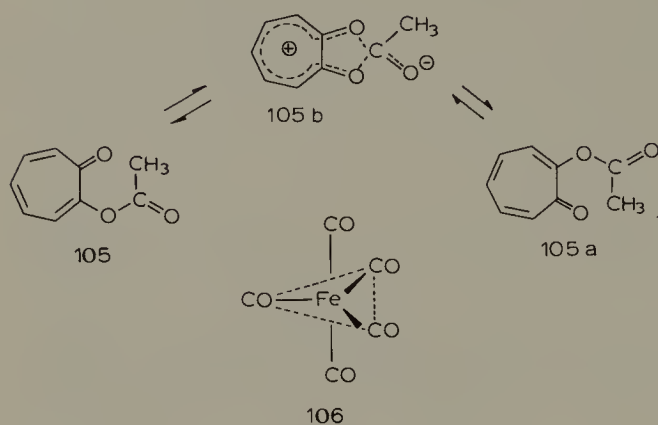
parameters for ring inversion in a variety of cyclohexane derivatives [135,136], and also for conformational barriers in ring systems as large as cyclotetradecane [137]. A recent examination [138] of cycloheptene oxide indicates that its lowest energy conformation should be of the chair type, i.e., (103) and (104) (3 : 2), and that the free energy of activation for the interconversion of (103) \rightarrow (104) is $7.5 \text{ kcal mol}^{-1}$ at the coalescence temperature (-116°).



Evidence for migration of the *O*-acetyl group of tropolone acetate (105) has been provided [139] by variable temperature studies. (The ¹H spectra were either deceptively simple or too complex for analysis). At 50° , only three ¹³C absorption signals are obtained, whereas at -70° the spectrum clearly accounted for each of the nine carbons. From the manner in which the ¹³C signals approach coalescence at intermediate temperatures, it has been proposed that an equilibrium exists between (105) and (105a), mediated by a species such as (105b).

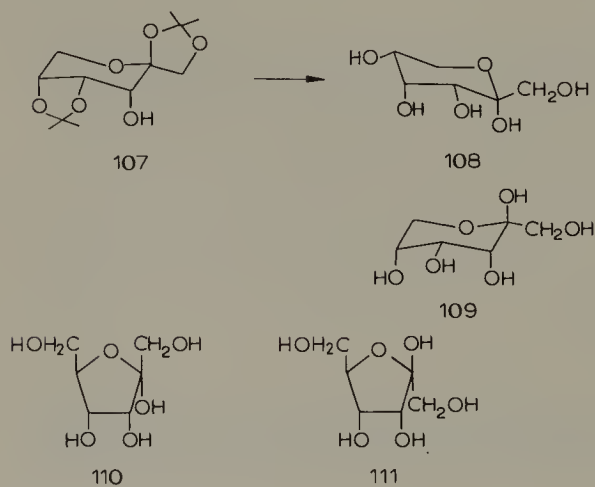
^a Similarly, for the determination of kinetic parameters in dynamic systems by “line shape” analysis [133], the availability of several (sometimes many) distinct signals in a ¹³C spectrum can enhance the reliability of such analyses.

It appears that some transformations occur at rates that are too rapid for practical detection by the n.m.r. method. Although it is generally accepted that iron pentacarbonyl (106) exists in a trigonal bipyramidal form, and hence should incorporate two



distinct carbonyl environments, its ^{13}C spectrum consists of only a single peak, even at -63°C [140,141]. It appears certain that this arises as a result of rapid intramolecular exchange of the $\text{C}=\text{O}$ moieties.

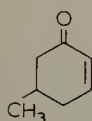
At the other extreme, when rates of interconversion between equilibrating species are relatively slow on the n.m.r. time scale, the spectrum at ambient temperatures is that of the individual components. ^{13}C n.m.r. spectroscopy then constitutes a direct means for detecting the number of species present and giving their proportions. The tautomeric equilibria of reducing sugars can be examined in this way [5,68,71], and though ^1H data for anomeric protons of aldoses have long been of immense value for this purpose, ^{13}C n.m.r. also permits a study of the equilibria of such compounds as ketoses [71–74], which do not contain anomeric protons. For instance, until recently virtually nothing was known in this context about D-psicose, a naturally-occurring 2-hexulose that is not known in a crystalline modification. The ^{13}C spectrum of the



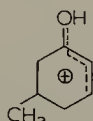
sugar in water prepared by mild acid hydrolysis of a suitable derivative (107), shows that it exists at equilibrium as a 2.5 : 2.5 : 4 : 1 mixture of α -pyranose (108), β -pyranose (109), α -furanose (110) and β -furanose (111). Information about preferred conformations of these various isomers has also been obtained from the ^{13}C spectrum, owing largely to the fact that some 20 individual signals, out of a possible 24, were distinguishable [72–74].

3. Charged species

A very active area of application deals with the characterization of organic ions. Thus, for example there are substantial deshielding changes that accompany the protonation of a carbonyl compound, and these are associated with the development of a more positive charge on the appropriate carbons [142]. For the α,β -unsaturated ketone, (112), the large downfield shift produced for C-3 when the compound is dissolved in $\text{HSO}_3\text{F-SbF}_3$, is estimated to be equivalent to 0.3 units of positive charge. By contrast, $\Delta\delta$ is very small for C-2 in this, as well as other α,β -unsaturated carbonyl



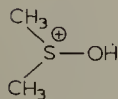
112



113

compounds, indicating that C-2 in such systems always bears little, if any, positive charge. In general, the results suggest that these ions are of a hydroxy allyl cationic nature (113).

Data on ethers, sulfides and ketones in sulfuric or trifluoroacetic acid show [143] that protonation causes a downfield shift of the resonance due to the carbon α to the protonation site, whereas those of the β and γ carbons shift upfield. According to the spectra of dimethyl- and diethyl-sulfoxides, the methyl and methylene carbons experience an increase in shielding, which suggests that these carbons are not α to the site of protonation. That is, the proton appears to reside on oxygen (114) (in accord with i.r. and acid–base equilibrium evidence), whereas ^1H data had been interpreted in

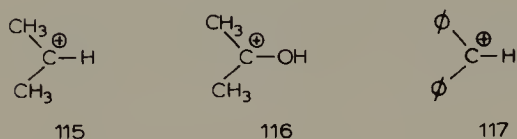


114

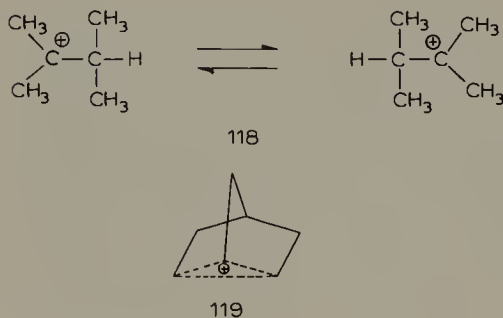
terms of a protonation of sulfur. Similarly, there has been ambiguity about the site of protonation of amides. ^1H data have suggested that *N,N*-dimethylformamide is predominantly *N*-protonated, or both *N* and *O*-protonated, because the *N*-methyl proton signals coalesce at intermediate acidities. However, the observation of two distinct methyl signals in the ^{13}C spectrum of *N,N*-dimethylformamide over the range 0–100%

sulfuric acid shows clearly that the predominant protonated form at all acidities is the *O*-protonated amide [144]. In amino acids and peptides, protonation of the amino group, and ionization of the carboxyl group, exhibit highly characteristic pH-induced ^{13}C chemical shift changes [145].

Carbocations have received a great deal of attention, as described in a recent review [146]. In this field, ^{13}C n.m.r. has been found frequently to be more informative than p.m.r., but on the whole less definitive than ESCA spectroscopy. The various types of cations show a wide range of chemical shifts, which generally accord well with expectation based on chemical experience and theoretical considerations of charge density distributions. Thus, the extreme low field resonance (δ , 320 p.p.m.) for the central carbon of the isopropyl ion (115) is taken as evidence that there can be little σ participation.



By contrast, the corresponding ^{13}C signals for ions such as (116) and (117) are at 250 p.p.m. and 200 p.p.m., respectively, consistent with *n*- and π -delocation processes that are anticipated with these species. For the dimethylisopropyl cation, the C-2 chemical shift of 198 p.p.m. has been interpreted in terms of a rapidly equilibrating pair (118), whereas the relatively upfield position (δ , 93 p.p.m.) and equivalence of signals for C-1,



-2 and -6 of the norbornyl cation are strong evidence in support of the view that this is a non-classical carbonium ion (119) [146].

IV. STEREOCHEMICAL ASPECTS OF ^{13}C COUPLING CONSTANTS

A. Measurement of $^{13}\text{C}-^1\text{H}$ coupling

As mentioned earlier, many observations on coupling between ^{13}C and ^1H (and, indeed, other magnetic nuclei) were reported several years before ^{13}C n.m.r. spectro-

scopy became an area of widespread interest. These early measurements utilized the ^{13}C satellite signals of ^1H spectra, i.e., weak absorption lines produced by coupling of protons with the 1.1% population of ^{13}C nuclei in the molecule. To offset the satellite's low intensity and the problem of an excessively complex splitting pattern, most of the spectra were of neat liquids and/or relatively simple molecules. ^{13}C -enrichment (to a level of 90% at present), although costly and laborious, has greatly facilitated studies of more complex molecules by giving rise to much stronger satellite signals in the ^1H spectrum, and currently is being used with increasing frequency [147]. With the advent of ^{13}C n.m.r. spectrometers, coupling information has become available from measurements of the splitting of ^{13}C resonances. Recent improvements in instrumentation and methodology – notably “gated” decoupling [30] – make this approach particularly attractive. Signal overlap, by obscuring the splitting pattern, can be a major problem in any measurement of coupling, although it is likely to be less serious with proton spectra of ^{13}C -enriched compounds than with ^1H -coupled ^{13}C spectra.

A ^{13}C nucleus exhibits coupling with a proton to which it is directly bonded ($^1J_{\text{C-H}}$), a proton from which it is separated by two bonds ($^2J_{\text{C-H}}$, “geminal”), or three bonds ($^3J_{\text{C-H}}$, vicinal); relatively few examples of longer range interactions are known. Values of 1J (commonly ~ 150 Hz) are very much larger than the others, and hence, with adequate resolution, are measurable with relative ease. By way of contrast, 2J and 3J for sp^3 carbons are normally smaller than 7–8 Hz, and may be difficult to detect, especially in spectra representing a three or four spin system. Primarily for this reason, the literature on geminal and vicinal coupling is not extensive. Nevertheless, because the magnitude of all of these couplings is dependent on molecular geometry, each category of $J_{\text{C-H}}$ merits examination as a source of valuable stereochemical information.

The sign of 1J is generally accepted to be positive [18]. Both negative and positive signs are found among values for 2J , whereas it appears that 3J is more likely to be positive in sign [148]. In most instances, the sign of coupling has not been determined, owing largely to experimental difficulties, and in some cases has been assumed by analogy. The two methods used most widely for sign determination deal with ^{13}C satellite spectra, and involve either the matching of the observed with computed spectra, or double resonance experiments [149]. Two more recently developed approaches – selective population inversion [150] and selective population transfer [151] – utilize the ^{13}C spectrum itself, and the sign of J may sometimes be obtained in the analysis of higher-order coupled ^{13}C spectra [28].

B. Coupling between directly-bonded ^{13}C and ^1H ($^1J_{\text{C-H}}$)

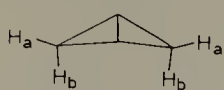
Values of 1J vary widely, e.g., ranging from 125 Hz for methane, through 156 Hz for ethane, to 249 Hz for acetylene [152], and generally are found to increase with a decrease in the magnetic shielding of the carbon [153]. These characteristics have led

to an interest in the 1J coupling parameter as a possible index of hybridization, a possibility that receives support on theoretical grounds [18,154,155]. Hence, studies such as those on carbocations cited above (Section III.E.3) have utilized not only ^{13}C chemical shifts but also ^{13}C – ^1H couplings: e.g. the central carbon of the isopropyl cation (115) exhibits $^1J = 169$ Hz which, by analogy with ethylene, is consistent with sp^2 hybridization [146].

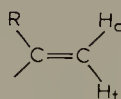
1J coupling may be affected strongly by other factors as well. Electronegative substituents induce a large increase as illustrated by the following series: CH_4 (125 Hz), CH_3Cl (150 Hz), CH_2Cl_2 (178 Hz) and CHCl_3 (209 Hz) [17,156]. Undoubtedly, the hybridization state of carbon in these compounds is not the same, but changes in the effective nuclear charge on carbon [157] or in the average excitation energy [158] are more likely to be the main source of these variations.

Although, as in studies on ^{13}C chemical shifts, it is difficult to apportion the contribution to 1J of a steric, as opposed to an electronic, influence, one may again examine in an empirical manner changes in the coupling constant that accompany a change in geometry. In this connection, even the relatively few data now available appear to show some inconsistencies.

Steric perturbations would be expected to affect 1J by altering the electron distribution in the ^{13}C – ^1H bond. A possible example is found [159] in bicyclo[1.1.0]butane (120), for which $^1J_{\text{C-Ha}}$ is 153 Hz and $^1J_{\text{C-Hb}}$, 169 Hz. Steric compression, which should be acute for the C–Hb bond, may contribute to its relatively large coupling constant.



120

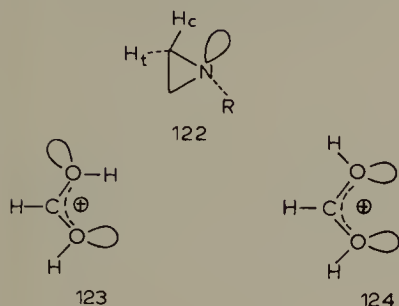


121

Results for alkenes are rather diverse. In 1-propene ((121), $\text{R}=\text{CH}_3$) the *cis* proton couples more strongly with C-1 (162.6 Hz) than does the *trans* proton (160.6 Hz) [160], whereas in 3,3-dimethyl-1-butene ((121), $\text{R}=t\text{-butyl}$) the situation is reversed: $^1J_{\text{C-Hc}} = 153.3$ Hz and $^1J_{\text{C-Ht}} = 157.2$ Hz [161]. As the halogen of vinyl halides ((121), $\text{R}=\text{halogen}$) is varied from F through I, opposite trends in coupling are observed [162–164]. That is, $^1J_{\text{C-Hc}}$ increases – 159.2, 162.6, 163.6 and 164.1 Hz – whereas $^1J_{\text{C-Ht}}$ decreases – 162.2, 160.3, 160.0 and 159.2 Hz. In such systems, of course, there is the possibility of polar influences being transmitted through the π bond, as well as of differences in geometric relationship between the C–H bond and the vinyl substituent, R.

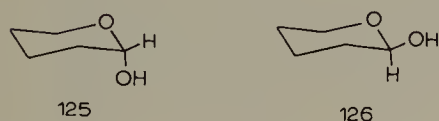
A rather consistent type of effect is observed when the orientation of the C–H bond is viewed with respect to adjacent non-bonding electrons. The question of the shape of lone pairs is itself a controversial one, and is the object of much theoretical concern [113,165]. Organic chemists usually represent lone pairs of electrons as lobes resembling sp^3 orbitals, and for the purpose of the present empirical treatment lone pairs are

depicted in this way. Accordingly, it has been noted for (122) that the C—H bond *syn* with respect to the lone pair has a larger 1J coupling (171 Hz) than the *trans* C—H bond (161 Hz) [166]. A comparable situation is found [167] with oxonium ions such

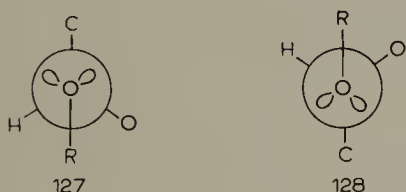


as (123) and (124), for which the respective 1J values are 244.8 Hz (*syn* lone pair) and 235.8 Hz (*trans*).

In the sugar series, there are many related examples. One-bond coupling at the anomeric centre of α and β -D-glucose (partial structures (125) and (126)), is 169 Hz and 161 Hz, respectively [68]. The equatorial C—H bond of the α -anomer may be re-



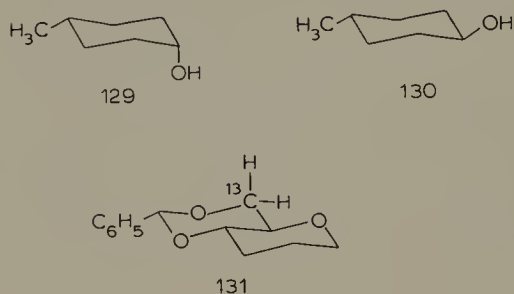
garded as *gauche* with respect to the two lone pairs of the ring O, whereas the axial β C—H bears one *gauche* and one *trans* relationship. This difference of close to 10 Hz is found consistently for a large number of anomeric pairs of sugars and derivatives [68,168–170], as well as for oligo- and polysaccharides [171]. Hence 1J can be useful in determining anomeric configuration, especially in the *D-manno* series where $^3J_{\text{H-H}}$ and chemical shifts are relatively uninformative. The disposition of the lone pairs on O-1, as in (127) and (128), also should have a bearing on these coupling constants. However, this might be a relatively constant factor for each anomeric configuration



because, unless there are gross differences in the nature of R, the rotamer population should be fairly constant for a given class of anomer (see p. 216).

That these α,β differences in 1J are not due to a factor such as greater steric crowding of the axial 1-OH substituent in (125) as compared with (126), is indicated by the

much smaller Δ^1J for *cis*- and *trans*-4-methylcyclohexanol ((129)^a and (130), respectively): 1J is 143 Hz for (129) and 140 Hz for (130) [169]. By contrast, coupling between C-6 of (131) and its appended equatorial and axial protons is 151 Hz and 141



Hz, respectively; i.e., $\Delta^1J \simeq \Delta^1J$ for anomeric sugars. Hence, it is noteworthy that in (131), as in the sugars, the orientational relationship between the eq. C—H bond and the oxygen lone pairs is *gauche, gauche*, whereas it is *gauche, trans* for the ax. C—H bond [169].

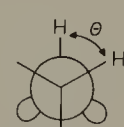
A calculation of the possible influence of the orientation of lone pair electrons on $^1J_{C-H}$, taking methanol as a model, is in qualitative agreement with the observations just discussed [172]. By using the CNDO/2 method and considering only the Fermi contact term, the results of Table 8 have been obtained. On this basis, it is indeed to be expected that coupling between directly bonded ^{13}C and 1H should increase as the lone pair electrons approach the $^{13}C-^1H$ bond.

C. Two bond $^{13}C-^1H$ coupling ($^2J_{C-H}$)

The nature of the two bond coupling pathway that links a ^{13}C nucleus with a proton can have a strong influence on the magnitude and sign of the coupling constant. The 2J value for ethane is -4.8 Hz, and is -2.4 Hz for ethylene [152]. In propyne or

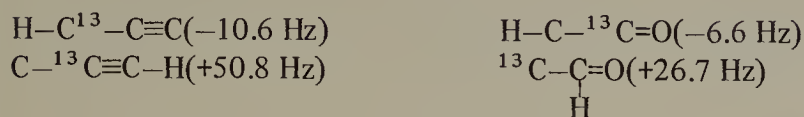
TABLE 8

INFLUENCE ON $^1J_{C-H}$ OF THE ORIENTATION OF THE OXYGEN LONE PAIR ELECTRONS RELATIVE TO THE C—H BOND. CALCULATIONS FOR CH_3OH

	θ°	$^1J_{C-H}$ (Hz)
	0	162.3
	60	165.0
	120	169.5
	180	171.3

^a The e CH_3 , a OH conformer is preponderant.

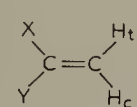
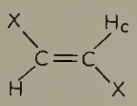
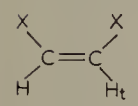
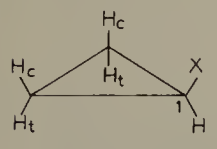
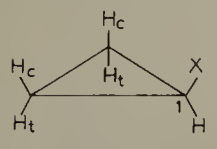
acetyldehyde, two different coupling pathways exist and are characterized by strikingly different values of 2J [173,174]:



Stereochemical changes also may be associated with a change in the sign of 2J coupling. Some notably consistent effects have been observed in this regard [162, 175, 176]. For a variety of olefin derivatives, coupling between the substituted carbon and a *cis* proton is negative (or less positive) whereas the *trans* proton exhibits positive coupling. Some representative data, given in Table 9, suggest that a halogen atom *anti* with respect to the coupling proton makes a positive contribution to 2J . A similar relationship may be cited [177] for bromo-, iodo- and chlorocyclopropane (Table 9), and this is emphasized by the fact that when the halogen is not located on the coupling carbon, 2J is unaffected.

TABLE 9

VARIATIONS IN $^2J_{\text{C-H}}$ ASSOCIATED WITH CHANGES IN THE CONFIGURATION OF SUBSTITUENTS RELATIVE TO THE COUPLING PATHWAY

	X	Y	2J (Hz)	
			C-H _c	C-H _t
	H	Br	-8.5	+7.5
	H	Cl	-8.3	+7.1
	phenyl	Cl	-6.3	+5.6
	H	CN	-4.4	+0.3
	Br	-	-0.4	-
	Cl	-	+0.3	-
	Br	-	-	+14.7
	Cl	-	-	+15.4
 (C-1, H-2)	Br	-	-5.4	-1.6
	Cl	-	-5.1	-1.2
	I	-	-5.5	-2.3
 (C-2, H-3)	Br	-	-2.9	-2.9
	Cl	-	-2.8	-3.1
	I	-	-2.9	-2.8

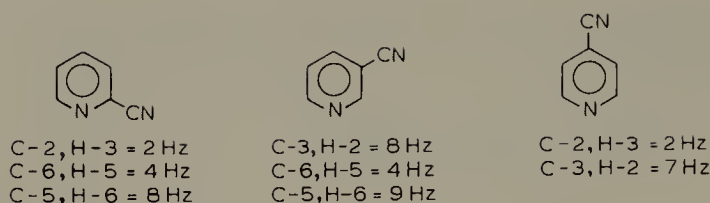
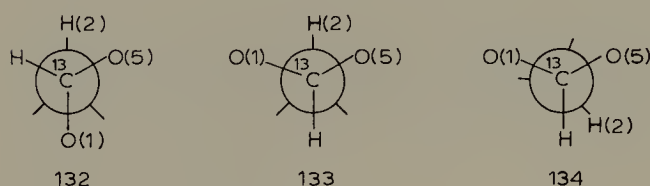


Fig. 5. Variations in ${}^2J_{\text{C-H}}$ (Hz) for 2-, 3- and 4-cyanopyridine.

Other examples of the importance of the disposition of an electro-negative atom relative to the coupling pathway are provided [178] by 2J coupling in cyanopyridines (Fig. 5). Hence 2J is either 2–4 Hz or 7–9 (of unknown sign) depending on the location of the nitrogen atom on the path of interaction between the ${}^{13}\text{C}$ and ${}^1\text{H}$. When the nitrogen is more remote from the coupling nuclei, 2J is close to that (+1.0 Hz) for benzene; i.e., in 2-, 3- and 4-cyanopyridine almost all contributions of 2J coupling involving C-3, C-4 or C-5 with H-3, H-4 or H-5 give rise to splittings of <1 Hz.

Two bond coupling between C-1 and H-2 of α and β -D-glucopyranose [68], as projected in (132) and (133), respectively, differs notably: 2J for the former is <1 Hz



for the latter -5.7 Hz [179]. The arrangement of the corresponding group of nuclei in 1,2 : 5,6-di-*O*-isopropylidene- α -D-glucofuranose is close to that shown in (134), for which the corresponding value of 2J is $+5.5$ Hz. These differences could be accounted for [179] if there is a positive contribution to 2J when an oxygen is *anti* to the coupled proton, and a negative contribution when they have a *gauche* relationship. That is, O-1 and O-5 are *gauche, gauche* with respect to H-2 in (133) (${}^2J = -5.7$ Hz), they are *gauche, anti* in 132 (${}^2J \sim 0$ Hz), and approach an *anti-clinal, anti-clinal* situation in (134) (${}^2J = +5.5$ Hz). Hence there appear to be close analogies between these orientation effects and those found with vinyl and cyclopropyl halides.

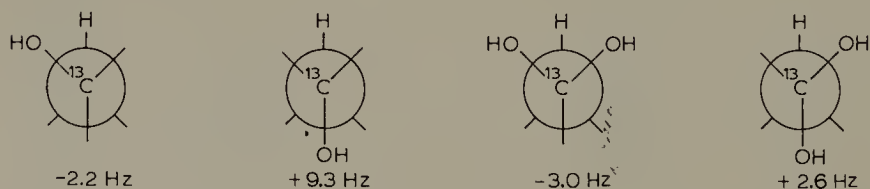


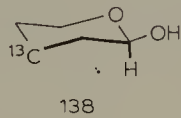
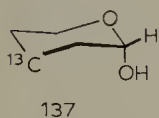
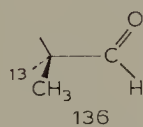
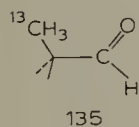
Fig. 6. Calculated values of ${}^2J_{\text{C-H}}$ (Hz) for ethanol and 1,1-ethanediol illustrating differences associated with various orientations of hydroxyl groups relative to the coupling pathway.

Calculations [179,180] of the sign and relative magnitude of ${}^2J_{\text{C-H}}$ for ethanol and 1,1-ethanediol are in qualitative accord with the experimental data for the carbohydrate molecules. Hence, the possibility that an *anti* oxygen makes a positive contribution, and a *gauche* oxygen a negative one, are clearly indicated by the calculated data (Fig. 6).

D. Coupling between vicinal ${}^{13}\text{C}$ and ${}^1\text{H}$ (${}^3J_{\text{C-H}}$)

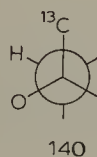
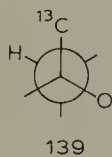
From the standpoint of stereochemical effects, spin-spin interactions between ${}^{13}\text{C}$ and ${}^1\text{H}$ nuclei separated by three bonds show much of the character of ${}^1\text{H}$ – ${}^1\text{H}$ coupling [147].

Carbon-3 of propanal is coupled to the formyl proton by 2.4 Hz, and it has been estimated that this 3J value consists of contributions of 3.5 Hz due to *anti* orientation (135) of the two nuclei and of 0.2 Hz for a *gauche* orientation (136) [181]. Experimentally, a difference of this general magnitude between *anti* and *gauche* ${}^{13}\text{C}$ – ${}^1\text{H}$



couplings — i.e., 5–6 Hz and 1–2 Hz, respectively — has been observed [68,168] in the spectra of α - and β -D-glucose ((137) and (138), partial structures). Other 3J data obtained with a variety of carbohydrate derivatives [44,168] and nucleosides [182, 183] show that the coupling between ${}^{13}\text{C}$ and ${}^1\text{H}$ is related to the dihedral (torsional) angle formed by the three bonds separating these nuclei — i.e., the relationship is analogous to that of the familiar Karplus curve [184,185] for protons; calculations of 3J [44,186] are in accord with these findings.

As is already well known for vicinal ${}^1\text{H}$ – ${}^1\text{H}$ coupling, a number of factors other than dihedral angle can contribute to the absolute value of ${}^3J_{\text{C-H}}$. These include such variables as the orientation of electronegative atoms appended to the interaction pathway: hence an *antiperiplanar* oxygen as in (139) is associated with a *gauche* ${}^{13}\text{C}$ – ${}^1\text{H}$



coupling of <1 Hz, whereas in (140) the coupling is 2–3 [168]. Vicinal ^{13}C – ^1H coupling involving an sp^2 carbon may be appreciably larger than for an sp^3 -hybridized carbon in a comparable geometric arrangement [168]. Another possibility is non-first-order splitting in ^1H -coupled ^{13}C spectra, which can lead to a significant difference between the measured and actual $^3J_{\text{C-H}}$ value [28].

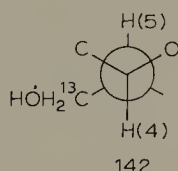
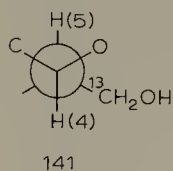
Conformational studies on acyclic systems have made substantial use of ^{13}C – ^1H coupling data. As an example, 3J coupling in propanal, which varies from 2.65 to 2.30 Hz as the temperature is varied from -65 to $+45^\circ$, has been taken as direct evidence of an increase in the relative population of the *gauche* rotamer (136) with temperature [181]. Similarly, changes in the populations of rotamers probably account for the fact that an increase in the size of the R group of an acyclic ether, $\text{R-CH}_2\text{-O-CH}_3$ (16)–(19), is accompanied by a decrease in coupling between the methyl carbon and methylene protons [187]. This may be illustrated with the following sequence of R groups and 3J values (in parenthesis):

H-(+5.7 Hz) , $\text{CH}_3\text{CH}_2\text{-(3.2 Hz)}$, $\text{CH}_3\text{CH}_2\text{CH}_2\text{-(3.1 Hz)}$,

$(\text{CH}_3)_2\text{CH-(3.05 Hz)}$ and $(\text{CH}_3)_3\text{C-(2.6 Hz)}$

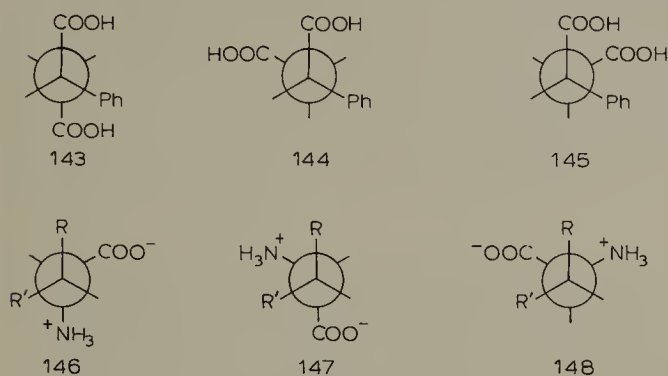
In *O*-methyl glycopyranosides, coupling of 3–4 Hz between the methyl carbon and the anomeric proton has been cited as evidence favouring the *gauche* orientations of nuclei depicted by (127) and (128), which is close to the conformations in the crystal-line state [188].

As noted above, one advantage of ^{13}C data is that it may be utilized in concert with other n.m.r. data thus providing mutual support. For example, vicinal coupling between protons-4 and -5 of 1,2-*O*-isopropylidene- α -D-glucopyranose and - β -L-idopyranose is 7.5–8.0 Hz, which is strongly indicative of a preference, respectively, for rotamers (141) and (142). It is reassuring, therefore, that the corresponding values for $^3J_{\text{C6-H4}}$ (*gluco*, 2.4 Hz; *ido*, <1 Hz) are in accord with the *gauche* relationship ex-



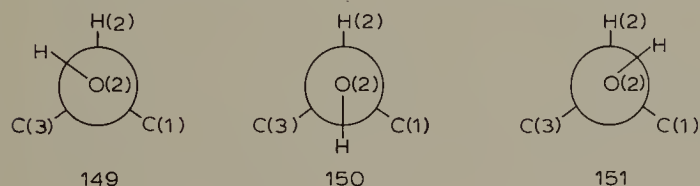
pected from the proton data; also, the fact that O-4 is *trans* to C-6 in (142) but *gauche* in (141) is consistent with the smaller coupling observed for the *ido* epimer [168]. From the effect on the proton spectrum of carboxyl ^{13}C -enrichment in phenylsuccinic acid, 3J values of ~ 11 Hz for the *trans* and ~ 4 Hz for a *gauche* ^{13}C -1, H-3 interaction have been deduced by computer simulation. On this basis, and the ^1H – ^1H coupling data for the compound, it has been concluded that the relative importance of the

conformers of phenylsuccinic acid is (143) > (144) \gg (145) [189]. In a related application, relative populations of the staggered rotamers of amino acids ((146), (147) and (148)) have been estimated by a combination of $^3J_{\text{C-H}}$ and $^3J_{\text{H-H}}$ data. Calcula-

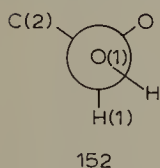


tion gave values of 11.9 and 0.4 Hz for *trans* and *gauche* orientations, respectively, of $^{13}\text{CO}_2^-$ and vicinal protons and, overall, the results indicated that the ratio of rotamers above is approximately 1 : 3 : 1 [190,191].

The combined use of ^{13}C and ^1H data is helpful also in defining preferred orientation in carbinols. OH-2 of α -D-glucose exhibits coupling of 2.0 Hz with C-1 [192]. This small 3J value suggests that the *anti* rotamer (149) is unimportant and that only (150) and (151) need be considered. Coupling between OH-2 and H-2 is 6.5 Hz, and since the values expected for (150) and (151) are respectively ~ 12 Hz and ~ 3 Hz, it ap-



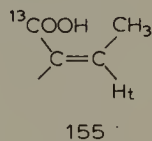
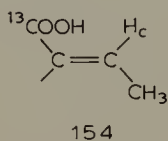
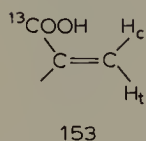
pears that (151) is sterically favoured over (150) by a factor of about two. An *antiperiplanar* arrangement of OH-1 and C-2 (152) in 2,3 : 4,5-di-*O*-isopropylidene- α -D-mannofuranose is highly likely because of their 3J coupling of 9.2 Hz [193]. On this basis,



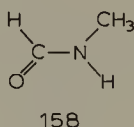
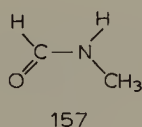
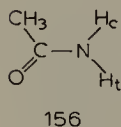
OH-1 and H-1 should subtend a dihedral angle of $\sim 60^\circ$; in fact, the observed coupling between these protons is 2.6 Hz, in close accord with expectation.

Cis and *trans* vicinal couplings in α,β unsaturated acids are widely different [194].

For acrylic acid (153), $^3J_{\text{C-H}_t}$ is +14.1 Hz and $^3J_{\text{C-H}_c} + 7.6$ Hz. Similarly, the *cis* arrangement in crotonic acid (154) gives $^3J = +6.8$ Hz, whereas the *trans* nuclei of isocrotonic acid (155) give $^3J = +14.5$ Hz. The magnitude of the *trans* values is noteworthy in being appreciably larger than the estimated values (11–12 Hz) cited above for *anti* rotamers of saturated acids, and much larger than $^3J_{\text{C-H}}$ values for *anti* orientations observed in other systems containing sp^2 carbon.

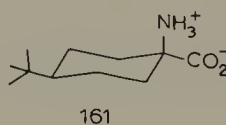
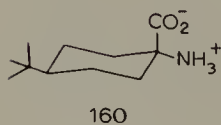
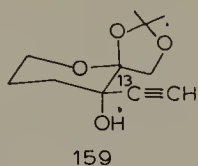


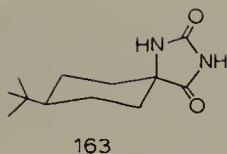
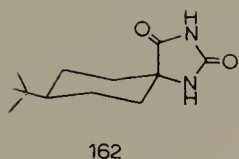
Amides, in which there is restricted rotation about the C–N bond, also show substantial coupling differences between *syn* and *anti* vicinal ^{13}C and ^1H nuclei [195]. However, the results available for simple amides are complex, and infer that applications of 3J to polypeptides may not prove to be straightforward (see ref. 188). The methyl carbon of acetamide (156) shows coupling ($^3J = 7.1$ Hz) with only one of the N protons, considered to be the *syn* H. Conversely, coupling between the *N*-methyl carbon and the formyl proton of *N*-methylformamide is ~ 5 Hz for conformer (157)



whereas 3J for (158) is too small to be resolved. Furthermore, in both acetamide and *N*-methylformamide, the dihedral angle in one conformation is expected to be about 180° , and in the other close to 0° . Hence, these results suggest that a Karplus type curve for the angular dependence of 3J does not apply for such compounds.

Vicinal ^{13}C – ^1H coupling offers a means for determining configuration at a quaternary centre in some classes of compounds [193]. For example, the configuration of the C-3 branch point shown in (159) has been designated on the basis of the small (1.5–2 Hz) 3J coupling between the methinyl ^{13}C -3' and H-4; i.e., a much larger coupling with H-4 was to be expected if this carbon was axially oriented. Similarly, the configurational assignments for amino acid (160) and (161), and related spiro deri-





vatives (e.g., (162) and (163)) have been based on 3J coupling measured in signals of the carboxyl (or carbonyl) carbons. Although the splittings of these signals were not adequately resolved, their line widths differed substantially: i.e., for (160) and (161) the values (half-widths) are 6.0 and 15.0 Hz, and for (162) and (163), are 7.0 and 15.0 Hz, respectively [196].

E. Coupling between ^{13}C and nuclei other than ^1H

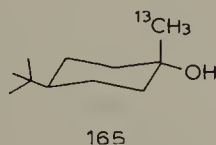
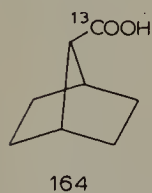
As is found for coupling between ^{13}C and ^1H , a good deal of study has been devoted to spin-spin interactions of ^{13}C with other nuclei from the standpoint of hybridization and electronegativity effects, or of coupling mechanisms, and only a minor part of the substantial literature on this general subject is concerned with stereochemical influences.

1. ^{13}C and ^{13}C

Due to the low natural abundance of ^{13}C , and hence the low probability of detecting spin-spin interactions between two such nuclei in a non-enriched molecule, isotopic labelling is employed for the measurement of coupling between two ^{13}C nuclei.

There are a number of parallels between ^{13}C – ^{13}C and ^{13}C – ^1H coupling [147]^a. Direct coupling ($^1J_{\text{C-C}}$) increases with an increase in the *s* character of carbon [152, 197], with the introduction of electronegative substituents [197–200], and with an increase in ring size from three to five carbons [201] (Table 10). The orientation of an electronegative substituent may have an influence, as suggested by the difference in ^{13}C -1, ^{13}C -2 coupling between α - and β -D-glucopyranose, which is 44.9 Hz and 47.1 Hz, respectively [68].

Studies on the angular dependence of $^3J_{\text{C-C}}$ suggest that in general there is a Karplus type of relationship. Thus, for a series of carboxyl-labelled acids of known geometry (eg., (164)) there are maxima of 2.5 Hz and 5.6 Hz at dihedral angles of 0° and



^a As noted above, this applies also for a comparison of the latter with ^1H – ^1H coupling. Consequently, $J_{\text{H-H}}$ values may be increasingly important in helping to establish correlations between $J_{\text{C-C}}$ and molecular structure [147].

TABLE 10

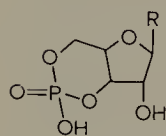
VARIATIONS IN $^1J_{C-C}$ Hz WITH CHANGES IN HYBRIDIZATION, SUBSTITUENTS AND RING SIZE

CH ₃ -CH ₃ 34.6	CH ₂ =CH ₂ 67.2	HC≡CH 170.6
CH ₃ -CH ₂ OH 37.7	CH ₃ -CHO 39.4	CH ₃ C≡N 56.5
cyclopropyl bromide	13.3	
cyclobutyl bromide	29.6	
cyclobutanone	29.7	
cyclopentanone	37.0	
cyclohexanone	37.3	

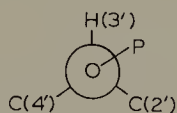
$\sim 165^\circ$, respectively, and a minimum of 0.5 Hz at $\sim 65^\circ$ [202]. Values obtained with ^{13}C -methyl carbinols (e.g., (165)) are maximal at 0° (5.4 Hz) and 180° (3.2 Hz) and give a minimum of ~ 0 Hz near 90° [203].

2. ^{13}C and ^{31}P

An orientational dependence of coupling between ^{13}C and ^{31}P has been demonstrated with various classes of compounds. In a series of 3',5' cyclic *O*-phosphates (166), which possess a relatively rigid ring system, coupling of the ^{31}P with an *anti-periplanar* C-2' was found to be 8 Hz, and ~ 2 Hz with *gauche* C-4' [204,205]. From these 3J values it has been estimated that the preferred orientation of the *O*-phosphate

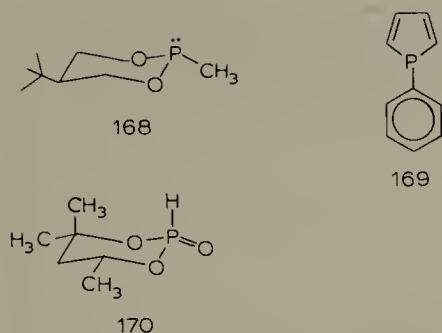


166



167

group in uridine-3'-phosphate is as shown in rotamer (167). Differences in two-bond coupling of the ^{31}P with C-3' and C-5' of (166) are essentially constant at 4.2 Hz and 7.2 Hz, respectively, which indicates that there are consistently different environments, or bond angles, at the C-3' and C-5' positions of the D-ribofuranoside ring; this difference is emphasized by the fact that 2J is essentially constant at 5.0 Hz in non-cyclic nucleotides [204]. The spatial disposition of the lone pair on the phosphorus of 1,3,2-dioxaphosphorinans (as in (168) and its *cis* isomer) noticeably affects the magnitude of 1J , 2J and 3J [206], and may also account for large differences in 2J observed for a series of compounds related to 1-phenylphosphole (169) [207]. With another 1,3,2-dioxaphosphorinan (170) it has been shown [208] that the vicinal coupling of ^{31}P with an equatorial $^{13}\text{CH}_3$ (dihedral angle $\sim 180^\circ$) is larger than with an axial $^{13}\text{CH}_3$



(dihedral angle $\sim 60^\circ$); the respective values of 5.9 Hz and 1.8 Hz parallel those obtained for (166).

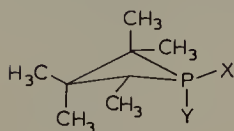
Phosphetane oxides (e.g., (171), $X=O$, $Y=CH_3$), which have been examined extensively [209], are characterized by distinctive values of 1J and 3J associated with the orientation of the oxygen and the second substituent on the phosphorus. Thus, coupling with a directly bonded axial $^{13}CH_3$ is substantially larger than with an equatorial one (Table 11). Noteworthy is the fact that 3J varies consistently as the X and Y substituents are interchanged, as seen typically in the data for 1-substituted 2,2,3,4,4-pentamethyl phosphetane oxides (171) (Table 11). The orientation of the oxygen is not the determining factor, however, for similar differences are found with isomeric pairs in which X or Y is methyl, phenyl or benzyl (Table 11). In 2,2,3,3,4-pentamethyl compounds (172) the ax. 3-methyl carbon exhibits a much smaller vicinal coupling with the ^{31}P than does the eq. CH_3 : for $X=Ph$ and $Y=O$ the respective 3J values are 1.6 Hz and 24.9 Hz. Since the $^{13}C-C-C-^{31}P$ dihedral angles corresponding to these values are expected to be about 90° and 180° , respectively, a Karplus-type of relation-

TABLE 11

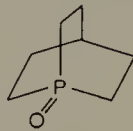
INFLUENCE OF SUBSTITUENT ORIENTATION ON $^{13}C-^{31}P$ COUPLING IN PHOSPHE-TANES (171)

	X	Y	1J (Hz)	3J (Hz)
<p>171</p>	O	CH_3	40.9	23.0
	CH_3	O	36.9	12.6
	O	CH_2Ph	34.8	22.9
	CH_2Ph	O	30.7	15.5
	O	OCH_3	—	23.8
	OCH_3	O	—	18.5
	Ph	CH_3	35.9	22.2
	CH_3	Ph	31.1	17.6

ship is indicated for three-bond coupling in this type of spin system ^a. Further evidence of such a relationship is provided [210] by the fact that coupling between the



172



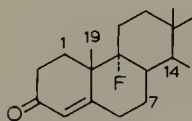
173

bridgehead ¹³C and ³¹P atoms in a bicyclic phosphine oxide (173) is large; i.e., ³*J* is 47 Hz, and the dihedral angle relating these two nuclei is ~0°.

3. ¹³C and ¹⁹F

The magnitude of both ¹*J* and ²*J* for coupling between ¹³C and ¹⁹F differs for *cis* and *trans* isomers of 1,2-difluoro-1,2-dihalo-ethylene, (174) and (175), although, curiously, the relative order of ¹*J* values is reversed for the chloro and bromo derivatives (Table 12) [211,212].

Data obtained [213] with 9- α -fluorocortisol ((176), partial structure) suggests that a Karplus relationship holds for vicinal coupling between ¹³C and ¹⁹F. Thus, coupling



176

of the fluorine with C-19 gives a ³*J* value of 6.0 Hz for an *anti* disposition of these two

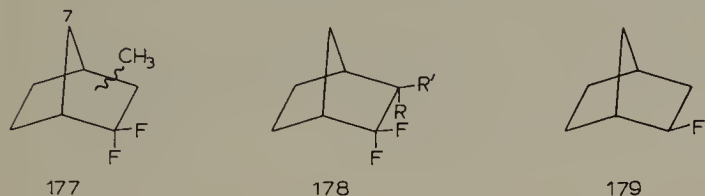
TABLE 12

¹³C-¹⁹F COUPLING IN GEOMETRIC ISOMERS OF 1,2-DIFLUORO-1,2-DIHALO-ETHYLENE

	X = Cl		X = Br	
	174	175	174	175
¹ <i>J</i>	299.0	291.0	324.7	355.0
² <i>J</i>	+37.0	+54.5	+35.8	+102.5

^a It is noteworthy that the *anti* orientation in this system gives about three times the ³*J* values as does the *anti* ¹³C-C-O-³¹P array of cyclic phosphates (166) or of (170).

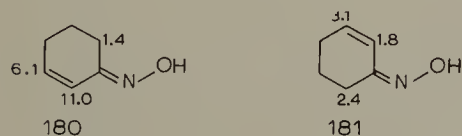
kinds of nuclei, whereas the couplings with *gauche* C-1, C-7 or C-14 are 1.5–3.1 Hz. Other data, available from studies on fluoronorbornanes [214], also conform to this type of interrelationship between 3J and dihedral angle. For example, C-7 of 2,2-difluoronorbornanes (177) exhibits coupling only with the *endo* ^{19}F ($^3J = \sim 5$ Hz), thus clearly differentiating between the *antiperiplanar* arrangement of these two nuclei and the *gauche* relationship between C-7 and the *exo* ^{19}F . Eclipsed arrangements are also characterized by a relatively large 3J : hence, coupling between the *endo* 3-methyl *endo* ^{19}F of (178) ($\text{R}=\text{CH}_3$, $\text{R}'=\text{H}$) is 14.1 Hz, and between the *exo* 3-methyl and *exo* ^{19}F of (178) ($\text{R}=\text{H}$, $\text{R}'=\text{CH}_3$) is 9.7 Hz. Because of the general consistency observed in the



series of 3-, 5-, 6- and 7-*exo* and *endo* methyl derivatives (177), ^{13}C – ^{19}F coupling data have proved to be highly useful for the assignment of signals in the ^{13}C spectra of these compounds. Nevertheless, considerable complexity may be noted within the overall data for fluoronorbornanes. For example, in *exo*-2-fluoronorbornane (179), vicinal coupling between the ^{19}F and *anti* C-6 is 9.8 Hz, whereas in the difluoro derivative ((178), R and $\text{R}'=\text{H}$) the analogous coupling pathway gives a reduced value of 6 Hz. Most striking are the values of 3.4 to 6.8 Hz for *gauche* coupling between C-6 and the *endo* ^{19}F of (177), which contrasts markedly with the *gauche* values of <1 Hz cited above.

4. ^{13}C and other nuclei

Substantial interest has been evinced in stereochemical aspects of coupling between ^{13}C and yet other nuclei. Coupling between ^{13}C and ^{15}N in oximes exhibits a geometric dependence that appears to be related to the orientation of the lone pair [215]. Some representative 2J and 3J values are given, (180) and (181), for *anti* (E) and *syn* (Z) isomers, respectively, of 2-cyclohexenone oxime- ^{15}N . A preliminary study [216]



of one-, two- and three-bond ^{13}C – ^{15}N coupling constants for *n*-propylamine- ^{15}N , raises possibilities for utilizing these parameters to define the conformations of alkylamines in solution. Research in this area, and also with ^{17}O as a tracer, will undoubtedly intensify greatly in the near future, particularly with biological systems.

Organometallics are receiving a good deal of attention. As an example, a Karplus

relationship between 3J and dihedral angle has been found [217] for the system $^{13}\text{C}-\text{C}-^{119}\text{Sn}$, and this information has been applied to benzylic tin compounds for determining the orientation of the benzylic $\text{C}-\text{Sn}$ bond with respect to the adjacent aromatic moiety. Also, some characteristics of coupling between ^{13}C and ^{57}Fe , ^{195}Pt , ^{199}Hg and ^{207}Pb have been described [217,218].

V. ^{13}C NUCLEAR SPIN RELAXATION

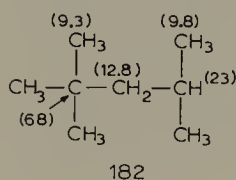
Spin-lattice relaxation times (T_1) of ^{13}C nuclei can now be determined in a relatively straightforward manner, especially as a result of recent innovations in pulsed FT techniques [219–221]. Since T_1 values provide a good deal of insight as to the motional behaviour of liquids or of molecules in solution, as well as important information about molecular structure, relaxation measurements are rapidly becoming integral features of ^{13}C n.m.r. studies ^a.

A. Influence of proton proximity on T_1

Generally speaking, spin-lattice relaxation takes place most importantly by dipole–dipole interaction between the ^{13}C nucleus and nearby protons [222,223] ^b. The efficiency of the dipolar mechanism is related to the number of interacting protons (N) and their distance (r) from the ^{13}C nucleus; i.e.,

$$1/T_1 \propto N/r^6$$

Accordingly, directly-bonded protons are most effective, and the relative order of T_1 values for carbons bearing three, two, one or no protons should increase ^c. This is clearly evident in data for isooctane ((182), values in s) [219].



Relaxation by spin-rotation may be important in small molecules. In cyclopropane, for example, dipolar and spin-rotation mechanisms contribute equally, but the dipolar

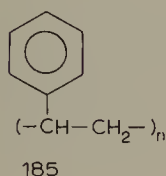
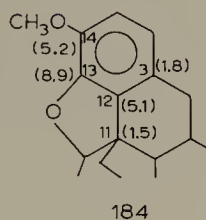
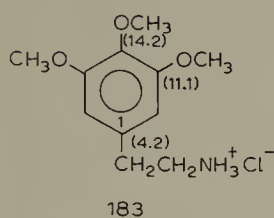
^a Even from the standpoint of optimal sensitivity in FT spectra, it is necessary to have an estimate of T_1 in order to select suitable delay times for the pulsing operation.

^b Or other neighbouring nuclei, such as ^{19}F , that possess a high gyromagnetic ratio.

^c In the absence of other effects, the ratio of T_1 values should be 1 : 2 : 3 when the number of protons attached to the ^{13}C is three, two or one, respectively [222,223].

contribution increases progressively in the cycloalkane series, and is the only effective relaxation mechanism in cyclohexane-to-cyclodecane [224].

Although protons not bonded directly to the ^{13}C nucleus are relatively inefficient dipoles, their contribution to T_1 need not be negligible. Hence ^{13}C signals produced by non-protonated carbons of mescaline (183) have been differentiated [225] on the basis of their T_1 values: i.e., the longest T_1 has been attributed to C-4 because it is more remote from H-2 and H-6 than are C-3 and C-5, and the shortest T_1 to C-1 because of its proximity to H-2, H-6 and the methylene protons. Similarly differences in T_1 have been utilized [226] in identifying ^{13}C signals of the quaternary carbons of



codeine ((184), partial formula) and brucine. Here, again, the smaller T_1 values have been correlated with the presence of protons on carbons α to the considered ^{13}C nucleus: i.e., in (184), T_1 of C-3 and C-11 is smaller than those of C-12, -13 and -14.

As noted above, variations in polymer tacticity are reflected in differences of ^{13}C chemical shifts. By contrast, no such distinction has been observed in spin-lattice relaxation measurements on synthetic polymers [227]. Thus, the values of T_1 for the methylene, methine and quaternary carbons of polystyrene (185) are, respectively, 32, 65 and 550 ms for isotactic material (see (11)), and 30, 60 and 550 ms for atactic. For $^{13}\text{CH}_2$ and ^{13}CH , this lack of dependence on configuration is perhaps to be expected because of the dominant dipolar relaxation role of bonded protons (note the 1 : 2 ratio of their T_1 's). The equality of T_1 values for the quaternary carbons, however, appears to arise because the average distance between each quaternary carbon and the protons of its monomer unit as well as nearest protons of neighbour monomer units is about the same for the two configurations. That is, an evaluation of conformational populations in polystyrene indicates that in solution there are probably 6–10 protons within 2–3 Å of each quaternary carbon. Furthermore, segmental motions (see below) in these polymers must be similar. Comparable T_1 data have been obtained for polyacrylonitrile and polyvinyl chloride of differing tacticities [228].

B. Influence of molecular motion on T_1

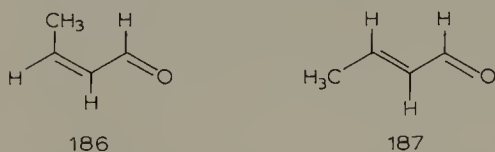
Spin-lattice relaxation *via* the dipolar mechanism is affected by changes in the local fluctuating magnetic field caused by reorientation of the dipole during molecular motion. For rapid motion ($<10^{-8}$ s/radian) the correlation time (τ_c) that characterizes the rate of reorientation is inversely proportional to T_1 ; i.e.

$$1/T_1 \propto \tau_c$$

These effects are well illustrated [229] by the relaxation behavior of some monosubstituted benzenes: whereas T_1 for benzene itself is 28 s, the shortened T_1 values (in s) denoted below (Fig. 7) are consistent with a progressive reduction in the (anisotropic) tumbling rates, caused by increasingly bulky substituent groups. T_1 values for the *para* carbons are consistently the smallest, which has been interpreted as evidence of a preferred rotation around the C_2 molecular symmetry axis coincident with the ring-to-substituent bond.

Ring size appears to have an influence on anisotropic motion. For alicyclic alcohols containing 4, 5, 6, 8 or 12 carbons, and their methyl ethers, variations in the pattern of T_1 values indicate that molecular motion becomes less anisotropic as the ring size increases [230]. Glycosides of anomeric pyranose sugars exhibit evidence of isotropic tumbling in solution, since each carbon has approximately the same correlation time [231,232]. Furthermore, a change in the anomeric configuration is not accompanied by detectable changes in T_1 .

Significantly different T_1 's are found, however, for *cis*- and *trans*-crotonaldehyde, (186) and (187) [233]. With this pair of isomers, it appears that the *cis* structure is



sufficiently more compact that it diffuses slightly faster. Hence it possesses a somewhat shorter correlation time than the more extended *trans* isomer, and exhibits larger T_1

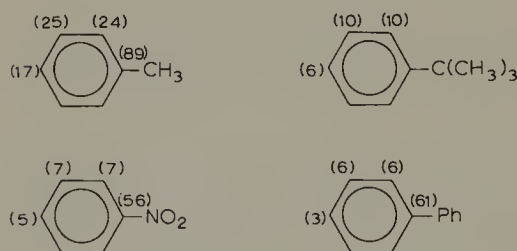


Fig. 7. Spin-lattice relaxation times (T_1 , s) for monosubstituted benzenes.

$\text{H}_2\text{C}^{(3.0)}-\text{CH}_2^{(3.9)}-\text{CH}_2^{(3.6)}-\text{CH}_3^{(4.2)}$	188
$\text{HO}^{(0.65)}-\text{CH}_2^{(0.77)}-(\text{CH}_2)_4^{(2.2)}-\text{CH}_2-\text{CH}_3^{(3.1)}$	189
$\text{H}_2\text{N}^{(13.4)}-\text{CH}_2^{(13.4)}-\text{CH}_2^{(15.0)}-\text{CH}_2-\text{CH}_3^{(12.1)}$	190
$\text{H}_3\text{N}^+^{(0.88)}-\text{CH}_2^{(1.54)}-\text{CH}_2^{(1.95)}-\text{CH}_2-\text{CH}_3^{(3.35)}$	191
$\begin{array}{c} (0.60) \text{CH}_3-\text{C}^{(1.10)}-\text{C}^{(0.12)}-\text{O}-\text{CH}_2-\text{CH}_2-\text{CH}_2-\text{CH}_3 \\ \quad \quad \quad \quad \quad \quad \\ (0.04) \quad \quad \quad \text{O} \quad \quad \quad (0.76) \quad \quad \quad (1.39) \\ \quad \quad \quad \quad \quad \quad \\ (0.07) \text{CH}_2 \end{array}$	192

Fig. 8. Variations in segmental motion, as reflected in differing patterns of spin-lattice relaxation times (T_1 , s).

values. Especially noteworthy, is the use of these relaxation data in conjunction with measurements of nuclear Overhauser enhancement and ^1H spin-lattice relaxation, to determine internuclear distances between all of the protons of (186) and (187), and hence to define in a precise manner the geometries of these molecules, including the rotational conformation of the methyl groups.

C. Segmental motion

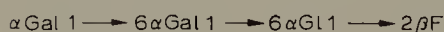
In some molecules, different segments exhibit distinct reorientation rates and give rise to substantial variations in T_1 between groups of carbons. A comparison of butanol (188) with octanol (189) shows (Fig. 8) that, although both must engage in intermolecular H-bonding, internal motions are obscured in the smaller aggregate by a relatively rapid overall reorientation. That is, T_1 's for the various carbons of butanol do not differ greatly, whereas the values within octanol differ markedly. *n*-Butylamine (190) exhibits longer T_1 values than butanol, and hence reorients faster, although the *n*-butylammonium ion (191) appears to be much more effectively anchored since it gives shorter T_1 values and shows large differences in segmental motion [234]. A more marked restriction is imposed on the mobility of the *n*-butyl chain in poly-*n*-butyl methacrylate (192) which is accompanied by even greater variations in segmental motion [235]^a.

Differential T_1 effects of this type find application in the biopolymer field, for de-

^a The very short T_1 of $^{13}\text{CH}_2$ of the polymer main chain is of the same order as for $^{13}\text{CH}_2$ of polystyrene; i.e., these values reflect the slow overall molecular reorientation rates (long τ_c) of high polymers.

tecting unfolding or denaturation due to temperature or environmental changes and for distinguishing between ordered and random structures within the same macromolecule. For example [236], the ϵ -methyl carbons of lysine residues in ribonuclease are seen to have relatively greater mobility than the α carbons of amino acid residues, as shown by the fact that the ratio of T_1 's for CH_3/CH is about 8 : 1. On acid denaturation, this ratio falls to about 3 : 1; an indication that in the random coil conformation of the protein the lysine side chains no longer possess a distinctive segmental motion.

An elegant application of differences in spin-lattice relaxation arising from variations in reorientation rates within a molecule has been demonstrated [237] in an analysis of the ^{13}C spectrum of the tetrasaccharide stachyose (193). Thus, the terminal α -D-galactopyranose residue (αGal) exhibits longer T_1 's than the internal, 1,6-linked-



193

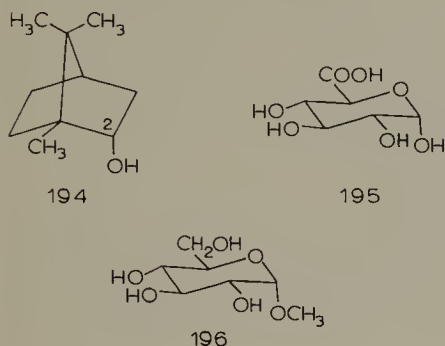
α -D-galactopyranose residue ($6\alpha\text{Gal}$), because of its greater freedom of mobility. These differences, visualized conveniently in the form of a "partially relaxed" FT spectrum, have permitted the ready distinction of closely spaced ^{13}C signals.

D. Intermolecular association

Other areas of application are concerned with changes in spin-lattice relaxation rates caused by intermolecular associations. Solvation effects, for example, are evident in the behavior of 1-octanol. As mentioned above, the high degree of segmental motion exhibited by 1-octanol was observed for the neat liquid and has been ascribed to molecular aggregation. Further evidence for this is provided by the marked reduction in segmental motion and the general increase in T_1 that occurs when the alcohol is examined as a dilute solution in carbon tetrachloride [238]. As another example, T_1 's of the *t*-butylammonium ion in water or methanol are substantially longer than those in less polar solvents (methylene chloride or dioxane). Hence the overall motion is greater in the polar media, presumably because the interaction of solvent and counter ion is less important for stability than is electrostatic stabilization.

Paramagnetic substances can induce an increase in spin-lattice relaxation rates because the unpaired electrons may compete very effectively with protons in dipole-dipole relaxation of ^{13}C [239]. Such paramagnetic reagents as iron trisacetylacetonate ($\text{Fe}(\text{acac})_3$) have accordingly been utilized to facilitate spectral assignments for compounds in somewhat the same way as the well-known use of shift reagents in n.m.r. spectroscopy. Thus, the addition of $\text{Fe}(\text{acac})_3$ to a solution of borneol (194) in benzene- d_6 causes a significantly larger decrease in the T_1 's of those carbons (C-1, -2, -3) closer to the interaction site than of more remote carbons. In aqueous solution, the lanthanide salt, gadolinium nitrate ($\text{Gd}(\text{NO}_3)_3$) is very effective in altering the ^{13}C

relaxation characteristics of uronic acids in a stereoselective manner [240]. An axial anomeric C—O bond, as in α -D-glucuronic acid (195) is accompanied by a striking decrease in the relative intensities of the ^{13}C -1 and ^{13}C -6 signals, whereas there is little



effect on the corresponding signals of the equatorial (β -) anomer.

Potentially, very interesting applications are to be found in areas of enzyme—substrate or antigen—antibody interactions. A recent study [232] of binding between methyl α -D-glucopyranoside (196) and Zn^{2+} and Mn^{2+} derivatives of concovallin A, a hemagglutinin protein, is illustrative. Using ^{13}C -enriched (196) to attain improved sensitivity, changes in T_1 's of the sugar caused by the paramagnetic ions at the binding site have been measured. Zn^{2+} was found to be less effective than Mn^{2+} in reducing T_1 , and the dipolar contributions estimated for the latter ion were used to obtain ^{13}C —Mn internuclear distances, and hence to determine the binding orientation of the sugar relative to the transition ion site in the protein.

ACKNOWLEDGEMENT

The kind assistance of Drs. N. Cyr, G.K. Hamer and J.A. Schwarcz is gratefully acknowledged.

REFERENCES

- 1 J.B. Stothers, *Carbon-13 NMR Spectroscopy*, Academic Press, New York, 1972.
- 2 G.C. Levy and G.L. Nelson, *Carbon-13 Nuclear Magnetic Resonance for Organic Chemists*, Wiley-Interscience, New York, 1972.
- 3 J.B. Stothers, *Quart. Rev.*, 19 (1965) 144.
- 4 E.F. Mooney and P.H. Winson, in E.F. Mooney (Ed.), *Annual Review of NMR Spectroscopy*, Vol. 2, Academic Press, New York, 1969, p. 153.
- 5 E. Breitmaier, G. Jung and W. Voelter, *Angew. Chem., Int. Ed. Engl.*, 10 (1971) 673.
- 6 G.C. Levy, *Acc. Chem. Res.*, 6 (1973) 161.
- 7 G.C. Levy (Ed.), *Topics in Carbon-13 NMR Spectroscopy*, Vol. 1, Wiley-Interscience, New York, 1974.

- 8 Nuclear Magnetic Resonance, Specialist Periodical Reports (R.K. Harris, Senior Reporter), The Chemical Society, London, 1972–1974, Vols. 1–3.
- 9 N.K. Wilson and J.B. Stothers, in E.L. Eliel and N.L. Allinger (Eds.), Topics in Stereochemistry, Wiley-Interscience, New York, 1974, p. 1.
- 10 P.C. Lauterbur, J. Am. Chem. Soc., 83 (1961) 1838.
- 11 P.C. Lauterbur, J. Am. Chem. Soc., 83 (1961) 1846.
- 12 H. Speisecke and W.G. Schneider, J. Chem. Phys., 35 (1961) 722, 731.
- 13 R.A. Friedel and H.L. Retcofsky, J. Am. Chem. Soc., 85 (1963) 1300.
- 14 D.M. Grant and E.G. Paul, J. Am. Chem. Soc., 86 (1964) 2984.
- 15 G.B. Savitsky and K. Namikawa, J. Phys. Chem., 68 (1964) 1956.
- 16 J.B. Stothers and P.C. Lauterbur, Can. J. Chem., 42 (1964) 1563.
- 17 J.A. Pople, W.G. Schneider and H.J. Bernstein, High-Resolution Nuclear Magnetic Resonance, McGraw-Hill, New York, 1959, p. 307.
- 18 J.H. Goldstein, V.S. Watts and L.S. Rattet, in J.W. Emsley, J. Feeney and L.H. Sutcliffe (Eds.), Progress in Nuclear Magnetic Resonance Spectroscopy, Vol. 8, part 2, Pergamon, Oxford, 1971, p. 103.
- 19 M. Tanabe and G. Detre, J. Am. Chem. Soc., 88 (1966) 4515.
- 20 A.G. McInnes, D.G. Smith, L.C. Vining and L.F. Johnson, Chem. Commun. (1971) 325.
- 21 J.B. Stothers, in G.C. Levy (Ed.), Topics in Carbon-13 NMR Spectroscopy, Vol. 1, Wiley-Interscience, New York, 1974, p. 229.
- 22 E.G. Paul and D.M. Grant, J. Am. Chem. Soc., 86 (1964) 2977.
- 23 R.R. Ernst and W.A. Anderson, Rev. Sci. Instrum., 37 (1966) 93.
- 24 H.J. Koch and A.S. Perlin, Carbohydr. Res., 15 (1970) 403.
- 25 F.J. Weigert and J.D. Roberts, J. Am. Chem. Soc., 89 (1967) 2967.
- 26 J.N. Shoolery, 3rd ENC, Pittsburgh, Pa., March, 1962.
- 27 R.A. Newmark and J.R. Hill, J. Am. Chem. Soc., 95 (1973) 4435.
- 28 N. Cyr, R.G.S. Ritchie, T.M. Spotswood and A.S. Perlin, Can. J. Spectrosc., 19 (1974) 190.
- 29 L.F. Johnson, cited in refs. 1 and 2.
- 30 O.A. Gansow and W. Shittenhelm, J. Am. Chem. Soc., 93 (1971) 4294.
- 31 K.S. Pitzer, J. Chem. Phys., 8 (1940) 711.
- 32 D.K. Dalling and D.M. Grant, J. Am. Chem. Soc., 86 (1967) 6612.
- 33 D.M. Grant and B.V. Cheney, J. Am. Chem. Soc., 89 (1967) 5315.
- 34 F.A.L. Anet, C.H. Bradley and G.W. Buchanan, J. Am. Chem. Soc., 93 (1971) 258.
- 35 A.S. Perlin and H.J. Koch, Can. J. Chem., 48 (1970) 2639.
- 36 B.V. Cheney and D.M. Grant, J. Am. Chem. Soc., 89 (1967) 5319.
- 37 B.V. Cheney, J. Am. Chem. Soc., 90 (1968) 5386.
- 38 D. Danneels and M. Anteunis, Org. Magn. Reson., 6 (1974) 617.
- 39 A. Saika and C.P. Slichter, J. Chem. Phys., 22 (1954) 26.
- 40 M. Karplus and J.A. Pople, J. Chem. Phys., 38 (1963) 2803.
- 41 G.J. Martin, M.L. Martin and S. Odier, Org. Magn. Reson., 7 (1975) 2.
- 42 N. Cyr, A.S. Perlin and M.A. Whitehead, Can. J. Chem., 50 (1972) 814.
- 43 N. Cyr, J.A. Schwarcz and A.S. Perlin, unpublished.
- 44 A.S. Perlin, N. Cyr, H.J. Koch and B. Korsch, Ann. N.Y. Acad. Sci., 222 (1973) 935.
- 45 W.H. Flygare and J. Goodisman, J. Chem. Phys., 49 (1968) 3122.
- 46 J. Mason, J. Chem. Soc., (1971) 1038.
- 47 J.D. Roberts, F.J. Weigert, J.I. Kroschwitz and H.J. Reich, J. Am. Chem. Soc., 92 (1970) 1338.
- 48 T. Pekk and E. Lippmaa, Eesti NSV Tead. Akad. Toim., Keem., Geol., 17 (1968) 287, 291.
- 49 T. Pekk and E. Lippmaa, Org. Magn. Reson., 3 (1971) 679.
- 50 H.J. Schneider and V. Hoppen, Tetrahedron Lett. (1974) 579.

- 51 E.L. Eliel, N.L. Allinger, S.J. Angyal and G.A. Morrison, *Conformational Analysis*, Interscience, New York, 1967, p. 44.
- 52 J. Schaefer, *Macromolecules*, 2 (1969) 210,533.
- 53 L.F. Johnson, F. Heatley and F.A. Bovey, *Macromolecules*, 3 (1970) 175.
- 54 C.J. Carman, A.R. Tarpley, Jr. and J.H. Goldstein, *Macromolecules*, 4 (1971) 445.
- 55 I.R. Peat and W.F. Reynolds, *Tetrahedron Lett.*, 1359 (1972).
- 56 J. Schaefer, in G.C. Levy (Ed.), *Topics in Carbon-13 NMR Spectroscopy*, Vol. 1, Wiley-Interscience, New York, 1974, p. 150.
- 57 F.A. Bovey, in E.B. Mano (Ed.), *Proceedings International Symposium on Macromolecules*, Elsevier, Amsterdam, 1974, p. 169.
- 58 C.J. Carman, A.R. Tarpley, Jr. and J.H. Goldstein, *J. Am. Chem. Soc.*, 93 (1971) 2864.
- 59 M. Christl, H.J. Reich and J.D. Roberts, *J. Am. Chem. Soc.*, 93 (1971) 3463.
- 60 W. McFarlane, *Chem. Commun.*, (1970) 418.
- 61 G.C. Levy and G.L. Nelson, *J. Am. Chem. Soc.*, 94 (1972) 4897.
- 62 P.S. Pregosin and E.W. Randall, *Chem. Commun.*, (1971) 399.
- 63 G. Binsch, in E.L. Eliel and N.L. Allinger (Eds.), *Topics in Stereochemistry*, Vol. 3, Interscience, New York, 1968, p. 97.
- 64 E. Lippmaa and T. Pekk, *Kem. Teollisuus*, 12 (1967) 1001.
- 65 D.E. Dorman, M. Jautelat and J.D. Roberts, *J. Org. Chem.*, 36 (1971) 2757.
- 66 J.W. de Haan and L.J.M. van de Ven, *Tetrahedron Lett.*, (1971) 3965.
- 67 E. Wenkert, M.J. Gasic, E.W. Hagaman and L.D. Kwart, *Org. Magn. Reson.*, 7 (1975) 51.
- 68 A.S. Perlin and B. Casu, *Tetrahedron Lett.*, (1969) 2921; A.S. Perlin, B. Casu and H.J. Koch, *Can. J. Chem.*, 48 (1970) 2596.
- 69 L.D. Hall and L.F. Johnson, *Chem. Commun.*, (1969) 509.
- 70 D.E. Dorman and J.D. Roberts, *J. Am. Chem. Soc.*, 92 (1970) 1355.
- 71 D. Doddrell and A. Allerhand, *J. Am. Chem. Soc.*, 93 (1971) 2779.
- 72 A.S. Perlin, P.C.M. Herve du Penhoat and H.S. Isbell, *Adv. Chem. Ser.*, 117 (1973) 39.
- 73 P.C.M. Herve du Penhoat and A.S. Perlin, *Carbohydr. Res.*, 36 (1974) 111.
- 74 L. Que, Jr. and G.A. Gray, *Biochemistry*, 13 (1974) 146.
- 75 D.E. Dorman, S.J. Angyal and J.D. Roberts, *J. Am. Chem. Soc.*, 92 (1970) 1351.
- 76 E. Breitmaier, W. Voelter, G. Jung and C. Tanzer, *Chem. Ber.*, 104 (1971) 1147.
- 77 D.R. Bundle, H.J. Jennings and I.C.P. Smith, *Can. J. Chem.*, 51 (1973) 3812.
- 78 N. Gurudata and F.J.M. Rajabalee, *Can. J. Chem.*, 51 (1973) 1797.
- 79 W.A. Szarek, D.M. Vyas, G. Lukacs and S.D. Gero, *Can. J. Chem.*, 52 (1974) 3394.
- 80 A.S. Perlin, *Can. J. Chem.*, 49 (1971) 1972.
- 81 F.G. Riddell, *J. Chem. Soc., B*, (1970) 331.
- 82 D. Wendisch, W. Naegle and H. Feltkamp, *Org. Magn. Reson.*, 2 (1970) 561; G. Ellis and R.G. Jones, *J. Chem. Soc., Perkin Trans. 2*, (1972) 437.
- 83 W.A. Szarek, D.M. Vyas, A.-M. Sepulchre, S.D. Gero and G. Lukacs, *Can. J. Chem.*, 52 (1974) 2041.
- 84 F.J. Weigert and J.D. Roberts, *J. Am. Chem. Soc.*, 92 (1970) 1347; D.H. Marr and J.B. Stothers, *Can. J. Chem.*, 45 (1967) 225.
- 85 M. Christl, H.J. Reich and J.D. Roberts, *J. Am. Chem. Soc.*, 93 (1971) 3463.
- 86 R.G.S. Ritchie, N. Cyr, B. Korsch, H.J. Koch and A.S. Perlin, *Can. J. Chem.*, 53 (1975) 1424.
- 87 M. Christl and J.D. Roberts, *J. Org. Chem.*, 37 (1972) 3443.
- 88 G. Mann, M. Mühlstädt, R. Muller, E. Kern and W. Hadeball, *Tetrahedron*, 24 (1968) 6941.
- 89 D. Zimmermann, R. Ottinger, J. Reisse, H. Cristol and J. Brugidou, *Org. Magn. Reson.*, 6 (1974) 346.
- 90 W.R. Wolfenden and D.M. Grant, *J. Am. Chem. Soc.*, 88 (1966) 1496.
- 91 N.K. Wilson and J.B. Stothers, *J. Magn. Reson.*, 15 (1974) 31.

- 92 S.H. Grover and J.B. Stothers, *Can. J. Chem.*, 52 (1974) 870.
- 93 H.J. Reich, M. Jautelat, M.T. Messe, F.J. Weigert and J.D. Roberts, *J. Am. Chem. Soc.*, 91 (1969) 7445.
- 94 E. Lippmaa and T. Pekk, *Eesti NSV Tead. Akad. Toim., Keem., Geol.*, 17 (1968) 287.
- 95 B. Balogh, D.M. Wilson and A.L. Burlingame, *Nature (London)*, 233 (1971) 261.
- 96 J.L. Gough, J.P. Guthrie and J.B. Stothers, *Chem. Commun.*, (1972) 979.
- 97 D. Leibfritz and J.D. Roberts, *J. Am. Chem. Soc.*, 95 (1973) 4996.
- 98 G. Lukacs, A. Pictot, X. Lusinchi, H.J. Koch and A.S. Perlin, *C.R. Acad. Sci. Paris*, 272 (1971) 2171.
- 99 R.T. Lalonde and T.N. Donvito, *Can. J. Chem.*, 52 (1974) 3778.
- 100 E. Lippmaa, T. Pekk, J. Paasivirta, N. Belikova and A. Platé, *Org. Magn. Reson.*, 2 (1970) 581.
- 101 J.B. Grutzner, M. Jautelat, J.B. Dence, J.A. Smith and J.D. Roberts, *J. Am. Chem. Soc.*, 92 (1970) 7107.
- 102 D. Zimmerman, J. Reisse, J. Coste, F. Plénat and H. Cristol, *Org. Magn. Reson.*, 6 (1974) 492.
- 103 K. Tori, M. Ueyama, T. Tsuji, H. Matsumura, H. Tanida, H. Iwamura, K. Kushida, T. Nishida and S. Satoh, *Tetrahedron Lett.*, (1974) 327.
- 104 G.E. Maciel, H.C. Dorn, R.L. Greene, W.A. Kleschick, M.R. Peterson, Jr. and G.H. Wahl, Jr., *Org. Magn. Reson.*, 6 (1974) 178.
- 105 J.B. Stothers, *Carbon-13 NMR Spectroscopy*, Academic Press, New York, 1972, p. 58.
- 106 J.B. Stothers, *Carbon-13 NMR Spectroscopy*, Academic Press, New York, 1972, p. 75.
- 107 J.I. Kroschwitz, M. Winokur, H.J. Reich and J.D. Roberts, *J. Am. Chem. Soc.*, 91 (1969) 5927.
- 108 S.H. Grover, J.P. Guthrie, J.B. Stothers and C.T. Tan, *J. Magn. Reson.*, 10 (1973) 227.
- 109 R.G.S. Ritchie, N. Cyr and A.S. Perlin, *Can. J. Chem.*, 54 (1976) 2301.
- 110 G.M. Kellie and F.G. Riddell, *J. Chem. Soc. B*, (1971) 1030; F.G. Riddell, *J. Chem. Soc., Perkin Trans. 2*, (1972) 252.
- 111 L. Radom and J.A. Pople, *J. Am. Chem. Soc.*, 92 (1970) 4286.
- 112 L.C. Allen, *Chem. Phys. Lett.*, 2 (1968) 597.
- 113 S. Wolfe, A. Rauk, L.M. Tel and I.G. Csizmadia, *J. Chem. Soc.*, (1971) 136.
- 114 A.J. Jones, E.L. Eliel, D.M. Grant, M.C. Knoeber and W.F. Bailey, *J. Am. Chem. Soc.*, 93 (1971) 4772.
- 115 E.L. Eliel, W.F. Bailey, L.D. Kopp, R.L. Willer, D.M. Grant, R. Bertrand, K.A. Christensen, D.K. Dalling, M.W. Duch, E. Wenkert, F.M. Schell and D.W. Cochran, *J. Am. Chem. Soc.*, 97 (1975) 322.
- 116 J.J. Burke and P.C. Lauterbur, *J. Am. Chem. Soc.*, 86 (1964) 1870.
- 117 G.E. Maciel and G.B. Sawitsky, *J. Phys. Chem.*, 69 (1965) 3925.
- 118 J.B. Stothers, *Carbon-13 NMR Spectroscopy*, Academic Press, New York, 1972, p. 270.
- 119 D.K. Dalling and D.M. Grant, cited in Ref. 1, p. 62.
- 120 C.H. Park and H.E. Simmons, *J. Am. Chem. Soc.*, 94 (1972) 7184.
- 121 R.K. Hill and D.W. Ladner, *Tetrahedron Lett.*, (1975) 989.
- 122 W.A. Gibbons, J.A. Sogn, A. Stern, L.C. Craig and L.F. Johnson, *Nature (London)*, 227 (1970) 840.
- 123 J.P. Snyder, L. Lee and D.G. Farnum, *J. Am. Chem. Soc.*, 93 (1971) 3816.
- 124 A. Solladité-Cavallo and G. Solladité, *Org. Magn. Reson.*, 7 (1975) 18.
- 125 A. Allerhand, D. Doddrell, V. Glushko, D.W. Cochran, E. Wenkert, P.J. Lawson and F.R.N. Gurd, *J. Am. Chem. Soc.*, 93 (1971) 544; A. Allerhand, R.F. Childers, R.A. Goodman, E. Oldfield and X. Ysern, *Am. Lab.*, 4 (1972) 19.
- 126 A.S. Perlin, N.M.K. Ng Ying Kin, S.S. Bhattacharjee and L.F. Johnson, *Can. J. Chem.*, 50 (1972) 2437.
- 127 H.J. Jennings and I.C.P. Smith, *J. Am. Chem. Soc.*, 95 (1973) 606.

- 128 P.A.J. Gorin, *Can. J. Chem.*, 51 (1973) 2375.
- 129 T. Usui, N. Yamaoka, K. Matsuda, K. Tuzimura, H. Sugiyama and S. Seto, *J. Chem. Soc., Perkin Trans. 2*, (1973) 2425.
- 130 O.A. Gansow, J. Killough and A.R. Burke, *J. Am. Chem. Soc.*, 93 (1971) 4298.
- 131 D.K. Dalling, D.M. Grant and L.F. Johnson, *J. Am. Chem. Soc.*, 93 (1971) 3678.
- 132 B.P. Roques, S. Combrisson and F. Wehrli, *Tetrahedron Lett.*, (1975) 1047.
- 133 D. Doddrell, C. Charrier, B.L. Hawkins, W.O. Crain, Jr., L. Harris and J.D. Roberts, *Proc. Natl. Acad. Sci. U.S.A.*, 67 (1970) 1588.
- 134 F.W. Buchanan, J.B. Stothers and S.T. Wu, *Can. J. Chem.*, 47 (1969) 3113.
- 135 H.-J. Schneider, R. Price and T. Keller, *Angew. Chem., Int. Ed. Engl.*, 10 (1971) 730.
- 136 O. Yamamoto, M. Yanagisawa, K. Hayamizu and G. Kotowycz, *J. Magn. Reson.*, 9 (1973) 216.
- 137 F.A.L. Anet, A.K. Cheng and J.J. Wagner, *J. Am. Chem. Soc.*, 94 (1972) 9250.
- 138 K.L. Servis, E.A. Noe, N. Roy Easton, Jr. and F.A.L. Anet, *J. Am. Chem. Soc.*, 96 (1974) 4185.
- 139 S. Masamune, A.V. Kemp-Jones, J. Green, D.L. Rabenstein, M. Yasunami, K. Takase and T. Nozoe, *Chem. Commun.*, (1973) 283.
- 140 F.A. Cotton, A. Danti, J.S. Waugh and R.W. Fessenden, *J. Chem. Phys.*, 29 (1958) 1427.
- 141 R. Bramley, B.N. Figgis and R.S. Nyholm, *Trans. Faraday Soc.*, 58 (1962) 1893; *J. Chem. Soc. A*, (1967) 861.
- 142 G.A. Olah, Y. Halpern, Y.K. Mo and G. Liang, *J. Am. Chem. Soc.*, 94 (1972) 3554; G.A. Olah, A.M. White and D.H. O'Brien, *Chem. Rev.*, 70 (1970) 561.
- 143 G. Gatti, A. Levi, V. Lucchini, G. Modena and G. Scorrano, *Chem. Commun.*, (1973) 25.
- 144 R.A. McClelland and W.F. Reynolds, *Chem. Commun.*, (1974) 824.
- 145 W.J. Horsley and H. Sternlicht, *J. Am. Chem. Soc.*, 90 (1968) 3738.
- 146 G.A. Olah, *Angew. Chem., Int. Ed. Engl.*, 12 (1973) 173.
- 147 J.L. Marshall, D.E. Müller, S.A. Conn, R. Seiwel and A.M. Ihrig, *Acc. Chem. Res.*, 7 (1974) 333.
- 148 J.B. Stothers, *Carbon-13 NMR Spectroscopy*, Academic Press, New York, 1972, p. 348.
- 149 E.D. Becker, *High Resolution NMR*, Academic, New York, 1969, p. 192.
- 150 A.A. Chalmers, K.G.R. Pachler and P.L. Wessels, *Org. Magn. Reson.*, 6 (1974) 445; K.G.R. Pachler and P.L. Wessels, *J. Magn. Reson.*, 12 (1973) 337.
- 151 S. Sorenson, R.S. Hansen and H.J. Jakobsen, *J. Magn. Reson.*, 14 (1974) 243.
- 152 D.M. Graham and C.E. Holloway, *Can. J. Chem.*, 41 (1963) 2114.
- 153 R.N. Lynden-Bell and N. Sheppard, *Proc. Roy. Soc. London, Ser. A*, 269 (1964) 385.
- 154 N. Muller and D.E. Pritchard, *J. Chem. Phys.*, 31 (1959) 768, 1471; J.N. Shoolery, *J. Chem. Phys.*, 31 (1959) 1427.
- 155 M. Karplus and D.M. Grant, *Proc. Natl. Acad. Sci. U.S.A.*, 45 (1959) 1269.
- 156 E.R. Malinowski, *J. Am. Chem. Soc.*, 83 (1961) 4479.
- 157 D.M. Grant and W.M. Litchman, *J. Am. Chem. Soc.*, 87 (1965) 3944.
- 158 N. Cyr and T.J.R. Cyr, *J. Chem. Phys.*, 47 (1967) 3082.
- 159 K. Wiithrich, S. Meiboom and L.C. Snyder, *J. Chem. Phys.*, 52 (1970) 230.
- 160 L. Lunazzi and F. Taddei, *Spectrochim. Acta, Part A*, 25 (1969) 611.
- 161 P.P. Nicholas, C.J. Carman, A.R. Tarpley, Jr. and J.H. Goldstein, *J. Phys. Chem.*, 76 (1972) 2877.
- 162 R.M. Lynden-Bell, *Mol. Phys.*, 6 (1963) 537.
- 163 R.E. Mayo and J.H. Goldstein, *J. Mol. Spectrosc.*, 14 (1964) 173.
- 164 F. Hruska, G. Kotowycz and T. Schaefer, *Can. J. Chem.*, 43 (1965) 2827.
- 165 R.F.W. Bader and H.J.T. Preston, *Can. J. Chem.*, 44 (1966) 1131.
- 166 T. Yonezawa and I. Morishima, *J. Mol. Spectrosc.*, 27 (1968) 210.

- 167 G.A. Olah and A.M. White, *J. Am. Chem. Soc.*, 89 (1967) 7072.
- 168 J.A. Schwarcz and A.S. Perlin, *Can. J. Chem.*, 50 (1972) 3667.
- 169 J.A. Schwarcz, Ph. D. Thesis, McGill University, Montreal, 1974.
- 170 K. Bock, J. Lundt and C. Pederson, *Tetrahedron Lett.*, (1973) 1073; K. Bock and C. Pederson, *J. Chem. Soc., Perkin Trans. 2*, (1974) 293.
- 171 G.K. Hamer and A.S. Perlin, *Carbohydr. Res.*, 49 (1976) 37.
- 172 N. Cyr, J.A. Schwarcz and A.S. Perlin, unpublished.
- 173 H. Dreeskamp, E. Sackmann and G. Stegmeier, *Ber. Bunsenges. Phys. Chem.*, 67 (1963) 860.
- 174 O. Yamamoto, W. Watabe and O. Kikuchi, *Mol. Phys.*, 17 (1969) 49.
- 175 F.J. Weigert and J.D. Roberts, *J. Phys. Chem.*, 73 (1969) 449.
- 176 R. Freeman, *J. Chem. Phys.*, 40 (1964) 3571.
- 177 K.M. Creceley, R.W. Creceley and J.H. Goldstein, *J. Phys. Chem.*, 74 (1970) 2680.
- 178 Y. Takeuchi and N. Dennis, *J. Am. Chem. Soc.*, 96 (1974) 3657; *Org. Magn. Reson.*, 7 (1975) 244.
- 179 J.A. Schwarcz, N. Cyr and A.S. Perlin, *Can. J. Chem.*, 53 (1975) 1872.
- 180 J.A. Pople and D.P. Santry, *Mol. Phys.*, 8 (1965) 1.
- 181 G.J. Karabatsos, C.E. Orzech, Jr. and N. Hsi, *J. Am. Chem. Soc.*, 88 (1966) 1817; G.J. Karabatsos and N. Hsi, *J. Am. Chem. Soc.*, 87 (1965) 2864.
- 182 R.U. Lemieux, T.L. Nagabushan and B. Paul, *Can. J. Chem.*, 50 (1972) 773.
- 183 L.T.J. Delbaere, M.N.G. James and R.U. Lemieux, *J. Am. Chem. Soc.*, 95 (1973) 7866.
- 184 M. Karplus, *J. Chem. Phys.*, 30 (1959) 11.
- 185 M. Karplus, *J. Phys. Chem.*, 64 (1960) 1793.
- 186 R. Wasylshen and T. Schaefer, *Can. J. Chem.*, 50 (1972) 2710.
- 187 D.E. Dorman, *Ann. N.Y. Acad. Sci.*, 222 (1973) 943.
- 188 R.U. Lemieux, *Ann. N.Y. Acad. Sci.*, 222 (1973) 915.
- 189 M.E. Rennekamp and C.A. Kingsbury, *J. Org. Chem.*, 38 (1973) 3959.
- 190 J. Feeney, P.E. Hansen and G.C.K. Roberts, *Chem. Commun.*, (1974) 465.
- 191 P.E. Hansen, J. Feeney and G.C.K. Roberts, *J. Magn. Reson.*, 17 (1975) 249.
- 192 A.S. Perlin, unpublished.
- 193 A.S. Perlin, N. Cyr, R.G.S. Ritchie and A. Parfondry, *Carbohydr. Res.*, 37 (1974) C1.
- 194 J.L. Marshall and R. Seiwel, *J. Magn. Reson.*, 15 (1974) 150.
- 195 D.E. Dorman and F.A. Bovey, *J. Org. Chem.*, 38 (1973) 1719.
- 196 J.T. Edward and C. Jitrangsri, *Can. J. Chem.*, 53 (1975) 3339.
- 197 K. Frei and H.J. Bernstein, *J. Chem. Phys.*, 38 (1963) 1216.
- 198 G.A. Gray, G.E. Maciel and P.D. Ellis, *J. Magn. Reson.*, 1 (1969) 407.
- 199 G.A. Gray, P.D. Ellis, D.D. Traficante and G.E. Maciel, *J. Magn. Reson.*, 1 (1969) 41.
- 200 F.J. Weigert and J.D. Roberts, cited in ref. 1, p. 370.
- 201 F.J. Weigert and J.D. Roberts, cited in ref. 1, p. 372.
- 202 J.L. Marshall and D.E. Müller, *J. Am. Chem. Soc.*, 95 (1973) 8305.
- 203 D. Doddrell, I. Burfitt, J.B. Grutzner and M. Barfield, *J. Am. Chem. Soc.*, 96 (1974) 1241.
- 204 H.H. Mantsch and I.C.P. Smith, *Biochem. Biophys. Res. Commun.*, 46 (1972) 808.
- 205 R.D. Lapper, H.H. Mantsch and I.C.P. Smith, *J. Am. Chem. Soc.*, 94 (1972) 6243.
- 206 W.G. Bentrude, K.C. Yee, R.D. Bertrand and D.M. Grant, *J. Am. Chem. Soc.*, 93 (1971) 797.
- 207 T. Brungaard and H.J. Jakobsen, *Tetrahedron Lett.*, (1972) 3353.
- 208 A.A. Borisenko, N.M. Sergayev, E. Ye. Nifant'ev and Yu. A. Ustynyuk, *Chem. Commun.*, (1972) 406.
- 209 G.A. Gray and S.E. Cremer, *J. Org. Chem.*, 37 (1972) 3458.
- 210 R.B. Wetzel and G.L. Kenyon, *Chem. Commun.*, (1973) 287.
- 211 R. Kaiser and A. Saika, *Mol. Phys.*, 15 (1968) 221.

- 212 J. Reuben and A. Demiel, *J. Chem. Phys.*, **44** (1966) 2114.
- 213 D.D. Giannini, P.A. Kollman, N.S. Bhacca and M.E. Wolff, *J. Am. Chem. Soc.*, **96** (1974) 5462.
- 214 J.B. Grutzner, M. Jautelat, J.B. Dence, R.A. Smith and J.D. Roberts, *J. Am. Chem. Soc.*, **92** (1970) 7107.
- 215 R.L. Lichter, D.E. Dorman and R. Wasylshen, *J. Am. Chem. Soc.*, **96** (1974) 930.
- 216 S. Berger and J.D. Roberts, *J. Am. Chem. Soc.*, **96** (1974) 6757.
- 217 W. Adcock, B.D. Gupta, W. Kitching, D. Doddrell and M. Geckle, *J. Am. Chem. Soc.*, **96** (1974) 7361.
- 218 M.H. Chisholm, H.C. Clark, L.E. Manzer and J.B. Stothers, *Chem. Commun.*, (1971) 1627; B.F. Mann, *Chem. Commun.*, (1971) 1173; W. Kitching, D. Prager, D. Doddrell, F.A.L. Anet and J. Krane, *Tetrahedron Lett.*, (1975) 759.
- 219 G.C. Levy and G.L. Nelson, *Carbon-13 Nuclear Magnetic Resonance for Organic Chemists*, Wiley-Interscience, New York, 1972, p. 76.
- 220 G.C. Levy and I.R. Peat, *J. Magn. Reson.*, **18** (1975) 500.
- 221 J.A. Lyerla, Jr. and G.C. Levy, in G.C. Levy (Ed.), *Topics in Carbon-13 NMR Spectroscopy*, Vol. 1, Wiley-Interscience, New York, 1974, p. 79.
- 222 K.F. Kuhlman, D.M. Grant and R.K. Harris, *J. Chem. Phys.*, **52** (1970) 3439.
- 223 A. Allerhand, D. Doddrell and R. Komoroski, *J. Chem. Phys.*, **55** (1971) 189.
- 224 S. Berger, F.R. Kreisel and J.D. Roberts, *J. Am. Chem. Soc.*, **96** (1974) 4348.
- 225 G.C. Levy, *Acc. Chem. Res.*, **6** (1973) 166.
- 226 F.H. Wehrli, *Chem. Commun.*, (1973) 379.
- 227 J. Schaeffer and D.F.S. Natusch, *Macromolecules*, **5** (1972) 416.
- 228 Y. Inoue, A. Nishioka and R. Chûjô, *J. Polym. Sci.*, **11** (1973) 2237.
- 229 G.C. Levy, J.D. Cargioli and F.A.L. Anet, *J. Am. Chem. Soc.*, **95** (1973) 1527.
- 230 G.C. Levy and R.A. Komoroski, private communication.
- 231 K. Bock and L.D. Hall, *Carbohydr. Res.*, **40** (1975) C3.
- 232 C.F. Brewer, D. Marcus, A.P. Grollman and H. Sternlicht, *Ann. N.Y. Acad. Sci.*, **222** (1973) 978.
- 233 R. Rowan III, J.A. McCammon and B.D. Sykes, *J. Am. Chem. Soc.*, **96** (1974) 4773.
- 234 G.C. Levy, *Chem. Commun.*, (1972) 768.
- 235 G.C. Levy, *J. Am. Chem. Soc.*, **95** (1973) 6117.
- 236 A. Allerhand, D.W. Cochran and D. Doddrell, *Proc. Natl. Acad. Sci., U.S.A.*, **67** (1970) 1093.
- 237 A. Allerhand and D. Doddrell, *J. Am. Chem. Soc.*, **93** (1971) 2777.
- 238 J.A. Lyerla, Jr. and G.C. Levy, in G.C. Levy (Ed.), *Topics in Carbon-13 NMR Spectroscopy*, Vol. 1, Wiley-Interscience, New York, 1974, p. 121.
- 239 G.C. Levy, R.A. Komoroski and J.A. Halstead, *J. Am. Chem. Soc.*, **96** (1974) 5456.
- 240 B. Casu, G. Gatti, N. Cyr and A.S. Perlin, *Carbohydr. Res.*, **41** (1975) C6.

KINETIC CARBON AND OTHER ISOTOPE EFFECTS IN CLEAVAGE AND FORMATION OF BONDS TO CARBON

ALFRED V. WILLI^a

Fachbereich Chemie, Universität Hamburg (West Germany)

I. INTRODUCTION AND SCOPE OF PRESENTATION

Early measurements of heavy atom kinetic isotope effects (KIEs) were mainly concerned with carbon-carbon bond cleavage in decarboxylations [1-7] and related reactions [8-10]. The work was performed for the purposes of demonstrating the existence of the KIE and comparison of experimental data with the Bigeleisen and Mayer theory [11]. Subsequent carbon KIE studies were carried out in the field of nucleophilic substitution [12-16]. In most cases, the position of isotopic substitution was at the central carbon atom of the alkyl halide, or at the attacking nucleophile (CN^-) in one example [15]. It was hoped that central carbon KIEs may serve as a criterion for distinction between mechanisms $\text{S}_{\text{N}}2$ and $\text{S}_{\text{N}}1$ [12]. Carbon-13 and carbon-14 KIEs would be equally useful for this purpose. Actually, the magnitude of the carbon KIE in a S_{N} reaction strongly depends on the mechanism [17]. The same refers to the α -hydrogen KIE which is a more sensitive criterion of distinction between mechanisms $\text{S}_{\text{N}}2$ and $\text{S}_{\text{N}}1$ [18]. For these reasons, it is useful to consider carbon and α -hydrogen KIEs together. This point of view becomes even more important when experimental data are compared with results of computer calculations of KIEs from force constants. Similarly, there is no special reason for the exclusion from this review of carbon-14 and other heavy atom KIE data, and such will be considered when required for completeness of the presentation. As far as S_{N} reactions are concerned, experimental data are available on primary chlorine-37 KIEs, also.

However, β - and γ -hydrogen KIEs are not within the scope of this review. If the position of isotopic substitution is separated from a reacting atom by more than one bond, the KIE mainly depends on the mechanism of transmission of electronic effects through several bonds. This is a different matter, and it will not be discussed here.

Reaction types discussed in this review are somewhat dependent on the particular interests of the writer. They include nucleophilic substitution, aromatic decarboxylation (of amino and hydroxy acids) in aqueous solution, and carbonyl addition reactions. In the section on aromatic decarboxylation, the emphasis is on the interplay of carbon and solvent hydrogen KIEs and the dependence of the KIE on the rate-determining step. The solvent hydrogen KIE is considered because it is really a primary isotope effect if hydrogen ion transfer is rate-determining.

^a Address for correspondence : Am Barkenkamp 8, D-2081 Hasloh, West Germany.

There is a connection between KIEs in nucleophilic substitution and carbonyl addition. In the latter reaction type, bond orbital hybridization at the central carbon atom changes from sp^2 to sp^3 . The reverse change occurs in a nucleophilic substitution. The section on carbonyl addition includes discussions of carbon, α -hydrogen, as well as other heavy atom KIEs. Some experimental data are available on primary oxygen and sulfur isotope effects in carbonyl additions.

II. CARBON, HYDROGEN, AND OTHER ISOTOPE EFFECTS IN NUCLEOPHILIC SUBSTITUTION

A. Isotope effect and mechanism

Bender and his associates found carbon-14 KIEs in the range of $k_{12}/k_{14} = 1.08$ to 1.14 in typical S_N2 reactions of methyl iodide with hydroxide ion, pyridine, and various aliphatic or aromatic amines [12,14]. On the other hand, in the S_N1 hydrolysis of *tert*-butyl chloride k_{12}/k_{14} was 1.027 [13]. The hydrolysis of methyl iodide in the presence of silver ion ($k_{12}/k_{14} = 1.086$) was considered a borderline case [12]. Furthermore, Kresge et al. [19] observed a small inverse carbon-13 isotope effect on the equilibrium constant of ionization of triphenylmethyl chloride in liquid sulfur dioxide, $K_{12}/K_{13} = 0.9833$ at 0° . It was suggested that carbon isotope effects are relatively high in S_N2 reactions and low or inverse in S_N1 reactions. This generalization was found to be valid for the results of more recent work by Stothers and Bourns [20] and Bron and Stothers [21] on the alcoholysis of 1-phenylethyl bromide.

The reverse is true for the α -hydrogen KIE; it is small in S_N2 reactions ($k_H/k_D < 1.05$ per D), and it is large in S_N1 reactions [18]. The high limit of k_H/k_D in "limiting" (S_N1) solvolysis depends on the leaving group. Therefore, the α -hydrogen KIE is a useful criterion of mechanism of S_N reactions. The limiting values of k_H/k_D for different leaving groups will be discussed in more detail in Section II.C. The magnitude of the carbon KIE is less well understood.

Recent work by Yukawa et al. [22] was concerned with a special mechanistic topic in the field of S_N reactions. With the aid of multiple isotope labeling, the Japanese authors succeeded in obtaining unambiguous, direct evidence for aryl participation in the solvolysis of 2-arylethyl arenesulfonates. This matter will be discussed in detail in Section II.E.

B. S_N2 Reactions

1. Isotope effects and transition state properties

Experimental data of carbon and α -hydrogen KIEs are collected in Tables 1 and 2. Table 2 also includes some data on chlorine KIEs. However, the main emphasis is on carbon and hydrogen KIEs. No attempt is made to achieve completeness as far as chlorine (and other) KIEs are concerned. Those entries of Table 1 that are based on separate kinetic experiments with methyl or methyl- d_3 halides refer to experiments in reaction

vessels with no or very little gas phase [23]. The reactions in Tables 1 and 2 may be divided into four groups with respect to the question of mechanism: (a) reactions of primary alkyl compounds (mostly halides) with relatively strong nucleophiles; (b) solvolyses of primary alkyl halides, sulfonic esters, or nitrates in water; (c) reactions of benzyl halides or sulfonic esters with various nucleophiles including water; and (d) reactions of α -phenylethyl halides with alkoxide ion.

Reactions of group (a) are clear-cut S_N2 processes [24]. The molecularity of a solvolysis reaction of group (b) cannot be discerned from the kinetic order since the solvent is present in large excess. However, there are good reasons for considering such a reaction of a primary alkyl compound a bimolecular process, as the tendency of primary alkyl groups to form carbonium ions is low. Final confirmation of the S_N2 mechanism is supplied by the α -deuterium KIE. (A detailed discussion of this matter will be given in Section II.C.)

The bimolecular nature of the mechanism of reactions of groups (c) and (d) is not so obvious. There are parallel reactions via the S_N1 pathway in several examples. Their relative contributions to the overall reaction will be discussed in a following paragraph.

2. Correlations of KIEs with free energy parameters

For 39 different S_N2 reactions, Seltzer and Zavitsas [25] found a correlation of values of k_H/k_D with $E_n - E_l$, the difference of nucleophilic constants [26] of entering and leaving groups. Different straight lines were obtained for reactions of methyl, ethyl, *n*-propyl, and isopropyl compounds, with much scattering and a few appreciable deviations. Another correlation was observed if values of carbon KIEs (k_{12}/k_{13}) were plotted versus $E_n - E_l$. Unfortunately, the data in the compilation of Seltzer and Zavitsas refer to different temperatures, and in some cases even to different solvents.

In the same way, values of k_H/k_D for reactions of methyl iodide with various nucleophiles may be correlated with ΔG^\ddagger values [27] of the reactions or with the Swain–Scott nucleophilic constants [28]. (In the latter case, it is advisable to apply *n* values for the halide ions given by Petty and Nichols [29].)

3. Computer calculations of KIEs

Kinetic isotope effects can be calculated from the isotopic partition function ratios of the transition state and the reactants on the basis of the Bigeleisen–Mayer theory [11]. The isotopic partition function ratios are dependent on the vibrational frequencies of reactants, transition state, and their isotopically substituted variants. Vibrational frequencies of stable compounds are available from spectroscopic measurements. However, they cannot be observed directly for transition states.

Preliminary attempts at theoretical calculations of KIEs were carried out by Miller [46] who assigned vibrational frequencies to the transition state by analogy with similar molecules. He also computed frequencies for simple three-center transition state models. Wolfsberg and Stern [47] calculated KIEs with the aid of an electronic computer, from vibrational force constants, on the basis of polyatomic models of reactants and transition

TABLE I

CARBON AND HYDROGEN KINETIC ISOTOPE EFFECTS IN S_N2 REACTIONS OF METHYL COMPOUNDS

Reaction	k_{12}/k_{13}	k_{12}/k_{14}	Solvent
$\text{CH}_3\text{I} + \text{S}_2\text{O}_3^{2-}$	1.071 ± 0.005		H_2O
$\text{CH}_3\text{I} + \text{CN}^-$			
$\text{CH}_3\text{I} + \text{N}_3^-$			
$\text{CH}_3\text{I} + \text{CH}_3\text{COO}^-$	1.0355 ± 0.0065	1.088 ± 0.010	H_2O 50% Diox.— H_2O
$\text{CH}_3\text{I} + \text{OH}^-$			
$\text{CH}_3\text{I} + \text{OH}^-$			
$\text{CH}_3\text{I} + ^*\text{I}^-$		1.102 ± 0.012	Benzene
$\text{CH}_3\text{I} + ^*\text{I}^-$			
$\text{CH}_3\text{I} + \text{Et}_3\text{N}$			
$\text{CH}_3\text{I} + n\text{-Pr}_3\text{N}$		1.142 ± 0.009	Benzene
$\text{CH}_3\text{I} + n\text{-Bu}_3\text{N}$			
$\text{CH}_3\text{I} + \text{pyridine}$			
$\text{CH}_3\text{I} + \text{pyridine}$			
$\text{CH}_3\text{I} + \text{pyridine}$			
$\text{CH}_3\text{I} + \text{pyridine}$			
$\text{CH}_3\text{I} + 2\text{-picoline}$			
$\text{CH}_3\text{I} + 2,6\text{-lutidine}$			
$\text{CH}_3\text{I} + \text{PhNMe}_2$			
$\text{CH}_3\text{I} + \text{PhNEt}_2$		1.117	MeOH
$\text{CH}_3\text{I} + o\text{-Me-C}_6\text{H}_4\text{NMe}_2$		1.120	MeOH
$\text{CH}_3\text{Br} + \text{CN}^-$		1.134	MeOH
$\text{CH}_3\text{Cl} + \text{CN}^-$	1.0815 ± 0.0068	1.086 ± 0.005	H_2O
$\text{CH}_3\text{I} + \text{H}_2\text{O}$	1.0711 ± 0.0078		H_2O
$\text{CH}_3\text{Br} + \text{H}_2\text{O}$			70% EtOH— $\text{H}_2\text{O} + \text{Ag}^+$
$\text{CH}_3\text{Cl} + \text{H}_2\text{O}$			
$\text{CH}_3\text{O}_3\text{S-C}_6\text{H}_4\text{-Me}(p) + \text{H}_2\text{O}$			
$\text{CH}_3\text{O}_3\text{S-Me} + \text{H}_2\text{O}$			
$\text{CH}_3\text{ONO}_2 + \text{H}_2\text{O}$			
$\text{CH}_3\text{Br} + \text{pyridine}$			
$\text{CH}_3\text{-O}_3\text{S-C}_6\text{H}_4\text{Me}(p) + \text{pyridine}$			
$\text{CH}_3\text{-O}_3\text{S-C}_6\text{H}_4\text{Me}(p) + \text{S}_2\text{O}_3^{2-}$			
$\text{CH}_3\text{-O}_3\text{S-Me} + \text{S}_2\text{O}_3^{2-}$			

^a Parts of this table have been reproduced by permission of the National Research Council of Canada from the Canadian Journal of Chemistry (ref. 32a, Table 1, and ref. 33, Table 1).

states of some S_N1 and S_N2 reactions, and applying the Schachtschneider program [48] for the calculation of vibrational frequencies from force constants. They demonstrated that KIEs are caused by force constant changes at the position of isotopic substitution which occur when going from reactant to transition state. With the aid of the Wolfsberg—Stern—Schachtschneider program, Willi [49] carried out model calculations of KIEs in S_N2 and S_N1 reactions of methyl iodide, in order to understand the causes of the KIE

Temp. (°C)	Ref.	k_{3H}/k_{3D}	Solvent	Temp. (°C)	Ref.
31	15	0.970 ± 0.003	H ₂ O	20	30
		0.913 ± 0.011	H ₂ O	20	31
		0.901 ± 0.007	H ₂ O	20	27
		0.882 ± 0.012	H ₂ O	40	27
11.4	15				
25	12				
25	12	1.10 ± 0.04	H ₂ O	20	25
		1.05 ± 0.01	MeOH	20	25
		0.877 ± 0.004	Benzene	50	32
		0.89	Benzene	50	32
25	12	0.896 ± 0.001	Benzene	50	32
		0.919 ± 0.002	Benzene	50	32
		0.891 ± 0.002	Nitrobenzene	50	32
		0.857 ± 0.002	2-Butanone	50	32
		0.882 ± 0.002	EtOH	50	32
		0.877 ± 0.002	Benzene	50	32
		0.876 ± 0.002	Benzene	50	32
48.5	14				
62.7	14				
62.7	14				
31	15				
31	15				
24.9	12	0.87	H ₂ O	70	33
		0.90	H ₂ O	79.9	33
		0.92	H ₂ O	89.8	33
		0.96	H ₂ O	70	33
		0.96	H ₂ O	60	33
		0.92	H ₂ O	100	33
		0.928	Nitrobenzene	50	32
		0.982	Nitrobenzene	50	32
		1.12	50% EtOH-H ₂ O	25	34
		1.11	50% EtOH-H ₂ O	25	34

and to gain insight into the nature of the transition states. Similar KIE calculations (with similar results) on reactions of benzyl compounds were done more recently by Sims et al. [50] and by Bron [51].

In the calculations on reactions of methyl iodide, the CH₃ group in the transition state I...CH₃...Y is considered to be planar, with carbon having sp^2 orbitals and the CH₃ plane being perpendicular to the straight line connecting the I, C, and Y atoms. Values of transition state force constants of C-H stretching, H-C-H bending, and C-H out-of-plane bending may be taken from related molecules with sp^2 carbon atoms.

TABLE 2

CARBON AND HYDROGEN ISOTOPE EFFECTS IN NUCLEOPHILIC SUBSTITUTION REACTIONS OF ALKYL AND ARYLALKYL COMPOUNDS

Reaction	k_{12}/k_{13}	k_{12}/k_{14}	Solvent
CH ₃ CH ₂ Br + S ₂ O ₃ ²⁻			
CH ₃ CH ₂ CH ₂ Br + S ₂ O ₃ ²⁻			
CH ₃ CH ₂ I + pyridine			
CH ₃ CH ₂ Br + pyridine			
CH ₃ CH ₂ CH ₂ Br + pyridine			
(CH ₃) ₂ CH-Br + pyridine			
PhCH ₂ Cl + CN ⁻		1.061 ± 0.003	80% EtOH-H ₂ O
PhCH ₂ Cl + CN ⁻		1.102	80% Dioxane-H ₂ O
<i>m</i> -Cl-C ₆ H ₄ CH ₂ -Cl + CN ⁻			
<i>p</i> -Cl-C ₆ H ₄ CH ₂ -Cl + CN ⁻		1.106	80% Dioxane-H ₂ O
<i>p</i> -Me-C ₆ H ₄ CH ₂ -Cl + CN ⁻		1.090	80% Dioxane-H ₂ O
<i>p</i> -MeO-C ₆ H ₄ CH ₂ -Cl + CN ⁻		1.012	80% Dioxane-H ₂ O
PhCH ₂ Cl + *Cl ⁻			
PhCH ₂ Cl + *Cl ⁻			
3-Thenyl chloride + *Cl ⁻			
2-Thenyl chloride + *Cl ⁻			
PhCH ₂ Cl + H ₂ O		1.085 ± 0.007	Acetone-H ₂ O
<i>p</i> -Me-C ₆ H ₄ CH ₂ Cl + H ₂ O		1.061 ± 0.007	Acetone-H ₂ O
PhCH ₂ Cl + N ₃ ⁻		1.130 ± 0.007	Acetone-H ₂ O
<i>p</i> -Me-C ₆ H ₄ CH ₂ Cl + N ₃ ⁻		1.096 ± 0.007	Acetone-H ₂ O
PhCH ₂ Br + MeO ⁻	1.0531 ± 0.0002		MeOH
PhCH(CH ₃)Br + EtO ⁻	1.0359 ± 0.0007		EtOH
<i>p</i> -CF ₃ -C ₆ H ₄ CH ₂ -O ₃ S-C ₆ H ₄ Br (<i>p</i>), solvolysis			
<i>p</i> -O ₂ N-C ₆ H ₄ CH ₂ -O ₃ S-C ₆ H ₄ Br (<i>p</i>), solvolysis			

DMF = Dimethylformamide

ME = 2-methoxyethanol

It is far more difficult to assign values to the force constants referring to reacting bonds, namely those of C—I and C—Y stretching, the interaction between these stretches, and H—C—I, H—C—Y bending. In an attempt at complete calculation of the KIEs in the reactions of methyl iodide with labeled iodide ion and cyanide ion, Willi [52] assumed the force constants f_{CI} , f_{CC} , f_{HCl} , and f_{HCC} to be half as large as in stable molecules. Values of the interaction force constants f_{12} were obtained from a one-dimensional, semi-empirical model of the energy barrier. Results for 25° were: $k_{12}/k_{13} = 1.060$, $k_{3\text{H}}/k_{3\text{D}} = 1.125$ for CH₃I + *I⁻; and $k_{12}/k_{13} = 1.055$, $k_{3\text{H}}/k_{3\text{D}} = 1.051$ for CH₃I + CN⁻. Agreement with experimental data is fair (see Table 1), when it is considered that the calculations are based on crude estimates of the transition state bending force constants.

Temp. (°C)	Ref.	$k_2\text{H}/k_2\text{D}$	Solvent	Temp. (°C)	Ref.
		1.068 ± 0.01	50% EtOH–H ₂ O	25	35
		1.075 ± 0.01	50% EtOH–H ₂ O	25	35
		0.967	Nitrobenzene	50	32
		0.967	Nitrobenzene	50	32
		0.960	Nitrobenzene	50	32
		0.958 ^a	Nitrobenzene	50	32
50	38				
40	39	1.023 ± 0.007	55% ME–H ₂ O	40	37
		0.995 ± 0.002	55% ME–H ₂ O	40	37
40	39				
40	39	1.261 ± 0.017	55% ME–H ₂ O	40	37
40	39				
		1.05 ± 0.03	DMF	40.1	41
		1.084 ± 0.012	DMF	35	42
		1.09 ± 0.03	DMF	40.1	41
		1.08 ± 0.03	DMF	40.1	41
60	43	1.006 ± 0.014	Acetone–H ₂ O	60	43
60	43	0.996 ± 0.014	Acetone–H ₂ O	60	43
60	43	1.033 ± 0.014	Acetone–H ₂ O	60	43
60	43	1.004 ± 0.014	Acetone–H ₂ O	60	43
0	16, 44				
0	16, 44				
		1.028 ± 0.001	90% EtOH–H ₂ O	25	45
		1.004 ± 0.001	90% EtOH–H ₂ O	25	25

^a $k_{\text{H}}/k_{\text{D}}$

However, a more important objective of the model calculations was to arrive at a better understanding of the dependence of the KIE on the transition state force constants. Extended studies of transition state models of S_N2 reactions led to the following results [49]. (a) The methyl carbon KIE mainly depends on the relative degrees of bond-breaking and bond-making in the transition state, as measured by the force constant ratio $f_{\text{CY}}/f_{\text{CI}}$ (k_{12}/k_{13} would be at its maximum value if $f_{\text{CY}} = f_{\text{CI}}$, e.g. if the transition state is “symmetric”). (b) It depends also on the curvature of the potential energy barrier as measured by $f_{\text{CI}} f_{\text{CY}} - f_{12}^2 = d < 0$ (the more negative d the higher k_{12}/k_{13}). (c) The stiffness of the transition state as measured by the sum of the bending force constants $f_{\text{HCl}} + f_{\text{HCY}}$ (k_{12}/k_{13} is decreased by an increase of $f_{\text{HCl}} + f_{\text{HCY}}$, though the change is relatively weak). The α -hydrogen KIE is strongly dependent on the sum

of the bending force constants $f_{\text{HCl}} + f_{\text{HCY}}$ ($k_{3\text{H}}/k_{3\text{D}}$ is decreased by an increase of $f_{\text{HCl}} + f_{\text{HCY}}$). The influence of f_{CI} , f_{CY} , and f_{12} is relatively small. On the other hand, the influence of the curvature of the energy barrier is not negligible (the stronger the curvature the smaller is $k_{3\text{H}}/k_{3\text{D}}$).

The entering group KIE was studied for the case of the reaction of methyl iodide with hydroxide ion. An increase of f_{CO} and/or a decrease of f_{CI} cause the oxygen KIE, k_{16}/k_{18} , to decrease. The dependence on $f_{\text{HCl}} + f_{\text{HCY}}$ is small.

Several series of calculations were carried out by the writer [49] in which the curvature parameter d and the bending force constants were kept constant while f_{CY} was increased and f_{CI} was decreased simultaneously, in order to vary the transition state model from reactant-like to product-like. It was found that the primary carbon KIE at first increases, then passes through a maximum value for the "symmetric" transition state (with equal degrees of bond-making and bond-breaking), and finally decreases. In the same series, the entering group KIE decreases in a monotonous manner and the α -hydrogen KIE remains almost constant. Sims et al. [50] report similar results of carbon and α -hydrogen KIE calculations for $\text{S}_{\text{N}}2$ reactions of benzyl chloride. Furthermore they find a monotonous increase of the leaving group (chlorine-37) KIE when the transition state model is varied from reactant-like to product-like. (In these calculations, the complete transition state model may be successfully replaced by an abbreviated model applying the cut-off procedure by Stern and Wolfsberg [53].)

Experimental examples of variable chlorine-37 KIEs have been reported by Bare et al. [54] for several $\text{S}_{\text{N}}2$ reactions of methyl chloride in 1,2-dimethoxyethane solution at 25° . In the reactions with triethylamine and *N*-ethyl-4-*tert*-butylpiperidine k_{35}/k_{37} is 1.0064, but in the reaction with NaI it is 1.0086, indicating a higher degree of C-Cl bond cleavage in the transition state of the latter reaction.

As soon as experimental KIE data on reactions of methyl iodide with various nucleophiles became available, further calculations were done by Willi and Won [27,30,31] with the purpose of gaining information on the transition states. It was hoped to obtain "experimental" values of $f_{\text{HCl}} + f_{\text{HCY}}$ by adjusting the sum of transition state bending force constants in the calculations to fit the experimental α -deuterium KIE. The relative values of f_{CY} and f_{CI} would then be adjusted to fit the experimental carbon KIE; the adjusted values would supply information on reacting bond orders in the transition states. These calculations could not be done without reasonable assumptions about the curvature of the potential energy barrier. Willi and his group applied three different models of an (one-dimensional) energy barrier:

(a) It is assumed (arbitrarily) that $f_{\text{CY}} = f_{\text{CI}} = 0.2 \text{ mdyn/\AA}$ and $f_{12} = 1.5 \text{ mdyn/\AA}$.

(b) The energy barrier is approximated by a truncated parabola (with additional consideration of restoring forces between C and I as well as C and Y) with a height corresponding to the experimental ΔG^\ddagger value and a width 10% of the sum of the CI and CY equilibrium bond lengths.

(c) The energy barrier is described with the aid of the semi-empirical model [52] mentioned above. This model includes the possibility of an asymmetric transition state.

TABLE 2b
CHLORINE ISOTOPE EFFECTS IN S_N2 REACTIONS

Reaction	k_{35}/k_{37}	Solvent	Temp. (°C)	Ref.
$\text{CH}_3\text{CH}_2\text{CH}_2\text{CH}_2\text{Cl} + \text{MeO}^-$	1.0074	MeOH	40	36
$\text{CH}_3\text{CH}_2\text{CH}_2\text{CH}_2\text{Cl} + n\text{-BuS}^-$	1.0081	MeOH	40	36
$\text{PhCH}_2\text{Cl} + \text{CN}^-$	1.0072 ± 0.0002	80% Dioxane– H_2O	30	40
$p\text{-Cl-C}_6\text{H}_4\text{CH}_2\text{Cl} + \text{CN}^-$	1.0060 ± 0.0002	80% Dioxane– H_2O	30	40
$p\text{-O}_2\text{N-C}_6\text{H}_4\text{CH}_2\text{Cl} + \text{CN}^-$	1.0057 ± 0.0002	80% Dioxane– H_2O	30	40
$p\text{-Me-C}_6\text{H}_4\text{CH}_2\text{Cl} + \text{CN}^-$	1.0079 ± 0.0003	80% Dioxane– H_2O	30	40
$p\text{-MeO-C}_6\text{H}_4\text{CH}_2\text{Cl} + \text{CN}^-$	1.0078 ± 0.0004	80% Dioxane– H_2O	30	40
$\text{PhCH}_2\text{Cl} + \text{MeO}^-$	1.0080	MeOH	20	36
$p\text{-O}_2\text{N-C}_6\text{H}_4\text{CH}_2\text{Cl} + \text{MeO}^-$	1.0076	MeOH	20	36

The barrier height is again set equal to ΔG^\ddagger and the shape of the barrier is described with the aid of a Johnston [55] type equation. (The energy difference between the reactant side and the product side of the barrier is set equal to a reasonable estimate. At the present time, experimental ΔG^\ddagger values are not available for most S_N2 reactions.)

Unfortunately, there are very few examples with experimental data on α -deuterium as well as carbon KIEs for the same S_N2 reaction. For one of these, the reaction of methyl iodide with cyanide ion, the experimental k_{12}/k_{13} value known today (Table 1) is a little higher than any calculated value based on a reasonable set of transition state force constants [49]. Therefore, the calculations had to be done in comparison to experimental deuterium KIEs alone.

For the reaction of methyl iodide with cyanide ion, calculations [31,52] were carried out with energy barrier models (a), (b), and (c). The sum of bending force constants was

TABLE 3
CALCULATED ISOTOPE EFFECTS FOR THE REACTION OF METHYL IODIDE WITH
CYANIDE ION (Refs. 31 and 52) ^a

Barrier model	f_{Cl}	f_{CC}	f_{12}	f_{HCl}	f_{HCC}	$k_{3\text{H}}/k_{3\text{D}}$ (25°)	$A_{\text{H}}/A_{\text{D}}$	$E_{\text{a}}^{\text{H}} - E_{\text{a}}^{\text{D}}$ cal	k_{12}/k_{13} (10°)
a	0.2	0.2	1.5	0.300	0.410	0.927	1.131	118	1.050
b	-0.8	0.2	1.8	0.300	0.395	0.925	1.124	116	1.054
c	1.12	2.25	3.95	0.300	0.390	0.927	1.124	114	1.052
Experimental results						0.926	1.124	116	

^a Stretching force constants are given in mdyne/Å and bending force constants are given in mdyne Å. Reproduced (in part) from ref. 31, Table 2, (and additional data) by permission of the American Chemical Society.

adjusted in such a way that the calculated deuterium KIE agreed with the experimental result at 25°. The adjusted value of $f_{\text{HCl}} + f_{\text{HCl}}^{\text{D}}$ (Table 3) depended very little on the choice of barrier model. An independent check of the meaningfulness of the models was possible by examining the temperature dependence of the deuterium KIE. Calculations were done for different temperatures, and (according to a suggestion by Wolfsberg and Stern [47]) Arrhenius parameters of the calculated KIE (in the temperature range of the experimental data) were computed with the aid of the least squares method. There was excellent agreement between experimental and calculated Arrhenius parameters for each of the three barrier models (Table 3).

Similar KIE calculations in comparison to experimental data of $k_{3\text{H}}/k_{3\text{D}}$ were performed for the reactions of methyl iodide with labeled iodide ion [49] (barrier models a and b), thiosulfate ion [30] (models a and c), and azide ion [27] (models a and c). There was also very little dependence of the adjusted value of $f_{\text{HCl}} + f_{\text{HCl}}^{\text{D}}$ on the choice of the barrier model in these examples. If $f_{\text{HCl}} + f_{\text{HCl}}^{\text{D}}$ was adjusted to fit the experimental deuterium KIE at one temperature, excellent agreement between experimental and calculated KIEs was reached over the whole temperature range of the experimental data for the latter two reactions. (However, the temperature dependence test is not so meaningful in these examples since the experimental data extend over temperature ranges of 20° or 30° only. On the other hand, the temperature range of the data for the reaction $\text{CH}_3\text{I} + \text{CN}^-$ extends over 40°.)

In Table 4 are collected the transition state bending force constants (involving one reacting bond) for different reactions. The Table also contains bending force constants for the corresponding bonds in stable molecules [27]. There is no relationship between the nucleophilic constant of Y^- (which decreases in the sequence $\text{S}_2\text{O}_3^{2-} > \text{CN}^- > \text{I}^- > \text{N}_3^-$) and the transition state bending force constant, $f_{\text{HCl}}^{\text{D}}$, or the ratio, $f_{\text{HCl}}^{\text{D}}/F_{\text{HCl}}^{\text{D}}$.

For a better understanding of these matters, it is necessary to look at the question whether there is a relationship between the isotope effect in different reactions and

TABLE 4

COMPARISON OF TRANSITION STATE BENDING FORCE CONSTANTS (Ref. 27) ^a

Reaction	Transition state		Stable molecule $F_{\text{HCl}}^{\text{D}}$ mdyn Å	$f_{\text{HCl}}^{\text{D}}/F_{\text{HCl}}^{\text{D}}$
	$f_{\text{HCl}} + f_{\text{HCl}}^{\text{D}}$ mdyn Å	$f_{\text{HCl}}^{\text{D}}$ mdyn Å		
$\text{CH}_3\text{I} + \text{S}_2\text{O}_3^{2-}$	0.595	0.300	0.525	0.572
$\text{CH}_3\text{I} + \text{CN}^-$	0.690	0.395	0.64	0.616
$\text{CH}_3\text{I} + \text{I}^-$	0.590	0.295	0.55	0.537
$\text{CH}_3\text{I} + \text{N}_3^-$	0.615	0.320	0.681	0.470

^a Reproduced from ref. 27, Table 3, by permission of the American Chemical Society.

the sum of transition state bending force constants, $f_{\text{HCl}} + f_{\text{HCY}}$. Actually, sample calculations with the same value of $f_{\text{HCl}} + f_{\text{HCY}}$ lead to different results of $k_{3\text{H}}/k_{3\text{D}}$ for transition states with different groups Y. For example, a higher value of $k_{3\text{H}}/k_{3\text{D}}$ has been calculated for the reaction with CN^- than for the reaction with N_3^- . Therefore, $f_{\text{HCl}} + f_{\text{HCY}}$ must be adjusted to a higher value in order to obtain agreement with the experimental isotope effect in the reaction with CN^- , even though the experimental value of $k_{3\text{H}}/k_{3\text{D}}$ is lower in the reaction with N_3^- . Obviously, the influence of masses and the geometry of Y is not negligible, as the KIE depends on the particular way in which the motions of H(D) and Y are coupled in some of the bending vibrational modes of the transition state. The influence of these factors is substantial in comparison to the relatively small range of observed values of $k_{3\text{H}}/k_{3\text{D}}$ in $\text{S}_{\text{N}}2$ reactions. On the basis of these considerations, and the results of sample calculations, a good correlation between $k_{3\text{H}}/k_{3\text{D}}$ and values of $f_{\text{HCl}} + f_{\text{HCY}}$ would not be expected for different transition states. The same applies to correlations between $k_{3\text{H}}/k_{3\text{D}}$ and the nucleophilic constant of Y^- , which affects the reacting bond order and transition state force constants involving reacting bonds.

A very good correlation between α -deuterium KIE and reactivity of Y^- does exist [25,27], however. Consequently, the models applied in these calculations cannot be fully adequate. In other words, matters appear to be much more simple than they ought to be on the basis of the model calculations. It will probably be necessary to consider solvation of reactants and transition states. The influence of masses and geometry of entering and leaving groups on the transition state bending frequencies will be smaller if these groups are solvated by clusters of associated water molecules. Solvation causes some restriction of the motions of I and Y in the transition state. (At the present time, it would not be worthwhile to discuss detailed models of solvated reactants and transition states, as the calculations have not yet been done.)

A similar conclusion referring to solvation of reactant was arrived at in a comparison of experimental ($k_{12}/k_{13} = 1.0149 \pm 0.0020$ at 11.4° [15]) and calculated values of the cyanide-C-13 KIE in the reaction of methyl iodide with cyanide ion [49]. It was suggested that the rotation of cyanide ion in aqueous solution is strongly hindered by solvation.

There is more direct evidence concerning the special role of solvation in $\text{S}_{\text{N}}2$ reactions in solution. As found by Bohme and Young [56], applying the flowing afterglow technique, the reactions of methyl chloride with hydroxide or alkoxide ions in the gas phase are fast. Experimental rate constants are of the same order of magnitude as calculated collision rate constants. The same is probably true for many other reactions of methyl halides with charge-localized anions in the gas phase. However, the rate of the gas phase reaction of methyl chloride with alkoxide ion is strongly decreased if the anion is hydrogen-bonded to one alcohol molecule. Furthermore, reactions of methyl halides with anions in solution are slow; they possess activation energies in the approximate range of 15–25 kcal. The rates of these reactions in solution are strongly dependent on the solvation of the anion [57]. In future calculations of KIEs, solvation is to be considered. In the transition state models, several solvent molecules must be bonded directly to the

entering nucleophile. According to the principle of microscopic reversibility, the leaving group in the transition state must be solvated also. Another way of describing the transition state of the reaction of a methyl halide with an anion would be as follows: the methyl halide and the attacking anion are in the same solvent cage, and the entering and leaving groups are strongly bonded to the walls of the cage.

It is expected that the solvent dependence of the KIE is not negligible in reactions of alkyl halides with amines. This has been confirmed by Leffek and Matheson [32] for the reaction of methyl iodide with pyridine in different solvents (Table 1). In these reactions, the relative degrees of bond cleavage and formation in the transition state may be dependent on the solvent.

4. Isotope effects in S_N2 reactions of benzyl and α -phenylethyl compounds

Examination of KIEs in reactions of benzyl and α -phenylethyl compounds must be done with some caution, since borderline (between S_N2 and S_N1) behavior has been observed in many examples. In a study of α -deuterium KIEs in reactions of benzyl chlorides with cyanide ion, Willi et al. [37] found that a substantial fraction of the overall reaction is first order solvolysis (via S_N2 or S_N1). In a treatment of the kinetic data, it is necessary to apply eqn. (1),

$$-d[\text{ArCH}_2\text{Cl}]/dt = k_2[\text{ArCH}_2\text{Cl}][\text{CN}^-] + k_1[\text{ArCH}_2\text{Cl}] \quad (1)$$

which, upon integration, leads to eqn. (2)

$$\ln \frac{A_0[A + (k_1/k_2) + B_0 - A_0]}{A[(k_1/k_2) + B_0]} = [B_0 - A_0 + (k_1/k_2)]k_2t \quad (2)$$

where $A = [\text{ArCH}_2\text{Cl}]$; $A_0 = [\text{ArCH}_2\text{Cl}]_0$; $B_0 = [\text{CN}^-]_0$

The rate constant k_1 may be determined in separate kinetic experiments in the same solvent mixture at the same ionic strength (addition of sodium perchlorate instead of sodium cyanide).

In the reaction of *p*-methylbenzyl chloride in the presence of CN^- , almost 60% of the overall reaction is caused by first order solvolysis, and the KIE of the additional reaction with CN^- (if treated as a second order process) is $k_{2\text{H}}/k_{2\text{D}} = 1.26$. If the overall reaction is treated as a pure first order process, then $k_{2\text{H}}/k_{2\text{D}} = 1.31$ which is equal to the value suggested by Shiner [18a] for the "limiting" S_N1 reaction. These findings indicate a carbonium ion (or ion pair) mechanism also in the reaction with CN^- . With the aid of Hammett's rule [58, 59] (utilizing σ^+ constants of Brown and Okamoto [59]), it is possible to crudely estimate the contribution of the carbonium ion pathway to the reactions of the other benzyl chlorides. For the reactions of benzyl chloride with CN^- and solvent, the possibility that about 10% of the overall reaction passes through a carbonium ion intermediate cannot be excluded. The corresponding reactions of *m*-chlorobenzyl chloride, however, may safely be considered as pure S_N2 processes, and the α -deuterium KIEs are equal to unity within experimental error [37] (Table 2). These conclusions concerning the contributions of different mechanisms refer only to the solvent

system used by Willi and his associates. It is well known that the relative contributions of the S_N2 and S_N1 mechanisms to the solvolyses of benzyl chlorides are strongly dependent on the solvent [45,60]. According to the results obtained by Raaen et al. [43] for the reactions of benzyl chlorides with water and azide ion in aqueous acetone, k_{2H}/k_{2D} is almost equal to unity. Consequently, the mechanism must be "pure" S_N2 . Under these conditions, the carbon KIEs are high ($k_{12}/k_{14} = 1.06$ to 1.13 , see Table 2).

In the chlorine KIE experiments reported by Hill and Fry [40] for reactions in 80% aqueous dioxane, however, the kinetic data (first order reactions – in some cases almost equal rates with CN^- and $S_2O_3^{2-}$) indicate parallel S_N2 and S_N1 reactions, with a dominating contribution from the S_N1 mechanism in the reaction of *p*-methoxybenzyl chloride. Accordingly, the carbon KIE (measured by Pearson and Fry [39]) is relatively low in the reaction of the *p*-methoxy compound. Chlorine KIEs (k_{35}/k_{37}) appear to be approximately 1.006 for S_N2 and 1.008 for S_N1 reactions. Shiner et al. [45] have presented evidence that the solvolyses of *p*-trifluoromethylbenzyl and *p*-nitrobenzyl sulfonic esters are pure S_N2 reactions since the α -deuterium KIEs are low and almost independent of solvent. In the reaction of α -phenylethyl bromide with ethoxide ion, the carbon KIE is relatively low [16,44] (Table 2), suggesting a possible contribution of the carbonium ion pathway parallel to the S_N2 mechanism.

C. Isotope effects in limiting (S_N1) solvolysis

1. Experimental data

Owing to the experimental difficulties, reported data on carbon and other heavy atom KIEs in solvolysis reactions are scarce (Table 5). The total number of papers on carbon KIEs published prior to 1970 is about 250, and nearly 40% of them are concerned with decarboxylations or decarbonylations [17]. Relatively little additional work has been done since then. Carbon KIEs are low or even inverse in typical S_N1 solvolyses such as those of *tert*-butyl chloride [13] or triphenylmethyl chloride [19]. The solvolysis of methyl iodide in the presence of silver ion is probably not a S_N1 process ($k_{12}/k_{14} = 1.09$) [12].

Much more work has been done on deuterium KIEs in solvolysis reactions, mainly by Shiner [18a], Robertson [33], Streitwieser [61], and their associates. It was found that in solvolysis reactions under suitable conditions, the α -deuterium KIE is appreciably larger than S_N2 reactions (Table 6). If the nucleophilic power of the solvents is sufficiently low, the α -deuterium KIE is nearly independent of solvent, which suggests that the mechanism must be S_N1 . In this manner, α -deuterium KIEs supply information on the mechanism of the reactions. Knowledge of mechanism is advantageous in a discussion of carbon and other heavy atom KIEs. Therefore, α -deuterium KIEs will be considered first.

2. α -Deuterium KIEs in solvolysis

In 1957, it was discovered that the α -deuterium KIE in the acetolysis of cyclopentyl

TABLE 5
CARBON ISOTOPE EFFECTS IN SOLVOLYSIS REACTIONS

Reactant	k_{12}/k_{13}	k_{12}/k_{14}	Solvent	Temp. (°C)	Ref.
Ph ₃ CCl (ratio of equilibrium constants)	0.9833 ± 0.0032		Liquid SO ₂	0	19
(CH ₃) ₃ C-Cl		1.027 ± 0.015	60% Dioxane-H ₂ O	24.8	13
<i>p</i> -MeO-C ₆ H ₄ CH ₂ Cl		1.034	80% Dioxane-H ₂ O	40	17
<i>p</i> -MeO-C ₆ H ₄ CH ₂ Cl addn. of 0.1 M NaClO ₄		1.009	80% Dioxane-H ₂ O	40	17
<i>p</i> -Me-C ₆ H ₄ CH ₂ Cl		1.057	80% Dioxane-H ₂ O	40	17
Ph-CH ₂ Cl		1.064	80% Dioxane-H ₂ O	40	17
<i>p</i> -Cl-C ₆ H ₄ CH ₂ Cl		1.071	80% Dioxane-H ₂ O	40	17
<i>p</i> -Me-C ₆ H ₄ CH(CH ₃)Br	0.9995 ± 0.0005		MeOH	0	21
Ph-CH(CH ₃)Br	1.0050 ± 0.0004		MeOH	0	21
<i>p</i> -Br-C ₆ H ₄ CH(CH ₃)Br	1.0127 ± 0.0006		MeOH	0	21

TABLE 6

DEPENDENCE OF THE α -DEUTERIUM ISOTOPE EFFECT ON REACTANT AND SOLVENT ^a

Solvolysis of	Solvent	Temp. (°C)	$k_H/k_{\alpha-D}$ per D	Ref.
PhCH(CH ₃)Cl	80% EtOH-H ₂ O	25	1.146	63
	70% EtOH-H ₂ O	25	1.149	63
	60% EtOH-H ₂ O	25	1.151	63
	50% EtOH-H ₂ O	25	1.153	63
	97% CF ₃ CH ₂ OH-H ₂ O	25	1.158	63
<i>m</i> -Br-C ₆ H ₄ CH(CH ₃)Cl	50% EtOH-H ₂ O	25	1.133	63
	9% Acetone-H ₂ O	25	1.149	63
<i>p</i> -F-C ₆ H ₄ CH(CH ₃)Cl	60% EtOH-H ₂ O	25	1.150	63
<i>m</i> -Me-C ₆ H ₄ CH(CH ₃)Cl	70% EtOH-H ₂ O	25	1.147	63
<i>p</i> -Me-C ₆ H ₄ CH(CH ₃)Cl	80% EtOH-H ₂ O	25	1.150	63
<i>p</i> -PhO-C ₆ H ₄ CH(CH ₃)Cl	95% EtOH-H ₂ O	25	1.149	63
<i>p</i> -MeO-C ₆ H ₄ CH(CH ₃)Cl	93% Acetone-H ₂ O	25	1.147	63
PhCH ₂ Cl	55% ME-H ₂ O	50	1.014	37
	H ₂ O	65	1.048	60
<i>p</i> -Me-C ₆ H ₄ CH ₂ Cl	55% ME-H ₂ O	50	1.034	37
	80% EtOH-H ₂ O	70	1.041	64
	50% EtOH-H ₂ O	45	1.080	63
	H ₂ O	25	1.132	60
	70% CF ₃ CH ₂ OH-H ₂ O	25	1.140	63
	94% CF ₃ CH ₂ OH-H ₂ O	25	1.145	63
	97% CF ₃ CH ₂ OH-H ₂ O	25	1.143	63
	80% EtOH-H ₂ O	45	1.09	64
	80% CF ₃ CH ₂ OH-H ₂ O	30	1.16	64
2,4,6-Me ₃ C ₆ H ₂ CH ₂ Cl	80% EtOH-H ₂ O	45	1.15	64
	80% CF ₃ CH ₂ OH-H ₂ O	45	1.126	63
2,4,6-(<i>t</i> -Bu) ₃ C ₆ H ₂ CH ₂ Cl	93% Acetone-H ₂ O	25	1.122	63
<i>p</i> -PhO-C ₆ H ₄ CH(CH ₃)Br	80% EtOH-H ₂ O	25	1.085	63
PhCH(CH ₃)Br	5% Acetone-H ₂ O	25	1.053	45
<i>p</i> -O ₂ N-C ₆ H ₄ CH(CH ₃)Br	95% EtOH-H ₂ O	25	1.060	45
PhCH ₂ -O ₃ S-C ₆ H ₄ Br (<i>p</i>)	90% EtOH-H ₂ O	25	1.074	45
	80% EtOH-H ₂ O	25	1.159	45
	80% CF ₃ CH ₂ OH-H ₂ O	25	1.173	45
	97% CF ₃ CH ₂ OH-H ₂ O	25	1.122	63
	50% CF ₃ CH ₂ OH-H ₂ O	25	1.140	63
	70% CF ₃ CH ₂ OH-H ₂ O	25	1.22	65
(CH ₃) ₂ CH-O ₃ S-C ₆ H ₄ Br (<i>p</i>)	CF ₃ COOH	25	1.114	68
PhCH ₂ -ONO ₂	H ₂ O	64	0.988	68
<i>m</i> -CF ₃ -C ₆ H ₄ CH ₂ ONO ₂	H ₂ O	70	1.119	68
<i>p</i> -Cl-C ₆ H ₄ CH ₂ ONO ₂	H ₂ O	60	1.113	68
<i>m</i> -MeO-C ₆ H ₄ CH ₂ ONO ₂	H ₂ O	56	1.177	68
<i>p</i> -Me-C ₆ H ₄ CH ₂ ONO ₂	H ₂ O	30	1.181	68
2,6-Me ₂ C ₆ H ₃ CH ₂ ONO ₂	H ₂ O	20	1.187	68
Cyclopentyl nitrate	H ₂ O	60		

^a Essential parts of this table have been reproduced from ref. 45, Table 1, and ref. 63b, Table 4, by permission of the American Chemical Society.

References pp. 280-283

tosylate is $k_H/k_D = 1.15$ [61,62]. Similar results were obtained for the acetolyses of other secondary tosylates or *p*-bromobenzenesulfonates [62]. It was concluded that these high values of k_H/k_D were representative of the S_N1 mechanism. It was assumed that they were a consequence of almost complete C—O bond cleavage in the transition state, whose H—C—O bending frequencies have become much smaller than those of the reactant. In subsequent investigations [63], it was found that k_H/k_D increases with decreasing nucleophilicity and increasing ionizing power of the solvent. It reaches a high limit in solvents with sufficiently low nucleophilicity and high ionizing power (Table 6). For all chlorides, the limiting value is $k_H/k_D = 1.15 \pm 0.01$ (per D); there is no dependence on structure or solvent. For the solvolysis reactions of the compounds $Z-C_6H_4CH(CH_3)Cl$ in 50% aqueous ethanol at 25°, k_H/k_D is between 1.151 and 1.157 if $Z = p-CH_3O$, $p-C_6H_5O$, $p-CH_3$, $p-F$, $m-CH_3$, or H [63]. It is obvious that the limiting value of the α -deuterium KIE refers to "limiting" S_N1 solvolysis — noticeable contributions of parallel reactions with rate-determining nucleophilic attack of solvent being absent. The limiting value of k_H/k_D merely depends on the leaving group [64–67] (Tables 6 and 7). The values for the solvolyses of *p*-methylbenzyl, *o,o'*-dimethylbenzyl, and cyclopentyl nitrates are 1.18 [68]. It is not certain, however, that this is the maximum value for nitrates. (The value of 0.988 for *m*-trifluoromethylbenzyl nitrate refers to an "almost pure" S_N2 mechanism.) Examples are given in Table 7 for solvolyses of 3-pentyn-2-yl [67] and 2-adamantyl [69,70] compounds.

The theoretical explanation [66] of these findings is based on the assumption that the bond between the central carbon and the leaving group is more or less completely broken in the transition state of the S_N1 reaction. Consequently, the isotopic partition function ratio of the transition state must be almost independent of the leaving group. Therefore, the α -deuterium KIE must be proportional to the inverse isotopic partition function ratio of the reactant.

Shiner et al. [66] calculated partition function ratios $Q(CH_2DX)/Q(CH_3X)$ for $X = Cl$, Br, and I. Starting from $k_H/k_D = 1.15$ for the S_N1 solvolysis of chlorides, they predicted

TABLE 7
LIMITING VALUES OF THE α -DEUTERIUM KIE IN SOLVOLYSIS REACTIONS

Reactant	Solvent	Temp. (°C)	k_H/k_D	Ref.
$CH_3-C\equiv C-CH(CH_3)Br$	70% $CF_3CH_2OH-H_2O$	25	1.123	67
$CH_3-C\equiv C-CH(CH_3)I$	70% $CF_3CH_2OH-H_2O$	25	1.089	67
$CH_3-C\equiv C-CH(CH_3)OTs$	70% $CF_3CH_2OH-H_2O$	25	1.226	67
2-Adamantyl tosylate	CF_3COOH	25	1.26 ± 0.02	69
2-Adamantyl 2,2,2-trifluoroethylsulfonate	70% $CF_3CH_2OH-H_2O$	25	1.225 ± 0.001	70
	97% $CF_3CH_2OH-H_2O$	25	1.228 ± 0.001	70

values of $k_{\text{H}}/k_{\text{D}} = 1.125$ for bromides, and 1.09 for iodides, in very good agreement with experimental results (Tables 6 and 7).

Shiner [18a] suggested that the rate-determining step in "limiting" solvolysis reactions is cleavage of the intimate ion pair. This is based on good experimental evidence (comparison of titrimetric and polarimetric rates, etc.) in examples concerning non-aqueous solutions. Certainly, the majority of experimental data of limiting solvolysis reactions refer to nonaqueous solvents or solvent mixtures with a high percentage of the nonaqueous component, and in these solvents ion-pairs are more important than free ions. However, matters may be different in more aqueous solvents. From the point of view of the KIE calculations, it is not necessary to assume *complete* cleavage of the C–X bond in the transition state. If, for example, there is only 80% or 90% bond cleavage, the transition state bending force constants f_{HCX} are small and the frequencies are low enough for almost complete excitation of the bending vibrations. They then behave like classical oscillators, and the isotopic partition function ratios are independent of the force constants [71]. These ideas also supply an explanation of the fact that the α -deuterium KIE is not dependent on the alkyl group. One would not expect that the degrees of bond cleavage in the transition state are exactly equal for an isopropyl compound and an α -phenylethyl or 2-adamantyl compound.

3. Carbon KIEs in $S_{\text{N}}1$ solvolysis

According to the results of the work on α -deuterium KIEs, there are considerable contributions from the $S_{\text{N}}2$ mechanism in the solvolyses of benzyl chlorides. If one examines the values of $k_{\text{H}}/k_{\text{D}}$ in the solvolyses of 4-methylbenzyl and 2,4,6-trimethylbenzyl chlorides in 80% aqueous ethanol [64] (Table 6), it is easily concluded that these reactions, as well as that of 4-methoxybenzyl chloride, would not be "limiting" $S_{\text{N}}1$ in 80% aqueous *dioxane* (whose ionizing power must be even lower than that of aqueous ethanol). Consequently, the entries of k_{12}/k_{14} for these reactions (Table 5) are not typical for $S_{\text{N}}1$ processes. It is not surprising to observe that the carbon-14 KIE for the 4-methoxy compound decreases from 1.034 to 1.009 if 0.1 M sodium perchlorate is added to the solution [17]. The increased ionic strength of the solvent favors the $S_{\text{N}}1$ mechanism. The remaining values of carbon KIEs (Table 5) are 1.013 (k_{12}/k_{13}) or lower.

In the solvolysis of α -phenylethyl chloride, $k_{\text{H}}/k_{\text{D}}$ is at the value for limiting solvolysis in almost all solvents studied. Since bromine is a better leaving group than chlorine, it may be expected that the solvolyses of α -phenylethyl bromide in methanol or ethanol are also pure $S_{\text{N}}1$ processes. Correspondingly, measured values of k_{12}/k_{13} are between 0.99 and 1.01. In these examples, an anomalous temperature dependence is observed, namely, k_{12}/k_{13} *increases* slightly with increasing temperature [21]. (In examples with large contributions from the $S_{\text{N}}2$ mechanism, k_{12}/k_{13} *decreases* with increasing temperature [21].) The probable cause of the anomalous temperature dependence may be a change in the solvation of the transition state [21].

From a comparison of the values for α -phenylethyl bromides with the substituents Br,

H, or CH₃ in the *para* position, it can be seen that k_{12}/k_{13} decreases with increasing electron-releasing ability of the substituent.

Sample calculations have been performed for the carbon KIEs in S_N1 reactions of triphenylmethyl chloride [19] and α -phenylethyl bromide [51], and it has been concluded that the experimental carbon KIEs are low because the carbon-carbon stretching force constants at the central carbon are increased in the transition state (or in the carbonium ion, respectively). The bonds between the central carbon and the aromatic carbon atoms are shortened and strengthened by resonance.

4. Chlorine isotope effects

In the solvolysis of *tert*-butyl chloride, the chlorine KIE is $k_{35}/k_{37} = 1.008 (\pm 0.0015)$ in aqueous ethanol (with NaOH) [72] and 1.0106 in methanol at 20° [36]. This is equal to, or a little higher than, respectively, the results for the reactions of 4-methoxybenzyl chloride with either cyanide ion or water [36, 40]. Experimental values of k_{35}/k_{37} for S_N2 reactions of benzyl chlorides with electron-withdrawing groups (Table 2b) are lower [40].

According to sample calculations carried out by various authors, the leaving group KIE must increase with increasing bond cleavage in the transition state [49,50]. Bond cleavage has proceeded further in the transition state of the S_N1 reaction. On the other hand, it must be considered that the developing chloride ion is solvated. This represents increased bonding relative to the reactant, which must decrease the chlorine KIE [73, 74]. The solvation effect must be more important in the S_N1 than in the S_N2 reaction. For a better understanding of the chlorine KIE in S_N1 and S_N2 reactions, it will be necessary to carry out improved sample calculations that include interactions of the leaving group with the solvent.

D. The Snee ion-pair mechanism versus the S_N2 and S_N1 mechanisms

It was suggested by Snee and Larsen [75] that S_N1 as well as S_N2 reactions go through common ion-pair intermediates. More recently, Graczyk and Taylor [76a] investigated chlorine-37 KIEs in the solvolysis of 4-methoxybenzyl chloride in 70% aqueous acetone. They found that k_{35}/k_{37} increases if azide ion is added to the solution. On the basis of a simple model of parallel first and second order reactions, one would expect k_{35}/k_{37} to decrease, since an increase of [N₃⁻] would cause the S_N2 pathway to become more important. Therefore, Graczyk and Taylor considered their observations as further support of Snee's ion-pair mechanism.

Actually, Graczyk and Taylor's experimental results are consistent with the findings of Willi et al. [37] concerning α -deuterium KIEs. In the reaction of 4-methylbenzyl chloride in 55% aqueous 2-methoxyethanol, $k_{\text{H}}/k_{\text{D}}$ was found to increase from 1.03 to the limiting value of 1.15 upon addition of 0.04 M cyanide ion. However, both observations do not permit any decisive conclusions to be drawn with respect to the pathway with nucleophilic participation. They merely indicate that the "limiting"

pathway must be more complicated; the latter may pass through ion-pairs as well as free ions. There is either internal or external return (from the intermediate to the reactant), which can be prevented by reaction of the intermediate with a strong nucleophile.

Raaen et al. [43] recently determined carbon-14 and α -deuterium KIEs in the solvolyses of benzyl chloride and 4-methylbenzyl chloride in aqueous acetone in the presence of azide ion (Table 2). Under the conditions of their experiments, deuterium KIEs are low and carbon KIEs are high. These findings require strong bonding in the transition state. They strongly support the picture of a classic S_N2 reaction and refute the Sneen mechanism in its generalized form.

E. Carbon and hydrogen isotope effects in solvolysis with aryl participation

Yukawa and co-workers [22] measured carbon-14 and deuterium KIEs in the solvolyses of 2-phenylethyl and 2-methyl-2-phenylpropyl arenesulfonates (Table 8). The most important feature of their results was the demonstration of substantial carbon-14 KIEs at the aryl-1 position. One would not expect a noticeable secondary carbon KIE at a position separated from the reacting carbon by two bonds. The authors concluded that the observed aryl-1- ^{14}C KIEs of the magnitude of 1.02–1.035 supply direct evidence of aryl participation in the formation of the transition state of the solvolysis. The KIEs indicate a considerable force constant change at the ring carbon, which may be caused by formation of a phenonium ion-like transition state. Previous suggestions of aryl participation have been based on observations of rearranged products and rate enhancements whose accurate magnitudes were difficult to evaluate. Some additional support had been obtained from determinations of α -deuterium KIEs [18b]. Yukawa and his associates also observed appreciable α and β ^{14}C KIEs, as well as α -deuterium KIEs (Table 8).

It may be surprising that the aryl-1- ^{14}C KIE for the solvolysis of 2-phenylethyl *p*-nitrobenzenesulfonate is increased from 1.002 to 1.022 by replacing the solvent acetic acid by formic acid. However, it has been reported by Saunders et al. [76b] that a corresponding increase of the α -deuterium KIE (from $k_{\text{H}}/k_{\text{D}} = 1.03$ to 1.105) occurs in the solvolysis of 2-phenylethyl tosylate for the same change of solvent.

Aryl participation involves some weak bond formation in the transition state. Therefore, one might ask the question why the observed aryl-1- ^{14}C KIE is not inverse. The writer suggests the following answer. When the aryl-1-carbon interacts with the α carbon atom, it increases the *p* character (from sp^2 toward sp^3) of the other three bonding orbitals, causing the stretching force constants of the three bonds to decrease. Furthermore, the α , β , and aryl-1 carbon atoms are to form a three-membered ring, and ring strain is equivalent to diminished orbital overlap, which leads to additional bond weakening. Bond weakening due to ring strain would also affect the β carbon, and this is probably the cause of the β - ^{14}C KIE value, $k_{12}/k_{14} = 1.014$.

The α - ^{14}C KIE is as large as has been observed in S_N2 reactions [22]. This may be

TABLE 8
CARBON AND DEUTERIUM EFFECTS IN THE SOLVOLYSIS OF 2-PHENYLETHYL ARENESULFONATES (Ref. 22) ^a

Reactant	Solvent	Temp. (°C)	Aryl-1- ¹⁴ C k_{12}/k_{14}	α - ¹⁴ C k_{12}/k_{14}	β - ¹⁴ C k_{12}/k_{14}	α -D k_{2H}/k_{2D}
PhCH ₂ CH ₂ -O ₃ S-C ₆ H ₄ -NO ₂ (<i>p</i>)	CH ₃ COOH	100	1.002 ± 0.001			
	HCOOH	60	1.022 ± 0.002			
	CF ₃ COOH	45	1.029 ± 0.002			
<i>p</i> -MeO-C ₆ H ₄ CH ₂ CH ₂ -O ₃ S-C ₆ H ₄ NO ₂ (<i>p</i>)	CH ₃ COOH	60	1.028 ± 0.001			
	HCOOH	30	1.026 ± 0.003			
	CF ₃ COOH	0	1.036 ± 0.009			
PhCMe ₂ CH ₂ -O ₃ S-C ₆ H ₄ -Br (<i>p</i>)	CH ₃ COOH	75	1.023 ± 0.001	1.093 ± 0.003	1.014 ± 0.001	1.21
	CF ₃ COOH	75	1.035 ± 0.001	1.141 ± 0.001	1.014 ± 0.001	1.24

^a Reproduced from ref. 22c, Table 1, by permission of Pergamon Press, Oxford.

expected, for the transition state is stabilized by weak neighboring group participation rather than by bond-strengthening electron release to the α carbon.

The α -deuterium KIEs reported by Yukawa et al. [22] are of a similar magnitude as those found previously for solvolyses with aryl participation [18b]. The values of k_{2H}/k_{2D} (referring to 2 Ds) are approximately in the middle of those for S_N2 and S_N1 reactions. It has been concluded that the transition state of solvolysis with aryl participation involves less bonding to entering and leaving groups than the S_N2 transition state. On the other hand, bond breaking has not proceeded as far as in a transition state of a limiting S_N1 solvolysis reaction [18b, 22, 76b].

Much more work has been done on hydrogen KIEs in solvolyses with neighboring group participation. The work was reviewed in 1969 by Sunko and Borčić [18b].

III. CARBON AND HYDROGEN ISOTOPE EFFECTS IN AROMATIC DECARBOXYLATIONS ^a

A. The mechanism of decarboxylation of aromatic acids with electron-releasing substituents

1. Rate-determining proton transfer

Carbon KIEs in the decarboxylation of various reactants, such as malonic acid [1–4, 6], trichloroacetate ion [5], and 2,4,6-trinitrobenzoate ion [77] (with the label at the carboxylic group) were found to be in the range $k_{12}/k_{13} = 1.028$ to 1.04. Surprisingly, Stevens et al. [78] observed no carbon KIE ($k_{12}/k_{13} = 1.00$ within experimental error) in the decarboxylation of anthranilic acid in aqueous acidic solution. The apparent discrepancy is caused by differences in mechanism. In the decarboxylation of anthranilic acid in weakly acidic solution, bond cleavage between aromatic ring and carboxylic group does not take place in the rate-determining step. In the slow step of the reaction, an intermediate is formed prior to elimination of carbon dioxide. This is the decarboxylation mechanism common to many aromatic acids carrying electron-releasing substituents. The decarboxylation reactions of these compounds provide good examples of interrelationships between carbon and solvent hydrogen KIEs and mechanism. These interrelationships are discussed in this section. On the other hand, it is not intended to present a full account of isotope effects in decarboxylations.

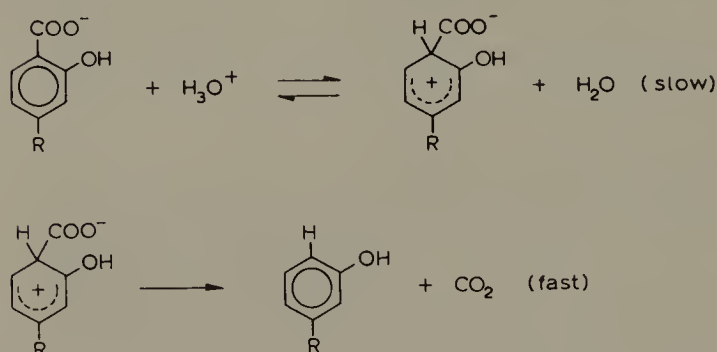
Schubert et al. [79] studied the decarboxylation kinetics of mesitoic and 2,4,6-trimethoxybenzoic acids in $H_2SO_4-H_2O$ mixtures. The reaction rate was found to increase with increasing acidity of the solvent. On the basis of certain aspects of the dependence of the rate on solvent composition, Schubert suggested that there is general acid catalysis by sulfuric acid, in addition to specific catalysis by H_3O^+ . Therefore, he concluded that these reactions are examples of rate-determining proton transfer. The decarboxylation kinetics of 2,4,6-trihydroxybenzoic acid [80] and some 4-substituted salicylic acids [81] could be investigated in dilute aqueous acid solutions. It was possible to carry

^a For another discussion of this topic, see Chapter 1 in this volume.

out experiments at a constant ionic strength, which led to the rate equation

$$v = k_2[\text{ArCOO}^-][\text{H}_3\text{O}^+] \quad (3)$$

The rate constant k_2 was found to increase with increasing electron-releasing ability of the substituent at the 4-position [81]. In the decarboxylation of 2,4,6-trihydroxybenzoic acid [80] and 4-aminosalicylic acid [81], general acid catalysis by some ammonium and pyridinium ions was detected. Furthermore, a kinetic solvent isotope effect of $(k_2)_{\text{H}_2\text{O}}/(k_2)_{\text{D}_2\text{O}} = 1.76$ (50°) was measured for the decarboxylation of 2,4-dihydroxybenzoic acid in the pH range 1.65–2.00 [82]. Consequently, the slow step of these reactions must be proton transfer from H_3O^+ to the ring carbon atom that carries the COO^- group. Willi [81] suggested that an intermediate is formed in analogy with other electrophilic aromatic substitutions, according to the following scheme



Confirmation of the two-step mechanism was supplied by Lynn and Bourns [83] who observed variable carbon-13 KIEs in the decarboxylation of 2,4-dihydroxybenzoic acid (label at the carboxylic group) with acetate buffers (Table 9). In the first experiment, with $[\text{CH}_3\text{COO}^-] = 0.067$ M, the carbon KIE is almost equal to unity since carbon–carbon bond cleavage is not rate-determining. At higher concentrations of the buffer base, however, the rate of proton abstraction from the intermediate (i.e. reversal of the first step) becomes comparable to the rate of elimination of carbon dioxide (i.e. the second step). As a consequence, the second step becomes partially rate-determining which causes a low carbon KIE.

TABLE 9

CARBON KIEs IN THE DECARBOXYLATION OF 2,4-DIHYDROXYBENZOIC ACID IN AQUEOUS ACETATE BUFFERS AT 50° ; IONIC STRENGTH 1 M (Ref. 83)

$[\text{CH}_3\text{COOH}]$ (M)	$[\text{CH}_3\text{COO}^-]$ (M)	k_{12}/k_{13}
0.10	0.067	1.005
0.05	0.15	1.011
0.33	1.00	1.018

The decarboxylation of aromatic aminoacids involves two parallel pathways which are represented by rate eqn. (4). In both of them, a proton is transferred to the ring carbon atom at position 1.

$$v = k_H^{\text{HA}} [\text{ArCOOH}] [\text{H}_3\text{O}^+] + k_H^{\text{A}} [\text{ArCOO}^-] [\text{H}_3\text{O}^+] \quad (4)$$

The reaction between ArCOOH and H_3O^+ is the more important one in the decarboxylation of 4-aminobenzoic [84,85] and anthranilic [86,87] acids at $\text{pH} = 3$ or below, but it is relatively unimportant in the decarboxylation of 4-aminosalicylic acid [81]. If acid-base equilibria (5) and (6) are considered, (of which eqn. (5) refers to the deprotonation of the NH_3^+ group,)

$$[\text{H}_3\text{O}^+][\text{ArCOOH}]/[\text{HArCOOH}^+] = K_0 \quad (5)$$

$$[\text{H}_3\text{O}^+][\text{ArCOO}^-]/[\text{ArCOOH}] = K_1 \quad (6)$$

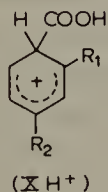
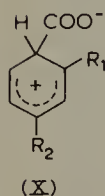
it follows from eqn. (4) that the pH dependence of the pseudo first order rate constant k ($v/(\text{overall concentration of substrate})$) is given by eqn. (7) [84].

$$k = \frac{K_0 k_H^{\text{HA}} [\text{H}_3\text{O}^+]^2 + K_0 K_1 k_H^{\text{A}} [\text{H}_3\text{O}^+]}{[\text{H}_3\text{O}^+]^2 + K_0 [\text{H}_3\text{O}^+] + K_0 K_1} \quad (7)$$

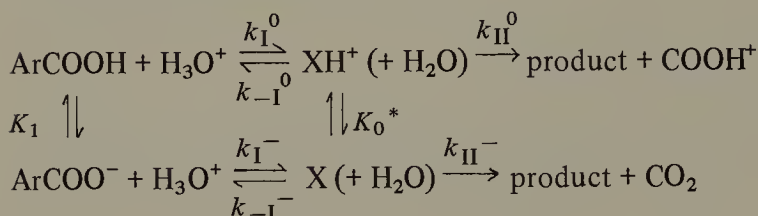
Equation (7) was found to be in agreement with experimental data for values of $[\text{H}_3\text{O}^+]$ below 0.04 M. A solvent isotope effect of $(k_H^{\text{HA}})_{\text{H}_2\text{O}}/(k_D^{\text{DA}})_{\text{D}_2\text{O}} = 1.7$ [84] can also be considered as sufficient proof of rate-determining proton transfer in the reaction between ArCOOH and H_3O^+ .

2. Change of the rate-determining step

It follows from eqn. (7) that the pseudo first order rate constant should attain a limiting value, $k = K_0 k_H^{\text{HA}}$, if $[\text{H}_3\text{O}^+]$ becomes large in comparison to K_0 and K_1 . However, Dunn et al. [86] observed that the decarboxylation rates of 4-methoxyanthranilic and 4-methylanthranilic acids pass through a maximum near $\text{pH} = 1$ and then decrease with increasing acidity of the solution. They concluded that the rate decreases are caused by a change of the rate-determining step. Similar rate decreases with increasing acidity of the solution have been found in the decarboxylation of some 2-substituted 4-aminobenzoic acids [85], anthranilic acid [87], 4-aminobenzoic acid [88], and 4-aminosalicylic acid [85,88]. A quantitative treatment of the data was carried out which included the possibility of a change of the rate-determining step. The method of the



stationary state was applied to the sum of concentrations of the intermediates X and XH^+ in the following general scheme



This procedure then led to the more complete eqn. (8)

$$k = \frac{k_1^0 K_0 [\text{H}_3\text{O}^+]^2 + k_1^- K_0 K_1 [\text{H}_3\text{O}^+]}{[\text{H}_3\text{O}^+]^2 + K_0 [\text{H}_3\text{O}^+] + K_0 K_1} \times \frac{k_{\text{II}}^- + k_{\text{II}}^0 [\text{H}_3\text{O}^+]/K_0^*}{k_{-1}^- + k_{\text{II}}^- + (k_{-1}^0 + k_{\text{II}}^0) [\text{H}_3\text{O}^+]/K_0^*} \quad (8)$$

The first factor of eqn. (8) is identical with the right side of eqn. (7). The second factor takes care of the decrease of the overall rate due to return from the intermediates XH^+ and X, and it must be equal to a constant for sufficiently low values of $[\text{H}_3\text{O}^+]$. For high values of $[\text{H}_3\text{O}^+]$, on the other hand, the first factor attains the constant value of $k_1^0 K_0$, and the second factor depends on the acidity of the solution. Equation (8) then may be replaced by the simpler expressions (8a) and (8b)

$$k = k_1^0 K_0 \frac{1 + m [\text{H}_3\text{O}^+]}{1 + q [\text{H}_3\text{O}^+]} = d \frac{1 + m [\text{H}_3\text{O}^+]}{1 + q [\text{H}_3\text{O}^+]} \quad (8a)$$

$$k = \frac{d}{1 + q h_0} \quad (8b)$$

In eqn. (8b), $[\text{H}_3\text{O}^+]$ has been replaced by h_0 which is defined by the Hammett acidity function, $h_0 = 10^{-H_0}$. Furthermore, $m h_0$ has been omitted since it is superfluous for the description of the experimental data (in the examples of anthranilic [87] and 4-aminosalicylic [88] acids). This means that the reaction step referring to k_{II}^0 (elimination of COOH^+ from XH^+) is negligible for the overall reaction.

The cause of the change of the rate-determining step may be visualized in the following way. The intermediate XH^+ cannot readily decompose to products before the carboxylic proton is split off to form the intermediate X. The latter subsequently expels CO_2 . If the solution becomes strongly acidic, the acid-base equilibrium between X and XH^+ must be far on the side of XH^+ . As a consequence, [X] will finally become too low to maintain a relatively fast rate of decomposition. The rate of return from XH^+ to $\text{ArCOOH} + \text{H}_3\text{O}^+$ will then be comparable to the rate of elimination of carbon dioxide, which means that the latter must be partially rate-determining. This will occur as soon as $q h_0$ becomes comparable to unity. The elimination step will be completely rate-determining when $q h_0$ becomes much greater than unity, and k must then be inversely proportional to h_0 . This indicates that the transition state of the slowest step

(whose structure is close to X) then contains one proton less than the principal form of the reactant (${}^+\text{H}_3\text{N}-\text{C}_6\text{H}_4\text{COOH}$) in the solution.

A change of the rate-determining step in strongly acidic solutions may also occur in the decarboxylation of substituted salicylic acids. These reactants, if they do not possess a basic group, are electrically neutral in acidic solution, and they possess as many acidic protons as their intermediate X. The decarboxylation rate then must be independent of h_0 , if the elimination step has become rate-determining.

The pseudo first order rate constant for the decarboxylation of 2,4-dihydroxybenzoic acid attains a constant value of $k_1^-K_1$ near $\text{pH} = 2$. If the acidity of the solution is raised to 0.1 M (HCl), or higher, k increases again. This must be due to a reaction between ArCOOH and H_3O^+ . However, in the acidity range of 3.5 to 6.1 M HCl ($H_0 = -1.2$ to -2.2), k has attained another constant plateau [89]. It may be concluded that elimination of carbon dioxide from X has become rate-determining under these conditions. Similar results have been found in the decarboxylation of 2,4,6-trihydroxybenzoic acid [90].

Conditions are particularly simple in the decarboxylation of azulene-1-carboxylic acid [91], since the only pathway with an appreciable rate starts with proton transfer from H_3O^+ to ArCOOH . It is possible to carry out experiments at a constant ionic strength of 0.5 M. The pseudo first order rate constant has been found to follow eqn. (9).

$$k = \frac{k_H[\text{H}_3\text{O}^+]}{1 + q[\text{H}_3\text{O}^+]} \quad (9)$$

k_H is the rate constant of proton transfer from H_3O^+ to the ring carbon atom of the reactant (ArCOOH). The value of q (at 25°) is 26.3 M^{-1} . That means that proton transfer must be rate-determining at $[\text{H}_3\text{O}^+] \leq 10^{-3} \text{ M}$ while, on the other hand, the plateau referring to rate-determining elimination of carbon dioxide is reached at $[\text{H}_3\text{O}^+] > 1 \text{ M}$.

B. Carboxyl- ^{13}C and D_2O solvent isotope effects in decarboxylations with changing rate-determining step

1. Acidity dependence of isotope effects

Carboxyl- ^{13}C and D_2O solvent KIEs in the decarboxylation of substituted salicylic [89,90,92,93], 4-aminobenzoic [90], anthranilic [90,94,95], and azulene-1-carboxylic [91,96] acids have been measured by various workers. It may be recognized from the data collected in Table 10 that the KIEs are variable under certain conditions, their magnitudes being dependent on the acidity of the solution. Furthermore, a negligible carbon KIE always corresponds to a high D_2O solvent KIE (usually > 3 , with the exception of azulene-1-carboxylic acid), — and a maximum carbon KIE always corresponds to a relatively low D_2O solvent KIE. (The low limit is dependent on the acid

TABLE 10

KINETIC CARBON-13 AND D₂O-SOLVENT ISOTOPE EFFECTS IN THE DECARBOXYLATION OF AROMATIC AMINO- AND HYDROXYACIDS (CARBON-13 AT THE CARBOXYLIC GROUP)

Reactant	*C _{HZ}	H ₀ or pH	Temp. (°C)	k ₁₂ /k ₁₃	k _{H₂O} /k _{D₂O}	Ref.
Anthranilic acid	1.71 ^b		115		3.57	94
	2.0 ^b	-0.84	115	1.001		94
	2.56 ^b	-1.13	115		3.20	94
	5.60 ^b	-2.51	115		3.21	94
	7.50 ^b	-3.60	115		3.07	94
	10.0 ^b	-4.89	115	1.037		94
	0.10 ^c	+0.98	85		4.67	90
	1.00 ^c	-0.20	85		3.64	90
	2.91 ^c	-1.03	85		3.28	90
	4.00 ^c	-1.40	85		3.14	90
	4.85 ^c	-1.74	85		2.95	90
	6.00 ^c	-2.12	85		2.89	90
4.Methoxyanthranilic acid formate buffer						
		4.0	60	1.0022		95
	HCl-KCl	1.3	60	1.0140		95
	2.00 ^c	-0.3	60	1.0416		95
4-Aminobenzoic acid	0.10 ^c	+0.98	85		3.50	90
	1.00 ^c	-0.20	85		2.71	90
	3.00 ^c	-1.05	85		2.76	90
2,4-Dihydroxybenzoic acid						
	0.002 ^a	+2.70	85	1.0063		92
	0.01 ^a	+2.00	85	1.0056		92
	0.02 ^a	+1.70	85	1.0061		92
	0.05 ^a	+1.30	85	1.0062		92
	0.10 ^a	+0.98	85	1.0061		92
	1.01 ^a	-0.22	85	1.0096		92
	3.00 ^a	-1.23	85	1.0218		92
	5.81 ^a	-2.72	85	1.0314		92
	7.81 ^a	-4.23	85	1.0361		92
	0.01 ^a	+2.00	50		6.05	82
	1.02 ^c	-0.20	50		1.99	89
	4.08 ^c	-1.41	50		1.47	89
	5.10 ^c	-1.77	50		1.35	89
	6.12 ^c	-2.14	50		1.33	89
	8.16 ^c	-3.03	50		1.26	89
2,4,6-Trihydroxybenzoic acid						
	0.001 ^a	+3.00	30	1.0042		93
	0.50 ^c	+0.20	30		5.38	90
	1.02 ^c	-0.20	30		5.41	90
	2.02 ^c	-0.69	30		4.32	90
	3.01 ^c	-1.05	30		3.86	90
	5.01 ^c	-1.76	30		3.10	90

TABLE 10 (continued)

Reactant	*C _{HZ}	H ₀ or pH	Temp. (°C)	k ₁₂ /k ₁₃	k _{H₂O} /k _{D₂O}	Ref.
	5.50 ^c	−1.93	30		2.12	90
	5.96 ^c	−2.11	30		1.79	90
	6.42 ^c	−2.31	30		1.56	90
	6.12 ^a	−2.88	30		1.33	93
	8.35 ^a	−4.45	30	1.041		93
Azulene-1-carboxylic acid						
	0.006 ^d			1.008		96
	0.010 ^d		25		2.15	91
	0.020 ^d		25		1.94	91
	0.32 ^d		25	1.043		96
	0.40 ^d		25		1.26	91
	0.50 ^d		25		1.17	91

*C_{HZ} = Concentration of strong acid in solvent.

^a Perchloric acid.

^b Sulfuric acid.

^c Hydrochloric acid.

^d Perchloric acid, ionic strength = 0.5 M.

type.) Small carbon and high solvent deuterium KIEs are observed in dilute acidic solutions, while noticeable carbon and low solvent deuterium KIEs are observed in moderately concentrated acidic solutions. This is in full accord with expectations based on the mechanism. The change of the rate-determining step from protonation to carbon–carbon bond cleavage occurs when the acidity of the solution is increased. Actually, the observed variations of the KIEs have been taken as additional evidence for the change of the rate-determining step [89–96].

There is even quantitative agreement with predictions derived from the observed kinetics. For the decarboxylation of anthranilic acid [87] at 85°, $q = 0.31 \text{ M}^{-1}$ (see eqn. 8b). In 0.1 M aqueous hydrochloric acid, $qh_0 \ll 1$ which indicates rate-determining proton transfer. Accordingly, $k_{\text{H}_2\text{O}}/k_{\text{D}_2\text{O}}$ is at its maximum value [90] (Table 10). (Unfortunately, no carbon KIE has been measured under the same conditions.) In 4.85 M hydrochloric acid ($h_0 = 10^{1.74} \text{ M} = 55 \text{ M}$), on the other hand, $qh_0 > 1$ which indicates predominant rate-determining carbon–carbon bond cleavage. (H_0 values have been taken from the review article by Paul and Long [97].) Correspondingly, $k_{\text{H}_2\text{O}}/k_{\text{D}_2\text{O}}$ has attained its low limit for this reaction.

For the decarboxylation of 4-aminobenzoic acid at 85° [88], $q = 4.35 \text{ M}^{-1}$, and $qh_0 \ll 1$ in 0.01 M (or more dilute) hydrochloric acid, while $qh_0 \gg 1$ in 2.0 M hydrochloric acid ($h_0 = 4.9 \text{ M}$). As expected, $k_{\text{H}_2\text{O}}/k_{\text{D}_2\text{O}}$ is already below its high limit in 0.1 M hydrochloric acid, and it is near its low limit in 1.0 M hydrochloric acid [90].

The q value is much higher in the decarboxylation of 4-methoxyanthranilic acid, $q = 935 \text{ M}^{-1}$ (equal to b/a in the paper by Dunn et al. [86]). At pH = 4.0, $qh_0 < 1$,

but it is not completely negligible in comparison to unity. It is difficult to judge whether the carbon-13 KIE at pH = 4.0 (Table 10) is merely a secondary effect, or if it already indicates a small contribution of rate-determining carbon–carbon bond cleavage. There is a primary carbon KIE at pH = 1.3, but it has not yet reached its full size. In 3.0 M hydrochloric acid, $h_0 = 10^{1.05} = 11$ M, $qh_0 \gg 1$, and there is a full carbon KIE as expected. (There are no data in 0.5 or 1.0 M hydrochloric acid.)

2. The magnitudes of the carbon and hydrogen isotope effects

Under conditions in which carbon–carbon bond cleavage is solely rate-determining, the carbon-13 KIEs in the decarboxylation of 2,4-dihydroxybenzoic, 2,4,6-trihydroxybenzoic, anthranilic, 4-methoxyanthranilic, and azulene-1-carboxylic acids were found to be in the range 1.036–1.043 (Table 10). The values are probably more dependent on temperature than on the individual reactant. Similar results have been obtained for the decarboxylation of other aromatic acids, such as 2,4,6-trinitrobenzoic acid [77] ($k_{12}/k_{13} = 1.036$ at 50° , no change of rate-determining step) and mesitoic acid [98] (1.037 at 61°). Carbon-13 KIEs in the decarboxylation of malonic acid [99] (1.0285 at 140.5°) and trichloroacetate ion [5] (1.0338 at 70.4°) were a little lower.

Theoretical KIE calculations with the aid of the heavy atom approximation [11] (on the basis of simple models) were attempted for malonic acid by Bigeleisen [100] ($k_{12}/k_{13} = 1.020$ at 400 K) and by Pitzer (1.07 at 400 K) [101]. Stern and Wolfsberg [102] carried out computer calculations from force constants on the basis of a “complete” model (with the loss of one carbon–carbon bond in the transition state) for the carbon-13 KIE in the decarboxylation of malonic acid. Their result was 1.023 at 400 K (per COOH group, ^{13}C at the carboxylic group). To the writer’s knowledge, no computer calculations of KIEs have been published for the decarboxylation of aromatic acids.

The carbon isotope effect is not exactly equal to unity under conditions in which carbon–carbon bond cleavage is not rate-determining (Table 10). As suggested by Bourns [93], the values of $k_{12}/k_{13} = 1.0042 \pm 0.0010$ (2,4,6-trihydroxybenzoic acid in 0.001 M aqueous perchloric acid) and 1.0063 ± 0.0010 (2,4-dihydroxybenzoic acid in 0.002 M aqueous HClO_4) are probably secondary carbon isotope effects. They are presumably caused by a decrease of the stretching force constant of the carbon–carbon bond (hybridization change from $sp^2 - sp^2$ to $sp^3 - sp^2$) in the formation of the transition state on the way to the intermediate.

For an understanding of the limiting values of the solvent deuterium KIE, it is necessary to examine the acid–base equilibria of reactant and intermediate. Aromatic acids without an NH_2 group are considered first. If H^+ transfer is rate-determining, the reaction rate is given by eqn. (4). As mentioned previously, the reaction pathway with H^+ transfer from H_3O^+ to ArCOOH (attack at the ring C atom) contributes to the overall reaction of substituted salicylic acids if the concentration of strong acid in the solution is 0.1 M or higher. It is useful to substitute the product $[\text{ArCOO}^-][\text{H}_3\text{O}^+]$ in eqn. (4) with the aid of eqn. (6), which leads to eqn. (10).

$$v = k_{\text{H}}^{\text{HA}} [\text{ArCOOH}] [\text{H}_3\text{O}^+] + k_{\text{H}}^{\text{A}} K_1 [\text{ArCOOH}] \quad (10)$$

For more dilute aqueous acid solutions (if $\text{pH} > 1.7$ in the case of 2,4-dihydroxybenzoic acid), it is sufficient to consider only the second part of the right side of eqn.

(10). If $\text{pH} < \text{p}K_1 - 1.3$, more than 95% of the reactant is present as the unionized acid, ArCOOH . One may then write for the observed first order rate constant:

$$v/[\text{reactant}] = k = k_{\text{H}}^{\text{A}} K_1 \quad (11)$$

The solvent isotope effect on the observed first order rate constant is then given by eqn. (12).

$$\frac{k_{\text{H}_2\text{O}}}{k_{\text{D}_2\text{O}}} = \frac{k_{\text{H}}^{\text{A}}}{k_{\text{D}}^{\text{A}}} \cdot \frac{(K_1)_{\text{H}}}{(K_1)_{\text{D}}} \quad (12)$$

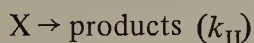
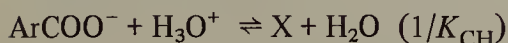
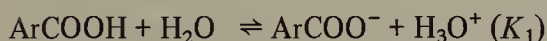
In the example of 2,4-dihydroxybenzoic acid, the values of K_1 in H_2O and D_2O have been determined directly [82], and the following value has been obtained for their isotopic ratio: $(K_1)_{\text{H}}/(K_1)_{\text{D}} = 3.6$ at 50° . From the ratio of observed rate constants in H_2O and D_2O (ca. 6), the following value was computed (eqn. 12) for the ratio of rate constants of the hydrogen ion transfer step [82] $k_{\text{H}}^{\text{A}}/k_{\text{D}}^{\text{A}} = 1.76$.

If the acidity of the solvent is increased to 1 M or higher, the first part of the right side of eqn. (10) becomes the more important, and the solvent isotope effect then decreases to the value given by eqn. (13),

$$k_{\text{H}_2\text{O}}/k_{\text{D}_2\text{O}} = k_{\text{H}}^{\text{HA}}/k_{\text{D}}^{\text{DA}} \quad (13)$$

which is of approximately the same magnitude [84] as the ratio $k_{\text{H}}^{\text{A}}/k_{\text{D}}^{\text{A}}$.

If elimination of CO_2 from X (carbon-carbon bond cleavage) is rate-determining, the reaction pathway from reactant to product is represented by two equilibrium steps and the final slow step.



The reaction rate is then given by eqn. (14),

$$v = k_{\text{II}} [\text{X}] = \frac{K_1}{K_{\text{CH}}} \cdot k_{\text{II}} [\text{ArCOOH}] \quad (14)$$

and the solvent isotope effect is given by eqn. (15)

$$\frac{k_{\text{H}_2\text{O}}}{k_{\text{D}_2\text{O}}} = \frac{(K_1)_\text{H}}{(K_1)_\text{D}} \cdot \frac{(K_{\text{CD}})_\text{D}}{(K_{\text{CH}})_\text{H}} \cdot \frac{(k_{\text{II}})_\text{H}}{(k_{\text{II}})_\text{D}} \quad (15)$$

The solvent isotope effects on the acidities of ArCOOH and X cancel each other to a large extent. The one acting upon the CH acid (X) is probably a little smaller, and the ratio of the two isotopic K ratios is estimated as 1.0 to 1.3. There is a secondary deuterium isotope effect acting upon k_{II} , which is somewhat similar to the one in limiting solvolysis (see Section B. 3). Since it is not expected that the extent of bond cleavage in the transition state is as great as in carbonium ion formation, the secondary KIE is estimated as $(k_{\text{II}})_\text{H}/(k_{\text{II}})_\text{D} = 1.0$ to 1.1. The magnitude of the solvent isotope effect on the observed rate constant then may be within the limits of $k_{\text{H}_2\text{O}}/k_{\text{D}_2\text{O}} = 1.0$ to 1.43. This estimate agrees well with the experimental low limits of $k_{\text{H}_2\text{O}}/k_{\text{D}_2\text{O}}$ (in strongly acidic solutions) for 2,4-dihydroxybenzoic acid [89], 2,4,6-trihydroxybenzoic acid [93], and azulene-1-carboxylic acid [91] (Table 10).

Aromatic aminoacids are to be considered separately because of the existence of the cation HArCOOH^+ , which is formed by N-protonation in strongly acidic solution. If $\text{pH} < \text{p}K_0 - 1.3$, at least 95% of the reactant is present as the cation. Under these conditions, the second part of the right side of eqn. (4) may be neglected. Substitution of the product $[\text{ArCOOH}][\text{H}_3\text{O}^+]$ with the aid of eqn. (5) leads to eqn. (16).

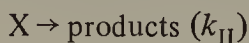
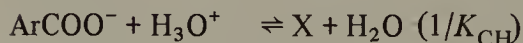
$$v = k_{\text{H}}^{\text{HA}} [\text{ArCOOH}][\text{H}_3\text{O}^+] = k_{\text{H}}^{\text{HA}} K_0 [\text{HArCOOH}^+] \quad (16)$$

Since almost all of the reactant is present as HArCOOH^+ , the observed first order rate constant is given by $k = k_{\text{H}}^{\text{HA}} K_0$. Furthermore, the solvent isotope effect in the case of rate-determining H^+ transfer must be equal to

$$\frac{k_{\text{H}_2\text{O}}}{k_{\text{D}_2\text{O}}} = \frac{k_{\text{H}}^{\text{HA}}}{k_{\text{D}}^{\text{DA}}} \cdot \frac{(K_0)_\text{H}}{(K_0)_\text{D}} \quad (17)$$

Again, $(K_0)_\text{H}/(K_0)_\text{D}$ approximately equals 3 (or 2.8 [84], respectively, at 85°), and $k_{\text{H}}^{\text{HA}}/k_{\text{D}}^{\text{DA}} \approx 1.6$ to 2. Consequently, the value expected for $k_{\text{H}_2\text{O}}/k_{\text{D}_2\text{O}}$ is within 4.5–6. This is in good agreement with the high limit of the experimental solvent KIE in the decarboxylation of 4-aminobenzoic [84] and anthranilic [90] acids.

If carbon–carbon cleavage is rate-determining, there are three equilibrium steps on the way from the N-protonated aminoacid (reactant) to the reactive intermediate X.



It follows that for the reaction rate,

$$v = k_{\text{II}}[\text{X}] = k_{\text{II}}(K_0K_1/K_{\text{CH}}h_0)[\text{HArCOOH}^+] \quad (18)$$

the observed first order rate constant is given by

$$k = k_{\text{II}}K_0K_1/K_{\text{CH}}h_0 \quad (19)$$

and the solvent isotope effect is

$$\frac{k_{\text{H}_2\text{O}}}{k_{\text{D}_2\text{O}}} = \frac{(K_0)_{\text{H}}}{(K_0)_{\text{D}}} \cdot \frac{(K_1)_{\text{H}}}{(K_1)_{\text{D}}} \cdot \frac{(K_{\text{CD}})_{\text{D}}}{(K_{\text{CH}})_{\text{H}}} \cdot \frac{(k_{\text{II}})_{\text{H}}}{(k_{\text{II}})_{\text{D}}} \quad (20)$$

The right side of eqn. (20) is equal to that of eqn. (15) multiplied by $(K_0)_{\text{H}}/(K_0)_{\text{D}}$. Therefore, $k_{\text{H}_2\text{O}}/k_{\text{D}_2\text{O}}$ is expected to lie between $2.8 \times 1.0 = 2.8$ and $3 \times 1.43 = 4.3$. The experimental low limits of the solvent KIE are 2.7 for aminobenzoic acid and 2.9 for anthranilic acid [90] (Table 10), in good agreement with the estimate.

IV. CARBON AND OTHER ISOTOPE EFFECTS IN CARBONYL ADDITION REACTIONS

A. Heavy atom isotope effects in ester hydrolysis and related reactions

1. General

Experimental work on carbon-14 KIEs in carbonyl addition reactions was initiated in 1949 and the early fifties. For a satisfactory understanding of the causes of the KIEs in these reactions, it is necessary to have available sufficient knowledge on the reaction mechanism and the rate-determining step. Conclusive experimental evidence concerning the mechanisms of various carbonyl addition processes had not been accumulated prior to the mid-fifties. Today, our knowledge of the mechanisms of these reactions is more complete, and we are in a much better position to discuss the magnitudes of the observed isotope effects.

2. Experimental data

The first report of a carbon-14 KIE in alkaline ester hydrolysis was given by Stevens and Attree [103] in 1949, who found $k_{12}/k_{14} = 1.16 \pm 0.017$ for the hydrolysis of ethyl benzoate-7- ^{14}C . Results obtained by Ropp and Raaen [104] in 1952 for the same reaction were somewhat lower (Table 11). Ropp and Raaen also studied the influence of *para*-substituents on the KIE [104,105]. In more recent work [106], the KIE in the alkaline hydrolysis of benzyl benzoate-7- ^{14}C was found to be appreciably larger ($k_{12}/k_{14} = 1.126$) than that reported by Ropp and Raaen for ethyl benzoate. Other experimental studies referring to ester hydrolysis were concerned with oxygen-18 KIEs [107–109] (Table 11). The work by Mitton and Schowen [107] was done with the aid of very precise, separate kinetic experiments with the ^{16}O and ^{18}O compounds.

TABLE 11
KINETIC ISOTOPE EFFECTS IN ESTER HYDROLYSIS OR SIMILAR REACTIONS

Reactant	Catalyst or attacking reagent	Solvent	Temp. (°C)	k_{12}/k_{14}	Ref.
$p\text{-MeO-C}_6\text{H}_4\text{*COOEt}$	OH^-	85% EtOH-H ₂ O	25	1.092	104,105
$p\text{-Me-C}_6\text{H}_4\text{*COOEt}$	OH^-	85% EtOH-H ₂ O	25	1.078	104,105
Ph*COOEt	OH^-	85% EtOH-H ₂ O	25	1.076	104,105
$p\text{-Cl-C}_6\text{H}_4\text{*COOEt}$	OH^-	85% EtOH-H ₂ O	25	1.081	104,105
$m\text{-Cl-C}_6\text{H}_4\text{*COOEt}$	OH^-	85% EtOH-H ₂ O	25	1.072	104,105
$m\text{-O}_2\text{N-C}_6\text{H}_4\text{*COOEt}$	OH^-	85% EtOH-H ₂ O	25	1.067	104,105
$\text{Ph*COOCH}_2\text{Ph}$	OH^-	50% MeOH-H ₂ O	50	1.126 ± 0.021	106
Ph*CO (prod. of k_{14} : $\text{Ph*COOEt} + \text{PhCOOH}$)	EtOH	EtOH	30	1.127	105b
Ph*CO (prod. of k_{14} : $\text{Ph*CONHAr} + \text{PhCOOH}$)	EtOH	EtOH	78	1.129	105b
	$p\text{-MeC}_6\text{H}_4\text{NH}_2$	"Dry hydrocarbon solvent"	30	1.073	105b
			138	1.071	105b
				Oxygen KIE k_{16}/k_{18}	
$\text{Ph-C=}^{18}\text{O} \cdot \text{O-C}_6\text{H}_4\text{Br (p)}$	MeO^-	MeOH	29.5	1.018 ± 0.005	107
$\text{Ph-C=}^{18}\text{O} \cdot \text{O-Ph}$	MeO^-	MeOH	29.5	1.024 ± 0.013	107
$\text{HCO} \cdot ^{18}\text{OMe}$	OH^-	H ₂ O, pH 10	25	1.0091 ± 0.0004	108
$\text{HCO} \cdot ^{18}\text{OMe}$	H_3O^+	H ₂ O, 0.5 M HCl	25	1.0009 ± 0.0004	108
$\text{HCO} \cdot ^{18}\text{OMe}$	N_2H_4	H ₂ O, pH 10	25	1.0048 ± 0.0006	108
$\text{HCO} \cdot ^{18}\text{OMe}$	N_2H_4	H ₂ O, pH 7.85	25	1.0621 ± 0.0008	108
$cis\text{-5-Methyl-2-cyclohexenyl}$ $p\text{-nitrobenzoate (ether-}^{18}\text{O)}$	H_2O	80% Acetone-H ₂ O	99.6	1.08 ± 0.02	109

3. Theoretical

The first attempt at a theoretical calculation of the carbon-14 KIE in ester hydrolysis was carried out by Bigeleisen [110] in 1952. It was a single frequency calculation based on the assumption that cleavage of the bond between acyl-C and ether-O would be rate-determining. Meanwhile, it has been established beyond any reasonable doubt that the slow step in the hydrolyses of primary alkyl and aryl benzoates is the addition of hydroxide ion to the carbonyl carbon [111]. Carbon–oxygen bond making nearly corresponds to the reaction coordinate; therefore, it does not contribute stretching vibrational zero-point energy to the transition state. On the other hand, during the course of the formation of the transition state, the carbonyl double bond is partially changed to a single bond. This leads to a decrease of zero-point energy in the transition state, which is the main cause of the observed “normal” isotope effect. According to calculations performed by Mitton and Schowen [107], based on the observed oxygen-18 KIE in the reaction of *p*-bromophenyl benzoate-carbonyl-¹⁸O with methoxide ion, the C–O stretching frequency is decreased from 1727 cm⁻¹ in the reactant to approximately 1300 cm⁻¹ in the transition state.

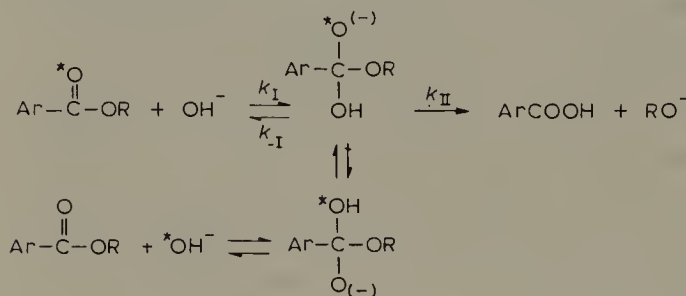
In the oxygen-18 work by Sawyer and Kirsch [108], the label is at the ether-O of the ester. The KIE is close to unity in the acid and base catalyzed hydrolyses and the hydrazinolysis at pH = 10 of methyl formate, indicating that bond cleavage between carbonyl-C and ether-O is not predominantly rate-determining in these examples. The observed values of $k_{16}/k_{18} = 1.0009$ and 1.0048 correspond to secondary isotope effects. The value of 1.0091 for the alkaline hydrolysis probably includes a weak contribution of a primary isotope effect, which is caused by some return from the tetrahedral intermediate formed in the first (slow) step. Obviously, carbonyl–oxygen bond cleavage is rate-determining in the hydrazinolysis of methyl formate at pH = 7.85. A change of the rate-determining step was expected because of an observed break in the pH–rate profile.

Sawyer and Kirsch calculated the primary KIE (for rate-determining carbon–oxygen bond cleavage) from observed frequencies of the ¹⁶O and ¹⁸O esters, assuming complete loss of zero-point energies of C–O stretching (1208.3(¹⁶O)/1187.4(¹⁸O) cm⁻¹) and methyl rocking (1162.3/1144.8 cm⁻¹) frequencies in the transition state. The result was $k_{16}/k_{18} = 1.052$. The experimental value is higher. (It is probably necessary to consider in the calculation more than two vibrational modes. According to the findings of Stern and Wolfsberg [102], in the complete calculation of the carbon KIE for the decarboxylation of malonic acid, “comparison of isotopic frequency shifts in reactants and transition states shows, in general, that changes occur over a large frequency range and are not localized.”)

It is worthwhile considering the observed dependence of k_{12}/k_{14} in ethyl benzoate hydrolysis on the ring substituent. It would be highly desirable if the conclusion could be drawn that the carbon-14 KIE decreases with increasing electron-withdrawing power of the substituent which indicates that cleavage of the carbonyl double bond and approach of OH⁻ in the transition state are diminished by the effect of the substituent.

It follows that the transition state of the hydrolysis of the more reactive ester is reached at an earlier stage, as expected on the basis of the Hammond postulate [112]. Unfortunately, matters are more complicated.

It was found by Bender et al. [111,113–115] that the hydrolysis of alkyl benzoates labeled with ^{18}O in the carbonyl group is always accompanied by oxygen exchange of the ester with the solvent. Hydrolysis and oxygen exchange pass through a common tetrahedral intermediate according to the scheme given below.



In the alkaline hydrolysis of ethyl benzoate in 33% aqueous dioxane, the ratio of the rate constants for oxygen exchange and hydrolysis is $k_{\text{ex}}/k_{\text{hy}} = 0.094$ [113]. Oxygen exchange occurs through return of the labeled oxygen (as *OH^-) from the intermediate, but reversal of the first step of the hydrolysis reaction occurs through return of either of the two oxygens (not bonded to R). Consequently, the ratio k_{-I}/k_{II} must be approximately twice as large as $k_{\text{ex}}/k_{\text{hy}}$. It follows that formation of the tetrahedral intermediate is predominantly but not exclusively rate-determining in ester hydrolysis, as the rate of return from the intermediate is not negligible in comparison to the rate of the second step. (This is not a contradiction to the statement that the first step is slow. $k_I[\text{OH}^-] \ll k_{-I} + k_{II}$ since the concentration of the intermediate is always low in comparison to that of the ester. Furthermore, $k_{-I} < k_{II}$ in all examples.)

Values of $k_{\text{ex}}/k_{\text{hy}}$ for various ring-substituted methyl benzoates (not ethyl benzoates) in 33% aqueous dioxane at 24.7° were determined by Bender and Thomas [114] (Table 12) and were found to be strongly dependent on the substituent. There

TABLE 12

RATIO OF RATES OF OXYGEN EXCHANGE AND ALKALINE HYDROLYSIS OF *p*-SUBSTITUTED METHYL BENZOATES-CARBONYL- ^{18}O IN 33% AQUEOUS DIOXANE AT 24.7° (Ref. 114) ^a

Substituent	$k_{\text{ex}}/k_{\text{hy}}$
<i>p</i> -NH ₂	0.033
<i>p</i> -CH ₃	0.091
H	0.19
<i>p</i> -Cl	0.16
<i>p</i> -NO ₂	0.36

^a Reproduced from ref. 114, Table 2, by permission of the American Chemical Society. (Values for $k_{\text{ex}}/k_{\text{hy}}$ were computed from values of $k_{\text{hy}}/k_{\text{ex}}$ given in the original table.)

is no reason to doubt that conditions are similar in the hydrolyses of ethyl benzoates. It is striking that the sequence of the values for different substituents in rising order is almost completely identical with that of the carbon-14 KIEs in decreasing order (Table 11), especially with respect to the unusual position of *p*-Cl. Consequently, the observed variations of the carbon KIE in the hydrolyses of ethyl benzoates are caused by different contributions of return from the intermediate. The overall rate constant is given by eqn. (21).

$$k_{\text{hy}} = k_{\text{I}} / (1 + k_{-\text{I}} / k_{\text{II}}) \quad (21)$$

None of the observed KIEs in the series of ethyl benzoates refers to the first step alone. Each of them corresponds to an intermediate value between those for the first and the second step being rate-determining, though it is closer to that of the first step. Since there is more return in the hydrolysis of the *p*-nitro ester, it may be concluded that the KIE referring to formation of the transition state of the second step (from the reactants) is smaller. (There is probably a substituent effect on the isotope effect in the first step — whose direction is unknown — but, unfortunately, it cannot be determined directly.)

It is not surprising that k_{12}/k_{14} is appreciably larger for the alkaline hydrolysis of benzyl benzoate [106], for according to the findings of Bender et al. [115], $k_{\text{ex}}/k_{\text{hy}}$ is of the order of magnitude of 0.01 in this reaction. This indicates that return from the intermediate is negligible.

B. Heavy atom isotope effects in the formation of derivatives of carbonyl compounds

Early work on carbon-14 KIEs (Table 13) in the formation of derivatives of carbonyl compounds [105,116,117] was carried out with the purpose of pointing to possible sources of error in conclusions drawn from labeling experiments. The work was done under the usual conditions of preparation of the derivatives, except that reacting solutions were thermostated. No particular attention was paid to control or measurement of pH of the solutions.

According to the findings of Jencks et al. [118], the slow step in the formation of oximes, substituted hydrazones, and semicarbazones is carbonyl addition (to form a "tetrahedral" intermediate) at low pH, and dehydration of the intermediate at high pH.

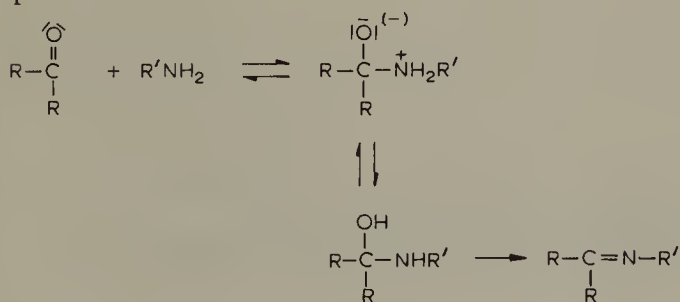


TABLE 13
CARBON KIEs IN THE FORMATION OF DERIVATIVES OF CARBONYL COMPOUNDS

Reactant and position of label	Derivative	Solvent	Temp. (°C)	k_{12}/k_{14}	Ref.
Ph-*COPh	2,4-Dinitrophenylhydrazone	EtOH-H ₂ O	27.8	1.099	116
Ph-*COPh	2,4-Dinitrophenylhydrazone	EtOH-H ₂ O	25	1.071	117
Ph-*COCH ₃	2,4-Dinitrophenylhydrazone	EtOH	25	1.057	117
Ph-*COCH ₃	2,4-Dinitrophenylhydrazone	EtOH	-75	1.100	117
Ph-*COCH ₃	2,4-Dinitrophenylhydrazone	EtOH	0	1.054 ± 0.002	124
Ph-*COCH ₃	2,4-Dinitrophenylhydrazone	EtOH	0	1.063 ± 0.001	124
Ph-*COCD ₃	2,4-Dinitrophenylhydrazone	MeOH	0	0.9916 ± 0.0004	123
PhCO*CH ₃	2,4-Dinitrophenylhydrazone	EtOH	0	0.9962 ± 0.0003	124
Ph-*COCH ₃	2,4-Dinitrophenylhydrazone	EtOH	0	1.052 ± 0.001	124
Ph-*COC(CH ₃) ₃	2,4-Dinitrophenylhydrazone	EtOH	0	0.9971 ± 0.0017	124
PhCO*C(CH ₃) ₃	2,4-Dinitrophenylhydrazone	EtOH	25	1.072	105
<i>p</i> -MeO-C ₆ H ₄ -*COCH ₃	2,4-Dinitrophenylhydrazone	EtOH	25	1.057	105
Ph-*COCH ₃	2,4-Dinitrophenylhydrazone	EtOH	78	1.043	105
Ph-*COCH ₃	2,4-Dinitrophenylhydrazone	EtOH	25	1.042	105
<i>m</i> -O ₂ N-C ₆ H ₄ -*COCH ₃	2,4-Dinitrophenylhydrazone	EtOH	25	1.057	122 ^a
β -Naphthaldehyde	Phenylhydrazone	H ₂ O, pH 1.8		1.052	122 ^a
β -Naphthaldehyde	Phenylhydrazone	H ₂ O, pH 5.0		1.066	122 ^a
β -Naphthaldehyde	Phenylhydrazone	H ₂ O, pH 7.2		1.055	122 ^a
β -Naphthaldehyde	Semicarbazone	H ₂ O, pH 5.0			122 ^a

^a No temperature has been given in ref. 122.

(Several steps are coalesced into one in the hydration step.)

Ropp and Raaen [105] employed "procedure 15" given by Shriner and Fuson [119] (presumably identical with procedure 18 of Shriner et al. [120]) in which the carbonyl compound is reacted with 2,4-dinitrophenylhydrazine and excess sulfuric acid in aqueous ethanol. It appears reasonable to assume that these experimental conditions lead to rate-determining carbonyl addition. The cause of the carbon KIE (label at carbonyl carbon) would then be the same as in alkaline ester hydrolysis, namely partial loss of zero-point energy of the carbonyl double bond in the transition state. Provided the assumption of a rate-determining carbonyl addition step is correct, the observed substituent effect upon the KIE (Table 13) indicates that C–N bond formation and simultaneous opening of the C=O double bond are more complete in the transition state of the reaction of the *p*-methoxy compound, as expected on the basis of the Hammond postulate.

In the transition state of the dehydration step, the C=O double bond has been opened completely (i.e. it is now a single bond) and a C=N double bond has been partially formed. As the C=N stretching force constant is lower than the C=O stretching force constant [121], the transition state of the dehydration step probably possesses less zero-point energy than that of the addition step. However, these considerations cannot be sufficiently precise to allow one to draw conclusions about the rate-determining step from the magnitude of the carbon KIE. On the other hand, Simon and Palm [122] found that the carbon-14 KIE in the formation of β -naphthaldehyde-phenylhydrazone is increased by raising the pH from 1.8 to 7.2 (Table 13), as expected for a change of the rate-determining step from carbonyl addition to dehydration.

Raaen and co-workers [123,124] also observed secondary α -carbon KIEs in the formation of acetophenone-2,4-dinitrophenylhydrazone (Table 13). These inverse isotope effects are probably caused by zero-point energies of bending vibrations occurring in the transition state, but not in the reactants.

Sheppard and Bourns [125] measured ^{34}S isotope effects on the equilibrium constant of addition of hydrogen sulfite ion to various carbonyl compounds (Table 14). The values of K_{32}/K_{34} are smaller than unity, as expected when there is increased bonding of the S atom in the addition compound. The sulfur-34 isotope effects on the rate constants of some of these reactions were studied by Sheppard et al. [126], and were found to be equal to unity within experimental error. This is not unexpected since the vibrational zero-point energy involving motions of S atoms cannot change appreciably during the course of the formation of the transition state. The stretching motion of the reacting C–S bond nearly corresponds to the reaction coordinate and it does not possess zero-point energy.

C. The Cannizzaro reaction

In an early study of the Cannizzaro reaction of benzaldehyde, Stevens and Attree [127] reported no carbon-14 isotope effect (within an experimental error of $\pm 1.5\%$).

TABLE 14

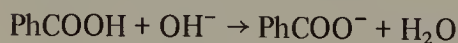
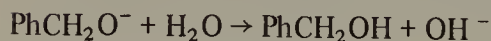
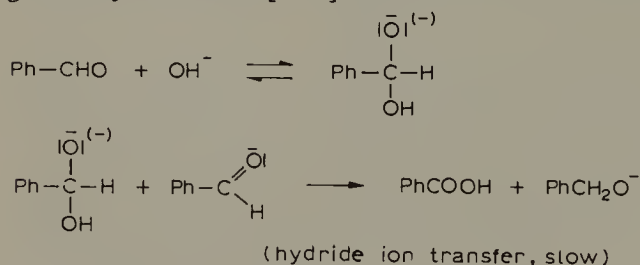
SULFUR-34 ISOTOPE EFFECTS ON THE EQUILIBRIUM CONSTANT OF ADDITION OF HYDROGEN SULFITE ION TO CARBONYL COMPOUNDS (Ref. 125) ^a

Reactant	K_{32}/K_{34} (25°)
Acetone	0.979
Butanone	0.978
4-Methyl-2-pentanone	0.981
Benzaldehyde	0.986
Heptanal	0.986
2-Heptanone	0.988
2-Octanone	0.987
Anisaldehyde	0.990

^a Reproduced in part by permission of the National Research Council of Canada from the Canadian Journal of Chemistry.

However, Downes and Harris [128] found $k_{12}/k_{14} = 1.060$ for the carbon KIE in the Cannizzaro reaction of formaldehyde in water with 0.5 M sodium hydroxide. More recently, Luther and Koch [106] found $k_{12}/k_{14} = 1.042 \pm 0.004$ for the Cannizzaro reaction of benzaldehyde-7-¹⁴C in 50% aqueous methanol with 1 M potassium hydroxide at 50°.

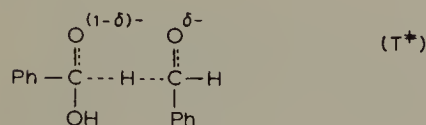
The kinetics of the Cannizzaro reaction of benzaldehyde are known to be of the third order, second order in benzaldehyde and first order in hydroxide ion [129]. If the reaction is carried out in D₂O solution, the products do not possess any carbon-bonded deuterium [130]. The generally accepted mechanism is a variant of that suggested by Hammett [131] in 1940.



Additional evidence for a hydrogen transfer (either H⁺, H, or H⁻) in the rate-determining step is supplied by the α-deuterium KIE of $k_{\text{H}}/k_{\text{D}} = 1.8 \pm 0.2$, measured by Wiberg [132].

The Hammett mechanism involves two subsequent additions of nucleophile to the carbonyl carbon, one to each of the participating benzaldehyde molecules. However, in the hydride transfer step, the C=O double bond of the second reactant molecule is

opened while that of the first is simultaneously restored. The transition state T^\ddagger possesses two partially opened (dashed lines) $C\cdots O$ double bonds. Since benzaldehyde-7- ^{14}C is present at a tracer level, only one of the two carbonyl groups may contain the label. (The probability for the existence of transition states with two carbon-14 atoms is very low.)



For these reasons, it is to be expected that the carbon KIE in the Cannizzaro reaction is lower than in more simple carbonyl addition reactions.

Luther and Koch [106] also measured α -tritium KIEs in the Cannizzaro reaction of benzaldehyde and a few other aromatic aldehydes. Results of k_H/k_T were in the range 1.2–1.4, appreciably lower than Wiberg's result of k_H/k_D for the Cannizzaro reaction of benzaldehyde. This is not surprising if it is considered that the deuterium KIE was determined with the aid of separate kinetic experiments with either the pure α -H or the pure α -D compounds, while tritium KIEs were determined by the competitive method at tracer levels of the T compound. The compound with "light" hydrogen is more reactive as a hydride donor because of the primary isotope effect. In addition, it is present in large excess. Consequently, hydride ions to be transferred are supplied mainly by "light" reactant molecules and tritiated benzaldehyde molecules mainly react by accepting hydride ions. Therefore, the contribution of the primary isotope effect to the observed tritium KIE must be relatively small.

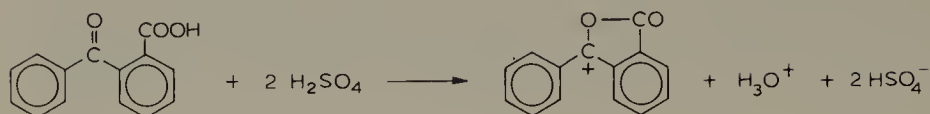
The α -deuterium isotope effect in the Cannizzaro reaction is composed of a primary isotope effect referring to the hydride (deuteride) being transferred and a secondary isotope effect of the α -hydrogen (deuterium) in the hydride acceptor molecule. α -Deuterium KIEs in various carbonyl addition reactions of benzaldehyde are inverse, with values of $k_H/k_D \sim 0.8$ [133]. It may be concluded that the real primary isotope effect in the Cannizzaro reaction of benzaldehyde is higher than the observed value of $k_H/k_D = 1.8$.

D. Miscellaneous reactions

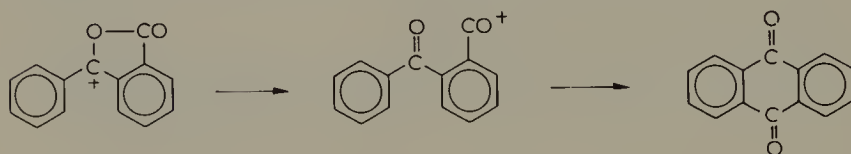
1. Cyclization of *o*-benzoylbenzoic acid

An early determination of the carbon KIE in the cyclization of *o*-benzoylbenzoic acid (to form anthraquinone), $k_{12}/k_{14} = 0.931$ [134], was later found to be erroneous. Ropp [135] reported a result of $k_{12}/k_{14} = 1.035$ for the same reaction (label at the carboxylic carbon) at 80° . The mechanism of this reaction has been investigated by Newman et al. [136]. When *o*-benzoylbenzoic acid is dissolved in sulfuric acid, a four-fold freezing point depression is found, indicating that protonation of the substrate is followed by elimination of H_2O which then adds another proton. As suggested by New-

man, the following reaction takes place immediately.



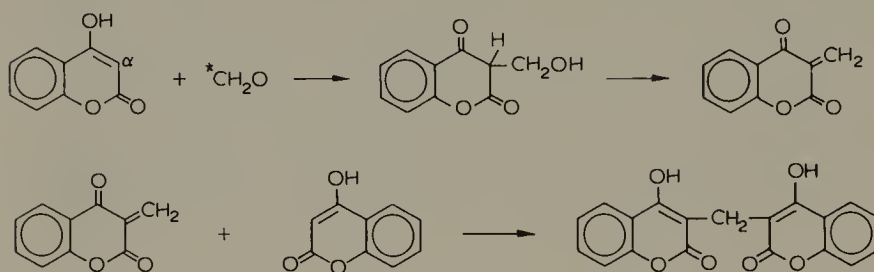
In the mechanism for the subsequent formation of anthraquinone (which occurs upon heating), the five-membered ring is opened by heterolytic bond cleavage between oxygen and carbonyl carbon. The benzene ring which carries the CO^+ group is then rotated in such a way that the group may attack a carbon atom of the other benzene ring, probably with formation of a σ complex intermediate.



It is expected that the bond cleavage step causes a normal isotope effect. The latter is probably counteracted by a small inverse isotope effect in the subsequent ring closure by formation of the σ complex.

2. Reaction of formaldehyde with 4-hydroxycoumarin

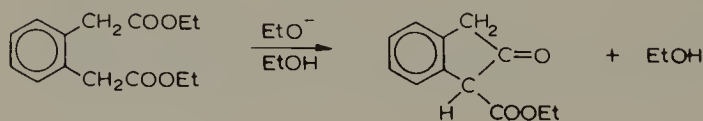
A relatively large carbon KIE was found by Lee and Spinks [137] in the reaction of labeled formaldehyde with 4-hydroxycoumarin, $k_{12}/k_{14} = 1.073 \pm 0.003$ in aqueous solution at 99.5° .



In extending the work, Fry and Rothrock [138] measured the α -carbon KIE in this reaction, $k_{12}/k_{14} = 1.115$. This KIE is large because an isotopic double fractionation takes place.

3. The Dieckmann condensation

Carrick and Fry [139] studied the carbon- ^{14}C KIE in the Dieckmann condensation.



The reactant was labeled either in the carboxylic or the methylene group. Relatively large KIEs were observed in both cases, $k_{12}/k_{14} = 1.087 \pm 0.018$ per COO whose carbon atom then becomes a member of the new ring, and $k_{12}/k_{14} = 1.085 \pm 0.015$ per CH_2 , both at 80° . These large KIEs were considered to be primary, and it was concluded that bond formation between carboxyl carbon and methylene carbon takes place in (or prior to) the rate-determining step.

The carboxyl-C KIE is of the usual magnitude of a carbonyl addition reaction. As far as the methylene-C KIE is concerned, however, one would rather expect an inverse isotope effect for rate-determining bond formation leading to ring closure. The cause of the observed "normal" isotope effect is unknown.

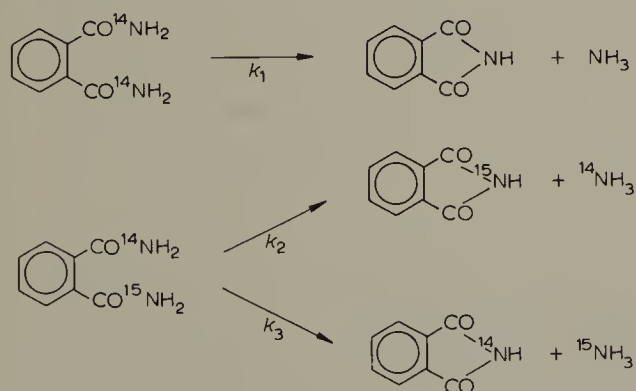
Carrick and Fry also measured the "intramolecular" KIE in the Dieckmann condensation, " k_2/k_3 " = 1.056 ± 0.009 , by evaluating the following ratio of labeled reaction products.



(Upon heating, these compounds readily decompose with elimination of carbon dioxide which, depending on the precursor, is either labeled or unlabeled.) It is possible to compute from this measurement (and the result of the "intermolecular" KIE) a secondary carbon KIE in which the labeled carboxyl carbon is adjacent to the methylene-carbon participating in the ring closure, $k_{12}/k_{14} = 1.087/1.056 = 1.029$. Unfortunately, this result is of little value, because of the accumulated experimental uncertainty of $0.009 + 0.018 = 0.027$ in the KIE.

4. The thermal deammonation of phthalamide

In 1952, Stacey et al. [140] measured nitrogen-15 KIEs in the thermal deammonation of phthalamide in the solid phase at 180° .

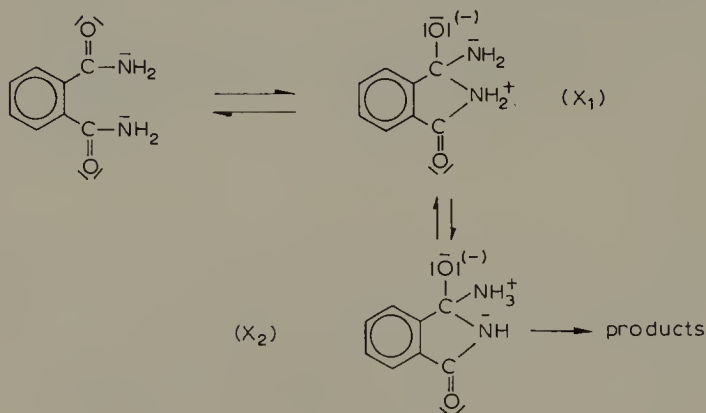


The results were $k_1/2k_2 = 0.994 \pm 0.001$ and $k_1/2k_3 = 1.006 \pm 0.001$. An early at-

tempt at a theoretical calculation of these KIEs was carried out by Bigeleisen [141] in the same year.

However, the causes of the KIEs may be understood much better if more information is available concerning the mechanism. It may be concluded from the following considerations that there is no carbon–nitrogen bond rupture in the transition state of the slow step.

It is reasonable to assume that a tetrahedral intermediate X_1 is formed in the first step. By prototropic change, it may go over to the intermediate X_2 , which then splits off NH_3 .



Because of the strong electron-withdrawing effect of the carbonyl group, intermediate (X_1) must be a much stronger acid than intermediate (X_2). Consequently, the equilibrium between (X_1) and (X_2) must be far (by several powers of ten) on the side of (X_2), and it may be expected that elimination of NH_3 from (X_2) occurs much more frequently than ring opening of (X_1). If the rate of the product-forming step is faster than that of reversal of the first step, the first step must be slow and rate-determining.

On the basis of these conclusions, the KIE in the reaction pathway leading to elimination of $^{15}\text{NH}_3$ is a secondary effect. One of its possible causes may be the hybridization change of the adjacent carbon from sp^2 to sp^3 in the formation of the intermediate. On the other hand, we have to expect a small inverse KIE in the formation of the intermediate (X_1) if the labeled N atom becomes a member of the new ring.

E. α -Deuterium isotope effects in carbonyl addition reactions of aldehydes

Secondary α -deuterium isotope effects are larger and easier to measure than primary carbon isotope effects, and this applies to S_{N} reactions as well as carbonyl addition processes. The mechanisms of reactions of aldehydes with various carbonyl reagents have been studied extensively, mainly by Jencks and co-workers [118]. It may be concluded from the pH dependence of the rates of these reactions that there is a change in the rate-determining step. In studies of the reactions of aldehydes with hy-

droxylamine, methoxyamine, semicarbazide, and hydrazine near neutral pH, it was found that the (tetrahedral) addition compound is formed first. It is then dehydrated to the final product (with a carbon–nitrogen double bond) in a subsequent slow step.



(At relatively high concentrations of the carbonyl reagent, it was possible to observe directly, by u.v. spectrophotometry, the initial formation of the addition compound.) Since the dehydration step was found to be rate-determining at the high pH side (near neutral) of the bell-shaped rate–pH profiles, it was concluded that formation of the addition compound must be rate-determining at the low pH side. Furthermore, it was generalized that the situation is similar in the reactions of aldehydes with aliphatic or aromatic amines [118].

Some work on α -deuterium KIEs in the formation of 2,4-dinitrophenylhydrazones was carried out by Raaen et al. [124] who utilized carbon-14 as a tracer for deuterium. Cordes and co-workers [133] carried out extensive direct studies of α -deuterium isotope effects on equilibrium and rate constants of various carbonyl addition reactions of aldehydes.

In the formation of the addition compound, the hybridization of the aldehyde carbon is changed from sp^2 to sp^3 . It is reasonable to assume that the α -deuterium KIE in this reaction is of a similar magnitude as the inverse value of the α -deuterium KIE in S_N1 solvolysis (in which hybridization changes from sp^3 to sp^2). The measured values of α -D isotope effects on the equilibrium constants in aqueous solution at 25° are $K^D/K^H = 1.276 \pm 0.002$ for the reaction of 4-methoxybenzaldehyde with hydrogen cyanide, and $K^D/K^H = 1.36 \pm 0.02$ for the reaction (formation of addition compound) of benzaldehyde with hydroxylamine [133]. These values are much larger than expected, probably because the stretching force constant of the aldehyde C–H bond is low in comparison to that for other $C(sp^2)$ –H bonds.

The α -D isotope effects on the rate constants of formation of semicarbazones and phenylhydrazones of benzaldehydes were found in the range $k_D/k_H = 1.13$ – 1.29 (most values being close to 1.22), under conditions in which carbinolamine formation is rate-determining [133]. (These KIEs are inverse, $k_H/k_D < 1$ and $k_D/k_H > 1$.) It follows from comparison of these results with the isotope effect on the equilibrium constant for the addition of hydroxylamine that carbon–nitrogen (single) bond formation in the transition states has proceeded to a large extent though not to completion. Under conditions in which dehydration of carbinolamine is rate-determining, the α -deuterium KIEs on these reactions were found to be in the range $k_D/k_H = 1.27$ – 1.31 (except for the formation of 4-nitrobenzaldehyde-semicarbazone, with $k_D/k_H = 1.20$). It may be concluded that large (inverse) KIEs correspond to transition states which resemble the carbinolamine. Carbon–oxygen bond cleavage did not proceed far in these transition states [133].

In another study [142], α -deuterium KIEs were determined for the hydrolysis of

substituted benzylidene-1,1-dimethylethylamines, $k_D/k_H = 1.20-1.22$. It was concluded that the carbon-oxygen bond formation and the opening of the carbon-nitrogen double bond are nearly complete in the transition state.

REFERENCES

- 1 J. Bigeleisen and L. Friedman, *J. Chem. Phys.*, **17** (1949) 998.
- 2 P.E. Yankwich and M. Calvin, *J. Chem. Phys.*, **17** (1949) 109.
- 3 A. Roe and M. Hellman, *J. Chem. Phys.*, **19** (1951) 660.
- 4 J.G. Lindsay, A.N. Bourns and H.G. Thode, *Can. J. Chem.*, **29** (1951) 192.
- 5 J. Bigeleisen and T.L. Allen, *J. Chem. Phys.*, **19** (1951) 760.
- 6 G.A. Ropp and V.F. Raaen, *J. Am. Chem. Soc.*, **74** (1952) 4992.
- 7 A. Fry and M. Calvin, *J. Phys. Chem.*, **56** (1952) 901.
- 8 G.A. Ropp, A.J. Weinberger and O.K. Neville, *J. Am. Chem. Soc.*, **73** (1951) 5573.
- 9 J.G. Lindsay, D.E. McElcheran and H.G. Thode, *J. Chem. Phys.*, **17** (1949) 589.
- 10 A. Fry and M. Calvin, *J. Phys. Chem.*, **56** (1952) 897.
- 11 J. Bigeleisen and M. Goeppert-Mayer, *J. Chem. Phys.*, **15** (1947) 261; J. Bigeleisen, *J. Chem. Phys.*, **17** (1949) 675; J. Bigeleisen and M. Wolfsberg, *Adv. Chem. Phys.*, **1** (1958) 15.
- 12 M.L. Bender and D.F. Hoeg, *J. Am. Chem. Soc.*, **79** (1957) 5649.
- 13 M.L. Bender and G.J. Buist, *J. Am. Chem. Soc.*, **80** (1958) 4304.
- 14 G.J. Buist and M.L. Bender, *J. Am. Chem. Soc.*, **80** (1958) 4308.
- 15 K.R. Lynn and P.E. Yankwich, *J. Am. Chem. Soc.*, **83** (1961) 53, 790, 3220.
- 16 J.B. Stothers and A.N. Bourns, *Can. J. Chem.*, **40** (1962) 2007.
- 17 A. Fry, Heavy Atom Isotope Effects in Organic Reaction Mechanism Studies, in C.J. Collins and N.S. Bowman (Eds.), *Isotope Effects in Chemical Reactions*, Van Nostrand Reinhold, New York, 1970, p. 364.
- 18 a. V.J. Shiner, Jr., Deuterium Isotope Effects in Solvolytic Substitution at Saturated Carbon, in C.J. Collins and N.S. Bowman (Eds.), *Isotope Effects in Chemical Reactions*, Van Nostrand Reinhold, New York, 1970, p. 90 (and further references therein).
b. D.E. Sunko and S. Borčić, Secondary Deuterium Isotope Effects and Neighboring Group Participation, in C.J. Collins and N.S. Bowman (Eds.), *Isotope Effects in Chemical Reactions*, Van Nostrand Reinhold, New York, 1970, p. 160 (and further references therein).
- 19 A.J. Kresge, N. Lichtin, K.N. Rao and R.E. Weston, *J. Am. Chem. Soc.*, **87** (1964) 437.
- 20 J.B. Stothers and A.N. Bourns, *Can. J. Chem.*, **38** (1960) 923.
- 21 J. Bron and J.B. Stothers, *Can. J. Chem.*, **46** (1968) 1435, 1825; **47** (1969) 2506.
- 22 Y. Yukawa, T. Ando, K. Token, M. Kawada and S.-G. Kim, *Tetrahedron Lett.*, (1969) 2367; (1971) 847; H. Yamataka, S.-G. Kim, T. Ando and Y. Yukawa, *Tetrahedron Lett.*, (1973) 4767.
- 23 R.B. Fahim and E.A. Moelwyn-Hughes, *J. Chem. Soc.*, (1956) 1035.
- 24 C.K. Ingold, *Structure and Mechanism in Organic Chemistry*, Cornell University Press, Ithaca, N.Y., 1953.
- 25 S. Seltzer and A.A. Zavitsas, *Can. J. Chem.*, **45** (1967) 2023.
- 26 J.O. Edwards, *J. Am. Chem. Soc.*, **76** (1954) 1540; **78** (1956) 1819; **84** (1962) 16.
- 27 C.M. Won and A.V. Willi, *J. Phys. Chem.*, **76** (1972) 427 (and further references therein).
- 28 C.G. Swain and C.B. Scott, *J. Am. Chem. Soc.*, **75** (1953) 141.
- 29 W.L. Petty and P.L. Nichols, *J. Am. Chem. Soc.*, **76** (1954) 4385.
- 30 A.V. Willi and C.M. Won, *Can. J. Chem.*, **48** (1970) 1452.
- 31 A.V. Willi and C.M. Won, *J. Am. Chem. Soc.*, **90** (1968) 5999.

- 32 K.T. Leffek and J.W. McLean, *Can. J. Chem.*, 43 (1965) 40; K.T. Leffek and A.F. Matheson, *Can. J. Chem.*, 50 (1972) 982, 986.
- 33 J.A. Llewellyn, R.E. Robertson and J.M.W. Scott, *Can. J. Chem.*, 38 (1960) 222.
- 34 G.E. Jackson and K.T. Leffek, *Can. J. Chem.*, 47 (1969) 1537.
- 35 K.T. Leffek, *Can. J. Chem.*, 42 (1964) 851.
- 36 E.P. Grimsrud and J.W. Taylor, *J. Am. Chem. Soc.*, 92 (1970) 739; C.R. Turnquist, J.W. Taylor and E.P. Grimsrud, *J. Am. Chem. Soc.*, 95 (1973) 4133.
- 37 A.V. Willi, C. Ho and A. Ghanbarpour, *J. Org. Chem.*, 37 (1972) 1185.
- 38 P.M. Nair, Ph.D. Dissertation, University of Arkansas, Fayetteville, Arkansas, 1956; Dissertation Abstr., 17 (1957) 1469; A. Fry, Heavy Atom Isotope Effects in Organic Reaction Mechanism Studies, in C.J. Collins and N.S. Bowman (Eds.), *Isotope Effects in Chemical Reactions*, Van Nostrand Reinhold, New York, 1970, p. 377.
- 39 N. Pearson and A. Fry, Heavy Atom Isotope Effects in Organic Reaction Mechanism Studies, in C.J. Collins and N.S. Bowman (Eds.), *Isotope Effects in Chemical Reactions*, Van Nostrand Reinhold, New York, 1970, p. 379.
- 40 J.W. Hill and A. Fry, *J. Am. Chem. Soc.*, 84 (1962) 2763.
- 41 B. Östman, *J. Am. Chem. Soc.*, 87 (1965) 3163.
- 42 H. Strecker and H. Elias, *Chem. Ber.*, 102 (1969) 1270.
- 43 V.F. Raaen, T. Juhlke, F.J. Brown, and C.J. Collins, *J. Am. Chem. Soc.*, 96 (1974) 5928.
- 44 J. Bron and J.B. Stothers, *Can. J. Chem.*, 46 (1968) 1825.
- 45 V.J. Shiner, Jr., M.W. Rapp and H.R. Pinnick, *J. Am. Chem. Soc.*, 92 (1970) 232.
- 46 S.I. Miller, *J. Phys. Chem.*, 66 (1962) 978.
- 47 M. Wolfsberg and M.J. Stern, *Pure Appl. Chem.*, 8 (1964) 225, 325; M.J. Stern and M. Wolfsberg, *J. Chem. Phys.*, 39 (1963) 2776; *J. Pharm. Sci.*, 54 (1965) 849.
- 48 J.H. Schachtschneider and R.G. Snyder, *Spectrochim. Acta*, 19 (1963) 117.
- 49 A.V. Willi, *Can. J. Chem.*, 44 (1966) 1889; *Z. Naturforsch., Teil A*, 21 (1966) 1377, 1385.
- 50 L.B. Sims, A. Fry, L.T. Netherton, J.C. Wilson, K.D. Reppond and S.W. Crook, *J. Am. Chem. Soc.*, 94 (1972) 1364.
- 51 J. Bron, *Can. J. Chem.*, 52 (1974) 903.
- 52 A.V. Willi, *Z. Phys. Chem. (Frankfurt am Main)*, 66 (1969) 317.
- 53 M.J. Stern and M. Wolfsberg, *J. Chem. Phys.*, 45 (1966) 4105.
- 54 T.M. Bare, N.D. Hershey, H.O. House and C.G. Swain, *J. Org. Chem.*, 37 (1972) 997.
- 55 H.S. Johnston, *Adv. Chem. Phys.*, 3 (1960) 131.
- 56 D.K. Bohme and L.B. Young, *J. Am. Chem. Soc.*, 92 (1970) 7354.
- 57 A.J. Parker, *J. Chem. Soc.*, (1961) 1328; *Q. Rev. (London)*, 16 (1962) 163; *Adv. Org. Chem.*, 5 (1965) 1.
- 58 L.P. Hammett, *Physical Organic Chemistry*, McGraw-Hill, New York, 1940, p. 184.
- 59 H.C. Brown and Y. Okamoto, *J. Am. Chem. Soc.*, 79 (1957) 1913; Y. Okamoto and H.C. Brown, *J. Org. Chem.*, 22 (1957) 485.
- 60 K.M. Koshy, R.E. Robertson and W.M.J. Strachan, *Can. J. Chem.*, 51 (1973) 2958.
- 61 A. Streitwieser, Jr., R.H. Jagow, R.C. Fahey and S. Suzuki, *J. Am. Chem. Soc.*, 80 (1958) 2326.
- 62 K. Mislow, S. Borčić and V. Prelog, *Helv. Chim. Acta*, 40 (1957) 2477.
- 63 V.J. Shiner, Jr., W. Dowd, R.D. Fisher, S.R. Hartshorn, M.A. Kessick, L. Milakowsky and M.W. Rapp, *J. Am. Chem. Soc.*, 91 (1969) 4838; V.J. Shiner, Jr., W.E. Buddenbaum, B.L. Murr and G. Lamaty, *J. Am. Chem. Soc.*, 90 (1968) 418.
- 64 L.R.C. Barclay, J.R. Mercer and J.C. Hudson, *Can. J. Chem.*, 50 (1972) 3965.
- 65 A. Streitwieser and G.A. Dafforn, *Tetrahedron Lett.*, (1969) 1236.
- 66 V.J. Shiner, Jr., M.W. Rapp, E.A. Halevi and M. Wolfsberg, *J. Am. Chem. Soc.*, 90 (1968) 7171.

- 67 V.J. Shiner, Jr. and W. Dowd, *J. Am. Chem. Soc.*, 93 (1971) 1029.
- 68 K.M. Koshy and R.E. Robertson, *J. Am. Chem. Soc.*, 96 (1974) 914.
- 69 J.M. Harris, R.E. Hall and P.v.R. Schleyer, *J. Am. Chem. Soc.*, 93 (1971) 2551.
- 70 V.J. Shiner, Jr. and R.D. Fisher, *J. Am. Chem. Soc.*, 93 (1971) 2553.
- 71 A.V. Willi, C. Ho and A. Ghanbarpour, *J. Org. Chem.*, 37 (1972) 1185, footnote 22.
- 72 R.M. Bartholomew, F. Brown and M. Lounsbury, *Can. J. Chem.*, 32 (1954) 979.
- 73 A. Fry, *Heavy Atom Isotope Effects in Organic Reaction Mechanism Studies*, in C.J. Collins and N.S. Bowman (Eds.), *Isotope Effects in Chemical Reactions*, Van Nostrand Reinhold, New York, 1970 p. 383.
- 74 E.R. Thornton, *Solvolysis Mechanisms*, Ronald Press, New York, 1964, p. 206.
- 75 R.A. Sneen and J.W. Larsen, *J. Am. Chem. Soc.*, 91 (1969) 362, 6031.
- 76 a. D.G. Graczyk and J.W. Taylor, *J. Am. Chem. Soc.*, 96 (1974) 3255.
b. W.H. Saunders, S. Aşperger and D.H. Edison, *J. Am. Chem. Soc.*, 80 (1958) 2421.
- 77 P. Riesz and J. Bigeleisen, *J. Am. Chem. Soc.*, 81 (1959) 6187.
- 78 W.H. Stevens, J.M. Pepper and M. Lounsbury, *Can. J. Chem.*, 30 (1952) 529.
- 79 W.M. Schubert, *J. Am. Chem. Soc.*, 71 (1949) 2639; W.M. Schubert, J. Donahue and J.D. Gardner, *J. Am. Chem. Soc.*, 76 (1954) 9; W.M. Schubert, R.E. Zahler and J. Robins, *J. Am. Chem. Soc.*, 77 (1955) 2293.
- 80 W.M. Schubert and J.D. Gardner, *J. Am. Chem. Soc.*, 75 (1953) 1401.
- 81 A.V. Willi and J.F. Stocker, *Helv. Chim. Acta*, 37 (1954) 1113; A.V. Willi, *Helv. Chim. Acta*, 40 (1957) 1053, 43 (1960) 644; *Trans. Faraday Soc.*, 55 (1959) 433.
- 82 A.V. Willi, *Z. Naturforsch., Teil A*, 13 (1958) 997.
- 83 K.R. Lynn and A.N. Bourns, *Chem. Ind. (London)*, (1963) 782.
- 84 A.V. Willi, *Z. Phys. Chem. (Frankfurt am Main)*, 27 (1961) 221.
- 85 J.M. Los, R.F. Rekker and C.H.T. Tonsbeek, *Rec. Trav. Chim.*, 86 (1967) 622.
- 86 G.E. Dunn, P. Leggate and I.E. Scheffler, *Can. J. Chem.*, 43 (1965) 3080.
- 87 A.V. Willi, C.M. Won and P. Vilk, *J. Phys. Chem.*, 72 (1968) 3142.
- 88 A.V. Willi and P. Vilk, *Z. Phys. Chem. (Frankfurt am Main)*, 59 (1968) 189.
- 89 A.V. Willi, M.H. Cho and C.M. Won, *Helv. Chim. Acta*, 53 (1970) 663.
- 90 A.V. Willi, M.H. Cho and W. Chen, *Z. Phys. Chem. (Frankfurt am Main)*, 91 (1974) 193.
- 91 J.L. Longridge and F.A. Long, *J. Am. Chem. Soc.*, 90 (1968) 3092.
- 92 A.N. Bourns, *Trans. R. Soc. Can., Vol. II, Ser. IV, Sect. III* (1964) 277.
- 93 A.N. Bourns, personal communication (1962).
- 94 G.E. Dunn and S.K. Dayal, *Can. J. Chem.*, 48 (1970) 3349.
- 95 G.E. Dunn and J. Buccini, *Can. J. Chem.*, 46 (1968) 563.
- 96 H.H. Huang and F.A. Long, *J. Am. Chem. Soc.*, 91 (1969) 2872.
- 97 M.A. Paul and F.A. Long, *Chem. Rev.*, 57 (1957) 1.
- 98 A.A. Bothner-By and J. Bigeleisen, *J. Chem. Phys.*, 19 (1951) 755; W.H. Stevens, J.M. Pepper and M. Lounsbury, *J. Chem. Phys.*, 20 (1952) 192.
- 99 P.E. Yankwich, A.L. Promislow and R.F. Nystrom, *J. Am. Chem. Soc.*, 76 (1954) 5893.
- 100 J. Bigeleisen, *J. Chem. Phys.*, 17 (1949) 344, 425.
- 101 K.S. Pitzer, *J. Chem. Phys.*, 17 (1949) 1341.
- 102 M.J. Stern and M. Wolfsberg, *J. Chem. Phys.*, 39 (1963) 2776.
- 103 W.H. Stevens and R.W. Attree, *Can. J. Res., Sect. B*, 27 (1949) 807.
- 104 G.A. Ropp and V.F. Raaen, *J. Chem. Phys.*, 20 (1952) 1823.
- 105 a. G.A. Ropp and V.F. Raaen, *J. Chem. Phys.*, 22 (1954) 1223.
b. V.F. Raaen and G.A. Ropp, *J. Chem. Phys.*, 21 (1953) 1902.
- 106 D. Luther and H. Koch, *Chem. Ber.*, 99 (1966) 2227.
- 107 C.G. Mitton and R.L. Schowen, *Tetrahedron Lett.*, (1968) 5803.
- 108 C.B. Sawyer and J.F. Kirsch, *J. Am. Chem. Soc.*, 95 (1973) 7375.

- 109 H.L. Goering, J.T. Doi and K.D. McMichael, *J. Am. Chem. Soc.*, 86 (1964) 1951.
- 110 J. Bigeleisen, *J. Phys. Chem.*, 56 (1952) 823.
- 111 M.L. Bender, *Chem. Rev.*, 60 (1960) 53 (and further references therein).
- 112 G.S. Hammond, *J. Am. Chem. Soc.*, 77 (1955) 334.
- 113 M.L. Bender, *J. Am. Chem. Soc.*, 73 (1951) 1626; M.L. Bender, R.D. Ginger and J.P. Unik, *J. Am. Chem. Soc.*, 80 (1958) 1044.
- 114 M.L. Bender and R.J. Thomas, *J. Am. Chem. Soc.*, 83 (1961) 4189.
- 115 M.L. Bender, H. Matsui, R.J. Thomas and S.W. Tobey, *J. Am. Chem. Soc.*, 83 (1961) 4193.
- 116 F. Brown and D.A. Holland, *Can. J. Chem.*, 30 (1952) 438.
- 117 G.A. Ropp, V.F. Raaen and A.J. Weinberger, *J. Am. Chem. Soc.*, 75 (1953) 3694.
- 118 W.P. Jencks, *Prog. Phys. Org. Chem.*, 2 (1964) 63 (and further references therein).
- 119 R.L. Shriner and R.C. Fuson, *Identification of Organic Compounds*, 2nd edn., Wiley, New York, 1940, p. 171.
- 120 R.L. Shriner, R.C. Fuson and D.Y. Curtin, *The Systematic Identification of Organic Compounds*, 5th edn., Wiley, New York, 1965, p. 253.
- 121 E.B. Wilson, J.C. Decius and P.C. Cross, *Molecular Vibrations*, McGraw-Hill, New York, 1955, p. 175.
- 122 H. Simon and D. Palm, *Chem. Ber.*, 93 (1960) 1289.
- 123 V.F. Raaen, A.K. Tsiomis and C.J. Collins, *J. Am. Chem. Soc.*, 82 (1960) 5502.
- 124 V.F. Raaen, T.K. Dunham, D.D. Thompson and C.J. Collins, *J. Am. Chem. Soc.*, 85 (1963) 3497.
- 125 W.A. Sheppard and A.N. Bourns, *Can. J. Chem.*, 32 (1954) 4.
- 126 W.A. Sheppard, R.F.W. Bader and A.N. Bourns, *Can. J. Chem.*, 32 (1954) 345.
- 127 W.H. Stevens and R.W. Attree, *J. Chem. Phys.*, 18 (1950) 574.
- 128 A.M. Downes and G.M. Harris, *J. Chem. Phys.*, 20 (1952) 196.
- 129 J. Hine, *Physical Organic Chemistry*, McGraw-Hill, New York, 1956, p. 261 (and further references therein).
- 130 H. Fredenhagen and K.F. Bonhoeffer, *Z. Phys. Chem., Abt. A*, 181 (1938) 379.
- 131 L.P. Hammett, *Physical Organic Chemistry*, McGraw-Hill, New York, 1940, p. 351.
- 133 L. do Amaral, H.G. Bull and E.H. Cordes, *J. Am. Chem. Soc.*, 94 (1972) 7579; L. do Amaral, M.P. Bastos, H.G. Bull and E.H. Cordes, *J. Am. Chem. Soc.*, 95 (1973) 7369.
- 134 W.H. Stevens and D.A. Crowder, *Can. J. Chem.*, 32 (1954) 792.
- 135 G.A. Ropp, *J. Chem. Phys.*, 23 (1955) 2196; *J. Org. Chem.*, 25 (1960) 1255.
- 136 M.S. Newman, *J. Am. Chem. Soc.*, 64 (1942) 2324; M.S. Newman, H.G. Kuivila and A.B. Garrett, *J. Am. Chem. Soc.*, 67 (1945) 704.
- 137 C.C. Lee and J.W.T. Spinks, *Can. J. Chem.*, 32 (1954) 327.
- 138 A. Fry and T.S. Rothrock, unpublished. A. Fry, *Heavy Atom Isotope Effects in Organic Reaction Mechanism Studies*, in C.J. Collins and N.S. Bowman (Eds.), *Isotope Effects in Chemical Reactions*, Van Nostrand Reinhold, New York, p. 400.
- 139 W.L. Carrick and A. Fry, *J. Am. Chem. Soc.*, 77 (1955) 4381.
- 140 F.W. Stacey, J.G. Lindsay and A.N. Bourns, *Can. J. Chem.*, 30 (1952) 135.
- 141 J. Bigeleisen, *Can. J. Chem.*, 30 (1952) 443.
- 142 J. Archila, H. Bull, C. Langenaur and E.H. Cordes, *J. Org. Chem.*, 36 (1971) 1345.

SUBJECT INDEX

- Acetic acid enriched, 42, 43, 62
 Acid catalysis, general, 258
 —, specific, 258, 269
 Activation energy, 55, 57, 77, 85
 2-Adamantyl compounds, 252
 Alicyclic systems, 56
 Aminobenzoic acids, 257, 259–263, 266, 267
 4-Aminosalicylic acid, 258, 260
 Anomeric equilibrium, 60, 67
 Ansamycins, 131
 Anthranilic acid, 15–17
 Antibiotic X-537 A, 144
 2-Arylethyl arenesulfonates, 238, 255–257
 Aryl participation, 255–257
 Ascochlorin, 148
 Asperentin, 118
 Asperlin, 117
 Aureothin, 144
 Avenaciolide, 126
 Azulene-1-carboxylic acid, 17, 261, 263–266
- Base catalysis, specific, 267–270
 Bending force constants, 241, 242, 245, 246, 253
 Bending vibrations, 241–246, 253
 o-Benzoylbenzoic acid, 275, 276
 Bromodecarboxylation, 32
 Bromomalonic acid, 29
- Camptothecin, 158
 Cannizzaro reaction, 273–275
 Carbanions, 96
 Carbenes, 80, 90
 Carbenium ion rearrangements, 67, 92
 Carbon-12, 49, 99
 Carbon-13, chemical shift, 50, 67, 73, 92–94
 —, depleted studies, 48, 99
 —, enriched studies, 43, 48, 62, 63, 66–72, 76, 78, 80–83, 88, 94, 97
 —, n.m.r. sensitivity, 41, 46
 —, quantitative analysis, 50
 —, satellite analysis, 41, 42, 46, 63, 66, 70, 71, 75, 78, 80, 82, 83
 Carbon-13 chemical shift characteristics, charge density, 178, 208
 —, C–H bond polarization, 177, 183
 —, “cog wheel” effect, 197
 —, deshielding by *anti-periplanar* heteroatoms, 198
 —, δ -deshielding effect, 194–197
 —, dynamic systems, 204
 —, enthalpy and free energy, 178, 179, 184, 188
 —, γ -*gauche* effect, 175–194
 —, interconversion of conformers, 205
 —, “overall” shielding differences, 175, 179, 184
 —, paramagnetic and diamagnetic contributions, 178, 179, 201
 —, protonation sites, 207
 —, range, 171
 —, restricted bond rotation, 182, 204
 —, ring size effects, 199
 —, substituent parameters, 175
 —, substituent size, effect of, 179
 —, symmetry considerations, 201
 —, tacticity of synthetic polymers, 180
 —, tautomeric equilibria, 206
 Carbon-13 chemical shifts steric effects in,
 alkanes, 176
 —, alkenes, geometric isomers of, 182
 —, amides, 182, 204, 207
 —, arenes, 189, 194
 —, bridged ring systems, 192–196, 202
 —, carbocations, 206, 207
 —, carbohydrates, 185–187, 195, 199, 203, 206
 —, cycloalkanes, 178, 187, 188, 199, 204
 —, fused ring systems, 190–192, 195, 202, 203
 —, polypeptides and proteins, 202–204
 —, saturated heterocyclic compounds, 185–187, 192, 197–199, 203
 —, spiro compounds, 189
 —, substituted alkanes, 181, 194
 —, substituted cycloalkanes, 176, 179, 186–188, 198, 205
 —, synthetic polymers, 179, 180
 Carbon-13– ^1H spin–spin coupling (1J , 2J , 3J),
 174, 208–219
 —, alkenes, differences between geometric isomers, 210, 213, 217

- , anomeric configuration of carbohydrates, 211
- , calculation of J , 212, 214, 215
- , configuration at a quaternary carbon, 218
- , conformations of acyclic systems, 216–218
- , dihedral (torsional) angle dependence of 3J , 215
- , effect of electronegative substituents, 210, 211, 214, 215
- , hybridization and magnitude of 1J , 210
- , orientational dependence of 2J , 213
- Carbon-13 n.m.r. spectroscopic techniques, ^{13}C -enrichment and measurement of $J_{\text{C-H}}$, 209
 - , ^{13}C – ^1H coupling, measurement of, 209
 - , effect of deuteration, 173
 - , gated decoupling, 174, 209
 - , ^1H -coupled, 174, 208
 - , ^1H -decoupled, 172
 - , $J_{\text{C-H}}$ sign determination, 209
 - , pulsed FT spectroscopy, 172
 - , selective ^1H -decoupling, 174
- Carbon-13 satellite signals, 172
- Carbon-13 spin-lattice relaxation times (T_1), 224–229
 - , and intermolecular association, 228
 - , and molecular motion, 226
 - , and proton proximity, 224
 - , and segmental motion, 227
 - , dipolar mechanism, 224
 - , paramagnetic substances, effect of, 228
 - , measurements on, alkaloids, 225
 - , —, alkyl chains, 225, 227
 - , —, antibody–antigen interactions, 229
 - , —, ring compounds, 224, 226
 - , —, synthetic polymers, 225, 227
 - , —, α,β -unsaturated aldehydes, 226
- Carbon-13 spin–spin coupling stereochemistry of, with ^{13}C , 219
 - , with ^{19}F , 222
 - , with ^1H , 174, 208–219
 - , with metals, 223
 - , with ^{15}N , 223
 - , with ^{31}P , 220
- Carbon-13, tracer in biosynthesis, 172
- Carbon-14, comparison with carbon-13, 46, 67–71, 74, 76
- Carbon dioxide, collection and purification, 10
- Carbon isotope effects, 237, 238, 240, 242, 245, 247, 249, 250, 253, 255–258, 261, 263, 264, 267–269, 271–273, 275–277
 - Carbonium ion, 67, 92
 - Carbonyl addition, 267–280
 - Cephalosporins, 139
 - Cerulenin, 128
 - Chlorine-37 KIEs, 244, 245, 249, 254
 - CIDNP, 86
 - Colchicin, 159
 - Complex formation, 60, 97, 99
 - Computer calculations of KIEs, 239–248, 264
 - Conformation studies, 50, 53, 56, 57
 - Coriolin, 150
 - Corrins, 152
 - Cyanocobalamin, 152
 - Cytochalasanes, 127
 - Cytochalasine B, 127
 - Cytochalasine D, 127
 - Decarboxylation, 237, 257–267
 - Deuterium, 73, 74, 78, 85, 86, 99
 - Dibenzhydryl oxalate, 33
 - Dicarboxylic acids, 6–9, 22
 - Dieckmann condensation, 276, 277
 - Diels–Alder reaction, 34
 - Dihydrolatumcidin, 111
 - Dihydroxybenzoic acid, 14
 - 2,4-Dihydroxybenzoic acid, 258, 261, 262, 264–266
 - Dimethyl phthalate as solvent for decarboxylation, 34
 - Dioxane as solvent for decarboxylation, 24, 28
 - Dynamic studies, 50
 - Energy barrier, models of, 244–248
 - Enzyme catalysis of decarboxylation, 12, 29–31
 - Epoxydon, 128
 - Equilibrium ^{13}C isotope effect, 27, 29
 - Equilibrium constants, 50, 62
 - Errors in calculation of isotope effects, 6
 - Ester decarboxylation, 33
 - Ester hydrolysis, 267–271
 - Exchange, 50, 53, 56
 - Extent of reaction, f , 6, 10
 - Fatty acids, 128
 - Ferric oxidation of oxalic acid, 38
 - Formic acid, 12
 - Free energy, 55–57, 61
 - Fusaric acid, 143
 - Fusidic acid, 150

- Geldanamycin, 136
 Glycerol as solvent for decarboxylation, 24
 Gramicidin S A, 161
 Griseofulvin, 107

 Halonium ions, 75, 91
 Hammett relationship, 92
 Helicobasidin, 147
 Hirsutic acid, 150
 Homoenolate ions, 78
 α -Hydrogen KIEs, 237, 238, 241, 243, 245, 247–249, 251–253, 255–257, 275, 278–280
 Hydrogen sulfite, addition to carbonyl compounds, 273, 274

 Intermolecular isotope effects, 5, 8, 9
 Internal rotation, 55
 Intramolecular isotope effects, 5, 7
 Inverse isotope effect, 2, 34, 35
 Ion-pair mechanism, 254, 255
 Isomer ratios, 50, 59, 60–62, 64
 β Isotope effect, 27

 Keto–enol tautomerism, 57, 67
 Ketone rearrangements, 64, 75

 β Lactam antibiotics, 139
 Lasalocid A, 144
 Latumecidin, 111
 Limiting values of α -D KIEs, 252, 253

 Malonic acid, 25–29, 257, 264
 Mechanistic investigations, 41, 42, 45, 66
 Mesitoic acid, 17, 257
 4-Methoxyanthranilic acid, 259, 262, 263
 4-Methylantranilic acid, 259
 Methyl iodide, 238, 240–246, 249
 Mollisin, 122
 Multicollic acid, 116
 Multicollosic acid, 116

 β -Naphthaldehyde, 272, 273
 Nigrifactin, 124
 Nitrogen-15 KIEs, 277, 278
 Normal isotope effects, 2
 Nuclear Overhauser Effect (NOE), 46, 47, 52, 59
 Nucleophilic constants, correlations with KIEs, 239, 246–248

 Nucleophilic substitution, 237–257
 Nybomycin, 131

 Ochratoxin A, 145
 Ochrephilone, 125
 Ovalicin, 147
 Oxalic acid, 22–25
 Oxalic acid- d_2 , 23
 Oxaloacetic acid, 29
 Oxidative decarboxylation, 36–38
 Oxime formation, 278, 279
 Oximes, 60, 91
 Oxygen exchange of esters, 270
 Oxygen-18 KIEs, 268, 269

 Paramagnetic reagents, 47, 52, 59
 Peak height-area, 45–48, 59, 63
 Penicillic acid, 113
 Penicillins, 139
 3-Pentyn-2-yl compounds, 252
 Permanganate oxidation of oxalic acid, 36, 37
 pH, 96
 Phenonium ion, 255
 1-Phenylethyl compounds, 238, 242, 249, 251, 254
 Phenylhydrazone formation, 272, 273, 279
 Phomin, 127
 Photodecarboxylation, 34, 38
 Phthalamide, 277, 278
 Picolinic acid, 18–21
 Picolinic acid hydrochloride, 21
 Piericidin A, 137
 Porphyrins, 152
 Prodigiosin, 141
 Protonation, site of, 67, 69, 94, 96
 Pyridinedicarboxylic acids, 31, 32
 Pyrrole-2-carboxylic acid, 18
 Pyrrolnitrin, 151

 Quantitative analysis, 41, 42, 45, 47, 50, 60, 63, 66
 Quinaldinic acid, 21
 Quinoline as solvent for decarboxylation, 13, 27, 28

 γ -Radiation induced decarboxylation, 35
 Radical reactions, 86, 96
 Radicinin, 109
 Rate constants, 50, 53, 92, 96
 Ratio $^{12}\text{C}/^{13}\text{C}$, 6, 10, 11

- Relaxation time, 45–47, 53
 Resonance structure contributions, 67, 92–94, 96
 Rifamycin S, 133
 Rifamycin W, 133
 Ring strain, cause of KIE, 255
 Rotational isomerism, 52

 Salicylic acid, 13
 Salicylic acids, 257–259, 261, 262, 264
 Satellite analysis, 42, 45, 46, 63, 66, 70, 71, 76, 78, 80, 82, 83
 Scytalone, 128
 Semicarbazone formation, 271, 272, 279
 Sepedonin, 145
 Shanorellin, 130
 Showdomycin, 130
 S_N1, 97
 S_N1 reactions, 238, 248–254
 S_N2, 97
 S_N2 reactions, 238–249, 254, 255
 Solvation-number, 62
 Solvation of transition state, 247, 248, 254
 Solvent dependence of isotope effect, 14, 18–21, 31, 33
 Solvent dependence of KIEs, 240, 241, 248
 Solvent isotope effects of D₂O, 258, 259, 261–263, 265–267
 Solvolysis, 248–257

 Stereoconfiguration, 62
 Sterigmatocystin, 119
 Streptovaricin D, 135
 Stretching force constants, 241–247, 254, 273
 Stretching vibrations, 269, 273
 Sulfur-34 isotope effects, 273, 274

 Tajixanthone, 128
 Tautomeric equilibrium, 57, 67, 77, 95–97
 Temperature dependence of isotope effect, 2, 3, 23–25, 27–29
 Tenellin, 129
 Terpenes, 146
 Thermozytocidin, 128
 Trichloroacetic acid, 12
 Trichothecolone, 150
 2,4,6-Trihydroxybenzoic acid, 257, 258, 262, 264–266
 2,4,6-Trimethoxybenzoic acid, 257
 2,4,6-Trinitrobenzoate ion, 257, 264
 Triphenylmethyl chloride, 238, 249, 250, 254
 Tritium isotope effect, 20

 Valence tautomerism, 85
 Variotin, 142
 Virescenol A, 149
 Viscosity, 46
 Vitamin B₁₂, 152

QD.466.5.C1.C317

CARBON-13 IN ORGANIC CHEMIST

RY /

*CIOCHE

N/2060/00605/8149X

stac
QD 466.5.C1 C317
Carbon-13 in organic chemistry



32060003205651

↑↑ TRINITY UNIV. MADDUX LIBRARY ↑↑



32060003205651